Gauge/Gravity Duality: Exploring Universal Features in Quantum Matter

Steffen Klug

München 2013

Dissertation

an der Fakultät für Physik
der Ludwig-Maximilians-Universität, München
vorgelegt von Steffen Klug geb. Müller
aus Stuttgart am 30. April 2013.

Erstgutachter:	Priv.-Doz. Dr. Johanna Karen Erdmenger
Zweitgutachter:	Prof. Dr. Dieter Lüst
Tag der mündlichen Prüfung:	09. Juli 2013

Max-Planck-Institut für Physik,
München, April 2013

To my lovely wife

Zusammenfassung

In der vorliegenden Arbeit wird mit Hilfe der verallgemeinerten Eichtheorie/Gravitations-Dualität, welche stark gekoppelte Eichtheorien mit schwach gekrümmten gravitativen Theorien verbindet, stark korrelierte Quantenzustände der Materie untersucht. Der Schwerpunkt liegt dabei in Anwendungen auf Systeme der kondensierten Materie, insbesondere Hochtemperatur-Supraleitung und kritische Quantenzustände bei verschwindender Temperatur. Die Eichtheorie/-Gravitations-Dualität entstammt der Stringtheorie und erlaubt eine Umsetzung des holographischen Prinzips. Aus diesem Grund wird eine kurze Einführung in die Konzepte der Stringtheorie und ihre Auswirkungen auf das holographische Prinzip gegeben. Für das tiefere Verständnis der effektiven Niederenergie-Feldtheorien wird zusätzlich die Supersymmetrie benötigt. Ausgestattet mit einem robusten Stringtheorie-Hintergrund wird die unterschiedliche Interpretation der Dirichlet- oder D-Branen, ausgedehnte Objekte auf denen offene Strings/Fäden enden können, diskutiert: Zum einen als massive solitonische Lösungen der Typ II Supergravitation und auf der anderen Seite, ihre Rolle als Quelle für supersymmetrische Yang-Mills Theorien. Die Verbindung dieser unterschiedlichen Betrachtungsweise der D-Branen liefert eine explizite Konstruktion der Eichtheorie/Gravitations-Dualität, genauer der $\mathrm{AdS}_5/\mathrm{CFT}_4$ Korrespondenz zwischen der $\mathcal{N} = 4$ supersymmetrischen $SU(N_c)$ Yang-Mills Theorie in vier Dimensionen mit verschwindender β-Funktion in allen Ordnungen, also eine echte konforme Theorie, und Type IIB Supergravitation in der zehn dimensionalen $\mathrm{AdS}_5 \times S^5$ Raumzeit. Darüber hinaus wird das Wörterbuch, das zwischen den Operatoren der konformen Feldtheorie und den gravitativen Feldern übersetzt, im Detail eingeführt. Genauer gesagt, die Zustandssumme der stark gekoppelten $\mathcal{N} = 4$ supersymmetrischen Yang-Mills Theorie im Grenzwert großer N_c, ist identisch mit der Zustandssumme der Supergravitation unter Berücksichtigung der zugehörigen Lösungen der Bewegungsgleichungen, ausgewertet am Rand des AdS-Raumes. Die Anwendung der perturbativen Quantenfeldtheorie und die Verbindungen zur quantenstatistischen Zustandssumme erlaubt die Erweiterung des holographischen Wörterbuchs auf Systeme mit endlichen Dichten und endlicher Temperatur. Aus diesem Grund werden alle Aspekte der Quantenfeldtheorie behandelt, die für die Anwendung der "Linear-Response"-Theorie, der Berechnung von Korrelationsfunktionen und die Beschreibung von kritischen Phänomenen benötigt werden, wobei die Betonung auf allgemeine Zusammenhänge zwischen Thermodynamik, statistischer Physik bzw. statistischer Feldtheorie und Quantenfeldtheorie liegt. Des Weiteren wird der Renormierungsgruppen-Formalismus zur Beschreibung von effektiven Feldtheorien und kritischen Phänomene im Kontext der verallgemeinerten Eichtheorie/Gravitations-Dualität ausführlich dargelegt. Folgende Hauptthemen werden in dieser Arbeit behandelt: Die Untersuchung der optischen Eigenschaften von holographischen Metallen und ihre Beschreibung durch das Drude-Sommerfeld Modell, ein Versuch das Homes'sche Gesetz in Hochtemperatur-Supraleitern holographisch zu beschreiben indem verschiedene Diffusionskonstanten und zugehörige Zeitskalen berechnet werden [1], das mesonische Spektrum bei verschwindender Temperatur und schlussendlich holographische Quantenzustände bei endlichen Dichten [2]. Entscheidend für die Anwendung dieses Rahmenprogramms auf stark korrelierte Systeme der kondensierten Materie ist die Renormierungsgruppenfluss-Interpretation der $\mathrm{AdS}_5/\mathrm{CFT}_4$ Korrespondenz und die daraus resultierenden emergenten, ho-

lographischen Duale, welche die meisten Beschränkungen der ursprünglichen Theorie aufheben. Diese sogenannten “Bottom-Up” Zugänge sind besonders geeignet für Anwendungen auf Fragestellungen in der Theorie der kondensierten Materie und der “Linear-Response”-Theorie, mittels des holographischen Fluktuations-Dissipations-Theorem. Die Hauptergebnisse der vorliegenden Arbeit umfassen eine ausführliche Untersuchung der R-Ladungs-Diffusion und der Impulsdiffusion in holographischen s- und p-Wellen Supraleitern, welche durch die Einstein-Maxwell Theorie bzw. die Einstein-Yang-Mills Theorie beschrieben werden, und eine Vertiefung des Verständnisses der universellen Eigenschaften solcher Systeme. Als zweites wurde die Stabilität der kalten holographischen Quantenzustände der Materie untersucht, wobei eine zusätzliche Diffusions-Mode entdeckt wurde. Diese Mode kann als eine Art “R-Spin-Diffusion” aufgefasst werden, die der Spin-Diffusion in Systemen mit frei beweglichen “itineranten” Elektronen ähnelt, wobei die Entkopplung der Spin-Bahn Kopplung die Spin-Symmetrie in eine globale Symmetrie überführt. Das Fehlen der Instabilitäten und die Existenz einer “Zero-Sound” Mode, bekannt von Fermi-Flüssigkeiten, deuten eine Beschreibung der kalten holographischen Materie durch eine effektive hydrodynamische Theorie an.

Abstract

In this dissertation strongly correlated quantum states of matter are explored with the help of the gauge/gravity duality, relating strongly coupled gauge theories to weakly curved gravitational theories. The main focus of the present work is on applications to condensed matter systems, in particular high temperature superconductors and quantum matter close to criticality at zero temperature. The gauge/gravity duality originates from string theory and is a particular realization of the holographic principle. Therefore, a brief overview of the conceptual ideas behind string theory and the ramifications of the holographic principle are given. Along the way, supersymmetry and supersymmetric field theories needed to understand the low energy effective field theories of superstring theory will be discussed. Armed with the string theory background, the double life of D-branes, extended object where open strings end, is explained as massive solitonic solutions to the type II supergravity equations of motion and their role in generating supersymmetric Yang-Mills theories. Connecting these two different pictures of D-branes will give an explicit construction of a gauge/gravity duality, the $\text{AdS}_5/\text{CFT}_4$ correspondence between $\mathcal{N} = 4$ supersymmetric $SU(N_c)$ Yang-Mills theory in four dimensions with vanishing β-function to all orders, describing a true CFT, and type IIB supergravity in ten-dimensional $\text{AdS}_5 \times S^5$ spacetime. Furthermore, the precise dictionary relating operators of the conformal field theory to fields in the gravitational theory is established. More precisely, the partitions functions of the strongly coupled $\mathcal{N} = 4$ supersymmetric Yang-Mills theory in the large N_c limit is equal to the on-shell supergravity partition evaluated at the boundary of the AdS space. Applying the knowledge of perturbative quantum field theory and its relation to the quantum partition function the dictionary may be extended to finite temperature and finite density states. Thus, all aspects of quantum field theory relevant for the application of linear response theory, the computation of correlation functions, and the description of critical phenomena are covered with emphasis on elucidating connections between thermodynamics, statistical physics, statistical field theory and quantum field theory. Furthermore, the renormalization group formalism in the context of effective field theories and critical phenomena will be developed explaining the critical exponents in terms of hyperscaling relations. The main topics covered in this thesis are: the analysis of optical properties of holographic metals and their relation to the Drude-Sommerfeld model, an attempt to understand Homes' law of high temperature superconductors holographically by computing different diffusion constants and related timescales [1], the mesonic spectrum at zero temperature and holographic quantum matter at finite density [2]. Crucially for the application of this framework to strongly correlated condensed matter systems is the renormalization flow interpretation of the $\text{AdS}_5/\text{CFT}_4$ correspondence and the resulting emergent holographic duals relaxing most of the constraints of the original formulation. These so-called bottom up approaches are geared especially towards applications in condensed matter physics and to linear response theory, via the central operational prescription, the holographic fluctuation-dissipation theorem. The main results of the present work are an extensive analysis of the R-charge- and momentum diffusion in holographic s- and p-wave superconductors, described by Einstein-Maxwell theory and the Einstein-Yang-Mills model, respectively, and the lessons learned how to improve the understanding of universal features in such systems. Secondly, the stability of cold holographic quantum

matter is investigated. So far, there are no instabilities detected in such systems. Instead, an interesting additional diffusion mode is discovered, which can be interpreted as an “R-spin diffusion”, resembling spin diffusion in itinerant electronic systems where the spin decouples from the orbital momenta and becomes an internal global symmetry. The lack of instabilities and the existence of a zero sound and diffusion mode indicates that cold holographic matter is closely described by an effective hydrodynamic theory.

Contents

List of Figures

List of Tables

List of Program Codes

1 Introduction

Modern physics is and has been very successful in approaching the explanation of physical phenomena by resting on two seemingly very different philosophies: The first approach has been dominating for centuries and followed the reductionist viewpoint of finding a unified fundamental description of all physical phenomena. The second approach takes into account the lessons learned from quantum mechanics and confusingly entangled systems to identify the dominating, emergent degrees of freedom characterizing the observed phenomena. Recently, these two approaches have been coming closer and may even be connected by a fascinating duality involving string theory and strongly coupled non-perturbative quantum field theories with the help of a new principle, known as the *holographic principle*, which is not fully understood yet.

Before the onset of modern physics in the 20^{th} century, the main driving idea of understanding the physical world was to find a accurate simplification and subsequent description in terms of the available contemporary mathematics. Every physical system described by a collection of experimentally measured data can be eventually described by a single closed theory that may even allow for predicting yet unobserved phenomena. Starting from Newton's theory of point particles extended by many physicist such as d'Alembert, Laplace, Lagrange, *etc*. which finally culminated in Hamilton's principle, describing our classical mechanical world by a simple quantity, known as the action. Ontologically[1], the physical world was viewed as a large, intricate mechanical system whose evolution in time is mathematically described by Hamilton's principle of an extremized action. The same reductionist approach even succeeded for systems with incredible large number of particles such as gases, liquids and solids. Their thermodynamic properties may be encoded in a single function, nowadays known as the entropy. It was possible to describe all known classical interactions, the magnetic and electric phenomena and of course gravity by a unified potential theory. By the end of the 19^{th} century the reductionist approach presented the physical knowledge in a deterministic closed theory, where the last closing links between the microscopic world of point particles and the macroscopic world of thermodynamics were filled in by Boltzmann's statistical mechanics.

[1] Ontology is a branch of philosophy that studies the structure of existence and reality; or simply put tries to answer the question 'what is?'.

In the beginning of the 20^{th} century physics radically shifted to completely new paradigms. Albert Einstein was one of the first that drastically shifted the understanding of nature and introduced the most powerful principle physicist heavily exploited afterwards: the invariance of the real physical world under symmetries and the equivalence principle. Before Einstein's special relativity, unifying space and time, symmetries were only considered as yet another property of a physical system that may be used to simplify its description. With the success of general relativity the new era heralded by symmetrizing and geometrizing physical phenomena attracted mathematicians such as Hermann Weyl, to find a unified framework were symmetries heavily constrain the possible realization of physical systems. Another even more drastic shift was discovered by Max Planck while trying to reconcile thermodynamic properties with an electromagnetic description by introducing the innocent constant $\hbar$ to make sense of the calculation. In contrast to the discovery of special and general relativity based more or less on pure theoretical reasoning, the development of quantum mechanics was driven by experiments such as the Stern-Gerlach experiment discovering the spin of the electron or spectroscopy on atomic and molecular gases. All these effects could be traced back to the existence of a discretized description of nature which approaches the continuous world for large energies, system size and time scales. However, the implications of this innocent discretization are tremendous: as worked out by many physicist such as Born, Heisenberg, Schrödinger, quantum mechanics radically breaks with the classical mechanical deterministic world view. In quantum mechanics the reality is no longer part of the physical framework, but is unveiled only by measurements in experiments. Ontologically, the existence of an electron is absolutely unclear and only manifests its properties when measured. Even so, its existence might be interpreted as a wave or a particle. As this bizarre theory unfolded the symmetry principle was let to victory in particular by Weyl unraveling the connection between intrinsic gauge symmetries and quantum mechanics. The properties being measured with certainty are exactly those which belong to an intrinsic symmetry of the system. All properties of a fundamental quantum object are encoded in the conserved quantum numbers under the symmetries of the system, regardless of its nature. Although, in a classical sense the "true" nature of the quantum object is entirely unknown, the fundamental symmetries of nature classify all fundamental quantum objects by their simple quantum numbers. The reductionist success of describing all the fundamental objects and their interactions in terms of symmetries culminated in the standard model of particle physics: explaining the strong and weak nuclear forces as well as electrodynamic interaction in a unified framework. Furthermore, all fundamental particles are classified according to their quantum numbers including flavor, color, baryon and lepton numbers as quarks, leptons, and gauge bosons transmitting the interactions. Some of the symmetries are actually broken in nature therefore not all of these quantum numbers are conserved [3].

The standard model of particle physics is dealing with relativistic theories at high energies. But quantum mechanics and symmetries had a tantamount impact on physics involving states of matter, where we need to deal with a large interacting ensemble of physical objects. With the help of quantum mechanical measurements the analysis of solids and molecular gases by spectroscopic methods such as Raman-, X-ray-, or electron spectroscopy, magnetic resonances or neutron scattering revealed the structure and composition of matter and its related symmetries. The scanning tunneling microscope may even illustrate the structure of matter by a quantum mechanical interaction between the probe and the sample. Symmetries allowed to classify all know stable phases of matter and phase transitions are described by a change of these symmetries. For example a simple melting process of a crystalline phase or solid to a liquid phase removes the point and space symmetries of the crystalline phase by introducing a simple translation and rotation symmetry of the liquid phase. This viewpoint is very different from the previous reductionist viewpoint on symmetries in physics. Here we are dealing with emergent symmetries, not funda-

mental symmetries. In both phases the underlying microscopic fundamental building blocks are interacting by the same electromagnetic interaction and their quantum numbers such as electric charge or spin are unchanged, let alone the quantum numbers involved in the standard model. However, the relevant degrees of freedom characterizing the symmetries of the system and the related quantum numbers are emergent degrees of freedom arising from collective excitations of the system, which are often called quasi-particles to distinguish these composite quantum objects from the fundamental quantum objects. So even if we can understand the small distance behavior in principle, the large scale macroscopic matter state is emerging and may be described by a simple set of properties such as the dimensionality of the system and its symmetries. The "standard model" of traditional condensed matter physics can be formulated as Landau's symmetry breaking theory in combination with the Wilsonian renormalization group formulation of effective theories and Fermi liquid theory. Considering the vacuum as a filled state of particles, the Fermi liquid theory describes small perturbations about this particular vacuum state that may be viewed as complicated entangled collective excitations of the particles creating the vacuum. Fermi liquid theory is relating interacting fermions to free fermions with redefined effective properties such as their masses or the specific heat. The Fermi surface and the respective Fermi momentum is not redefined due to Luttinger's theorem. Interestingly, this seemingly very crude approximation is perturbatively very successful although the strong Coulomb interaction is much larger than the level spacing of different states close to the Fermi surface. Nearly all properties of metals, semiconductors, insulators, magnetic materials, superconductors and superfluids may be described by this theory and the different phases and phase transitions are characterized by the Landau-Wilson symmetry breaking scheme. This seems to work for conventional matter even close to zero temperature. Apart from thermal phase transition, there are also quantum phase transitions triggered by quantum fluctuations at (quantum) critical points. For example the superfluid-insulator transition can be understood as a quantum phase transition connecting two different phases with different conserved quantum numbers. In the insulating phase we find a definite particle number n of excited states and corresponding holes but their phase is totally randomized. On the other hand in the superfluid phase the global $U(1)$ symmetry describing the phase φ of the quantum mechanical state is broken and the excitations of the system involve vortices and anti-vortices with highly fluctuating particle numbers. Both quantum numbers cannot be conserved due to Heisenberg's uncertainty principle, *i.e.* $[\hat{n}, \hat{\varphi}] = \mathrm{i}\hbar$ with $\Delta n \Delta\varphi = \hbar/2$.

As the reader is surely aware, this picture is not complete. Both "standard models" in condensed matter physics and in particle physics fail to describe a huge amount of known phenomena. First of all, gravity as a fundamental interaction is missing in the standard model of particle physics. So far gravity defied any description in terms of the quantum field theory framework. From the reductionist viewpoint the problems arises due to the complicated nature of the symmetries in general relativity. The general covariance forces us to quantize space and time itself and attribute quantum numbers to spatial and time measurements. From effective field theory viewpoint gravity is perturbatively non-renormalizable, so the high-energy completion is not accessible by a typical renormalization group flow. Additionally, the origin of dark energy, dark matter and the role of the cosmological constant are far from being understood. *String theory*, which originally arose in the context of explaining the strong nuclear force prior to the invention of quantum chromodynamics, is a strong candidate for providing a theory that treats all fundamental forces in a unifying framework. The main idea is quite simple: point particles are replaced by strings with finite length. Different elementary particles are generated by different low-energy excitations of the fundamental string. There are also higher dimensional non-perturbative solitonic objects that can be viewed as membranes or hyperplanes in the ten-dimensional background spacetime required for consistency. While string theory is a promising candidate for a unified

theory including gravity, the precise details are not completely understood so far,[2] yet it gives rise to astonishing mathematical relations that shed light on different areas of theoretical and mathematical physics, mostly in the form of "unexpected" dualities. One of these amazing relations, the gauge/gravity duality and its applications to quantum matter is the main focus of this thesis. The gauge/gravity duality is a particular realization of the holographic principle of gravitational systems. The holographic principle follows from the unusual thermodynamic behavior of black holes and in a wider sense every mass distribution that will eventually collapse to a black hole. A black hole is the simplest spherical symmetric solution to Einstein's equations characterize only by its mass, charge and angular momentum. In particular its entropy is related to the event horizon and thus scales as the area of the black hole and not the volume. Taking the holographic principle seriously, it suggest that the complete information of a four dimensional physical theory is encoded in a three dimensional horizon. The gauge/gravity duality connects a four dimensional strongly coupled quantum field theory to a five dimensional weakly curved gravitational system. The strong/weak duality is essentially needed to evade the Weinberg-Witten theorem stating that gravity cannot emerge from a four dimensional local quantum field theory. In this sense gauge/gravity teaches us two important lessons: A strongly coupled quantum theory characterizing strongly correlated quantum states of matter can be described by a simple classical gravitational theory in one dimension higher. Intricate entangled theories with emergent excitations, *e.g*. quantum liquids, are simple related to properties of black hole horizons. Thus, in a wider sense we may view the gauge/gravity duality not only as a strong/weak duality, but also as a unification of emergent phenomena with reductionistic fundamental theories. Both of these lessons will play an important role in applying the gauge/gravity duality to condensed matter systems exhibiting exotic quantum phases of matter.

The condensed matter "standard model" is fairly incomplete as well. There are condensed matter systems that cannot be described by the Fermi liquid theory in conjunction with the traditional Wilsonian effective theory viewpoint. Two very prominent systems that demands a new classification scheme for quantum matter are the fractional quantum Hall effect and high temperature superconductivity. The former arises in two-dimensional cold electron systems subject to large magnetic fields with plateaus in the transverse resistivity at fractional values of the ratio of particle number to magnetic flux quanta in contrast to the integer quantum Hall effect with integer values. This particular state of matter, an incompressible gapped liquid, cannot be described by a long-range ordered phase and the conventional symmetry breaking mechanism, but rather by a new kind of order arising from topological quantities. The discovery of novel phases of quantum matter boosted the need for a new classification scheme in condensed matter physics to characterize these exotic states of matter. Tremendous support came with the discovery of high temperature superconductors, that ultimately heralded the new era of modern condensed matter physics. Recently, experimental progress in controlling strongly correlated electronic systems and the exploration of strongly coupled fermionic/bosonic systems with the help of ultracold gases presented a new picture of nature. Famous examples of novel quantum matter states are spin liquids, high temperature superconductors, heavy fermion compounds, topological insulators, quantum critical regions – sometimes called strange metals – connected to quantum critical points, and as explained above the (fractional) quantum Hall states[3] Let us give a brief overview

[2] The lack of success in explaining natural phenomena is surely not to blame on the theory itself, since the theory is far from being understood. From my point of view it might be almost impossible to work out a physical theory without experimental data. It would have been certainly impossible to identify the relevant degrees of freedom of the effective low-energy theory of QCD, without studying/knowing hadrons. Similarly, no one could have guessed that electrons interacting via the strong Coulomb interaction give rise to a simple quasi-particle description if not nature would have experimentally told us so.

[3] See *e.g*. [4–8] and references therein.

of the possible proposed classifications [9]:

- Looking at low-energy excitations of quantum matter with long-range entanglement
  - **Gapped** quantum matter, *i.e*. systems without zero energy excitations ⟶ spin liquids, quantum Hall liquids.
  - **Conformal** quantum matter, *i.e*. system with relativistic dispersion relations ⟶ antiferromagnets, graphene at zero voltage, ultracold atoms *e.g*. in superfluid insulator transition in optical lattices
  - **Compressible** quantum matter, *i.e*. systems with ground states that changes smoothly the expectation value of conserved charges ⟶ Fermi liquids, Graphene at finite chemical potential, strange metals in high temperature superconductors, superfluids, (super-)solids, spin liquids
- Looking at ordering mechanism of zero temperature ground states
  - **Gapped** topological order, *i.e*. systems with topological degenerate ground states ⟶ fractional quantum Hall liquids, spin liquids, superconductors
  - **Gapless** quantum order, *i.e*. systems described by quantum phase transitions without symmetry breaking ⟶ Fermi liquids, strange metals

The classifications might not even be complete and we may hope to find more exotic quantum states of matter. For example one might think of a gapless topological state protecting gapless fermionic excitations or even massless gauge bosons in the spirit of the bosonic Nambu-Goldstone modes arising in the symmetry breaking formalism [4]. These different phases characterized by different quantum order are connected by quantum phase transitions [6], *c.f*. Figure 1.1, exhibiting singularities in the ground state energy functional upon variation of external parameters in the corresponding Hamiltonian. Several of the above system are strongly correlated liquids not susceptible to perturbative methods. In particular kinetic theory and quasi-particle concepts fail to accurately describe the quantum phases, for example in the above mentioned superfluid-insulator transition the results are highly contradictory upon approaching the quantum critical point (see [10] and references therein). In the strongly interacting cases, the "mapping" between the relevant degrees of freedom in the low-energy regime and the microscopic degrees of freedom are far from being clear and understood. Furthermore, it seems that quantum field theory alone is not enough to tackle strongly correlated systems and to explain these new states of quantum matter. In particular solving strongly coupled quantum field theories poses some challenges. First, there is no analytic recipe to calculate correlation functions or thermodynamic properties. Thus one needs to resort to numerical analysis. This is usually done by lattice gauge theories, working with discretized path integrals that can be handled by numerical approaches such as the quantum Monte-Carlo method. This already leads to some problems. First, it is not mathematically clear if the lattice gauge theory represents the entire continuous gauge theory in the limit of vanishing lattice spacing. Secondly, for fermionic systems whose functional integral representation cannot be bosonized the infamous sign problem renders any computation totally useless. In general, this applies to high-density fermionic matter as found in strongly correlated electronic systems, nuclear matter in neutron stars or heavy nuclei, the ground state properties of quarks and the QCD phase diagram, *c.f*. Figure 1.2. Furthermore, transport properties needs to be calculated in real time which introduces a highly oscillatory integrand $\mathrm{e}^{\mathrm{i}S}$. The same is generically true for all hydrodynamic processes and non-equilibrium calculations. In order to understand quantum matter/order at zero temperature and finite density we seem to have reached an impasse.

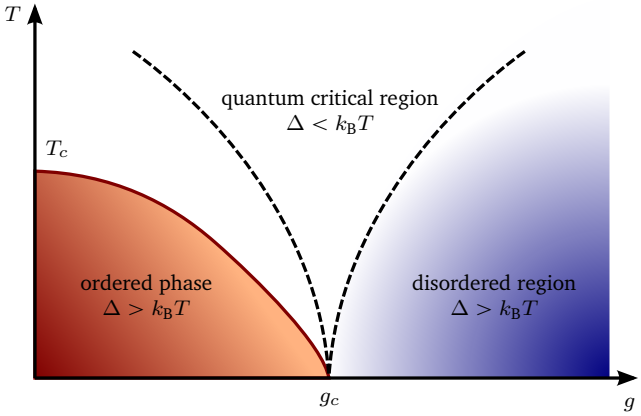

Figure 1.1. A quantum phase transition is indicated by a non-analyticity in the ground state energy which is driven by quantum fluctuations at zero temperature. Tuning the external parameter g in the full Hamiltonian close to the critical value, the characteristic energy scale Δ, associated with the low-energy excitations above the ground state, approaches zero. For an infinite lattice this amounts to the limit of an avoided or an actual level-crossing. For continuous quantum phase transitions, $\Delta \sim J\,|g - g_c|^{z\nu}$ close to the quantum critical point where J denotes the intrinsic/microscopic energy scale of the system, z and ν are the dynamical scaling exponent and a critical exponent, respectively. The correlation length of the quantum fluctuations diverges at the critical point *i.e.* $\xi^{-1} \sim \lambda\,|g - g_c|^{\nu}$ with λ being the inverse lattice spacing. In the finite temperature case, we may find a thermal phase transition indicated by the solid line (—). Typically this thermal phase transition is of BKT type *i.e.* topological, since the quantum ordered phase does not break any symmetries. Above the quantum critical point we find the quantum critical region characterized by quantum *and* thermal fluctuations for $\Delta < k_B T$, exhibiting a long-range quantum entanglement. In this region the classical description breaks down since the imaginary time path integral is not sufficient to capture both thermal fluctuations *and* quantum fluctuations and hence we need to resort to a full complex valued functional in the partition function. Typically the classical theory of thermal phase transitions can only be applied close to the thermal phase transition line (—) terminating at the quantum critical point. The dashed lines (- - -) denote crossovers from the quantum critical region into the effectively classical regions $\Delta > k_B T$ where quantum effects may be neglected since the timescale of the relevant long-distance fluctuations is $\tau \gg \hbar/k_B T$. On the other hand in the quantum critical region we are close to the shortest possible equilibration time allowed by the uncertainty principle, *i.e.* $\tau \sim \hbar/k_B T$. Quantum critical points are found in heavy fermion compounds, pnictides, magnetic insulators and are suspected in high temperature superconductors under the superconducting dome, where the strange metal phase corresponds to the quantum critical region (see [7] and references therein).

Luckily, as explained above gauge/gravity duality provides yet another trick to deal with strongly correlated systems. Although, the original gauge/gravity duality originates from string theory involving a conformal supersymmetric gauge theory and supergravity in a particular ten dimensional spacetime, these constraints can be subsequently removed.

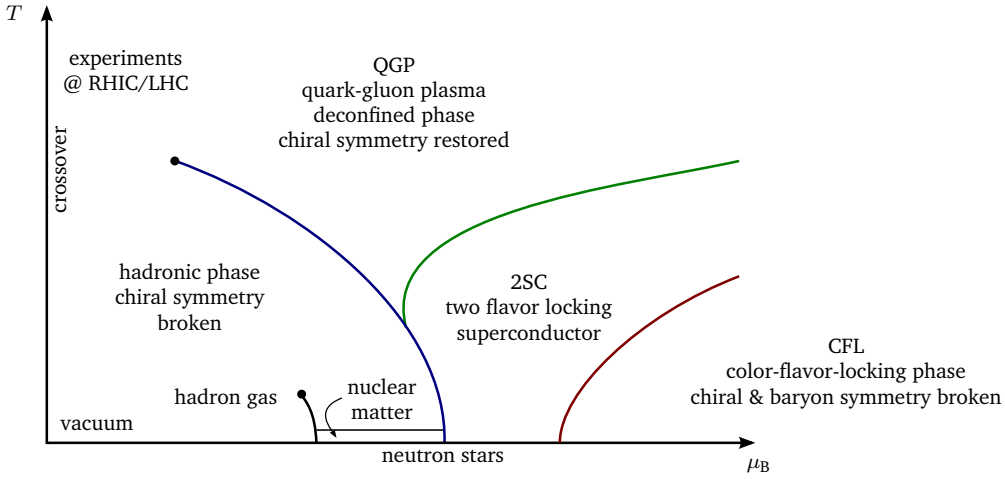

Figure 1.2. This is the state of the art QCD diagram including experimental data, lattice simulations and educated guesses. The experimental accessible region to study the quark-gluon plasma lies at small densities and high temperatures, by smashing heavy ions at high speed. In particular the critical endpoint of the first order chiral phase transition line (—) separating the confined hadronic phase from the deconfined quark-gluon plasma (QGP) phase has been found in heavy ion collisions. Note that so far we do not have sufficient data to understand the QGP phase in detail. For finite light quark masses of the up u and d down quarks compared to heavy strange s quarks, we find a crossover for small baryon densities. In the hadronic phase the chiral symmetry is explicitly broken by the finite quark masses. Cranking up the baryon chemical potential at low temperature, leads to a hadron gas of individual nucleons, in the spirit of very small droplets of hadronized matter until we reach the condensing phase where we find a nuclear matter liquid. For extremely low temperature, a cold nuclear superfluid is formed which is believed to be found in the degenerated matter of neutron stars. For extremely high densities, the difference of the u, d and s quarks are negligible, so flavor and color degrees of freedom are locked in a collective mode, forming cooper pairs with common Fermi momenta. There are two different phases of color superconductivity due to the hierarchy of the quark masses with the strange quark mass much larger as the up and down quark masses, $m_s \gg m_d \approx m_u$. If only the flavors of the up and down quark are locked to the colors red and green, say, chiral symmetry is restored and we find the two color superconducting phase denoted by 2SC. The color symmetry group is broken from $SU(3)_c$ to $SU(2)_c$, hence $8 - 3 = 5$ gluons become massive. However it is not a superfluid since there are no broken global symmetries. Due to the restored chiral symmetry, the 2SC phase is separated from the hadronic phase by a first order phase transition (—). The phase transition between the 2SC phase and the full color superconductor CFL phase (—) is also of first order since the CFL phase again breaks chiral symmetry. Furthermore, the CFL phase is a true superfluid with all symmetries broken and massive gluons exhibiting the Meißner-Ochsenfeld effect known from electromagnetic $U(1)$ superconductors. Finally, we expect a first order phase transition separating the confined 2SC phase from the deconfined QGP phase (—). Due to the strongly correlated nature of the liquid QCD phases and the high densities required to experimentally prepare such a state of matter, the phase diagram is neither theoretically nor experimentally well known. More details about the QCD phase diagram can be found in [11, 12] and in [13] for lattice results.

So far, no counterexample has been found that forbids a generalization of the original duality to finite temperature, densities, non-supersymmetric backgrounds *etc*. Therefore, we simply need to find an appropriate gravity theory that describes the essential key features of our strongly coupled field theory and solve the corresponding classical gravity theory.

Strongly correlated condensed matter and gauge/gravity duality

Gauge/gravity duality has proved to be a valuable tool for exploring strongly coupled regimes of field theories. The best studied example so far for applications to experimentally accessible strongly coupled systems is the application to the quark-gluon plasma. A very important calculation is the derivation of the famous result for the ratio of the shear viscosity and the entropy density [14],

$$\frac{\eta}{s} = \frac{1}{4\pi}\frac{\hbar}{k_{\mathrm{B}}}. \tag{1.1}$$

Here the physical constants $\hbar$ and k_{B} are written out explicitly in order to illustrate the influence of quantum mechanics and thermal physics. The result seems to be supported by lattice gauge theory computations and measurements conducted at RHIC. Recently the anomalous behavior of strongly correlated liquids and thermalization processes are in the focus to be tackled by gauge/gravity methods [15]. The even more exotic phases of QCD are under investigation *e.g*. [16], however, results should be taken carefully especially outside the experimentally reachable regimes since the holographic dual of QCD may *not* reproduce all features correctly. It has been shown [17–19] that the universal result for the ratio of shear viscosity over entropy density applies universally for any isotropic gauge/gravity duality model based on an Einstein-Hilbert action on the gravity side. Exceptions are found by considering higher curvature corrections [20] or anisotropic configurations, see [21, 22] and [23].

As explained above condensed matter physics presents a huge plethora of experimentally controlled and well-studied quantum states of matter, where a theoretical description is lacking. For example, the pairing mechanism of the high-temperature superconductors and the existence of a quantum critical point below the superconducting dome are pressing open questions, *c.f*. Figure 1.3. Recently, the focus of applying the tools of the gauge/gravity duality has been widened to other strongly coupled systems in physics, especially to problems in condensed matter physics [24]. In particular, significant progress has been made in describing holographic fermions (see [25–27] and references therein), superconductors/superfluids (for instance [28–32] and references therein) and to some extent also to lattices [33–39]. For obtaining a solid general framework for condensed matter applications of the gauge/gravity duality, it would be very useful to derive a universal relation, similar in importance to (1.1), designed in particular for applications in condensed matter physics. Interestingly, the result (1.1) may be understood in the context of condensed matter physics by a time scale argument. Here, the properties of quantum critical regions [6, 7] give rise to a universal lower bound

$$\tau_{\hbar} = \frac{\hbar}{k_{\mathrm{B}}T}, \tag{1.2}$$

sometimes called "Planckian dissipation" [40] which can be compared to the possible lower bound for η/s given in (1.1). This seems to imply that the "strange metal phase" is a nearly perfect fluid without a quasi-particle description as is the quark-gluon plasma, since both cases do not allow for long-lived excitations compared to the energy

$$\frac{\hbar}{\tau} \ll \epsilon, \tag{1.3}$$

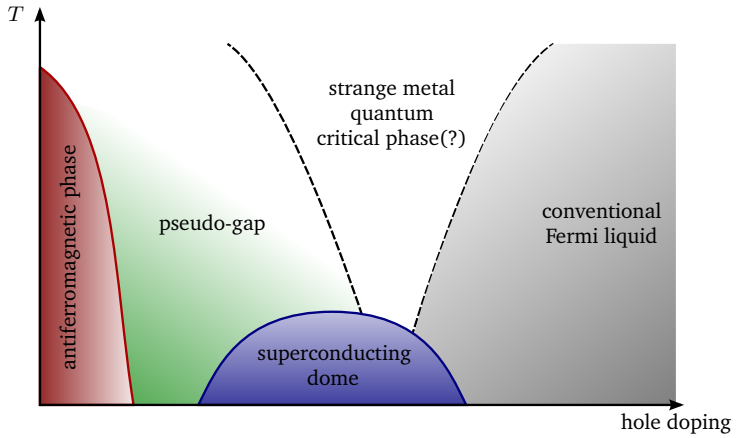

Figure 1.3. The phase diagram of a typical high temperature superconductor: many unconventional high temperature superconductors, known as cuprates, feature an effectively two-dimensional electronic system in a copper-oxide (CU_2) layer background. The low-doping ground state of many oxides is described by an antiferromagnetic phase. Upon increasing the hole doping, the system enters the so-called pseudo-gap region, describe by states with partial energy gaps in the Fermi surface. The superconducting phase exhibiting the Meißner-Ochsenfeld effect, expelling magnetic fields characterizing an ideal diamagnet, and vanishing direct current resistivity is often called superconducting dome due to its shape. Optimal doping refers to the top of the dome where the critical temperature is maximized. Above the superconducting dome there is a non-Fermi liquid phase with unusual thermodynamic properties deviating from the Fermi liquid behavior. It is conjectured that this phase might be a quantum critical phase with a quantum critical point, located somewhere below the superconducting dome. At high doping we again find a conventional Fermi liquid. The pairing or gluing mechanism inducing superconductivity is still unknown, but it is highly unlikely a phonon induced attraction of electrons since no isotope effect has been detected. Since electron carries charge and spin, there are other possibilities *e.g.* the exchange of spin fluctuations/magnons or exotic quantum ordered states facilitate charge-spin separation. The phase diagram of electron doped high temperature superconductors is roughly the mirrored image along the temperature axis.

but rather describe a regime characterized by

$$\tau \sim \frac{\hbar}{\epsilon}. \tag{1.4}$$

In the case of the quark-gluon plasma, a possible characteristic time scale can be defined by

$$\eta \sim \epsilon\tau. \tag{1.5}$$

In typical condensed matter problems at quantum critical points, the relevant energy scale ϵ is set by the thermal energy $\epsilon \sim k_B T$. A very interesting universality shown by almost all types of superconductors is *Homes' law*. Thus, it is an exciting candidate to find a universal relation for strongly coupled condensed matter systems [41] where the usual quasi-particle picture seems to fail. Interestingly, the universality of Homes' law seems to go beyond the "artificial" distinction

between traditional and modern condensed matter physics since it displays a relation that works for conventional superconductors and high temperature superconductors which can be regarded as representatives of the old and the yet to be developed framework. So the main focus of the present work lies in universal properties of quantum states of matter and their appropriate realization as holographic models.

Outline of the thesis

The main topics covered in this thesis are: the analysis of optical properties of holographic metals and their relation to the Drude-Sommerfeld model, an attempt to understand Homes' law holographically by computing different diffusion constants and related timescales, the mesonic spectrum at zero temperature and holographic quantum matter at finite density. The thesis is structured as follows: In Chapter 2 we will extensively cover the all aspects of quantum field theory relevant for the application of linear response theory, computing correlation functions, and describing critical phenomena. In particular, the emphasis lies on elucidating connections between thermodynamics, statistical physics, statistical field theory and quantum field theory. The renormalization group formalism in the context of effective field theories and critical phenomena will be developed explaining the critical exponents in terms of hyperscaling relations. The chapter is concluded by a discussion of conformal field theories arising at critical points in thermal field theory. In Chapter 3 we give a brief overview of the conceptual ideas behind string theory and the ramifications of the holographic principle. Along the way we will discuss supersymmetry and supersymmetric field theories needed to understand the low energy effective field theories of superstring theory. Armed with the string theory background, we move on to explain the double life of D-branes, extended object where open strings end, as massive solitonic solutions to the type II supergravity equations of motion and their role in generating supersymmetric Yang-Mills theories. Connecting these two different pictures of D-branes will give an explicit construction of a gauge/gravity duality, the $\text{AdS}_5/\text{CFT}_4$ correspondence between $\mathcal{N}=4$ supersymmetric $SU(N_c)$ Yang-Mills theory in four dimensions with vanishing β-function to all orders, describing a true CFT, and type IIB supergravity in ten-dimensional $\text{AdS}_5 \times S^5$ spacetime. Furthermore, we will establish the precise dictionary relating operators of the conformal field theory to fields in the gravitational theory. More precisely, the partitions functions of the strongly coupled $\mathcal{N}=4$ supersymmetric Yang-Mills theory in the large N_c limit is equal to the on-shell supergravity partition evaluated at the boundary of the AdS space. Applying our knowledge of perturbative quantum field theory and its relation to the quantum partition function we may extend the dictionary to finite temperature and finite density states. The last part of this chapter deals with the renormalization flow interpretation of the $\text{AdS}_5/\text{CFT}_4$ correspondence and the resulting emergent holographic duals relaxing most of the constraints of the original formulation. These so-called bottom up approaches are geared especially towards applications in condensed matter physics and to linear response theory, closing the chapter with the central operational prescription, the holographic fluctuation-dissipation theorem. In Chapter 4 we will discuss holographic s- and p-wave superconductors. In particular, we discuss the bottom-up approaches to model the properties of superconductors or more precisely superfluids, *i.e.* the Einstein-Maxwell theory and the Einstein-Yang-Mills model. The full holographic s-wave fluctuation equations in d spacetime dimensions are derived and the respective correlation functions in the metallic phase are investigated. The nature of the optical conductivity of the strongly coupled metallic phase is compared to the Drude-Sommerfeld model in the regime $\omega \ll T$. For large frequencies the conformal limit set by the scaling dimensions of the current operator is recovered. Furthermore, the s-wave and p-wave phase diagram is computed numerically with backreaction and for various masses of the scalar condensate characterizing the s-wave superconducting phase. In order to

calculate universal features of real world superconductors a holographic realization of Homes' law is proposed. Homes' law as explained above is not directly accessible to holographic calculations due to the very different nature of the gravitational dual. Thus, we explicitly rewrite the original Homes' law relation in terms of a simple universal statement about diffusive processes *i.e.* $D(T_c)T_c = \text{const.}$. The chapter concludes with an extensive analysis of the R-charge diffusion and momentum diffusion in holographic s- and p-wave superconductors and the lessons learned how to improve our understanding of universal features in such systems. In Chapter 5 we investigate the stability of a top-down construction describing cold holographic quantum matter. As already realized in the previous chapter an intriguing quantum critical point arises in the zero temperature finite density gravity background with finite entropy density, indicating a large ground state degeneracy. The existence of charged bosonic and fermionic degrees of freedom let us anticipate a non-trivial meta-stable state of quantum matter. Studying mesonic fluctuations described by the fluctuations of the worldvolume fields of a single D_7-brane embedded in a zero temperature and finite density background *does* not reveal any instability and seems to imply that the finite density AdS_2 ground state is stable. In order to conduct the numerical quasi-normal mode analysis we need to devise a new numerical scheme dubbed the "zig-zag" method to deal with numerical instabilities arising from irregular singular points in the fluctuation equations about the finite density background. After complexifying the radial integration variable, we invent an integration contour that avoids the entanglement of in- and outgoing waves and allows for an easy extraction of the correct solution while avoiding branch cuts in the complex radial plane of the finite density solution. Along the way, we discover an interesting additional diffusion mode, which can be interpreted as an "R-spin diffusion", resembling spin diffusion in itinerant electronic systems where the spin decouples from the orbital momenta and becomes an internal global symmetry. The lack of instabilities and the existence of a zero sound and diffusion mode indicates that cold holographic matter is closely described by an effective hydrodynamic theory. The final Chapter 6 gives an extensive discussion of the results obtained and how to improve the approaches to gain an even deeper knowledge of universal features and the nature of the strongly coupled ground states. An outlook to extend the top-down program to fermionic excitations and to check Luttinger's theorem in hyperscaling violating backgrounds is given.

Main results of this thesis

In the following the main results of this thesis are listed. Let me emphasize that all analytic and numerical computation presented in this thesis have been executed by myself. Most of the work reproduces known results in a different context and is used as a consistency check of my derivations and extension. Yet some of the work is original and other parts have been derived in close collaboration with the authors of [1, 2].

- **Universality in high temperature superconductors/Homes' law:**

  The original empirically found relation by Homes et al. [42, 43] between the superfluid density at vanishing temperature and the direct current conductivity measured at the critical temperature times the critical temperature, *i.e.* $\rho_s = C\sigma_{DC}(T_c)T_c$, is not amenable to a direct holographic formulation. We first reformulate Homes' law in a way that we can relate it to the aforementioned "Planckian dissipation" following [40] and construct a holographic function describing the proportionality constant of Homes' law in terms of the black hole charge in our gravity dual. The proposed holographic version of Homes' law is given by

$$C_M\big|_{d=3} = 4\pi T_c D_M(T_c) = \left(1 + \frac{4\bar{Q}^2}{3-\bar{Q}^2}\right)^{-1},$$

$$C_{\mathrm{R}}\big|_{d=4} = 4\pi T_c D_{\mathrm{M}}(T_c) = \frac{(2-\bar{Q}^2)(2+\bar{Q}^2)}{2(1+\bar{Q}^2)}, \tag{1.6}$$

$$C_{\mathrm{M}}\big|_{d=4} = \left(1+\frac{3\bar{Q}^2}{2-\bar{Q}^2}\right)^{-1}.$$

where Homes' law holds for these functions to be constant. This is true in the probe limit $\bar{Q} = 0$, where we neglect the backreaction of the matter content onto the background geometry. Unfortunately, the black hole charge $\bar{Q}$ as a function of the critical chemical potential is not constant but rather monotonically decreasing. The ramifications of this result are discussed in detail in Chapter 6. Independent of Homes' law the derivation of the phase diagram and the computation of the diffusion constant yield invaluable insight into holographic superconductors/superfluids, such as a non-trivial relation between the density of a holographically ideal conductor and the superfluid density in the superconducting phase.

- **Properties of cold holographic matter:**

  We compute the quasi-normal mode spectrum of mesonic operators in a zero temperature, finite density background described by a certain embedding function of a D_7-brane. As there is some circumstantial evidence that the system might be unstable, such as finite entropy density at zero temperature and charged degrees of freedom, our quasi-normal analysis does not reveal any instabilities. We discover a diffusive mode related to an internal global $SU(2)$ symmetry that resembles a spin diffusion process known in itinerant electronic condensed matter systems. All results are computed numerically, where the presence of irregular singular points forced us to devise a numerical integration scheme adapted to the problem.

2
Field Theory

In this chapter we will lay the groundwork for understanding thermal properties and dynamical processes of complex physical systems. These systems typically involve a large amount of interacting entities and thus we need to adapt our mathematical language to efficiently deal with the essential information we want to extract. One of the major tools to treat such systems are field theoretic methods, encoding the minimal amount of information, crucial to understand and reproduce measurable effects. The main concern lies on systems that are related to condensed matter phenomena found in nature, such as metals and superconductors. In particular we will see that the field theoretic methods developed and explained here fail to cope with novel types of condensed matter system that cannot be classified using the traditional scheme of symmetry breaking and renormalization.

2.1. Quantum Field Theory

Overview

- Why use field theory?
  → calculate measurable observables, *e.g.* correlators of operators, spectral densities,... .
- Quantum mechanics is just a $0+1$ dimensional field theory.
- Thermal field theory/statistical field theory is related to quantum field theory.

There are several ways to approach field theories. What is common to all approaches is the removal of any discrete entities by an averaging prescription in such a way that the physically measurable quantities are unchanged. This can be done since averaging lies at the very heart of any measuring device. In principle there is always a finite resolution, so there are no exact "point-like" measurements.[1] Here we will start from the quantum mechanical viewpoint and

[1] Experimentally, it is possible to do a single measurement to determine the spin of a single atom, for instance. The

extend it to infinitely many degrees of freedom. This procedure is somewhat strange because we will restructure the theory which is usually known under the (misleading) term “second quantization”.

2.1.1. Path integral formulation of quantum mechanics

Quantum mechanics is an intrinsically probabilistic theory. Although the time evolution is deterministic, it is not possible to predict the outcome of an experiment. Even worse, the experiment has to be iterated many times to obtain meaningful information about the system under the same initial conditions. If an experimenter would be allowed to do an experiment only once, the result would be absolutely meaningless. This statistical nature will be made explicit in the functional integral formulation of quantum mechanics. In quantum mechanics the path integral defines expectation values of quantum operators. It encodes the basic principle of quantum mechanics, *i.e*. the superposition principle: we can view the path integral as a weighted summation over all possible paths of the system in phase space. Since the physical time is a true parameter in quantum mechanics (there is no time operator $\hat{t}$), we can understand this sum as the complete possible/accessible history of the physical system.[2] The derivation is quite simple and will be outlined with emphasis on the physical implications:

i View the path integral as a limit of n-slits placed at N discrete points, which effectively describes free space in the limit $n \to \infty$ and $N \to \infty$. Since we will construct the path integral in phase space (parametrized by the position q and the momentum p) we can apply the $n \to \infty$ limit at the beginning.

ii Take the unitary time evolution operator

$$\mathcal{U}(t',t) = \mathrm{e}^{-\frac{\mathrm{i}}{\hbar}\mathcal{H}(t'-t)}\,\Theta(t'-t), \qquad \big|\,\Psi(t')\,\big\rangle = \mathcal{U}(t',t)\,\big|\,\Psi(t)\,\big\rangle, \tag{2.1}$$

where $\Theta(t'-t)$ denotes the Heaviside distribution defined as

$$\Theta(t) = \begin{cases} 1 & t > 0 \\ 0 & t < 0 \end{cases} \tag{2.2}$$

The time evolution operator is applied N times with discrete time step $\Delta t = {}^{(t'-t)}\!/_{N}$ to describe the time evolution of the system from the fixed initial state $|\,q_i\,\rangle$ at $t = 0$ to the final state $|\,q_f\,\rangle$ at $t' = t$. The transition/probability amplitude for this process is given by

$$\begin{aligned}\left\langle q_f \left| \left[\,\mathrm{e}^{-\frac{\mathrm{i}}{\hbar}\mathcal{H}\Delta t}\,\right]^N \right| q_i \right\rangle = \int \prod_{k=1}^{N-1} \mathrm{d}q_k \left\langle q_f \left| \,\mathrm{e}^{-\frac{\mathrm{i}}{\hbar}\mathcal{H}\Delta t}\, \right| q_{N-1} \right\rangle \\ \times \left\langle q_{N-1} \left| \cdots \right| q_1 \right\rangle \left\langle q_1 \left| \,\mathrm{e}^{-\frac{\mathrm{i}}{\hbar}\mathcal{H}\Delta t}\, \right| q_i \right\rangle,\end{aligned} \tag{2.3}$$

where we inserted the resolution of identity

$$\int \mathrm{d}q_k\,|\,q_k\,\rangle\langle\,q_k\,| = \mathbb{1}, \tag{2.4}$$

at each intermediate time step in the q representation and omitted the limiting process $N \to \infty$.

statement "point-like" should be taken mathematically, *i.e*. it is impossible to read off an absolutely exact value instantaneously.

[2] This idea goes back to Dirac and was later refined and truly appreciated by Feynman.

Look at a single infinitesimal transition amplitude and note that the Hamiltonian generically depends on both phase space variables q and p, so we need to insert a complete set of $|\,p\,\rangle$ states as well

$$\begin{aligned}\left\langle\, q_{k+1} \,\middle|\, \mathrm{e}^{-\frac{\mathrm{i}}{\hbar}\mathcal{H}\Delta t} \,\middle|\, q_k \,\right\rangle &= \int \mathrm{d}p_k \left\langle\, q_{k+1} \,\middle|\, p_k \,\right\rangle\!\left\langle\, p_k \,\middle|\, \mathrm{e}^{-\frac{\mathrm{i}}{\hbar}\mathcal{H}(q,p)\Delta t} \,\middle|\, q_k \,\right\rangle \\ &= \int \mathrm{d}p_k \left\langle\, q_{k+1} \,\middle|\, p_k \,\right\rangle\!\left\langle\, p_k \,\middle|\, \mathrm{e}^{-\frac{\mathrm{i}}{\hbar}H(q_k,p_k)\Delta t + \mathcal{O}(\Delta t^2)} \,\middle|\, q_k \,\right\rangle \\ &\approx \int \mathrm{d}p_k \,\langle\, q_{k+1} \,|\, p_k \,\rangle\langle\, p_k \,|\, q_k \,\rangle\, \mathrm{e}^{-\frac{\mathrm{i}}{\hbar}H(q_k,p_k)\Delta t}\,, \end{aligned} \tag{2.5}$$

where we used the Baker-Campell-Hausdorff formula to expand the product

$$\mathrm{e}^{-\frac{\mathrm{i}}{\hbar}\mathcal{H}(q,p)\Delta t} = \mathrm{e}^{-\frac{\mathrm{i}}{\hbar}\mathcal{T}(p)\Delta t}\, \mathrm{e}^{-\frac{\mathrm{i}}{\hbar}\mathcal{V}(q)\Delta t}\, \mathrm{e}^{\frac{1}{2}\left(-\frac{\mathrm{i}}{\hbar}\right)^2\left[\mathcal{T}(p),\mathcal{V}(q)\right]\Delta t^2}\, \mathrm{e}^{\mathcal{O}\left(\Delta t^3\right)}\,. \tag{2.6}$$

The factorization is exact only if $\left[\mathcal{T}(p), \mathcal{V}(q)\right] = 0$. Alternatively and more general, we can write all p operators to the left of all q operators in the Hamiltonian up to linear order in Δt. Interestingly, this implies that for very short timescales the kinetic/momentum contributions disentangle from the potential/position contributions. Since we are considering infinitesimal time steps in the limit $N \to \infty$ we can discard all (Δt^2) terms. Additionally, the momentum space representation is the Fourier transform of the position space representation

$$|\,q\,\rangle = \int \mathrm{d}p\,|\,p\,\rangle\langle\, p \,|\, q\,\rangle = \int \frac{\mathrm{d}p}{2\pi\hbar}\, \mathrm{e}^{\frac{\mathrm{i}}{\hbar}qp}\,|\,p\,\rangle, \qquad \langle\, p \,|\, q\,\rangle = \frac{1}{2\pi\hbar}\, \mathrm{e}^{\frac{\mathrm{i}}{\hbar}qp}\,, \tag{2.7}$$

so we finally get

$$\begin{aligned}\left\langle\, q_{k+1} \,\middle|\, \mathrm{e}^{-\frac{\mathrm{i}}{\hbar}\mathcal{H}\Delta t} \,\middle|\, q_k \,\right\rangle &\approx \int \mathrm{d}p_k \,\langle\, q_{k+1} \,|\, p_k \,\rangle\langle\, p_k \,|\, q_k \,\rangle\, \mathrm{e}^{-\frac{\mathrm{i}}{\hbar}H(q_k,p_k)\Delta t} \\ &= \int \frac{\mathrm{d}p_k}{2\pi\hbar}\, \mathrm{e}^{-\frac{\mathrm{i}}{\hbar}q_{k+1}p_k}\, \mathrm{e}^{\frac{\mathrm{i}}{\hbar}q_k p_k}\, \mathrm{e}^{-\frac{\mathrm{i}}{\hbar}\mathcal{H}(q_k,p_k)} \\ &= \int \frac{\mathrm{d}p_k}{2\pi\hbar}\, \mathrm{e}^{-\frac{\mathrm{i}}{\hbar}\left[\frac{q_{k+1}-q_k}{\Delta t}p_k + H(q_k,p_k)\right]\Delta t}\,. \end{aligned} \tag{2.8}$$

Insert (2.8) into (2.3) to obtain

$$\begin{aligned}\left\langle\, q_f \,\middle|\, \left[\mathrm{e}^{-\frac{\mathrm{i}}{\hbar}\mathcal{H}\Delta t}\right]^N \,\middle|\, q_i \,\right\rangle \approx \int &\left(\prod_{k=1}^{N-1} \mathrm{d}q_k\right)\left(\prod_{k=0}^{N-1} \frac{\mathrm{d}p_k}{2\pi\hbar}\right) \\ &\times \exp\left[-\frac{\mathrm{i}}{\hbar}\Delta t \sum_{k=0}^{N-1} \frac{q_{k+1}-q_k}{\Delta t}p_k + H(q_k,p_k)\right]. \end{aligned} \tag{2.9}$$

Note that we have an additional integration over p_0 coming from $\langle\, q_1 \,|\, \ldots \,|\, q_i = q_0 \,\rangle$ as well as an additional summand $k = 0$ in the exponential.

iii Finally, take the $N \to \infty$ and $\Delta t \to 0$ limit (keeping $t = {}^{N}/_{\Delta t}$ fixed) which yields the continuous path integral. The measure will be denoted by

$$\mathcal{D}[q,p] = \lim_{N\to\infty} \prod_{k=1}^{N-1} \mathrm{d}q_k \prod_{k=0}^{N-1} \frac{\mathrm{d}p_k}{2\pi\hbar}. \tag{2.10}$$

Furthermore, the sum over the discrete set turns into an integral over the dense time interval $[0,t]$ and the difference quotient ${}^{\Delta q}/_{\Delta t}$ converges to the derivative

$$\Delta t \sum_{k=0}^{N-1} \xrightarrow[N\to\infty]{\Delta t\to 0} \int_0^t \mathrm{d}t', \qquad \frac{q_{k+1}-q_k}{\Delta t} \xrightarrow[N\to\infty]{\Delta t\to 0} \frac{\partial q(t')}{\partial t'} \equiv \dot{q}(t), \tag{2.11}$$

so the Hamiltonian form of the path integral is given by

$$\left\langle q_f \middle| \mathrm{e}^{-\frac{\mathrm{i}}{\hbar}\mathcal{H}t} \middle| q_i \right\rangle = \int_{\substack{q_f=q(t)\\ q_i=q(0)}} \mathcal{D}[q,p] \exp\left[\frac{\mathrm{i}}{\hbar}\int_t^0 \mathrm{d}t' \Big(p(t')\dot{q}(t') - H(q(t'),p(t'))\Big)\right]. \tag{2.12}$$

The path integral can be viewed as a collection of infinitely many integrals summed up for each point in time and weighted by the classical action in Hamiltonian form for all paths/configurations starting in q_i and ending in q_f. Quantum mechanically it describes the propagation of the quantum system from the state $|\, q_i \,\rangle$ to the state $|\, q_f \,\rangle$ with respect to the Hamiltonian $\mathcal{H}$

There are mathematical issues which may impact physical calculations as well, so it is advisable to carry out the steps *iii* and *iii* on page 15 explicitly for the problem at hand. Even for calculating the free quantum propagator the path integral should be evaluated in discretized form in order to regularize divergences. For quantum mechanical calculations we will ignore (at least for all practical purposes) the following mathematical problems:

- The path integral measure is in general ill-defined for arbitrary path integrals. However, for Gaussian integrals[3] we can define a Wiener measure which is mathematically sound (see Section 2.1.3)
- The weight function is a complex function and so weighting is strictly speaking not possible because the complex numbers defy any ordering. So in principle we are not able to distinguish important contributions from insignificant contribution. It is also not clear if the integral does converge at all. We can argue that physically the contributions with large classical action will be highly fluctuating and should average to zero. This argument is based on the stationary phase approximation (see Infobox Stationary Phase Approximation on page 18)

After introducing functional integrals we will see that there are remedies to the problem when considering stochastic functional integrals (see Section 2.1.4 and Table 2.1). Apart from the fact that the path integral is (maybe the most) "natural" representation of the quantum superposition principle mentioned above, there are further advantages:

- The classical limit can be easily obtained. In fact we can view the path integral as being composed of the classical solution (obeying the Hamilton equations of classical mechanics) and the quantum corrections due to quantum fluctuations.

[3] Unfortunately, these are the only integrals we are able to solve, so we will use good approximation and/or transformations to obtain a Gaussian integral from a more complex path integral.

- Non-perturbative effects such as the instanton solution to the quantum double well/tunneling problem can be easily constructed.
- Path integrals can be easily extended to functional integrals describing physics in $d+1$ dimensional spacetime. In this case the time slicing in the construction of the path integral (see step *iii* on page 14) naturally gives rise to a time ordered correlations function of operators.

Lagrangian formulation of the path integral

The path integral in Hamiltonian form (2.12) can be transformed into a Lagrangian version if the momentum dependence of the Hamiltonian is purely quadratic

$$H(q,p) = \frac{p^2}{2m} + V(q), \tag{2.13}$$

or can be brought into quadratic form by completing the square and shifting the integration variable such that we have a factorization of the position integral and a true Gaussian integral over the momentum p

$$\left\langle q_f \left| \, \mathrm{e}^{-\frac{\mathrm{i}}{\hbar}\mathcal{H}t} \, \right| q_i \right\rangle = \int_{\substack{q_f=q(t)\\ q_i=q(0)}} \mathcal{D}[q] \; \mathrm{e}^{-\frac{\mathrm{i}}{\hbar}\int_t^0 \mathrm{d}t' \, V(q(t'))} \int \mathcal{D}[p] \; \mathrm{e}^{\frac{\mathrm{i}}{\hbar}\int_t^0 \mathrm{d}t' \left(p(t')\dot{q}(t') - \frac{p(t')^2}{2m} \right)} . \tag{2.14}$$

The momentum integral evaluates to (using $p \longrightarrow \sqrt{\hbar/\mathrm{i}}p$ and Gaussian integrals defined in Appendix B.1)

$$\begin{aligned}
\mathfrak{I}[p] = & \lim_{N\to\infty} \int \left(\prod_{k=0}^{N-1} \frac{\mathrm{d}p_k}{2\pi\sqrt{\mathrm{i}\hbar}} \right) \exp\left\{ \sum_{k=0}^{N-1} \left[\sqrt{\frac{\mathrm{i}}{\hbar}} \Delta q_k p_k - \frac{1}{2} p_k \left(\frac{t}{Nm} \right) p_k \right\} \right] \\
= & \lim_{N\to\infty} \left\{ \frac{(2\pi)^{N/2}}{\left(2\pi\sqrt{\mathrm{i}\hbar}\right)^N} \det\left[\left(\frac{t}{Nm} \right) \mathbb{1}_N \right]^{-1/2} \right. \\
& \left. \cdot \exp\left[\frac{1}{2} \frac{t}{N} \sum_{k=0}^{N-1} \left(\sqrt{\frac{\mathrm{i}}{\hbar}} \Delta q_k \right) \left(\frac{t}{Nm} \right)^{-1} \left(\sqrt{\frac{\mathrm{i}}{\hbar}} \Delta q_k \right) \right] \right\} \\
= & \lim_{N\to\infty} \left\{ \frac{1}{(2\pi\mathrm{i}\hbar)^{N/2}} \left(\frac{t}{Nm} \right)^{-N/2} \exp\left[\frac{\mathrm{i}}{\hbar} \sum_{k=0}^{N-1} \frac{1}{2} m \left(\Delta q_k \right)^2 \right] \right\} .
\end{aligned} \tag{2.15}$$

Here we strictly evaluate the discrete time sliced integral and take the continuum limit $N \to \infty$. This is the reason why the time t sneaked into the denominator of the prefactor, which could have been easily missed by just applying the Gaussian integration formula. Executing the continuum limit on both sides of (2.15) and inserting it into (2.14) yields the path integral formulation with the classical action in Lagrangian from

$$\begin{aligned}
\left\langle q_f \left| \, \mathrm{e}^{-\frac{\mathrm{i}}{\hbar}\mathcal{H}t} \, \right| q_i \right\rangle = & \int_{\substack{q_f=q(t)\\ q_i=q(0)}} \mathcal{D}[q] \; \mathrm{e}^{\frac{\mathrm{i}}{\hbar}\int_t^0 \mathrm{d}t' \, \frac{1}{2} m \dot{q}(t')^2 - V(q(t'))} \\
= & \int_{\substack{q_f=q(t)\\ q_i=q(0)}} \mathcal{D}[q] \; \mathrm{e}^{\frac{\mathrm{i}}{\hbar}\int \mathrm{d}t' \, L(q(t'),\dot{q}(t'))} = \int_{\substack{q_f=q(t)\\ q_i=q(0)}} \mathcal{D}[q] \; \mathrm{e}^{\mathrm{i}/\hbar S[q,\dot{q}]} .
\end{aligned} \tag{2.16}$$

The path integral measure $\mathcal{D}[q]$ has been rescaled such that the prefactor in (2.16) is absorbed

$$\mathcal{D}[q] = \lim_{N\to\infty} \left(\frac{Nm}{t2\pi\mathrm{i}\hbar}\right)^{\frac{N}{2}} \prod_{k=1}^{N-1} \mathrm{d}q_k \,. \tag{2.17}$$

For non-quadratic momentum integrals we need to employ the so-called stationary phase approximation:

Stationary Phase / Saddle Point Approximation

For a contour integral over a complex analytic function $f(z)$ of the form

$$\mathfrak{I} = \int_{\mathcal{C}} \mathrm{d}z\, h(z)\, \mathrm{e}^{tf(z)} \underset{t\to\infty}{\approx} h(z_0)\, \mathrm{e}^{tf(z_0)}\,, \qquad \text{where} \qquad \frac{\mathrm{d}}{\mathrm{d}z} f(z)\Big|_{z_0} = 0,$$

in the limit $t \to \infty$ the value of $\mathfrak{I}$ is best approximated at points where $f(z)$ is extremized or equivalently, the first derivative of $f(z)$ vanishes. The contour $\mathcal{C}$ must be chosen such that

- the real part of $f(z)$ is maximized,
- the imaginary part is stationary $\longrightarrow$ small fluctuations,

in order to obtain the correct approximation/asymptotic behavior of $\mathfrak{I}$.

This follows from the analyticity condition of complex functions, where both the real and imaginary part have to solve the Laplace equations. Thus, neither the imaginary part nor the real part can have an absolute extremum on the complex plane (except at the origin). In fact, Laplace equations for the real and imaginary part yields a saddle point such that the maximum along a certain contour is a minimum along another. The stationary curves for $\mathrm{Im}\, f(z) = \text{const.}$ are tangent to the gradient of $\mathrm{Re}\, f(z)$, so the optimal contour follows the curve where the absolute value of the function is maximally decreasing when moving through the saddle point. Therefore, this approximation is sometimes called the "steepest descent method".

Applying the stationary phase approximation to the Hamiltonian version of the path integral (2.12) we see that the Hamiltonian equations of motion

$$\frac{\partial}{\partial p(t)} \Big(p(t)\dot{q}(t) - H(q(t), p(t))\Big) = \dot{q}(t) - \frac{\partial H(q(t), p(t))}{\partial p(t)} \overset{!}{=} 0, \tag{2.18}$$

satisfies the stationarity condition. Solving the Hamilton equations for $\dot{q}(t)$ and inserting this into the integrand, removes the $p(t)$ dependence since it corresponds to the Legendre transformation from the Hamiltonian formulations to the Lagrangian formulation. Thus, the momentum integration over p is dropped and the remaining factors can be absorbed into the definition of $\mathcal{D}[q]$ following (2.17). In general this can always be done since the Hamiltonian equation (2.18) is local in $\dot{q}$ and p and so it must hold for arbitrary k or at each time step, respectively. In the case of quadratic integrals (2.13) the stationary phase approximation becomes exact (up to the previous calculated normalization factor of the Gaussian integral).

Semi-classical approximation

The stationary phase approximation can be used to define the validity of the semi-classical limit and allows the "splitting" into the classical path and quantum fluctuations about the classical

solution which arise as corrections in $1/\hbar$. The solution to the saddle point equation are the classical equations of motion (2.18) that minimizes the classical action. Thus, we can expand about the saddle point solution up to quadratic order in the fluctuations

$$S[q] \approx S[q_{\text{cl}}] + \frac{1}{2}\int \mathrm{d}t\,\mathrm{d}t'(q-q_{\text{cl}})(t)\left.\frac{\delta^2 S[q]}{\delta q(t)\delta q(t')}\right|_{q=q_{\text{cl}}}(q-q_{\text{cl}})(t'). \tag{2.19}$$

Note that $S[q]$ is strictly a functional and so we need to apply second order functional derivatives. The first order functional derivative of $S[q]$ vanishes when evaluated on solutions of the equations of motion q_{cl}. Note also that the second order functional derivative is positive definite since the classical solution minimizes the action and hence the convergence of the Gaussian integral is ensured. The stationary path integral reads then

$$\int_{\substack{q_f=q(t)\\ q_i=q(0)}} \mathcal{D}[q]\ \mathrm{e}^{\mathrm{i}/\hbar S[q]} = \sum_{\ell} \mathrm{e}^{\mathrm{i}/\hbar S[q_{\text{cl}}^{(\ell)}]}\ \det\left(\frac{\mathrm{i}}{2\pi\hbar}\frac{\delta^2 S[q^{(\ell)}]}{\delta q_f^{(\ell)}\delta q_i^{(\ell)}}\right)^{-1/2}, \tag{2.20}$$

where the sum over ℓ runs over the contribution from different saddle point solutions. For $\hbar \to 0$ this is the dominant/leading term in the asymptotic expansion. To make the argument mathematically more rigorous one should start from the analytic continuation and expand to higher orders in the fluctuations. Then, the method of steepest descend ensures the convergence of the Gaussian integrals and enables us to choose the constant phase such that the derivatives of the function are real. For an even complex function $f(z)$ we find

$$\mathfrak{I} = \int_{\mathcal{C}} \mathrm{d}z\ \mathrm{e}^{tf(z)} \approx \sqrt{\frac{2\pi}{tf''(z)}}\exp\left[tf(z_0) + \frac{3f^{(\mathrm{iv})}(z_0)}{tf''(z_0)}\right], \tag{2.21}$$

where we see that higher order terms are suppressed with higher powers of t. This power counting carries over to non-Gaussian integrals arising from higher order fluctuation terms in the action $S[q]$.[4] In general we would find contributions to the path integral (2.20) scaling with

$$\int_{\substack{q_f=q(t)\\ q_i=q(0)}} \mathcal{D}[q]\ \mathrm{e}^{\mathrm{i}/\hbar S[q]} \sim \exp\left[\hbar^{-1}\left(S[q_{\text{cl}}] + \sum_{\substack{n>2\\ n\ \text{even}}} \hbar^{n/2}\ \frac{\delta^n S[q]}{\delta q^n}\Big/\left.\frac{\delta^{n/2} S[q]}{\delta q^{n/2}}\right|_{q=q_{\text{cl}}}\right)\right], \tag{2.22}$$

where n denotes the (even!) expansion order in the fluctuation. Again for $\hbar \to 0$ the classical action is the leading term in the asymptotic expansion. Since this is an asymptotic expansion, we can only truncate the series for systems where quantum fluctuations are small. With this final remark we conclude our discussion on path integrals. For a more in-depth discussion and detailed insight see the excellent textbooks [44, 45].

2.1.2. Functional integrals & quantum field theory

When we switched to the path integral formulation of quantum mechanics something miraculous happened. The position and momentum operators somehow vanished from the actual calculations and were replaced by a classical action relying only on classical position and momentum functions. Therefore, we are naturally led to the idea of demoting the position operator to a classical parameter such as the time and thus allowing us to treat space and time on the same

[4] These higher order terms have to be expanded in order to perform the integral.

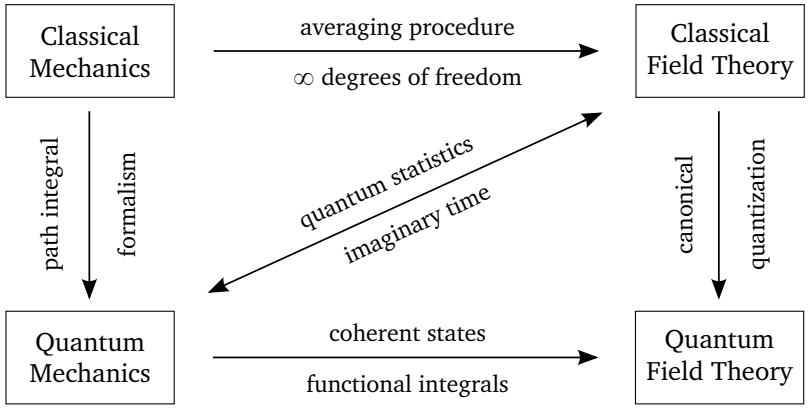

Figure 2.1. Various connection between the corner stones of theoretical physics. Formal similarities and analogs in mathematical representation allows for interconnections and methodical transfer between conceptual different physical frameworks. One of the most fruitful and interesting connection is the mapping of quantum statistics onto (classical) field theory.

footing.[5] This gives way to a formulation where the quantum mechanical structure is implemented in field valued operators $\varphi(t, \mathbf{x})$ describing the creation/annihilation of excitations from a vacuum state at given time t and point $\mathbf{x}$, in close analogy to wavelike excitations in classical field theory (see Figure 2.1) The right eigenstates of the annihilation operators a_k are called coherent states

$$|\,\varphi\,\rangle = \exp\left(\sum_k \varphi_k a_k^\dagger\right)|\,0\,\rangle, \qquad a_k\,|\,\varphi\,\rangle = \varphi_k\,|\,\varphi\,\rangle \;\forall k. \tag{2.23}$$

Note that the "excitation number" is not constant and thus we cannot have an eigenstate for the creation operator. It is possible to take the Hermitian conjugate of (2.23) to define a left eigenstate for the creation operator $a^\dagger$. So for the functional integrals we will write the Hamiltonian in the coherent state representation replacing the momentum and position eigenstates of the path integral. Following the same steps *ii* to *iv* on page 15 as for the derivation of the path integral we find the functional integral for quantum fields in $d+1$ dimensions. The conceptional difference lies in the interpretation of the transition amplitude. Now all calculations are done with respect to the vacuum state $|\,0\,\rangle$ which removes our knowledge of the preparation of the state and thus the boundary conditions of the initial and final state are removed

$$\langle\,\varphi_f(\mathbf{x}); t_f\,|\,\varphi_i(\mathbf{x}); t_i\,\rangle = \int_{\substack{\varphi(t_i,\mathbf{x})=\varphi_i(\mathbf{x})\\ \varphi(t_f,\mathbf{x})=\varphi_f(\mathbf{x})}} \mathcal{D}\varphi\; \mathrm{e}^{\mathrm{i}S[\varphi]} \quad \longrightarrow \quad \langle\,0;\infty\,|\,0;-\infty\,\rangle = \int \mathcal{D}\varphi\; \mathrm{e}^{\mathrm{i}S[\varphi]}\,. \tag{2.24}$$

Note that we now need to use the Heisenberg picture where the state vectors are time independent in order to compare to time dependent field operators, so we end up with the vacuum to vacuum transition amplitude at $t \to \pm\infty$. We see that the propagator is now a correlation function of two field operators inserted at the spacetime points where excitations are created and

[5] This choice amounts to a quantum mechanical unitary position operator. One might wonder if there could be a way to promote the classical parameter time t to a true Hermitian quantum operator $\hat{t}$ (implying that time becomes measurable). This leads us in the realm of "quantum spacetime". Interesting ideas (also about the different meanings of time) can be found in [46].

annihilated

$$\langle\, q_f; t_f \,|\, q_i; t_i \,\rangle \quad \longrightarrow \quad \langle\, 0; \infty \,|\, \varphi(t_f, x_f)\varphi(t_i, x_i) \,|\, 0; -\infty \,\rangle\,. \tag{2.25}$$

Furthermore, we can view quantum mechanics as a $0+1$ dimensional quantum field theory, where the pair of conjugated creation and annihilation operators $\{a, a^\dagger\}$ is mapped to the conjugated position and momentum operator $\{q, p\}$ by a canonical transformation.

Correlation functions and generating functionals

In quantum field theory we are concerned with the correlation functions (or correlators) of operators inserted at different spacetime points. The information about the quantum system is encoded in the correlation functions of all physical operators. The correlation functions are defined as the functional expectation value of a product of operators $\varphi(x)$[6]

$$\langle\, \varphi(x_1) \cdots \varphi(x_n) \,\rangle = \frac{1}{Z} \int \mathcal{D}\varphi\, \varphi(x_1) \cdots \varphi(x_n)\, \mathrm{e}^{\mathrm{i}S[\varphi]}\,. \tag{2.26}$$

Note that by construction the functional integral is time ordered so a time ordering operator is implicitly assumed in all expectation values. The functional Z is called partition function, which encodes the vacuum structure of the theory, an is used as a normalization factor. As we will see in Section 2.1.4 it is the primary object of statistical field theory. Here it ensures the right normalization of the expectation value

$$Z = \int \mathcal{D}\varphi\; \mathrm{e}^{\mathrm{i}S[\varphi]} \qquad \Leftrightarrow \qquad \langle\, \mathbb{1} \,\rangle = \frac{1}{Z} \int \mathcal{D}\varphi\, \mathbb{1}\, \mathrm{e}^{\mathrm{i}S[\varphi]} = 1. \tag{2.27}$$

All correlation functions can be constructed by taking functional derivatives of the so-called generating functional which is the partition function with an additional source term preparing the system in the state $\varphi(x)$. The preparation is usually done by an external device (a filter projecting the quantum state onto the particular state the system is prepared in) described by the external source field J. Therefore, the full action $S[\varphi; J]$ is described by an additional interaction between the field φ and its source J

$$Z[J] = \int \mathcal{D}\varphi \exp\left[\mathrm{i} \int \mathrm{d}^d x\, (\mathscr{L} + \varphi J)\right] = \int \mathcal{D}\varphi\; \mathrm{e}^{\mathrm{i}S[\varphi; J]}\,. \tag{2.28}$$

In principle there are various ways to prepare the system so there are different source fields $\tilde{J}$ that define different generating functional $Z[\tilde{J}]$. But any measurements described by an observable must be independent of the specific preparation (*e.g.* a specific experimental setup) and thus we need to set $J = \tilde{J} = 0$ to obtain an objective observable

$$\langle\, \varphi(x_1) \cdots \varphi(x_n) \,\rangle = \frac{(-\mathrm{i})^n}{Z[0]} \left.\frac{\delta^n Z[J]}{\delta J(x_1) \cdots \delta J(x_n)}\right|_{J=0}, \tag{2.29}$$

where the functional derivative is defined as

$$\frac{\delta J(x)}{\delta J(y)} = \delta(x - y) \qquad \longrightarrow \qquad \frac{\delta}{\delta J(y)} \int \mathrm{d}^d x\, J(x)\varphi(x) = \varphi(y). \tag{2.30}$$

[6] In the following we will use units such that $\hbar = 1$.

The correlation functions (2.29) encode, as their name suggest, the correlations between two field operators at different spacetime points. If the amplitudes of the fields fluctuate independently then the correlation function will vanish. Due to the non-local nature of quantum fluctuations, non-zero correlation functions describe the entanglement of the respective operators. There are two special correlation functions, namely the vacuum expectation value of a field $\langle\, \varphi(x) \,\rangle$ and the propagator $\langle\, \varphi(x)\varphi(y) \,\rangle$ describing the propagation of the influence of the operator over the range $|x-y|$. A prominent example is the creation of a particle at the spacetime point x and the annihilation at the spacetime point y which amounts to a particle propagating form x to y. The correlation functions defined so far include also lower order correlations which are (topologically) disconnected from each other describing lower order entanglement. The logarithmic derivative of the partition function removes these disconnected parts such that only connected terms remain. We therefore define the connected correlation function as

$$\langle\!\langle\, \varphi(x_1)\cdots\varphi(x_n) \,\rangle\!\rangle = (-\mathrm{i})^n \left.\frac{\delta \ln Z[J]}{\delta J(x_1)\cdots\delta J(x_n)}\right|_{J=0} . \tag{2.31}$$

For instance the propagator can be split into

$$\begin{aligned}\langle\!\langle\, \varphi(x)\varphi(y) \,\rangle\!\rangle &= \langle\, \varphi(x)\varphi(y) \,\rangle - \langle\, \varphi(x) \,\rangle\langle\, \varphi(y) \,\rangle \\ &= \big\langle \big(\varphi(x) - \langle\, \varphi(x) \,\rangle\big)\big(\varphi(y) - \langle\, \varphi(y) \,\rangle\big) \big\rangle ,\end{aligned} \tag{2.32}$$

where we explicitly see that we removed the lower order vacuum expectation value. Therefore, the connected propagator really describes the field excitations above the vacuum. This can be generalized to include the so-called quantum chain rule, see Appendix B.2. In this case the quantum chain rule is not needed because our fields in the path integral are mere complex numbers so we can commute them in an arbitrary fashion. This is also the reason why the functional integral yields a time ordered correlation function.

Gaussian integrals and Wick's theorem

Now let us look at a very simple case that can be solved explicitly using Gaussian integration. In fact a lot of techniques used in field theory rely on the transformation of a more complicated functional integral into a Gaussian integral which can be solved exactly. Completing the square, we can solve integrals of the type

$$\begin{aligned}&\int \mathcal{D}\varphi \exp\left[\mathrm{i}\left(\frac{1}{2}\int \mathrm{d}^d x\, \mathrm{d}^d y\, \varphi(x)\mathscr{G}^{-1}(x,y)\varphi(y) - \int \mathrm{d}^d x\, \varphi(x) J(x)\right)\right] \\ &\qquad = \mathcal{N}\sqrt{\det(\mathrm{i}\mathscr{G})}\exp\left(\frac{1}{2}\int \mathrm{d}^d x\, \mathrm{d}^d y\, J(x)\mathscr{G}(x,y)J(y)\right) .\end{aligned} \tag{2.33}$$

In the special case $J = 0$ the integral reduces to the square root determinant of the operator kernel (or Green function) $\mathscr{G}$. The determinant is understood as a determinant of an Hermitian operator.[7] Since we are dealing with a bilinear form we can take functional derivatives of (2.33) with respect to $\mathscr{G}(x',y')^{-1}$ and $J = 0$. The left hand side gives rise to

$$\frac{\mathrm{i}}{2}\int \mathcal{D}\varphi\, \varphi(x')\varphi(y') \exp\left(\frac{\mathrm{i}}{2}\int \mathrm{d}^d x\, \mathrm{d}^d y\, \varphi(x)\mathscr{G}^{-1}(x,y)\varphi(y)\right) = \mathcal{N}\sqrt{\det(\mathrm{i}\mathscr{G})}\frac{\mathrm{i}}{2}\langle\, \varphi(x')\varphi(y') \,\rangle \tag{2.34}$$

[7] In principle one needs to be very careful to distinguish between self-adjoint and Hermitian operators and to make sure that there are no residual contributions (*c.f.* also the discussion in Appendix B.3).

and the right hand side (see Appendix B.1)

$$\mathcal{N}\frac{\delta\sqrt{\det(\mathrm{i}\mathscr{G})}}{\delta\,\mathscr{G}(x',y')^{-1}}=\mathcal{N}\frac{\mathrm{i}}{2}\sqrt{\det(\mathrm{i}\mathscr{G})}\mathscr{G}(x',y')$$

Equating (2.34) and (2.35) yields

$$\big\langle\,\varphi(x')\varphi(y')\,\big\rangle=\mathscr{G}(x',y') \tag{2.35}$$

Acting again with the functional derivative $\delta/\delta\mathscr{G}^{-1}$ on (2.35) we obtain

$$\begin{aligned}\big\langle\,\varphi(x_1)\varphi(x_2)\varphi(x_3)\varphi(x_4)\,\big\rangle=\mathscr{G}(x_1,x_2)\mathscr{G}(x_3,x_4)+\mathscr{G}(x_1,x_3)\mathscr{G}(x_2,x_4)\\+\mathscr{G}(x_1,x_4)\mathscr{G}(x_2,x_3).\end{aligned} \tag{2.36}$$

For more technical details (using discretized matrices) see Appendix B.1. Taking the derivatives with respect to $\mathscr{G}^{-1}$ can be iterated to generalize (2.36) to express arbitrary even correlation functions in terms of all possible pairings of "contracted" two-point correlation function

$$\big\langle\,\varphi(x_1)\cdots\varphi(x_{2n})\,\big\rangle=\sum_{\substack{\mathcal{P}\{\text{pairings}\\ \text{of }(x_1,\ldots,x_{2n})\}}}\mathscr{G}(x_{i_1},x_{i_2})\cdots\mathscr{G}(x_{i_{2n-1}},x_{i_{2n}}). \tag{2.37}$$

Note that all correlation functions with odd insertions vanish due to the structure of a bilinear form. As a matter of fact they cannot be generated by virtue of the symmetric/Hermitian form of the operator. Using the full form (2.33) and taking functional derivatives with respect to $J(x')$ (as in the prescription (2.29)) we see that all odd correlation functions must vanish since an odd integrand is integrated to zero over a symmetric range $(-\infty,\infty)$.

This only holds true for the free theory. As explained in the next Section 2.1.3 we can include interactions by looking at perturbations. All these concepts can be derived for fermions as well. Due to the anti-commuting nature of fermions one needs to introduce Grassmann numbers and Grassmann valued fields. Since we will use field theoretical methods in the context of effective field theories for critical phenomena, we will not have to deal with fermionic fields since order parameters or condensates are bosonic objects due to the strange property that fermions are always excited/created in pairs. So the total number of fermions must be an even integer. This non-local constraint gives rise to non-local excitations [4]. This "pairing" constraint also prohibits any macroscopic object such as a condensate to behave like a truly fermionic object. Therefore, macroscopic observables must be bosonic.

2.1.3. Perturbation theory

This section is only included for completeness. Thus, we will be quite brief in our exposition since the ideas of perturbation theory can be found in any classic textbook on quantum field theory.[8] In order to simplify the expressions and illustrate the transition to statistical field theory we will work in imaginary or Euclidean time.

[8] Personal favorites are [47–50]

Euclidean Functional Integral

The transformation to imaginary time is sometimes called Wick rotation because it can be viewed as a rotation in the complex plane

$$t \longrightarrow -\mathrm{i}\tau, \qquad \mathrm{d}t \longrightarrow -\mathrm{i}\,\mathrm{d}\tau, \qquad \partial_t \longrightarrow \mathrm{i}\partial_\tau \qquad \Rightarrow \qquad \mathrm{i}S \longrightarrow -S.$$

Applying the Wick rotation to the exponential of the action in the functional integral will yield a true weighting function which is entirely real and does not diverge for any value of the action

$$Z[J] = \int \mathcal{D}\varphi \; \mathrm{e}^{-S[\varphi;J]}\,.$$

Particularly, the potential term in the Euclidean action is flipped *i.e.* $V \longrightarrow -V$.

An interacting field theory may be described by the following Euclidean action

$$S[\varphi;J] = S^{(0)}[\varphi;J] + S_{\text{int}}[\varphi], \tag{2.38}$$

where the free field part includes the source term

$$S^{(0)} = \frac{1}{2}\int \mathrm{d}^d x\,\mathrm{d}^d y\,\varphi(x)\Delta^{-1}(x,y)\varphi(y) - \int \mathrm{d}^d x\,J(x)\varphi(x), \tag{2.39}$$

and $\Delta(x,y)$ denotes the free field propagator

$$\Delta^{-1}(x-y) = -\partial_x^2 + m^2\delta(x-y), \tag{2.40}$$

which only depends on the distance between x and y due to translational invariance. For a free field the propagator can be written as a Fourier transform[9]

$$\Delta(x-y) = \int \frac{\mathrm{d}^d q}{(2\pi)^d}\frac{\mathrm{e}^{\mathrm{i}q(x-y)}}{q^2+m^2-\mathrm{i}0^+} \qquad \Leftrightarrow \qquad \Delta^{-1}(x-y)\Delta(x-y) = \delta(x-y), \tag{2.41}$$

being the Green function of the free field differential operator $\Delta^{-1}(x,y)$ with regulator $\mathrm{i}0^+$ to assure convergence. For brevity we introduce the functional scalar product

$$\left(\varphi\,,\,\Delta^{-1}\varphi\right) = \int \mathrm{d}^d x\,\mathrm{d}^d y\,\varphi(x)\Delta^{-1}(x,y)\varphi(y), \tag{2.42}$$

and we can introduce a mathematically well-define measure for Gaussian integrals which is the kernel

$$\mathrm{d}\mu(\Delta|\varphi) = \mathcal{D}\varphi\;\mathrm{e}^{-1/2\left(\varphi\,,\,\Delta^{-1}\varphi\right)}\,. \tag{2.43}$$

This is known as the Wiener measure. Using these definitions the free field partition function with and without source field is defined as

$$Z^{(0)}[J] = \int \mathrm{d}\mu(\Delta|\varphi)\;\mathrm{e}^{(J\,,\,\varphi)} = Z^{(0)}[0]\,\mathrm{e}^{\frac{1}{2}(J\,,\,\Delta J)}\,, \tag{2.44}$$

where

$$Z^{(0)}[0] = \int \mathrm{d}\mu(\Delta|\varphi) = \mathcal{N}\det\Delta, \tag{2.45}$$

[9] Note that all products implicitly use the Minkowski metric *i.e.* $qx = -q^0x^0 + \mathbf{q}\cdot\mathbf{x}$.

respectively. Note that the actual normalization is not physically accessible since physical observables are only connected to correlators where $Z[0]$ is factored out. The full interaction partition function is obtained by inserting (2.38) and splitting the interaction exponential into the free field term, the source term, and the interacting term

$$\begin{aligned} Z[J] &= \int \mathrm{d}\mu(\Delta|\varphi)\ \exp\left(-S_{\text{int}}[\varphi]\right) \exp\left[\,(J\,,\,\varphi)\,\right] \\ &= Z^{(0)}[0] \exp\left(-S_{\text{int}}\left[\frac{\delta}{\delta J}\right]\right) \exp\left[\frac{1}{2}\,(J\,,\,\Delta J)\right] \\ &= \exp\left(-S_{\text{int}}\left[\frac{\delta}{\delta J}\right]\right) Z^{(0)}[J]. \end{aligned} \tag{2.46}$$

where we reduced (2.46) into a Gaussian integral by expanding the interaction in the couplings. The expansion is generated by expanding the interaction part of the action where the field operators are replaced by the functional derivative with respect to the source field. Once we have the interacting generating functional $\ln Z[J]$ we can calculate correlators and apply Wick's theorem (2.37). This expansion is an asymptotic expansion with vanishing radius of convergence. The perturbative expansion will break down when the partial sums over the combinatorial factors, arising from the expanded powers of the interacting field, will outnumber the smallness of the coupling constant (see also [51]). From a mathematical point of view the series is convergent for positive coupling constants and divergent for negative coupling constants. Since we are expanding about zero, the radius of convergence is also zero. If we happen to start with a strongly interacting field theory the first terms will already lead to a divergent sum such that the partial summation is not possible.[10] The breakdown of the asymptotic expansion for strong coupling is a serious obstacle which will be explored further in the following sections. This is also the main driving force of searching for and employing weak-strong dualities. Finally the weak-strong duality we are interested in will be the gauge/gravity duality explained in Section 3.4.

2.1.4. Thermal field theory & statistical field theory

The Wick rotation not only allows us to define the functional integral more rigorously, but also defines the partition function of classical statistical field theory[11]

$$Z = \int \mathcal{D}\varphi\ \mathrm{e}^{-1/\hbar S[\varphi]} \sim \int \mathcal{D}\varphi\ \mathrm{e}^{-\beta H[\varphi]}\,, \tag{2.47}$$

where the action describes the static energy functional H of a statistical configuration φ in d dimensions. Note that the Euclidean time is yet another direction/dimension of the configuration space and must not be confused with temporal evolution. Thus, we may conclude that Euclidean quantum field theory in d dimensional spacetime can be identified with classical statistical field theory with Boltzmann weight

$$\mathrm{e}^{-1/\hbar S[\varphi]} \sim \mathrm{e}^{-\beta H[\varphi]} = \mathrm{e}^{-H[\varphi]/k_{\mathrm{B}}T} \qquad \longrightarrow \qquad \hbar \sim k_{\mathrm{B}}T = \beta^{-1}, \tag{2.48}$$

[10] Compare to the statement of strong quantum fluctuations in the semi-classical limit below (2.22). In fact the semi-classical expansion of the saddle-point method follows the same logic as the perturbative expansion of the interacting field theory.

[11] In this section we explicitly write out the factors of $\hbar$ and k_{B} to elucidate the nature of the mapping.

where the temperature T is identified with the inverse of the Planckian action $\hbar^{-1}$. In general the temperature of the classical statistical field theory is *not* related to the temperature of the quantum system, but to the dimensionless coupling constant of the quantum theory. Note that the removal of the temporal evolution yields the identification of an action functional with an energy functional

$$\begin{aligned} S[\varphi] &= \int \mathrm{d}^d x\, \mathscr{L} = \int \mathrm{d}\tau\, \mathrm{d}^D\mathbf{x} \Big[\left(\partial_\tau \varphi(\tau,\mathbf{x})\right)^2 + \left(\nabla\varphi(\tau,\mathbf{x})\right)^2 + V(\varphi) \Big], \\ H[\varphi] &= \int \mathrm{d}^d x\, \mathscr{E} = \int \mathrm{d}^{D+1}\mathbf{x} \Big[\left(\nabla\varphi(\mathbf{x})\right)^2 + V(\varphi) \Big], \end{aligned} \tag{2.49}$$

where the spacetime dimensionality of the *quantum field theory* is given by $d = D + 1$ and D denotes the number of spatial dimensions.

The mapping between Euclidean quantum field theory and classical statistical field theory can be extended to partition functions of quantum statistical systems. This follows directly from the definition of the quantum partition function

$$\mathcal{Z} = \operatorname{tr} \mathrm{e}^{-\beta\mathcal{H}} = \sum_n \Big\langle\, n \,\Big|\, \mathrm{e}^{-\beta\mathcal{H}} \,\Big|\, n \,\Big\rangle, \tag{2.50}$$

We can retrace steps *i* and *ii* on page 15 of constructing the path integral, but this time with imaginary time τ running from 0 to β and under periodic boundary conditions identifying $|\, q_i \,\rangle \equiv |\, n \,\rangle$ and $|\, q_f \,\rangle \equiv |\, n \,\rangle$ by virtue of the identification

$$\Big\langle\, q_f \,\Big|\, \mathrm{e}^{-\mathrm{i}/\hbar\mathcal{H}(t_f - t_i)} \,\Big|\, q_i \,\Big\rangle = \Big\langle\, q(\tau_f) \,\Big|\, \mathrm{e}^{-1/\hbar\mathcal{H}(\tau_f - \tau_i)} \,\Big|\, q(\tau_i) \,\Big\rangle \sim \Big\langle\, n \,\Big|\, \mathrm{e}^{-\beta\mathcal{H}} \,\Big|\, n \,\Big\rangle, \tag{2.51}$$

implying

$$\hbar\beta = \tau_f - \tau_i \qquad \text{and} \qquad |\, q_f \,\rangle = |\, q(\tau_f) \,\rangle = |\, q(\tau_f + \hbar\beta) \,\rangle = |\, q_i \,\rangle. \tag{2.52}$$

The periodic boundary conditions (2.52) yield a non-trivial topology[12] so the quantum partition function is equivalent to an imaginary time evolution over a circle S^1 with circumference

$$L_T = \frac{\hbar}{k_\mathrm{B} T} = \hbar\beta. \tag{2.53}$$

Extending the path integral representation to a functional integral representation for a higher dimensional systems, introducing coherent states, we can identify a Euclidean quantum field theory on $S^1 \times \mathbb{R}^D$ with a quantum statistical system in $\mathbb{R}^D$[13]

$$\mathcal{Z} = \operatorname{tr} \mathrm{e}^{-\beta\mathcal{H}} = \int \mathcal{D}\varphi \exp\Big[- \oint_{S^1} \mathrm{d}\tau \int \mathrm{d}^D\mathbf{x}\, \mathscr{L} \Big]. \tag{2.54}$$

Remarkably, thermal quantum field theory in equilibrium is obtained by compactifying the imaginary time direction on a circle S^1 with radius $L_T/2\pi$. As an additional side effect the Fourier

[12] For fermions one obtains antiperiodic boundary conditions due to the anticommuting nature of fermionic coherent states.

[13] Note that the coherent states do introduce the proper $p\dot{q}$ term such that the Hamiltonian density is transformed into the Lagrange density see *e.g.* [51]

transform of the imaginary time becomes discrete, the so-called Matsubara frequency representation

$$\varphi(\tau,\mathbf{x}) = \sum_n \varphi_n(\mathbf{x})\,\mathrm{e}^{-\mathrm{i}\omega_n\tau}\,, \qquad \varphi_n(\mathbf{x}) = \frac{1}{\beta}\int_0^\beta \mathrm{d}\tau\,\varphi(\tau,\mathbf{x})\,\mathrm{e}^{\mathrm{i}\omega_n\tau}\,. \tag{2.55}$$

where the Matsubara frequencies are given by[14]

$$\omega_n = 2\pi n T, \qquad n\in\mathbb{Z}. \tag{2.56}$$

The discreteness of the Matsubara frequencies can pose a problem to obtain the proper analytic continuation of the imaginary time correlation functions (*e.g.* the analytic continuation of a function only defined on discrete points is not unique). Furthermore, for more complex applications the analytic continuation becomes highly non-trivial and might not be feasible at all. Even worse, any approximation made to obtain an analytic continuation might be totally uncontrolled and could in principle lead to spurious real time results. These issues become important when dealing with linear response and transport coefficients where we need to look at fluctuations about the equilibrium state, yet the measurements are done in real time (see Section 2.2.2).

From the quantum partition function (2.54) we have access to all thermodynamic properties by introducing thermal (equilibrium) averages and employing the statistical density operator describing the quantum statistical canonical ensemble or a quantum system in a mixed state

$$\langle\,\varphi\,\rangle = \mathrm{tr}\,(\hat{\rho}\varphi) \qquad \text{where} \qquad \hat{\rho} = \frac{1}{\mathcal{Z}}\,\mathrm{e}^{-\beta\mathcal{H}}\,. \tag{2.57}$$

Note that we can easily include the chemical potential μ by simply shifting the Hamiltonian $\mathcal{H} \longrightarrow \mathcal{H} - \mu\mathcal{N}$ where $\mathcal{N}$ denotes the number operator (of a species). Thus, we allow the number of certain particle species to fluctuate where the average number is fixed by the respective chemical potential. This is the quantum grand canonical ensemble or a quantum system described by Gibbs states. In Table 2.1 the correspondence between Euclidean quantum field theory and quantum statistical field theory is shown including all "identifications" of the concepts we defined in Section 2.1.2. Futhermore, we can look at two interesting limits of thermal field theories:

- The zero temperature limit $T \to 0$, $\beta \to \infty$ effectively removes the time circle S^1 since the circumference becomes infinite. Therefore, we recover the quantum field theory over infinite spacetime $\mathbb{R}^d$
- In the high temperature limit $T \to \infty$, $\beta \to 0$ the circle S^1 shrinks to zero and so we effectively remove the imaginary time dimension completely. The Euclidean quantum field theory is now defined over $\mathbb{R}^D$. This is in agreement with the statement that for high temperatures the quantum nature of a system is lost and hence we end up with a classical statistical field theory. In this case we recover the correspondence between Euclidean quantum field theory and classical statistical field theory of the same total dimension.

The last point can be understand physically as the suppression of quantum fluctuations at high temperatures. Following the saddle point method (2.19) the classical action is time independent and the quantum fluctuations up to quadratic order contribute a term quadratic in Matsubara frequencies

$$S_{\text{fluct}} = \sum_{\omega_n} \omega_n^2 \delta q(\omega_n,\mathbf{x})\delta q(-\omega_n,-\mathbf{x}). \tag{2.58}$$

[14] Fermionic Matsubara frequencies read $\omega_n = (2n+1)\pi T$ with $n\in\mathbb{Z}$.

Euclidean quantum field theory		Quantum statistical systems
d dimensional Euclidean spacetime $(\tau, \mathbf{x}) \in S^1 \times \mathbb{R}^{d-1}$	$\Leftrightarrow$	D dimensional space $\mathbf{x} \in \mathbb{R}^D$
Correlation functions	$\Leftrightarrow$	(generalized) moments
Generating functional $\ln Z$	$\Leftrightarrow$	Thermodynamic potentials $\Omega = -\beta^{-1} \ln \mathcal{Z}$
Connected correlation functions	$\Leftrightarrow$	Cumulants
Wick's theorem	$\Leftrightarrow$	"Corresponding theorem" (for moments in Gaussian theory)
Perturbative expansion in interactions	$\Leftrightarrow$	Cumulant expansion of interaction term

Table 2.1. Euclidean quantum field theory can be related to statistical field theory for quantum statistical systems. All concepts derived in quantum field theory can be carried over immediately to concepts in statistical physics. In particular the machinery to generate connected correlation functions determines the thermodynamic potentials. From a mathematical point of view, the formulation of quantum field theory by means of stochastic functional integration puts it on a firm mathematical basis.

If the quantum fluctuation energy $\omega_n \sim T$ exceeds the characteristic energy scale set by the classical action all non-vanishing Matsubara modes can be neglected. In imaginary time representation the increase of the quantum fluctuation energy corresponds to the shrinking of the imaginary time interval $\tau \in [0, \beta]$ which increases the contributions of the gradient terms (through steeper slopes) by $\partial_\tau \delta q(\tau, \mathbf{x}) \sim \beta^{-1} \sim T$. This argument is crucial in understanding the interplay of quantum and thermal fluctuations of quantum phase transitions in particular the shape of the quantum critical region, *c.f.* Figure 1.1. As a final remark we may combine the correspondence between classical statistical field theory and Euclidean quantum field theory with the correspondence to quantum statistical theories. Thus, we end up with an mapping from D dimensional quantum systems onto $D+1$ dimensional classical systems. Moreover, the D dimensional imaginary time correlation functions are mapped to correlation function in the $D+1$ dimensional classical field theory. This mapping becomes precise for large correlation lengths such that the discrete microscopic details of the theories are averaged out by a proper renormalization to obtain a true effective field theory. In any case the universal thermodynamic properties must not depend on the underlying microscopic model.

2.2. Linear Response Theory

Overview

- Linear responses are measurable via experimental techniques to determine
  - thermodynamic properties
  - transport coefficients
  - spectroscopic information.

- Response functions are related to analytic continuations of imaginary time correlation functions.
- Understanding of physical connection between
  - fluctuations & dissipation
  - causality & analyticity.

Physical properties (of many-body systems) are measured by probing the system with external forces and ascertaining the evoked response of the system. In general the response encodes additional dynamic and structural information not accessible by thermodynamic measurements. Experimentally, the physical system under investigation is driven out of its equilibrium state by a (small) perturbation and is carefully observed returning to its equilibrium state. This process usually generates non-vanishing expectation values of certain observables connected to the external perturbing force. Theoretically, the response functions need to obey two conditions

- **Causality:** The perturbation of the system is the source for the measured response. Thus, the response functions must be related to retarded correlation functions.
- **Memory:** The response function needs to incorporate memory effects such as the temporal connection between source and response.

2.2.1. External sources & response functions

The most general functional relation between external sources and expectation values fulfilling both conditions are the so-called Volterra series for continuous[15] time invariant systems

$$\langle O_j(t,\mathbf{x})\rangle = \sum_{n=0}^{\infty}\frac{1}{n!}\int_{-\infty}^{\infty}\mathrm{d}t_1\cdots\mathrm{d}t_n\int\mathrm{d}^D\mathbf{x}_1\cdots\mathrm{d}^D\mathbf{x}_n\,\chi_{jk}^{(n)}(t-t_1,\ldots,t-t_n;\mathbf{x},\mathbf{x}_1,\ldots,\mathbf{x}_n)$$
$$\times\,\mathcal{F}_k(t-t_1,\mathbf{x}_1)\cdots\mathcal{F}_k(\mathbf{x}_n,t-t_n), \quad (2.59)$$

where $\mathcal{F}_k$ are the external force operators (experimentally controllable observables) and $\langle O_j\rangle$ are the response expectation values of the system. The integral (or Volterra) kernel $\chi_{jk}^{(n)}$ describes only intrinsic properties of the system sensitive to the external perturbation and is thus called a response function or generalized susceptibility, weighting the system's response. Note that the response function depends only on the difference of the time coordinate due to the time invariance of the system. For a system without memory we obtain the usual Taylor series where the response depends only on the external sources at the same spacetime point, *i.e.* there is no connection to the history of the system. In this case the response function does not depend on the spacetime coordinates and the convolution integrals are reduced to pure products. From now on we will assume that the external perturbation is sufficiently weak which is valid for many experimental measurements, but of course there are very intriguing systems *e.g.* in non-linear optics that needs to be treated with higher order terms. In any case the Volterra series expansion will break down if one is dealing with strongly non-linear systems. Thus, we can drop all higher

[15] For discrete systems the Volterra series is defined by convolution sums instead of convolution integrals.

order terms in the external forces and deal only with the leading term in the Volterra kernel of (2.59),

$$\langle\, O_j(t,\mathbf{x})\,\rangle = \langle\, O_j(t,\mathbf{x})\,\rangle_{\mathcal{F}_k=0} + \int \mathrm{d}t' \int \mathrm{d}^D\mathbf{x}'\, \chi_{jk}(t-t';\mathbf{x},\mathbf{x}')\mathcal{F}_k(t',\mathbf{x}'), \tag{2.60}$$

so we will drop the superscript n in the following. Note that the zeroth order term in the Volterra expansion is just the expectation value without external forces perturbing the system and may be set to zero (*e.g.* by carefully preparing the experimental setup). To make contact with field theory, we will couple the external forces to the corresponding operator by introducing an interaction/perturbation term

$$S[\varphi, O; J, \mathcal{F}] = S^{(0)}[\varphi; J] + S_{\text{per}}[O; \mathcal{F}]. \tag{2.61}$$

The perturbation term will give rise to a response expectation value following (2.31) for sourcing operators

$$\langle\, \varphi(x)\,\rangle = -\left.\frac{\delta \ln \mathcal{Z}[J,\mathcal{F}_k]}{\delta J(x)}\right|_{J=0}. \tag{2.62}$$

Note that in general the response is not measured using the same observable O that is connected directly, but some other well prepared observable (*e.g.* a laser beam used in spectroscopy) denoted by φ. Because the external force $\mathcal{F}_k$ is considered to be weak, we can expand the generating functional $\ln \mathcal{Z}[J,\mathcal{F}_k]$ to linear order in $\mathcal{F}_k$

$$\ln \mathcal{Z}[J,\mathcal{F}_k] = \ln \mathcal{Z}[J,0] + \int \mathrm{d}^d x'\, \left.\frac{\delta \ln \mathcal{Z}[J,\mathcal{F}_k]}{\delta \mathcal{F}_k(x')}\mathcal{F}_k(x')\right|_{\mathcal{F}_k=0}, \tag{2.63}$$

and insert (2.63) into (2.62) to obtain

$$\begin{aligned}\langle\, \varphi(x)\,\rangle &\approx -\left.\frac{\delta \ln \mathcal{Z}[J,0]}{\delta J(x)}\right|_{J=0} - \frac{\delta}{\delta J(x)}\int \mathrm{d}^d x'\, \left.\frac{\delta \ln \mathcal{Z}[J,\mathcal{F}_k]}{\delta \mathcal{F}_k(x')}\mathcal{F}_k(x')\right|_{\mathcal{F}_k=0} \\ &= -\langle\, \varphi(x)\,\rangle_{\mathcal{F}_k=0} - \int \mathrm{d}^d x'\, \left.\frac{\delta^2 \ln \mathcal{Z}[J,\mathcal{F}_k]}{\delta J \delta \mathcal{F}_k(x')}\right|_{J=\mathcal{F}_k=0} \mathcal{F}_k(x')\end{aligned} \tag{2.64}$$

Comparing with the linear term in the Volterra expansion, we see that the response function is given by the imaginary time two-point correlator (or Green function) in thermal equilibrium where we may assume/set $\langle\, \varphi(x)\,\rangle_{\mathcal{F}_k=0} = 0$. Moreover, we can treat the external force and the source term for the measurement on the same footing by setting $J = \mathcal{F}'_j$ and $\varphi = O'$.

Fluctuation-Dissipation Theorem

In linear response theory the spontaneous (quantum) fluctuations about the thermal equilibrium are related directly to the dissipative behavior of the perturbed non-equilibrium system characterized by the linear response relaxation

$$\chi_{jk}(x,x') = -\left.\frac{\delta^2 \ln \mathcal{Z}[\mathcal{F}]}{\delta\mathcal{F}'_j(x)\delta\mathcal{F}_k(x')}\right|_{\mathcal{F}'_j=\mathcal{F}_k=0}$$
$$= -\left\langle\!\!\left\langle\, \mathcal{O}'(x)\mathcal{O}(x') \,\right\rangle\!\!\right\rangle = -\left\langle \left(\mathcal{O}'(x) - \left\langle\, \mathcal{O}'(x) \,\right\rangle\right)\left(\mathcal{O}(x') - \left\langle\, \mathcal{O}(x') \,\right\rangle\right) \right\rangle$$

where the susceptibility $\chi_{jk}(x,x')$ describes the distribution of the external perturbation/energy over the intrinsic excitations which are turned into entropy/heat. Note that for vanishing vacuum expectation values the connected imaginary time Green function reduce to a simple imaginary time correlator.

If the external perturbing operator and the observed operator are identical we can drop the tilde on the observables and the external force. Strictly speaking we may only deal with static susceptibilities since we are still working in imaginary time. For dynamical processes we need a prescription to obtain real-time correlators. The fluctuation-dissipation theorem can also be related to the Kubo formula derived from time-dependent perturbation theory in quantum mechanics. Since the Kubo formula will play a crucial role in our holographic calculations *e.g.* in Chapter 4, we will take a small detour and outline its derivation briefly. We start again with an external perturbation

$$\mathcal{H}(t) = \mathcal{H}^{(0)} + F(t)\mathcal{O}(t), \tag{2.65}$$

and expand the unitary time evolution operator to linear order in $F(t)$

$$\mathcal{U}(t',t) = \mathcal{T}\left[\,\mathrm{e}^{-\mathrm{i}\int_t^{t'}\mathrm{d}t''\,\mathcal{H}(t'')}\,\right] \approx\ \mathrm{e}^{-\mathrm{i}\mathcal{H}^{(0)}(t'-t)}\left(\mathbb{1} - \mathrm{i}\int_t^{t'}\mathrm{d}t''\,F(t'')\mathcal{O}(t'')\right). \tag{2.66}$$

In the interaction picture the time dependence is encoded in the following way

$$|\,n(t)\,\rangle = \ \mathrm{e}^{\mathrm{i}\mathcal{H}^{(0)}t}\,\mathcal{U}(t,t')\,|\,n(t')\,\rangle\,. \tag{2.67}$$

Since we are not interested in intrinsic properties of the system that must not depend on the initial conditions, we define the initial state to be at $t \to -\infty$

$$\lim_{t'\to-\infty}|\,n(t)\,\rangle = \ \mathrm{e}^{\mathrm{i}\mathcal{H}^{(0)}t}\,\mathcal{U}(t,-\infty)\,|\,n\,\rangle \qquad \text{where} \qquad |\,n\,\rangle = \lim_{t'\to-\infty}|\,n(t')\,\rangle\,. \tag{2.68}$$

Thus, inserting (2.66), the thermal average of a response operator $\mathcal{O}'(t)$ is given by

$$\begin{aligned}
\left\langle\, \mathcal{O}'(t) \,\right\rangle &= \frac{1}{\mathcal{Z}^{(0)}}\sum_n \left\langle\, n \,\right|\mathcal{U}(t,-\infty)^\dagger\mathcal{O}'(t)\,\mathcal{U}(t,-\infty)\left|\, n \,\right\rangle \mathrm{e}^{-\beta E_n} \\
&\approx \frac{1}{\mathcal{Z}^{(0)}}\sum_n \left\langle\, n \,\right|\mathcal{O}'(t)\left|\, n \,\right\rangle \mathrm{e}^{-\beta E_n} \\
&\quad - \mathrm{i}\int_{-\infty}^{t}\mathrm{d}t'\,F(t')\left[\frac{1}{\mathcal{Z}^{(0)}}\sum_n \left\langle\, n \,\right|\mathcal{O}'(t)\mathcal{O}(t') - \mathcal{O}(t')\mathcal{O}'(t)\left|\, n \,\right\rangle\right] \\
&= \left\langle\, \mathcal{O}'(t) \,\right\rangle_{\mathcal{H}^{(0)}} - \mathrm{i}\int_{-\infty}^{\infty}\mathrm{d}t'\,\Theta(t-t')\left\langle \left[\mathcal{O}'(t),\mathcal{O}(t')\right] \right\rangle F(t')
\end{aligned} \tag{2.69}$$

Note that we introduced the Heaviside distribution $\Theta(t-t')$ *c.f.* (2.2) to extend the upper integral limit to infinity. Comparing with the linear Volterra series (2.60) we see that the response function reads

$$\chi(t,t') = -\mathrm{i}\Theta(t-t')\left\langle \left[O'(t), O(t')\right]\right\rangle \tag{2.70}$$

where the Heaviside distribution/step function allows only for responses for $t > t'$. (2.70) is called the general Kubo formula. Here the physical observable can be obtained directly in a more or less intuitive fashion since we are led immediately to the retarded response function obeying causality. This is a striking advantage of the real time formalism. An alternative way to deal with real-time response is the Keldysh formalism discussed in Section 3.5.2 which allows a more general derivation of the Fluctuation-Dissipation Theorem on page 30. In the following section we will show how to obtain the retarded response function by analytic continuation.

2.2.2. Analytic structure of imaginary time correlation functions

Note that we used the machinery to generate imaginary time correlation functions in the previous section, but real dynamical processes are measured in real time. Why did we not start with a true real time formalism.[16] The reason is that we defined our thermal field theory with compactified imaginary time to introduce thermal averages (2.57) via the quantum partition function. For thermodynamic properties imaginary time correlators are sufficient since we only extract static information. For transport processes/coefficient we need to do an analytic continuation of the imaginary correlators and extract the real time information. Basically this is done by reversing the Wick rotation $\tau \longrightarrow \mathrm{i}t$ (see Infobox Euclidean Functional Integral on page 24). But we have to ensure not to pass over a pole or a branch cut to obtain the correct real time correlation function. Therefore it is necessary to understand the pole structure of the correlation functions.

Let us start with the sought real time correlation functions, or to be more precise the two point correlators related to the real time response function, which for simplicity we will call Green function from now on. We may define three different types of real time Green functions (with the factor i coming form the reversed Wick rotation and the additional -1 from the definition of the response function)

$$\begin{aligned} G^{\mathbb{T}}(x,x') &= -\mathrm{i}\left\langle O'(t,\mathbf{x})O(t',\mathbf{x}')\right\rangle, \\ G^{\mathrm{R}}_{\mathrm{A}}(x,x') &= \mp\mathrm{i}\Theta\big(\pm(t-t')\big)\left\langle\left[O'(t,\mathbf{x}), O(t',\mathbf{x}')\right]\right\rangle, \end{aligned} \tag{2.71}$$

where $G^{\mathbb{T}}$ denotes the (real time-ordered) Green function we obtain from functional integration, G^{R} is the retarded Green function and G^{A} the advanced Green function, respectively. Physically, we are looking for the retarded Green function as confirmed by the Kubo formula derivation (2.70) and how to express it in terms of the imaginary time Green function defined in the fluctuation-dissipation theorem. In order to obtain the pole structure we need to express the Heaviside distribution in terms of a Fourier transform

$$\begin{aligned} \pm\mathrm{i}\int\frac{\mathrm{d}\omega}{2\pi}\Theta(t-t')\,\mathrm{e}^{-\mathrm{i}\omega(t-t')} &= \mp\mathcal{P}\left[\frac{1}{\omega}\right] \pm \mathrm{i}\pi\delta(\omega), \\ \pm\mathrm{i}\int\frac{\mathrm{d}\omega}{2\pi}\Theta(t-t')\,\mathrm{e}^{-\mathrm{i}\omega(t-t')\pm\epsilon|t|} &= \mp\frac{1}{\omega\mp\mathrm{i}\epsilon}, \end{aligned} \tag{2.72}$$

[16] There are several approaches to avoid imaginary time correlators most notable the Keldysh contour integration (Schwinger-Keldysh formalism) or the direct formulation of linear response in real time. In our holographic context we will explicitly use a real time approach directly applicable to extract dynamical properties/transport coefficients. For a nice exposition of real time linear response see *e.g.* [52]

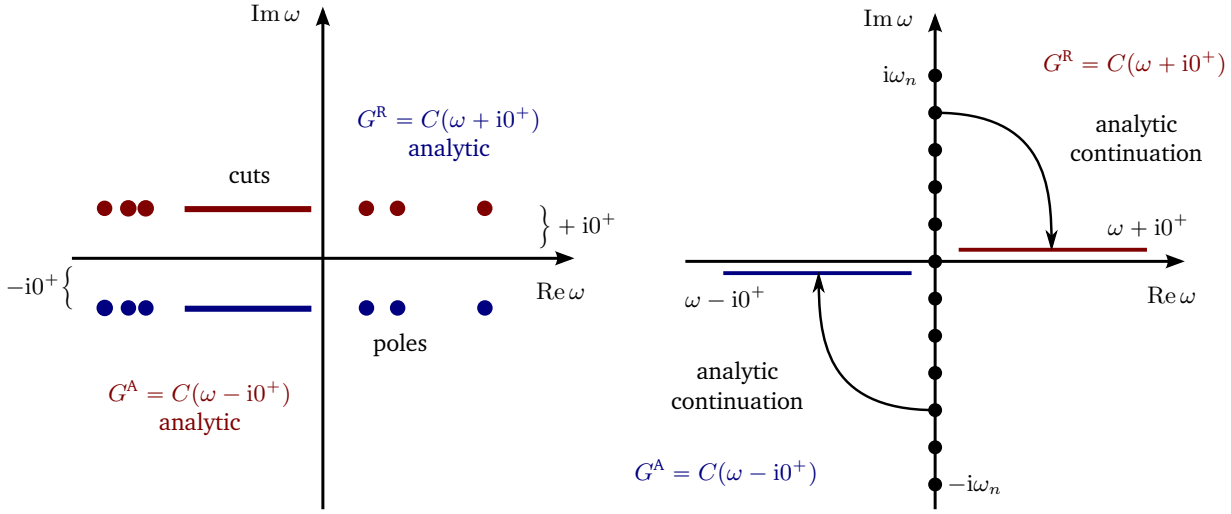

Figure 2.2. The retarded Green function $G^{\mathrm{R}}(\omega)$ is analytic in the upper half plane. The resonance frequencies $\omega = E_a - E_b$ lead to poles that describe the single particle spectrum of the physical system. In the case of a continuous spectrum the dense poles form a cut. The convergence factor moves the poles in the lower half-plane (dissipation) generating a retardation. This connects the analyticity to the causal structure. For the advanced Green function $G^{\mathrm{A}}(\omega)$ the pictures is reversed (due to complex conjugation), so the poles are in the upper half-plane which leads to analyticity in the lower half-plane and anticausality.

where the second expression involves a convergence factor (physically we can think of this factor as a dissipation process damping of the resonant modes) that regulates the Dirac distribution and removes the singularity to obtain a well defined Fourier transform. Note that we have to take the Cauchy principal value denoted by $\mathcal{P}[.]$ when removing the regulator $\epsilon \to 0$. This limit yields the Dirac identity,

$$\frac{1}{\omega \mp \mathrm{i}0^+} = \mathcal{P}\left[\frac{1}{\omega}\right] \pm \mathrm{i}\pi\delta(\omega). \tag{2.73}$$

The regularized Fourier transform of (2.71) in the eigenbasis of the system[17] with $\mathcal{H}\,|\,\Phi\,\rangle = E\,|\,\Phi\,\rangle$ and $O_{ab} = \langle\,\Phi_a\,|\,O\,|\,\Phi_b\,\rangle$ reads[18]

$$\begin{aligned} G^{\mathbb{T}}(\omega) &= \frac{1}{\mathcal{Z}} O'_{ab} O_{ba} \left(\frac{\mathrm{e}^{-\beta E_a}}{\omega + \mathrm{i}0^+ + (E_a - E_b)} - \frac{\mathrm{e}^{-\beta E_b}}{\omega - \mathrm{i}0^+ + (E_a - E_b)} \right), \\ G^{\mathrm{R/A}}(\omega) &= \frac{1}{\mathcal{Z}} O'_{ab} O_{ba} \frac{\mathrm{e}^{-\beta E_a} - \mathrm{e}^{-\beta E_b}}{\omega \pm \mathrm{i}0^+ + (E_a - E_b)}. \end{aligned} \tag{2.74}$$

We see that the real time ordered Green function $G^{\mathbb{T}}(\omega)$ has poles in the upper and lower complex frequency half-plane whereas the retarded Green function $G^{\mathrm{R}}(\omega)$ possess poles in the lower and the advanced Green function $G^{\mathrm{A}}(\omega)$ (being the complex/Hermitian conjugate of the retarded

[17] Note that the knowledge of the complete eigenbasis implies a full solution to the problem at hand and thus there would be no need to calculate/measure any correlation or response functions. The eigenbasis is only used to extract the analytic properties of the Green functions.

[18] For clarity the dependence on the spatial coordinates is suppressed in the following.

Green function) poles in the upper half-plane as shown in Figure 2.2. Remarkably, one can show, using the Dirac identity connected to (2.72), that all three Green functions $G^{\mathbb{T}}$, G^{R}, G^{A} are related to each other and carry the same information content of the physical system.

Let us redo the calculation with the imaginary time Green functions denoted by G^{τ} with the only difference that the Fourier transform will employ discrete Matsubara frequencies ω_n *c.f.* (2.56)

$$G^{\tau}(\mathrm{i}\omega) = \frac{1}{\mathcal{Z}} O'_{ab} O_{ba} \frac{\mathrm{e}^{-\beta E_a} - \mathrm{e}^{-\beta E_b}}{\mathrm{i}\omega + E_a - E_b}, \tag{2.75}$$

In addition we can define a complex Green function

$$C(z) = \frac{1}{\mathcal{Z}} O'_{ab} O_{ba} \frac{\mathrm{e}^{-\beta E_a} - \mathrm{e}^{-\beta E_b}}{z + E_a - E_b}, \tag{2.76}$$

which is analytic in the entire complex frequency plane except for the real axis since $(E_a - E_b) \in \mathbb{R}$. Now we can connect the retarded Green function $G^{\mathrm{R}} = C(\omega + \mathrm{i}0^+)$ to the imaginary time Green function $G^{\tau} = C(\mathrm{i}\omega_n)$ using the fact that two analytic functions are identical on a discrete sequence limiting in the domain of both functions. Therefore, it is enough to calculate the complex Green function for all positive Matsubara frequencies (up to $\mathrm{i}\infty$) and simply read off the value $C(\omega + \mathrm{i}0^+)$. This procedure corresponds to a well defined reversed Wick rotation in the Matsubara representation due to the analyticity of the complex Green function in the upper half-plane. We see that causality and analyticity are intimately connected. Using the Fourier transform of the Heaviside distribution (2.72) we see that an analytic function in the upper complex frequency plane vanishes for negative times and is therefore causal. For the advanced Green function $G^{\mathrm{A}} = C(\omega - \mathrm{i}0^+)$ we need to approach the real axis from below and thus we need to ensure the analyticity in the lower complex frequency half-plane. Therefore, the limit of the discrete sequence must be $-\mathrm{i}\infty$, so in order to determine the advanced Green function we need to compute the imaginary time Green function G^{τ} for all negative Matsubara frequencies. Again the analyticity in the lower half-plane yields a function that vanishes for positive times which is called anticausal (*c.f.* Figure 2.2). The only issue that remains, as mentioned below (2.56), is related to the problem of being unable to obtain the imaginary time Green function for all Matsubara frequencies due to some approximation or a limited knowledge of the theory such as an effective field theory only valid below some (cut-off) energy/frequency. In these cases the imaginary time response functions are of no use to determine transport coefficients. This happens *i.a.* in strongly coupled theories where only low-energy approximations are known or in strongly correlated systems where the Volterra approach breaks down in any case. Note that for zero temperature the discrete Matsubara frequencies become continuous and thus the analytic continuation is “trivial”.

2.2.3. Spectral functions, sum-rules & Kramers-Kronig relations

Once we have computed one of the Green or response function we can construct further physical quantities of interest. Specifically, for interacting theories such as strongly correlated fermions, the spectral (density) function $\mathscr{A}(\omega)$ and the respective spectral measure $\mathscr{R}(\omega)$ play a central role in understanding the distribution of the strongly interacting degrees of freedom. The spectral function is defined as the anti-Hermitian part of the retarded Green function

$$\mathscr{A}(\omega) = \mathrm{i}\left(G^{\mathrm{R}}(\omega) - G^{\mathrm{R}^{\dagger}}(\omega)\right), \tag{2.77}$$

and the trace over all possible states is defined as the corresponding spectral measure

$$\mathscr{R}(\omega) = \operatorname{tr} \mathscr{A}(\omega). \tag{2.78}$$

Note that in general the response function might be a multi-component or matrix-valued complex function and the trace in the spectral measure will be taken over all occurring indices. In the case of a simple function (2.77) and (2.78) reduce to

$$\mathscr{A}(\omega) = -2 \operatorname{Im} G^{\mathrm{R}}(\omega) = \mathscr{R}(\omega), \tag{2.79}$$

For a non-interacting theory the spectral function is given by a collection of δ-peaks. By turning on interaction the δ-peaks are resolved or broadened due to the entanglement of the quantum states describing the degrees of freedom. Interacting systems cannot be described by single particle states and corresponding eigenvalues/energies, so we expect a continuum of correlated states. The spectral weight carried by an excitation thus gets distributed over a broad range of many-body states. Nonetheless, there are some exact (mathematical) identities, usually called sum rules, which are independent of the physical system at hand. Important sum rules are:

- Static susceptibility sum rules
- Oscillator strength sum rules (f-sum rules/Thomas-Reiche-Kuhn sum rules) in atomic transitions (also valid for solids)
- Conductivity sum rules
- Spectral weights sum rules in superconductors (Tinkham-Glover-Ferrell sum rule).

Apart from these sum rules conserving degrees of freedom there are exact mathematical relations between the response/Green functions and the spectral function. The most profound of these relations are the Kramers-Kronig relations following from

$$\mathscr{A}(\omega) = \mathrm{i}\left(G^{\mathrm{R}}(\omega) - G^{\mathrm{A}}(\omega)\right), \tag{2.80}$$

where we used the fact that the advanced Green function is the Hermitian conjugate of the retarded Green function. Equation (2.80) allows us to write the complex Green function in terms of the spectral function as an integral over the real frequency line

$$C(z) = \int_{-\infty}^{\infty} \frac{\mathrm{d}\omega}{2\pi} \frac{\mathscr{A}(\omega)}{z-\omega}, \tag{2.81}$$

since in the upper complex half-plane $\operatorname{Im} z > 0$ only the residues of the analytic retarded Green function contribute whereas the contribution of the advanced Green functions vanishes. Thus, we can close the contour in the upper half-plane as shown in Figure 2.3 and use the theorem of residues to compute

$$\begin{aligned}
\int_{-\infty}^{\infty} \frac{\mathrm{d}\omega}{2\pi} \frac{\mathscr{A}(\omega)}{z-\omega}\bigg|_{\operatorname{Im} z>0} &= \oint_{\mathcal{C}^+} \frac{\mathrm{d}\omega}{2\pi} \frac{\mathscr{A}(\omega)}{z-\omega} - \left(|\omega| \to \infty\right) \\
&= \mathrm{i} \oint_{\mathcal{C}^+} \frac{\mathrm{d}\omega}{2\pi} \frac{G^{\mathrm{R}}(\omega)}{z-\omega} - \mathrm{i} \oint_{\mathcal{C}^+} \frac{\mathrm{d}\omega}{2\pi} \frac{G^{\mathrm{A}}(\omega)}{z-\omega} - \left(|\omega| \to \infty\right) \\
\Rightarrow \int_{-\infty}^{\infty} \frac{\mathrm{d}\omega}{2\pi} \frac{\mathscr{A}(\omega)}{z-\omega}\bigg|_{\operatorname{Im} z>0} &= -\frac{1}{2\pi\mathrm{i}} \oint_{\mathcal{C}} \mathrm{d}\omega \, \frac{G^{\mathrm{R}}(\omega)}{z-\omega} = C(z)
\end{aligned} \tag{2.82}$$

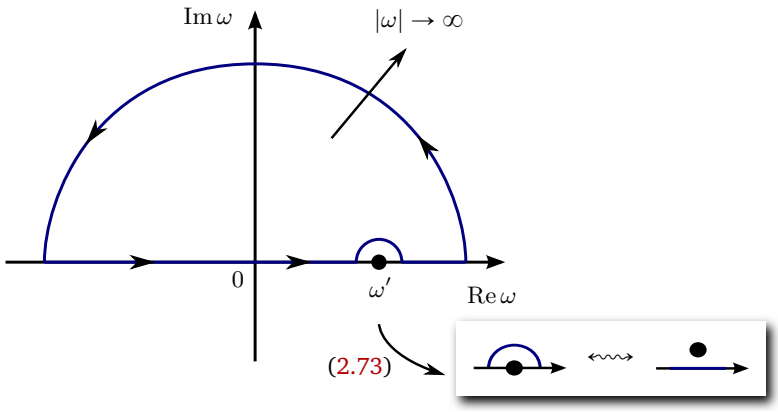

Figure 2.3. The is the contour used to derive the Kramers-Kronig relations. The inset is the graphical representation of the Dirac identity (2.73) used in the main derivation. Note also that the same contour is used to derive the relation between the integral over the spectral function and the complex Green function (2.81) with the additional poles structure of the retarded Green function in the upper half-plane.

Note that the length of the real line segment is given by $|\omega|$ but the integrand decays faster than $1/\omega$ so there are no additional contributions coming from $|\omega| \to \infty$. The last equality sign follows from Cauchy's integral formula where the additional minus sign is picked up by moving the imaginary unit in the denominator. Analogously, we can redo this computation for the lower complex half-plane $\mathrm{Im}\, z < 0$ using the contour integral over the advanced Green function, which yields the same result (the additional minus sign of G^{A} in (2.80) is compensated by the clockwise closure of the contour) and hence proving (2.81). We see that the spectral function (being the imaginary part of the complex Green function) completely determines the complex Green function. But this relation is only valid if the spectral function/imaginary part of the complex Green function is known for all frequencies. Then the Kramers-Kronig relations simply follow from $G^{\mathrm{R}}(\omega) = C(\omega + \mathrm{i}0^+)$ inserted into (2.82) which yields

$$G^{\mathrm{R}}(\omega) = -\frac{1}{2\pi\mathrm{i}} \oint_{\mathcal{C}} \mathrm{d}\omega' \, \frac{G^{\mathrm{R}}(\omega')}{\omega - \omega' + \mathrm{i}0^+}. \tag{2.83}$$

Using the Dirac identity from (2.73)

$$\frac{1}{\omega \mp \mathrm{i}0^+} = \mathcal{P}\left[\frac{1}{\omega}\right] \pm \mathrm{i}\pi\delta(\omega), \tag{2.84}$$

we remove the singularity on the real axis by "kicking" it in the upper complex frequency half-plane (see inset in Figure 2.3). Thus, we are left over with the real line integral as in (2.82), so

$$G^{\mathrm{R}}(\omega) = -\frac{1}{2\pi\mathrm{i}} \int_{-\infty}^{\infty} \mathrm{d}\omega' \, G^{\mathrm{R}}(\omega') \mathcal{P}\left[\frac{1}{\omega - \omega'}\right] + \frac{1}{2} \int_{-\infty}^{\infty} \mathrm{d}\omega' \, \delta(\omega - \omega') G^{\mathrm{R}}(\omega')$$

$$\Rightarrow G^{\mathrm{R}}(\omega) = -\frac{1}{\mathrm{i}\pi} \mathcal{P} \int_{-\infty}^{\infty} \mathrm{d}\omega' \, \frac{G^{\mathrm{R}}(\omega')}{\omega - \omega'}. \tag{2.85}$$

Kramers-Kronig Relation

The Kramers-Kronig relations relate the imaginary part to the real part of the retarded Green function and vice versa

$$\mathrm{Re}\, G^{\mathrm{R}}(\omega') = \frac{1}{\pi}\mathcal{P}\int_{-\infty}^{\infty} \mathrm{d}\omega' \, \frac{\mathrm{Im}\, G^{\mathrm{R}}(\omega')}{\omega' - \omega}, \qquad \mathrm{Im}\, G^{\mathrm{R}}(\omega') = -\frac{1}{\pi}\mathcal{P}\int_{-\infty}^{\infty} \mathrm{d}\omega' \, \frac{\mathrm{Re}\, G^{\mathrm{R}}(\omega')}{\omega' - \omega}.$$

Physically, the Kramers-Kronig relation connects dissipative effects/energy loss (*e.g.* absorption) with dispersive effects/energy transport (*e.g.* refraction).

We will make heavy use of the sum rules and the Kramers-Kronig relations when discussing the physics behind the metal/superconductor transition in condensed matter and holography, see for example Section 4.3, where we will also give a more detailed and physically inclined interpretation of the Kramers-Kronig relations.

2.3. Critical Phenomena & Renormalization

Overview

- Stable phases of matter are described by effective quantum field theories characterized by universal properties such as symmetries, conserved currents, and dimensionality.
- Phase transitions are related to (spontaneous) symmetry breaking and long-range fluctuations.
- Mean field solutions break down for strong fluctuations. Critical phenomena are best described by scaling and renormalization schemes.

In this section we will connect statistical/thermal field theory to critical phenomena and show how the Wilsonian renormalization scheme generates the effective field theories describing stable phases of matter. Combined with Landau's symmetry breaking theory of (continuous) phase transitions, we will elucidate the intimately connected concepts of spontaneous symmetry breaking, long-range order/fluctuations, and the breakdown of mean field theory. First we will give an overview of the basic types of phase transitions characterized by singularities in the free energy. Followed by a discussion of symmetries and symmetry breaking in quantum field theory, the appearance of long-range fluctuations/correlations in the broken symmetry phases destroy the simple mean field picture of critical phenomena. Thus, we will use "renormalization group" methods to analyze the importance of fluctuations. This will enable us to determine the nature of the free energy singularities and understand the critical behavior of the physical system in terms of fixed points under the action of the renormalization group. Finally, we will look at a special type of phase transition not induced by thermal but by quantum fluctuations, at zero temperature known as quantum phase transition.

2.3.1. Classification of phase transitions

Phase transitions originate from the competition between the minimization of a system's (internal) energy and the maximization of its entropy/disorder. The interplay between energy,

minimizing order, and the system's impulse to realize as many different microscopic configurations as possible, is controlled by intensive thermodynamic quantities (thermodynamic forces) usually the temperature, which can be easily controlled in experiments. Thus, phase transitions are captured by singularities in the free energy

$$F(T, V, \{N_i\}) = E(T, V, \{N_i\}) - TS(T, V, \{N_i\}) = -T \ln Z \tag{2.86}$$

or its derivatives with respect to thermodynamic variables. In the traditional Ehrenfest classification of thermal phase transitions, the order of the phase transition is set by the lowest derivative of the free energy with respect to a thermodynamic variable that displays a singularity, typically a discontinuity in the conjugated extensive variable. From a modern perspective this classification is rather artificial because it does not capture the essential physical properties underlying the type of the phase transition. Also higher order phase transitions are very close to second order phase transitions with respect to their physical properties. A modern classification distinguishes three different types of phase transitions:

- **First order** or **discontinuous** phase transitions:

  These phase transitions are characterized by a discontinuous change in the order parameter (an extensive variable distinguishing ordered from disordered phases) and a finite amount of energy transfer without temperature change (owing to the discontinuity in the first derivative of the free energy with respect to the temperature and the divergence of the second derivative, the heat capacity, at the stability limits between the two phases). Thus, the two states describing the respective phases in the thermodynamic configuration space must be distinct, hence the shift from one local equilibrium with minimal energy to the other needs a finite amount of energy. In terms of a potential function (like the famous Mexican hat potential, but here tilted in such a way that the minima can be distinguished) the phase transition changes the shape of the potential function. In a sense the symmetry of the potential is explicitly broken. Another consequence of the finite latent heat is the coexistence of both phases as a mixture, which in turn implies a finite correlation length.

  Examples:

  - Water/vapor, gas/liquid transitions
  - Order/disorder transitions in metallic alloys
  - Bose-Einstein condensation.

- **Second order** or **continuous** phase transitions:

  Here the order parameter vanishes continuously at the phase transition and the first derivative of the free energy is continuous as well. Thus, there is no latent heat and the correlation length of order parameter fluctuations diverges at the critical point where the phase transition occurs and decays in a power law fashion. Futhermore, the susceptibilities and heat capacity display power law singularities determined by universal critical exponents. Phenomenologically, continuous phase transitions are described by a Mexican hat potential (Landau's famous φ^4 theory), where the system spontaneously picks one of the many contiguous thermodynamic configurations. This can be viewed as a spontaneous symmetry breaking induced by a finite order parameter.

  Examples:

  - Superfluid/normal fluid and superconductor/metal transitions
  - Ferromagnetic/paramagnetic order/disorder transitions.

- **Infinite order** or **topological** phase transitions:

  The derivatives of the free energy do not exhibit any discontinuity at the phase transition but nonetheless the free energy possesses an essential singularity. In this sense it is an infinite order phase transition (where the order parameter shows an exponential behavior near the critical point), which is continuous but cannot break any symmetries. Thus, the different phases are distinguished by their topology and not by their symmetries. A famous example is the BKT transition in the two dimensional XY-model without a true long-range ordered phase. Yet there are two phases, one with topological configurations called vortices and a paramagnetic phase without topological excitations [53].

  Examples:

  - BKT phase transition
  - Quantum phase transitions in low dimensional electron systems.

  The topological phase transitions clearly show a departure from the aforementioned Landau symmetry breaking classification scheme where different phases and the related internal structure of different states of matter are described by their respective symmetries (*e.g.* order/disorder). The quantum phase transitions and the fractional quantum hall effect points toward a richer yet unknown classification including different types of quantum matter. See also [4, 9] for more details.

Second order phase transitions are much better understood than first order phase transitions (at least theoretically) due to the absence of the latent heat and the divergent correlation length of the fluctuations of the order parameter. This divergence renders the short-range interactions/behavior of the system irrelevant and only the long wavelength excitation of the order of the large correlation length scale near the critical point are important. Right at the critical point we expect the system to be scale invariant, which will yield a special type of quantum field theory, a conformal field theory. This scaling behavior of thermodynamic properties is the reason why we expect universal features to be encoded in simple effective field theories derived from Wilson's renormalization scheme.

2.3.2. Symmetries in quantum field theories

As explained in the previous section, the continuous phase transition between ordered and disordered (symmetric) phases is described by spontaneous symmetry breaking. Let us recapitulate symmetries in physics, first in classical field theory and finally in quantum field theory. If the action is invariant under a certain set of symmetry operations belonging to a symmetry group, we say the corresponding theory is invariant under this symmetry transformations

$$\begin{aligned} \Phi^i(x) \longrightarrow \Phi^i(x) - \mathrm{i}\varepsilon^a g_a \Phi^i(x) = \Phi^i(x) + \mathrm{i}\varepsilon^a \mathscr{F}^i{}_a(x), \\ \Rightarrow \delta_a S[\Phi] = \mathrm{i}\varepsilon^a \int \mathrm{d}^d x \, \frac{\delta S[\Phi]}{\delta \Phi^i(x)} \mathscr{F}^i{}_a(x) \stackrel{!}{=} 0, \end{aligned} \tag{2.87}$$

where g^a denotes the generators of the symmetry group and $\mathscr{F}^i{}_a$ the action of the group generators on the fields. Note that the Hamiltonian can be viewed as the generator of the dynamical evolution of the system since the equations of motion always leave the action invariant (Hamilton's principle of stationary action)

$$\delta S[\Phi] = \int \mathrm{d}^d x \, \delta \mathscr{L}(\Phi, \partial_\mu \Phi) = \int \mathrm{d}^d x \left[\frac{\partial \mathscr{L}}{\partial \Phi^i} - \partial_\mu \left(\frac{\partial \mathscr{L}}{\partial(\partial_\mu \Phi^i)} \right) \right] \delta \Phi^i, \tag{2.88}$$

for vanishing variations on the boundary $\Phi^i|_\partial = 0$.

We can also distinguish several types of symmetries:

- Global symmetries, acting on the entire system at every point, such as the Poincaré symmetry or the internal isospin $SU(2)$ symmetry.

- Local symmetries, depending on local coordinate representations of the base manifold such as the spacetime, *i.e.* $\varepsilon = \varepsilon(x)$.

Additionally, we can discriminate between

- Physical symmetries, act on physical states and commute with the microscopic Hamiltonian. More precisely, the physical states transform in some representation of the symmetry group (*e.g.* for the Lorentz symmetry this classifies all one particle states). The Hamiltonian commutes with all generators and thus the eigenvalues are called quantum numbers that label the physical states.

- "Gauge" symmetries[19] characterizing the mathematical redundancy in describing the same physical state of the system. Thus, this symmetry relates redundant degrees of freedom in the theory. Observables and physical states cannot transform under gauge symmetries.

Of course there are local and global gauge redundancies/symmetries, but physical symmetries can only be global, because physical local symmetries can only exist for free theories (*e.g.* in effective theories with Gaussian fixed point or in the $T \to \infty$ limit of a statistical system). All symmetries can be continuous, described by Lie groups, or discrete, described by a symmetry group with finite order. Futhermore, there are purely internal symmetries acting only on internal degrees of freedom. In Table 2.2 and 2.3 we list some physical systems and their corresponding symmetries. For global continuous symmetries there is a powerful theorem relating conserved "charges" (constants of motion) and "currents" to the respective generators of the symmetry group:

Noether's Theorem

Under an arbitrary symmetry operation

$$\Phi^i(x) + \mathrm{i}\varepsilon^a(x)\mathscr{F}^i_{\ a}(x),$$

the variation of the action is given by

$$\delta_a S[\Phi] = \int \mathrm{d}^d x \, J^\mu_a(x) \, \frac{\partial \varepsilon^a(x)}{\partial x^\mu}$$

Every continuous global symmetry yields a classical conserved current (not related to forces/interactions) for each symmetry transformation labeled by a

[19] A better parlance for gauge symmetry is gauge redundancy since gauge symmetry is no symmetry in a strict mathematical sense and cannot be broken in principle.

Discrete symmetries	n	Classical system	Quantum system
Global $\mathbb{Z}_n$	1	Potts model	—
	2	Ising model	quantum Ising model
	∞	XY model	quantum rotor boson Hubbard model
Local gauge $\mathbb{Z}_n$	2	Ising lattice gauge theory	(topological)quantum liquids

Table 2.2. Overview of some common discrete symmetries encountered in physical theories/ models. The different global $\mathbb{Z}_n$ models are sometimes called n-state Potts model, vector Potts model or more generally the clock model. The Ising and the XY model may be realized as continuous vector symmetries as well, *c.f.* Table 2.3.

$$\delta_a S[\Phi] = -\int \mathrm{d}^d x\, \varepsilon^a \partial_\mu J_a^\mu(x) \stackrel{!}{=} 0$$

for variations (2.88) vanishing at the boundary. There exists a corresponding conserved charge

$$Q_a = \int \mathrm{d}^D\mathbf{x}\, J_a^0 \qquad \text{where} \qquad \partial_t Q_a = -\int \mathrm{d}^D\mathbf{x}\, \partial_i J_a^i = -\int \left(\partial\, \mathrm{d}^D\mathbf{x}\right)_i J_a^i \approx 0$$

for sufficiently decaying currents near the boundary. Note that Noether's theorem relies on the on-shell action and the classical equations of motion. The off-shell quantum version of Noether's theorem implicitly assumes expectation values and therefore the symmetry applies only to correlation functions. The related operator identities using equations of motion for correlation functions are called Ward-Takahashi identities.

If the Lagrangian or even the Lagrangian density is invariant we can write explicit formulae for the conserved currents[20]

$$J_a^\mu = \left(\frac{\partial \mathscr{L}}{\partial(\partial_\mu \Phi^i)}\partial_\nu \Phi^i - \delta^\mu{}_\nu \mathscr{L}\right)\delta x_a^\nu - \frac{\partial \mathscr{L}}{\partial(\partial_\mu \Phi^i)}\mathscr{F}_a{}^i = \frac{\partial \mathscr{L}}{\partial(\partial_\mu \Phi^i)}\mathrm{i}g_a \Phi^i - \mathscr{L}\delta x_a^\mu, \tag{2.89}$$

where the action of the generators on the fields is generalizes to

$$\mathrm{i}g_a \Phi^i(x) = \partial_\mu \Phi(x)^i \delta x_a^\mu - \mathscr{F}_a{}^i. \tag{2.90}$$

For an exhaustive discussion of symmetries and conserved currents see [54]. Applying Noether's Theorem on page 40 to spacetime translation we find the definition of the conserved energy-momentum tensor

$$T^\mu{}_\nu = \frac{\mathscr{L}}{\partial(\partial_\mu \Phi^i)}\partial_\nu \Phi^i - \delta^\mu{}_\nu \mathscr{L}, \tag{2.91}$$

[20] Only the second term follows from a invariant Lagrangian density, since spacetime variations $x^\mu \longrightarrow x + \varepsilon^a \delta_a x^\mu$ do not leave the Lagrangian density invariant.

Continuous symmetry	n	Classical system	Quantum system
Global $O(n)$	1	Ising model	quantum Ising model
	2	XY model	$O(2)$ quantum rotor model boson Hubbard model
	3	Heisenberg model	$O(3)$ quantum rotor model
	4	Higgs sector toy model	—
Global $U(n)$	1	vector/axial symmetry	—
	2	—	isospin symmetry
Gauge $U(n)$	1	electrodynamics	quantum electrodynamics
	2	—	weak interactions
	3	—	quantum chromodynamic

Table 2.3. Continuation of the overview of common symmetry groups in physical models. Enhancing the discrete symmetries to continuous symmetries allows for true vector models. A very prominent model with continuous symmetry is the standard model of elementary particle physics given by the product group $SU(3) \times SU(2) \times U(1)/\mathbb{Z}_6$. There are also approximate symmetries such as the $SU(3)_{\text{flavor}}$ and the chiral symmetry of QCD $U(2)_{\text{L}} \times U(2)_{\text{R}} = SU(2)_{\text{L}} \times SU(2)_{\text{R}} \times U(1)_{\text{vector}} \times U(1)_{\text{axial}}$ which are only realized for massless quarks. The $SU(2)_{\text{L}} \times SU(2)_{\text{R}}$ is spontaneously broken by a finite quark condensate and due to its approximate nature the corresponding Nambu-Goldstone bosons (the three pions) are massive, *c.f.* Table 2.4.

where the corresponding charge is the conserved total energy and the spatial momentum because the time-spatial components T^{0i} are the momentum density current and the T^{00} component is the energy density. The complete discussion carries over to quantum field theories (replacing Poisson brackets with commutators) but with the caveat of so-called "anomalies". These anomalies change the functional integral measure which in turn changes the action or the Lagrangian of the quantum field theory. The name "anomalies" is more or less a misnomer since their origin lies in the fact that we need to take the Jacobian of a coordinate transformation into account. As stated above, symmetries in classical physics leave the action invariant (2.87) but symmetries in quantum physics need to be realized on the level of the quantum states and hence the partition function needs to be invariant, so the functional integral measure must be preserved in addition to the classical action

$$\delta S[\Phi] = 0 \qquad \Leftrightarrow \qquad \delta Z = \delta \int \mathcal{D}\Phi \; \mathrm{e}^{-S[\Phi]} = 0. \tag{2.92}$$

Therefore, anomalies are symmetries which hold at the classical level but are broken at the quantum level because

$$\mathcal{D}\Phi \longrightarrow \mathcal{J}\, \mathcal{D}\tilde{\Phi} \neq \mathcal{D}\Phi\,. \tag{2.93}$$

A well known anomaly is the axial anomaly. Classically the current corresponding to the global axial symmetry

$$\Psi \longrightarrow \mathrm{e}^{\mathrm{i}\varepsilon\gamma^5}\,\Psi \qquad \text{in} \qquad \mathscr{L} = \mathrm{i}\overline{\Psi}\gamma^\mu\partial_\mu\Psi \qquad \text{where} \qquad \Psi = \left(\psi_{\text{L}}, \psi_{\text{R}}\right)^{\mathsf{T}}, \tag{2.94}$$

is conserved, but in quantum field theory, there are non-zero contributions arising from what are known as triangular diagrams due to quantum fluctuations [50]. We will see in Section 2.3.3 that quantum fluctuations can not only destroy symmetries but also dynamically restore them.

Theories with gauge redundancy are described by the action of the gauge group generators In particular we need to modify the derivatives by introducing a gauge connection relating different "gauges" of the physical quantities to each other. These gauge fields naturally give rise to interactions transmitted between the fields transforming under the gauge group. A famous (and to my knowledge the only classical example) is Maxwell's theory of electromagnetic interactions with a $U(1)$ gauge group. The theory can be written entirely in the language of differential forms allowing immediate extension to curved spacetime if necessary

$$A \longrightarrow A + \mathrm{d}\lambda(x) \quad \Rightarrow \quad \mathscr{L}_{\text{em}} = -\frac{1}{4}(\mathrm{d}A)^2 \longrightarrow -\frac{1}{4}(\mathrm{d}A + \mathrm{d}^2\lambda(x))^2 = \mathscr{L}_{\text{em}}, \tag{2.95}$$

Turning to quantum physics, we show that the phase invariance (describing a true gauge redundancy) of a complex quantum field implies the existence of an interaction mediated by a gauge field. Charged matter can be described (microscopically) by quantum operators and their respective excitations from the vacuum state such as charged fermionic particles (electrons) transforming in the fundamental representation of the $U(1)$. In a heuristic picture, we can view the different states of an electron connected by the $U(1)$ symmetry

$$\Psi \longrightarrow \mathrm{e}^{-\mathrm{i}e\lambda(x)}\,\Psi, \qquad \text{length of } \nearrow = \left|\mathrm{e}^{-\mathrm{i}e\lambda(x)}\right| = 1, \qquad \text{position of } \nearrow = \lambda(x), \tag{2.96}$$

as internal indicators (displaying the phase of the wavefunction) carried by each electron. Now the photon exchanged by two electrons plays the role of transmitting the position of the indicator from an electron to the other in such a way that both electrons can retain their respective choice of phase. Therefore for an external observer it is impossible to extract the actual phase of an electron, because any measurement done by interchanging photons can only detect phase changes. This "reality" of the gauge field was demonstrated by the experimental realization of the Aharonov-Bohm effect. It can be shown that local phases accumulated by contractible loops are represented by forces (here the magnetic force) but global phases of non-contractible loops are not related to any classical force [4]

$$\varphi_{\text{local}} = \mathrm{i}q \oint \mathrm{d}\mathbf{x}\cdot\mathbf{A} = \mathrm{i}q \int \mathrm{d}\mathbf{n}\cdot\mathbf{B}, \qquad \varphi_{\text{global}} = \mathrm{i}q n_w \Phi_{\text{magnetic flux}}, \tag{2.97}$$

where n_w denotes the winding number and the magnetic flux is confined to a small non-accessible region (*e.g.* a single flux tube), hence the loop is non-contractible. Nonetheless the free quantum particle will be subject to some interaction since its quantum properties are changed, but the classical equations of motion are only affected by local phases generated by non-zero gauge fields. Mathematically, the local phase is related to the holonomy of the gauge connection whereas the global gauge are related to the monodromy. In differential geometry parlance this holonomy can be viewed as a parallel transport around a closed loop

$$W[\mathcal{C}] = \mathrm{tr}\left[\mathcal{P}\exp\left(\mathrm{i}\oint_{\mathcal{C}} A\right)\right], \tag{2.98}$$

where the trace is the character of the irreducible representations of the gauge group and $\mathcal{P}$ denotes the path ordering analogous to the time ordering in the path integral since the gauge

one-forms may not commute at different points on the loop. In physics, (2.98) is called the Wilson loop and is an important gauge invariant quantity in (thermal) gauge theories. The spacetime derivative is supplemented by a gauge connection in order to define gauge invariant derivatives and the corresponding field strength tensor is then interpreted as the curvature form

$$\mathrm{D}\,\Phi = \mathrm{d}\,\Phi - \mathrm{i}gA\Phi = \mathrm{d}\,\Phi - \mathrm{i}g\,[A,\Phi]\,, \qquad \mathrm{i}gF = \mathrm{D}\wedge\mathrm{D} = [\mathrm{D},\mathrm{D}]\,, \tag{2.99}$$

which yields the dynamical terms for the gauge field. The conservation law for currents *cannot* be determined by Noether's theorem since it only holds for global symmetries. Instead, conserved currents arise from the identity $\mathrm{d}^2 = 0$ which is also valid for non-Abelian gauge groups if we take the proper covariant extension *i.e.* the corresponding Bianchi identities. Note that the corresponding charges are not conserved since for non-Abelian gauge groups the gauge field are not neutral/uncharged. The full gauge invariant $U(1)$ Lagrangian of quantum electrodynamics describing charged particles/electrons ($q = -e$) and photons can then be written as

$$\begin{aligned}\mathscr{L}_{\text{QED}} &= -\frac{1}{4}F^2 + \overline{\Psi}\,(\mathrm{i}\gamma^\mu\,\mathrm{D}_\mu - m)\,\Psi \\ &= -(\partial_\mu A_\nu - \partial_\nu A_\mu)(\partial^\mu A^\nu - \partial^\nu A^\mu) + \mathrm{i}\overline{\Psi}\gamma^\mu\partial_\mu\Psi - e\overline{\Psi}\gamma^\mu A_\mu\Psi\end{aligned} \tag{2.100}$$

where the gauge covariant derivative induces an interaction $q\overline{\Psi}\gamma^\mu A_\mu\Psi$ between the fermionic fields (electrons) mediated by the gauge connection/field (photons). In quantum theories of elementary particles there exist two more forces, with no classical counterpart, the weak interaction transmitted by an $SU(2)$ gauge field and the strong interaction described by quantum chromodynamics, an $SU(3)$ gauge theory. Equation (2.95) for general non-Abelian $SU(N)$ gauge groups reads

$$\mathscr{L}_{\text{YM}} = -\frac{1}{2}\,\mathrm{tr}\,F^2 = -\frac{1}{4}F^{a\mu\nu}F^a_{\mu\nu} \qquad \text{where} \qquad F^a_{\mu\nu} = \partial_\mu A^a_\nu - \partial_\nu A^a_\mu + g_{\text{YM}} f^{abc} A^b_\mu A^c_\nu \tag{2.101}$$

and the corresponding field theories are called Yang-Mills theories. In particular the gauge field excitations or gauge bosons, being in the adjoint representation, carry charges for non-Abelian gauge theories. The adjoint representation of the $U(1)$ gauge group is trivial and hence the photon, and all other possible excitations transforming in the adjoint representation, are uncharged

$$gXg^{-1} \longrightarrow \mathrm{e}^{\mathrm{i}q\lambda}\,X\,\mathrm{e}^{-\mathrm{i}q\lambda} = X \qquad \Rightarrow \qquad [X,Y] = 0. \tag{2.102}$$

yet

$$A \longrightarrow \mathrm{e}^{\mathrm{i}q\lambda}\,A\,\mathrm{e}^{-\mathrm{i}q\lambda} + \mathrm{e}^{\mathrm{i}q\lambda}\,\mathrm{d}\,\mathrm{e}^{-\mathrm{i}q\lambda} = A - \mathrm{i}q\,\mathrm{d}\lambda\,. \tag{2.103}$$

A nice book discussing Yang-Mills theories and its application to particle physics is [55]. Classically, we can also consider gravity as a gauge theory (in the broader sense that gauge symmetries describe mathematical redundancies) but here we need to be careful. The active diffeomorphism invariance of general relativity is not a true redundancy but rather a change of reference frame. Observers in different reference frames *do* measure different results for the same event. But events are independent of the underlying parametrization of the spacetime manifold as shown by Einstein's hole argument; see for example [46, 56].

2.3.3. Symmetry breaking, massless excitations & massive "gauge" fields

Different phases of physical systems are related to different symmetries, so for a phase transition to happen we need to break the symmetry of the theory. For global symmetries we can have two distinct symmetry breaking mechanisms:

- **Explicit symmetry breaking:**
  The symmetry is explicitly broken in the Lagrangian of the theory, *i.e.* a symmetry breaking term is added, which will give rise to gapped low-energy excitations. For critical phenomena/phase transitions this approach cannot connect different phases by varying a (thermodynamic) parameter since the symmetry is always broken.

- **Spontaneous symmetry breaking:**
  In this case only the symmetry of the vacuum state is broken whereas the Lagrangian remains invariant. In quantum theories a symmetry of the vacuum must also be a symmetry of the Hamiltonian but *not* vice versa. An invariant Hamiltonian which commutes with conserved charges allows for two possible realizations

$$[\mathcal{H}, Q_a] = 0 \Rightarrow \begin{cases} Q_a \,|\, 0 \rangle = 0 \Leftrightarrow \\ \mathrm{e}^{\mathrm{i}\varepsilon^a Q_a} \,|\, 0 \rangle = |\, 0 \rangle \\ Q_a \,|\, 0 \rangle \neq 0 \end{cases} \qquad \begin{array}{l} \langle\, 0 \,|\, \Phi^\dagger \mathcal{H} \Phi \,|\, 0 \,\rangle \overset{21}{=} \left\langle\, 0 \,\middle|\, \tilde{\Phi}^\dagger \mathcal{H} \tilde{\Phi} \,\middle|\, 0 \,\right\rangle \\ \textit{e.g.}\ \langle\, \delta_a \Phi \,\rangle = \mathrm{i} \langle\, 0 \,|\, [Q_a, \Phi] \,|\, 0 \,\rangle \neq 0 \end{array} . \tag{2.104}$$

  The first case can be generalized to show the invariance of arbitrary correlation functions leading to the Ward-Takahashi identities hinted at in the Infobox Noether's Theorem on page 40. Since for all ε^a the vacuum state is invariant, all generators must annihilate the vacuum state. Here the symmetric vacuum state possess a finite energy gap as well. In the second case at least one of the correlation functions is not invariant under the symmetry, usually the vacuum expectation value of a field, which is identified as the order parameter, by acquiring a fixed value. Additionally, a non-zero two point correlation function of the order parameter imply long range order

$$\lim_{|x-x'| \to \infty} \langle\, \Phi(x) \Phi(x') \,\rangle \neq 0 \tag{2.105}$$

  and the spontaneously broken symmetry phase describes a ordered system on a global scale.

Strictly speaking, a spontaneous symmetry breaking can only occur in the thermodynamic limit $N \to \infty$, $V \to \infty$ while $N/V = \text{const}$. Mathematically, the order parameter is a logarithmic derivative of the partition function which is composed of a finite sum of weighting factors and thus cannot be a singular function. Only in the continuous limit a singularity may emerge. Physically, thermal and/or quantum fluctuations will destroy the uniform (fixed) value of the order parameter and thus dynamically restore the symmetry (see also Section 2.3.4 and Infobox Coleman-Mermin-Wagner Theorem on page 53). Thermal fluctuations vanish in the thermodynamic limit and for quantum field theories the infinite number of degrees of freedom decouple different vacuum/ground states since the mixed matrix elements of the Hamiltonian are zero and there is no quantum superposition of different vacuum states anymore. So the vacuum state characterized by the order parameter is stable and it takes an infinite time to fluctuate into a different vacuum state.

The fact that the vacuum expectation is not invariant under the symmetry leads to the celebrated Goldstone theorem for spontaneously broken continuous global symmetries:[22]

[21] This follows directly from

$$\left\langle\, 0 \,\middle|\, \Phi^\dagger \mathcal{H} \Phi \,\middle|\, 0 \,\right\rangle = \left\langle\, 0 \,\middle|\, \mathrm{e}^{-\mathrm{i}\varepsilon Q} \tilde{\Phi}^\dagger \mathrm{e}^{\mathrm{i}\varepsilon Q} \mathcal{H} \mathrm{e}^{-\mathrm{i}\varepsilon Q} \tilde{\Phi} \mathrm{e}^{\mathrm{i}\varepsilon Q} \,\middle|\, 0 \,\right\rangle = \left\langle\, 0 \,\middle|\, \tilde{\Phi}^\dagger \mathcal{H} \tilde{\Phi} \,\middle|\, 0 \,\right\rangle$$

yielding vacuum/ground states with degenerate energy.

[22] While a discrete symmetry may also give rise to degenerate (non-contingent) vacuum states, it is not possible to move from one symmetry-breaking vacuum state to another with zero energy fluctuations. For an infinite system (*e.g.* in

Physical system	Broken symmetry	Excitation	Quasi-particle
Fluids	Galilean symmetry	density/sound waves	phonons
Solids	translational & rotational	lattice vibrations	crystal phonons
Magnets	rotational	spin waves	magnons
Superfluids	global $U(1)$	density waves	phonons
QCD	chiral-flavor	quark-antiquark	pions*

Table 2.4. The Nambu-Goldstone excitations are universal features of physical systems exhibiting spontaneous symmetry breaking. The massless/gapless modes are independent of the microscopic details as long as the (microscopic) interactions are sufficiently short-ranged. The corresponding quasi-particles are characterized by the same quantum numbers as the respective generators. Note that the chiral symmetry breaking yields massive pseudo-Goldstone bosons due to the quark condensate's explicit symmetry breaking.

Goldstone's Theorem

A spontaneously broken continuous symmetry in a system with sufficiently short-ranged interactions leads to massless excitations along the directions spanned by the generators of the symmetry (more precisely, the coset space) that *do not* leave the vacuum/ground states invariant because

$$\left.\frac{\partial V\left(\mathrm{e}^{-\mathrm{i}\varepsilon^a Q_a}\,\Phi\right)}{\partial\varepsilon^a}\right|_{\varepsilon^a=0} = \frac{\partial V}{\partial\Phi^j}\left.\frac{\partial\left(\mathrm{e}^{-\mathrm{i}\varepsilon^a Q_a}\right)}{\partial\Phi^j}\right|_{\varepsilon^a=0} = -\mathrm{i}\frac{\partial V}{\partial\Phi^j}Q_a\Phi^j \stackrel{!}{=} 0$$

$$\Rightarrow \frac{\partial}{\partial\Phi^k}\left(\frac{\partial V}{\partial\Phi^j}Q_a\Phi^j\right) = \frac{\partial^2 V}{\partial\Phi^k\partial\Phi^j}Q_a\Phi^j + \frac{\partial Q_a\Phi^j}{\partial\Phi^k}\frac{\partial V}{\partial\Phi^j} = 0$$

$$\Rightarrow \left.\frac{\partial^2 V}{\partial\Phi^k\partial\Phi^j}\right|_{\Phi^j=\Phi^k=\Phi^{(0)}} Q_a\Phi^{(0)} = \mathcal{M}^2_{jk}Q_a\Phi^{(0)} = 0$$

where the mass operator squared is defined as the curvature of the potential functional V and the vacuum states are defined as the minima of V, *i.e.* $\partial V/\partial\Phi^j\big|_{\Phi^j=\Phi^{(0)}} = 0$. For all generators $Q_a\Phi^{(0)} \neq 0$ the corresponding eigenvalue of $\mathcal{M}^2_{jk}$ are zero. The remaining generators, leaving the broken symmetry vacuum state invariant, correspond to the residual symmetry gauge group. Excitations along these directions possess an energy gap related to the shape of the potential (*i.e.* the non-zero eigenvalues of $\mathcal{M}^2_{jk}$). The manifold of degenerate vacuum states may be parametrized by a continuous field describing the effective low-energy dynamics of the massless excitations.

The massless low-energy excitations are called Nambu-Goldstone modes and can be related to quasi-particles in various systems, *c.f.* Table 2.4. In Fourier representation these modes will manifest themselves as zero momentum poles of the corresponding correlation functions. For

the thermodynamic limit) the energy cost is infinite and the system is said to be rigid with respect to this broken symmetry.

continuous phase transitions the onset of the ordered phase can be probed by computing the pole structure of the respective susceptibilities in the unbroken phase. Upon approaching the critical point the zero momentum pole of the susceptibilities related to the order parameter fluctuations will cross the origin of the complex frequency plane indicating an instability due to the expansion around the "false vacuum". Therefore, assuming well behaved low-energy effective theories, the critical point can be determined without computing thermodynamic properties such as the free energy in the broken and unbroken phase. This method will come into its own when applied to holographic systems, where calculations in the ordered phase may become intractable, see *e.g.* Section 4.5 and 5.3.

In principle gauge symmetries/redundancy cannot be broken spontaneously. This is the essence of Elitzur's theorem [57] and as a consequence we cannot construct a Landau type local order parameter. The different phases in a gauge theory can be characterized by a gauge invariant physical quantity, the Wilson loops introduced in (2.98). The high-temperature phase displays an exponential decay determined by the enclosed area of the loop

$$W[\mathcal{C}] \sim \left. \mathrm{e}^{-\text{const.}\cdot\text{Area}[\mathcal{C}]} \right|_{T>T_c} \qquad \text{(area law)} \tag{2.106}$$

whereas the low-temperature phase is related to the length of the Wilson loop

$$W[\mathcal{C}] \sim \left. \mathrm{e}^{-\text{const.}\cdot|\mathcal{C}|} \right|_{T<T_c} \qquad \text{(perimeter law)} \tag{2.107}$$

For a (lattice) $U(1)$ gauge theory the gapped/confined phase with linear flux tubes connecting opposite charges is described by the area law whereas the deconfined/Coulomb phase exhibit the perimeter law. In non-perturbative/strongly coupled QCD the Wilson loops can be used to distinguish the hadronic phase from the deconfined quark-gluon plasma phase, *c.f.* Figure 1.2. The area law of the Wilson loop for the hadronic phase can be understood as being proportional to the flux tube area which in turn is proportional to the separation of antiquark/quark pairs. Mesons as bound states of antiquark/quark pairs contain two Wilson loops almost canceling each other which yields a small area enclosed by the total loop. The Wilson loop in the deconfined phase is proportional to the path traced out by "free" antiquark/quark pairs which is characterized by the perimeter law.

Nonetheless, we can choose a particular gauge where the gauge symmetry may be hidden in the vacuum states, such that the gauge transformations of the gauge group become trivial. This symmetry breaking mechanism follows from the observation that we can "gauge away" the "artificial" or spurious Nambu-Goldstone mode by a redefinition of the gauge field. This is the famous Anderson-Higgs mechanism explaining massive photons in superconductors and the mass of the weak force gauge bosons.

Anderson-Higgs Mechanism

The Anderson-Higgs mechanism gives rise to massive "gauge" fields for a particular choice of gauge that encodes only the true physical degrees of freedom. The "symmetry breaking" turns the original gauge field into a massive gauge invariant vector field by removing the unphysical massless Goldstone mode.

The number of degrees of freedom is conserved and the action is still manifestly gauge invariant. Thus, the term "spontaneously broken gauge symmetry" should be read as "gauge symmetry/transformation becomes trivial". Historically, the terms Anderson-Higgs mechanism and spontaneously broken gauge symmetry are used synonymously due to their formal equivalence. For an elucidating discussion on these matters see the excellent review about spontaneously violated gauge symmetries in superconductors [58].

Experimentally, there is strong evidence that our universe is actually in a condensed phase where a non-zero vacuum expectation value of a scalar field provides the electroweak symmetry breaking mechanism in the standard model and thus gives rise to massive gauge bosons and generates masses of the elementary particles. Last year a new bosonic particle was discovered at the Large Hadron Collider in Geneva which seems to have the properties predicted by the standard model calculations. The mass of the particle is about $126\,{}^{\mathrm{GeV}}/_{\mathrm{c}^2}$ but if it is a scalar spin zero particle has yet to be ascertained.[23] If the new particle is the so-called Higgs particle, the collective excitation of the condensed scalar field, the particle/field content of the standard model of elementary particle physics would be complete. Studying the new particle more closely could yield more information about the properties of the (current) phase or state of our universe. In principle it could be possible that the Higgs field is of composite nature and the corresponding collective excitations are an emergent phenomenon.[24] Funnily enough, in condensed matter physics a Higgs-like mode has been detected (even prior to the discovery at CERN) in an quantum antiferromagnet displaying a dimerized disorder to magnetic long range order transition [61] and recently in an ultracold atoms system close to the critical point of the superfluid-insulator transition [62]. A Higgs mode can only exist in a relativistic theory but in condensed matter the low-energy excitations are non relativistic (*i.e.* the mass gap is not equal to the dynamic mass of the excitation). However, in quantum phase transitions the ordered and disorder phase as well as the quantum critical point is described by relativistic Lagrangians. In addition to the gapless Goldstone modes, quantum critical systems possess gapped low-energy excitations with a mass gap proportional to the curvature of the minimized potential. In the superfluid-insulator experiment [62] the experimental visibility is obscured due to the low-dimensionality of the system. The Higgs mode can decay into multiple Goldstone modes and the respective amplitude of such a process in two dimensions has an infrared singularity.[25]

2.3.4. Mean field theory & universality

The simplest case to generate unique field theories from the microscopic Hamiltonian/Lagrangian in order to study universal properties are mean-field theories employing the so-called mean-field approximation. Once we have determined the "right" degrees of freedom (not necessarily simply related to microscopic degrees of freedom) and the respective ground state, we can compute physical properties by expanding about the stable ground state. Singularities in physical observables, such as response functions, imply instabilities and missing relevant degrees of freedom indicating the expansion about the wrong reference ground state. In the following we will briefly

[23] Due to the decay channels measured so far it can be ruled out to be a spin one particle $\mathrm{H} \longrightarrow \gamma\gamma$ following the Landau-Yang theorem [59, 60]. In order to rule out a spin two particle we need to find the $\tau\tau$ and $\bar{\mathrm{b}}\mathrm{b}$ decay channels that have not been confirmed yet.

[24] Personally, I am very suspicious that the Higgs field is really elementary and I hope particle physics will discover a window to a whole new world.

[25] Numerical confirmation of the experimental results and theoretical predictions [63–65] has been obtained by a Monte Carlo simulation of the Bose-Hubbard model [66].

outline the mean field methods and its breakdown which is connected to strong fluctuations destroying the mean field solution.

Mean Field Approximation

The central argument of the mean field theory relies on the fact that quantum fluctuations are irrelevant and the quantum operators can be effectively replace by classical complex numbers

$$\Delta O = O - \langle O \rangle \qquad \Leftrightarrow \qquad O = \langle O \rangle + \Delta O.$$

The solution fixing the mean field $\langle O \rangle$ must be found self-consistently. As the name suggest the complicated many-body Hamiltonian is reduced to a single quantum operator where the effect of the interaction/entanglement with all other operators is reduced to an averaged background field, the so-called mean field

$$\begin{aligned} O'O &= O' \langle O \rangle + \langle O' \rangle O - \langle O' \rangle \langle O \rangle + \Delta O' \Delta O \\ &\approx O' \langle O \rangle + \langle O' \rangle O. \end{aligned}$$

This scheme can be carried over to field theoretic methods, where we introduce an additional field φ by means of the so-called Hubbard-Stratonovich transformation (being the inverse of the Gaussian identity (2.44))

$$\exp\left(-\frac{1}{2} O_i \mathcal{V}_{ij} O_j\right) \approx \exp\left(-\frac{1}{2}\left(\Phi\,,\, \mathcal{V}\Phi\right)\right) = \int \mathcal{D}\varphi \exp\left(-\frac{1}{2}\left(\varphi\,,\, \mathcal{V}^{-1}\varphi\right) - \mathrm{i}\left(\varphi\,,\, \Phi\right)\right) \tag{2.108}$$

Note that the left-hand side of the Hubbard-Stratonovich transformation may involve a sum over discrete degrees of freedom, so in this case the averaging process can be accomplished by a single operation. This is not always possible. The integration over the original fields Φ composed of complicated microscopic fields is now replaced by the integration over the auxiliary field φ. We can view the Hubbard-Stratonovich transformation (2.108) as a decoupling of the Φ interaction by introducing the effect of the mean field φ on a single composite field Φ. The self-consistent mean field solution is determined by a stationary phase approximation (which is valid since the mean field is a averaged quantities over a large number of microscopic degrees of freedom providing the existence of a large parameter), *i.e.* $\varphi = \varphi^\star$. Finally, the expansion about the stationary phase solution yields the relevant/important low-energy excitations above the ground state.

It is straight forward to describe critical phenomena using mean field methods. Since we are dealing with a low-energy effective theory encoding only the relevant information independent of the microscopic nature, we can immediately identify the mean field as the order parameter of a continuous phase transition. The ground or reference state mentioned above is identified with the stable phase *e.g.* $\varphi^\star \equiv 0$. Upon approaching the critical point, response functions will show singular behavior due to large fluctuations indicating the aforementioned instabilities[26]. Thus, we are forced to adopt a new ground/reference state naturally arising from the new emergent minima in the field theory potential. This parallels exactly our discussion about spontaneously symmetry breaking in Section 2.3.3. The new reference state will be characterized by a spontaneously broken symmetric ground state with non-zero order parameter/mean field $\varphi^\star \neq 0$. The

[26] Strictly speaking, as we will see at the end of this section, mean field theories fail to describe the critical point accurately, except above a certain spatial dimension called the upper critical dimension D_c.

Physical quantity	Definition	Behavior near critical point $\lvert T-T_c\rvert$	
		$T>T_c$	$T<T_c$
Susceptibility	$\chi=-\left.\frac{\delta^2 F[\varphi;J]}{\delta J^2}\right\rvert_{J=0}$	γ	γ'
Specific heat	$C=-T\frac{\partial^2 f}{\partial T^2}$	α	α'
Order parameter	$\langle\varphi\rangle=\left.\frac{\delta F[\varphi;J]}{\delta J}\right\rvert_{J=0}$	$(\varphi^\star=0)$	β
Correlation length	ξ	$-\nu$	$-\nu'$
		$T>T_c$	$T=T_c$
Source field	J		$(\varphi^\star)^\delta$
Correlator	$\langle\!\langle\,\varphi(\mathbf{x})\varphi(\mathbf{y})\,\rangle\!\rangle$	$\lvert\mathbf{x}-\mathbf{y}\rvert^{-D+1/2}\,\mathrm{e}^{-\lvert\mathbf{x}-\mathbf{y}\rvert/\xi}$	$\lvert\mathbf{x}-\mathbf{y}\rvert^{-D+2-\eta}$

Table 2.5. The free energy functional is defined as $F[\varphi;J]=-T\ln\mathcal{Z}[J]$ and the free energy density $f=T/L^D S[\varphi^\star;J]$ is an implicit function of the temperature. The order parameter is the thermal expectation value and may be sourced by an external field J. Although the connected correlation function of the order parameter $G_\varphi(\mathbf{x},\mathbf{y})=-\langle\!\langle\,\varphi(\mathbf{x})\varphi(\mathbf{y})\,\rangle\!\rangle$ is related to the response function/susceptibility by the fluctuation-dissipation theorem, the thermodynamic susceptibility χ encodes imaginary time/thermal fluctuations only and not spatial fluctuations of the order parameter field. The deeper understanding of the critical exponents will become clear when we will apply the renormalization group scheme in Section 2.3.5.

low-energy excitations or Goldstone modes are the relevant low-energy excitations obtained by expanding about the non-zero stationary phase solution.

The microscopic theories are thus classified according to their universal low energy behavior encoded in the critical exponents listed in Table 2.5. All microscopic models that can be described by the same effective model/theory are said to be members of the same universality class, *i.e.* they possess the same universal properties (symmetries, dimensionalities, range of interactions,...) independent of their microscopic origin. For each of the models in Table 2.2 and 2.3 we may find a universality class with unique critical exponents. For instance, the Landau-Ginzburg theory (sometimes called φ^4 theory or Mexican hat potential theory)

$$S[\varphi;J]=\int \mathrm{d}^D\mathbf{x}\left[\frac{b}{2}(\nabla\varphi)^2+\frac{r}{2}\varphi^2+\frac{u}{4!}\varphi^4-\varphi J\right] \tag{2.109}$$

where b denotes the stiffness,[27] r is the reduced temperature $(T-T_c)/T_c$ and u describes effective interactions, is the effective field theory of the Ising universality class. Equation (2.109) can

[27] Strictly speaking, for $b\neq 0$ we do note have a true mean field theory. The spatially uniform theory consisting solely of a free energy functional is usually called Landau theory, whereas the inclusion of spatial fluctuations is known as Landau-Ginzburg theory. In order to determine ν and η and to understand the breakdown of the mean field theory it

Critical exponent	$D = 1$ Ising	$D = 2$ Ising	$D = 3$ Ising (computed)	Mean field theory
α	1	$0(\log)$	0.110(1)	0
β	0	$1/8$	0.3265(3)	$1/2$
γ	1	$7/4$	1.2372(5)	1
δ	∞	15	4.789(2)	3
ν	1	1	0.6301(4)	$1/2$
η	1	$1/4$	0.0364(5)	0

Table 2.6. The one and two dimensional Ising model can be solved analytically by duality techniques or the transfer matrix method. The three dimensional Ising model values are obtained form high temperature expansion and Monte Carlo methods taken from [67] and are in close agreement with experimental results. As can be seen, the critical exponents depend on the dimensionality of the system. For increasing dimensionality the system approaches the mean field behavior due to the decreasing importance of fluctuations (see also Infobox Ginzburg Criterion on page 52).

be "derived" from the Ising Hamiltonian by applying a Hubbard-Stratonovich transformation (2.108) and takeing a successive continuum limit. The Ising universality class describes phase transitions in ferromagnetic materials and the liquid gas phase transition, whereas the superfluid/normal fluid phase transition is effectively described by the XY model, *i.e.* it belongs to the XY model universality class. A very comprehensive and detailed overview concerning the properties of the $O(n)$ universality classes and classification of physical phase transitions can be found in [67]. The critical exponents of the mean field theory are derived by inserting the saddle point solution

$$\left.\frac{\delta S}{\delta \varphi}\right|_{\varphi=\varphi^\star} = -b\nabla^2\varphi^\star + r\varphi^\star + \frac{u}{6}\left(\varphi^\star\right)^3 - J \stackrel{!}{=} 0 \tag{2.110}$$

$$\stackrel{J=0}{\Longrightarrow} \begin{cases} \varphi^\star = 0, & r > 0, \quad (T > T_c) \\ |\varphi^\star| = \sqrt{-\dfrac{6\,|r|}{u}}, & r < 0, \quad (T < T_c) \end{cases}, \tag{2.111}$$

displaying degenerate minima, into the Landau-Ginzburg action (2.109)

$$S[\varphi^\star] = \frac{L^D}{T}\left(\frac{r}{2}\left|\varphi^\star\right|^2 + \frac{u}{4!}\left|\varphi^\star\right|^4 - \varphi^\star J\right) = \frac{L^D}{T}\begin{cases} 0, & r > 0, \quad (T > T_c) \\ -\dfrac{3}{2}\dfrac{r^2}{u}, & r < 0, \quad (T < T_c) \end{cases} \tag{2.112}$$

We see that for $T < T_c$ the energetic preferred configuration $f = -3r^2/2u$ is the asymmetric solution with finite order parameter. Applying all definitions of Table 2.5 to (2.110), (2.111) and (2.112) yields the mean field critical exponents shown in Table 2.6.

Unfortunately, the mean field theory has some serious drawbacks, most importantly it fails to reproduce computational and experimental results in two and three spatial dimensions (as can

is instructive to include these fluctuations. In Section 2.3.5 we will see that the correlation length scales like $\xi \sim \sqrt{b}$ so the microscopic interaction range is related to b motivating the colloquial term "stiffness".

be seen in Table 2.6) and even worse it predicts the existence of (finite temperature) phase transitions in one and two dimensional systems. The reasons for this failure lies in the relevance of fluctuations in low-dimensional systems which destroys the naïve mean field solution. In order to estimate the range of applicability of the mean field approximation we require the fluctuations to be sufficiently smaller than the mean field "strength". This is the so-called Ginzburg criterion:

Ginzburg Criterion

The mean field approximation yields a self-consistent solution if the correlated spatial fluctuations about the mean field $\langle \Delta\varphi(\mathbf{x})\Delta\varphi(\mathbf{y}) \rangle$ are sufficiently small

$$G_\varphi(\mathbf{x},\mathbf{y}) \ll \langle \varphi \rangle^2$$

In Fourier representation the Landau Ginzburg correlator close to the critical point reads

$$G_\varphi(\mathbf{x}-\mathbf{y}) \sim \int \frac{\mathrm{d}^D\mathbf{k}}{(2\pi)^D} \frac{\mathrm{e}^{\mathrm{i}\mathbf{k}\cdot(\mathbf{x}-\mathbf{y})}}{r+bq^2} \xrightarrow{r\to 0} G_\varphi(\xi) \sim \int \frac{\mathrm{d}^D(k\xi)}{(2\pi)^D} \frac{\xi^2}{1+b(k\xi)^2} \mathrm{e}^{\mathrm{i}(k\xi)} \sim \xi^{-D+2}$$

where we neglected the interaction term due to its irrelevance and we assume that all dimensionful quantities scale with the correlated fluctuations over the length scale $|\mathbf{x}-\mathbf{y}| = \xi$.[28] Written in terms of critical exponents

$$G_\varphi \sim r^{(D-2)\nu} \ll r^{2\beta} \sim \langle \varphi \rangle^2 \qquad \longrightarrow \qquad (D-2)\nu > 2\beta$$

the Ginzburg criterion states that the mean field approximation is only consistent in $D > 2\beta/\gamma + 2$. In particular for the Ising universality class we find $D > 4$.

In general, *i.e.* for all universality classes above the respective upper critical dimension D_c, fluctuations can be neglected and the mean-field approximation yields a valid solution. The same holds true for quantum fluctuations and quantum critical points at zero temperature. Only for dimensions larger than the upper critical dimension the quantum fluctuations can be neglected and the semi-classical approximation is valid. Therefore, only for $D > D_c$ the semi-classical theory describes quantum critical points correctly. There is also a lower critical dimension usually denoted by D_ℓ. Only systems with larger dimension then D_ℓ exhibit finite temperature phase transitions. Heuristically, this dimension can already be seen from the expression of the correlator in Table 2.5

$$G_\varphi(\mathbf{x},\mathbf{y}) \sim |\mathbf{x}-\mathbf{y}|^{-D+2-\eta} \qquad \text{for} \qquad T \approx T_c \tag{2.113}$$

If we neglect the so-called "anomalous" scaling dimension[29] η we see that for $D = 2$ the long-range correlations in the broken/condensed phase are virtually non-existent, as well as the associated long-range order.

[28] For a full justification of the scaling behavior and irrelevance of interactions see the following Section 2.3.5 on renormalization.

[29] Strictly speaking a misnomer, since it only hints at another important microscopic length scale besides the correlation length which is connected to ultra-violet divergences. In principle all other critical exponents may be corrected by additional "anomalous" coefficient which is usually not represented by a special symbol. From the renormalization perspective (developed in Section 2.3.5) the "anomalous" scaling dimensions arise from the influence of irrelevant operators/fields which might be still important close to the critical point, *e.g.* correlations on all length scales imply contributions of the microscopic lattice spacing or the short wavelength cut-off.

Coleman-Mermin-Wagner Theorem

A continuous symmetry cannot be broken spontaneously in physical systems with sufficiently short-ranged interactions. This implies that there are no finite temperature phase transitions due to the existence of long-range fluctuations favoring the disordered high-temperature phase, thus destroying long-range order. The Landau Ginzburg correlator for fluctuations about the vacuum state reads

$$\langle\, \delta\varphi(\mathbf{x})\delta\varphi(\mathbf{y})\,\rangle = \int \frac{\mathrm{d}^D\mathbf{q}}{(2\pi)^D}\,\frac{\mathrm{e}^{\mathrm{i}\mathbf{q}\cdot(\mathbf{x}-\mathbf{y})}}{q^2} \sim \int_0^\infty \frac{\mathrm{d}q\, q^{D-1}}{q^2}$$

The small momenta long-wavelength (infrared) divergence, due to quantum fluctuations of the massless Nambu-Goldstone modes, persists only in systems with spatial dimensions $D \leqslant 2$. A proper and well-explained derivation of this theorem from a statistical viewpoint can be found in [68].

For systems with discrete symmetry breaking we can use Peierl's argument to obtain the lower critical dimension $D_\ell = 1$. Comparing energy cost and entropy gain, we see that the free energy of a disordered discrete one-dimensional system is always favored at finite temperature since the entropy is logarithmically diverging with the system size. But for a two-dimensional system the energy cost for introducing disorder scales with the length of the domain wall L, separating different degenerate ground state configurations, as does the entropy. Thus, the free energy difference of the ordered and disordered phase approaches zero at a finite critical temperature. Quantum fluctuations cannot alter this result since we do not have massless modes connecting the different ground states, as in the continuous symmetry case. For completeness let us mention again that the lower critical dimension of gauge/symmetries is formally ∞ due to Elitzur's theorem.

2.3.5. Effective theories & renormalization

We finally arrive at the central section of our adventure into (thermal) field theory. As we learned in the previous section, true universality of physical systems is encoded in the fluctuations at the critical point. In order to understand the phase diagram of a physical system, we need to determine the stable phases and the phase transitions at the phase boundaries. Thus, for systems exhibiting continuous or second order phase transitions we have to deal with long-range order, large/diverging correlation lengths and fluctuations on a global scale at the critical point. The best framework known so far is Wilson's renormalization group method of generating effective field theories. Effective field theories itself are the most important concept in field theory and we have used the term already several times so we finally will give a definition. An effective theory is constructed by integrating out high-energy/fast fluctuating fields up to an certain cut-off λ, generating an effective low-energy theory, which encodes the "relevant" degrees of freedom at the particular energy scale

$$S_{\text{eff}}\left[\varphi\big|_{k<\lambda}\right] = \ln\left[\int \mathcal{D}\varphi\,\big|_{k\geqslant\lambda}\, \mathrm{e}^{-S[\varphi]}\right]. \tag{2.114}$$

There are different schemes for decimating the amount of degrees of freedom, *e.g.* in (2.114) we used the so-called fast-fluctuation integration which needs to be combined with a proper regularization scheme due to the occurrence of divergences. Alternatives are real space RG methods, such as block-spin transformations or the momentum shell integration, where we only integrate

	Euclidean QFT	Critical phenomena
Momentum/inverse lattice spacing (UV cut-off) λ	∞	fixed
reduced temperature/mass (IR cut-off) r	fixed	0
$d \geqslant 4$	UV difficult	IR simple
$d < 4$	UV simple	IR difficult
Intrinsic energy scale J	∞	fixed
Characteristic energy scale (excitations) Δ	fixed	0
Correlation length ξ	fixed	∞

Table 2.7. For critical phenomena applications we remove the effective IR[30] cut-off which is equivalent to a massless theory at the critical point. From this viewpoint the microscopic degrees of freedom are irrelevant for the effective description, yet the short distance (UV) physics is very well known. Thus, the difficulties lie in the low-energy behavior (IR) at small frequencies and wave vectors such as collective excitations of electrons in metals. On the other hand for high-energy physics applications we remove the effective UV cut-off which is equivalent to a theory without lattice spacing or at arbitrary short distances. Here the high-energy description is well understood but the low-energy long distance degrees of freedom are hard to describe. Note that both pictures are equivalent since the dimensionless ratios $\lambda/r \to \infty$ and $J/\Delta \to \infty$ approach the same limit.

out a small range of momenta controlled by the cut-off $\lambda/c < k < \lambda$ and an additional scaling parameter c. In any case we need to employ a method generically called "renormalization" that allows us to retain a well-behaved field theory after the decimation process. This viewpoint on renormalization is drastically digressing from the "technical" tool to remove diverging sub-diagrams in perturbation theory. We now have to deal with cut-off dependent quantities which ultimately needs to be expressed in terms of physical observables. There are two types of effective theories

- **Renormalizable theories:**

  Low-energy physics is decoupled from high-energy excitations. High-energy physics can be encoded in a finite number of cut-off independent physical constants.

- **Non-renormalizable theories:**

  High-energy physics becomes important at a particular energy scale, usually close to the cut-off scale, where the effective field theory is not reliable. Physical quantities do not fully encode the high-energy physics and hence are cut-off dependent.

Interestingly, if we combine the "high-energy" and "condensed matter" viewpoint on effective field theory (*c.f.* Table 2.7) we assert that non-renormalizability is not really an issue. For all

[30] In RG parlance, "IR" stands for "infra-red" and its context dependent meaning describes low-energy, long distance, small momenta and slow mode behavior, whereas "UV" stands for "ultra-violet"and describes the high-energy, short distance, large momenta and fast mode behavior of an effective theory.

we know, we can only describe the appropriate degrees of freedom accessible in experiments which may not be related to the "real" microscopic degrees of freedom in a simple way. In order to understand the phase diagram structure upon varying a physical parameter we need to look at the flow along infinitely many infinitesimal "renormalization group[31]" steps. A single renormalization step is (formally) conducted as follows:

i. Rescaling the system by a scaling transformation

$$x \longrightarrow \frac{x}{c}, \qquad \lambda \longrightarrow c\lambda, \tag{2.115}$$

where c parametrizes the scale at which the system is investigated. For $c > 1$ we can view the scaling transformation (2.115) as zooming out where the distances between two points is shrinking. Equivalently, the momentum cut-off is increased to retain longer wavelengths only.

ii. After zooming out, we decimate the degrees of freedom by an appropriate averaging process. Aiming for effective field theory applications of renormalization, a simple decimation procedure is to increase the cut-off and integrate out fast fluctuations. Occurring divergences, in addition to initial singularities, are removed by introducing counter terms. This can be done by adding appropriate operators to the effective action designed in such a way not to alter the physical content of the theory (*e.g.* total derivative terms). Generically new operators are generated by this averaging procedure, which must be included in the original action, so we need to iterate this step until we have a closed set of operators O_a and their respective coupling g^a. The complete effective action reads

$$S_{\text{eff}}[\varphi] = g^a O_a[\varphi] \tag{2.116}$$

where the operators O_a are all occurring combinations of the original fields φ (including higher gradient terms) respecting the symmetry of the physical system.

iii. Next we need to renormalize all occurring fields φ in such a way that we can compare to the original system *before* the rescaling step *i.*

$$\varphi \longrightarrow \varphi' = c^{\Delta_\varphi}\varphi, \tag{2.117}$$

where Δ_φ denotes the scaling dimension of the field. In order to fix the field renormalization we need to single out the operators controlling the free field theory, *i.e.* the part of the theory which must be invariant under renormalization for physical reasons. The (canonical) scaling dimensions of the coordinates fixes uniquely the scaling dimension of the fields. Finally the couplings g^a are adjusted such that the renormalized effective action is "form invariant"

$$S_{\text{eff}}[\varphi] = g^{a\prime} O'_a[\varphi']. \tag{2.118}$$

Thus, we can read the single renormalization step as a mathematical mapping between coupling constants of the form

$$g^{a\prime}(c) = \mathcal{R}_c(\{g^a\}) \qquad \text{or} \qquad \mathbf{g}'(c) = \mathcal{R}_c[\mathbf{g}] \tag{2.119}$$

[31] Mathematically speaking, it is not a group but rather a semi group since there exists no inverse to a renormalization step. The non-existence of an inverse lies at the heart of generating effective theories via renormalization since we can only loose information by integrating out degrees of freedom/fluctuations on length scales but not generate information by "zooming in" on small length scales.

Taking the finite scaling parameter to be infinitesimally small, we can define a flow equation for the couplings. It is customary to "invert" the exponential map and define $\ell = \ln c$. Then (2.119) can be written as

$$\mathbf{g}'(c) = \lim_{\substack{n\to\infty \\ \ell\to 0}} \Big[\mathcal{R}_c[\mathbf{g}]\Big]^n \approx \lim_{\substack{n\to\infty \\ \ell\to 0}} \left[\mathbb{1} + n\mathcal{R}_\ell\right][\mathbf{g}] = \mathbf{g} + R(\mathbf{g})\,\mathrm{d}\ell \qquad \Rightarrow \qquad \frac{\mathrm{d}\mathbf{g}}{\mathrm{d}\ell} = R(\mathbf{g}) \tag{2.120}$$

which defines the change in the coupling under a smooth zooming out process. We can compare this expression to the Callan-Symanzik equation (2.142) arising from correlation function renormalization[32] and identify the flow equation (2.120) as the generalized (coupling dependent) β-function.

2.3.6. Fixed points & renormalization flow diagrams

The renormalization group flow equation, sometimes called Gell-Mann-Low equation, (2.120) may be analyzed by mapping out its direction field diagram and determine the stability of stationary points. In RG parlance the stationary points are called fixed points and are defined as

$$\frac{\mathrm{d}\mathbf{g}}{\mathrm{d}\ell}\Big|_{\mathbf{g}=\mathbf{g}^\star} \overset{!}{=} 0 \qquad \Leftrightarrow \qquad R(\mathbf{g}^\star) = 0 \tag{2.121}$$

The fixed point condition implies that the system does not change under the single RG steps outlined in *i*–*iii* on page 55, in particular the system exhibits self similarity under spacetime rescaling. Furthermore, the intrinsic length scale of the system, such as the correlation length ξ describing the exponential decay of correlation functions (*c.f.* Table 2.5), must be invariant under the scaling transformation (2.115). Thus, at a RG fixed point the correlation length is either zero ($\xi = 0$) or diverges $\xi = \infty$). The former describes a totally uncorrelated free system, whereas the latter is indicating a second order phase transition, where at its critical point the system exhibit fluctuations on all length scales. Therefore, critical phenomena are best studied by analyzing the fixed points and stability structure of the effective description of critical systems and at the same time the RG methods allow us to circumvent the problems (*e.g.* fluctuations) encountered by simple mean field analysis. The nature of fixed points from a critical phenomena perspective can be classified as follows:

- **Strong coupling fixed point:**
  $g^a \to \infty$ describing fluids (*e.g.* liquid phase)[33]
- **Weak coupling fixed point:**
  $g^a \to 0$ describing single (quasi-)particle collisions (*e.g.* gaseous phase).
- **Critical fixed point:**
  $g^a = g_c$ describes the (fine-tuned) critical couplings.

Stable phases of matter are described by (stable) strong or weak coupling fixed points while critical fixed points characterize phase transitions. The very different nature of the fixed points allows us to consider each fixed point as a distinct scale invariant effective theory describing separate physical phenomena. In this sense the Wilsonian approach to effective field theory can be summarized as follows:

[32] The Callan-Symanzik equation plays the central role in sub-diagram renormalization of n-point vertex functions.

[33] The term fluid designate strongly correlated systems described by hydrodynamic equations. For sufficiently long length scales, gases and liquids behave as fluids. On microscopic length scales, weakly coupled systems are characterized by short range single particle collisions. In this sense, gases are weakly coupled whereas liquids are typically more strongly correlated. Strongly coupled systems behave as fluids on all length scales, hence the strongly coupled fixed point.

i. Find all scale invariant theories with the additional symmetries imposed by the given universality class, *i.e.* determine all possible scale covariant[34] operators and their scaling dimension.

ii. Analyze the local behavior of all scale invariant effective theories by deformations close to their fixed points. This amounts to the analog of higher loop calculation in perturbative QFT, which can be viewed as quantum corrections to the naïve or engineering dimension of the scale covariant operators. Map out the local RG flows by solving the linearized RG flow equations near the fixed points.

iii. Connect all fixed points by extending the local RG flows to integrated global RG flows.

The last point is usually intractable and only possible for weak coupling fixed points. This is the arena where the Gauge/Gravity Duality will step in and (may) provide invaluable insight, add more strongly coupled scale invariant theories and new calculational tools for tackling strongly coupled RG flows (see Chapter 3 and in particular Section 3.4). The stability analysis close to the fixed points $\mathbf{g}^\star$ follows the stability analysis of first order differential equations. Linearizing the generalized β-function

$$R(\mathbf{g}) = R(g^\star) + \nabla R(\mathbf{g})\big|_{\mathbf{g}=\mathbf{g}^\star}(\mathbf{g}-\mathbf{g}^\star) \qquad \Rightarrow \qquad R^a{}_b = \left.\frac{\partial R(g^a)}{\partial g^b}\right|_{g=g^\star}, \tag{2.122}$$

the stability is controlled by the eigensystem of the in general non-symmetric linear mapping $R^a{}_b$. In RG parlance the components of the left-eigenvector of $R^a{}_b$ are (dangerously) called scaling fields and obey the simple flow equation with the (trivial) exponential solution

$$\frac{\mathrm{d}v^a}{\mathrm{d}\ell} = y^a v^a \qquad \Rightarrow \qquad v^a = C\,\mathrm{e}^{\ell y^a}\,. \tag{2.123}$$

Note also that the corresponding operator scales with $\Delta_O = D - y^a$. The solution of (2.123) allows for three different types of scaling fields:

- $\mathrm{Re}(y^a) > 0$ **(relevant)**:
  For increasing ℓ (zooming out) the system is driven away from the fixed point and thus the corresponding scaling field is called relevant. Starting with a small relevant deformation, the system flows to a different fixed point with a possibly different effective theory/universality class.

- $y^a = 0$ **(marginal)**:
  Invariant scaling fields under the RG flow (2.123) are called marginal and do not contribute to the flow. However, the second order derivatives along marginal directions allow for a more subtle classification, *i.e.* positive values are marginally relevant whereas negative values are marginally irrelevant. In any case on approaching the fixed point the flow of a marginal field will decrease until it is stationary at the fixed point.

- $\mathrm{Re}(y^a) < 0$ **(irrelevant)**:
  For increasing ℓ the system is attracted to the fixed point and the corresponding scaling field is termed irrelevant. Under a small irrelevant deformation close to the fixed point, the theory will flow back to the fixed point.[35]

[34] Operators that transform under the scale transformation, *i.e.* respect the scaling symmetry of the theory.

[35] There are also dangerously irrelevant scaling fields inducing singularities in the free energy which usually leads to violations of hyperscaling.

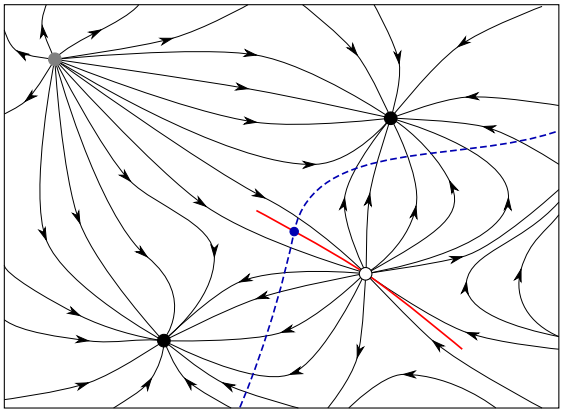

Figure 2.4.
A typical yet intricate renormalization flow diagram connecting stable fixed points (•) to unstable (•) and mixed fixed points (○), where the flow direction is indicated by the arrows. The mixed or critical fixed point defines a critical surface (—) spanned by the irrelevant directions. Tuning the coupling of the physical system is represented by the blue dashed line (----) and the critical point (•) is given by the intersection with the critical surface. Crossing the critical surface allows the system to flow to a different stable fixed point (stable phase of matter), whereas right at the intersection point the system flows to the critical fixed point, describing a phase transition with universal features.

The local behavior of the RG flow close to the fixed point leads to the following stability classification:

- **Stable fixed points:**
  A stable fixed point possesses no relevant scaling fields. Thus, small microscopic differences in the initial theory cannot deform the effective theory under rescaling and so we can identify stable fixed points with stable states of matter.
- **Unstable fixed points:**
  Unstable fixed points possess only relevant scaling fields. In principle, these fixed points are not accessible by any RG flow and are unphysical yet important artifacts that control the global RG flow behavior.
- **Mixed fixed points:**
  A mixed fixed point has relevant and irrelevant directions. The irrelevant scaling fields define a tangent space denoted as critical surface. Any set of coupling constants describing a point on the critical surface will be attracted to the mixed fixed point. A small deviation away from the critical surface will drive the system to other fixed points in the respective directions of the relevant scaling fields. In this sense, a mixed fixed point is related to a phase transition and the existence of such a fixed point implies the existence of a stable fixed point (where the relevant scaling fields will be irrelevant). However, the critical point of a second order phase transition is in general not identical to a mixed or critical fixed point, it is sufficient to cross the critical surface in the vicinity of the actual critical point, *c.f*. Figure 2.4

In order to elucidate the power of the renormalization group method, let us apply it to the simple scalar field theory describing the vector $O(n)$ universality class we already investigated in Section 2.3.4 with mean field methods. Starting with the total effective theory involving all possible terms respecting the $O(n)$ symmetry

$$S[\varphi; J] = \int \mathrm{d}^D\mathbf{x} \left[\sum_j g^{(j)} \left(\nabla^j \varphi\right)^2 + \sum_k g^{(k)} \varphi^k - \varphi J \right], \tag{2.124}$$

we can easily determine the scaling behavior of the coupling and the field by a simple dimensional analysis. First the action must be dimensionless under rescaling by construction, so $[S]_c = 0$ and the scaling transformation (2.115) implies $[x]_c = -1$. Furthermore, we fix the scaling dimension of the field φ by identifying the leading gradient term as the free field dimensionless contribution

$$[S[\varphi;J]]_c = 0 \quad \Rightarrow \quad \left[\int \mathrm{d}^D\mathbf{x}\,(\nabla\varphi)^2\right]_c = 0 \quad \wedge \quad [x]_c = -1 \quad \Rightarrow \quad [\nabla]_c = 1, \tag{2.125}$$

to obtain

$$[\varphi]_c = \frac{D-2}{2} \quad \Rightarrow \quad \left[g^{(j)}\right]_c = 2(j-1), \quad \left[g^{(k)}\right]_c = k - \left(\frac{k}{2}-1\right)D, \quad [J]_c = \frac{D+2}{2}. \tag{2.126}$$

The corresponding RG flow equations are found by linearizing the scaling transformation $g^a \longrightarrow c^{[g^a]}g^a$. The trivial fixed point is $g^\star = 0$ which is called Gaussian fixed point for reasons that will become apparent in a moment. Let us determine the irrelevant operators of the Gaussian fixed point. The gradient terms are independent of the dimensionality and the leading free field gradient is the only marginal gradient term of the action (2.124) since

$$\frac{\mathrm{d}g^{(j)}}{\mathrm{d}\ell} = 2(1-j)g^{(j)} \qquad \longrightarrow \qquad 2(1-j) < 0, \;\; j > 1 \tag{2.127}$$

whereas the power series terms in the fields yields

$$\frac{\mathrm{d}g^{(k)}}{\mathrm{d}\ell} = k - \left(\frac{k}{2}-1\right)Dg^{(k)} \qquad \longrightarrow \qquad k > 4 \wedge \begin{cases} 4 < D \\ \dfrac{2k}{k-2} < D < 4. \end{cases} \tag{2.128}$$

We immediately rediscover the Ginzburg Criterion on page 52 and obtain the Gaussian/free field critical exponents. For $D > 4$ all higher interaction terms are irrelevant and the system is flowing to the Gaussian fixed point described by the Gaussian model

$$S[\varphi;J] = \int \mathrm{d}^D\mathbf{x}\left[\frac{b}{2}(\nabla\varphi)^2 + \frac{r}{2}\varphi^2\right]. \tag{2.129}$$

Note that the φ^2 term is always relevant (the mass term introduces an energy scale breaking conformal invariance) as well as the source term which naturally must be a relevant deformation as an external force preparing the system in a particular state. The RG flow diagram and generalized β-function are shown in Figure 2.5. We see that the Gaussian fixed point in $D > 4$ dimensions is actually a mixed fixed point denoting a phase transition at the critical point $r^\star = 0$ and $u^\star = 0$. If we consider for example the Ising universality class then the coupling r can be identified with the reduced temperature (2.109) and the stable $r^\star = \infty$ fixed point describes the paramagnetic (high-temperature) phase whereas for $r < 0$ we are flowing to the $r^\star = -\infty$ fixed point describing the (low-temperature) ferromagnetic phase. However, for $D < 4$ we see in (2.128) that the interaction terms are becoming more and more relevant where φ^4 is the leading relevant term. The effective theory is therefore given by the Landau φ^4-theory (2.109)

$$S[\varphi;J] = \int \mathrm{d}^D\mathbf{x}\left[\frac{b}{2}(\nabla\varphi)^2 + \frac{r}{2}\varphi^2 + \frac{u}{4!}\varphi^4 - \varphi J\right]. \tag{2.130}$$

Relevant deformations/perturbations in u renders the Gaussian fixed point unstable in $D < 4$ and the system is flowing to a new fixed point $r^\star \neq 0$ and $u^\star \neq 0$, known as the Wilson-Fisher

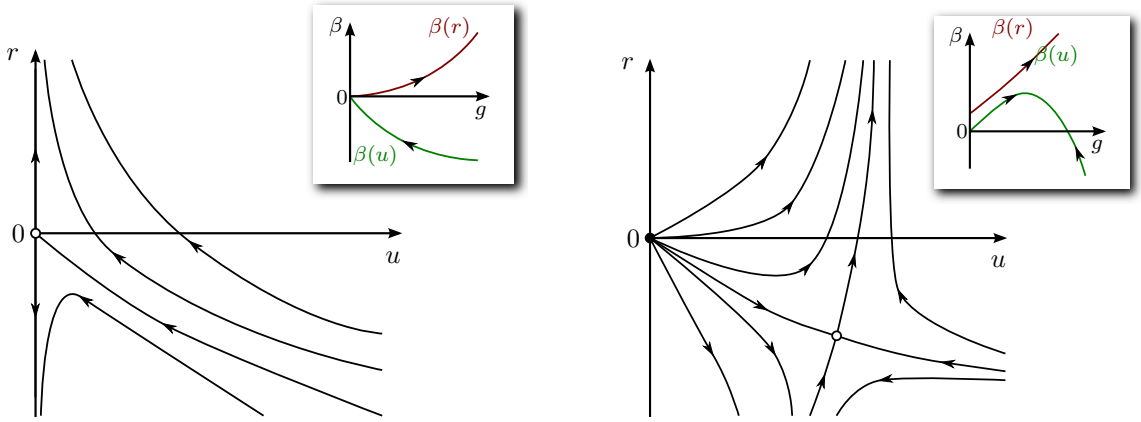

Figure 2.5. In the left panel we show the renormalization group flow for $D > 4$. In this case we find a critical fixed point at $r^\star = 0$ and $u^\star = 0$ where the scaling field r is relevant and the scaling field u is irrelevant. The Gaussian fixed point $(r^\star = 0, u^\star = 0)$ describes a phase transition with mean field critical exponents between the stable disordered high-temperature fixed point $r \to \infty$ (paramagnetic phase) and the stable ordered low-temperature fixed point $r \to -\infty$ (ferromagnetic phase). In the right panel we show the situation in the case of $D < 4$. Here the Gaussian fixed point destabilizes and a new critical fixed point emerges, the so-called Wilson-Fisher fixed point. Due to the importance of the fluctuations, the mean field solution is modified and for $r < 0$ a flow to the disordered phase is possible. The insets describe the functional dependence of the β-function in (2.131).

fixed point, *c.f.* Figure 2.5. For the Landau-Wilson effective theory the fast fluctuation modes and the slow fluctuating modes are not decoupled as in the Gaussian model, so the local RG flow equations cannot be determined from the scaling behavior alone. Corrections to the leading RG behavior can be computed by various schemes *e.g.* momentum shell renormalization or the operator product expansion of the local operators close to the critical point. The renormalized effective action (at the one loop level regularized by dimensional regularization) leads to the following RG flow equations[36]

$$\begin{aligned} \frac{\mathrm{d}r}{\mathrm{d}\ell} &= 2r + \frac{(n+2)C}{6}\frac{u}{r+\lambda^2}, \\ \frac{\mathrm{d}u}{\mathrm{d}\ell} &= (4-D)u - \frac{(n+8)C}{6}\frac{u^2}{(r+\lambda^2)^2}, \end{aligned} \tag{2.131}$$

where n denotes the number of components of the $O(n)$ vector model and C describes the phase space factor of the momentum integration. The Wilson-Fisher fixed point is determined by

$$\begin{aligned} r^\star &= -\frac{(n+1)C}{12}\frac{u^\star}{r^\star+\lambda^2}, \\ u^\star &= 6\frac{(r^\star+\lambda^2)^2}{(n+8)C}(4-D), \end{aligned} \tag{2.132}$$

[36] The details are outlined in almost all books about QFT and renormalization, a particular nice exposition can be found in [6, 68]

which can be solved by an expansion in $\epsilon = 4 - D$[37]

$$\begin{aligned} r^\star &= -\frac{n+2}{2(n+8)}\epsilon + \mathcal{O}(\epsilon^2), \\ u^\star &= \frac{6}{C(n+8)}\epsilon + \mathcal{O}(\epsilon^2), \end{aligned} \tag{2.133}$$

and expressing all length in units of λ^{-1} for convenience. The linearized RG equations for the scaling fields close to the Wilson-Fisher fixed point read

$$\frac{\mathrm{d}v^1}{\mathrm{d}\ell} = 2 - \frac{n+2}{n+8}\epsilon + \mathcal{O}(\epsilon^2), \qquad \frac{\mathrm{d}v^2}{\mathrm{d}\ell} = -\epsilon + \mathcal{O}(\epsilon^2), \tag{2.134}$$

where v^a are linear combination of r and u according to the transformation matrix

$$\begin{pmatrix} v^1 \\ v^2 \end{pmatrix} = \begin{pmatrix} \frac{12(n+3\epsilon+8)}{(n+2)(6\epsilon n+n+12\epsilon+8)} & 1 \\ 0 & 1 \end{pmatrix} \begin{pmatrix} r \\ u \end{pmatrix}. \tag{2.135}$$

We see that the Wilson-Fisher fixed point is the critical/mixed fixed point, where the new scaling field v^1 is now a non-trivial combination of the old couplings r and u. Again the Wilson-Fisher fixed point resides at $v^1 = v^\star = 0$ and we may regard the coupling v^1 as the reduced "temperature" describing deviations away from the critical point. Note that in term of the "old" couplings, for sufficiently strong interactions u, the phase transition from the ferromagnetic to paramagnetic phase might occur for $r < 0$. Due to the strong fluctuations, the ferromagnetic phase is disfavored and thus even for $r < 0$ the system will flow to the disordered fixed point at $r^\star = \infty$. The punchline of this example is to show that once we determine the right coupling in the vicinity of the critical fixed point, we automatically include the effects of fluctuations. Applying the scaling theory, which is briefly explained in the following paragraph, we are able to determine all critical exponent including all "anomalous" contributions.

Scaling & Critical Phenomena

To make contact with experiments we need to connect the RG flow results to the measurable correlation functions. The correlators must be independent of the purely theoretical renormalization steps which allows us to write

$$C(x; \mathbf{v}) = c^{n\Delta_\varphi} C(c^{-1}x; \{c^{y^a} v^a\}) = \mathrm{e}^{n/2(D-2+\eta)\ell}\, C(c^{-1}x; \{c^{y^a} v^a\}), \tag{2.136}$$

where we used the general scaling behavior of n fields φ (2.126). Note that x stands for all coordinates where φ is inserted. Taking the most relevant scaling field to be the leading deformation,[38] we can rescale the correlation function by fixing the rescaling parameter of the most relevant scaling field $v^1 = v$ to be $c^{y^1} v^1 = c^y v = 1$ since (2.136) must be true for arbitrarily chosen ℓ and hence

$$\begin{aligned} C(x; v, v^a) &= v^{-2\Delta_\varphi/y} C\left(v^{1/y} x, 1, v^{-y^a/y} v^a\right) \\ &\overset{v\to 0}{=} v^{-2\Delta_\varphi/y} F\left(v^{1/y} x\right) = \xi^{D-2+\eta} F\left(\frac{x}{\xi}\right) \end{aligned} \tag{2.137}$$

[37] Note that dimensional regularization introduced a real valued dimensionality.
[38] Usually for most fixed points after proper diagonalization there is only one relevant scaling field left.

The function F is an universal scaling function encoding the relevant contribution close to the critical point. Approaching the critical point $v \to 0$ all other scaling field contributions vanish and the intrinsic characteristic length scale diverges. Therefore, we may assign to the relevant scaling field v the intrinsic characteristic length scale of correlation functions, the correlation length ξ. Comparing with Table 2.5 the relevant RG eigenvalue can be related to the critical exponent ν via

$$\xi \sim v^{-1/y} \sim |T - T_c|^{-\nu} \qquad \Rightarrow \qquad \nu = \frac{1}{y}. \tag{2.138}$$

This relation is commonly known as a hyperscaling relation. Strictly speaking this relation is only true for *one* relevant scaling field. If there are more competing relevant scaling fields the physical description is more complex and there are competing length/energy scales related to the behavior near the critical point. Indeed for thermodynamic or global transport properties at zero momentum (static equilibrium) the second most relevant deformation will play the role of the reference scale. In this case (2.137) is modified to

$$C(v^1, v^2) = \left(v^1\right)^{-n(\Delta_\varphi/y^1)} F\left[\left(v^1\right)^{-y^2/y^1} v^2\right]. \tag{2.139}$$

All other critical exponents can be related to the leading relevant scaling fields. The derivation follows the same steps as above, where we apply the RG method to the reduced free energy density $f = S[\varphi; J]/L^d$ of the Landau-Ginzburg action (2.112). According to (2.126), the external source field and the reduced temperature are the most relevant terms, whereas all irrelevant scaling fields with $y^a < 0$ are denoted by v^a

$$\begin{aligned} f(r, J, v^a) &= c^{-D} f\left(c^{y_r} r, c^{y_J} J, c^{-|y^a|} v^a\right) \\ &= r^{D/y_r} f\left(\pm 1, r^{-y_J/y_r} J, r^{|y^a|/y_r} v^a\right) = r^{D/y_J} f_{\text{sing}}\left(r^{-y_J/y_r} J\right), \end{aligned} \tag{2.140}$$

with f_{sing} being the singular part of the reduced free energy density at the critical point $r \to 0$. Taking the definitions from Table 2.5 one can show that the following scaling relations hold true

$$\alpha = 2 - \frac{D}{y_r}, \qquad \beta = \frac{D - y_J}{y_r}, \qquad \gamma = \frac{2y_J - D}{y_r}, \qquad \delta = \frac{y_J}{D - y_J}. \tag{2.141}$$

Note that Fisher's scaling law $\gamma = (2 - \eta)\nu$ can be directly derived by integrating (2.137) and comparing to the definition of the susceptibility in Table 2.5. Using the reduced free energy, Fisher's scaling law takes the form $\eta = 2 + D - 2y_J$. Eliminating the eigenvalues of the scaling fields from (2.141) yields the thermodynamic scaling relations between α, β, γ and δ. Expressions involving the critical exponents related to the correlation functions η and ν are called hyperscaling relations, which may be violated by dangerously irrelevant scaling fields impacting on correlation functions and Euclidean actions/free energies, differently. As an aside the scaling behavior of the correlation function is instrumental in deriving the Callan-Symanzik equations, usually defined not in terms of length scales but an energy scale μ

$$\frac{\mathrm{d}}{\mathrm{d}\mu} C(x; g) = 0 \qquad \Rightarrow \qquad \left(\mu \frac{\partial}{\partial \mu} + \beta(g) \frac{\partial}{\partial g} + n\gamma(g)\right) C(x; g) = 0. \tag{2.142}$$

where the β and γ-function are defined as

$$\beta(g) = \mu \frac{\partial g}{\partial \mu}, \qquad \gamma(g) = \mu \frac{\partial \ln \sqrt{Z_\varphi}}{\partial \mu}. \tag{2.143}$$

Of course the physical content of (2.142) and the combination of the RG flow equations with the scaling functions is equivalent.

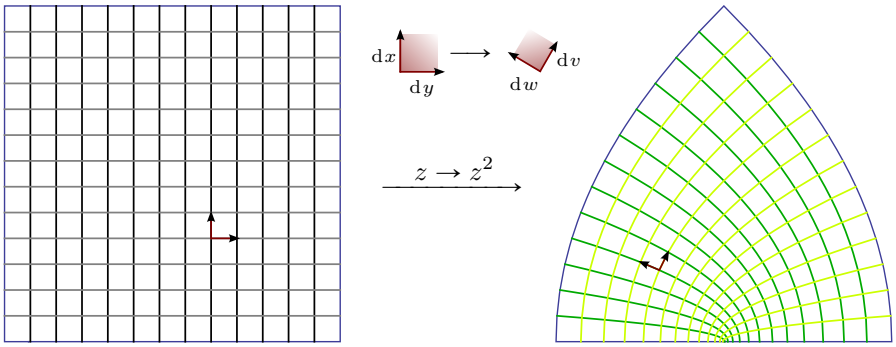

Figure 2.6. Holomorphic complex functions describe conformal maps between their domain complex plane $z = x+\mathrm{i}y$ and the image complex plane $f(z) = \mathrm{Re}\, f(z)+\mathrm{i}\,\mathrm{Im}\, f(z) = w + \mathrm{i}v$. In the above figure the analytic function $f(z) = z^2$ is shown. As one can see the angles of the intersection of the coordinate functions x and y are preserved, but not the area enclosed by contour lines. Moreover, the plots indicate that the transformation of an infinitesimal area element $\mathrm{d}x\,\mathrm{d}y \to \mathrm{d}w\,\mathrm{d}v$ can be composed of a scaling and a rotation as shown in the inset.

2.3.7. Scale invariant theories & conformal field theories

Scale invariant field theories can be extended to conformal field theories, if the theory is in addition invariant under Poincaré transformations. Conformal coordinate transformations preserve oriented angles (directions and magnitude of the angle between two coordinate lines). For infinitesimal transformations the local angles and the shape are preserved, but global properties such as the global size may change. In differential geometry parlance every object can be represented by a manifold endowed with a set of coordinate functions x^μ and a certain notion of distance between coordinate points. This distance is defined as the metric

$$\mathrm{d}s^2 = g_{\mu\nu}\,\mathrm{d}x^\mu\,\mathrm{d}x^\nu, \tag{2.144}$$

which can be represented as a symmetric cotensor of rank two and can be understand as the "scalar" product of two tangent vectors. Since infinitesimal conformal mappings are described by a Jacobian composed of a rotation and a scaling (*c.f.* Figure 2.6), the metric will change by the square of an overall scale factor[39]

$$g'_{\mu\nu}(\mathsf{x}') = \Omega(\mathsf{x})^2 g_{\mu\nu}(\mathsf{x}). \tag{2.145}$$

For $\Omega(\mathsf{x}) = 1$ we recover the Poincaré symmetry being a subgroup of the full conformal group. Infinitesimal transformations can be parametrized by a vector field v, *i.e.* $\mathsf{x} \longrightarrow \mathsf{x}'(\mathsf{x}) + \mathsf{v}(\mathsf{x})$. If the metric is invariant under the symmetry described by the transformation v, its Lie derivative must vanish

$$g \longrightarrow g' = g - \mathcal{L}_\mathsf{v} g \stackrel{!}{=} g \qquad \Rightarrow \qquad \mathcal{L}_\mathsf{v} g = 0, \tag{2.146}$$

[39] For coordinate transformation $\mathsf{x} \longrightarrow \mathsf{x}'(\mathsf{x})$ the Jacobian is defined as $\mathrm{d}\mathsf{x} = \mathcal{J}\,\mathrm{d}\mathsf{x}'$ and can be written in matrix form as

$$J^\mu{}_\nu = \frac{\partial x^\mu(x')}{\partial x'^\nu}.$$

Therefore, the metric tensor, transforming as a rank two cotensor under coordinate transformations, can be written in terms of the Jacobian matrix as $g' = J^\mathsf{T} J g$ or $g'_{\kappa\lambda} = J^\nu{}_\mu J^\mu{}_\kappa g_{\nu\lambda}$. For conformal coordinate transformation $J = \Omega R$, where R is a orthogonal rotation matrix $R^\mathsf{T} R = \mathbb{1}$ and Ω a scaling factor, the metric will only be scaled by Ω^2.

since the metric field $g(x)$ does not change when "flowing" along $\mathbf{v}$. For a conformal transformation of the metric (2.145) the Killing equation (2.146) is modified to

$$\mathcal{L}_{\mathbf{v}} g = 2\sigma(\mathbf{x}) g \qquad \xrightarrow[\text{coordinates}]{\text{local}} \qquad \nabla_\mu v_\nu + \nabla_\nu v_\mu = 2\sigma g_{\mu\nu}, \tag{2.147}$$

[40]

where $\Omega(\mathbf{x}) = 1 - \sigma(\mathbf{x})$ follows from the linearized relation $g' = \Omega^2 g \approx g - \mathcal{L}_{\mathbf{v}} g$. Exponentiating the infinitesimal transformation defined by $\sigma(x)$ shows that a conformal transformations is in fact a Weyl rescaling

$$g'_{\mu\nu}(\mathbf{x}') = \mathrm{e}^{-2\sigma(\mathbf{x})}\, g_{\mu\nu}(\mathbf{x}). \tag{2.148}$$

In local coordinates the trace of the conformal Killing equation (2.147) yields

$$2\nabla_\mu v^\mu = 2\sigma d \qquad \Rightarrow \qquad \sigma = \frac{1}{d}\nabla_\mu v^\mu. \tag{2.149}$$

Inserting (2.149) into the conformal Killing equation allows to construct various constraint equations depending on the dimension d, and respective solutions for the vector field $\mathbf{v}$. For a comprehensive and exhaustive treatment of the conformal invariance/group see *e.g.* [69]. We will be content with understanding the different solutions for $d = 1, 2$ and $d > 2$. We see that for $d = 1$ (2.147) is trivially satisfied, so any vector field $\mathbf{v}$ describes a conformal transformation, due to the fact that the concept of angles between tangent vectors is meaningless in one dimension. For $d = 2$ (2.147) reduces to the Cauchy-Riemann equations, so the vector field $\mathbf{v}$ can be constructed by all holomorphic functions. Thus, the two dimensional conformal group possesses an infinite number of generators and an infinite number of associated conserved currents/charges. In dimensions $d > 2$, the vector field $\mathbf{v}$ can in general be expressed as follows

$$v^\mu = a^\mu + c x^\mu + \omega^\mu{}_\nu x^\nu - x_\nu x^\nu b^\mu + 2 b_\nu x^\nu x^\mu, \tag{2.150}$$

where a^μ describes infinitesimal translations, the antisymmetric $\omega_{\mu\nu}$ infinitesimal rotations, c infinitesimal scaling transformations or dilation, and b^μ so-called special conformal transformations. In general the Poincaré symmetry and scale invariance is not fully equivalent to conformal symmetry due to the existence of the special conformal transformations. Constructing the associated generators, one can show that the Poincaré group including scale transformations form a subgroup of the conformal group. Futhermore, by constructing appropriate generators analogous to the Poincaré generators it can be shown [69] that the conformal group is isomorphic to $SO(d+1, 1)$ in Euclidean spacetime and $SO(d, 2)$ in Minkowski spacetime, respectively.

Conformal Field Theory

Operators[41] transforming under the conformal group can be constructed by representing the Lie derivative in local coordinates of the conformal transformation $O' = O - \mathcal{L}_{\mathbf{v}} O$ in the following way

$$\mathcal{L}_{\mathbf{v}} = v^\mu \nabla_\mu + \Delta\sigma - \frac{1}{2}\left(\nabla_\mu v_\nu - \nabla_\nu v_\mu\right) S^{\mu\nu}, \tag{2.151}$$

[40] The local coordinate representation of the metric Lie derivative in terms of simple covariant derivatives is only valid for a metric connection, *i.e.* $\nabla g = 0$.

[41] Note that the CFT community developed a slightly different jargon as usually used in QFT: fields are called operators, and to add to the confusion there are two special classes of operators which are called primary and quasi-primary fields. Primary fields transform in a simple "tensorial" manner under local and global conformal transformations, whereas quasi-primary fields transform only under global conformal transformations. In two dimensions primary fields have the simplest energy-momentum operator product expansion with at most second order poles.

where Δ denotes the scaling dimension of the operator O as defined in (2.117) and explained in Section 2.3.5, whereas $S^{\mu\nu}$ denotes the $O(d)$ generators. A scalar conformal covariant operator transforming in a simple "tensorial" way under global conformal transformations is called quasi-primary. This transformation law can be derived from the conformal generators following (2.90) and is given by

$$\varphi(x) \longrightarrow \varphi'(x') = \left|\frac{\mathrm{d}x'}{\mathrm{d}x}\right|^{-\Delta_\varphi/d} \varphi(x) = \Omega(x)^{\Delta_\varphi}\varphi(x), \tag{2.152}$$

where we have inserted the Jacobian of the coordinate transformation $x \longrightarrow x' = \Omega^{-1}x$. Due to this additional transformation behavior, the two-point and three-point correlation functions are highly constrained

$$\begin{aligned} \big\langle \varphi_1'(x_1')\varphi_2'(x_2') \big\rangle &= \Omega^{\Delta_1+\Delta_2} \big\langle \varphi_1(\Omega x_1')\varphi_1(\Omega x_2') \big\rangle \\ \Rightarrow \big\langle \varphi_1(x_1)\varphi_2(x_2) \big\rangle &= \frac{C_{12}}{|x_1-x_2|^{\Delta_1+\Delta_2}}, \end{aligned} \tag{2.153}$$

where C_{12} is a constant coefficient and we implicitly used translation and rotation invariance. Using the special conformal transformation, one can show that the correlator is only non-zero if $\Delta_1 = \Delta_2$, *i.e.* only quasi-primary fields with the same scaling dimension are correlated

$$\big\langle \varphi_1(x_1)\varphi_2(x_2) \big\rangle = \frac{C_{12}}{|x_1-x_2|^{2\Delta}}. \tag{2.154}$$

Comparing with the definition of the critical exponent for correlators η in Table 2.5 we find $2\Delta_\varphi = d-2+\eta$ or $\eta = 2-d+2\Delta_\varphi$. This is in agreement with the hyperscaling relation $\eta = 2+d-2y_J$ (as expected!) where the scaling dimension of the operator is related to the scaling of the relevant source field J by $y_J = d-\Delta_\varphi$. In the same way, the three point function is fixed up to a constant C_{123} as

$$\big\langle \varphi_1(x_1)\varphi_2(x_2)\varphi_3(x_3) \big\rangle = \frac{C_{123}}{|x_1-x_2|^{\Delta_1+\Delta_2-\Delta_3}\,|x_2-x_3|^{\Delta_2+\Delta_3-\Delta_1}\,|x_1-x_3|^{\Delta_3+\Delta_1-\Delta_2}}. \tag{2.155}$$

Higher order correlation functions cannot be constrained by the scaling and special conformal transformation alone because here we can construct conformally invariant dimensionless cross ratios such as $\frac{|x_1-x_2|}{|x_1-x_3|}\frac{|x_3-x_4|}{|x_2-x_4|}$. The non-existence of conformal invariants for two and three point functions, due to the special conformal transformation, allows for the totally fixed simple forms in (2.154) and (2.155). Apart from the constraints imposed on the correlation functions, there are additional constraints for the conserved currents related to the Poincaré symmetry, in particular the energy-momentum tensor.

Polyakov's Theorem

Using Noether's theorem we can define a tensor field by varying the action under symmetry transformations as

$$\delta_{\mathbf{v}} S = \int \mathrm{d}^d x\, T^{\mu\nu}\nabla_\mu v_\nu \overset{!}{=} 0.$$

For translational invariance $v_\nu = a_\nu$ we find the conservation of charge or divergence condition

$$\nabla_\mu T^{\mu\nu} = 0,$$

whereas the rotational invariance implies a symmetric energy-momentum tensor since its generator is totally antisymmetric

$$T^{\mu\nu}\omega_{\mu\nu} = 0 \quad \wedge \quad \omega_{\mu\nu} = -\omega_{\nu\mu} \quad \Rightarrow \quad T^{\mu\nu} = T^{\nu\mu}.$$

Finally, conformal symmetry together with the conservation law and the symmetry condition gives rise to a traceless condition

$$T^{\mu}{}_{\mu} = 0.$$

This follows from demanding that the conservation law must hold for conformal transformations, see Appendix D of [70].

Formally, the traceless condition for the energy-momentum tensor can be derived directly from the general source term of a quantum field theory. Lorentz invariance (or translational and rotational invariance) imposes already strong constraints on the possible source terms. In general, there is no consistent interacting theory for massless fields with higher spin excitations than spin two in flat spacetime.[42] Heuristically, a higher spin field possess more independent components that cannot be fixed by symmetries which in turn yields unphysical degrees of freedom, *e.g.* in $d = 4$ a massless field has only two physical degrees of freedom. Therefore, the most general source term is given by

$$S_{\text{source}} = \int \mathrm{d}^d x \left(\phi\lambda + j_\mu A^\mu + T_{\mu\nu} g^{\mu\nu}\right). \tag{2.156}$$

Physically, we can view the scalar source term λ as a Lagrange multiplier fixing the value of the scalar, the vector source terms are usually related to gauge connections such as the electromagnetic $U(1)$ gauge field A^μ or, conversely, a charged current j_μ induces an interaction mediated by the gauge field (see the discussion in Section 2.3.2 below (2.96)). Considering Poincaré invariant theories, the related massless excitations to the energy-momentum tensor are spin two excitations, so we naturally expect the metric as the source term. But even for non-relativistic theories the deformation of a physical object due to external stresses is described by a displacement field changing distances compared to the free reference metric. In this cases $T_{\mu\nu}$ is usually called stress-energy tensor related to the strain tensor of the deformed object. Applying a conformal coordinate transformation to (2.156) and inserting the generating functional for the energy-momentum tensor yields

$$\delta_{\mathsf{v}} \ln Z[g_{\mu\nu}] = \int \mathrm{d}^d x \, \frac{\delta \ln Z[g_{\mu\nu}]}{\delta g^{\mu\nu}} \delta_{\mathsf{v}} g^{\mu\nu} = \int \mathrm{d}^d x \, T_{\mu\nu} \left(\mathcal{L}_{\mathsf{v}} g^{\mu\nu}\right) = 2 \int \mathrm{d}^d x \, \sigma T_{\mu\nu} g^{\mu\nu} \stackrel{!}{=} 0, \tag{2.157}$$

which directly implies the traceless condition for arbitrary conformal deformations σ

$$g^{\mu\nu} T_{\mu\nu} = T^{\mu}{}_{\mu} = 0. \tag{2.158}$$

This also holds true for quantum field operators, where the corresponding Ward identities can be derived for the translation, rotation (Lorentz) and scaling symmetry. Nonetheless, conformal symmetry can be broken by quantum effects leading to a conformal anomaly. Since we learned from the RG approach that the critical fluctuations are correlated on length scales of the inverse reduced temperature (2.138) or the mass operator, conformal anomalies introduce a characteristic length scale signaling the breakdown of the effective theory description in the chosen degrees

[42] An interesting possible interacting higher spin theory with massless excitations is Vasiliev's higher spin gravity in AdS_4 spacetime, see [71]

of freedom. For example in chiral QCD the conformal anomaly sets the scale for color confinement and the acquired mass of the confined quarks/composite hadrons (since the quark masses $\sim \mathcal{O}(1\,\mathrm{MeV})$ are much smaller than the confinement scale $\sim \mathcal{O}(1\,\mathrm{GeV})$). As we will see in Section 3.1.2, for a consistent string theory the conformal anomaly of the local Weyl symmetry must be removed which leads to a constraint on the numbers of spacetime dimensions. For purely bosonic string theory the critical dimension is $d = 26$, whereas the supersymmetric string theories are consistent in ten dimensional spacetime. For condensed matter applications some of the symmetries might not be present in the system. Usually, the Poincaré symmetry is broken due to anisotropies (no rotation invariance), lattices (no translation invariance) or non-relativistic degrees of freedom (no boosts). This allow for different scaling behavior of space and time which is classified by yet another exponent the so-called dynamical scaling exponent z defined as

$$\begin{aligned} t &\longrightarrow \frac{t}{c^z}, & \mathbf{x} &\longrightarrow \frac{\mathbf{x}}{c}, \\ \omega &\longrightarrow c^z \omega, & \mathbf{k} &\longrightarrow c\mathbf{k}. \end{aligned} \tag{2.159}$$

For $z = 1$ we recover relativistic scaling symmetries found in one-dimensional electron liquids or in two-dimensional Graphene sheets. These systems can be described by a chiral quantum field theory and show a linear massless dispersion relation when tuned to their critical point. A non-relativistic analogue of the conformal group is the Schrödinger group [72] where the Schrödinger scaling (see Schrödinger equation) yields $z = 2$. More complicated scaling symmetries, depending on the effective dispersion relation, might involve non-integer values for the dynamical scaling exponent. In certain gravity duals one finds a particular scaling behavior called Lifshitz scaling as well as more complicated scaling symmetries of AdS-spaces. Additionally, there exists a spacetime metric that allows for hyperscaling violation, parametrized by another scaling exponent [73].

To conclude the section about renormalization, I hope the reader is convinced that renormalization elegantly connects the microscopic world with the macroscopic world and in the same way different scale invariant theories that describe distinct physical phenomena. It is one of the most powerful methods to extract relevant degrees of freedom/information of complicated microscopic theories and relates them to universal effective theories. In Chapter 3 we show that the Gauge/Gravity duality geometrize this wonderful method in a fascinating way and at the same time allows us to deal with new classes of strongly coupled, scale invariant theories and extend the applicability of the RG method.

3

Gauge/Gravity Duality

In this chapter we will establish the "original" AdS_5/CFT_4 correspondence devised in [74] and somewhat refined in [75, 76]. In this case AdS_5 stands for the five dimensional Anti-de Sitter spacetime, a hyperbolic spacetime with a boundary, which is a solution to Einstein's classical equations of gravity with negative cosmological constant. On the other side of the duality we have a supersymmetric conformal field theory in four dimensions with vanishing β-function at all energy/length scales even with regard to perturbative and non-perturbative quantum corrections. The duality belongs to the very powerful class of weak/strong dualities, *i.e.* we can map a strongly coupled conformal field theory with some additional properties to a weakly curved classical gravity. Furthermore, the AdS_5/CFT_4 correspondence is an example of the holographic nature of (quantum) gravity as is exemplified by its unusually thermodynamic behavior near black holes. Therefore, we will start with a small survey of interesting features of gravity, then move on to explain a possible way to quantize gravity, which gives rise to a vast mathematical web of theories (see Figure 3.8) and are known under the name of (super) string theories. Again dualities play an important role to map between these different string theories. In order to understand the AdS_5/CFT_4 correspondence, we will only explain the crucial objects originating from a certain type of string theory. Clearly, this exposition of string theory will not do justice to the huge and still intricate subject, but I hope the more stringy inclined reader does not mind the writer's lack of expertise on the subject. As a next step, we will employ the equivalence of the partition function to construct generating functionals and incorporate symmetry breaking mechanism [77], as explained in Section 2.3. Most importantly, we will utilize the recipe of calculating response and Green functions [78] — a real time fluctuation-dissipation theorem connected to the Schwinger-Keldysh approach to Green functions [79] — to compile a dictionary relating equilibrium and dynamical properties of strongly correlated systems to a simple gravitational computation. Finally, we focus on generalizations of the original correspondence and show its deep and intriguing connection to renormalization group flows and to extend the dictionary to finite temperature/density calculations designed to tackle problems within condensed matter theory. As we will see, the generalized gauge/gravity duality, understood as a weak/strong duality, is a powerful tool for extending field theoretic methods into previously inaccessible regimes.

3.1. Quantum Gravity & the Holographic Principle

Overview

- Gravity incorporated as curved spacetime with diffeomorphism invariance is incompatible with flat space quantum field theory. Canonical quantization using the Dirac quantization scheme yields an ill-defined and intractable equation, *e.g.* the Wheeler De-Witt equation [80].
- String theory is a promising candidate for quantum gravity and a unified description of all four (known) fundamental forces.
- The holographic principle states that the entire information content of physical theories may be encoded into their boundaries, in particular the black hole information paradox is resolved.

3.1.1. Black hole thermodynamics

Classical gravity is described by the Einstein-Hilbert action and can be viewed as a purely geometric manifestation, where the gravitational force is removed via the equivalence principle such that free falling observers follow geodesics in curved space. The Einstein Hilbert action is fixed by the coordinate invariance condition

$$S_{\text{EH}} = \frac{1}{2\kappa^2}\int \mathrm{d}^4x\,\sqrt{-g}\left(R + 2\kappa^2\mathscr{L}_{\text{matter}}\right), \tag{3.1}$$

which yields the Einstein equations

$$R_{\mu\nu} - \frac{1}{2}Rg_{\mu\nu} = \kappa^2 T_{\mu\nu}, \tag{3.2}$$

where the energy momentum tensor arises from the matter Lagrangian via

$$T_{\mu\nu} = -\frac{2}{\sqrt{-g}}\frac{\partial\left(\sqrt{-g}\mathscr{L}_{\text{matter}}\right)}{\partial g^{\mu\nu}}. \tag{3.3}$$

By comparison with the non-relativistic limit, the gravitational coupling constant can be related to Newton's gravitational constant and the speed of light[1] $\kappa^2 = {}^{8\pi G}/_{c^4}$. Physically, (3.2) relates the energy content of our spacetime to the curvature/gravitational force, which heuristically can be understood as the manifestation of the energy/mass equivalence as a source for the gravitational field with field strength tensor R and "gauge" field ω, summarized by Cartan's structure equations

$$T_{(2)} = \mathrm{d}e + \omega \wedge e = 0, \qquad R = \mathrm{d}\omega + \omega \wedge \omega. \tag{3.4}$$

The first equation describes the vanishing torsion two form $T_{(2)}$ of classical gravity. It relates the gravitational field encoded in the so-called frame fields, which do not have an analogue in gauge

[1] Note that one has to be careful with defining unit systems to maintain the right dimensions. For example, setting $\hbar = 1$ and $c = 1$ yields the energy dimension of inverse length, whereas $G = 1$ and $c = 1$ yields the energy dimension of length, which is convenient in defining the Schwarzschild radius of stars/black holes in terms of their mass.

theory, to the spin connection one-form ω. The second equation describes the curvature two form entering the Einstein-Hilbert action (3.1). From this construction we immediately see the non-renormalizability of the Einstein-Hilbert action by expanding about a flat reference spacetime $g_{\mu\nu} = \eta_{\mu\nu} + \kappa h_{\mu\nu}$. We redefined the quantum excitations to have a canonically normalized kinetic term

$$S_{\text{EH}} = \int \mathrm{d}^4x (\partial h)^2 \left[1 + \kappa h + \kappa^2 h^2 + \dots\right], \tag{3.5}$$

where in the IR (low-energy/long wavelength regime) there is a stable weak coupling fixed point $\kappa^\star = 0$ and κ is an irrelevant scaling field. Thus, we can view classical gravity as an effective theory only valid up to energies $E\kappa \sim 1$ or even below which can be translated into $E \sim M_{\text{P}}$, where $M_{\text{P}} \sim \mathcal{O}(10^{28}\,\text{eV})$ denotes the Planck mass. Due to the irrelevant nature of the coupling in the IR, gravity is a non-renormalizable theory, *i.e.* adding additional irrelevant fields does not change the UV behavior, so we need an infinite number of counter terms to cure divergences in loop integrals. At high energies $E \sim M_{\text{P}}$ the low-energy effective theory must be replaced by a new theory containing UV degrees of freedom. A different resolution would be the existence of a UV fixed point in the theory.

Another interesting property of gravity is its unusual thermodynamic behavior, *i.e.* violating one of the three "axiomatic" properties that define thermodynamics, the so-called entropy postulates:

- **Homogeneity**, *i.e.* the entropy is a homogeneous function of order one $S(cX) = cS(X)$ for $c > 0$. This shows the extensivity of the entropy and insures that a thermodynamic system cannot be described by intrinsic variables alone ("the size of the system matters!").
- **Convexity** describes a function with values larger or equal to a secant between two points or, if its derivative exists, a tangent that is larger or equal to the functional values $f''(x) \geqslant 0$. Stability requires a convex entropy function implying the second law for conventional matter.
- **Superadditivity** is the following property $S(x_1 + x_2) \leqslant S(x_2) + S(x_1)$ valid for all $x_{1,2}$ in the domain of S. In particular, it implies the third law of thermodynamics $S(0) = 0$.

As can be shown, not all of the three postulates are independent. Two of the above properties imply the third one. Normal matter as microscopic constituents of statistical systems obeys all three postulates but gravitating matter such as stars or black holes[2] violate the convexity postulate. Note that this does not violate the second law of thermodynamics, but can rather be seen as a consequence of it. Uniformly distributed matter can be considered as the most ordered state regarding the gravitational interaction, whereas extreme density differences (*e.g.* randomly distributed massive objects in almost empty space) yield a very high disorder on long length scales where the gravitational interaction dominates. So introducing a small density fluctuation in a uniformly matter distribution, a gravitational system tends to amplify these deviations in contrast to conventional statistical systems. For example, the specific heat of huge gravitating objects is negative, *i.e.* adding more matter yields a decrease in temperature. Thus, massive black holes are colder than lighter black holes.

Taking the so-called Unruh effect into account, an accelerating observer sees a heat bath with

[2] A black hole can be viewed as a massive gravitational object that does not allow for light to escape its event horizon. Strictly speaking, a black hole constitutes a causally disconnected spacetime region, where "information is trapped" and observers inside the black hole cannot communicate or escape to the outside of a black hole. However, matters are more complicated as we will see once we look at the Unruh effect and the Hawking radiation. For a detailed discussion of the peculiarities of black holes see [81].

temperature

$$T_{\mathrm{U}}(x) = \frac{a(x)}{2\pi}, \tag{3.6}$$

compared to a freely falling observer. This implies that the vacuum state of a quantum field theory depends on the state of the observer and cannot be compared since the canonical commutation relations are defined in the local coordinates of the free falling and the accelerated observer.[3] If we apply the equivalence principle of acceleration and gravity, we would expect that a stationary observer close to the horizon of a black hole measures a black body temperature given by the surface gravity $\kappa(r_{\mathrm{H}})$ at the horizon of the black hole

$$T_{\mathrm{H}} = \frac{\kappa(r_{\mathrm{H}})}{2\pi}. \tag{3.7}$$

In fact this temperature has been independently discovered by Hawking, yet to date there is no conclusive even indirect experiment to measure this effect experimentally.[4] Additionally to the thermal radiation, there is a related evaporation process, since the thermal heat bath consists of virtual particle/anti-particle pairs, created at the horizon. A consistent extension of the local heat bath allows for a leakage of some of the virtual particle pairs escaping to infinity and thus becoming real. Thus, a black hole emits radiation, loses mass/energy and increases its temperature in the process until it is completely evaporated (unless the mass influx from other sources leads to a positive net increase in the black hole energy).[5] For a Schwarzschild black hole the Hawking temperature at the event horizon $r_{\mathrm{H}} = 2MG$, $\kappa = (2r_{\mathrm{H}})^{-1}$ is given by $T = (8\pi MG)^{-1}$ and we see that the temperature is inversely proportional to the black hole mass. This implies the following entropy relation, known as the Bekenstein-Hawking entropy

$$\mathrm{d}M = T\,\mathrm{d}S = \frac{1}{8\pi MG}\,\mathrm{d}S \qquad \Rightarrow \qquad S_{\mathrm{BH}} = 4\pi M^2 G = \frac{A(r_{\mathrm{H}})}{4G}, \tag{3.8}$$

suggesting that the information content of the black hole is encoded in its area and *not* in its volume. The extensivity of the entropy in ordinary thermodynamic systems scales with the volume of the system and since the maximal entropy is a measure for the total degrees of freedom needed to describe the system, we conclude that the degrees of freedom to describe a quantum gravity system scale only with its area.

Quantum mechanically, this poses the problem of naïvely violating some of the fundamental laws of nature, *i.e.* the conservation of information. Unitary evolution does not allow a pure state to evolve into a mixed quantum state characterizing a thermal ensemble. So an observer outside of the black hole should in principle retrieve information (after the initial entropy is halved due to evaporation) that once entered the black hole. The problem intensifies once we take the quantum no-cloning theorem into account which asserts that a quantum state cannot be duplicated without violating the linearity of quantum mechanics and hence the Heisenberg

[3] So far, it is not clear if the Unruh effect is real and measurable, but there are experiments devised for possible direct detection, see [82].

[4] However, there exists an analogous table-top experiment, in the sense of emergent gravity, using phonons in perfect fluids where the fluid is flowing faster than the local speed of sound trapping the phonons. The change from supersonic speed of the fluid to subsonic speed creates a event horizon where the frequency of the phonons approaches zero. A possible realization using Bose-Einstein condensates might be expandable to detect a phononic Hawking radiation [83]

[5] Interestingly, a free falling observer crossing the event horizon would not detect any thermal heat bath. Every spacetime point on its infalling trajectory close to the horizon would consist of the usually vacuum state. Furthermore, the event horizon is not special since the free falling observer "sees" only a weakly curved locally flat Minkowski spacetime.

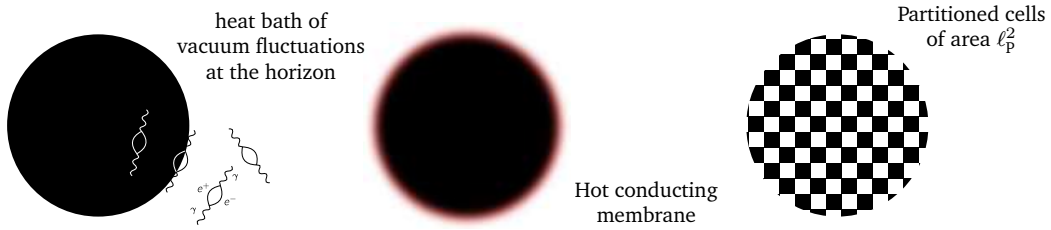

Figure 3.1. Due to the Unruh effect, a stationary observer close to the black hole, will observe a heat bath with temperature $T_{\mathrm{U/H}}$. Hawking radiation allows for emission of virtual particles becoming real particles away from the black hole horizon, thus rendering the black hole a thermal ideal black body (left panel). Additionally infalling matter is observed by a distant observer as frozen in time, "heated up" and spread over the black hole horizon because of the IR/UV connection $\Delta x \Delta t \sim \ell_{\mathrm{P}}^2$. This stretched horizon can be described by a hydrodynamic theory incorporating dissipation effects such as viscosity and resistivity (middle panel). Statistically, we can view the black hole horizon as a "holographic" projection (see also Infobox Holographic Principle on page 74) of the degrees of freedom residing "inside" the black hole, which are partitioned into Plank area ℓ_{P}^2 cells (right panel).

uncertainty principle [84]. We could imagine an external observer B, sufficiently close to the horizon, collecting information by observing an infalling observer A and eventually entering the black hole to retrieve again the identical/duplicated information from observer A. This is equivalent to duplicate the information at the horizon, where one copy of the information enters the black hole and the other copy is sent out, thus violating the no-cloning theorem. A possible resolutions to this paradox, which violates neither the no-cloning theorem nor the conservation of information, is called black hole complementarity stating that the external observer "sees" the black hole as a complex system with information stored in its degrees of freedom, counted by the area scaling of the entropy, where the infalling observer carries its information freely through the horizon. The information paradox is resolved by taking into account that sending the information requires at least one quantum, such as a photon, with a definite frequency/energy. In order for A to send the information before B hits the singularity, the energy required by the observer is larger than the black hole mass. So we conclude that *in principle* it is not possible for the external observer to receive the same information outside of the horizon and inside the black hole. In this sense, the black hole complementarity avoids a violation of quantum mechanics and the equivalence principle. An alternative approach to resolve the puzzle, the black hole firewalls [85], sparked a still ongoing hot debate *c.f.* [86]. It departs from the idea that the horizon is a simple coordinate singularity and propose that once the black hole reaches the "age" where information can be retrieved (after evaporating half of its initial entropy), the event horizon turns into an impenetrable firewall burning the infalling observer. In the following, we will assume that there exist two different viewpoints of black holes which are complementary in the above sense of avoiding any violation of the fundamental laws observed and verified so far.

- For a distant observer (in asymptotically flat spacetime at infinity) the black hole can be described by a nearly perfect fluid with dissipative properties, such as viscosity and electrical resistivity in addition to its temperature/entropy, covering the black hole horizon. This so-called "stretched horizon" [87] yields a hot conducting membrane with properties explicitly computed by the membrane paradigm [88, 89]. The reason for this membrane picture to work lies in the gravitational redshift of the infalling matter. For the distant ob-

server the infalling matter never reaches the black hole horizon in finite time, but is frozen infinitesimally close to the horizon, forming a membrane stretched over the horizon. The properties of this membrane can be described by an effective hydrodynamic description using a non-gravitational quantum field theory defined on the lower dimensional horizon with d dimensions, say. Adding more matter to the black hole is seen as disturbing the stretched horizon which gives rise to wave-like excitations of the fluid. In particular, due to the quite unintuitive IR/UV connection, which states that with increasing energies we are probing *larger*(!) length scales (for a detailed discussion see [81]),[6] the information stored in the infalling matter will be uniformly spread over the stretched horizon, as shown in Figure 3.1.

- On the other hand, an infalling observer does not observe any of the properties of the stretched horizon. On the contrary, such an observer will only approach an effectively zero-temperature gravitating object with increasing tidal forces which can be described by the full $d+1$ gravitational theory.

Furthermore, these two pictures can be related to each other by the holographic principle, which states that the full information content encoded in the entropy and its distribution over the (internal) degrees of freedom in the theory, characterized by the partition function, are equivalent if we reduce the dimensionality of one of the two descriptions. As the name suggests we draw from the analogue of optical holograms storing three dimensional information in an effectively two dimensional object.

Holographic Principle

The holographic principle[7] asserts that the maximal information of a physical system is encoded in its boundary area measured in units of $\hbar$. For black holes/gravity this can be understood in terms of a collapsing shell of matter which is teleologically[8] equivalent to a black hole of the same mass and entropy $S_{\text{BH}} = A/4G$. Therefore, any thermodynamic system satisfying the second law of thermodynamics with given energy and entropy is bounded by the mass of the black hole of area A and entropy S_{BH}. The microscopic degrees of freedom of such a thermodynamic system are distributed over the boundary of the system with a partition of one degree of freedom per Planck area ℓ_{P}^2. Two physical descriptions are equivalent if the same information is encoded, *i.e.* the maximal entropy, the number of degrees of freedom and the partition functions must be equal. Therefore, the partition function of the thermodynamic system, described by (Euclidean) quantum field theory, must be defined in one dimension lower than the gravitating mass distribution forming the black hole.

The emergence of the holographic principle draws heavily from semi-classical considerations. Thus, to understand these peculiarities, a true theory of quantum gravity is needed[9]. There have

[6] Resolving distances of the order of the Planck mass requires energies comparable to black hole masses, which in turn creates a singularity shielded by the event horizon. This yields the relations $\Delta x \sim E$ and the corresponding spacetime uncertainty $\Delta x \Delta t \sim \ell_{\text{P}}^2$ and so we are not able to probe distances smaller than the Planck length ℓ_{P}.

[7] A nice review about the holographic principle and its realization in terms of the AdS/CFT correspondence can be found in [90] and an explicit AdS/CFT calculation involving the stretched horizon is conducted in [14], determining the viscosity of black membranes.

[8] The Schwarzschild radius $r_{\text{s}} = 2MG$ can be viewed as "real" for any mass distribution that eventually will collapse in a spherical region with a smaller radius $r < r_{\text{s}}$.

[9] Due to the Weinberg-Witten theorem [91] a perturbative QFT cannot describe classical gravity. Thus, the hydrodynamic QFT of the hot membrane must describe a non-local or strongly correlated system. On the other hand the near horizon area of a black hole cannot be completely captured by classical gravity.

been many attempts to formulate a quantum theory of gravity, such as loop quantum gravity [46, 92–94], string theory [95–99], non-commutative geometry [100], string-net condensates [101–104], just to name a few. To my knowledge, only string theory has been successful to incorporate the holographic principle and allows for explicit realizations, for example

- **Matrix Theory:** M-Theory[10] is conjectured to be dual to D_0-branes (particles) in ten dimensions, providing a second quantization scheme of M-Theory in flat space in a certain set of limits (the infinite momentum frame $N/R \to \infty$ [105]). Thus, the eleven dimensional membranes (extended objects of M-theory) emerge from point like fundamental degrees of freedom in ten dimensions described in terms of supersymmetric ($N \times N$ matrix) quantum mechanics with $N \to \infty$. The additional dimension is removed by compactification on a circle with radius $R = g_s \ell_s$ related to the string coupling g_s and the string length ℓ_s. The eleven dimensional M-theory is recovered by the strong coupling limit $R \to \infty$. For more details the reader is urged to consult the comprehensive review [106]. A major difference to the AdS/CFT correspondence lies in the fact that matrix theory deals with an infinite volume Minkowski space, whereas the AdS spacetime possess a boundary with a well defined Cauchy problem, *i.e.* the boundary conditions of the "AdS box" introduce sources for the interacting bulk fields. An overview of the connection between matrix theory and AdS/CFT can be found in [107].

- **AdS/CFT Correspondence:** The $\text{AdS}_5/\text{CFT}_4$ correspondence connects holographically a conformal $\mathcal{N} = 4$ supersymmetric $SU(N_c)$ Yang-Mills theory in four dimensions to type IIB string theory on $\text{AdS}_5 \times S^5$. This holographic duality will be explained in the subsequent sections and extended in a way to geometrize the renormalization group method.

3.1.2. Bosonic string theory

In this section we will introduce the primary objects descending from string theory to give a precise statement of the AdS/CFT correspondence. Therefore, we will give a short pictorial survey over string theory and its main features. String theory replaces point particles by a string with string length $\ell_s = \sqrt{\alpha'}$ or tension $T_s = (2\pi\alpha')^{-1}$, respectively. Thus, the particle worldline invariant under reparametrization transformations[11] is replaced by a two dimensional worldsheet, *c.f.* Figure 3.2 and Figure 3.3, with the following symmetries[12]

- **Global Poincaré transformations** act globally on the target space coordinate functions

$$x^a \longrightarrow \Lambda^a{}_b x^b + a^a. \tag{3.9}$$

- **Local diffeomorphisms** describe a reparametrization of the worldsheet by redefining the worldsheet coordinates

$$\sigma^\alpha \longrightarrow f^\alpha(\{\sigma\}). \tag{3.10}$$

[10] The "M" in M-Theory might stand for "mother", "mysterious", "membrane" or in the present context for "matrix".

[11] In special relativity this reparametrization invariance of the action describing a relativistic point particle is usually used to define the proper time measured by a co-moving observer.

[12] The worldsheet coordinates will be denoted by Greek indices with letter from the beginning of the alphabet $\alpha, \beta, \ldots$, whereas the Latin indices from the beginning of the alphabet a, b label the d dimensional target spacetime coordinates. The worldsheet indices are not to be confused with the four dimensional spacetime indices with Greek letters from the middle of the alphabet typical $\mu, \nu, \ldots$. When we consider supersymmetric theories spinor indices will be denoted by Latin indices from the middle of the alphabet, typically $r, s, \ldots$ and local Lorentz frame indices will be underline *e.g.* $\underline{a}, \underline{\alpha}, \ldots$.

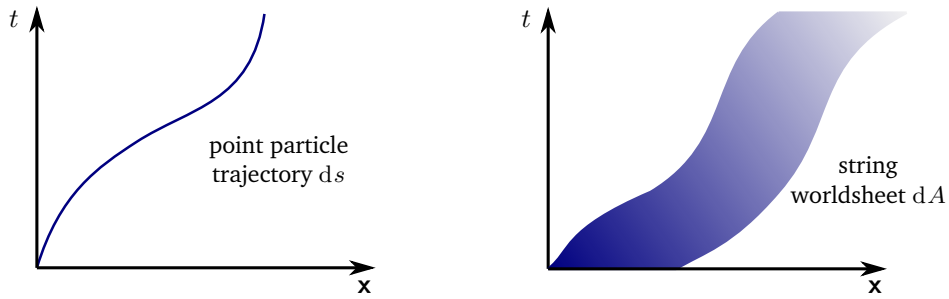

Figure 3.2. A relativistic point particle is described by the action $S = -m\int \mathrm{d}s$, where $\mathrm{d}s^2 = g_{\mu\nu}\,\mathrm{d}x^\mu\,\mathrm{d}x^\nu$ describes the relativistic worldline. The particles trajectory is determined by the coordinate functions $x^\mu(\tau)$ parametrized by the worldline parameter τ. A one dimensional string traces out a worldsheet in two dimensional spacetime with the corresponding Nambu-Goto action $S = -T_\mathrm{s}\int \mathrm{d}A$, where the particles mass is replaced by the string tension T_s, defined as (potential) energy over the spatial string length.

This is a gauge symmetry on the worldsheet where the coordinate functions transform as scalars and the induced metric transforms as a rank two cotensor

$$h'_{\alpha\beta}(\sigma') = \frac{\partial\sigma^\gamma}{\partial\sigma'^\alpha}\frac{\partial\sigma^\delta}{\partial\sigma'^\beta}h_{\gamma\delta}(\sigma), \tag{3.11}$$

or for infinitesimal transformations $f^\alpha(\{\sigma\}) = \sigma^\alpha + \epsilon^\alpha(\{\sigma\})$,

$$x^a \longrightarrow x^a - \epsilon^\alpha\partial_\alpha x^a, \qquad h_{\alpha\beta} \longrightarrow h_{\alpha\beta} - \left(\nabla_\alpha\epsilon_\beta + \nabla_\beta\epsilon_\alpha\right). \tag{3.12}$$

- **Weyl rescaling** as defined in (2.148)

$$h_{\alpha\beta} \longrightarrow \mathrm{e}^{-2w(\tau,\sigma)}\,h_{\alpha\beta}, \tag{3.13}$$

which allows to conformally deform the worldsheet and to describe the worldsheet by a two dimensional CFT. The different conformally equivalent worldsheets can be viewed as different gauges describing the same physical state.

The classical Polyakov (string sigma model) action

$$S_\mathrm{s} = -\frac{T_\mathrm{s}}{2}\int \mathrm{d}^2\sigma\,\sqrt{-h}h^{\alpha\beta}g_{ab}(x)\partial_\alpha x^a\partial_\beta x^b, \tag{3.14}$$

is invariant under the above mentioned symmetries. The Polyakov action can be derived from the Nambu-Goto action explained in Figure 3.2 by eliminating the square root of the area term. This yields an additional auxiliary field $h^{\alpha\beta}$ which can be viewed as the induced metric on the worldsheet up to a conformal factor. Thus, we can unleash the full power of two dimensional conformal symmetry described by holomorphic functions. The two parametrization transformations arising from the local diffeomorphism invariance may be used to write a conformally flat metric $h_{\alpha\beta} = \Omega(\tau,\sigma)^2\eta_{\alpha\beta}$ which can be viewed as a certain gauge choice called the conformal gauge. Together with the Weyl rescaling we may fix the three independent components of the two dimensional induced metric such that the worldsheet can be written in flat Minkowski coordinates *i.e.* $h_{\alpha\beta} = \eta_{\alpha\beta}$. Moreover, let us first work with a flat target spacetime $g_{ab}(x) = \eta_{ab}$

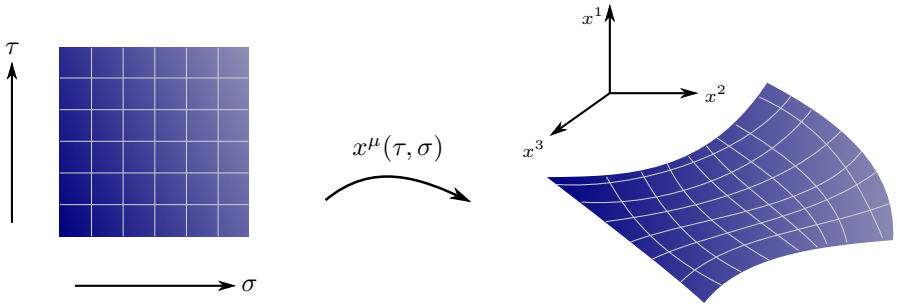

Figure 3.3. The worldsheet of a string moving in the target spacetime is parametrized by two parameters τ and σ and the area in the Nambu-Goto action $S = -T_\mathrm{s}\int \mathrm{d}A$ can be written in terms of the induced metric on the worldsheet given by the pullback of the coordinate functions, *i.e.* $\mathcal{P}[G]_{\alpha\beta} = g_{ab}\,\frac{\partial x^a}{\partial\sigma^\alpha}\,\frac{\partial x^b}{\partial\sigma^\beta}$, as $\mathrm{d}A = \sqrt{-\det\left(\mathcal{P}[G]_{\alpha\beta}\right)}\,\mathrm{d}^2\sigma$ with $\mathrm{d}^2\sigma = \mathrm{d}\tau\,\mathrm{d}\sigma$. This idea is easily extended to higher dimensional objects such as membranes tracing out a worldvolume and the corresponding hypersurface enters the action with a volume element. Note that the embedding of the string is not restricted to three dimensions as suggested by the labels of the target space coordinate system.

and later generalize to a curved spacetime. The equations of motion in the conformal gauge corresponding to (3.14) are simply given by the free wave equation

$$\partial_\alpha\partial^\alpha x^a = \left(\partial_\tau^2 - \partial_\sigma^2\right) x^a(\tau,\sigma) = 0, \tag{3.15}$$

with the additional constraint that the conformal energy-momentum tensor vanish

$$\partial_\tau x^a \partial_\sigma x_a = 0, \qquad (\partial_\tau x)^2 + (\partial_\sigma x)^2 = 0. \tag{3.16}$$

Solutions of (3.15) in light cone coordinates $\sigma^\pm = \tau \pm \sigma$ yield left and right moving waves

$$x^a(\tau,\sigma) = x^a_\mathrm{L}(\sigma^+) + x^a_\mathrm{R}(\sigma^-). \tag{3.17}$$

The constraints (3.16) relate the Fourier modes of the left and right moving waves to the effective mass of the string. Additionally, we need to impose the periodicity condition $x^a(\tau,\sigma) = x^a(\tau,\sigma+2\pi)$ for closed strings and boundary conditions for open strings. There are two types of boundary conditions, called Neumann and Dirichlet, as shown in Figure 3.4. The Dirichlet boundary conditions define a hypersurface in space, a so called D_p-brane, where p determines the number of spatial directions, *i.e.* a D_0-brane is a particle, a D_1-brane a string, and $D_{p>2}$-branes are higher dimensional membranes. Interestingly, the D_p-branes are dynamical charged solitonic objects (where D_{-1}-branes can be considered as instantons). A soliton is a kink-like solution interpolating between two different (vacuum) states and hence are related to unstable vacua and spontaneous symmetry breaking. In higher dimensions solitonic solutions are related to vortices determined by their winding numbers which can be viewed as the classification of maps from circles to circles or for arbitrary dimensions the homotopy groups of spheres. Indeed, D_P-branes are dynamical solutions to the supergravity equations of motion. The connection of supergravity to string theory will be elucidated at the end of the section, *c.f.* Figure 3.8. Detailed accounts of D-branes and their role in string theory can be found in [109, 110].

After quantizing (3.17) physical states arise from the oscillatory states of the string according to

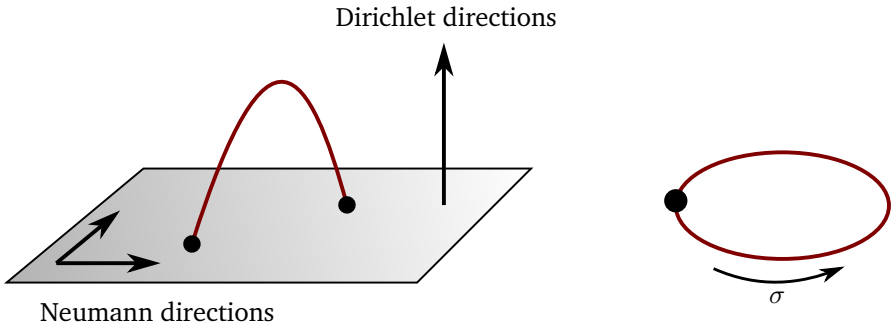

Figure 3.4. Open string solutions must be supplemented with two types of boundary conditions, Dirichlet boundary conditions defined by $x^a|_{\sigma=0,\pi} = \text{const.}$ and Neumann boundary conditions given by $\partial_\sigma x^a|_{\sigma=0,\pi} = 0$. Dirichlet boundary conditions define a $p+1$ dimensional hypersurface in d dimensional spacetime positioned at $x^b = c^b$ with $b = p+1,\ldots,d-1$ (Dirichlet directions) where along the $p+1$ hypersurface directions Neumann conditions apply, *i.e.* $\partial_\sigma x^a = 0$ with $a = 0,\ldots,p$ (Neumann directions). These so-called D_p-branes break the global Lorentz group $SO(1,d-1)$ into $SO(1,p)\times SO(d-1-p)$. In [108] the true meaning of a D_p-brane apart from defining the Dirichlet boundary conditions was discovered. In the context of superstring theories D_P-branes carry Ramond-Ramond charges. From a supergravity point of view D_p-branes are solitonic charged objects preserving half of the supersymmetric generators with tension scaling as the inverse string coupling g_s^{-1} (see also Section 3.2). For closed strings the boundary conditions reduce to the periodicity condition $x^a(\tau,\sigma) = x^a(\tau,\sigma+2\pi)$.

the decomposition of $SO(d-1)$ for massive and $SO(d-2)$ for massless single particle states. To quantize the classical string theory we can go about in various ways *e.g.* in a specific gauge, such as the lightcone gauge or covariant quantization imposing the constraints as operator equations, or the gauge invariant path integral method following the BRST[13] quantization scheme. In all three cases the consistency of the theory fixes the spacetime dimensions[14] *i.e.* the requirement of massless (massive) particles to transform under the little group $SO(d-2)$ ($SO(d-1)$) of the Lorentz symmetry or the absence of the conformal anomaly

$$\langle T^{\alpha}{}_{\alpha} \rangle = -\frac{c}{12}R = -\frac{c_{\text{Ghosts}} + c_{\text{CFT}}}{12}R = -\frac{-26+d}{R} \overset{!}{=} 0 \qquad \Rightarrow \qquad d = 26, \tag{3.18}$$

assuming the d dimensional coordinate functions to be free scalar fields with central charge $c = 1$. The critical dimension for bosonic string theory is $d = 26$. The spectrum of the closed strings is formed by a tachyonic ground state, indicating the instability of the bosonic string theory, three massless field arising from the first excited state which can be described in terms of irreducible representations, *i.e.* the trace representation, describing the spin zero dilaton $\tilde{\Phi}$, the antisymmetric representation, describing the spin one Neveu-Schwarz two form B, and the symmetric traceless representation, describing the metric/spin two graviton G. Higher excitations are massive with masses scaling as $\alpha'^{-1} = \ell_s^2$ which are quite large for small strings. For example, for a fundamental theory including quantum gravity the string length will be close to

[13] Named after Becchi, Rouet, Stora and Tyutin see [111, 112]

[14] In the BRST quantization scheme this is not completely true since any CFT with the opposite central charge of the ghosts, *i.e.* $c = 26$ removes the conformal anomaly, *i.e.* there is no need to choose d free scalar fields.

Figure 3.5.
Modes of open strings contains states that transforms as "photons" under the Lorentz group, whereas closed strings admit states that transform under symmetric traceless representations of the Lorentz group and hence can be identified as "gravitons". The graviton arises as the quadrupole fluctuation of a closed string.

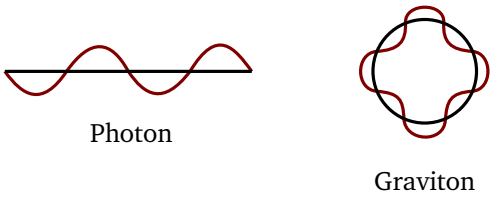

Figure 3.6.
The replacement of point particles with extended strings yields a purely topological smooth Feynman diagram. Locally, every point of the worldsheet diagram looks like a free propagating string, interactions are only affecting global properties of the worldsheet. Note that conformal invariance allows only to compute on-shell correlation functions.

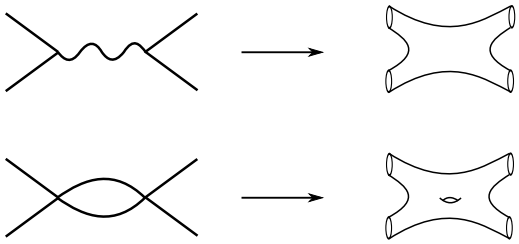

the Planck length $\ell_{\rm P}$ and the higher excited states carry masses close to the Planck mass $M_{\rm P}$. The open string sector spectrum consists of a tachyonic ground state confined to the brane and for the first excited state we find two types of massless excitations, longitudinal and transverse to the brane. The longitudinal excitation describes a spin one gauge boson on the brane transforming under the brane Lorentz group $SO(1,p)$, which can be identified as a "photon", whereas the transverse excitations transform as scalars under the $SO(1,p)$ and as vectors under the remaining $SO(d-p-1)$. A simple visualization of physical particles corresponding to the excited string states is displayed in Figure 3.5. In the open string sector the tachyonic state signals the instability of the brane decaying into a state of closed strings. This state is only a local minimum of the potential, however, there exists an additional global minimum with value $-\infty$. Considering interactions as shown in Figure 3.6, the topology of the worldsheet is modified depending on the particular string emission or absorption process. Since two dimensional gravity is purely topological, we include a topological term encoding the type of interaction process which, according to the Gauss-Bonnet theorem, yields a weighting factor given by the Euler number χ of the worldsheet

$$S_{\rm s} = S_{\rm s}^{(0)} + \frac{\lambda}{4\pi}\int \mathrm{d}^2\sigma\,\sqrt{-h}R = S_{\rm s}^{(0)} + \lambda\chi. \tag{3.19}$$

An expansion of the above action allows us to identify $g_{\rm s} = \mathrm{e}^{\lambda}$ as the closed string coupling since an emission and subsequent re-absorption changes the genus by one — switching from the sphere topology to the torum topology — and hence the Euler number by two via, $\chi = 2(1-\#\text{handles}) = 2(1-\text{genus})$. Clearly, an open string emission and re-absorption process will change the Euler number only by one due to the effect of boundaries $\chi = 2(1-\#\text{handles}) - \#\text{boundaries}$, so the open string coupling is given by $\sqrt{g_{\rm s}}$. As we will see in the effective low-energy action in curved spacetime (3.21), the parameter λ is dynamical and not a free parameter. Turning to strings in curved backgrounds, we can write the generalized action including all three closed string fields

$$S_{\rm s} = -\frac{1}{4\pi\alpha'}\int \mathrm{d}^2\sigma\,\sqrt{-h}\left(h^{\alpha\beta}G_{ab}(x)\partial_\alpha x^a\partial_\beta x^b + \mathrm{i}\epsilon^{\alpha\beta}B_{ab}(x)\partial_\alpha x^a\partial_\beta x^b + \alpha'\tilde{\Phi}R^{(h)}\right). \tag{3.20}$$

Conformal invariance is broken after quantization, so we have to determine the corresponding β-functions in the energy-momentum tensor and set them to zero. This is done by expanding the action (3.20) in the string length parameter $\ell_s = \sqrt{\alpha'}$ to obtain an interacting quantum field theory and calculate corrections to the naïve scaling dimension up to $\mathcal{O}(\alpha'^2)$, which amounts to a one loop β-function. Then, the Weyl invariance/traceless condition of the energy-momentum tensor can be generated from a low-energy effective action in the curved spacetime fields

$$S_{\text{eff-closed}} = -\frac{1}{2\kappa_0}\int \mathrm{d}^{26}x\,\sqrt{-G}\,\mathrm{e}^{-2\tilde{\Phi}}\left(R - \frac{1}{12}H_{abc}H^{abc} + 4\nabla_a\tilde{\Phi}\nabla^a\tilde{\Phi} + \mathcal{O}(\alpha')\right), \tag{3.21}$$

where the three form is the exterior derivative $H = \mathrm{d}B$ and the Ricci scalar R is calculated from the curved spacetime background metric G. Comparing with (3.19), we see that the expectation value of the dilaton field determines the string coupling via $g_s = \exp(\langle\tilde{\Phi}\rangle)$, so the string length $\kappa_0^2 \sim \ell_s^{24}$ is the only free parameter in the theory. For the open string sector the effective action of tree-level physics to leading order in α' is given by

$$S_{\text{eff-open}} = -\frac{1}{4q}\int \mathrm{d}^{26}x\;\mathrm{e}^{-\tilde{\Phi}}\left[\mathrm{tr}\left(F_{ab}F^{ab}\right) + \mathcal{O}(\alpha')\right]. \tag{3.22}$$

The low-energy effective action is of Yang-Mills type (2.101), where the trace is taken over the representation of the non-Abelian gauge group. The gauge fields A couple to the boundary of the worldsheet

$$\int_{\mathcal{C}} A = \int \mathrm{d}x^a\,A_a = \int \mathrm{d}\tau\,\partial_\tau x^a A_a, \tag{3.23}$$

which can be interpreted as open string ends carrying gauge field charges. This is an important ingredient when connecting open strings to D_p-branes. We will utilize this fact in the AdS/CFT correspondence, *c.f.* Section 3.2.

Let us conclude the (hopefully quite intriguing to the reader) bosonic string theory section by taking stock of the impact of extended fundamental objects to quantum theory:

- Interaction and free propagation is "unified" by removing the "singular points" in interaction diagrams. The properties of the interaction diagram are invariant under Lorentz transformations and hence the "disappearance" of the fixed interaction point cures the UV divergences in perturbative quantum gravity. Technically, this arises from the expansion of the low-energy effective action in curved spacetime (3.21) in orders of α' about the point particle limit $\alpha' \to 0$. Each additional factor of α' adds another "loop" in the sense of the semi-classical expansion explained in (2.22) ($\alpha' \leftrightarrow \hbar$) and an extra factor of Ricci curvature *e.g.* at two loops $R^{(2)} = R(1 + \alpha' R)$ which is reminiscent of the perturbative expansion in (3.5). In this sense, the controlled expansion in α' and g_s allows to compute the coefficient of the finite counter terms and therefore cures the UV divergences. This is known up to two loops and for supersymmetric string theories in the pure-spinor formalism up to five loops.
- Different known fundamental forces are "unified", *e.g.* forces transmitted by spin one and spin two bosons. To be more precise, the high-dimensional critical spacetime should be reduced to our "perceived" four dimensional spacetime by a compactification of the additional spacetime directions in the sense of the old Kaluza-Klein theory unifying electromagnetism and gravity. The unification of gauge interactions and gravity can also arise from D-branes, where closed strings (describing gravity) exchanged between D-branes are viewed as loops of open strings (describing gauge interactions). Moreover, from a reductionist point of view, fundamental particles with different intrinsic properties arise dynamically from a single entity, the fundamental string.

3.1.3. Supersymmetry

Nonetheless, we encountered two problems with bosonic string theory. First, the ground state is not stable and second we do not have fundamental fermionic degrees of freedom in our theory. Both problems can be cured once we enhance the symmetry of our theory. The only possible symmetry we can include is supersymmetry which follows directly from the Coleman-Mandula theorem:[15]

Coleman-Mandula Theorem

Considering quantum field theories with non-trivial interactions and symmetries described by Lie algebras, the only possible conserved charges transforming as tensors under the Lorentz group are the generators of translations P^μ and the generators of boost and rotations $J^{\mu\nu}$. Thus, the only possible symmetry extension is to include charges of internal symmetry generators commuting with P^μ and $J^{\mu\nu}$, *i.e.* spin-independent Lorentz scalars.

The only way to evade the Coleman-Mandula theorem in enhancing the symmetry is to include a symmetry that connects bosonic degrees of freedom with fermionic degrees of freedom $Q\,|\,\text{boson}\,\rangle \sim |\,\text{fermion}\,\rangle$. Therefore the generators of this symmetry, called supersymmetry, must be components of spinors satisfying anticommutation relations instead of commutation relations, *i.e.*

$$\begin{aligned}\left\{Q_r^i, \bar{Q}_s^j\right\} &= 2\,(\gamma^\mu)_{rs}\,P_\mu \delta^{ij},\\ \left[Q_r^i, P^\mu\right] &= 0,\\ \left[Q_r^i, J^{\mu\nu}\right] &= \mathrm{i}\,(\gamma^{\mu\nu})_{rs}\,Q_s^i,\end{aligned} \tag{3.24}$$

where the spinor indices are denoted by r, s and i, j runs over the number of supersymmetries $\mathcal{N}$. In case of $\mathcal{N} > 1$ one speaks of an extended supersymmetry. The decomposition of the spinor Q^i in Weyl spinors[16] define

$$Q = \begin{pmatrix} Q_\alpha \\ \bar{Q}_{\dot\alpha}\end{pmatrix} \quad \Rightarrow \quad \gamma^\mu = \begin{pmatrix} 0 & \sigma^\mu \\ \bar\sigma^\mu & 0\end{pmatrix} \quad \text{where} \quad \sigma^\mu = \begin{pmatrix} -\mathbb{1}_2 \\ \sigma^i_{2\times 2}\end{pmatrix} \quad \text{and} \quad \bar\sigma^\mu = \begin{pmatrix} -\mathbb{1}_2 \\ -\sigma^i_{2\times 2}\end{pmatrix} \tag{3.25}$$

in terms of the 2×2 canonical Pauli matrices. The anticommuting nature of the Clifford algebra elements leads to the definition of

$$(\gamma^{\mu\nu})_{rs} = \frac{1}{2}\,(\gamma^\mu\gamma^\nu - \gamma^\nu\gamma^\mu)_{rs}\,. \tag{3.26}$$

Writing the supersymmetry anticommutation relations (3.24) in Weyl spinors (with spinor indices denoted by α, β and $\dot\alpha, \dot\beta$) yields

$$\left\{Q_\alpha^i, \bar{Q}_{\dot\beta}^j\right\} = 2\,(\sigma^\mu)_{\alpha\dot\beta}\,P_\mu\delta^{ij}, \qquad \left\{Q_\alpha^i, Q_\beta^j\right\} = 2\epsilon_{\alpha\beta}Z^{ij}, \tag{3.27}$$

[15] For the time being we will discuss supersymmetry in $d = 4$ dimensions and later generalize to arbitrary dimension d. Note that there are limits to be discussed on the spacetime dimensionality to define a local quantum field theory with asymptotic states with supersymmetry *i.e.* $d \leqslant 11$.

[16] Weyl spinors are transforming under the irreducible Lorentz transformations for even dimensions *e.g.* $SO(1,3) \cong SU(2)_\mathrm{L} \times SU(2)_\mathrm{R}$ where the four component Dirac spinor arises as bispinor of a two-component left-handed and a two-component right-handed Weyl spinor. The Weyl spinors are retrieved from Dirac spinors by projections $\mathcal{P}_\mathrm{L}$ and $\mathcal{P}_\mathrm{R}$, respectively.

Spacetime dimensionality d	Spinor type	Number of components of minimal spinor d_{min}
2	Majorana-Weyl	1
3	Majorana	2
4	Majorana	4
5	symplectic	8
6	symplectic Weyl	8
7	symplectic	16
8	Majorana	16
9	Majorana	16
10	Majorana-Weyl	16

Table 3.1. The minimal number of components needed to define irreducible spinorial representations of the Clifford algebra in various flat Minkowski spacetime dimensions d. The representations have periodicity of eight in d, where the minimal number of spinor components is multiplied by 16 for $d \longrightarrow d + 8$.

where the antisymmetric Z^{ij} are the so-called central elements/charges commuting with all supersymmetry generators and $\epsilon^{\alpha\beta}$ denotes the total antisymmetric symbol. Due to its antisymmetry the central charge is zero for $\mathcal{N} = 1$. The number of supersymmetries $\mathcal{N}$ is determined by the number of Majorana spinors[17]/charges Q^i. The number of supercharges are the real degrees of freedom of the Majorana fermions and hence depends on the spacetime dimension d since the representation of the Clifford algebra has dimensionality of $2^{d/2}$ for d even and $2^{(d-1)/2}$ for d odd[18]. Thus,

$$\#\,(\text{supercharges}) = d_{\text{min}}\mathcal{N}, \tag{3.28}$$

where d_{min} denotes the minimal spinor dimension, *c.f*. Table 3.1). Due to the anticommuting nature of the generators $(Q^i)^2 = 0$, the massless supermultiplets, containing an equal number of bosonic and fermionic degrees of freedom, are bounded by the number of available supersymmetries *i.e*. $\mathcal{N}_{\text{max}} = \mathcal{N}/4$, where states with all helicities $-\mathcal{N}/2, \ldots, \mathcal{N}/2$ are present. Without reference to the dimensionality of spacetime more than 32 supercharges (being the components of the supersymmetry generating spinors) yields theories with higher spin particles $s > 2$ where it is not possible to remove the unphysical states considering interactions. Thus, we will consider 32 the maximal number of supercharges for supersymmetric theories including gravity or supergravity[19] theories and 16 the maximal number for non-gravitational supersymmetric theories. According to (3.28), in $d = 4$ only massless supermultiplets with $\mathcal{N} = 1, 2, 4, 8$ can be defined consistently with interactions, where $\mathcal{N} = 8$ is only possible including gravity. A list of the different supermultiplets is given in Table 3.2. Note that the supersymmetric nomenclature for the superpartner of bosons adds an -ino to the root (as in graviton ↔ gravitino) whereas for the fermionic superpartners an additional 's' is prefixed (*e.g*. electron ↔ selectron). The same

[17] A Majorana spinor is a real representation of the Dirac spinor and thus reduces the number of independent components by two due to the reality conditions.

[18] More details on representation of Clifford algebra in various spacetime dimensions can be found in [96, 113, 114].

[19] For supergravity the supersymmetry is a local symmetry such that the translation generator of the Poincaré group in (3.24) is replaced by general coordinate transformations (diffeomorphisms).

<table>
<tr><td colspan="4">$\mathcal{N}=1$</td></tr>
<tr><td>Chiral (matter) multiplet
$(h_0=0)$</td><td>Vector (gauge) multiplet
$(h_0=1/2)$</td><td>Gravitino multiplet
$(h_0=1)$</td><td>Graviton multiplet
$(h_0=3/2)$</td></tr>
<tr><td>$(0,1/2)\oplus(-1/2,0)$</td><td>$(1/2,1)\oplus(-1,-1/2)$</td><td>$(1,3/2)\oplus(-3/2,-1)$</td><td>$(3/2,2)\oplus(-3/2,-2)$</td></tr>
<tr><td>complex scalar & Weyl spinor</td><td>vector & adjoint Weyl spinor</td><td>inconsistent without graviton
due to Weinberg-Witten theorem</td><td>graviton & supersymmetric
partner gravitino</td></tr>
<tr><td colspan="4">$\mathcal{N}=2$</td></tr>
<tr><td>Hyper (matter) multiplet
$(h_0=-1/2)$</td><td>Vector (gauge) multiplet
$(h_0=0)$</td><td>Gravitino multiplet
$(h_0=-3/2)$</td><td>Graviton multiplet $(h_0=-2)$</td></tr>
<tr><td>$\left(-1/2,0^2,1/2\right)\oplus\left(-1/2,0^2,1/2\right)$</td><td>$\left(0,1/2^2,1\right)\oplus\left(-1,-1/2^2,0\right)$</td><td>$\left(-3/2,-1^2,-1/2\right)\oplus\left(1/2,1^2,3/2\right)$</td><td>$\left(-2,-3/2^2,-1\right)\oplus\left(1,3/2^2,2\right)$</td></tr>
<tr><td>scalar transforms as $SU(2)_{\mathrm{R}}$
doublet $\longrightarrow$ CPT completion</td><td>one vector, two adjoint Weyl
spinors & one complex scalar</td><td></td><td>one graviton, two gravitinos &
one graviphoton</td></tr>
<tr><td colspan="2">$\mathcal{N}=4$ Vector (gauge) multiplet $(h_0=-1)$
$\left(-1,-1/2^4,0^6,1/2^4,1\right)$
CPT self-dual multiplet:
a vector $SU(4)_{\mathrm{R}}$ singlet, four fundamental $SU(4)_{\mathrm{R}}$ Weyl
fermions & six real scalars in fundamental $SO(6)\cong SU(4)_{\mathrm{R}}$</td><td colspan="2">$\mathcal{N}=4$ Supergravity multiplet $(h_0=0)$
$\left(0,1/2^4,1^6,3/2^4,2\right)$
contains i.a. four Weyl fermions & two gravitons</td></tr>
<tr><td colspan="4">$\mathcal{N}=8$ Supergravity multiplet $(h_0=-2)$
$\left(-2,-3/2^8,-1^{28},-1/2^{56},0^{70},1/2^{56},1^{28},3/2^8,2\right)$</td></tr>
</table>

Table 3.2. Physically interesting massless irreducible representation of extended supersymmetries. Under the discrete **CPT** (simultaneous charge conjugation **C**, parity **P** and time reversal transformation **T**) the helicity is flipped since the momentum is a polar vector but the spin is an axial vector, so the projection of the spin onto the momentum must change sign. So for supermultiplets with a non-symmetrically distributed helicity we need to add the **CPT** conjugate supermultiplet. **CPT** self-conjugate supermultiplets with centered helicity distributions are only possible for a "Clifford vacuum" with helicity $h_0=-\mathcal{N}/4$. Each supercharge increases the helicity/spin of the state by $1/2$. Due to the fermionic nature, each supercharge can only act once. Since we focus only on local interacting quantum field theories, supermultiplets with $h_0=2$ do not exist due to the Weinberg-Witten theorem. Of course for supergravities there are also $\mathcal{N}=3,5,6,7$ multiplets which we omitted here, *c.f.* [114].

classification can be done for massive supermultiplets with an additional subtlety. Massive states are characterized by their spin instead of helicity and additional central elements/charges Z^{ij} commuting with all supersymmetry generators arise. The positivity of the creation operators constructed from the supercharges gives rise to a mass bound set by the eigenvalues

$$|Z_i| \geqslant 2m, \qquad i = 1, \ldots, \frac{\mathcal{N}}{2}. \tag{3.29}$$

Thus, we end up with three different lengths of multiplets usually called long multiplets with $2^{2\mathcal{N}-1}$, short multiplets with $2^{2(\mathcal{N}-k)-1}$ and ultra-short multiplets with $2^{\mathcal{N}-1}$ bosonic and fermionic degrees of freedom each. k denotes the number of supersymmetries preserved, where the long multiplets have $k = 0$ and ultra-short multiplets have $k = {}^{\mathcal{N}}/_{2}$, respectively. So all short multiplets are supersymmetry preserving *i.e.* they are annihilated by supersymmetry generators associated to central charge eigenvalues that saturate the mass bound (3.29). In general, preserved supersymmetries are described by vanishing supersymmetry transformations of the (classical) background or vacuum solutions and fluctuations above these solutions amount to quantum corrections in the spirit of Section 2.3.3. Thus, the supersymmetry transformation acting on fermions must vanish for supersymmetry preserving generators *i.e.* $Q\,|\,\text{fermion}\,\rangle = 0$ forming a global subset of the generically local or global supersymmetries. Furthermore, these short-multiplets contain so-called BPS[20] states (satisfying the BPS bound (3.29)) and thus can be related to solitons where the central charge corresponds to physical topological charges. These topological charges protect the BPS states against quantum corrections [117]. Generically there are ${}^{k}/_{\mathcal{N}}$ BPS states with $k = 1, \ldots, {}^{\mathcal{N}}/_{2}$. Note that massless multiplets always have vanishing central charges $Z^{ij} = 0$, so the length of the ultra-short multiplets equals the length of massless supermultiplets, with rearranged fields to account for the massive states. In the massive case we only want to mention the case of $\mathcal{N} = 4$ due to its importance in the $d = 4$, $\mathcal{N} = 4$ supersymmetric Yang-Mills theory being an integral part of the $\text{AdS}_5/\text{CFT}_4$ correspondence discussed in more detail in Section 3.2.2. In this case long-multiplets are not possible if one excludes massive spin two particles via the Weinberg-Witten theorem [91] for local quantum field theories, thus restricting the theory to include only an ultra-short supermultiplet. Taking the massless vector multiplet for $\mathcal{N} = 4$ listed in Table 3.2 we only need to incorporate one of the bosonic degrees of freedom of the scalar fields in the massive vector. Thus, we end up with one massive vector field, four Weyl fermions or two Dirac fermions, respectively and five instead of six scalar fields.

Additionally, there is a symmetry transformation relating different supercharges. In $d = 4$ and $d = 8$ the global symmetry group of the transformation is given by $U(\mathcal{N})_{\text{R}}$. In the case of $d = 10$ we have Majorana-Weyl spinors and so the R-symmetry is realized by a $SO(\mathcal{N}_L) \times SO(\mathcal{N}_r)$ symmetry. Note that the R-symmetry generator *do not* commute with the supercharges of supersymmetry. In the case of $\mathcal{N} = 1$ we find a global $U(1)_{\text{R}}$ symmetry group which can be broken to a discrete subgroup $\mathbb{Z}_2$ called R-parity. For example, in supersymmetric extensions to the standard model of particle physics, standard model particles possess R-parity of one whereas their supersymmetric partners have R-parity of -1. More details about technical aspects can be found in [114, 118, 119]. Physical applications of supersymmetry are explained in [113]. Note that we only discussed supersymmetric representation of asymptotic states. In order to define a supersymmetric quantum field theory it is convenient to introduce a so called superspace to define supersymmetric fields and a respective representation of the supersymmetric generators in terms of superspace differentials. Some of these concepts are introduced in Section 3.3, when we discuss the $\mathcal{N} = 4$ supersymmetric Yang-Mills theory in four dimensions.

[20] Named after Bogomol'nyi, Prasad, Sommerfield inequalities for solutions of partial differential equations related to topological homotopy classes [115, 116].

3.1.4. Superstring & supergravity

After introducing supersymmetry we finally want to give an overview of supersymmetric string theories or shorthand superstring theories. There are two equivalent ways to construct supersymmetric string theories, the so-called Green-Schwarz formalism being supersymmetric in ten-dimensional spacetime, and the Ramond-Neveu-Schwarz formalism which is supersymmetric on the worldsheet. Following the latter approach, the bosonic string theory action (3.14) is supplemented with fermionic degrees of freedom on the worldsheet

$$S_{\mathrm{s}} = -\frac{T_{\mathrm{s}}}{2}\int \mathrm{d}^2\sigma\,\sqrt{-h}\left(h^{\alpha\beta}g_{ab}(x)\partial_\alpha x^a\partial_\beta x^b + g_{ab}(x)\bar{\psi}^a\gamma^\alpha\,\mathrm{D}_\alpha\,\psi^b\right), \tag{3.30}$$

where $\gamma^\alpha = e_{\underline{\alpha}}{}^\alpha\gamma^{\underline{\alpha}}$ are two dimensional Dirac matrices satisfying the Clifford algebra in a local Lorentz frame, defined by the frame fields $e^{\underline{\alpha}}{}_\alpha$, $\left\{\gamma^{\underline{\alpha}},\gamma^{\underline{\beta}}\right\} = 2\eta^{\underline{\alpha\beta}}\mathbb{1}_2$, and $\mathrm{D}_\alpha = \partial_\alpha + \frac{1}{4}\omega_{\underline{\beta\gamma}\alpha}\gamma^{\underline{\beta}}\gamma^{\underline{\gamma}}$ denotes the spinorial covariant derivative including the spin connection $\omega_{\underline{\alpha\beta}\gamma}$. In flat spacetime $g_{ab} = \eta_{ab}$ and conformal gauge $h_{\alpha\beta} = \Omega(\tau,\sigma)^2\eta_{\alpha\beta}$ the supersymmetric Polyakov action (3.30) is invariant under the on-shell infinitesimal global supersymmetry transformation

$$\delta_\epsilon x^a = \bar{\epsilon}^r\psi^a_r, \qquad\qquad \delta_\epsilon\psi^a_r = \left(\gamma^\alpha\epsilon\right)_r\partial_\alpha x^a, \tag{3.31}$$

parametrized by a constant infinitesimal Majorana spinor ϵ with components ϵ^r. Redoing all steps done for the bosonic string theory we again find left and right moving waves equations in lightcone coordinates $\sigma^\pm = \tau \pm \sigma$

$$\partial_{\sigma^+}\psi^a_- = 0, \qquad\qquad \partial_{\sigma^-}\psi^a_+ = 0, \tag{3.32}$$

where we have chosen the basis $\gamma^0 = -\mathrm{i}\sigma^2$ and $\gamma^1 = \sigma^1$ for the two dimensional Dirac matrices using canonical Pauli matrices. The boundary conditions for open strings at $\sigma = 0$ are chosen to be $\psi^a_+(\tau,0) = \psi^a_-(\tau,0)$ and at $\sigma = \pi$ they split into two sectors

$$\begin{aligned} &\psi^a_+(\tau,\pi) = \psi^a_-(\tau,\pi) && \text{Ramond sector (R)},\\ &\psi^a_+(\tau,\pi) = -\psi^a_-(\tau,\pi) && \text{Neveu-Schwarz sector (NS)}. \end{aligned} \tag{3.33}$$

After quantization the excited string-states are constructed by acting with the creation operators arising from the mode expansion of the wave equation onto the vacuum state. The NS sector only admits bosonic string states since its vacuum state is bosonic (and tachyonic). The first excited state is again a massless vector boson. The R sector degenerate vacua are massless spinors with different chirality in spacetime and the excited states describe massive spacetime fermions. Thus, the target spacetime supersymmetry in the Ramond-Neveu-Schwarz formalism arises from the two different open string sectors. In general, worldsheet supersymmetry does not imply target spacetime supersymmetry. Spacetime supersymmetry can be achieved by truncating the spectrum of the NS and R sector to include only physical states with even fermion number, the so-called GSO[21] projection. Therefore, in the NS sector we are left with states created by an odd number of creation operators only, removing the tachyon respecting the supersymmetry, *i.e.* at each mass level the number of bosonic and fermionic degrees of freedom coincide. For the closed string the periodic boundary conditions consists of all combination of the two open string sectors (NS & R) since left and right movers are not related to each other (in the open string the reflected mode of a left mover is right moving, so the closed string has twice as many

[21] Named after Gliozzi, Scherk and Olive [120]. The GSO projection originates from the modular invariance of the two-tori partition function.

Figure 3.7.
In string theory a new duality arises since strings as extended objects can wrap around non-trivial geometries such as cylinders or tori and hence are sensitive to the topology of the space. For example in order to reduce the number of dimensions, some dimensions may be curled up on a circle with radius R and this compactification yields so-called Kaluza-Klein modes with quantized momentum given by $p = {}^{n}/_{R}$ with $n \in \mathbb{Z}$. Closed strings (*i.e.* the endpoints of the string are identified) can also wrap around the circle which yields so-called winding modes quantized as ${}^{wR}/_{\ell_s^2}$, where w is the winding number, that describes how often the string wraps around the circle. The spectrum of string theory is invariant under the exchange of the number of winding modes and the number of momentum modes $w \longleftrightarrow n$ and a change of radius $R \longleftrightarrow {}^{\ell_s^2}/_{R}$. For example the type IIA and type IIB are T-dual to each other. Note that the T-duality transformation exchange Dirichlet and Neumann boundary conditions and so a D_p-brane becomes a D_{p+1}-brane. Conversely a D_p-brane wrapping a circle becomes a D_{p-1}-brane located at a fixed point on the circle. This agrees with the stability of D_p-branes in type IIA and type IIB string theories.

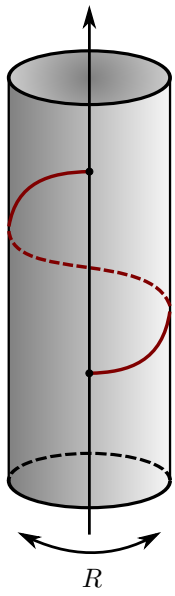

degrees of freedom as the open string). The NS-NS and R-R sector contain spacetime bosons whereas the NS-R and R-NS sector contain spacetime fermions, respectively. The NS-NS sector of oriented massless string states are identical to the bosonic massless excitations, *i.e.* the graviton G, the Neveu-Schwarz two form B, and the dilaton $\tilde{\Phi}$. The NS-R and R-NS states contain the supersymmetric partners of the NS-NS states, *i.e.* the gravitino and the dilatino. Due to the degeneracy of the R sector ground state, the R-R sector gives rise to two different superstring theories, namely the so-called type IIA and type IIB. The critical dimension of the superstring theories can be elegantly determined from the Weyl anomaly arising after BRST quantization. The additional fermionic degrees of freedom corresponding to the extra gauge symmetry, the worldsheet supersymmetry, give rise to more ghosts with total central charge of $c_{\text{SuSyGhosts}} = 11$. But the CFT must be invariant under supersymmetry as well, so if we add d bosonic scalar fields with central charge $c = 1$ we also need to add d fermionic fields with central charge $c = {}^{1}/_{2}$. Then the conformal anomaly (3.18) is modified to

$$\begin{aligned} \langle T^{\alpha}{}_{\alpha} \rangle &= -\frac{c_{\text{total}}}{12} R = -\frac{c_{\text{Ghosts}} + c_{\text{SuSyGhosts}} + c_{\text{CFT}}}{12} R \\ &= -\frac{-26 + 11 + (1 + \frac{1}{2})d}{12} R \stackrel{!}{=} 0, \end{aligned} \tag{3.34}$$

and the critical dimension of the superstring theories is $d = 10$. Let us give an overview of the different superstring theories connected either by S[22]- or T-dualities, *c.f.* Figure 3.7 or via their connection to M-theory. Since we can choose which combinations of fermionic boundary conditions we want to impose, there are two types of string theories, one with left and right moving fermions and one only with fermions moving in one direction, with each type having two different realizations:

[22] S-duality is a weak/strong duality connecting a theory with coupling constant g to a theory with coupling constant ${}^{1}/_{g}$. In two-dimensional lattice theories (*e.g.* $\mathbb{Z}_n$ or $U(1)$ models *c.f.* Table 2.2) the S-duality is known as Kramers-Wannier duality relating high-temperature phases of a Ising model $K \ll 1$ to the low-temperature phase with $\tilde{K} \gg 1$, *e.g.* see [121]. In four dimensions one can find lattice gauge theories where the S-duality relates lattice models with different gauge groups *e.g.* electric and magnetic fields swapped.

- **Type II** superstrings with left and right moving fermions and 32 supercharges in $d = 10$ dimensions (minimal spinor representation being 16 dimensional) are related to $\mathcal{N} = 2$ supersymmetries.
  - **Type IIA:** The R-sector vacuum state for the left and right moving sector has the opposite chirality in spacetime, so this theory is chirality preserving. Furthermore, the massless R-R bosons describe one and three form gauge fields $C_{(1)}$ and $C_{(3)}$, respectively. Since the open string tachyon is removed, we find stable D_p-branes with p even and unstable D_p-branes for p being odd. The stability is related to the fact that D_p-branes are charged under the R-R fields [108].
  - **Type IIB:** The R-sector vacuum state for the left and right moving sector has the same chirality in spacetime, so we have a parity violating theory. The massless R-R bosons give rise to scalar, a two and a four form gauge field denoted by $C_{(0)}$, $C_{(2)}$ and $C_{(4)}$, respectively and D_p-branes that are stable for p odd and unstable for p even.
- **Heterotic** superstrings with conventionally right-moving fermions only and 16 supercharges *i.e.* an $\mathcal{N} = 1$ spacetime supersymmetry. They do not possess R-R fields and no finite energy D_p-branes since right movers cannot be reflected into left movers.
  - **Heterotic** $SO(32)$: Contains the $SO(32)$ non-Abelian gauge group and gives rise to a ten-dimensional $SO(32)$ Yang-Mills theory.
  - **Heterotic** $E_8 \times E_8$: Contains the $E_8 \times E_8$ non-Abelian gauge group and gives rise to a ten-dimensional $E_8 \times E_8$ Yang-Mills theory.

So far these string theories are oriented. Additionally there is the unoriented string theory called type I with $\mathcal{N} = 1$ supersymmetries which contains both open and closed strings. As in the bosonic string theory we can derive an effective low-energy theory for the superstring theories. For the AdS/CFT correspondence we are interested in string theories with stable charged D-branes in particular in the type IIB string theory. In addition to the bosonic low-energy effective action, $\alpha' \to 0$, for closed strings (3.21) we find dynamical terms for the bosonic R-R fields and a topological Chern-Simons term

$$S_{\text{type IIA}} = S_{\text{eff-closed}} - \frac{1}{2\kappa_0^2}\int \mathrm{d}^{10}x\,\sqrt{-G}\frac{1}{2}\left[F_{(2)}^2 + \left(F_{(4)} - C_{(1)} \wedge H_{(3)}\right)^2\right] - \frac{1}{4\kappa_0^2}\int B_{(2)} \wedge F_{(4)} \wedge F_{(4)}, \tag{3.35}$$

$$S_{\text{type IIB}} = S_{\text{eff-closed}} - \frac{1}{2\kappa_0^2}\int \mathrm{d}^{10}x\,\sqrt{-G}\frac{1}{2}\left[F_{(1)}^2 + \left(F_{(3)} - C_{(0)} \wedge H_{(3)}\right)^2 + \frac{1}{2}\tilde{F}_{(5)}^2\right] - \frac{1}{4\kappa_0^2}\int C_{(4)} \wedge H_{(3)} \wedge F_{(3)}, \tag{3.36}$$

where 2κ is related to string coupling by $2\kappa_0^2 g_s^2$ where $g_s = \mathrm{e}^{\tilde{\Phi}_\infty}$ is given by the asymptotic value of the dilaton. The field strengths are defined as $F_{(i+1)} = \mathrm{d}C_{(i)}$ and $H_{(3)} = \mathrm{d}B_{(2)}$. The type IIB five form

$$\tilde{F}_{(5)} = \mathrm{d}C_{(4)} - \frac{1}{2}C_{(2)} \wedge H_{(3)} + \frac{1}{2}B_{(2)} \wedge F_{(3)}, \tag{3.37}$$

must be supplemented by a self-duality condition involving the Hodge dual, *i.e.* $\tilde{F}_{(5)} = \star\tilde{F}_{(5)}$. Due to the self-duality condition for the four form $C_{(4)}$, a Lorentz covariant Lagrangian formulation of type IIB action is not feasible.

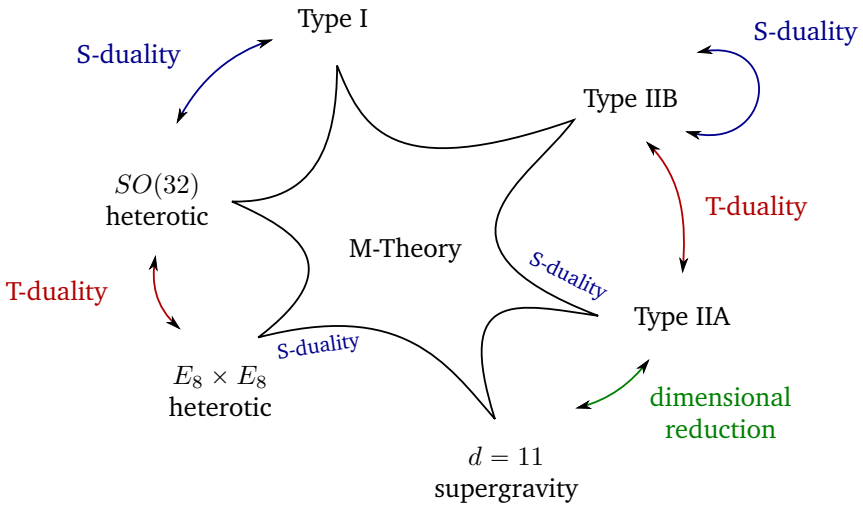

Figure 3.8. M-theory can be understood as a "unifying framework" underlying all superstring theories. The S-duality relation of type IIA to M-theory should be understood as a strong coupling limit where the additional dimension arise as $R = g\ell_s$. The $d = 11$, $\mathcal{N} = 1$ supergravity is the low-energy effective field theory of the eleven dimensional M-theory and can be related to the type IIA supergravity by dimensional reduction on a circle $\mathcal{M} \times S^1$ which is in turn the low-energy effective field theory of type IIA superstring theory. Similar constructions are possible for heterotic string theories; more details can be found in [122]

The full effective low-energy theory including the fermionic degrees of freedom are the type IIA and type IIB supergravities, respectively, because both type II supersymmetric actions possess 32 supercharges in ten-dimensions and hence are the unique supergravities invariant under $\mathcal{N} = 2$ supersymmetries. There exists another single unique $\mathcal{N} = 1$ supergravity in eleven dimensions which is the maximal dimension where supergravities can exist

$$S_{11d} = -\frac{1}{2\kappa_{11}^2}\left[\int \mathrm{d}^{11}x\, e\left(R - \frac{1}{2}F_{(4)}^2 - \psi_a\gamma^{abc}\,\mathrm{D}_b\,\psi_c\right) + \frac{1}{6}\int A_{(3)} \wedge F_{(4)} \wedge F_{(4)}\right], \tag{3.38}$$

where e denotes the determinant of the frame field $e^{\underline{a}}{}_a$ and $F_{(4)} = \mathrm{d}A_{(3)}$. Note that the gravitino field Ψ_a carries a vector index transforming in the **128** of the little group $SO(9)$ while the bosonic degrees of freedom are distributed in the **44**, the Elfbein $e^{\underline{a}}{}_a$, and the **84**, the field $A_{(3)}$, of the $SO(9)$ [118]. For the gravitino field we need to introduce three inverse frame fields converting $\gamma^{abc} = e_{\underline{a}}{}^a e_{\underline{b}}{}^b e_{\underline{c}}{}^c \gamma^{\underline{abc}}$ to local Lorentz frames. The type IIA supergravity can be obtained by dimensional reduction on a circle *e.g.* $\mathcal{M} \times S^1$ from $d = 11$ to $d = 10$. The eleven dimensional, 32 component Majorana spinor splits into two 16 component ten dimensional Majorana-Weyl spinors with opposite chirality, the eleven dimensional frame field splits into the ten dimensional frame field, a one form identified with $C_{(1)}$ and the dilaton $\tilde{\Phi}$. The $A_{(3)}$ form may be split into a ten dimensional three form identified with $C_{(3)}$ and the NS two form $B_{(2)}$. The eleven dimensional supergravity (3.38) is understood as the effective low-energy action of M-theory which in turn can be understood as a strong coupling limit of type IIA string theory since the compactification of the x^{11} direction on the circle with radius R relates to the string coupling $R = g_s\ell_s$. Thus, removing the circle $R \to \infty$ corresponds to the limit $g_s \to \infty$. An overview of the

connection between the various superstring theories and M-theory as the strong coupling/UV completion of perturbative string theory is shown in Figure 3.8.

3.2. D-branes & AdS/CFT Correspondence

Overview

- D-branes arise as non-perturbative objects in string theory where open strings can end. Massless open strings connecting D-branes may be understood as a supersymmetric non-Abelian gauge theory.
- Alternatively, D-branes can be viewed as macroscopic charged solitonic solutions to the low-energy effective field theory of string theory.
- The AdS/CFT correspondence is a weak/strong duality arising from the two different "viewpoints" on D-branes

3.2.1. D-branes

The central objects of the AdS/CFT correspondence are the D_p-branes and their seemingly two different interpretation from the open and closed string viewpoint. D_p-branes were taken seriously after they became real dynamical objects carrying R-R charges [108] and where relieved of their existence as strange, poorly understood boundary conditions.

Open string viewpoint

Naturally, D_p-branes are connected to open strings providing the Dirichlet boundary conditions as hyperplanes in ten-dimensional spacetime. Generalizing the Nambu-Goto action for the open string worldsheet to higher dimensional "branes" and their respective worldvolumes yields

$$S_{D_p} = -T_p \int \mathrm{d}V_p \,. \tag{3.39}$$

Including the fact that string ends carry charges (3.23) we include the respective field strength on the worldvolume $F = \mathrm{d}A$ with $A = A_\alpha \,\mathrm{d}\xi^\alpha$ and the NS two-form arising from the string tension. Thus, the effective theory of the bosonic sector for D_p-branes is described by the so-called Dirac-Born-Infeld action

$$S^{\mathrm{DBI}}_{D_p} = -\mu_p \int \mathrm{d}^{p+1}\xi \; \mathrm{e}^{-\tilde{\Phi}} \sqrt{\det\left(\mathcal{P}[G] + \mathcal{P}[B] + 2\pi\alpha' F\right)}, \tag{3.40}$$

as a charged membrane with generalized charge μ_p embedded in ten-dimensional spacetime. The pullback of the metric and NS two form is given by

$$g_{\alpha\beta} = \left(\mathcal{P}[G]\right)_{\alpha\beta} = \frac{\partial x^a}{\partial \xi^\alpha}\frac{\partial x^b}{\partial \xi^\beta} G_{ab}, \qquad B_{\alpha\beta} = \left(\mathcal{P}[B]\right)_{\alpha\beta} = \frac{\partial x^a}{\partial \xi^\alpha}\frac{\partial x^b}{\partial \xi^\beta} B_{ab}, \tag{3.41}$$

where the worldvolume of the D_P-brane is parametrized by the worldvolume coordinates ξ^α and the worldvolume directions are indexed by Greek letters from the beginning of the alphabet

$\alpha, \beta, \ldots$. The D_p-brane is invariant under $\mathcal{N} = 1$ supersymmetries, so it is characterized by a BPS state and hence is stabilized by carrying R-R charges. The R-R fields are encoded in a Chern-Simons term of the following form

$$S^{\text{CS}}_{D_p} = \pm\mu_p \int \mathrm{d}^{p+1}\xi \sum_q^p \mathcal{P}[C_{(q+1)}] \wedge \mathrm{tr}\left(\mathrm{e}_\wedge^{\mathscr{F}}\right) \tag{3.42}$$

where the sum over the R-R fields includes only odd (type IIA) or even (type IIB) forms depending on the type of string theory and the exponential is understood as a series expansion in polynomials of wedge products of $\mathscr{F}$ up to the order of a total $p+1$ form. The positive sign in (3.42) refers to a D_p-brane and the negative sign to an anti $\overline{D_p}$-brane, respectively. The D_p-brane tension is given by

$$T_p = \frac{\mu_p}{g_\text{s}} = (2\pi)^{-p}\alpha'^{-\frac{p+1}{2}} g_\text{s}^{-1}. \tag{3.43}$$

Comparing to the fundamental string tension $T_\text{s} = 2\pi\alpha'^{-1}$ a D_1-brane includes an additional factor of g_s^{-1}. Thus D_p-branes are non-perturbative objects where the brane tension scales as g_s^{-1} due to the presence of $\mathrm{e}^{-\tilde{\Phi}}$ with the shifted dilaton including the asymptotic value $\tilde{\Phi} \longrightarrow \tilde{\Phi} + \tilde{\Phi}_\infty$ set by the string coupling constant (see also discussion below (3.36)). In the following we will consider a constant dilaton field with fixed asymptotic value $\tilde{\Phi}_\infty$. The DBI action can be expanded to lowest order in the generalized field strength $\mathscr{F} = \mathcal{P}[B] + 2\pi\alpha' F$ with the help of the identity (A.9) in Appendix A.1.2, *i.e.*

$$\det(\mathbb{1} + \mathscr{F}) = \mathrm{e}^{\mathrm{tr}[\ln(\mathbb{1}+\mathscr{F})]} \approx 1 - \frac{1}{4}\,\mathrm{tr}\,\mathscr{F}^2, \tag{3.44}$$

yielding a generalized Yang-Mills action[23]

$$S^{\text{DBI-YM}} = -T_p \int \mathrm{d}^{p+1}\xi \sqrt{-\det \mathcal{P}[G]} \left[1 - \frac{1}{4}\,\mathrm{tr}\left(\mathscr{F}^2\right)\right], \tag{3.45}$$

where the Yang-Mills coupling is given by $g^2_{\text{YM}} = T_p^{-1}$, *c.f.* (2.101)). Taking N_c D_p-branes[24] we find a $U(1)$ gauge group, arising from the string ends as in (3.23), on each of the branes yielding a product group of $U(1)^{\times N_c}$ encoded in the so-called Chan-Paton factors that keep track of the D_p-branes connected by open strings, *i.e.* Ξ_{ij} labels an oriented string starting from the i^{th} brane and ending on the j^{th} brane. From a target spacetime point of view the Chan-Paton factors give rise to an element of a Lie algebra. So for N_c coincident D_p-branes the $U(1)$ gauge group of the brane gauge field $A = A_\alpha\,\mathrm{d}\xi^\alpha$ is enhanced to a $U(N_c) = SU(N_c) \times U(1)$. For the particular case of D_3-branes the expanded effective DBI action reduces to an $\mathcal{N} = 4$ $SU(N_c)$ supersymmetric Yang-Mills theory in the point particle limit $\alpha' \to 0$

$$S^{\text{YM}}_{D_3} = \frac{(2\pi\alpha')^2 T_3}{4} \int \mathrm{d}^4\xi \sqrt{-\det \mathcal{P}[G]}\,\mathrm{tr}\left(F^2\right), \tag{3.46}$$

effectively removing the NS two form field, *i.e.* $\mathscr{F} = 2\pi\alpha' F$, with coupling $g^2_{\text{YM}} = 2\pi g_\text{s}$. The R-symmetry group arises from the transverse directions of the D_3-branes invariant under the global $SO(6) \cong SU(4)$ symmetry.

[23] For a more detailed calculation see the explicit constructions in Chapter 5.

[24] One may think of N_c as the number of colors, but effectively the subscript c is only needed to distinguish this gauge group from other gauge groups arising in D_p-brane intersections, as explained in Section 5.1.

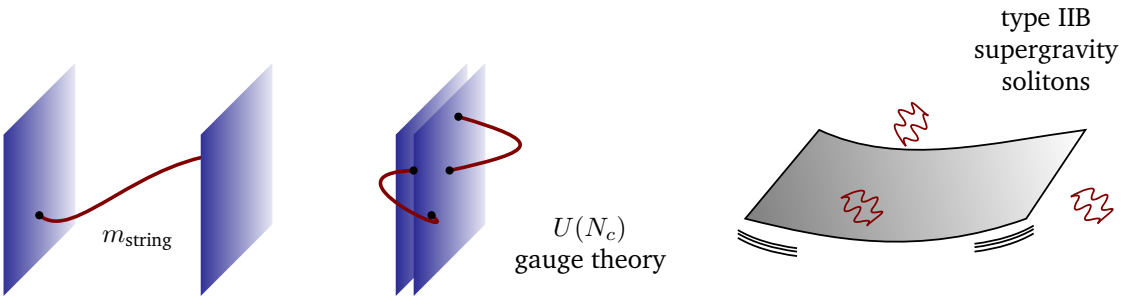

Figure 3.9. The left panel shows the open string viewpoint of D_p-branes with strings stretching between different D_p-branes. For separated D_p-branes the strings will acquire a finite tension/mass m proportional to the distance between the branes, whereas for N_c coincident D_p-branes we find a massless $U(N_c)$ gauge theory arising from the Lie algebra of Chan-Paton factors. In the right panel the closed string viewpoint of massive solitonic D_p-branes curving the surrounding spacetime is shown. In particular for N_c coincident D_p-branes the characteristic length scale of the curved space scales with $N_c g_s$.

Closed string viewpoint

From the closed string perspective, including the graviton excitations, the D_p-branes are massive (gravitating) solitonic objects solving the equations of motions arising from the type IIA and type IIB supergravity actions (3.35) and (3.36). Technically, we can view the D_p-brane solutions as $1/2$ BPS solitons preserving half of the supercharges and leaving a $p+1$ dimensional hypersurface invariant under the Poincaré group $\mathbb{R}^{p+1} \times SO(1,p)$. Embedded in ten dimensional spacetime the full symmetry of a D_p-brane is given by $\mathbb{R}^{p+1} \times SO(1,p) \times SO(9-p)$. A possible Ansatz solving the type IIB supergravity equations of motions is given by the (extremal) BPS solution

$$\begin{aligned} \mathrm{d}s^2 &= H_p^{-1/2} \eta_{\mu\nu}\, \mathrm{d}x^\mu\, \mathrm{d}x^\nu + H_p^{1/2}\, \mathrm{d}y \cdot \mathrm{d}y, \\ \mathrm{e}^{2\tilde{\Phi}} &= g_s^2 H_p^{(3-p)/2}, \\ C_{(p+1)} &= -(H_p^{-1} - 1) g_s^{-1}\, \mathrm{d}x^0 \wedge \cdots \wedge \mathrm{d}x^p, \end{aligned} \tag{3.47}$$

where x are the brane worldvolume coordinates and y denotes the direction transverse to the brane. The harmonic function H_p depends only on the distance in the transverse direction $r = \sqrt{\mathrm{d}y \cdot \mathrm{d}y}$ and is fixed by the condition that far away from the D_p-brane, $r \to \infty$, we need to recover flat space *i.e.* no gravity. Thus, H_p can be written as

$$H_p(r) = 1 + \left(\frac{L}{r}\right)^{d-p-3}, \tag{3.48}$$

with the length scale L related to the only dimensionful parameter of type IIB supergravity

$$L^{d-p-3} = (4\pi)^{(5-p)/2} \Gamma\left(\frac{7-p}{2}\right) g_s N_c \alpha'^{(d-p-3)/2}. \tag{3.49}$$

We are now ready to collect all the pieces we have learned about superstrings and D_p-branes to assemble them in a intriguing way which will give rise to the $\mathrm{AdS}_5/\mathrm{CFT}_4$ correspondence.

3.2.2. The AdS$_5$/CFT$_4$ correspondence

The AdS$_5$/CFT$_4$ correspondence arises from the two different viewpoints of a stack of D_3-brane in a particular limit. String theory admits two expansions, the string coupling expansion which yields higher loop corrections characterized by higher genera of the string worldsheet, and the expansion in the inverse string tension α' characterizing the stringiness away from the point particle limit. Various forms of the AdS$_5$/CFT$_4$ correspondence may be generated by looking at the two string expansions in g_s and α'. The strongest form of the AdS$_5$/CFT$_4$ correspondence can be stated in the following way:

AdS$_5$/CFT$_4$ correspondence

Field theory side:		**String theory side:**
$\mathcal{N}=4$ supersymmetric $SU(N_c)$ Yang-Mills theory in $d=4$ spacetime dimensions	$\rightleftharpoons$	$d=10$ dimensional type IIB superstring theory on AdS$_5 \times S^5$

The field theory side is characterized by the Yang-Mills coupling g_{YM}[25] and the number of "colors" of the gauge group N_c, while the string theory side is described by the dimensionless parameters g_s and $L/\sqrt{\alpha'} = L/\ell_s$ with L denoting the radius of curvature of the AdS$_5$ and S^5 space. The free parameters of both sides can be mapped to each other by virtue of (3.43) and (3.49) of a D_3-brane with $p=3$

$$g_{\text{YM}}^2 = 2\pi g_s \qquad\qquad g_{\text{YM}}^2 N_c = \frac{L^4}{2\alpha'^2} = \frac{L^4}{2\ell_s^4}$$

Let us give a sketch of the derivation of the correspondence in a particular limit suited to work with low-energy supergravity theories as presented in [74]; see [123] for an in-depth review. Consider type IIB superstring theory with a stack of N_c D_3-branes in ten dimensional spacetime. As explained in Section 3.2 the stack of D_3-branes give rise to a low-energy effective theory with massless excitations which can be split into a ten-dimensional supergravity term S_{bulk}, a D_3-brane term S_{brane} given by (3.40) and (3.42) with $p=3$ and a bulk-brane interaction term

$$S_{\text{eff}} = S_{\text{bulk}} + S_{\text{brane}} + S_{\text{int}} \tag{3.50}$$

In the point-particle limit $\alpha' \to 0$, the interaction terms in S_{bulk} and the brane-bulk interaction term vanishes, so we are left with free supergravity of massless excitations and the $\mathcal{N}=4$ supersymmetric Yang-Mills theory on the D_3 brane (3.46). On the other hand, the closed string viewpoint describes the stack of D_3 branes by the metric (3.47)

$$\mathrm{d}s^2 = \left(1+\frac{L^4}{r^4}\right)^{-1/2} \eta_{\mu\nu}\,\mathrm{d}x^\mu\,\mathrm{d}x^\nu + \left(1+\frac{L^4}{r^4}\right)^{1/2} \left(\mathrm{d}r^2 + r^2\,\mathrm{d}\Omega_5^2\right) \tag{3.51}$$

where r denotes the transverse distance from the stack of branes and $\mathrm{d}\Omega_5^2$ denotes the metric of the spherical symmetric five sphere. Far away from the stack of N_c D_3-branes, $r \to \infty$, we recover flat ten dimensional spacetime whereas close to the stack, $r \to 0$, the metric becomes singular. In this near-horizon or Maldacena limit the effective metric reduces to the metric of

[25] As we will see in Section 3.3.1, the coupling g_{YM} will not run due to protection from supersymmetry. Therefore the field theory side is described by a four dimensional CFT denoted CFT$_4$.

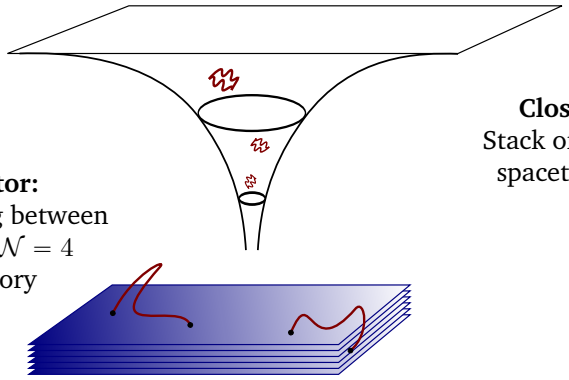

Open string sector:
Open strings stretching between N_c D_3-branes yield $\mathcal{N} = 4$ $SU(N_c)$ SYN theory

Closed string sector:
Stack of N_c D_3-branes warp spacetime into $\text{AdS}_5 \times S^5$ geometry

Figure 3.10. The $\text{AdS}_5/\text{CFT}_4$ correspondence arise from the near horizon decoupling limit $N_c \to \infty$ of a stack of N_c D_3-branes. The closed string sector yields free supergravity and massless excitations trapped in the "throat" generated by the massive D_3-branes. In the point particle limit the open string sector decouples free supergravity and a supersymmetric Yang-Mills theory on the D_3-branes. This allows us to identify the low-energy effective theories arising from the open and closed sector. Note that the fundamental degrees of freedom are completely different, but their effective theories are conjectured to describe the same physics in different perspectives.

$\text{AdS}_5 \times S^5$ with isometry group $SO(2,4) \times SO(6)$ and radius $L^4 = 4\pi g_s N_c \alpha'^2$.[26] The redshift factor of the metric (3.51) is a geometric representation of approaching the low-energy regime. For an observer in asymptotic flat spacetime at $r \to \infty$ the energy of an object close to the horizon of the D_3-brane stack is shifted by

$$E_\infty = \left(1 + \frac{L^4}{r^4}\right)^{-1/4} E. \tag{3.52}$$

The near horizon limit decouples two types of low-energy excitations, massless excitations in the bulk ($r \neq 0$) and the near horizon excitations at $r \to 0$. The former are again described by a free supergravity with massless excitations, whereas the latter describes massless excitations in $\text{AdS}_5 \times S^5$ spacetime. Combining both perspectives we can identify the free supergravity parts of the open and closed viewpoint and hence conjecture that the physical content of $\mathcal{N} = 4$ supersymmetric Yang-Mills theory in four dimensions is identical to the low-energy effective field theory of type IIB superstring theory. So the same physical system is described by different viewpoints as shown in Figure 3.10. If this conjecture is proven to be true the physics of $\mathcal{N} = 4$ supersymmetric Yang-Mills theory can be mapped onto type IIB superstring theory. In this sense the $\text{AdS}_5/\text{CFT}_4$ correspondence obeys the holographic principle and is a special case of a gauge/-gravity duality. Let us give an overview of the different forms of the $\text{AdS}_5/\text{CFT}_4$ correspondence:

- **Strongest form:** This is the conjecture stated in the Infobox $\text{AdS}_5/\text{CFT}_4$ correspondence on page 92. Here the field theory parameters g_{YM} and N_c can take arbitrary values and the supersymmetric Yang-Mills theory is exactly equivalent to type IIB superstring theory

[26] Note that AdS-space is a hyperbolic space, so in this sense the radius should be understood as the "negative radius" of a sphere. Therefore, the curvature of AdS_5 is equal to the negative curvature of S^5 and hence the overall curvature of $\text{AdS}_5 \times S^5$ is zero.

on $AdS_5 \times S^5$. This form is poorly understood and cannot be tested since so far no non-perturbative quantization of string theory exists.

- **Strong form:** Here we keep the 't Hooft coupling $\lambda = g_{YM}^2 N_c$ fixed while we take the large N_c limit, $N_c \to \infty$, which corresponds to an expansion in $1/N_c$ on the field theory side and an perturbative expansion in the string coupling $g_s \sim \lambda/N_c \ll 1$, so we effectively work with classical/tree-level string theory

$$\left.\begin{aligned} N_c &\to \infty \\ \lambda = g_{YM}^2 N_c &= \text{const.} \end{aligned}\right\} \quad \rightleftharpoons \quad \begin{cases} g_s = \dfrac{\lambda}{2\pi N_c} \to 0 \\ \alpha'^2 = \dfrac{L^4}{2\lambda} \end{cases} \tag{3.53}$$

- **Weak form:** As shown in Figure 3.10 and explained above we additionally take the limit $\lambda \gg 1$. In this case a strongly coupled supersymmetric Yang-Mills theory with perturbative expansion in $\lambda^{-1/2}$ about the strong coupling limit $\lambda \to \infty$ corresponds to classical supergravity expanded in α' about the point-particle limit $\alpha' \to 0$

$$\left.\begin{aligned} N_c &\to \infty \\ \lambda &\to \infty \end{aligned}\right\} \quad \rightleftharpoons \quad \begin{cases} g_s \to 0 \\ \alpha' \to 0 \end{cases} \tag{3.54}$$

The weak form of the AdS/CFT correspondence is one of the most fascinating strong/weak dualities and particularly interesting for applications to strongly correlated condensed matter system. If we are able to find a gravitational dual capturing the essential feature of particular condensed matter system, all the perturbative tools developed in Chapter 2 can be applied to solve strongly coupled problems as mentioned in the introduction, by simple solving classical (super)gravity in the saddle point approximation (see Infobox Saddle Point Approximation on page 18). So the main task for applying the AdS/CFT correspondence to challenging physical problems is to find a suitable D_p-brane setup and identify the physically relevant fields to describe the problem. However, for condensed matter applications we need to understand how to include physical properties such as temperature and densities known from thermal field theory. Therefore, we will take a broader perspective on the gauge/gravity duality which is in fact a geometrization of the renormalization group scheme as explained in detail in Section 3.4. Interesting reviews and introductory lecture notes are [124–135] and more technical details are covered in [123,136–139]. Let us conclude with an overview of other gauge/gravity dualities discovered so far

- **Mesons in AdS/CFT:** This is a holographic dual describing bilinear quarks or mesons by constructing a D_3-D_7-brane intersection to allow for flavor degrees of freedom [140,141]. This setup allows to add matter in the fundamental representation.

- **Sakai-Sugimoto model:** A holographic dual describing large N_c QCD with massless pions. The gravity dual arises from D_8 and anti $\overline{D}_8$-branes put into a supersymmetry breaking background created by D_4-branes [142].

- **ABJM model:** Here ABJM stands for the initials of the authors of [143]. This model introduces a topological Chern-Simons matter theory with gauge groups $U(N) \times U(N)$. In the large N limit the gravitational dual is M-theory on $AdS_4 \times S^7$ generated by N M_2-branes. Interesting lecture notes connecting the ABJM model to matrix model techniques are [144]

- **Higher Spin/Vector $O(N)$ models:** Vasiliev's higher spin gravity in AdS_4 is a possible gravitational dual to three dimensional large N, $O(N)$ vector models [145–147]. For a nice review see *e.g.* [148].

Other extensions including Wilson loops and scattering amplitudes as well as connections to concepts of string theory are described in several nice reviews [149–153]. Of course in the wider perspective of the so-called bottom-up approaches, reviewed in [154, 155], we find even more possible gauge/gravity dualities [156–159], applications to QCD [15, 160–165], and most notably the fluid/gravity correspondence [166–170] relaxing most of the requirements explained above. In particular the gauge/gravity constructions geared towards application in condensed matter physics are explained in [10, 28, 41, 171–179], and will be extensively used in the context of holographic superfluids/superconductors [29–31, 180] in Chapter 4. Furthermore, there are constructions for holographic non-Fermi liquids, strange metals and quantum criticality [181–184], as well as holographic fermions [27, 185]. The philosophy behind these generalized gauge/gravity dualities will be motivated and discussed in Section 3.4.

3.3. Holographic Dictionary

Overview

- The weak/strong duality between a strongly coupled supersymmetric non-Abelian gauge theory and a weakly curved classical gravity theory, allows to tackle strongly coupled problems, by solving Einstein's equations.
- The other way round, strongly coupled quantum gravity can be mapped in principle onto a weakly coupled perturbative quantum field theory.
- The holographic dictionary allows us to connect various objects of the field theory side to the gravity side.

In this section we will shortly establish the dictionary between the field theory side operators and the supergravity side fields. Let us start with a closer description of $\mathcal{N}=4$ $SU(N_c)$ supersymmetric Yang-Mills theory in four dimensions.

3.3.1. Overview of $d=4$, $\mathcal{N}=4$ supersymmetric $SU(N_c)$ Yang-Mills Theory

The Lagrangian belonging to the vector multiplet of $\mathcal{N}=4$ as listed in Table 3.2 is given by

$$\mathscr{L}_{\text{SYM}} = \operatorname{tr}\Bigg[-\frac{1}{2g_{\text{YM}}} F\wedge\star F + \frac{\theta}{8\pi^2} F\wedge F - \mathrm{i}\sum_{a=1}^{4}\bar{\lambda}^a\,(\bar{\sigma}\cdot\mathrm{D})\,\lambda_a - \sum_{i=1}^{6}\left(\mathrm{D}\,x^i\right)^2 + g_{\text{YM}}\sum_{a,b,i} C^{ab}{}_i\,\lambda_a\left[x^i,\lambda_b\right] + g_{\text{YM}}\sum_{a,b,i}\bar{C}_{abi}\bar{\lambda}^a\left[x^i,\lambda^b\right] + \frac{g_{\text{YM}}^2}{2}\sum_{ij}\left[x^i,x^j\right]^2\Bigg]. \tag{3.55}$$

The gauge field is described by the field strength and the **CP** violating term is parametrized by the instanton number θ, which will be set to zero in the following. The trace is running over the representation of the $SU(N_c)$ gauge group and the $C^{ab}{}_i$ are the structure constants of the

R-symmetry group $SU(4)_{\mathrm{R}}$. The λ^a denotes the four Weyl fermions and x^i the six scalars, respectively. The scaling dimension of the coupling g_{YM} is zero because the field strength tensors has scaling dimension two. Thus, on the classical level, considering only scaling dimension, the theory is conformal. After quantization, one can show that the one loop corrections to the β-function vanish. Supersymmetry protects the theory against loop corrections up to all orders, so the $\mathcal{N} = 4$ $SU(N_c)$ supersymmetric Yang-Mills theory is non-perturbatively conformal in $d = 4$, *i.e.* $\beta \equiv 0$ or in different terms exactly marginal. Since (3.55) describes a true CFT on the quantum level, the conformal group and supersymmetry can be combined in the superconformal group $SU(2,2|4)$ where the conformal subgroup $SO(2,4)$ commutes with the R-symmetry subgroup $SU(4)_{\mathrm{R}} \cong SO(6)_{\mathrm{R}}$. In the following we will work with superconformal primary operators (generalized concept of primary operators in CFTs as defined in Section 2.3.7) in particular with single trace $1/2$ BPS operators defined as

$$O = \mathrm{str}\left[x^{i_1} x^{i_2} \dots x^{i_n}\right], \tag{3.56}$$

where str denotes the gauge invariant symmetrized trace. There are two different types of supersymmetric vacua where the scalar potential must vanish, *i.e.* $\left[x^i, x^j\right] = 0$ for all i, j; either all scalar fields x^i are identically zero or only one scalar field acquires a non-zero expectation value. The former is called superconformal phase whereas the latter, called Coulomb phase, introduces a length scale set by the vacuum expectation value that explicitly breaks conformal invariance. As noted in the previous section the isometries of AdS_5 are given by the isometry group $SO(2,4)$ which is precisely the conformal group in four dimensions of CFT_4. Furthermore, the R-symmetry group $SU(4)_{\mathrm{R}} \cong SO(6)_{\mathrm{R}}$ relates to the isometry group of the S^5 part. The identification of the isometry groups of $\mathrm{AdS}_5 \times S^5$ with those of the field theory is known as symmetry matching.

Let us also comment on the large N_c limit[27] involved in the AdS/CFT correspondence, *i.e.* $N_c \to \infty$, which has a profound impact on the diagrams contributing in a perturbative expansion in $1/N_c$ [186]. Drawing the Feynman diagrams in double line notation, where each line carries a gauge or color index, one can show that any gauge invariant Feynman diagram with genus zero and no index lines crossing, can only be drawn on a two-dimensional flat sheet of paper. Accordingly, a Feynman diagram with a given genus and no index lines crossing can only be drawn on a surface with the same genus, *e.g.* a diagram with genus one can be drawn only on a torus without line crossing. For every physical observable, such as the free energy, the loop expansion in g_{YM} can be written as a double expansion in N_c and the 't Hooft coupling $\lambda = g_{\mathrm{YM}}^2 N_c$ in the following way

$$F = N^{\#} \sum_{g=0}^{\infty} \frac{f_g(\lambda)}{N_c^{2g}}, \tag{3.57}$$

where $f_g(\lambda)$ denotes the sum of all diagrams with genus g. For $N_c \to \infty$ only the leading term with genus $g = 0$ will contribute to the value of the observable. Thus, in the large N_c limit only planar diagrams contribute. Moreover, the vacuum expectation values of single trace operators defined in (3.56) factorize in the large N_c limit rendering the Mean Field Approximation on page 49 exact

$$\langle\, O_1 O_2 \,\rangle = \langle\, O_1 \,\rangle \langle\, O_2 \,\rangle + \mathcal{O}\left(\frac{1}{N_c}\right), \tag{3.58}$$

[27] This limit is often known as thermodynamic limit in statistical theories in order to apply the saddle-point method. For many condensed matter applications the large N limit is needed for a rigorous derivation providing the applicability of the mean field methods. Unlike the thermodynamic limit the degrees of freedom of a single constituent is considered to be large.

since the disconnected diagrams naturally include more loops than the connected diagrams, yielding additional powers of N_c. Therefore, in the large N_c limit gauge theories are described by a double expansion in $1/N_c$ controlling the genus of the diagrams and operator factorization, and $\lambda = g_{\text{YM}}^2 N_c$, which yields perturbative corrections and determines the anomalous dimension of the operators via their expectation values. This is reminiscent of the double expansion of string theory in the string coupling g_s, controlling the genus of the worldsheet or number of loops, respectively, and α' playing the analogous role of λ. Together with the symmetry matching this fact can be viewed as evidence for the sanity of the strong form of the AdS/CFT correspondence as outlined in (3.53).

3.3.2. Field-operator map

In this paragraph we will discuss the precise mapping of the classical fields in type IIB supergravity on $\text{AdS}_5 \times S^5$ onto gauge invariant operators of the $\mathcal{N} = 4$ $SU(N_c)$ supersymmetric Yang-Mills theory. As explained in Section 3.2 the basic claim of the AdS/CFT correspondence and gauge/-gravity duality in general is the reorganization of a d-dimensional CFT into a $d+1$-dimensional (quantum) theory of gravity. Independent of the internal distribution of the degrees of freedom the partition functions of both theories must agree in order to encode the equivalent physical information in both theories. Therefore, the first entry in the holographic dictionary is given by [76]

$$Z_{\text{QFT}}^{(d)}[J] = Z_{\text{QG}}^{(d+1)}[\varphi]\Big|_{\varphi_{\partial(\text{AdS})}=J}, \tag{3.59}$$

where the operators of the field theory are sourced by J which are determined by the boundary values of the quantum gravity fields. Operationally, the quantum gravity partition function is not known, so we have to take the classical limit on the gravity side. For a well defined classical gravity the curvature must be small compared to the Planck length ℓ_P in order to suppress quantum corrections and additionally small compared to the string length ℓ_s suppressing stringy corrections, thus

$$\frac{\ell_\text{P}}{L} \ll 1, \qquad \frac{\ell_\text{s}}{L} \ll 1. \tag{3.60}$$

This is exactly satisfied by the Maldacena limit and the conditions of the weak form of the AdS/CFT correspondence (3.54). So the second entry in the holographic dictionary relates the local degrees of freedom N_c and the 't Hooft coupling λ to the string length (following from (3.49) with $p = 3$) and the Planck length following from the Holographic Principle on page 74

$$N_c^2 \sim \left(\frac{L}{\ell_\text{P}}\right)^{d-1}, \qquad \lambda \sim \left(\frac{L}{\ell_\text{s}}\right)^{d}. \tag{3.61}$$

In the large N_c and strong coupling limit, we can find weakly curved classical supergravity in the saddle-point approximation which reduces (3.59) to

$$\left\langle \, \mathrm{e}^{-\int \mathrm{d}^d x \, J(x) O(x)} \, \right\rangle_{\text{QFT}} = Z_{\text{QFT}}^{(d)}[J] = Z_{\text{SUGRA}}^{(d+1)}[\varphi]\Big|_{\varphi_{\partial(\text{AdS})}=J} \approx \mathrm{e}^{-I_{\text{SUGRA}}}\Big|_{\varphi_{\partial(\text{AdS})}=J}. \tag{3.62}$$

Note that in the saddle-point approximation I_{SUGRA} is the regularized Euclidean on-shell action evaluated on the classical solution to the saddle-point equations (2.18) (see Infobox Saddle Point Approximation in Section 2.1.1 for more details). From the relation between quantum statistical partition functions and Euclidean QFT we can deduce that thermodynamic quantities scale with N_c^2, and λ amounts to a scale setting the anomalous dimensions. Thus (3.62) constitutes a

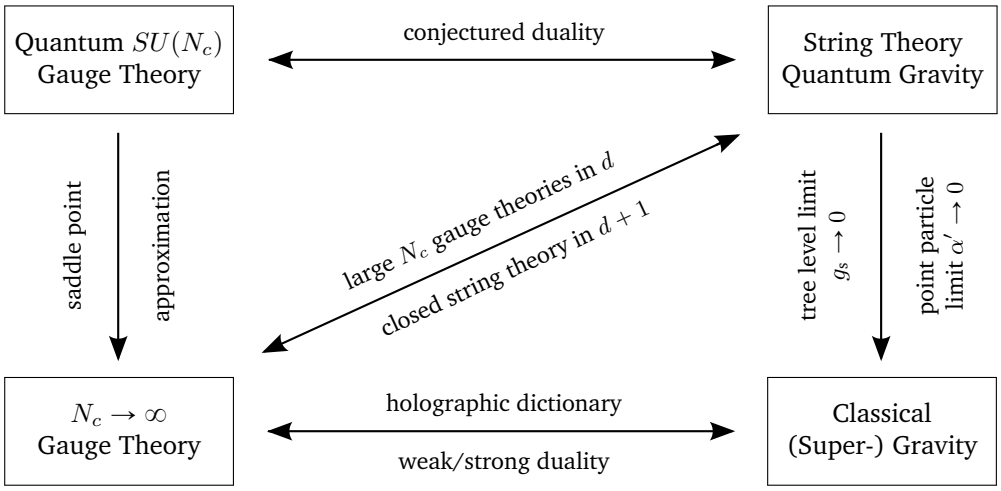

Figure 3.11. Conceptual overview of the generalized gauge/gravity duality. Strongly coupled large N_c gauge theory is effectively described by classical gravity. The Weinberg-Witten theorem [91] is evaded by the holographic principle allowing gravity to emerge from a gauge theory in a lower spacetime dimensions as the gravitational theory.

typical weak/strong duality, where a strongly coupled non-perturbative QFT is mapped onto a weakly curved gravity. In this sense the quasi particle description of perturbative QFT is replaced by a geometrical description in terms of gravity when flowing to strong coupling. Correlation functions of the strongly coupled QFT in d dimensions are calculated by functional derivatives of the regularized on-shell action I_{SUGRA} with the boundary condition $\varphi_{\partial(\text{AdS}_{d+1})} = J = 0$. The main connection drawn from the holographic dictionary is summarized in Figure 3.11.

Let us derive the explicit relation between the fields in type IIB supergravity on AdS_{d+1}. In order to make contact with the original $\text{AdS}_5 \times S^5$ supergravity, let us do the calculation in the simplest case of a scalar field in the $\text{AdS}_{d+1} \times S^{9-d}$ background where we generalize it to arbitrary dimensionality of the AdS-space. In this case we can look at the effective saddle-point action with the most relevant terms. As we have learned in Section 3.1.4 the Euclidean action for a scalar field reads

$$S_{\text{eff}} = -\frac{1}{2\kappa_0}\int \mathrm{d}^{10}x\,\sqrt{-g}\,(R + 4\nabla_a\Phi\nabla^a\Phi)\,. \tag{3.63}$$

The $\text{AdS}_{d+1} \times S^{9-d}$ metric is given by (3.51) in the near horizon limit $r \to 0$. It is convenient to write the metric in more suitable coordinates $u = {}^{L^2}\!/_r$ which are local coordinates on the Poincaré patch of global AdS-space (for details see *e.g.* [125])

$$\mathrm{d}s^2 = \frac{L^2}{u^2}\left(-\,\mathrm{d}t^2 + \mathrm{d}\mathbf{x}^2 + \mathrm{d}u^2\right) + L^2\,\mathrm{d}\Omega_5^2\,. \tag{3.64}$$

The $d = D + 1$ spatial coordinates will be denoted by $x = (t, \mathbf{x})$, the radial coordinate of AdS-space by u and the coordinates on the S^{9-d} by $\mathbf{y}$. First, we remove the extra dimensions of the S^{9-d} by dimensional reduction where we expand the fields in spherical harmonics $\mathcal{Y}(\mathbf{y})$. As a simple example, we may consider a one dimensional analog: the compactification yields a

"Kaluza-Klein tower" following from the periodicity of compact spaces[28]

$$\Phi(x,u,y)=\sum_{n\in\mathbb{Z}}\varphi_n(x,u)\,\mathrm{e}^{\mathrm{i}ny/L}\qquad\longrightarrow\qquad\left(\nabla_A\nabla^A-\frac{n^2}{L^2}\right)\varphi_n(x,u)=0. \tag{3.65}$$

In the case of spherical harmonics $\mathcal{Y}(\mathbf{y})$ the ten-dimensional Klein-Gordon equation arising from (3.63) acquires an additional mass term

$$\Phi(x,u,\mathbf{y})=\sum_{\Delta=0}^{\infty}\varphi^{\Delta}(x,u)\mathcal{Y}_{\Delta}(\mathbf{y})\qquad\longrightarrow\qquad(-\nabla^2+m_{\Delta}^2)\varphi^{\Delta}(x,u)=0, \tag{3.66}$$

where the mass of the scalar field is given by

$$m_{\Delta}^2L^2=\Delta(\Delta-d). \tag{3.67}$$

Note that the dimensional reduction of the action (3.63) yields the effective action of a scalar in AdS_{d+1} space with the most relevant terms included being a Gaussian theory as explained in Section 2.3.6 and (2.129)[29]

$$S_{\text{eff}}[\varphi]=\frac{1}{2}\int\mathrm{d}^{d+1}x\,\sqrt{-g}\left(g^{AB}\nabla_A\varphi^{\Delta}\nabla_B\varphi^{\Delta}+m_{\Delta}^2\varphi^{\Delta}\right). \tag{3.68}$$

In the following we will suppress the index Δ on φ and m. The Laplacian, or more precisely the Laplace-Beltrami operator, ∇^2 for scalar fields can be reduced to

$$\begin{aligned}\nabla_A\nabla^A\varphi(x,u)&=\frac{1}{\sqrt{-g}}\partial_A\left(\sqrt{-g}g^{AB}\partial_B\varphi(x,u)\right)\\&=\frac{1}{L^2}\left(u^2\partial_u^2-(d-1)u\partial_u+u^2\partial_\mu\partial^\mu\right)\varphi(x,u).\end{aligned} \tag{3.69}$$

The equation of motion (AdS_{d+1} Klein-Gordon equation) (3.66) in momentum space with the Fourier transform of the scalar field, imposed by Lorentz invariance,

$$\varphi(x,u)=\int\frac{\mathrm{d}^dk}{(2\pi)^d}\varphi(k,u)\,\mathrm{e}^{\mathrm{i}k_\mu x^\mu}, \tag{3.70}$$

replacing $\partial_\mu\partial^\mu\longrightarrow-k_\mu k^\mu$ is given by

$$\left[\partial_u^2-\frac{d-1}{u}\partial_u-\left(k_\mu k^\mu+\frac{m^2L^2}{u^2}\right)\right]\varphi(k,u)=0. \tag{3.71}$$

According to [187] (10.13.4), the solution to (3.71) can be written in terms of modified Bessel functions of the first $\mathcal{K}_\nu(ku)$ and second kind $\mathcal{I}_\nu(ku)$

$$\varphi(k,u)=u^{d/2}\left[\varphi_{\text{reg}}\mathcal{K}_\nu(ku)+\varphi_{\text{irreg}}\mathcal{I}_\nu(ku)\right], \tag{3.72}$$

[28] The AdS directions are labeled by capitalized Latin indices $A,B,\ldots$ and the S^{9-d} direction are indexed by lower case Latin characters $a,b,\ldots$.

[29] There are two possibilities to write the effective action. Firstly, we can write the action with covariant derivatives allowing us to simply deduce the equations of motion due to the metric property $\nabla g=0$, so the integration by parts can be conducted easily. Note that the covariant Laplacian of a scalar field involves connection terms arising from $\nabla_A(\partial^A\varphi)$, where the gradient of the scalar field needs to be treated as a vector. This gives rise to connection terms in the fully expanded Laplacian. Secondly, we know that the covariant derivative of a scalar field reduce to partial derivatives, so we can write the effective action in terms of partial derivatives. Here the integration by parts introduces derivatives of the metric since the partial derivative *does not* commute with the metric. Of course, both approaches will yield the same equations of motion.

where $\nu = \Delta - {}^{d}/_{2}$ and $k = \sqrt{k_\mu k^\mu}$. Note that Δ denotes the larger solution of (3.67), *i.e.*

$$\Delta_\pm = \frac{d}{2} \pm \frac{1}{2}\sqrt{d^2 + 4m^2L^2} \quad \longrightarrow \quad \Delta_+ + \Delta_- = d \quad \Rightarrow \quad \Delta_+ \equiv \Delta, \quad \Delta_- = d - \Delta. \tag{3.73}$$

Expanding the solution in the deep interior of the AdS-space $u \to \infty$, we see that the modified Bessel functions are exponentially increasing $\mathcal{I}_\nu(ku) \sim \mathrm{e}^{ku}$ or decaying $\mathcal{K}_\nu(ku) \sim \mathrm{e}^{-ku}$. Imposing regularity requires the irregular coefficient to vanish, $\varphi_{\text{irreg}} = 0$[30]. Expanding the solution (3.72) at the AdS boundary $u \to 0$ yields

$$\varphi(k,u) \approx \varphi_{d-\Delta}(k)u^{d-\Delta} + \varphi_\Delta(k)u^\Delta. \tag{3.74}$$

Considering the equivalence of the partition functions (3.59), we immediately see that Δ sets the scaling dimensions of the operator O sourced by the leading term $\varphi_{d-\Delta}(k)$ (for more details see the discussion in Section 3.4). Here some clarifications are in order. First, the scaling dimension must be real which requires the mass of the scalar to be larger than $-{}^{d^2}/_{4L^2}$, the so-called Breitenlohner-Freedman bound [188]. Due to the hyperbolic form of the AdS-space, which is a maximally symmetric space with negative curvature, some peculiar properties arise *e.g.* there is a boundary at infinity which can be reached in finite time. In fact, AdS-space acts as an isotropic and homogeneous harmonic box, so a photon sent out inside AdS will run to the boundary and return in finite time. This harmonic box-like structure allows stable fields with negative m^2 terms. The instability expected from flat space is removed by the harmonic potential generated by the AdS-space[31]. Moreover, for $m^2L^2 > 1 - {}^{d^2}/_{4}$ we can characterize the two independent solutions by their asymptotic behavior. Defining the norm on a constant time slice of AdS-space

$$(\varphi_1\,,\,\varphi_2) = \int \mathrm{d}^{d-1}x\,\mathrm{d}z\,\sqrt{-g}g^{tt}\left(\varphi_1^*\partial_t\varphi_2 - \varphi_2^*\partial_t\varphi_1\right), \tag{3.75}$$

we see that

$$\varphi(k,u) \sim \begin{cases} u^{d-\Delta} & \text{non-normalizable} \\ \\ u^\Delta & \text{normalizable.} \end{cases} \tag{3.76}$$

In order to have a well-posed variational problem of the action in (3.68), we need to fix the non-normalizable mode $\varphi_{d-\Delta}$ by boundary conditions at $u \to 0$ which can be identified with the source for the dual operator with proper wave function renormalization[32]

$$J(k) \equiv \varphi_{d-\Delta}(k) = \lim_{u\to 0} u^{\Delta-d}\varphi(k,u), \tag{3.77}$$

[30] In Minkowski signature this amounts to an outgoing mode, where the in-going mode is normalized by φ_{reg}. When considering finite temperature, we will deal with a black hole horizon in the deep interior of the modified AdS-space, so physically only the in-falling boundary condition will yield the correct causal structure for the Green functions, see Section 2.2.2.

[31] Furthermore, black holes in AdS-space are thermodynamically stable objects, *i.e.* their specific heat is positive. Thus, adding energy/matter to the black hole increases its temperature unlike the flat space black holes and therefore AdS black holes can come to an equilibrium state. Heuristically, this follows again from the harmonic box property, where any radiation (or even gravity) cannot leave the AdS-space, so the evaporation radiation will fall back into the black hole.

[32] For brevity we have omitted a proper discussion on holographic renormalization. It follows the same logic of perturbative QFT renormalization in removing divergent terms. The QFT correlation functions computed in a holographic context suffer from UV divergences which can be regularized by a near boundary cut-off. Due to the IR/UV connection of holographic theories (see Figure 3.1), the UV divergences of the field theory are related to IR divergences of the gravitational theory [189]. Heuristically, this IR divergence arises from the infinite spacetime volume of AdS-space. The holographic renormalization proceeds as follows. First, we integrate only to a shell near the boundary $u \to \epsilon$ and isolate the divergent terms under $\epsilon \to 0$. Then, we introduce appropriate counterterms respecting all symmetries to remove the divergences. In the scalar field case discussed in the main text, the renormalization was easy to obtain, but in generic situations a true holographic renormalization must be performed. An important counterterm of the

Supergravity field	Mass of field	Scaling of dual operator
Scalar	$m^2L^2 = \Delta(\Delta - d)$	$\Delta_\pm = \frac{1}{2}\left(d \pm \sqrt{d^2 + 4m^2L^2}\right)$
massless spin two	$m^2L^2 = 0$	$\Delta = d$
p-form	$m^2L^2 = (\Delta - p)(\Delta + p - d)$	$\Delta_\pm = \frac{1}{2}\left(d \pm \sqrt{(d-2p)^2 + 4m^2L^2}\right)$
spinors	$\lvert m\rvert L = \Delta - \frac{d}{2}$	$\Delta = \frac{1}{2}\left(d + 2\lvert m\rvert L\right)$

Table 3.3. Considering different types of supergravity fields, one can derive relations between the mass of the supergravity field in $d+1$ dimensions and the scaling of the dual sourced operator in the d dimensional supersymmetric Yang-Mills CFT. Many results are obtained by various groups, for references see [191].

adding another piece to our dictionary. In the case of $-{}^{d^2}/_4 < m^2L^2 < 1 - {}^{d^2}/_4$ we can have two different quantizations [77] where we find operators with scaling dimension Δ and $d-\Delta$, respectively. The field theory with operator scaling $d-\Delta$ is unstable against relevant double-trace deformations and thus will flow to the theory with operator scaling Δ. Exactly at the BF bound, the two scaling dimensions are identical, which usually gives rise to additional log-like terms in the boundary expansion. To conclude, the scalar field solution is completely fixed by the regularity condition deep in the AdS-space, which connects the coefficient of the normalizable solution to the non-normalizable solution as computed by setting $\varphi_{\text{irreg}} = 0$ in the boundary expansion of (3.72)

$$\varphi_\Delta = 2^{d/2-\Delta}\frac{\Gamma(\frac{d}{2}-\Delta)}{\Gamma(\Delta-\frac{d}{2})}k^{2\Delta-d}\varphi_{d-\Delta}. \tag{3.78}$$

This calculation can be generalized to other types of fields on the gravity side in particular for vector fields (p-form fields), spinors and massless spin two fields. The relation between the field's masses and the scaling of the dual operator sourced by the supergravity field are listed in Table 3.3. Finally, let us determine the dictionary entries for correlation functions, in particular the vacuum expectation values and the Green functions related to the scalar field sourced operator. Applying the general formula for correlation functions from generating functionals (2.31) to the partition function of supergravity in the saddle-point approximation (3.62) yields

$$\langle\!\langle\, O(x_1)\cdots O(x_n)\,\rangle\!\rangle = (-1)^{n+1}\frac{\delta^n I_{\text{SUGRA}}}{\delta J(x_1)\cdots\delta J(x_n)}\bigg|_{J=\varphi_{\partial(\text{AdS})}}. \tag{3.79}$$

The expectation value can be calculated from a single functional derivative with respect to the boundary value of the field. From Hamilton-Jacobi theory we know that the variation of the action with respect to the boundary value of a generalized coordinate yields the canonical conjugate momentum at the boundary. Treating the radial coordinate as "time" and applying the

Einstein action leading to AdS spacetime is the Gibbons-Hawking-York term given by

$$S = \frac{1}{\kappa^2}\int_{\partial\mathcal{M}} \mathrm{d}^d x\,\sqrt{|\gamma|}K$$

where γ denotes the determinant of the induces metric $\gamma^{\mu\nu}$ on the near boundary shell and K is the extrinsic curvature given by

$$K = \gamma^{\mu\nu}\nabla_\mu n_\nu$$

with n_ν being the outward pointing normal vector to the tangent surface of the near boundary shell. More details can be found in [190].

Leibniz integral rule or for higher dimensions the Reynold's transport theorem, the functional derivative at the boundary reduces to a normal gradient to the boundary (with normal vector pointing in the interior of AdS-space)

$$\Pi(k,u) = \frac{\delta I_{\text{SUGRA}}[\varphi]}{\delta \varphi_{\partial(\text{AdS})}} = -\sqrt{-g} g^{uu} \partial_u \varphi(k,u) \tag{3.80}$$

$$\Rightarrow \langle\, O(k) \,\rangle = \frac{\delta I_{\text{SUGRA}}[\varphi]}{\delta \varphi_{d-\Delta}(k)} = \lim_{u\to 0} u^{d-\Delta} \Pi(k,u). \tag{3.81}$$

Note that the factor $u^{d-\Delta}$ arises from the wavefunction renormalization of the source from the boundary value in (3.77) and the "functional chain rule". Inserting the boundary expansions (3.74) and the definition of the canonical conjugate momentum yields

$$\langle\, O(k) \,\rangle = \frac{2\Delta - d}{L} \varphi_\Delta(k), \tag{3.82}$$

so the vacuum expectation value of an operator is given by the coefficient of the subleading term in the boundary expansion φ_Δ, characterizing the normalizable solution according to (3.76). The two-point correlation function is now easily obtained. Following the "traditional" way, we would take another derivative with respect to the source of the regularized Euclidean on-shell action I_{SUGRA}, but we can do much better: we already know that the two boundary solutions are connected by the regularity condition in the deep AdS-space interior $u \to \infty$ as shown in (3.78). Therefore, we can take directly the derivative with respect to $J = \varphi_{d-\Delta}$ of the conjugate momentum Π

$$\langle\!\langle\, O(k) O(-k) \,\rangle\!\rangle = \frac{\delta^2 I_{\text{SUGRA}}}{\delta \varphi_{d-\Delta}^2} = \frac{\delta \Pi}{\delta \varphi_{d-\Delta}} \overset{33}{\simeq} \frac{2\Delta - d}{L} \frac{\partial \varphi_\Delta}{\partial \varphi_{d-\Delta}}. \tag{3.83}$$

Inserting the relation between φ_Δ and $\varphi_{d-\Delta}$ yields

$$\langle\!\langle\, O(k) O(-k) \,\rangle\!\rangle = \frac{2\Delta - d}{L} 2^{d/2-\Delta} \frac{\Gamma(\frac{d}{2} - \Delta)}{\Gamma(\Delta - \frac{d}{2})} k^{2\Delta - d}, \tag{3.84}$$

and transforming (3.84) to real space reads

$$\langle\!\langle\, O(x_1) O(x_2) \,\rangle\!\rangle = \frac{2\Delta - d}{L} \frac{\Gamma(\Delta)}{\pi^{d/2} \Gamma(\Delta - \frac{d}{2})} \frac{1}{|x_1 - x_2|^{2\Delta}}. \tag{3.85}$$

which is exactly the conformal correlator of a quasi primary field with scaling Δ as shown in (2.154). In more complicated cases we cannot find an analytic solution to the classical equation of motion in the bulk AdS-space. Therefore, we must resort to matched asymptotic expansions or even numerical methods to determine the relation between φ_Δ and $\varphi_{d-\Delta}$. This is extensively shown in all applications in Chapter 5 and 4. For fermions there are more subtleties. Let us just hint at the fact that the Dirac equation for spinors is already a first order differential equation, so imposing boundary conditions in the AdS interior and the AdS boundary would overdetermine the system of differential equations. Therefore half of the spinor components are related to the other half, usually in a decomposition with respect to a projector constructed from the radial Dirac matrix [192]. The dictionary discussed so far is summarized in Table 3.4. Further entries will be added when systems with deformed IR geometry will be discussed.

[33] Proper renormalization of all quantities involved is already taken into account, *i.e.* working directly with the coefficients of the boundary expansion includes all limit-taking processes.

Boundary field theory in d dimensions				Bulk gravity in $d+1$ dimensions
#(degrees of freedom)	N_c^2	$\rightleftharpoons$	$\frac{L^{d-1}}{\kappa^2} = \left(\frac{L}{\ell_\mathrm{p}}\right)^{d-1}$	AdS radius/curvature $[\ell_\mathrm{p}]$
Interaction strength	λ	$\rightleftharpoons$	$\left(\frac{L}{\ell_s}\right)^{d}$	AdS radius/curvature $[\ell_\mathrm{s}]$
QFT partition function	$Z^{(d)}_{\mathrm{QFT}}[J]$	$\rightleftharpoons$	$Z^{(d+1)}_{\mathrm{QG}}[\varphi]$	Quantum gravity partition function
Strongly coupled QFT	$Z^{(d)}_{\mathrm{QFT}}[J]\Big\vert_{N,\lambda\gg 1}$	$\rightleftharpoons$	$\mathrm{e}^{-I^{(d+1)}}$	Classical Gravity
Operator	$O(x)$	$\rightleftharpoons$	$\varphi(x,u)$	Field
Scaling dimensions	Δ_O	$\rightleftharpoons$	m	mass carried by the field
Source of operator	$J(x)$	$\rightleftharpoons$	$\varphi(x,u)\vert_{\partial(\mathrm{AdS})}$	Field at boundary
Vacuum expectation value	$\langle O \rangle$	$\rightleftharpoons$	$\Pi(x,u)\vert_{\partial(\mathrm{AdS})}$	Conjugate momentum at boundary
Quantum numbers	n_O	$\rightleftharpoons$	n	Properties of fields
Global symmetry	G_{global}	$\rightleftharpoons$	G_{local}	Local Symmetry
Global charge of operator	Q_O	$\rightleftharpoons$	q	gauge charge carried by the field

Table 3.4. The holographic dictionary as explained in the text so far. In general, a gravity dual to a certain field theory is found by incorporating all the symmetry properties, dimensionality and the nature of the interesting operators. However, the implementation of the field theory properties might not be simple, so in many cases one has to work with a universal QFT, capturing the relevant properties (the so-called bottom-up approach). The dictionary for additional symmetries follows from the fact that gauge symmetries include so-called large gauge transformations which are reduced to global symmetries at the spacetime boundary. The quantum numbers of the field theory (*e.g.* angular momentum/spin of the operator) are encoded in certain properties of the fields. This also includes certain constraints on the metric (which is viewed as yet another field on the gravity side), so conserved quantum numbers from global symmetries may appear as additional dimensions in the gravity dual (*e.g.* the Schrödinger metric [193]).

From the holographic principle we already know that black holes can be described as charged objects with temperature and entropy. Thus, AdS-black hole geometries will give rise to finite density and temperature field theories as explained in the RG context in Section 3.4.

3.3.3. Test of the AdS/CFT correspondence

There are several tests to check the AdS/CFT correspondence calculating gauge invariant quantities on the field and gravity side such as

- Exact equivalence of the three point functions of $1/2$ BPS operators in $\mathcal{N} = 4$ supersymmetric Yang-Mills theory [194] and the corresponding gravity counterpart [195]. This check is independent of the coupling.
- Coupling dependent checks can be conducted using integrability methods such as Bethe Ansätze and spin chains. An nice overview can be found in [196] and [197] with the following 22 publications.

In the next section we will tackle the gauge/gravity duality from a different viewpoint and thus motivate it without relying on supersymmetry, string theory and supergravity. In fact, the generalized gauge/gravity dualities have proven to be quite independent of their string theory origin and are extended to non-supersymmetric and/or non-conformal quantum field theories, including Lifshitz/Schrödinger symmetries [156–158, 193], hyperscaling violation metrics [73, 198] and even translational symmetry breaking configurations/lattices [33–35]. So far, all these extensions have passed all sanity checks, so one might even conjecture that gauge/gravity duality is a general yet unproven fact of quantum field theory and quantum gravity, regardless of its concrete physical realization. This is much in spirit of the holographic principle arising in (quantum) gravity.

3.4. Gauge/Gravity Duality & Renormalization

Overview

- The general gauge/gravity duality is intimately connected to the RG flow of field theories. In fact the characteristic RG length/energy scale gives rise to an emergent dimension ⟶ RG flow is geometrized.
- Strongly correlated effects at finite temperature and density are geometrized by certain IR geometries that correspond to deformations by relevant scaling fields ⟶ global RG flow of strongly coupled theories.

Now let us switch gears and motivate the gauge/gravity duality from a very different angle and reconstruct the basic ingredients of the dictionary in a bottom-up approach, *i.e.* without explicit use of string theory or supersymmetry. As already mentioned at the end of the previous section, the original discovery of holography and in particular the AdS/CFT correspondence is build on supersymmetric string theories and requires conformal invariance, the more general holographic dualities allow for relaxation of these constraints. Geared towards condensed matter applications, the renormalization flow viewpoint developed in Section 2.3.5 on holography has been proven very powerful in understanding strongly correlated systems at finite temperature and density. In a wider sense, the RG flow viewpoint of holography resembles the theme of emergent phenomena found in various intricate many-body systems.

3.4.1. Emergent holography

Let us start with a generic effective action (2.116) generated by a decimation process as explained in step *iii* of the RG prescription on page 55 which includes a closed set of operators O_a respecting the symmetry of the system

$$S_{\text{eff}} = \int \mathrm{d}^d x \, g(x)^a \, O_a(x). \tag{3.86}$$

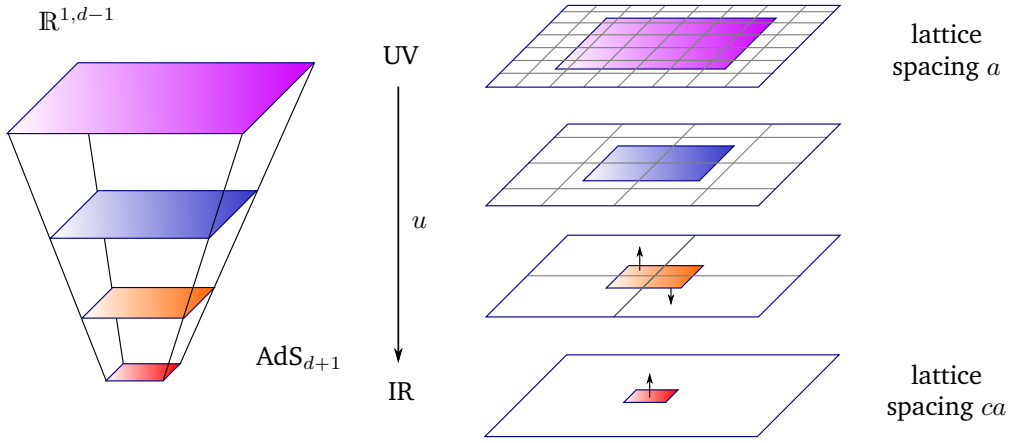

Figure 3.12. The RG flow prescription outlined in Section 2.3.5 as a local operation of an energy scale u can be geometrized by including the energy scale as an additional direction. Under each RG step the degrees of freedom are reduced by an averaging process. Keeping the "space" in the averaging process fixed corresponds to a rescaling of the characteristic length scale. Thus, AdS_{d+1} can be understood as an emergent space where each radial slice can be viewed as a step in the coarse-graining of the degrees of freedom. The running couplings in the UV are then identified according to the holographic dictionary with the boundary value of a field in AdS space. The RG flow of the boundary quantum field theory to the IR is determined by the equations of motion of the gravitational dual.

Note that we are looking at a statistical theory which can be mapped onto a Euclidean field theory, where we made the discretization of the effective action explicit which is encoded in the spatial positions x of the operators on a lattice. Generically, the couplings can vary between each lattice site, *i.e.* $g^a = g^a(x)$. Iterating the RG steps $\dot{\epsilon}$ to $\dot{\epsilon}\dot{\epsilon}\dot{\epsilon}$ on page 55 increases the lattice spacing where the degrees of freedom on the larger lattice represent a well-defined average of the degrees of freedom of the original lattice. The couplings are adjusted in such a way to preserve the physical content of the low-energy excitations above the ground state. Therefore, we can view the couplings as functions that depend on the lattice/spatial position and on the characteristic length scale u probing the system $g^a(x,u)$. The RG flow, as combined operation of infinite many infinitesimal RG steps, of the couplings $g^a(x,u)$ is encoded in the β-function (2.120) or (2.143) which is local in the characteristic length scale, or alternatively, in the energy scale $\mu \sim u^{-1}$

$$\frac{\mathrm{d}g^a(x,u)}{\mathrm{d}u} = R(g^a(x,u),u), \qquad \mu\,\frac{\partial g^a(x,\mu)}{\partial \mu} = \beta(g^a(x,\mu),\mu), \tag{3.87}$$

Thus, from the locality of the RG flow emerges another dimension, so we can view the couplings as fluctuating fields in $d+1$ dimensional space described by the original d dimensional spatial direction x and an additional direction, the characteristic length or energy scale of the RG flow u. In this sense the RG flow is geometrized, where $u \to 0$ denotes the flow to the UV and $u \to \infty$ the flow to the IR. The geometry of the system must encode the scaling transformation (2.115) $x \longrightarrow c^{-1}x$. Heuristically, the decimation process is then carried over to a "shrinking" process of the (lattice) space. Pictorially, this is shown in Figure 3.12. The nature of the underlying geometry can be uncovered by taking the Wilsonian view of the RG method. Here we start with

all known scale invariant theories describing the fixed points in the global RG flow diagram (see Figure 2.4) and try to connect them by global RG flows as outline in the Wilsonian approach *i* to *iii* on page 57. Scale invariant theories with Poincaré symmetries give rise to conformal theories which are invariant under the conformal group $SO(2,d)$ in d dimensions. Since at the fixed point the couplings remain invariant under a change in the characteristic length scale u, the geometry of scale invariant fixed point theories must be scale invariant under $x \longrightarrow c^{-1}x$ and $u \longrightarrow c^{-1}u$, which is realized by the AdS-space with metric[34]

$$\mathrm{d}s^2 = \frac{L^2}{u^2}\left(-\mathrm{d}t^2 + \mathrm{d}\mathbf{x}^2 + \mathrm{d}u^2\right). \tag{3.88}$$

Note that the isometries of the AdS-spacetime in $d+1$ dimensions $SO(2,d)$ is exactly the conformal group in d dimensions. The crucial question arises, which fixed point is described by the AdS-spacetime. Clearly, we need to start with the microscopic theory in the UV in order to define the couplings g^a of the underlying lattice theory in terms of physical microscopic interaction strengths J^a. Thus, we rediscover the holographic dictionary entry that the field living in the bulk geometry of the AdS-spacetime must correspond to the microscopic couplings in the UV, *i.e.*

$$g^a(x)\Big|_{\mathrm{UV}} = J^a(x) = \varphi^a(x,u)\Big|_{u=0} = \varphi^a(x)\Big|_{\partial(\mathrm{AdS})}. \tag{3.89}$$

Here we can make the relation between the scaling dimension and the nature of the associated operator clear. The coefficient $\varphi_{d-\Delta}$ of the leading term in the boundary expansion of the field scales with $d-\Delta$ under scaling transformations, which is exactly the eigenvalue y_J of a scaling field close to the fixed point (see (2.123)). The scaling dimension of the operator is related to the scaling of the source field by $y_J = d - \Delta_O$. The behavior in the vicinity of the fixed point is thus controlled by the mass of the bulk field. According to Table 3.3, for a scalar field with mass m the corresponding scaling field of the operator is relevant when $y_J > 0$ which corresponds to $\Delta < d$ and $-d^2/4L^2 < m^2 < 0$. For $m = 0$ we find $\Delta = d$ and thus a marginal operator $y_J = 0$, whereas for $m > 0$, $\Delta > d$ and $y_J < 0$ the operator is irrelevant. Similarly, for all other bulk fields listed in Table 3.3 we can do the same analysis. Additionally, from (3.89) follows that the bulk fields in AdS-spacetime must carry the same quantum numbers and charges as the corresponding couplings. Since the effective action at an RG fixed point is a conformal field theory we can extend the dictionary by identifying the coupling with the sources of the effective CFT action (2.156)

$$S_{\mathrm{source}} = \int \mathrm{d}^d x \left(\varphi^a(x)\mathcal{O}_a(x) + A^a_\mu J^\mu_a + g_{\mu\nu}T^{\mu\nu}\right), \tag{3.90}$$

which in turn correspond to the associated bulk fields via (3.89) with the same structure, *i.e.* the effective action of the bulk theory includes scalar fields $\varphi(x,u)$ for each scalar operator $\mathcal{O}$, vector (gauge) fields $A_A(x,u)$ for each current J^μ and a spin-two field g_{AB} for the canonical energy momentum tensor $T^{\mu\nu}$, arising due to Polyakov's Theorem on page 65. The existence of a spin-two field is the key to the gauge/gravity correspondence. According to the Weinberg-Witten theorem, and precursors [91, 199], a Lorentz invariant spin-two field theory describes a topological theory which would not affect the couplings/sources of the QFT side or couple universally due to the equivalence principle which effectively describes gravity. Thus, the AdS-spacetime arises

[34] Strictly speaking we work in Euclidean signature which corresponds to a statistical system, but we like to replace the computation of physical quantities such as thermodynamic and transport properties by a gravitational computation with the gravity dual. As we will shortly see, we can extend the holographic dictionary to include calculations involving correlation functions by real-time calculations as is made explicit in the holographic fluctuation-dissipation theorem (3.102) discussed in Section 3.5.1.

from a gravitational theory described by classical gravity with negative cosmological constant $\Lambda = {}^{d(d-1)}/_{2L^2}$

$$S_{\text{AdS}} = \frac{1}{2\kappa^2}\int \mathrm{d}^{d+1}x\,\sqrt{-g}\Big(R - 2\Lambda + \mathscr{L}_{\text{matter}}[\varphi, A_A]\Big). \tag{3.91}$$

Note that the energy-momentum tensor of the gravitational bulk theory is given by (3.3)

$$T_{AB} = -\frac{2}{\sqrt{-g}}\frac{\delta(\sqrt{-g}\mathscr{L}_{\text{matter}})}{\delta g^{AB}} = -2\frac{\delta\mathscr{L}_{\text{matter}}}{\delta g^{AB}} + g_{AB}\mathscr{L}_{\text{matter}}, \tag{3.92}$$

or[35]

$$T^{AB} = \frac{2}{\sqrt{-g}}\frac{\delta(\sqrt{-g}\mathscr{L}_{\text{matter}})}{\delta g_{AB}}, \tag{3.93}$$

and must not be confused with the energy-momentum tensor of the boundary conformal field theory. In summary, the UV fixed point conformal quantum field theory in d dimensions can be viewed as the boundary of a $d+1$ dimensional gravitational theory described by an AdS-spacetime. The source of the conformal energy-momentum tensor is the boundary value of the spacetime metric and the matter fields in the bulk AdS-spacetime describe the dynamics of the couplings under the RG flow of the quantum field theory operators. The boundary values of these matter fields correspond to the UV fixed point couplings.

3.4.2. Finite temperature & density deformations

In order to understand the global RG flow diagram and critical phenomena, we need to deform the fixed point CFT by relevant deformations allowing us to flow to other fixed points. Generically, the β-functions encoding the global RG flow are not accessible in complicated strongly coupled or strongly correlated systems. A holographic realization of fixed point deformation is realized by deforming the spacetime geometry in such a way that we recover the AdS-spacetime asymptotically. This amounts to a theory with a UV fixed point and a non-trivial IR behavior. Such a scenario is known from almost all condensed matter theories, where the short-range microscopic theory is known, but the long-range/low-energy behavior emerges non-trivially from the microscopic degrees of freedom. There are many possibilities for non-trivial IR geometries, but the holographic principle provides us already with the most simple ones. In order to define a field theory with thermodynamic properties as temperature, entropy and a free energy, we may consider a black hole geometry with horizon at $u = u_{\text{H}}$ which approaches AdS-spacetime asymptotically for $u \to 0$. Two well-known AdS-black hole solutions to Einstein's equations with negative cosmological constant are given by the AdS-Schwarzschild and AdS-Reissner-Nordström black hole, extensively discussed in Chapter 4 and applied to render a holographic dual of superconductors and charged superfluids. Therefore, our holographic dictionary can be extended by including thermal field theories with finite temperature, set by the Hawking temperature (3.7) T_{H}, finite entropy, defined by the black hole horizon or the Bekenstein-Hawking entropy S_{BH} (3.8) and a finite chemical potential related to the charge of the Reissner-Nordström black

[35] The minus sign arises from

$$\delta\left(g^{AB}g_{BC}\right) = 0 \qquad \Rightarrow \qquad \delta g^{AB} = -g^{AC}g^{BD}\delta g_{CD}$$

and

$$g_{AC}g_{BD}T^{AB} = T_{CD} = \frac{2}{\sqrt{-g}}\underbrace{g^{AC}g^{BD}\frac{\delta g^{CD}}{\delta g_{AB}}}_{=-1}\frac{\delta(\sqrt{-g}\mathscr{L}_{\text{matter}})}{\delta g^{CD}}.$$

Boundary field theory in d dimensions				Bulk gravity in $d+1$ dimensions
Global current	$J^\mu(x)$	$\rightleftharpoons$	$A_A(x,u)$	Gauge field
	$A_\mu(x)$	$\rightleftharpoons$	$A_A(x,u)\big\vert_{\partial(\text{AdS})}$	
	$\langle J^\mu(x)\rangle$	$\rightleftharpoons$	$\Pi[A]^A(x,u)\big\vert_{\partial(\text{AdS})}$	
Energy-momentum tensor	$T^{\mu\nu}(x)$	$\rightleftharpoons$	$g_{ab}(x,u)$	spacetime metric
	$g^{\mu\nu}(x)$	$\rightleftharpoons$	$g_{AB}(x,u)\big\vert_{\partial(\text{AdS})}$	
	$\langle T^{\mu\nu}(x)\rangle$	$\rightleftharpoons$	$\Pi[g]^{AB}(x,u)\big\vert_{\partial(\text{AdS})}$	
Entropy	S	$\rightleftharpoons$	S_{BH}	Bekenstein-Hawking entropy
Free energy	F	$\rightleftharpoons$	I_{Gravity}	Euclidean on-shell action
Temperature	T	$\rightleftharpoons$	T_{H}	Hawking Temperature
Chemical potential	μ	$\rightleftharpoons$	Q_{BH}	Charge of black hole

Table 3.5. From the holographic RG flow viewpoint the couplings of the strongly coupled QFT correspond to the fields with the same symmetries, quantum numbers and tensorial structure in the gravitational theory. The UV fixed point couplings are the sources of the fixed point CFT operators that correspond to the boundary values of the fields in asymptotic AdS spacetime.

hole. According to Table 2.1, once we have a thermal field theory, the thermodynamic potentials such as the free energy are determined by the logarithm of the partition function. In the case of gauge/gravity dualities we may employ the saddle-point approximation to the gravitational theory for strongly coupled field theories and thus the thermodynamic potentials reduce to the regularized Euclidean on-shell action. The extended holographic dictionary is listed in Table 3.5. The non-trivial geometry arises from a matter Lagrangian[36] $\mathscr{L}_{\text{matter}}$ designed in such a way that the boundary values of the matter fields correspond to the sources of the strongly coupled QFT we want to describe holographically. In general, the so-called backreaction of the matter fields onto the simple AdS geometry generates the non-trivial IR geometries which arise as consistent solutions of Einstein's equations with negative cosmological constant, *c.f*. Figure 3.13. Apart from the black hole solutions there are scaling solutions for non-trivial IR fixed points and there are other geometries like hard-wall solutions with a hard cut-off in the geometry introducing a mass-gap, or solitonic solutions connecting two AdS-spaces with different radii. There are also more exotic black hole solutions, such as the dionic black hole, including sources for magnetic fields. The main task to apply holography to physical systems is to identify the correct gravitational dual encoding the properties of the system and consistently solve the coupled equations of motion with two constraints. The first constraint arises from regularity in the IR, *i.e*. infalling boundary conditions at the black-hole horizon, that fixes one of the two solutions of the bulk equations of motion. The second constraint is that the geometry must be asymptotically AdS at the boundary, *i.e*. approach the UV fixed point CFT. In the next section, we will describe how

[36] In the following, we typically denote every Lagrangian including non-gravitational degrees of freedom as matter Lagrangian, including gauge fields or other massless fields.

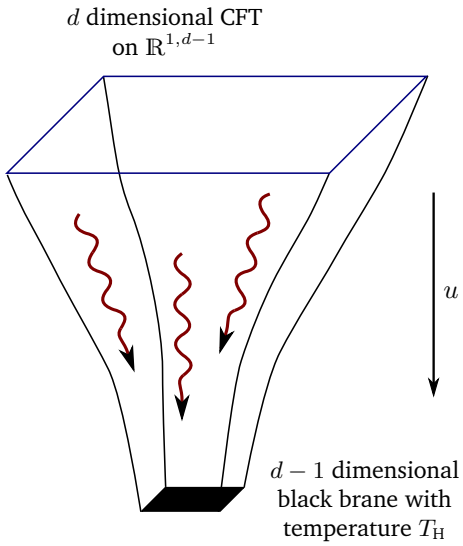

Figure 3.13.
The IR geometry is deformed by a relevant operator which corresponds to a AdS-black-hole geometry, where the boundary is still asymptotic AdS-space corresponding to a UV fixed point CFT. More accurately, the black hole is a spatially infinite black brane extending across the flat spatial direction of the field theory. The black brane horizon sets the temperature of the deformed UV fixed point CFT, but the matter content on the gravity side is introduced at zero temperature. As explained in Section 3.5, fluctuations about the background solution to the full Einstein equations are related to dissipative effects described by the infalling bulk field fluctuations. For charged black branes, the electric flux emanating from the black brane horizon sets the charge density on the boundary field theory.

to retrieve physical properties in terms of response functions by applying linear response theory from Section 2.2 to our holographic setup.

3.5. Linear Response & Holography

Overview

- Transport processes of strongly correlated systems can be computed via the holographic fluctuations-dissipation theorem.
- Response functions are related to correlators of fluctuations about background solutions of Einstein's equation.
- Finite temperature relaxation can be traced back to fluctuations being "swallowed" by black holes/branes.

As we have seen in the previous section, thermodynamic properties of physical systems are holographically described by asymptotically AdS-black-hole geometries. In order to probe the systems beyond thermodynamics to determine their transport behavior and to extend the holographic dictionary to general response functions, we need to reformulate the Fluctuation-Dissipation Theorem on page 30 in terms of bulk field fluctuations.

3.5.1. Holographic fluctuation-dissipation theorem

In Section 3.4.1 we already derived correlation functions which can be reduced easily to linear response Green functions. The linear response Green function is defined as the ratio of the response of the system $\langle O \rangle$ to an infinitesimal external source J. This allows us to reduce the functional derivative to a simple division due to the linear dependence of the expectation value to the source. According to the holographic dictionary listed in Table 3.4 and 3.5, the vacuum expectation value of an operator is given by the subleading term in the boundary expansion φ_Δ

and the corresponding source by the leading term $\varphi_{d-\Delta}$, respectively. Applying the holographic dictionary and inserting (3.82) we find

$$G(k) = \frac{\langle\, O(k)\,\rangle}{J(k)} = \lim_{u\to 0} u^{2(\Delta-d)}\,\frac{\Pi(k,u)}{\Phi(k,u)}. \tag{3.94}$$

However, to compute the Green function of real-time processes in this manner poses a serious problem. First of all, the Euclidean Green function should by analytically continued, which is only possible if an analytic solution relating φ_Δ to $\varphi_{d-\Delta}$ is known. As we already hinted at in the last paragraph of Section 3.4.2 for general bulk fields this solution cannot be obtained in closed analytical form and we need to resort to asymptotic expansions or even numerical solutions. Secondly, a direct calculation in real time is not feasible because we would need to modify the holographic dictionary concerning the equivalence of the partition functions of the field theory and the gravity side to

$$\left\langle\, \mathrm{e}^{\mathrm{i}\int \mathrm{d}^d x\, J(x)O(x)} \,\right\rangle_{\mathrm{QFT}} = \mathrm{e}^{\mathrm{i}S_{\mathrm{GR}}}\Big|_{\varphi_{\partial(\mathrm{AdS})}=J}. \tag{3.95}$$

As discussed in [78, 200] for real-time Minkowski spacetime the regularity condition at the black hole horizon is insufficient to obtain a unique solution. This corresponds to the existence of multiple real-time Green functions, the retarded G^{R}, the advanced G^{A} and the time-ordered Green function G^{T} (2.74) in contrast to the unique imaginary time Green function G^{τ} (2.75). Luckily, there exists a powerful method, known as the Keldysh formalism, that circumvents various problems arising in treatments of complex systems[37] *i.a.* equilibrium and close-to-equilibrium problems where the analytical continuation from Matsubara frequencies fails. Let us postpone the discussion of the Keldysh formalism to Section 3.5.2 and give the correct prescription to compute response functions in holography via the fluctuation-dissipation theorem:

i. Solve the background equations of motions arising from the effective classical gravity action of the holographic dual to the field theory. The solution describes the stationary thermal equilibrium state.

ii. Expand the classical effective action in fluctuations about the background $\delta\varphi = \varphi - \varphi^{\mathrm{B}}$ up to second order. The solution φ^{B} to the "classical" background equations of motion minimizes the action and hence the first order term in the expansion vanishes. This is in direct analogy to the saddle-point expansion in (2.19) where the classical solution corresponds to the background solution φ^{B} of the system in equilibrium and the time corresponds to the radial direction u

$$S[\varphi] \approx S[\varphi^{\mathrm{B}}] + \frac{1}{2}\int \mathrm{d}t\,\mathrm{d}t' \int \mathrm{d}^{d-1}\mathbf{x}\,\mathrm{d}^{d-1}\mathbf{x}' \int \mathrm{d}u\,\mathrm{d}u' \times \left[\delta\varphi(t,\mathbf{x},u)\,\frac{\delta^2 S[\varphi]}{\delta\varphi(t,\mathbf{x},u)\delta\varphi(t',\mathbf{x}',u')}\Big|_{\delta\varphi=0}\,\delta\varphi(t',\mathbf{x}',u')\right]. \tag{3.96}$$

For homogeneous and isotropic fluctuations and a time translational invariant system the fluctuation action may be Fourier transformed in time and spatial coordinates

$$\varphi(t,\mathbf{x},u) = \int \frac{\mathrm{d}\omega\,\mathrm{d}^{d-1}\mathbf{k}}{(2\pi)^d}\,\mathrm{e}^{-\mathrm{i}\omega t + \mathrm{i}\mathbf{k}\cdot\mathbf{x}}\,\varphi(\omega,\mathbf{k},u), \tag{3.97}$$

[37] To whet the reader's appetite for the versatility of the Keldysh formalism let us advertise some of its advantages and range of applications: non-equilibrium systems, determination of the full statistics of quantum observables, and treatment of disordered systems/metals/superconductors.

so (3.96) reduces to

$$S[\varphi] \approx S[\varphi^{\mathrm{B}}] + \frac{1}{2}\int \frac{\mathrm{d}\omega\, \mathrm{d}^{d-1}\mathbf{k}}{(2\pi)^d}\, \mathrm{d}u\, \delta\varphi(-\omega,-\mathbf{k},u)\mathcal{G}(\omega,\mathbf{k},u)\delta\varphi(\omega,\mathbf{k},u). \tag{3.98}$$

iii Solve the respective linearized equations of motions for the fluctuations in Fourier space with fixed boundary conditions at the asymptotically AdS boundary u_{B} *i.e.* $\varphi(u_{\mathrm{B}}) = \varphi_0$

$$\delta\varphi(\omega,\mathbf{k},u) = \delta\varphi_{\partial(AdS)}(\omega,\mathbf{k}) f_{\text{bulk}}(\omega,\mathbf{k},u), \qquad f_{\text{bulk}}(\omega,\mathbf{k},u_{\mathrm{B}}) = 1, \tag{3.99}$$

and infalling wave conditions at the black hole horizon u_{H}

$$f_{\text{bulk}}(\omega,\mathbf{k},u) \sim (u_{\mathrm{H}} - u)^{-\mathrm{i}\omega\gamma}, \tag{3.100}$$

where $\gamma > 0$ describes wave propagation into the black hole. Here, the ingoing boundary condition at the horizon corresponds to the retarded Green functions $G^{\mathrm{R}}(k)$, whereas the outgoing boundary condition corresponds to the advanced Green function $G^{\mathrm{A}}(k) = [G^{\mathrm{R}}(k)]^* = G^{\mathrm{R}}(-k)$ due to "time reversal" in $k \longrightarrow -k$ or $\omega \longrightarrow -\omega$.

iv Insert the solution to obtain the boundary on-shell action[38] quadratic in the fluctuations

$$S_{\text{on-shell}} = \frac{1}{2}\int \frac{\mathrm{d}\omega\, \mathrm{d}^{d-1}\mathbf{k}}{(2\pi)^d} \delta\varphi_0(-\omega,-\mathbf{k})\mathcal{G}(\omega,\mathbf{k},u)\Big|_{u_{\mathrm{B}}}^{u_{\mathrm{H}}} \delta\varphi_0(\omega,\mathbf{k}). \tag{3.101}$$

According to the holographic dictionary, the Green function is given by the second derivative of the regularized Euclidean(!) on-shell action. Since we are looking for a real-time solution we cannot rely on the naïve prescription following from the dictionary. Here the solution of the Keldysh formalism is crucial, which can be obtained explicitly from a genuine Keldysh calculation as done in [79]. Thus, the retarded Green function only takes contributions from the boundary into account, whereas surface terms from the horizon are omitted

$$G^{\mathrm{R}}(\omega,\mathbf{k}) = -2\mathcal{G}(\omega,\mathbf{k},u)\Big|_{u=u_{\mathrm{B}}}. \tag{3.102}$$

Heuristically, this is quite clear, since the Keldysh formalism is ignorant to the interior of the AdS-spacetime, only the radial evolution under the proper boundary conditions can affect the Green function, but not the boundary conditions at the horizon.

This prescription will be heavily applied in all the subsequent calculation and is the cornerstone of applied holography. Pictorially, the infalling wave condition at the black hole horizon renders the dissipation of the system, allowing for the relaxation to its equilibrium state, whereas the fluctuation about the background solution can be viewed as the initial perturbation of the field theory at the boundary propagating into the bulk and being swallowed by the black hole.

3.5.2. Short introduction to the Keldysh formalism

For completeness, we give a short overview of the Keldysh formalism [201], originally constructed for non-equilibrium problems. As it turned out, it is quite useful for a large variety of complicated interacting, disordered, or stochastic systems. Let us first recall how to calculate

[38] If needed, apply the holographic renormalization prescription to obtain a regularized finite on-shell action.

equilibrium expectation values (2.57) of observables in closed time contour as shown in Figure 3.14,

$$\langle\, O(t)\,\rangle = \frac{\mathrm{tr}(O\hat{\rho}(t))}{\mathrm{tr}\,\hat{\rho}(t)} = \frac{\mathrm{tr}(\mathcal{U}(-\infty,t)O\mathcal{U}(t,-\infty)\hat{\rho}(-\infty))}{\mathrm{tr}\,\hat{\rho}(-\infty)}, \tag{3.103}$$

where the unitary time evolution operator $\mathcal{U}(t',t)$ is defined in (2.1). In the last equality we used the cyclicity of the trace and the invariance under unitary evolution. Physically, the expression (3.103) can be viewed as an evolution of an equilibrium system described by the initial density matrix $\hat{\rho}(-\infty) = \hat{\rho}_0$ to the time t where the system is subject to measurement represented by the operator O and finally brought back to its initial equilibrium configuration at $t = -\infty$. The forward-backward evolution can be avoided for systems in equilibrium under the assumption that the ground state of the system evolves adiabatically, while interactions are slowly switched on. Therefore, extending the time evolution of the system to the distant future, $t \to \infty$ amounts to adding a phase factor $\langle\, 0 \,|\, \mathcal{U}(\infty,-\infty) = \langle\, 0 \,|\, \mathrm{e}^{\mathrm{i}\alpha}$. The additional phase factor can be factored out and so the backward segment of the closed time contour can be removed by subtracting the disconnected diagrams. However, for non-equilibrium systems the initial and final states are in general not identical, so the system could be relaxing into a different equilibrium state after it was driven out of the initial equilibrium state. The main idea to circumvent this problem is to keep the full closed time contour, where we start and end with a "trivial" description of our system, adiabatically switch on the "non-trivial" interactions and switch them off on our way back, *i.e.*

$$\langle\, O(t)\,\rangle = \frac{\mathrm{tr}(\mathcal{U}(-\infty,\infty)\mathcal{U}(\infty,t)O\mathcal{U}(t,-\infty)\hat{\rho}(-\infty))}{\mathrm{tr}\,\hat{\rho}(-\infty)}. \tag{3.104}$$

In this case we do not need to know the state of the system at $t \to \infty$ nor do we accumulate a phase and so there is no denominator and no need to subtract diagrams. As a consequence the partition function reads

$$Z[0] = \frac{\mathrm{tr}(\mathcal{U}_{\mathcal{C}}\hat{\rho}(-\infty))}{\mathrm{tr}\,\hat{\rho}(-\infty)} = 1, \tag{3.105}$$

since $\mathcal{U}_{\mathcal{C}} = \mathcal{U}(-\infty,\infty)\mathcal{U}(\infty,-\infty) = \mathbb{1}$. For interacting systems the symmetry between the forward (upper) and backward (lower) parts of the contour is broken, so $\mathcal{U}_{\mathcal{C}}[V] \neq \mathbb{1}$. Nonetheless, the denominator in the definition of the correlation functions (2.29) is absent.[39] Now redoing the steps of constructing the functional integral $\mathcal{ii}$ to $\mathcal{iii}$ on page 15, we obtain for the closed time contour partition function

$$Z = \frac{1}{\mathrm{tr}(\hat{\rho}_0)} \int \left(\prod_{k=1}^{2N} \mathrm{d}\varphi_k \right) \exp\left(\mathrm{i} \sum_{i,j=1}^{2N} \varphi_i G^{-1}_{ij} \varphi_j \right), \tag{3.106}$$

with indices i, j, k running from one to $2N$ in the discretization of the closed time contour as shown in Figure 3.14. The propagator is given by a $2N \times 2N$ matrix of the form

[39] This drastically simplifies the treatment of disordered systems and poses an alternative to replica [202] or supersymmetric approaches [203] in removing the denominator.

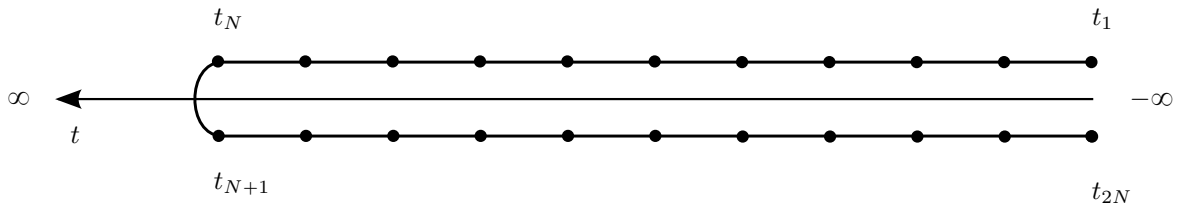

Figure 3.14. Discretized close time contour used to determine the expectation value of a physical observable. The computation must be independent of the initial conditions/-preparation of the system, so we can take $t_1 \to -\infty$ where the system is in equilibrium described by $\hat{\rho}(-\infty) = \hat{\rho}_0$. The system is measured at a specific time t by an insertion of the respective operator and then brought back to its equilibrium state at t_{2N}. For a symmetric extension of the adiabatically increased interactions, we can enhance the time evolution domain to ∞. For equilibrium measurements the backward time evolution amounts to a phase factor $\mathrm{e}^{\mathrm{i}\alpha}$ which can be removed by subtracting the disconnected diagrams. For non-equilibrium systems the initial state at $t = -\infty$ and the final state at $t = \infty$ are in general not identical equilibrium states, so the backward evolution cannot be omitted. The full propagator of the closed time contour consists of forward propagation from t_1 to t_N, backward propagation from t_{N+1} to t_{2N}. The points t_N and t_{N+1} are identified as well as t_1 and t_{2N} which are controlled by the density matrix $\hat{\rho}_0$ describing the equilibrium system. Sometimes the density matrix is resolved as imaginary time evolution from t_{2N} to $t_{2N} - \mathrm{i}\beta$ which is then identified with t_1.

$$\mathrm{i}G^{-1} = \left(\begin{array}{ccccc|ccccc} -1 & & & & & & & & & \hat{\rho}_0 \\ h_- & -1 & & & & & & & & \\ & h_- & -1 & & & & & & & \\ & & \ddots & \ddots & & & & & & \\ \hline & & & & 1 & -1 & & & & \\ & & & & & h_+ & \ddots & & & \\ & & & & & & \ddots & -1 & & \\ & & & & & & & h_+ & -1 & \end{array}\right), \tag{3.107}$$

where $h_\pm = 1 \pm \mathrm{i}H(\varphi_i, \varphi_{i-1})\Delta t$ follows from the time evolution from step t_i to $t_{i+1} = t_i + \Delta t$ and the diagonal entries from the resolution of unity. The top-left block describes the forward time evolution whereas the bottom-right block describes the backward evolution and the bottom-left and top-right the correlation between forward and backward evolution and vice versa. Thus, the single entry in the forward-backward block follows from the identification of t_N with t_{N+1} and the upper right entry in the backward-forward block from the matrix element of the density matrix connecting the equilibrium states at t_{2N} and t_1. The last step *iii* on page 15 in the program of constructing a true field theory poses some problems. Naïvely taking the continuum limit we lose the correlation between the different contours, in particular the statistical information encoded in the equilibrium density matrix ρ_0. To keep the correlations between the forward and backward parts of the closed time contour, we need to introduce fields with two independent components related to the forward and backward branch. Then the action in (3.106) is written

as

$$S = \int \mathrm{d}t\,\mathrm{d}t' \begin{pmatrix} \varphi^+ & \varphi^- \end{pmatrix}(t) \begin{pmatrix} G^{++} & G^{+-} \\ G^{-+} & G^{--} \end{pmatrix}^{-1} (t,t') \begin{pmatrix} \varphi^+ \\ \varphi^- \end{pmatrix}(t'). \tag{3.108}$$

Computing the formal[40] Gaussian integral (2.45) yields the individual Green functions

$$\begin{aligned}
\left\langle \varphi^+\varphi^+ \right\rangle &= \mathrm{i}G^{++}(t,t') = \mathrm{i}G^{\mathbb{T}}(t,t') = \frac{1}{\det(-\mathrm{i}G^{-1})} \lim_{\substack{N\to\infty \\ \Delta t\to 0}} (h_-)\,, \\
\left\langle \varphi^+\varphi^- \right\rangle &= \mathrm{i}G^{+-}(t,t') = \mathrm{i}G^{<}(t,t') = \frac{\rho_0}{\det(-\mathrm{i}G^{-1})} \lim_{\substack{N\to\infty \\ \Delta t\to 0}} (h_+h_-)\,, \\
\left\langle \varphi^-\varphi^+ \right\rangle &= \mathrm{i}G^{-+}(t,t') = \mathrm{i}G^{>}(t,t') = \frac{1}{\det(-\mathrm{i}G^{-1})} \lim_{\substack{N\to\infty \\ \Delta t\to 0}} (h_+h_-)\,, \\
\left\langle \varphi^-\varphi^- \right\rangle &= \mathrm{i}G^{--}(t,t') = \mathrm{i}G^{\overline{\mathbb{T}}}(t,t') = \frac{1}{\det(-\mathrm{i}G^{-1})} \lim_{\substack{N\to\infty \\ \Delta t\to 0}} (h_+)\,,
\end{aligned} \tag{3.109}$$

where $G^{\overline{\mathbb{T}}}$ denotes the anti-time ordered Green function. Using

$$\begin{aligned}
G^{\mathbb{T}}(t,t') &= \Theta(t-t')G^{>}(t,t') + \Theta(t'-t)G^{<}(t,t'), \\
G^{\overline{\mathbb{T}}}(t,t') &= \Theta(t'-t)G^{>}(t,t') + \Theta(t-t')G^{<}(t,t'),
\end{aligned} \tag{3.110}$$

one can show that not all of the above Green functions are independent, in fact

$$G^{\mathbb{T}} + G^{\overline{\mathbb{T}}} = G^{<} + G^{>}. \tag{3.111}$$

This identity holds for all $t \neq t'$, whereas for $t = t'$ it is violated. This follows from the relationship to the spectral function $\mathscr{A}$ defined in (2.77)

$$\mathscr{A}(t,\mathbf{x},t'\mathbf{x}) = \mathrm{i}\left(G^{\mathrm{R}}(t,\mathbf{x},t'\mathbf{x}) - G^{\mathrm{A}}(t,\mathbf{x},t'\mathbf{x})\right) = \mathrm{i}\left(G^{<}(t,\mathbf{x},t'\mathbf{x}) - G^{>}(t,\mathbf{x},t'\mathbf{x})\right), \tag{3.112}$$

where for $t = t'$ the spectral function is independent of the state of the system and thus given by $\mathscr{A}(t,\mathbf{x},t','x) = \delta(\mathbf{x}-\mathbf{x}')$. Mathematically, this forces us to take the normalization of the Heaviside distribution $\Theta(0) = 1$. Thus, in order to work with the "physical" Green functions we apply the so-called Keldysh rotation, a linear transformation in the two dimensional Keldysh space

$$G \longrightarrow G = UGU^{-1} = \begin{pmatrix} G^{\mathrm{K}} & G^{\mathrm{R}} \\ G^{\mathrm{A}} & 0 \end{pmatrix} \qquad \text{with} \qquad U = \frac{1}{\sqrt{2}} \begin{pmatrix} 1 & 1 \\ 1 & -1 \end{pmatrix}, \tag{3.113}$$

and

$$\varphi \longrightarrow U\varphi = \begin{pmatrix} \varphi^{\mathrm{cl}} \\ \varphi^{\mathrm{q}} \end{pmatrix} = \frac{1}{\sqrt{2}} \begin{pmatrix} \varphi^+ + \varphi^- \\ \varphi^+ - \varphi^- \end{pmatrix}, \tag{3.114}$$

[40] The convergence of the integral is ensured by the Keldysh component of the Keldysh rotated Green function (3.117).

with the Green function definitions

$$\begin{aligned} G^{\mathrm{R}}(t,t') = G^{\mathrm{cl\,q}} &= \frac{1}{2}\left(G^{\mathbb{T}} - G^{\overline{\mathbb{T}}} + G^{>} - G^{<}\right) = \Theta(t-t')\left(G^{>} - G^{<}\right), \\ G^{\mathrm{A}}(t,t') = G^{\mathrm{q\,cl}} &= \frac{1}{2}\left(G^{\mathbb{T}} - G^{\overline{\mathbb{T}}} - G^{>} + G^{<}\right) = \Theta(t'-t)\left(G^{<} - G^{>}\right), \\ G^{\mathrm{K}}(t,t') = G^{\mathrm{cl\,cl}} &= \frac{1}{2}\left(G^{\mathbb{T}} + G^{\overline{\mathbb{T}}} + G^{>} + G^{<}\right) = G^{<} + G^{>}. \end{aligned} \tag{3.115}$$

Note that the Keldysh Green function is antihermitian, *i.e.* $(G^{\mathrm{K}})^{\dagger} = -G^{\mathrm{K}}$. Taking the inverse of the Keldysh rotated Green function (3.113) leads to the action in Keldysh form

$$S\left[\varphi^{\mathrm{cl}}, \varphi^{\mathrm{q}}\right] = \int \mathrm{d}t\, \mathrm{d}t' \begin{pmatrix} \varphi^{\mathrm{cl}} & \varphi^{\mathrm{q}} \end{pmatrix}(t) \begin{pmatrix} 0 & \left(G^{\mathrm{A}}\right)^{-1} \\ \left(G^{\mathrm{R}}\right)^{-1} & \left[G^{-1}\right]^{\mathrm{K}} \end{pmatrix}^{-1} (t,t') \begin{pmatrix} \varphi^{\mathrm{cl}} \\ \varphi^{\mathrm{q}} \end{pmatrix}(t'). \tag{3.116}$$

where the inverse of the 2×2 matrix yields a non-trivial inverse for the Keldysh component

$$\left[G^{-1}\right]^{\mathrm{K}} = \left(G^{\mathrm{R}}\right)^{-1} F - F \left(G^{\mathrm{A}}\right)^{-1}, \tag{3.117}$$

parametrized by the Hermitian matrix F to ensure the antihermiticity of the Keldysh Green function. In general, the Wigner transform of the F matrix yields the instantaneous particle distribution function at given time t. Some comments about the notation and physical interpretation of the action (3.116) are in order: First the superscripts 'q' and 'cl' stand for "quantum" and "classical", respectively. This notation is chosen because generically the classical-classical component of the action is zero, *i.e.* $S\left[\varphi^{\mathrm{cl}}, 0\right] = 0$, since we are dealing with a quantum statistical system. Secondly, the antihermitian quantum-quantum component ensures the convergence of the functional integral and encodes the information about the distribution function of the statistical system. Last, but not least, the classical-quantum components encode the causal structure of the physical system. In particular, the Fluctuation-Dissipation Theorem on page 30 can be restated using the Keldysh Green function as

$$G^{\mathrm{K}}(\omega) = 2\mathrm{i}\,\mathrm{Im}\, G^{\mathbb{T}}(\omega). \tag{3.118}$$

We see that the imaginary part of the response function $\mathrm{Im}(\omega)$ characterizing the dissipation of the system is related to the equilibrium fluctuations encoded in $G^{\mathrm{K}}(\omega)$. More details about applications of the Keldysh formalism can be found in [51, 52, 204]. In the holographic context the Keldysh formalism has been used to prove (3.102) explicitly [79]. The causality structure of the Keldysh action is only satisfied if we define the retarded (advanced) Green function as

$$G^{\mathrm{R}}(\omega, \mathbf{k}) = -2\mathcal{G}(\omega, \mathbf{k}, u)\Big|_{u=u_{\mathrm{B}}}. \tag{3.119}$$

On the other hand, the Euclidean Green function can be converted into the Keldysh formalism which allows us to identify the correlation functions for thermal theories in equilibrium with the Green functions in the Keldysh formalism. Of course, this is applicable only to transport problems in equilibrium, for non-equilibrium calculations the holographic dictionary needs to be extended.[41]

[41] Approaches to render the equilibration process in holographic duals involve black hole generations by colliding gravitational shock waves.

With the working prescription for linear response theory, we close our survey of holography and apply it to concrete physical systems and their respective gravitational duals. In particular, all the machinery derived in this chapter and Chapter 2 can be used to tackle strongly correlated systems where the intractable field theoretical treatment without quasi particles is mapped to weakly coupled gravity duals, that allow for the applicability of our beloved perturbative tools again unfolding their power to describe physical systems.

4

Universal Properties in Holographic Superconductors

Our first application of the holographic dictionary and the weak/strong duality will be a bottom-up approach geared towards condensed matter applications. As advertised in the introduction to this thesis, we are looking for universal physical quantities that do not depend on the microscopical details but are rather defined by universality classes in the Wilsonian sense. In particular for the classification of novel states of quantum matter arising in quantum critical regions, strongly correlated quantum liquids or high temperature superconductors, the gauge/gravity duality can provide valuable insight and might even succeed to quantify some of the dimensionless functions that are not fixed by symmetries of the effective field theory. In this chapter we will explore the holographic superconductors aiming at the understanding of universal features, such as *Homes' law* and some of its cousins as *Tanner's law* to be explained in detail below. The holographic superconductors are endowed with key features reminiscent of real superconductors, *e.g.* there is a charged condensate which gives rise to a massive vector boson in the spirit of the Higgs mechanism, although the Meißner-Ochsenfeld effect is absent. Yet, a redistribution of spectral weight opens an energy gap in the optical conductivity and allows for an infinite DC conductivity or vanishing resistivity. The removed local $U(1)$ gauge symmetry on the gravity side translates to a removed global $U(1)$ gauge symmetry, so the holographic superconductor may be viewed as a strongly correlated charged superfluid. In this sense there is no true dynamical photon on the field theory side since the gauge field only sources the charged density of the system. However, we may allow for local transformation of the external source which in turn lifts the global $U(1)$ symmetry to a background local $U(1)$ symmetry. As explored in [205], the additional background local $U(1)$ symmetry permits the computation of response functions related to strongly coupled superconductors described by an effective Abelian Higgs model. The order parameter for the superconducting phase transition is identified with the vacuum expectation value of the operator dual to a bulk field with no source turned on in order to mimic a spontaneous symmetry breaking mechanism. To date there are holographic duals known for s- and p-wave superconductivity [206–208] and there are some ideas how to construct a d-wave type holographic superconductor [209–211]. Holographic superconductors have been studied extensively, numerically

as well as analytically [212–214]. There are also explicit top-down constructions employing a true D-brane setup where the field theory is explicitly known [215–217].

In this chapter I will present my work on holographic superconductors. Operationally, I have verified most of the numerical calculations presented in [218,219] in order to test the validity of my numerical approach for applications of the holographic dual to open questions in real world superconductors. In particular, the empirically found *Homes' law* to be discussed in Section 4.4 is the central focus of my work on holographic superconductors. All results obtained to understand a holographic realization of Homes' law presented in Section 4.4 are original and first published in [1]. To my knowledge, the s-wave equations of motion for arbitrary values of the charged scalar field's mass and the system's dimensionality have not been explicitly derived so far. In the first part of this chapter we will discuss the properties of holographic s- and p-wave superconductors and determine their phase diagrams. In the second part, an empirically found universal relation, the so-called *Homes' law*, between the superfluid density at zero temperature and the conductivity at the critical temperature times the critical temperature is explained and a possible holographic realization is proposed. In a way, our approach to Homes' law can be viewed analogously to the famous ratio of shear viscosity to entropy density η/s of the quark-gluon plasma with an important difference: for a hydrodynamic calculation the shear viscosity is determined by the metric fluctuations about the background metric. Thus the universality of η/s follows directly from the equivalence principle, *i.e.* the metric must couple globally to all forms of energy with a single coupling constant. Adding another coupling constant characterizing the charge of the scalar field which is independent of the metric field, however, complicates this simple universality in a non-trivial way. Finally, in the last part the results obtained from our proposed holographic realization of Homes' law, are analyzed.

4.1. Holographic s-Wave Superconductor

Overview

- Einstein-Maxwell action with minimally coupled scalar field
  $\longrightarrow$ Abelian-Higgs model describes holographic superconductors.
- Background solutions with/without backreaction in condensed/normal phase
  $\longrightarrow$ charged/uncharged black brane with/without scalar hair.
- General linearized fluctuation equations for arbitrary values of the dimensionality and the scalar field mass.

Following the original construction of holographic s-wave superconductor [207, 218] we introduce the holographic Abelian Higgs model given by the Einstein-Maxwell action with a minimally coupled charged scalar field. The holographic dictionary relates the bulk $U(1)$ gauge field A_a to global $U(1)$ current J^μ and the charged scalar field Φ to a fermion condensate operator $O = \overline{\Psi}\Psi$, turning the massless gauge field into a massive vector field employing the Anderson-Higgs Mechanism on page 47. First, we will derive the full set of equations of motion for the bulk fields and then consider various special cases. Analytic solutions, if possible, are given for $d = 3$ and $d = 4$ and numerical solutions are determined using *Mathematica*. The concrete numerical setup will be explained in detail, some pedagogical simple excerpts are listed in Appendix D.

4.1.1. Einstein-Maxwell action & equations of motion

The best known (bottom up) holographic model to describe s-wave superconductivity is given by the Einstein-Maxwell action coupled to a charged scalar on the gravity side dual to a field theory with a conserved $U(1)$ current and an operator describing the condensate [29, 207, 218]. The Abelian Higgs model is given by the following action with a $U(1)$ gauge field A and the complex scalar field Φ

$$S = \frac{1}{2\kappa^2}\int \mathrm{d}^{d+1}x\,\sqrt{-g}(R-2\Lambda) + \int \mathrm{d}^{d+1}x\,\sqrt{-g}\left(-\frac{1}{4}F_{ab}F^{ab} - |\nabla\Phi - \mathrm{i}eA\Phi|^2 - V(|\Phi|)\right), \quad (4.1)$$

where R denotes the Ricci scalar, Λ the cosmological constant, F_{ab} the electromagnetic field strength, and $V(|\Phi|)$ is a potential for the charged scalar Φ, respectively. The indices a, b are running over the bulk coordinates, *i.e.* $a, b = 0, \ldots, d+1$, where d denotes the dimensionality of the physical system under consideration. Rescaling the gauge field $A \to eA$ and the scalar field $\Phi \to e\Phi$ allows us to write the action in the form

$$S = \int \mathrm{d}^{d+1}x\,\sqrt{-g}\left[\frac{1}{2\kappa^2}(R-2\Lambda) - \frac{1}{e^2}\left(\frac{1}{4}F_{ab}F^{ab} - |\nabla\Phi - \mathrm{i}A\Phi|^2 - V(|\Phi|)\right)\right]. \quad (4.2)$$

We can redefine the gravity coupling constant κ^2 and the electromagnetic coupling constant e^2 in a way to give a clear exposition when we need to consider the backreaction of the charged degrees of freedom on the geometry. Factoring out $1/2\kappa^2$, the action (4.2) can be rewritten as

$$\begin{aligned} S &= \frac{1}{2\kappa^2}\int \mathrm{d}^{d+1}x\,\sqrt{-g}\left[R - 2\Lambda - \frac{2\kappa^2}{e^2}\left(\frac{1}{4}F_{ab}F^{ab} + |\nabla\Phi - \mathrm{i}A\Phi|^2 + V(|\Phi|)\right)\right] \\ &= \frac{1}{2\kappa^2}\int \mathrm{d}^{d+1}x\,\sqrt{-g}\left[\mathscr{L}_{\mathrm{EH}} + \frac{2\kappa^2}{e^2}\mathscr{L}_{\mathrm{M}}\right] = S_{\mathrm{EH}} + S_{\mathrm{M}}. \end{aligned} \quad (4.3)$$

From the dimensionality of the fields in the action

$$[R] = [\Lambda] = (\text{length})^{-2}, \qquad [A_a] = [\Phi] = (\text{length})^{-1}, \qquad [F_{ab}] = (\text{length})^{-2}, \quad (4.4)$$

we can read off the dimensionality of the couplings

$$\left[\kappa^2\right] = (\text{length})^{d-1}, \qquad \left[e^2\right] = (\text{length})^{d-3}, \quad (4.5)$$

that renders the action S dimensionless. We can define a dimensionless coupling constant as a ratio of the two coupling constants κ and e, with the additional factor L^{-2} *i.e.*

$$\alpha^2 L^2 = \frac{\kappa^2}{e^2}, \qquad \left[\alpha^2\right] = 1, \quad (4.6)$$

describing the strength of the backreaction onto the geometry exerted by the gauge field and the scalar field. On the field theory side, this parameter describes the ratio of charged degrees of freedom to the total degrees of freedom and thus can be considered as an effective chemical potential or in a loose sense some kind of "doping". Operationally, e controls the charged degrees of freedom of the CFT related by the central charge connected to the current J^μ, dual to the gauge field $c_{\langle J_\mu J_\nu\rangle} \sim 1/e^2$, whereas κ controls the total degrees of freedom via $c_{\langle T_{\mu\nu}T_{\lambda\sigma}\rangle} \sim L^2/\kappa^2$ [220], so[1]

$$\alpha^2 \sim \frac{\kappa^2}{L^2e^2} \sim \frac{c_{\langle J_\mu J_\nu\rangle}}{c_{\langle T_{\mu\nu}T_{\mu'\nu'}\rangle}} \sim \frac{\#\text{ charged dof}}{\#\text{ total dof}}. \quad (4.7)$$

[1] In a true top-down approach the backreaction amounts to $\alpha^2 \sim \frac{\#\text{charged dof}}{\#\text{total dof}} = \frac{N_c N_f}{N_c^2}$.

The equations of motions for the complex valued, massive, charged scalar field Φ with mass m and charge e are given by

$$\begin{aligned}(\nabla_a + \mathrm{i}A_a)(\nabla^a + \mathrm{i}A^a)\Phi^* - \frac{1}{2}V'(|\Phi|)\frac{\Phi^*}{|\Phi|} = 0,\\ (\nabla_a - \mathrm{i}A_a)(\nabla^a - \mathrm{i}A^a)\Phi - \frac{1}{2}V'(|\Phi|)\frac{\Phi}{|\Phi|} = 0.\end{aligned} \tag{4.8}$$

By varying with respect to the gauge field A we find Maxwell's equations

$$\nabla^a F_{ab} = \mathrm{i}\left[\Phi^*(\nabla_b - \mathrm{i}A_b)\Phi - \Phi(\nabla_b + \mathrm{i}A_b)\Phi^*\right] = j_b, \tag{4.9}$$

with the current j_b defined as the right-hand side of the Maxwell equations. This expression can be simplified since for completely antisymmetric tensor fields the divergence is identical to that of a vector field which can be reduced to

$$g^{ab}\nabla_a A_b = \frac{1}{\sqrt{-g}}\partial_c\left(\sqrt{-g}g^{cd}A_d\right), \tag{4.10}$$

so we only need to consider

$$g^{st}\nabla_s F_{ta} = \frac{1}{\sqrt{-g}}g_{ab}{}^{2}\partial_c\left(\sqrt{-g}g^{bd}g^{ce}F_{ed}\right) = \frac{1}{\sqrt{-g}}g_{ab}\partial_c\left(\sqrt{-g}F^{cb}\right), \tag{4.11}$$

where we can work with simple partial derivatives ∂_a instead of the Levi-Civita connection ∇_a. Finally, varying with respect to the metric yields the Einstein equations

$$R_{ab} - \frac{1}{2}Rg_{ab} + \Lambda g_{ab} = -\frac{2}{\sqrt{-g}}\frac{\kappa^2}{e^2}\frac{\delta\left(\sqrt{-g}\mathscr{L}_{\mathrm{M}}\right)}{\delta g^{ab}} = \alpha^2 L^2 T_{ab}, \tag{4.12}$$

where the left-hand side represents the Einstein tensor G^{ab} and the right-hand side is the energy-momentum tensor of the rescaled fields $A \to eA$ and $\Phi \to e\Phi$ which give the additional factor $1/e^2$. The matter Lagrangian density $\mathscr{L}_{\mathrm{M}}$ is defined without the coupling constants, so the ratio $2\kappa^2/e^2$ is written as an explicit factor, in order to retain the usual definition of the energy-momentum tensor. The energy momentum tensor of $\mathscr{L}_{\mathrm{M}}$ can be split into two parts, an electromagnetic contribution denoted T^{em}_{ab} and the contribution T^{Φ}_{ab} arising from the charged scalar field

$$T_{ab} = T^{\mathrm{em}}_{ab} + T^{\Phi}_{ab}, \tag{4.13}$$

where

$$T^{\mathrm{em}}_{ab} = g^{cd}F_{ac}F_{bd} - \frac{1}{4}g_{ab}F_{cd}F^{cd}, \tag{4.14}$$

$$\begin{aligned}T^{\Phi}_{ab} = {}&(\nabla_a\Phi^* + \mathrm{i}A_a\Phi^*)(\nabla_b\Phi - \mathrm{i}A_b\Phi) + (\nabla_a\Phi - \mathrm{i}A_a\Phi)(\nabla_b\Phi^* + \mathrm{i}A_b\Phi^*)\\ &- g_{ab}(\nabla_c\Phi^* + \mathrm{i}A_c\Phi^*)(\nabla^c\Phi - \mathrm{i}A^c\Phi) - g_{ab}V(|\Phi|).\end{aligned} \tag{4.15}$$

The most general planar and rotational symmetric solution to the set of equations (4.8),(4.9), and (4.12) is the AdS-Reissner-Nordström black brane solution with scalar hair. In general, there are four different possibilities we can consider: With and without backreaction and solution with zero and non-zero scalar field. In the following sections we will discuss these background solutions; an overview is listed in Table 4.1.

[2]The additional metric factor g_{ab} is needed because we want to have a covector in the end.

	$\alpha = 0$ (probe limit)	$\alpha \neq 0$ (backreaction)
$\Phi = 0$	AdS-Schwarzschild black brane analytic solution	AdS-Reissner-Nordström black brane analytic solution
$\Phi \neq 0$	AdS-Schwarzschild black brane numerical solution for Φ and A_t	AdS-Reissner-Nordström black brane with scalar hair numerical solution for Φ, A_t and g_{ab}

Table 4.1. The parameter α describes the backreaction onto the geometry, whereas $\Phi \neq 0$ describes the condensation of the dual operator sourced by the scalar field, *i.e.* $\langle O_\Phi \rangle \neq 0$. Note that in the normal phase of the holographic superconductor analytic solutions for the background field equations of motions are feasible, whereas the condensed phase solutions can be found only numerically. In the probe limit the non-trivial profile of Φ related to the condensation does not affect the geometry of the spacetime since Φ is decoupled from Einstein's equations. The fixed probe limit geometry is given by the AdS-Schwarzschild black brane solution discussed in Section 4.1.4. With backreaction the finite charge density on the boundary must be sourced by a finite charge at the horizon geometry which leads to an AdS-Reissner-Nordström black brane geometry outlined in Section 4.1.3.

4.1.2. Background equations of motion for scalar hair black branes

Let us first derive the complete set of equations for the holographic s-wave superconductor background in arbitrary dimensions d. To my knowledge, this calculation has not been done in full generality, so allow me to be a little more detailed in the derivation. Starting with the Einstein equations in AdS$_{d+1}$

$$R_{ab} - \frac{1}{2} R g_{ab} - \frac{d(d-1)}{2L^2} g_{ab} = \alpha^2 L^2 T_{ab}, \tag{4.16}$$

we have inserted the AdS$_{d+1}$ cosmological constant where L denotes the AdS-radius, related to the curvature of the AdS-space. The main ingredients of a holographic superconductor are a charged black brane that may "grow scalar hair", *i.e.* a condensate described by a charged scalar field Φ and a respective $U(1)$ gauge field. Due to Lorentz symmetry the fields can only depend on the radial AdS coordinate u and it is sufficient to have a non-zero time component of the gauge field, acting as a chemical potential at the boundary. Thus, we may take the Ansatz

$$\Phi = \Phi(u), \qquad A = A_t(u)\,\mathrm{d}t, \qquad \mathrm{d}s^2 = \frac{L^2}{u^2}\left(-f(u)\,\mathrm{e}^{-\chi(u)}\,\mathrm{d}t^2 + \mathrm{d}\mathbf{x}^2 + \frac{\mathrm{d}u^2}{f(u)}\right), \tag{4.17}$$

and for simplicity, we will assume a special scalar potential namely,

$$V(|\Phi|) = m^2\,|\Phi|^2\,, \tag{4.18}$$

where the mass of the potential needs to be fixed to a value above the Breitenlohner-Freedman bound $m^2L^2 \geqslant -d^2/4$. Note that it is sufficient to assume that only quadratic terms are present in the potential $V(|\Phi|) = m^2\,|\Phi|^2$, since we are only interested in the behavior near the critical point where higher order interactions do not contribute. Deep in the condensed phase, *i.e.* close to zero temperature, the ground state of the holographic superconductor depends heavily on the from of the scalar field potential. Inserting the Ansatz (4.17) into the equations of motions of

the scalar field (4.8) yields

$$\Phi''(u)+\left(\frac{f'(u)}{f(u)}-\frac{\chi'(u)}{2}-\frac{d-1}{u}\right)\Phi'(u)+\left(\frac{A_t(u)^2\,\mathrm{e}^{\chi(u)}}{f(u)^2}-\frac{L^2m^2}{u^2f(u)}\right)\Phi(u)=0. \tag{4.19}$$

The $U(1)$ gauge field Ansatz in (4.17) gives rise to the field strength

$$F=\mathrm{d}A=\partial_u A_t(u)\,\mathrm{d}u\wedge\mathrm{d}t=-\partial_u A_t(u)\,\mathrm{d}t\wedge\mathrm{d}u \qquad\Rightarrow\qquad F_{tu}=-A_t'(u), \tag{4.20}$$

and the gauge field equation of motions (4.9) for $b=t$, read

$$A_t''(u)+\left(\frac{\chi'(u)}{2}-\frac{d-3}{u}\right)A_t'(u)-\frac{2L^2\left|\Phi(u)\right|^2}{u^2f(u)}A_t(u)=0. \tag{4.21}$$

The second non trivial Maxwell equation for $b=u$, yields a reality condition for the scalar field

$$\Phi^*\partial_u\Phi-\Phi\partial_u\Phi^*=0. \tag{4.22}$$

For arbitrary $\Phi(u)=|\Phi(u)|\,\mathrm{e}^{\mathrm{i}\varphi(u)}$ this reduces to

$$2\mathrm{i}\varphi(u)\varphi'(u)=0. \tag{4.23}$$

Therefore we can conclude that $\varphi'=0\Rightarrow\varphi=$ const. and we can choose without loss of generality $\varphi=0\Leftrightarrow\Phi\in\mathbb{R}$. Hence, the current can be reduced to $j_b=2\Phi^2A_b$.

For the Einstein tensor G_{ab} we need to calculate the Christoffel symbols $\Gamma^a{}_{bc}$, the Riemann tensor R_{abcd}, the Ricci tensor R_{ab} and the Ricci scalar R. The non-vanishing Christoffel symbols defined by

$$\Gamma^a_{bc}=\frac{1}{2}g_{ab}\big(\partial_b g_{dc}+\partial_c g_{ab}-\partial_d g_{bc}\big), \tag{4.24}$$

read

$$\begin{gathered}\Gamma^t_{ut}=\Gamma^t_{tu}=-\frac{1}{u}+\frac{f'(u)}{2f(u)}-\frac{\chi'(u)}{2}, \qquad \Gamma^i_{iu}=\Gamma^i_{ui}=-\frac{1}{u},\\ \Gamma^u_{tt}=\frac{1}{2}f(u)^2\left(-\frac{2}{u}+\frac{f'(u)}{f(u)}-\chi'(u)\right), \qquad \Gamma^u_{ii}=\frac{f(u)}{u}, \qquad \Gamma^u_{uu}=-\frac{1}{u}-\frac{f'(u)}{2f(u)}.\end{gathered} \tag{4.25}$$

The Riemann tensor

$$R_{abcd}=\frac{1}{2}\big(\partial_d\partial_a g_{bc}-\partial_d\partial_b g_{ac}+\partial_c\partial_b g_{ad}-\partial_c\partial_a g_{bd}\big)-g_{ef}\left(\Gamma^e_{ac}\Gamma^f_{bd}-\Gamma^e_{ad}\Gamma^f_{bc}\right), \tag{4.26}$$

with all indices lowered, has the following symmetries

- $R_{[ab][cd]}$, *i.e.* antisymmetric in its first two and last two indices
- $R_{abcd}=R_{cdab}$, *i.e.* symmetric under the interchange of the first and the last pair of indices
- $R_{a[bcd]}=0$, the first or algebraic Bianchi identity

The only non-vanishing components thus read

$$R_{ijij} = R_{jiji} = -R_{ijji} = -R_{jiij} = -g_{uu}\left(\Gamma^u_{ii}\right)^2 = -\frac{L^2}{u^4}f(u),$$

$$R_{titi} = R_{itit} = -R_{itti} = -R_{tiit} = -g_{uu}\Gamma^u_{tt}\Gamma^u_{ii} = \frac{L^2 f(u)}{u^4}\left[1 - \frac{u}{2}\left(\frac{f'(u)}{f(u)} - \chi'(u)\right)\right]\mathrm{e}^{-\chi(u)},$$

$$R_{iuui} = R_{uiiu} = -R_{iuiu} = -R_{uiui} = \frac{1}{2}\partial_u^2 g_{ii} - g_{ii}\left(\Gamma^i_{iu}\right)^2 + g_{uu}\Gamma^u_{ii}\Gamma^u_{uu} = {}^{3}L^2\frac{2f(u) - uf'(u)}{2u^4 f(u)}$$

$$R_{utut} = R_{tutu} = -R_{uttu} = -R_{tuut} = \frac{1}{2}\partial_u^2 g_{tt} - g_{tt}\left(\Gamma^t_{tu}\right)^2 + g_{uu}\Gamma^u_{uu}\Gamma^u_{tt},$$

$$= \frac{L^2}{u^4}\left[f(u) - uf'(u) + \frac{u^2}{2}f''(u) + \frac{u}{2}\left(f(u) - \frac{3}{2}uf'(u) + \frac{u}{2}f\chi'(u)\right)\chi'(u) - \frac{u^2}{2}f(u)\chi''(u)\right].$$

The Ricci tensor can be derived from the Riemann tensor by $R_{ac} = g^{bd}R_{abcd}$ which yield a symmetric tensor. The non-zero components are

$$R_{tt} = g^{bd}R_{tbtd} = \sum_{i=1}^{d-1} g^{ii}R_{titi} + g^{uu}R_{tutu}$$

$$= \frac{\mathrm{e}^{-\chi(u)}}{u^2}\left[df(u)^2 - \frac{d+1}{2}uf(u)f'(u) + \frac{u^2}{2}f(u)f''(u)\right.$$

$$\left. + \frac{u}{2}\left(df(u)^2 - \frac{3}{2}uf(u)f'(u) + \frac{1}{2}uf(u)^2\chi'(u)\right)\chi'(u) - \frac{u^2}{2}f(u)^2\chi''(u)\right],$$

$$R_{ii} = g^{bd}R_{ibid} = g^{tt}R_{itit} + \sum_{j=1}^{d-1} g^{jj}R_{ijij}\,{}^{4} + g^{uu}R_{iuiu} = \frac{f(u)}{u^2}\left[-d + u\left(\frac{f'(u)}{f(u)} - \frac{\chi'(u)}{2}\right)\right],$$

$$R_{uu} = g^{bd}R_{ubud} = g^{tt}R_{utut} + \sum_{i=1}^{d-1} g^{ii}R_{uiui}$$

$$= \frac{1}{u^2}\left\{-d + (d+1)\frac{u}{2}\frac{f'(u)}{f(u)} - \frac{u^2}{2}\frac{f''(u)}{f(u)} - \frac{u}{2}\left[1 - \frac{u}{2}\left(3\frac{f'(u)}{f(u)} - \chi'(u)\right)\right]\chi'(u) + \frac{u^2}{2}\chi''(u)\right\},$$

and we find a diagonal Ricci tensor reflecting our spherical symmetric Ansatz and matching the diagonal form of the energy-momentum tensor T_{ab}. Finally, the Ricci scalar is the trace of the Ricci tensor

$$R = g^{ab}R_{ab} = g^{tt}R_{tt} + \sum_{i=1}^{d-1} g^{ii}R_{ii} + g^{uu}R_{uu}$$

[3] No summation over i; original term of the form $g_{ef}\Gamma^e_{iu}\Gamma^f_{ui}$ allows only one term, *i.e.* when $i = e = f$.
[4] $\sum_{j=1}^{d-1} g^{jj}R_{ijij}$ has one zero summand, namely $g^{ii}R_{iiii} = 0$, so this sum yields a factor of $(d-2)$.

$$= -\frac{1}{L^2}\Big[d(d+1)f(u) - 2duf'(u) + u^2 f''(u) + u\left(df(u) - \frac{3}{2}uf'(u) + \frac{u}{2}f(u)\chi'(u)\right)\chi'(u) - u^2 f(u)\chi''(u)\Big]. \tag{4.27}$$

We are now able to write the three different Einstein equations as

$$\begin{aligned}
&\frac{d(d-1)\big(f(u)-f(u)^2\big) + (d-1)uf(u)f'(u)}{2u^2\,\mathrm{e}^{\chi(u)}} = \alpha^2 L^2 T_{tt},\\
&-\frac{1}{2u^2}\Big[d(d-1) - d(d-1)f(u) + 2(d-1)uf'(u) - u^2 f''(u)\\
&+uf(u)\left(-d+1+\frac{3}{2}u\frac{f'(u)}{f(u)} - \frac{u}{2}\chi'(u)\right)\chi'(u) + u^2 f(u)\chi''(u)\Big] = \alpha^2 L^2 T_{ii},\\
&-\frac{d(d-1) - d(d-1)f(u) + (d-1)u\big[f'(u) - f(u)\chi'(u)\big]}{2u^2 f(u)} = \alpha^2 L^2 T_{uu}.
\end{aligned} \tag{4.28}$$

The right-hand side of the Einstein equations are the full energy-momentum tensor defined in (4.13)–(4.15). The gauge field energy-momentum tensor reads

$$T^{\mathrm{em}}_{ab} = g^{tt}F_{at}F_{bt} + \sum_{i=1}^{d-1} g^{ii}F_{ai}F_{bi} + g^{uu}F_{au}F_{bu} - \frac{1}{2}g_{ab}g^{tt}g^{uu}\left(F_{tu}\right)^2. \tag{4.29}$$

The only non-vanishing components are

$$\begin{aligned}
T^{\mathrm{em}}_{tt} &= \left(g^{uu} - \frac{1}{2}g_{tt}g^{tt}g^{uu}\right)\left(F_{tu}\right)^2 = \frac{1}{2}g^{uu}\left(F_{tu}\right)^2 = \frac{1}{2}\frac{u^2 f(u)}{L^2}\,\mathrm{e}^{\chi(u)}\,A_t'(u)^2,\\
T^{\mathrm{em}}_{jj} &= -\frac{1}{2}g_{jj}g^{tt}g^{uu}\left(F_{tu}\right)^2 = \frac{1}{2}\frac{u^2}{L^2}A_t'(u)^2,\\
T^{\mathrm{em}}_{uu} &= \left(g^{tt} - \frac{1}{2}g_{uu}g^{tt}g^{uu}\right)\left(F_{tu}\right)^2 = \frac{1}{2}g^{tt}\left(F_{tu}\right)^2 = -\frac{1}{2}\frac{u^2}{L^2 f(u)}\,\mathrm{e}^{\chi(u)}\,A_t'(u)^2.
\end{aligned} \tag{4.30}$$

The energy-momentum tensor for the scalar field (4.15) can be reduced to

$$\begin{aligned}
T^{\Phi}_{tt} &= A_t(u)^2\left|\Phi(u)\right|^2 - g_{tt}\left(g^{uu}\partial_u\Phi^*(u)\partial_u\Phi(u) - m^2\left|\Phi\right|^2\right),\\
T^{\Phi}_{ii} &= -g_{ii}\left(g^{tt}A_t(u)^2\left|\Phi(u)\right|^2 + g^{uu}\partial_u\Phi^*(u)\partial_u\Phi(u) - m^2\left|\Phi\right|^2\right),\\
T^{\Phi}_{uu} &= \partial_u\Phi^*(u)\partial_u\Phi(u) - g_{uu}\left(g^{tt}A_t(u)^2\left|\Phi(u)\right|^2 - m^2\left|\Phi\right|^2\right).
\end{aligned} \tag{4.31}$$

Inserting the metric Ansatz (4.17) and the reality condition (4.22) simplifies the full Einstein equations to

$$\begin{aligned}
0 = &\frac{d(d-1)}{u^2} + \frac{d-1}{u}f'(u) - \frac{d(d-1)}{u^2}f(u)\\
&- 2\alpha^2 L^2\left[f(u)\Phi'(u)^2 + \left(\frac{\mathrm{e}^{\chi(u)}\,A_t(u)^2}{f(u)} - \frac{m^2L^2}{u^2}\right)\Phi(u)^2\right] - \alpha^2 u^2\,\mathrm{e}^{\chi(u)}\,A_t'(u)^2,
\end{aligned} \tag{4.32}$$

$$
\begin{aligned}
0 = & \frac{d(d-1)}{u^2} - f''(u) + \left(\frac{2(d-1)}{u} + \frac{3}{2}\chi'(u)\right) f'(u) - \frac{d(d-1)}{u^2} f(u) \\
& + \left[\chi''(u) - \left(\frac{d-1}{u} + \frac{1}{2}\chi'(u)\right)\chi'(u)\right] f(u) \\
& + 2\alpha^2 L^2 \left(\mathrm{e}^{\chi(u)} \frac{A_t(u)^2}{f(u)} + \frac{m^2 L^2}{u^2}\right) \Phi(u)^2 - 2 f(u) \Phi'(u)^2 + \alpha^2 u^2 \mathrm{e}^{\chi(u)} A_t'(u)^2, \qquad (4.33) \\
0 = & -\frac{d(d-1)}{u^2} - \frac{d-1}{u} f'(u) + \left(\frac{(d-1)\chi'(u)}{u} + \frac{d(d-1)}{u^2}\right) f(u) \\
& - 2\alpha^2 L^2 \left[f(u)\Phi'(u)^2 + \left(\frac{\mathrm{e}^{\chi(u)} A_t(u)^2}{f(u)} + \frac{m^2 L^2}{u^2}\right)\Phi(u)^2\right] + \alpha^2 u^2 \mathrm{e}^{\chi(u)} A_t'(u)^2. \qquad (4.34)
\end{aligned}
$$

The horizon of the scalar hair AdS-Reissner-Nordström black brane defines a temperature according to (3.7)

$$
\begin{aligned}
T_{\mathrm{H}} &= \frac{1}{2\pi}\left[\frac{1}{\sqrt{g_{uu}}}\frac{\mathrm{d}}{\mathrm{d}u}\sqrt{-g_{tt}}\right]_{u=u_{\mathrm{H}}} \\
&= \frac{\mathrm{e}^{-\chi(u)/2}}{4\pi u}\left[u f'(u) - f(u)\left(u\chi'(u) + 2\right)\right]\Big|_{u=u_{\mathrm{H}}}. \qquad (4.35)
\end{aligned}
$$

We may use either the tt (4.32) or uu (4.34) Einstein equation to eliminate $f'(u)$ and the regularity conditions at the horizon, *i.e.* $f(u_{\mathrm{H}}) = 0$ and $A_t(u_{\mathrm{H}}) = 0$, which reduces the Hawking temperature to

$$
T_{\mathrm{H}} = \mathrm{e}^{-\chi_{\mathrm{H}}/2} \frac{d(d-1) - 2\alpha^2 m^2 L^4 \Phi_{\mathrm{H}}^2 + \alpha^2 u_{\mathrm{H}}^4 \mathrm{e}^{\chi_{\mathrm{H}}} {A_t'}_{\mathrm{H}}^2}{4\pi(d-1)u_{\mathrm{H}}}, \qquad (4.36)
$$

where we have a set of four parameters, the horizon radius u_{H} set by $f(u_{\mathrm{H}}) = 0$, the scalar field at the horizon $\Phi(u_{\mathrm{H}}) = \Phi_{\mathrm{H}}$, the electrical field perpendicular to the horizon $A_t'(u_{\mathrm{H}}) = {A_t'}_{\mathrm{H}}$ and the metric field $\chi_{\mathrm{H}} = \chi(u_{\mathrm{H}})$. In order to identify the black brane temperature T_{H} with the temperature of the boundary (Euclidean) field theory, we need the proper normalization of the gravitational redshift and thus the emblackening factor has to approach one, $f \to 1$ for $u \to 0$, at the boundary. Therefore the additional constraint $\chi \to 0$ as $u \to 0$ must be imposed on the solutions of the Einstein equations. The equations of motion, the metric and the one form are invariant under the scaling symmetry

$$
t \longrightarrow ct, \qquad A_t \longrightarrow c^{-1} A_t, \qquad \mathrm{e}^{\chi} \longrightarrow c^2 \mathrm{e}^{\chi}, \qquad (4.37)
$$

which we can use to set $\chi = 0$ at the boundary. Furthermore, there are two more scaling symmetries[5]

$$
\begin{aligned}
& t \longrightarrow ct, \qquad \mathbf{x} \longrightarrow \mathbf{x}, \qquad u \longrightarrow cu, \qquad \mathrm{d}s^2 \longrightarrow c^2 \mathrm{d}s^2, \\
& m \longrightarrow c^{-1} m, \qquad L \longrightarrow cL, \qquad A_t \longrightarrow c^{-1} A_t, \qquad \Phi \longrightarrow c^{-1}\Phi,
\end{aligned} \qquad (4.38)
$$

[5] The rescaling of the metric can be absorb in a Weyl rescaling.

and

$$(t, \mathbf{x}) \longrightarrow c(t, \mathbf{x}), \qquad u \longrightarrow cu, \qquad A_t \longrightarrow c^{-1} A_t, \tag{4.39}$$

which can be used to set $L = 1$ and $u_\mathrm{H} = 1$, respectively. This will be done in numerical calculations in order to work with purely dimensionless equations of motion, but we will keep the factors in all expressions which allows for easy identification of their correct dimensionality. Effectively, the temperature depends only on the remaining set of parameters $(\Phi_\mathrm{H}, A'_{t\,\mathrm{H}})$ and the additional external parameters α, m and d, that changes the theory of the holographic superconductor.

Numerical solution

The solution to the equations of motion (4.19), (4.21) and (4.32)–(4.34) can be obtained only by numerical integration. We will employ the following procedure:

i. Determine the asymptotic solution to the equations of motion in a power series about the regular singular point at the horizon $u_\mathrm{H} = 1$ under the regularity conditions $f(u_\mathrm{H}) = 0$ and $A_t(u_\mathrm{H}) = 0$. This approach is known as the Frobenius method. The numerical value of the asymptotic solution close to the horizon $u \lesssim 1$ is used as the initial data depending on the initial conditions set by $(\Phi_\mathrm{H}, A'_{t\,\mathrm{H}}, \chi_\mathrm{H})$. From a naïve counting we would expect six initial conditions for a set of three coupled, second order, ordinary differential equations. However, the Einstein equations are reduced to two first order differential equations and imposing the regularity condition $f(u_\mathrm{H}) = 0$ reduces the number of initial conditions to one, namely χ_H. The four initial conditions of the scalar and Maxwell equations are reduced to the remaining two Φ_H and $A'_{t\,\mathrm{H}}$ by imposing the regularity condition $A_t(u_\mathrm{H}) = 0$.

ii. Determine the boundary asymptotic near the asymptotic AdS-spacetime boundary $u \to 0$. Again a power series expansion will yield the asymptotic solution. In order to have a well-defined boundary variational problem, we need to use a holographic renormalization scheme to regularize the boundary on-shell action. Apart from the standard gravitational counterterms, *i.e.* the Gibbons-Hawking term and a boundary cosmological constant term, we need counterterms for the scalar field. The total counterterm reads

$$\begin{aligned} S_\text{counter} &= \int \mathrm{d}^\mathrm{d}x \sqrt{-\gamma} \left[2\gamma^{\mu\nu}\nabla_\mu n_\nu - \frac{2(d-1)}{L} + \frac{2\,|\Phi|}{L} + (\Phi^* n^\mu \partial_\mu \Phi + \Phi n^\mu \partial_\mu \Phi^*) \right] \Big|_{u=0^+} \\ &= 2 \int \mathrm{d}^\mathrm{d}x \sqrt{-\gamma} \left(\gamma^{\mu\nu}\nabla_\mu n_\nu - \frac{(d-1)}{L} + \frac{\Phi}{L} + \Phi n^\mu \partial_\mu \Phi \right) \Big|_{u=0^+}, \end{aligned} \tag{4.40}$$

where γ describes the induced metric on a shell close to the boundary and n^ν is the outward pointing normal vector on the boundary shell.

iii. Finally, integrate the equations of motion from the horizon $u_\mathrm{H} = 1$ to the boundary $u_\mathrm{B} = 0$. After stabilizing the numerical integration by choosing suitable values close to $u_\mathrm{H} = 1$ and $u_\mathrm{B} = 0$, the solution is fitted to the boundary expansion in order to obtain the coefficients of the leading and subleading terms. Formally, the integration defines the map

$$(\Phi_\mathrm{H}, A'_{t\,\mathrm{H}}, \chi_\mathrm{H}) \mapsto (\mu, \Phi_\mathrm{B}, \chi_\mathrm{B}), \tag{4.41}$$

where $A_{t\,\mathrm{B}} = \mu$ is the chemical potential of the dual field theory, fixing the charge density. For non-zero Φ_B the background $U(1)$ symmetry is explicitly broken, whereas spontaneous

symmetry breaking is induced by a non-zero vacuum expectation value of the dual field operator. Thus, we need to impose the boundary conditions $\Phi_{\mathrm{B}} = 0$ and as mentioned above for a well-define temperature of the field theory $T = T_{\mathrm{H}}$, the condition $\chi_{\mathrm{B}} = 0$. Using a so-called "shooting method" where we fix the boundary values in (4.41) to $(\mu, 0, 0)$ we determine the horizon initial conditions by searching for roots of the difference function between the integrated solution and the desired values. Operationally, we fit the numerical solution to the boundary expansion

$$\Phi_{\mathrm{B}} = \Phi_{\mathrm{B}}^{(1)} u^{d-\Delta} + \Phi_{\mathrm{B}}^{(2)} u^{\Delta} = \Phi_{\mathrm{B}}^{(1)} u^{\frac{1}{2}\left(d-\sqrt{d^2+4m^2}\right)} + \Phi_{\mathrm{B}}^{(2)} u^{\frac{1}{2}\left(\sqrt{d^2+4m^2}+d\right)}, \tag{4.42}$$

$$A_{t\,\mathrm{B}} = \mu + \rho u^{d-2}. \tag{4.43}$$

This method allows us to invert the map (4.41) and express the horizon initial conditions in terms of the dimensionless[6] boundary chemical potential $\bar{\mu}$, *i.e.* $\Phi_{\mathrm{H}}(\bar{\mu})$, $A'_{t\,\mathrm{H}}(\bar{\mu})$ and $\chi_{\mathrm{H}}(\bar{\mu})$. We are thus left with a one parameter family for each set of the external parameters d, m and α of solutions for different $\bar{\mu}$. The remaining physical quantities of the dual field theory are then completely determined by inserting the inverted map, *e.g.* the temperature $T(\bar{\mu})$ via (4.36), the charge density n, the order parameter of the superconducting phase transition $\langle\, O_\Delta \,\rangle$ and the energy density ϵ as

$$\begin{aligned} \langle\, O_\Delta \,\rangle &= \lim_{u\to 0} \frac{1}{\sqrt{\gamma}} \frac{\delta S_{\text{on-shell}}}{\delta \Phi_{\mathrm{B}}}, \\ n = \langle\, J^t \,\rangle &= \lim_{u\to 0} \frac{1}{\sqrt{\gamma}} \frac{\delta S_{\text{on-shell}}}{\delta A_{t\,\mathrm{B}}}, \\ \epsilon = \langle\, T^{00} \,\rangle &= \lim_{u\to 0} \frac{1}{\sqrt{\gamma}} \frac{\delta S_{\text{on-shell}}}{\delta g_{tt\,\mathrm{B}}}. \end{aligned} \tag{4.44}$$

Note that working with fixed chemical potential relates to the grand canonical ensemble and the grand canonical thermodynamic potential $\Omega(T, V, \mu)$. At the critical value of μ_c or T_c the boundary conditions $(\Phi(u_{\mathrm{H}}), A'_t(u_{\mathrm{H}}))$ are such that a non-zero vacuum value of $\mathcal{O}$ leads to a condensation of the charged scalar field, hovering over the charged black brane, at the critical chemical potential/temperature $\bar{\mu}_c$. Due to the geometry of the AdS-space there is a stable solution where the electrostatic repulsion cancels the gravitational attraction.

The numerical integration is executed by *Mathematica*. For simplicity, only the probe limit *Mathematica* code is presented in D.1, since all the key features are outlined and the extension to include the backreaction is straightforward, whereas the pedagogical value would be drastically reduced by the increased complexity of the more complicated equations of motion. In the following let us discuss the remaining special cases listed in Table 4.1.

4.1.3. Background equation of motion in the normal phase

In the following we will consider the normal phase, *i.e.* we take the trivial solution to the background equation of motions for the scalar field $\Phi = 0$ and no hair for the black brane Ansatz, *i.e.* $\chi = 0$. In this case the Einstein equations (4.32)–(4.34) reduce to a dynamical equation arising

[6] Barred math symbols denote dimensionless quantities.

from the spatial components

$$f''(u) - \frac{2(d-1)}{u} f'(u) + \frac{d(d-1)}{u^2} f(u) - \frac{d(d-1)}{u^2} - \alpha^2 u^2 A_t'(u)^2 = 0, \tag{4.45}$$

and a constraint equations coming from the tt and uu components where the tt equation equals the uu equation up to a global minus sign

$$\frac{d-1}{u} f'(u) - \frac{d(d-1)}{u^2} f(u) + \frac{d(d-1)}{u^2} - \alpha^2 u^2 A_t'(u)^2 = 0. \tag{4.46}$$

Accordingly, the Maxwell equation can be written as

$$A_t''(u) - \frac{d-3}{u} A_t'(u) = 0. \tag{4.47}$$

Since there is no $f(u)$ appearing in (4.47), we can solve this equations with the boundary condition $A_t(u = u_\mathrm{H}) = 0$, assuming we have a charged black brane with horizon located at $u = u_\mathrm{H}$. This boundary condition avoids a conical singularity at the horizon and thus yields a well-defined one form A. The solution to this equation is given by

$$A_t(u) = \mu \left(1 - \frac{u^{d-2}}{u_\mathrm{H}^{d-2}} \right), \tag{4.48}$$

where μ is the chemical potential, describing the difference in the electric potential between the horizon of the black brane at $u = u_\mathrm{H}$ and the boundary of the AdS space, at $u = 0$, and thus the energy of adding another charged particle to the black brane. Inserting this solution into the two Einstein equations (4.45) and (4.46), we can solve the differential equation for the blackening factor $f(u)$ obeying the boundary condition $f(u_\mathrm{H}) = 0$ which yields

$$f(u) = 1 - \underbrace{\left(\frac{d-2}{d-1} \mu^2 u_\mathrm{H}^2 \alpha^2 + 1 \right)}_{=\bar{M}} \frac{u^d}{u_\mathrm{H}^d} + \underbrace{\left(\frac{d-2}{d-1} \mu^2 u_\mathrm{H}^2 \alpha^2 \right)}_{=\bar{Q}^2} \frac{u^{2(d-1)}}{u_\mathrm{H}^{2(d-1)}}. \tag{4.49}$$

Rewriting (4.49) in the form of an Reissner-Nordström black brane with dimensionless mass $\bar{M}$ and charge $\bar{Q}$, we find the following relations

$$\bar{M} = \bar{Q}^2 + 1, \qquad \bar{Q} = \sqrt{\frac{d-2}{d-1}} \mu u_\mathrm{H} \alpha. \tag{4.50}$$

The temperature defined by the horizon of the Reissner-Nordström black brane is given by

$$\begin{aligned} T &= \frac{1}{2\pi} \left[\frac{1}{\sqrt{g_{uu}}} \frac{\mathrm{d}}{\mathrm{d}u} \sqrt{-g_{tt}} \right]_{u=u_\mathrm{H}} = \frac{1}{2\pi} \left[u \sqrt{f(u)} \frac{\mathrm{d}}{\mathrm{d}u} \left(\frac{\sqrt{f(u)}}{u} \right) \right]_{u=u_\mathrm{H}} \\ &= \frac{1}{4\pi} \left(f'(u) - \frac{2f(u)}{u} \right) \Big|_{u=u_\mathrm{H}} = \frac{|f'(u)|_{u=u_\mathrm{H}}}{4\pi} \\ &= \frac{d - (d-2)\bar{Q}^2}{4\pi u_\mathrm{H}} = \frac{d - \frac{(d-2)^2}{d-1} \mu^2 u_\mathrm{H}^2 \alpha^2}{4\pi u_\mathrm{H}}, \end{aligned} \tag{4.51}$$

which is in agreement with the general temperature (4.36) of the hairy black brane for $\chi_{\mathrm{H}} = 0$ and $\Phi_{\mathrm{H}} = 0$. Since we are dealing with a scale invariant theory in the UV, the only dimensionless physical parameter is the ratio T/μ which will be controlled numerically by the dimensionless chemical potential $\bar{\mu} = \mu u_{\mathrm{H}}$. Using (4.50) we may write this ratio in terms of the charge of the black brane,

$$\frac{T}{\mu} = \frac{d - \frac{(d-2)^2}{d-1}\bar{\mu}^2\alpha^2}{4\pi\bar{\mu}} = \frac{d-(d-2)\bar{Q}^2}{\frac{4\pi}{\alpha}\sqrt{\frac{d-1}{d-2}}\bar{Q}}, \tag{4.52}$$

and conversely

$$\bar{Q}_{\pm} = \frac{-2\pi\sqrt{d-1}\left(\frac{T}{\mu}\right) \pm \sqrt{4\pi^2(d-1)\left(\frac{T}{\mu}\right)^2 + d(d-2)^2\alpha^2}}{\alpha(d-2)^{\frac{3}{2}}}. \tag{4.53}$$

This expression can be used to rewrite the Reissner-Nordström black brane metric in term of T/μ. In order to find agreement with the probe limit $\alpha \to 0$, *c.f.* Section 4.1.4, we have to choose $Q = Q_+$ as the correct solution. The two possible limits can be easily read off from (4.53) using the l'Hospital rule for "$0/0$"

$$\lim_{\alpha\to 0} \bar{Q}_- = -\infty, \qquad \lim_{\alpha\to 0} \bar{Q}_+ = 0. \tag{4.54}$$

Furthermore, we are interested in the relation between the field theory side quantities like energy, entropy and charge density in terms of the black brane charge $\bar{Q}$. Since we are working with a fixed chemical potential we need to work in the grand canonical ensemble related to the grand canonical (thermodynamic) potential $\Omega(T, V, \mu)$. From the AdS/CFT correspondence in the large N and strong coupling limit, we know that the partition function is related to the gravitational action in the saddle point approximation

$$Z \approx \mathrm{e}^{-S_{\mathrm{E}}} \qquad \longrightarrow \qquad \ln Z = -I, \tag{4.55}$$

where I denotes the regularized Euclidean on-shell action. The free energy $F(T, V, N)$ is related to the canonical partition function via

$$F = -\frac{1}{\beta}\ln Z = -\frac{1}{\beta}\ln \mathrm{e}^{-I} = \frac{1}{\beta}I = k_{\mathrm{B}}TI, \tag{4.56}$$

where $\beta = (k_{\mathrm{B}}T)^{-1}$ and in the same way we can generalize (4.56) to the grand canonical ensemble using the grand canonical partition function and the grand canonical potential

$$\Omega = \frac{1}{\beta}I = k_{\mathrm{B}}TI. \tag{4.57}$$

The field theory quantities are given by [221]

$$\mathscr{N} = -\frac{\partial\Omega}{\partial\mu} = \frac{1}{\beta}\frac{\partial \ln Z}{\partial\mu} = -\frac{1}{\beta}\frac{\partial I}{\partial\mu} = -k_{\mathrm{B}}T\frac{\partial I}{\partial\mu}, \tag{4.58}$$

$$\begin{aligned} E &= -\frac{\partial \ln\left(Z\,\mathrm{e}^{-\beta\mu N}\right)}{\partial\beta} = -\frac{\partial \ln Z}{\partial\beta} + \mu\mathscr{N} = \frac{\partial I}{\partial\beta} - \frac{\mu}{\beta}\frac{\partial I}{\partial\mu} \\ &= \frac{\partial T}{\partial\beta}\frac{\partial I}{\partial T} - k_{\mathrm{B}}T\mu\frac{\partial I}{\partial\mu} = -k_{\mathrm{B}}T\left(T\frac{\partial I}{\partial T} + \mu\frac{\partial I}{\partial\mu}\right), \end{aligned} \tag{4.59}$$

$$S = -\frac{\partial\Omega}{\partial T} = -\frac{\partial\beta}{\partial T}\frac{\partial\Omega}{\partial\beta} = \frac{1}{k_{\mathrm{B}}T^2}\frac{\partial\left(-\beta^{-1}\ln Z\right)}{\partial\beta} = k_{\mathrm{B}}\left(\beta\frac{\partial I}{\partial\beta} - I\right) = -k_{\mathrm{B}}\left(T\frac{\partial I}{\partial T} + I\right). \tag{4.60}$$

Finally, the regularized on-shell action reads

$$I = -\frac{1}{2\kappa^2}\int_0^\beta \mathrm{d}t \int \mathrm{d}^{d-1}x \int_{u_\mathrm{B}}^{u_\mathrm{H}} \mathrm{d}u\, \mathscr{L}_{\text{on-shell}}(u) = -\frac{L^{d-1}}{2\kappa^2}\frac{V_{d-1}}{k_\mathrm{B}T}\int_{u_\mathrm{B}}^{u_\mathrm{H}} \mathrm{d}u\, \mathscr{L}_{\text{on-shell}}(u)$$
$$= -\frac{L^{d-1}}{2\kappa^2}\frac{V_{d-1}}{k_\mathrm{B}T}\frac{1}{u_\mathrm{H}}\left(1+\frac{d-2}{d-1}\mu^2 u_\mathrm{H}^2\alpha^2\right), \tag{4.61}$$

and thus (4.59) and (4.58) read

$$\begin{aligned} S &= \frac{4\pi}{2\kappa^2}\frac{L^{d-1}V_{d-1}}{u_\mathrm{H}^{d-1}}, \\ E &= \frac{d-1}{2\kappa^2}L^{d-1}V_{d-1}\frac{\bar{M}}{u_\mathrm{H}^d} = \frac{L^{d-1}V_{d-1}}{2\kappa^2}\frac{1}{u_\mathrm{H}^d}\Big[(d-1)+(d-2)\mu^2u_\mathrm{H}^2\alpha^2\Big], \\ \mathscr{N} &= (d-2)\frac{L^{d-1}V_{d-1}}{\kappa^2}\frac{\mu\alpha^2}{u_\mathrm{H}^{d-2}}, \end{aligned} \tag{4.62}$$

where the horizon u_H is understood as a function of μ/T given by solving (4.51) for u_H.

4.1.4. Background equations of motion in the probe limit

In the large charge limit, *i.e.* $\kappa^2/e^2 \ll L^2$, neglecting backreaction on the geometry, we actually consider an uncharged background described by an AdS-Schwarzschild black brane. We can derive its metric directly form the previous Reissner-Nordström black brane by setting the backreaction to zero, *i.e.* $\alpha = 0$. Therefore the Einstein equations reduce to

$$R_{ab} - \frac{1}{2}Rg_{ab} - \frac{d(d-1)}{2L^2}g_{ab} = 0. \tag{4.63}$$

This equations are solved by the AdS-Schwarzschild metric for an $d+1$ dimensional asymptotic AdS-space

$$ds^2 = \frac{L^2}{u^2}\left(-f(u)\,\mathrm{d}t^2 + \mathrm{d}\mathbf{x}^2\right) + \frac{L^2}{u^2}\frac{\mathrm{d}u^2}{f(u)}, \tag{4.64}$$

with

$$f(u) = 1 - \frac{u^d}{u_\mathrm{H}^d}. \tag{4.65}$$

The horizon of the Schwarzschild black brane u_H gives rise to the temperature

$$T = \frac{1}{2\pi}\left[\frac{1}{\sqrt{g_{uu}}}\frac{\mathrm{d}}{\mathrm{d}u}\sqrt{-g_{tt}}\right]_{u=u_\mathrm{H}} = \frac{|f'(u)|_{u=u_\mathrm{H}}}{4\pi} = \frac{d}{4\pi u_\mathrm{H}}, \tag{4.66}$$

in agreement with (4.36) for $\alpha = 0$. The dimensionless chemical potential $\bar{\mu} = \mu u_\mathrm{H}$ is identical to the dimensionless ratio

$$\frac{\mu}{T} = \frac{4\pi\mu u_\mathrm{H}}{d} = \frac{4\pi}{d}\bar{\mu}. \tag{4.67}$$

We see that the AdS-Schwarzschild solution in the probe limit and all its properties can be directly derived from the AdS-Reissner-Nordström black brane by setting $\alpha = 0$ or equivalently $Q = Q_+ = 0$. In the normal phase the equation for the background gauge field A_t does not change

and yields the same solution as in (4.48). The physical difference lies in the missing relation between the chemical potential of the charged particles and the charge of the black brane Q. Since we neglect the backreaction on the geometry, the black brane is not charged and cannot be influenced by the charged probes. In the condensed phase we are still dealing with the AdS-Schwarzschild black brane solution for the geometry, but with a non-trivial solution to the equations of motion of Φ. For completeness, we again state the equations of motion (4.19) and (4.21) with $\chi(u) = 0$ and $f(u)$ being the emblackening factor of the AdS-Schwarzschild (4.64)

$$\Phi''(u) + \left(\frac{f'(u)}{f(u)} - \frac{d-1}{u}\right)\Phi'(u) + \left(\frac{A_t(u)^2}{f(u)^2} - \frac{L^2 m^2}{u^2 f(u)}\right)\Phi(u) = 0, \tag{4.68}$$

$$A_t''(u) - \frac{d-3}{u}A_t'(u) - \frac{2L^2\left|\Phi(u)\right|^2}{u^2 f(u)}A_t(u) = 0. \tag{4.69}$$

Numerical solution

The condensed phase solution of (4.68) and (4.69) can only be obtained by numerical integration analogous to the backreacted case. Following *i* to *iii* on page 126, a numerical solution shown in Figure 4.1, is computed using the *Mathematica* code shown in detail in Appendix D and listed in Mathematica Code D.2.

4.1.5. Fluctuations about background fields

According to the holographic fluctuation-dissipation theorem explained in Section 3.5.1, the linear response functions are related to the linearized equations of motions in the fluctuations about the background solutions. Thus, in this section we will derive the full probe limit and backreaction linearized equations of motion of the field fluctuations.

Fluctuation in the probe limit

We now look at fluctuations of the scalar field $\Phi(u)$ and the gauge field $A(u)$ about there fixed background values with the scalar potential $V(\Phi) = m^2\Phi^2$. The metric will be fixed to the Schwarzschild solution since we do not consider any backreaction. The complex scalar field and the gauge field will be replaced by

$$\Phi \longrightarrow \Phi + \delta\phi, \qquad A_a \longrightarrow A_a + a_a, \tag{4.70}$$

with $\Phi \in \mathbb{R}$ as stated in (4.23), but $\delta\phi \in \mathbb{C}$. We allow a dependence on all coordinates for the fluctuations, *i.e.* $\delta\phi = \delta\phi(t, \mathbf{x}, u)$ and $a_a = a_a(t, \mathbf{x}, u)$. Expanding the action (4.1) up to quadratic order in the fluctuations we find

$$S_{\mathrm{F}} = S_{\mathrm{F}}^{(0)} + S_{\mathrm{F}}^{(1)} + S_{\mathrm{F}}^{(2)}, \tag{4.71}$$

where

$$S_{\mathrm{F}}^{(0)} = S_{\mathrm{M}}, \tag{4.72}$$

$$S_{\mathrm{F}}^{(1)} = \frac{1}{e^2}\int \mathrm{d}^{d+1}x\,\sqrt{-g}\left[-\frac{1}{4}\left(\delta F_{ab}F^{ab} + F_{ab}\delta F^{ab}\right) - \nabla_a\Phi\nabla^a\left(\delta\phi + \delta\phi^*\right)\right. \tag{4.73}$$

$$
\begin{aligned}
&- \mathrm{i}A_a\nabla^a\left(\delta\phi-\delta\phi^*\right)\Phi+\mathrm{i}\nabla_a\Phi A^a\left(\delta\phi-\delta\phi^*\right)\\
&- A_aA^a\Phi\left(\delta\phi+\delta\phi^*\right)-2A_aa^a\Phi^2-m^2\Phi\left(\delta\phi+\delta\phi^*\right)\Big],
\end{aligned}
\tag{4.74}
$$

$$
\begin{aligned}
S_{\mathrm{F}}^{(2)}=\frac{1}{e^2}\int \mathrm{d}^{d+1}x\,\sqrt{-g}\Big[&-\frac{1}{4}\delta F_{ab}\delta F^{ab}-\nabla_a\delta\phi\nabla^a\delta\phi^*+\mathrm{i}A_a\nabla^a\left(\delta\phi^*\right)\delta\phi\\
&- \mathrm{i}A_a\nabla^a\left(\delta\phi\right)\delta\phi^*-\mathrm{i}a_a\nabla^a\left(\delta\phi-\delta\phi^*\right)\Phi+\mathrm{i}\nabla_a\Phi a^a\left(\delta\phi-\delta\phi^*\right)\\
&- A_aA^a\delta\phi\delta\phi^*-2A_a^{\mathrm{B}}a^a\Phi\left(\delta\phi+\delta\phi^*\right)-a_aa^a\Phi^2-m^2\delta\phi\delta\phi^*\Big].
\end{aligned}
\tag{4.75}
$$

Variations with respect to the fluctuations of $S_{\mathrm{F}}^{(0)}$ are vanishing, while the variation of $S_{\mathrm{F}}^{(1)}$ gives rise to the equations of motions of the background fields as expected, since this is the usual variation procedure. The variations of the quadratic action in the fluctuations yield the linearized equations of motions for the fluctuations

$$
\left(\nabla_a-\mathrm{i}A_a\right)\left(\nabla^a-\mathrm{i}A^a\right)\delta\phi-m^2\delta\phi-\mathrm{i}\nabla_a\left(a^a\Phi\right)-\mathrm{i}a_a\nabla^a\Phi-2A_aa^a\Phi=0, \tag{4.76}
$$

$$
\nabla^a\delta F_{ab}+\mathrm{i}\nabla_b\Phi\left(\delta\phi-\delta\phi^*\right)-\mathrm{i}\nabla_b\left(\delta\phi-\delta\phi^*\right)\Phi-2A_b\Phi\left(\delta\phi+\delta\phi^*\right)-2a_b\Phi^2=0, \tag{4.77}
$$

where δF_{ab} is given by

$$
\delta F_{ab}=\partial_a\left(A_b+a_b\right)-\partial_b\left(A_a+a_a\right)-\partial_aA_b+\partial_bA_a=\partial_aa_b-\partial_ba_a. \tag{4.78}
$$

In order to work out the quasi-normal modes we apply a Fourier transformation and assume plain wave behavior for the spatial dependence

$$
\begin{aligned}
\delta\phi(t,\mathbf{x},u)&=\int\frac{\mathrm{d}\omega\,\mathrm{d}^{d-1}\,\mathbf{k}}{(2\pi)^d}\,\mathrm{e}^{-\mathrm{i}\omega t+\mathrm{i}\mathbf{k}\cdot\mathbf{x}}\,\delta\phi(u),\\
a_a(t,\mathbf{x},u)&=\int\frac{\mathrm{d}\omega\,\mathrm{d}^{d-1}\,\mathbf{k}}{(2\pi)^d}\,\mathrm{e}^{-\mathrm{i}\omega t+\mathrm{i}\mathbf{k}\cdot\mathbf{x}}\,a_a(u).
\end{aligned}
\tag{4.79}
$$

Thus, we end up with the following equation of motion for the scalar fluctuations

$$
\begin{aligned}
\delta\phi''(u)+\left(\frac{f'(u)}{f(u)}-\frac{d-1}{u}\right)\delta\phi'(u)+\left[\frac{(\omega+A_t(u))^2}{f(u)^2}-\frac{\mathbf{k}^2}{f(u)}-\frac{L^2m^2}{u^2f(u)}\right]\delta\phi(u)\\
+\left[\left(\frac{\omega+2A_t(u)}{f(u)^2}\right)a_t(u)+\frac{1}{f(u)}\mathbf{k}\cdot\mathbf{a}(u)\right]\Phi(u)\\
-\mathrm{i}\Phi a_u'(u)-\mathrm{i}\left[\left(\frac{f'(u)}{f(u)}-\frac{d-1}{u}\right)\Phi(u)+2\Phi'(u)\right]a_u(u)=0,
\end{aligned}
\tag{4.80}
$$

and for the gauge field fluctuations we have

$$a_t''(u) - \frac{d-3}{u}a_t'(u) - \left(\frac{\mathbf{k}^2}{f(u)} + \frac{2L^2\Phi(u)^2}{u^2 f(u)}\right)a_t(u) - \frac{\omega}{f(u)}\mathbf{k}\cdot\mathbf{a}(u)$$
$$- \frac{L^2}{u^2 f(u)}\Big[\big(\omega + 2A_t(u)\big)\delta\phi(u) - \big(\omega - 2A_t(u)\big)\delta\phi^*\Big]\Phi(u)$$
$$+ \mathrm{i}\omega\left(a_u'(u) - \frac{d-3}{u}a_u(u)\right) = 0, \quad (4.81)$$

$$\mathbf{a}''(u) + \left(\frac{f'(u)}{f(u)} - \frac{d-3}{u}\right)\mathbf{a}'(u) + \left(\frac{\omega^2}{f(u)^2} - \frac{\mathbf{k}_\perp^2}{f(u)} - \frac{2L^2\Phi(u)^2}{u^2 f(u)}\right)\mathbf{a}(u)$$
$$+ \frac{\mathbf{k}}{f(u)}\big(\mathbf{k}_\perp\cdot\mathbf{a}(u)\big) + \frac{\omega\mathbf{k}}{f(u)^2}a_t(u) + \frac{L^2\mathbf{k}}{u^2 f(u)}\big(\delta\phi(u) - \delta\phi^*(u)\big)\Phi(u)$$
$$- \mathrm{i}\mathbf{k}\left[a_u'(u) + \left(\frac{f'(u)}{f(u)} - \frac{d-3}{u}\right)a_u(u)\right] = 0, \quad (4.82)$$

$$\frac{\omega}{f(u)}a_t'(u) + \mathbf{k}\cdot\mathbf{a}'(u) - \mathrm{i}\left(\mathbf{k}^2 - \frac{\omega^2}{f(u)} + \frac{2L^2\Phi(u)^2}{u^2}\right)a_u(u)$$
$$- \frac{L^2}{u^2}\Big[\big(\delta\phi(u) - \delta\phi^*(u)\big)\Phi'(u) - \big(\delta\phi'(u) - \delta\phi'^*(u)\big)\Phi(u)\Big] = 0, \quad (4.83)$$

where $\mathbf{k}_\perp$ denotes the transverse vector orthogonal to the directions given by the particular equations for the component of $\mathbf{a}(u)$. For instance, we can look at the equation for one of the $d-1$ spatial components, $\mathbf{a}(u) = a_x(u)\mathbf{e}_x$ say, so $\mathbf{k}_\perp = k_y\mathbf{e}_y + k_z\mathbf{e}_z + \cdots$ and hence $\mathbf{k}_\perp\cdot\mathbf{a}$ couples the complementary components to the one chosen, *i.e.* $a_y(u), a_z(u), \ldots$. Furthermore, assuming $\mathbf{k} = k_x\mathbf{e}_x$, we see that the equations of the $a_x(u)$ component couples only with the $a_t(u)$ component (in this case $\mathbf{k}_\perp = \mathbf{0}$), whereas the equations for all other $d-2$ spatial components decouple. Looking at the transverse directions *e.g.* $\mathbf{k} = k_y\mathbf{e}_y + k_z\mathbf{e}_z + \cdots$, the equation for the fluctuations in the x-direction will decouple from all other $d-2$ fluctuation equations, but the equations for the remaining $d-2$ fluctuations will couple with each other and $a_t(u)$. The background solutions are given by the AdS-Schwarzschild solutions for $f(u)$ (4.65) and the numerical integrated solution for the coupled system (4.68) and (4.69).

Fluctuations with backreaction

Turning on the backreaction we need to consider the fluctuations of the metric field, too,

$$g_{ab} = G_{ab} + h_{ab}, \quad (4.84)$$

Thus, we need to expand the determinant of the metric up to quadratic order

$$\delta^{(2)}g = \det(G_{ab} + h_{ab}) - \det G_{ab}$$
$$= \frac{\partial(\det G)}{\partial G_{ab}}h_{ab} + \frac{1}{2}\frac{\partial^2(\det G)}{\partial G_{ab}G_{cd}}h_{ab}h_{cd}, \quad (4.85)$$

and the square root of (4.85)

$$\begin{aligned}\delta^{(2)}\sqrt{-g} &= \frac{\partial\sqrt{\text{-}\det G}}{\partial\det G}\frac{\partial\det G}{\partial G_{ab}}h_{ab} + \frac{1}{4}\left(\frac{\partial}{\partial G_{ab}}\frac{\partial\sqrt{\text{-}\det G}}{\partial G_{cd}} + \frac{\partial}{\partial G_{cd}}\frac{\partial\sqrt{\text{-}\det G}}{\partial G_{ab}}\right)h_{ab}h_{cd} \\ &= \sqrt{-\det G}\left[\frac{1}{2}G^{ab}h_{ab} + \left(\frac{1}{8}G^{ab}G^{cd} - \frac{1}{4}G^{bc}G^{ad}\right)h_{ab}h_{cd}\right], \end{aligned} \tag{4.86}$$

where we symmetrized the second partial derivative in its indices and inserted the well known relation

$$\frac{\partial\sqrt{\text{-}\det G}}{\partial G_{ab}} = \frac{1}{2}\sqrt{-G}G^{ab}. \tag{4.87}$$

Up to linear order in the fluctuations the indices of the metric fluctuations h_{ab} are raised and lowered by the background metric G_{ab}, so we can rewrite (4.86) as

$$\sqrt{\det(G+h)} = \sqrt{\det G}\left[1 + \frac{1}{2}\operatorname{tr}h - \frac{1}{4}\operatorname{tr}\left(h^2\right) + \frac{1}{8}\left(\operatorname{tr}h\right)^2\right], \tag{4.88}$$

which can be compared to the expansion using $\det(\mathbb{1}+M) = \exp\left(\operatorname{tr}\ln(\mathbb{1}+M)\right)$ as given in Appendix A.1.2, (A.10). This will lead to additional terms in (4.74) and (4.75) coming form the quadratic expansion of $\sqrt{-g}$ in the fluctuations

$$\begin{aligned}\mathscr{L}_{\mathrm{M}}^{(1)} = \sqrt{-G}\Bigg[&-\frac{1}{4}G^{ce}G^{df}\left(F_{cd}\delta F_{ef} + \delta F_{cd}F_{ef}\right) + G^{cd}\mathscr{L}_{\phi cd}^{(2)} \\ &- \frac{1}{4}\left(G^{cs}G^{et}h_{st}G^{df} + G^{ds}G^{ft}h_{st}G^{ce} + \frac{1}{2}G^{st}h_{st}G^{ce}G^{df}\right)F_{cd}F_{ef} \\ &+ \left(G^{cs}G^{dt}h_{st} + \frac{1}{2}G^{st}h_{st}G^{cd}\right)\mathscr{L}_{\phi cd}^{(0)}\Bigg], \end{aligned} \tag{4.89}$$

$$\begin{aligned}\mathscr{L}_{\mathrm{M}}^{(2)} = \sqrt{-G}\Bigg\{&-\frac{1}{4}G^{ce}G^{df}\delta F_{cd}\delta F_{ef} + G^{cd}\mathscr{L}_{\phi cd}^{(2)} \\ &- \frac{1}{4}\left(G^{cs}G^{et}h_{st}G^{df} + G^{ds}G^{ft}h_{st}G^{ce} + \frac{1}{2}G^{st}h_{st}G^{ce}G^{df}\right)\left(F_{cd}\delta F_{ef} + \delta F_{cd}F_{ef}\right) \\ &+ \left(G^{cs}G^{dt}h_{st} + \frac{1}{2}G^{st}h_{st}G^{cd}\right)\mathscr{L}_{\phi cd}^{(1)} \\ &- \frac{1}{4}\Bigg[G^{cs}G^{et}h_{st}G^{dm}g^{fn}h_{mn} + \frac{1}{2}G^{mn}h_{mn}\left(G^{cs}G^{et}h_{st}G^{df} + G^{ds}G^{ft}h_{st}g^{ce}\right) \\ &+ \left(\frac{1}{8}g^{st}G^{mn} - \frac{1}{4}G^{tm}G^{sn}\right)h_{st}h_{mn}G^{ce}G^{df}\Bigg]F_{ce}F_{df} \\ &+ \left[\frac{1}{2}G^{st}h_{st}G^{cm}G^{dn}h_{mn} + \left(\frac{1}{8}G^{st}G^{mn}h_{st}h_{mn} - \frac{1}{4}G^{tm}G^{sn}\right)h_{st}h_{mn}G^{cd}\right]\mathscr{L}_{\phi cd}^{(0)}\Bigg\}. \end{aligned} \tag{4.90}$$

Note that here we write the total action in the form

$$S = \frac{1}{2\kappa^2}\int \mathrm{d}^{d+1}x\left(\mathscr{L}_{\mathrm{EH}} + 2\alpha^2 L^2 \mathscr{L}_{\mathrm{M}}\right) = S_{\mathrm{EH}} + S_{\mathrm{M}}, \tag{4.91}$$

and the scalar field Lagrangian $\mathscr{L}_{\phi cd}$ is given by

$$\begin{aligned}
\mathscr{L}^{(0)}_{\phi cd} =& -\left(\nabla_c\Phi + \mathrm{i}A_c\Phi\right)\left(\nabla_d\Phi - \mathrm{i}A_d\Phi\right) - m^2\Phi^2,\\
\mathscr{L}^{(1)}_{\phi cd} =& -\nabla_c\delta\phi^*\nabla_d\Phi - \nabla_d\delta\phi\nabla_c\Phi + \mathrm{i}\nabla_c\Phi A_d\delta\phi - \mathrm{i}\nabla_d\Phi A_c\delta\phi^* - \mathrm{i}A_c\nabla_d\delta\phi\Phi\\
&+ \mathrm{i}A_d\nabla_c\delta\phi^*\Phi - A_cA_d\Phi\left(\delta\phi + \delta\phi^*\right) - \left(A_ca_d + A_da_c\right)\Phi^2 - m^2\Phi\left(\delta\phi + \delta\phi^*\right),\\
\mathscr{L}^{(2)}_{\phi cd} =& -\nabla_c\delta\phi\nabla_d\delta\phi^* - \mathrm{i}A_c\nabla_d\delta\phi\delta\phi^* + \mathrm{i}A_d\nabla_c\delta\phi^*\delta\phi - \mathrm{i}a_c\nabla_d\delta\phi\Phi + \mathrm{i}a_d\nabla_c\delta\phi^*\Phi\\
&+ \mathrm{i}\nabla_c\Phi a_d\delta\phi - \mathrm{i}\nabla_d\Phi a_c\delta\phi^* - A_cA_d\delta\phi\delta\phi^* - \left(A_ca_d + A_da_c\right)\left(\delta\phi + \delta\phi^*\right)\\
&- a_aa_b\phi^2 - m^2\delta\phi^*\delta\phi.
\end{aligned} \tag{4.92}$$

The Einstein-Hilbert term expanded up to quadratic order in the fluctuations can be casted in the following form

$$\mathscr{L}^{(1)}_{\mathrm{EH}} = \sqrt{-G}\delta^{(1)}R + \delta^{(1)}\sqrt{-g}\left(R - 2\Lambda\right), \tag{4.93}$$

$$\mathscr{L}^{(2)}_{\mathrm{EH}} = \sqrt{-G}\delta^{(2)}R + \delta^{(1)}\sqrt{-g}\delta^{(1)}R + \delta^{(2)}\sqrt{-g}\left(R - 2\Lambda\right), \tag{4.94}$$

where

$$\delta^{(2)}R = -h^{ab}\nabla^{(G)}_c\nabla^{(G)c}h_{ab} - \frac{3}{4}G^{ab}\partial_a h^{cd}\partial_b h_{cd} - g^{ab}\partial_a\ln\sqrt{-\det h}\partial_b\ln\sqrt{-\det h}, \tag{4.95}$$

with $\nabla^{(G)}$ denoting the background curved space covariant derivative constructed only out of the background metric G_{ab}. The full backreacted equations of motions are listed in Appendix C, where we applied the Fourier transformation for all fluctuations *i.e.*

$$\begin{aligned}
\delta\phi(t,\mathbf{x},u) &= \int\frac{\mathrm{d}\omega\,\mathrm{d}^{d-1}\,\mathbf{k}}{(2\pi)^d}\,\mathrm{e}^{-\mathrm{i}\omega t + \mathrm{i}\mathbf{k}\cdot\mathbf{x}}\,\delta\phi(u),\\
a_a(t,\mathbf{x},u) &= \int\frac{\mathrm{d}\omega\,\mathrm{d}^{d-1}\,\mathbf{k}}{(2\pi)^d}\,\mathrm{e}^{-\mathrm{i}\omega t + \mathrm{i}\mathbf{k}\cdot\mathbf{x}}\,a_a(u),\\
h_{ab}(t,\mathbf{x},u) &= \int\frac{\mathrm{d}\omega\,\mathrm{d}^{d-1}\,\mathbf{k}}{(2\pi)^d}\,\mathrm{e}^{-\mathrm{i}\omega t + \mathrm{i}\mathbf{k}\cdot\mathbf{x}}\,h_{ab}(u).
\end{aligned} \tag{4.96}$$

For most of the computations, conducted in Section 4.3 and 4.4, involved in applications to linear response and Homes' law, the normal phase equations of motions are sufficient. The normal phase $\Phi = 0$ and $\chi = 0$ equations of motion for the scalar field fluctuations are given by

$$\delta\phi''(u) + \left(\frac{f'(u)}{f(u)} - \frac{d-1}{u}\right)\delta\phi'(u) + \left[\frac{(\omega + A_t)^2}{f(u)^2} - \frac{\mathbf{k}^2}{f(u)} - \frac{L^2m^2}{u^2f(u)}\right]\delta\phi(u) = 0. \tag{4.97}$$

The gauge field equations are extended by metric fluctuations as well, where $\mathbf{h}_t(u), \mathbf{h}_u(u)$ denotes the spatial entries of the corresponding row/column

$$a_t''(u) - \frac{d-3}{u}a_t'(u) - \left(\frac{\mathbf{k}^2}{f(u)}\right)a_t(u) - \frac{\omega}{f(u)}\mathbf{k}\cdot\mathbf{a}(u) + \mathrm{i}\omega\left(a_u'(u) - \frac{d-3}{u}a_u(u)\right)$$
$$- \frac{3u^2A_t'(u)}{2L^2f(u)}h_{tt}'(u) + \frac{u^2A_t'(u)}{2L^2}\sum_{i=1}^{d-1}h_{ii}'(u) + \frac{3u^2f(u)A_t'(u)}{2L^2}h_{uu}'(u)$$
$$+ \frac{u}{L^2}A_t'(u)\sum_{i=1}^{d-1}h_{ii}(u) + \frac{\mathrm{i}uA_t'(u)}{L^2}\sum_{i=1}^{d-1}h_{ui}(u)k_i + \frac{3}{2}\frac{u^2f(u)}{L^2}\left(\frac{f'(u)}{f(u)} + \frac{2}{u}\right)A_t'(u)h_{uu}(u) = 0, \tag{4.98}$$

$$\mathbf{a}''(u) + \left(\frac{f'(u)}{f(u)} - \frac{d-3}{u}\right)\mathbf{a}'(u) + \left(\frac{\omega^2}{f(u)^2} - \frac{\mathbf{k}_\perp^2}{f(u)}\right)\mathbf{a}(u) + \frac{\mathbf{k}}{f(u)}(\mathbf{k}_\perp\cdot\mathbf{a}(u))$$
$$+ \frac{\omega\mathbf{k}}{f(u)^2}a_t(u) - \mathrm{i}\mathbf{k}\left[a_u'(u) + \left(\frac{f'(u)}{f(u)} - \frac{d-3}{u}\right)a_u(u)\right]$$
$$- \frac{u^2A_t'(u)}{L^2f(u)}\mathbf{h}_t'(u) - \frac{2uA_t'(u)}{L^2f(u)}\mathbf{h}_t(u) - \frac{\mathrm{i}u^2\omega A_t'(u)}{L^2f(u)}\mathbf{h}_u(u) = 0, \tag{4.99}$$

$$\frac{\omega}{f(u)}a_t'(u) + \mathbf{k}\cdot\mathbf{a}'(u) - \mathrm{i}\left(\mathbf{k}^2 - \frac{\omega^2}{f(u)}\right)a_u(u)$$
$$- \frac{3}{2}\frac{u^2\omega A_t'(u)}{L^2f(u)^2}h_{tt}(u) - \frac{u^2A_t'(u)}{L^2f(u)}\sum_{i=1}^{d-1}h_{ti}k_i + \frac{u^2\omega A_t'(u)}{2L^2f(u)}\sum_{i=1}^{d-1}h_{ii}(u) + \frac{3}{2}\frac{u^2\omega A_t'(u)}{L^2}h_{uu}(u) = 0. \tag{4.100}$$

Note that in the normal phase the background solution for the metric is given by the AdS-Reissner-Nordström black brane, so $f(u)$ is given by (4.49), as well as $A_t(u)$ by (4.48).

Numerical solution

Numerical solutions are integrated by adapting the Mathematica Code D.2 for fluctuations. In particular, we need to modify the asymptotic expansion at the horizon to use an index associated with infalling boundary conditions, as explained in detail in Section 4.3.6, in order to extract the retarded response function according to the holographic fluctuation-dissipation theorem outlined in *i* to *iv* on page 111. The numerical response function is defined as the ratio of the subleading coefficient to the leading coefficient in the boundary expansion. The numerically obtained key features of holographic superconductors are shown in Figure 4.1

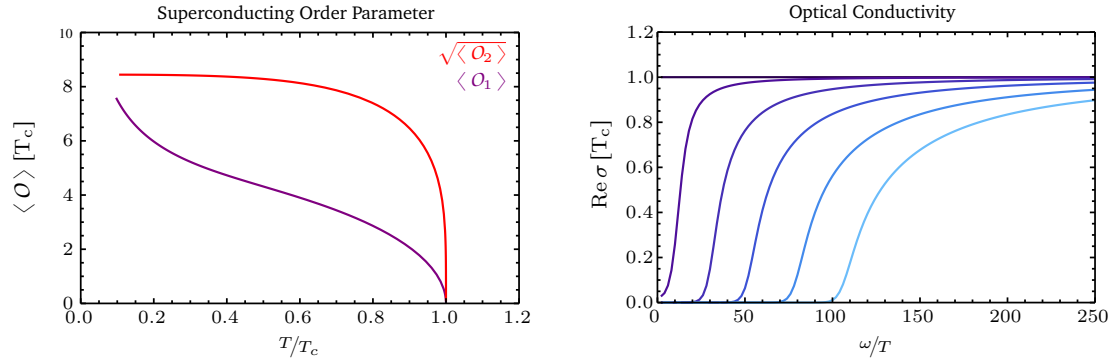

Figure 4.1. In the left panel, the expectation value of the dual operator is shown which serves as a order parameter for the superconducting phase transition for $\alpha = 0$, $d = 3$ and $m^2L^2 = -2$. In this case we may define two dual operators, O_Δ and $O_{d-\Delta}$, since $-9/4 < m^2L^2 < -5/4$ as explained below (3.77). In order to compare the curves for the dimension one and two operator we need to take the square root of $O_{\Delta=2}$. In the following we will only work with the dimension two operator O_Δ with RG scaling field $d - \Delta = 1$. The continuous phase transition is of mean-field type with the critical exponent $\beta = 1/2$, *c.f.* Table 2.6. The right panel shows the response function of the spatial gauge field fluctuation corresponding to the optical conductivity $\sigma(\omega)$. The real part measures the dissipation of the system, *c.f.* Section 4.3.2, which is exponentially suppressed in the superconducting phase. The normal phase solutions for $d = 3$ is given by a frequency independent optical conductivity. This is a general properties of conformal theories [181]. For IR deformation induced by the non-trivial profile of the scalar field solution in the limit $\omega \ll T$, the conformal solution is lost and a superconducting condensate allows for nearly dissipationless transport. The curves are color coded as follows: $T/T_c = 1, 0.5274, 0.2464, 0.165, 0.1212, 0.0974$. Generically, upon approaching the conformal limit in the UV, $\omega \gg T$, the optical conductivity is proportional to ω^{d-3} for $d > 2$ as derived in (4.190). Deeper implications of the gap in the real part of the optical conductivity and its connection to the superfluid strength is discussed extensively in Section 4.4.1.

4.2. Holographic p-Wave Superconductor

Overview

- Einstein Yang-Mills action describes condensation of internal gauge field component.
- Condensate breaks $U(1)_3$ and spatial rotations $SO(3)$ to $SO(2)$
  $\longrightarrow$ vector hair AdS-Reissner-Nordström black brane solution.
- Explicit top-down construction from D_p-brane embeddings possible.

Holographic p-wave superconductors are described by a non-Abelian gauge theory, or Yang-Mills theory. The order parameter is of p-wave type and due to the universal coupling of the metric to all fields we additionally find a spatial anisotropy. Therefore, the holographic p-wave superconductor should be thought of as a nematic superconductor, or a nematic superfluid,

respectively. The p-wave superconductor may be connected directly to a top-down setup utilizing two probe branes in a large N_c D_3-brane background [217, 222]. Here we start with a $U(2) \cong U(1)_{\mathrm{B}} \times SU(2)_{\mathrm{I}}$ symmetry, where 'B' stands for the baryon number and 'I' for the flavor isospin symmetry. Introducing a chemical potential explicitly breaks the isospin symmetry to a so-called $U(1)_3$ which is generated by the remaining unbroken generator τ_3. This generator can be chosen to be diagonal *e.g.* in the canonical choice for the Pauli matrices as representation of the $SU(2)_{\mathrm{I}}$. The condensate arises from the spontaneous breaking of the remaining $U(1)_3$ symmetry as well as the spatial $SO(3)$ symmetry of the metric. As in the s-wave holographic superconductor, the $U(1)_3$ symmetry breaking condensate is identified with the superconducting condensate of the charged degrees of freedom. Technically, we will not be able to detect the Meißner-Ochsenfeld effect since the local $U(1)_3$ is a global symmetry in the dual field theory, yet it can be made local by local background transformations. Strictly speaking, we are dealing with a rotational symmetry breaking superfluid which can be viewed as a nematic superfluid. The p-wave superfluid has been extensively studied in [169, 219, 222, 223] as well as the effects arising from its anisotropy [22, 224]. In this section we will first motivate the bottom-up Einstein-Yang-Mills action by expanding the top-down D_p-brane DBI action (3.40). Then we will discuss the general Ansatz to construct vector-hair AdS-Reissner-Nordström solutions. For our final application to understand Homes' law, we do not need to fully construct the fluctuations, as is further explained in Section 4.5.1.

4.2.1. Einstein-Yang-Mills action & equations of motion

In addition to gravity, non-Abelian gauge fields transforming under a non-Abelian gauge group are considered. This system is described by the Einstein-Yang-Mills action. In the following, we specialize to $(4+1)$-dimensional asymptotically AdS space and to the gauge group $SU(2)$ with field strength tensor (2.101) in the adjoint representation

$$F^a_{\mu\nu} = \partial_\mu A^a_\nu - \partial_\nu A^a_\mu + \epsilon^{abc} A^b_\mu A^c_\nu, \tag{4.101}$$

with $f^{ABC} = \epsilon^{ABC}$, where ϵ^{ABC} denotes the total antisymmetric tensor with the normalization $\epsilon^{123} = +1$. Due to the analogy to QCD, the $SU(2)_{\mathrm{I}}$ is dubbed isospin symmetry. The Einstein-Yang-Mills action is thus given by[7]

$$S = \int \mathrm{d}^5x \sqrt{-g} \left[\frac{1}{2\kappa_5^2}(R - \Lambda) - \frac{1}{4g_{\mathrm{YM}}^2} F^A_{ab} F^{Aab} \right], \tag{4.102}$$

where κ_5 is the five dimensional gravitational constant, $\Lambda = -12/L^2$ is the cosmological constant for $d = 5$, with L being the AdS radius and g_{YM} denotes the Yang-Mills coupling. The Yang-Mills part of the action (4.102) can be derived from the D_p-brane DBI action expanded to leading order in α', *i.e.* [8]

$$S^{\mathrm{DBI}}_{D_p} = -T_{D_p} N_f \int \mathrm{d}^{p+1}\xi \sqrt{-g} \left[1 + \frac{1}{2} \left(2\pi\alpha'\right)^2 \mathrm{tr}\left(F_{ab} F^{ab}\right) \right], \tag{4.103}$$

where $N_f = 2$ is the number of flavors and T_{D_p} describes the tension of the brane given in (3.43). The Einstein-Yang-Mills action yields the Einstein and Yang-Mills equations of motion

[7] The internal indices running over the generators in the adjoint representation are denoted by capitalized Latin letters, *i.e.* $A = A^A_a T^A \, \mathrm{d}x^a$, where T^A are the generators of the gauge group in a certain representation.

[8] The detailed derivation can be found in Section 5.2, where we work completely in a top-down fashion to analyze holographic matter at zero temperature and finite density.

$$R_{ab} + \frac{4}{R^2} g_{ab} = \kappa_5^2 \left(T_{ab} - \frac{1}{3} T^c{}_c \, g_{ab} \right), \qquad \nabla^a F^A_{ab} = -f^{ABC} A^{Ba} F^C_{ab}, \tag{4.104}$$

where the Einstein equations are brought into the "trace-reversed" form suitable for further manipulations. The Yang-Mills energy-momentum tensor $T_{\mu\nu}$ is defined as

$$T_{ab} = \frac{1}{g_{\text{YM}}^2} \left[F^A_{ac} F^A{}_b{}^c - \frac{1}{4} g_{ab} F^A_{cd} F^{Acd} \right]. \tag{4.105}$$

4.2.2. Numerical solutions of the p-wave background equations of motion

Let us first consider the probe limit solutions with $\alpha = \kappa_5 / g_{\text{YM}} = 0$. Since the Einstein equations decouple, they can be solved by the AdS-Schwarzschild solution discussed in the previous section. This is in agreement with the top-down solution of a D-brane wrapping P AdS_5 directions and Q S^5 directions, where the background metric generated by the D_3-branes is exactly the $\text{AdS}_5 \times S^5$-Schwarzschild metric (4.64) with temperature $T = 1/\pi u_{\text{H}}$. As explained in the introduction the $SU(2)_{\text{I}}$ will be explicitly broken to a $U(1)_3$ which in turn is subsequently broken by a spontaneously generated condensate. Thus the Ansatz for the gauge field is of the form

$$A = A^1_x(u) \tau_1 \, \mathrm{d}x + A^3_t(u) \tau_3 \, \mathrm{d}t \, . \tag{4.106}$$

On the field theory side this corresponds to the introduction of an isospin chemical potential by the boundary values of the time components of the gauge field A^3_t. This breaks the $SU(2)_{\text{I}}$ symmetry down to a diagonal $U(1)_3$ which is generated by τ^3. In order to study the transition to the superfluid state, we allow solutions with non-zero $\langle J^1_x \rangle$, such that we include the dual gauge field A^1_x in the gauge field Ansatz. Since we consider only isotropic and time-independent solutions in the field theory, the gauge fields exclusively depend on the radial coordinate u. With this Ansatz the Yang-Mills energy-momentum tensor defined in (4.105) is diagonal. The gauge field Ansatz (4.106) reduces the Yang-Mills equations to

$$\begin{aligned} A^{3\prime\prime}_t(u) + \frac{4-P}{u} A^{3\prime}_t(u) - \frac{\left(A^1_x\right)^2}{\pi^2 T^2 f(u)} A^3_t = 0, \\ A^{1\prime\prime}_x(u) + \left(\frac{f'(u)}{f(u)} + \frac{4-P}{u} \right) A^{1\prime}_x(u) + \frac{\left(A^3_t\right)^2}{\pi^2 T^2 f(u)^2} A^1_x = 0, \end{aligned} \tag{4.107}$$

where we work in dimensionless radial coordinates $u \longrightarrow u u_{\text{H}}$. Furthermore for numerical calculations the temperature can be set to $T = 1$ by rescaling the gauge fields $A^3_t \longrightarrow T A^3_t$ and $A^1_x \longrightarrow T A^1_x$. The asymptotic expansions of the gauge fields at the horizon and the boundary are determined via the Frobenius method, implemented in Mathematica Code D.1. The asymptotic expansions at the horizon $u_{\text{H}} = 1$ read

$$A^3_{t\text{H}}(u) = C a^3_t (u-1) - C a^3_t \left(2 - \frac{1}{2} P + \frac{\left(C a^1_x\right)^2}{8\pi^2 T^2} \right) (u-1)^2 \tag{4.108}$$

$$+ C a^3_t \frac{\left(C a^1_x\right)^4 - 12\pi^2 \left(C a^1_x\right)^2 (P-5) T^2 + 32\pi^4 \left(P^2 - 9P + 20\right) T^4}{192 \pi^4 T^4} (u-1)^3, \tag{4.109}$$

$$+ \mathcal{O}\left((u-1)^4\right) \tag{4.110}$$

	0	1	2	3	4	5	6	7	8	9
$N_c D3$	•	•	•	•	–	–	–	–	–	–
$N_f D5$	•	•	•	–	•	•	•	–	–	–
$N_f D7$	•	•	•	•	•	•	•	•	–	–
x^a	x^0	x^1	x^2	x^3	u	θ^1	θ^2	θ^3	θ^4	θ^5

Table 4.2. The directions wrapped by the D_p-branes are listed with a •. The spatial directions are denoted by x^μ, the radial AdS coordinate by u and the S^5 angles by θ^i. As explained in the main text the D_5-brane wraps $P = 4$ AdS directions and $Q = 2$ S^5 directions with a $d = 3$ field theory, while for the $d = 4$ field theory the $N_f = 2$ D_7-branes yields $P = 5$ and $Q = 3$. Note that $D3/D_p$-brane embeddings with $P-Q = 2$ are supersymmetric [225].

$$A^1_{x\mathrm{H}}(u) = Ca^1_x - \frac{\left(Ca^3_t\right)^2 Ca^1_x}{64\pi^2 T^2}(u-1)^2 + \frac{\left(Ca^3_t\right)^2 Ca^1_x\left(\left(Ca^1_x\right)^2 + 3(13-2P)\pi^2T^2\right)}{576\pi^4T^4}(u-1)^3 + \mathcal{O}\left((u-1)^4\right). \tag{4.111}$$

Due to the regularity conditions $A^3_t(u_\mathrm{H}) = 0$ we have only a two parameter family left at the horizon determined by Ca^3_t and Ca^1_x. For the numerical integration we actually used a asymptotic horizon expansion up to $\mathcal{O}\left((u-1)^8\right)$. The boundary asymptotic solution at $u_\mathrm{B} = 0$ is given by

$$\begin{aligned} A^3_{t\mathrm{B}}(u) &= \mu - \rho^3_t \frac{u^{P-3}}{(\pi T)^{P-3}}, \\ A^1_{x\mathrm{B}}(u) &= \rho^1_x \frac{u^{P-3}}{(\pi T)^{P-3}}, \end{aligned} \tag{4.112}$$

where we included directly the vanishing source constraint for the dual operator J^1_x. For the numerical solution the temperature T is set to one, so all dimensionful physical quantities are given in units of T, *e.g.* the numerical values of the isospin chemical potential are in fact μ/T. For a $d = 3$ dimensional field theory we may consider a D_3/D_5-brane setup where the D_5-brane wraps $P = 4$ directions of the AdS_5 space and $Q = 2$ directions of the S^5, whereas a $d = 4$ dimensional field theory may be described by a D_3/D_7-brane setup with $P = 5$ and $Q = 3$. The precise extensions of the branes are listed in Table 4.2. Solving these equations numerically with the help of the *Mathematica* program outlined in Mathematica Code D.2 yields the map

$$(Ca^3_t, Ca^1_x) \mapsto (\mu, 0). \tag{4.113}$$

Note that in general this map is not unique since there are higher excitation solutions with one or more nodes which are associated to higher energy states in analogy to higher modes of a harmonic oscillator in a box. However, we need to pick the ground state solution in order to apply the holographic dictionary. The isospin chemical potential μ_I of the $U(1)_3$ will be set as a free parameter, whereas the spontaneous symmetry breaking operator must not be sourced *i.e.* the coefficient of the leading term must be zero. The result of the shooting yields the inverse

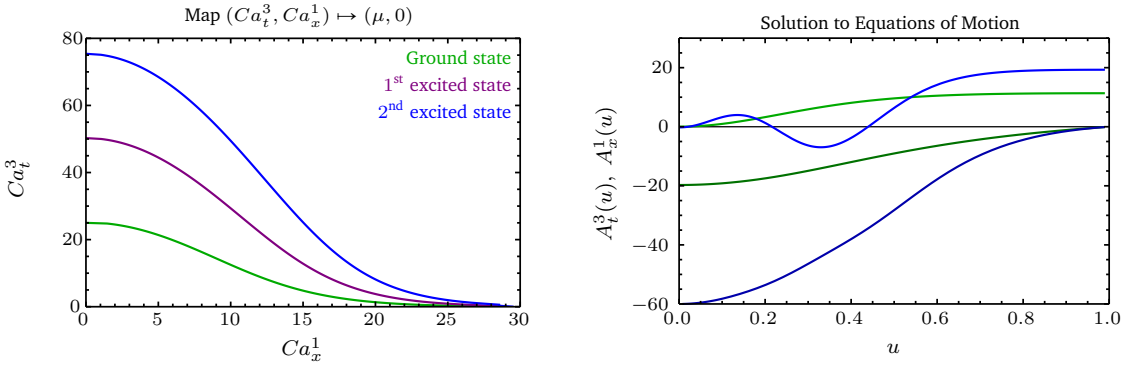

Figure 4.2. The left plot shows the mapping of the numerically obtained solutions with boundary values $A^3_{t\,\mathrm{B}} = \mu$ and $A^1_{x\,\mathrm{B}} = 0$ for a D_7-brane setup. The critical temperature is read off at $Ca_x^1 = 0$ from $Ca_t^3 \approx 24$ and hence according to (4.114) $\mu \approx 12 \approx 3.18\pi$. Note that the curves corresponding to the ground state solutions and the 1st and 2nd excited state of Ca_t^3 are approaching each other for large values of the free parameter Ca_x^1 at the horizon. Thus, it is virtually impossible to numerically distinguish the sought ground state solutions from the higher excitation solutions since not only the first and second, but all higher excitations approaching each other. Physically, this follows from the fact that for $Ca_t^3 \to 0$, $A_t^3 = 0$, the system is described by the totally disordered high temperature phase. The right plots shows the respective ground state solutions and the 2nd excited state solutions with two nodes in the $A_x^1(u)$ profile.

map displayed in Figure 4.2 The critical temperature can be read off directly from Figure 4.2 since for $Ca_x^1 = 0$ we find the trivial solution $A_x^1 = 0$, so the initial condition Ca_t^3 is identical to μ according to the analytic solution of A_t^3 in the normal phase (4.48)[9]

$$A_t^3(u) = -Ca_t^3 \frac{1-u^{P-3}}{P-3} \qquad \Rightarrow \qquad \mu = -\lim_{u\to 0} A_t^3(u) = \frac{Ca_t^3}{P-3}. \tag{4.114}$$

The critical value is $\mu/T_c \approx 3.81\pi$. The expectation value of the operators dual to the gauge fields is determined via the holographic dictionary[10]

$$\begin{aligned}\left\langle J_\mu^A \right\rangle &= \frac{\delta I^{\mathrm{DBI}}_{D_p}}{\delta \mu} = T_{D_p} N_f \left(2\pi\alpha'\right)^2 \rho_\mu^A = (2\pi)^{-p+2} \left(\frac{2\pi}{g_{\mathrm{YM}}^2}\right) \left(\frac{2g_{\mathrm{YM}}^2 N_c}{L^4}\right)^{(p-3)/4} N_f \rho_\mu^A \\ &= (2\pi)^{-p+2}\, 2^{(p-3)/4} L^{-p+3} \left(g_{\mathrm{YM}}^2 N_c\right)^{(p-7)/4} N_c N_f \rho_\mu^A, \end{aligned} \tag{4.115}$$

where in the last line the expression is written entirely in terms of field theory quantities via ${g_{\mathrm{s}}}^{-1} = {2\pi}/{g_{\mathrm{YM}}^2}$ and $\alpha' = \sqrt{2g_{\mathrm{YM}}^2 N_c / L^4}^{-1}$. Plotting the subleading term of the numerical solution, which determines the expectation value of the dual current, we see again the typical mean-field behavior in Figure 4.3. In the backreacted case $\alpha \neq 0$, the normal phase solution $\left\langle J_x^1 \right\rangle = 0$ or $A_x^1 = 0$, respectively, are the AdS-Reissner-Nordström black brane solution discussed in Section

[9] Strictly speaking the two function differ by an overall sign of the chemical potential, but this is a matter of convention what we call a D_p-brane or an anti $\overline{D_p}$-brane. In the following we will choose the convention that $\mu > 0$.

[10] P and p must not be confused, the former denotes the number of AdS directions wrapped by the brane, whereas the latter numbers the spatial dimensionality of the brane.

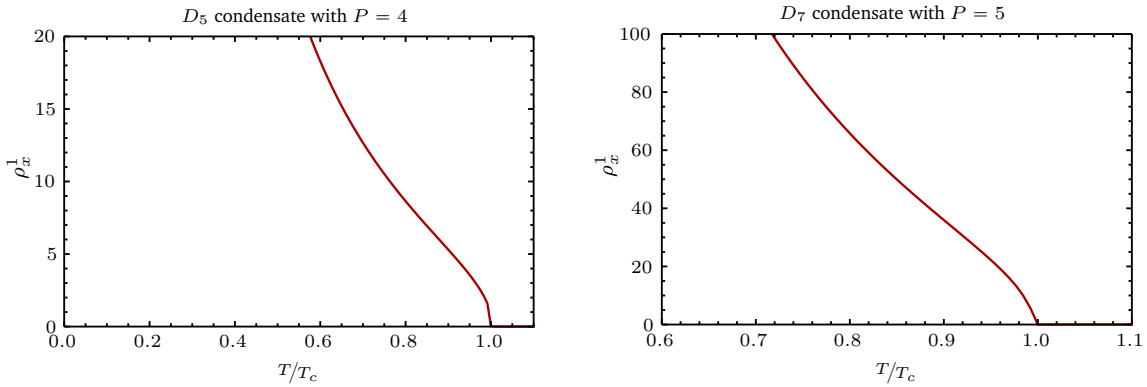

Figure 4.3. The condensate arising from the non-zero expectation value of the dual operator $\langle J_x^1 \rangle$ is plotted in the D_5 and D_7 case. In the probe limit, we find again a typical mean-field behavior with $\beta = 1/2$ for the second order superconducting phase transition.

4.1.3. The gauge field solution is given by (4.48)

$$A = \mu \left(1 - \frac{u^2}{u_{\mathrm{H}}^2}\right) \tau^3 \, \mathrm{d}t, \tag{4.116}$$

where $\tau^3 = \sigma^3/2\mathrm{i}$ with σ^3 the third Pauli matrix. We consider the diagonal representations of the gauge group since we may rotate the flavor coordinates until the chemical potential lies in the third isospin direction. Furthermore, the condensed phase is described by the solution to the full set of Einstein and Yang-Mills equations regarding the Yang-Mills energy-momentum tensor (4.105). This is the main difference to the background solutions of the holographic s-wave superconductors listed in Table 4.1: the AdS-Reissner-Nordström black brane solution with scalar hair is replaced by a vector hair solution. The numerical calculation seems to be more convenient and simpler in r-coordinates given by $r = L^2/u$, so in the following we will work in these coordinates. Given that the Yang-Mills energy-momentum tensor is diagonal, a diagonal metric is consistent

$$\mathrm{d}s^2 = -N(r)\sigma(r)^2 \, \mathrm{d}t^2 + \frac{1}{N(r)} \, \mathrm{d}r^2 + r^2 f(r)^{-4} \, \mathrm{d}x^2 + r^2 f(r)^2 \left(\mathrm{d}y^2 + \mathrm{d}z^2\right), \tag{4.117}$$

with

$$N(r) = -\frac{2m(r)}{r^2} + \frac{r^2}{L^2}. \tag{4.118}$$

Solutions with $\langle J_x^1 \rangle \neq 0$ also break the spatial rotational symmetry $SO(3)$ down to $SO(2)$[11] such that our metric Ansatz will respect only $SO(2)$. In addition, the system is invariant under the $\mathbb{Z}_2$ parity transformation $P_{\parallel} : x \longrightarrow -x$ and $A_x^1 \longrightarrow -A_x^1$. Inserting our Ansatz into the Einstein and Yang-Mills equations leads to six equations of motion for $m(r)$, $\sigma(r)$, $f(r)$, $\phi(r)$, $w(r)$ and one constraint equation from the rr component of the Einstein equations, where the

[10] In principle, equations of motions can be converted to different coordinates related by arbitrary bijective coordinate transformations (*c.f.* Appendix A.3). However, for a set of coupled equations of motions it is advisable to start again from the coordinate free formulation.

[11] Note that the finite temperature and chemical potential already break the Lorentz group down to $SO(3)$.

gauge fields $A_t^3 = \phi$ and $A_x^1 = w$ have been renamed in order to comply with the general naming scheme commonly used in the p-wave literature. The dynamical equations may be written as

$$\begin{aligned}
m' &= \frac{\alpha^2 r f^4 w^2 \phi^2}{6N\sigma^2} + \frac{r^3\alpha^2\phi'^2}{6\sigma^2} + N\left(\frac{r^3 f'^2}{f^2} + \frac{\alpha^2}{6} r f^4 w'^2\right), \\
\sigma' &= \frac{\alpha^2 f^4 w^2 \phi^2}{3rN^2\sigma} + \sigma\left(\frac{2rf'^2}{f^2} + \frac{\alpha^2 f^4 w'^2}{3r}\right), \\
f'' &= -\frac{\alpha^2 f^5 w^2 \phi^2}{3r^2 N^2 \sigma^2} + \frac{\alpha^2 f^5 w'^2}{3r^2} - f'\left(\frac{3}{r} - \frac{f'}{f} + \frac{N'}{N} + \frac{\sigma'}{\sigma}\right), \\
\phi'' &= \frac{f^4 w^2 \phi}{r^2 N} - \phi'\left(\frac{3}{r} - \frac{\sigma'}{\sigma}\right), \\
w'' &= -\frac{w\phi^2}{N^2\sigma^2} - w'\left(\frac{1}{r} + \frac{4f'}{f} + \frac{N'}{N} + \frac{\sigma'}{\sigma}\right).
\end{aligned} \tag{4.119}$$

The equations of motion are invariant under scaling transformations analogous to the s-wave superconductor. As illustrated for the probe limit solution where we rescaled the gauge fields to remove u_{H} we can apply this rescaling to the complete set of equations (4.119) via

$$r \longrightarrow cr, \qquad m \longrightarrow c^4 m, \qquad w \longrightarrow cw, \qquad \phi \longrightarrow c\phi. \tag{4.120}$$

to set r_h to one. By a similar scaling symmetry

$$r \longrightarrow cr, \qquad m \longrightarrow c^2 m, \qquad L \longrightarrow cL, \qquad \phi \longrightarrow c^{-1}\phi, \qquad \alpha \longrightarrow c\alpha, \tag{4.121}$$

the AdS radius may be set to $L = 1$. More importantly, the metric at the boundary needs to be asymptotically AdS spacetime, so we use the scaling

$$f \longrightarrow cf, \qquad w \longrightarrow c^{-2} w, \tag{4.122}$$

to set the boundary value $f(r_{\mathrm{B}}) = 1$ and

$$\sigma \longrightarrow c\sigma, \qquad \phi \longrightarrow c\phi, \tag{4.123}$$

in order to fix the boundary value $\sigma(r_{\mathrm{B}}) = 1$.

4.3. Applied Holography of Optical Properties of Solids

Overview

- Drude-Sommerfeld model captures key features of dissipative charge carrier transport in metals related to conductivity/resistivity.
- Linear response connects polarization and current-current correlators via the Einstein relations.
- Holographic calculations of strongly correlated metals without quasi particle description.
- Breakdown of the Drude-Sommerfeld model for large frequencies approaching conformal limit ⟶ no well-defined plasma frequency.

In this section we will develop the necessary tools to analyze response function characterizing different types of metals. In our case we are aiming for strongly correlated metals that allow for a relativistic scaling symmetry such as metallic systems close to the critical point, heavy fermions, high temperature superconductors, or graphene close to zero electrical potential. The holographic normal phase in the probe limit may be used to describe conformal matter and introducing a finite density, by fixing the chemical potential, the holographic calculation with backreaction extends to compressible matter. First, we will discuss the general Maxwell equations in d dimensions and define the dielectric function characterizing the response of matter in the presence of external electric and magnetic fields. The connection to the optical conductivity and the polarization will be elucidated as well as the Drude-Sommerfeld model for the conductivity in solids. Next, we define the plasma frequency and its relation to the dielectric function, the spectral weight, and the conductivity via the Kramers-Kronig relations. Finally, we give a detailed account of a holographic normal phase calculation on the Abelian-Higgs model and discuss the ramification and problems of holographically modeling the plasma frequency. The insight gained by this warming up exercise will guide us in order to devise and understand a possible holographic dual to tackle Homes' law in the following section.

4.3.1. Maxwell equations in $d = D + 1$ dimensions

Maxwell Equations in manifestly covariant form in curved space are given by

$$\nabla^A F_{AB} = j_B, \tag{4.124}$$

where $F = \mathrm{d}A$ is the field strength two-form of the gauge potential one-form A and j is the current three-form. The indices $A, B, \ldots$ are running from $0, \ldots, d-1$. We can split the field strength two-form into a $D = d - 1$ dimensional covector and a $1/2 D(D-1)$ dimensional antisymmetric tensor

$$E_a = F_{0a}, \qquad B_{ab} = \frac{1}{2}\sqrt{-g}\epsilon_{abcd}F^{cd}, \tag{4.125}$$

where the indices a and b are running from $1, \ldots, D = d - 1$, i.e. they are running only over the spatial components of the given spacetime. In a flat comoving local reference frame the fields can be written in terms of potentials ϕ and A_a[12]

$$E_a = -\partial_a \phi - \partial_0 A_a, \qquad B_{ab} = \partial_a A_b - \partial_b A_a. \tag{4.126}$$

In the local reference frame, the D dimensional Maxwell equations in E_a and $B^a = 1/2 \epsilon^{abc} B_{bc}$ take the form

$$\begin{aligned} \partial_a E^a &= 4\pi\rho, & \epsilon^{abc}\partial_b B_c - \partial_0 E^a &= 4\pi j^a, \\ \epsilon^{abc}\partial_b E_c + \partial_0 B^a &= 0, & \partial_a B^a &= 0. \end{aligned} \tag{4.127}$$

In the presence of matter the inhomogeneous equations are modified by contributions arising from polarization/magnetization of the matter

$$\partial_a D^a = 4\pi\rho_{\text{free}}, \qquad \epsilon^{abc}\partial_b H_c - \partial_0 D^a = 4\pi j^a_{\text{free}}, \tag{4.128}$$

[12] From now on the indices should be underlined since they are denoting the coordinates of the local reference frame in order to distinguish them from the curved spacetime coordinates. However, in the following we will only work in local reference frames so the underline is omitted.

where $D_a = E_a + 4\pi P_a$ and $H_a = B_a - 4\pi M_a$.[13] If we restrict to linear responses the polarization/magnetization is given in terms of the generating fields

$$P^a = (\chi^{\mathrm{e}})^a{}_b E^b, \qquad M^a = (\chi^{\mathrm{m}})^a{}_b H^b, \tag{4.129}$$

which allows us to rewrite the fields D^a and B^a in terms of E^a and H^a as

$$D^a = \underbrace{\left(\delta^a{}_b + 4\pi\,(\chi^{\mathrm{e}})^a{}_b\right)}_{\tilde{\epsilon}^a{}_b} E^b, \qquad B^a = \underbrace{\left(\delta^a{}_b + 4\pi\,(\chi^{\mathrm{m}})^a{}_b\right)}_{\mu^a{}_b} H^b. \tag{4.130}$$

For historical reason the role of B^a and H^a is reversed, so one should actually write $H^a = \tilde{\mu}^a{}_b B^b$ with $\left(\tilde{\mu}^{-1}\right)^a{}_b = \mu^a{}_b$, since the physical fields are the E and B fields, *i.e.* they are describing the change of energy density in space, *e.g.* by moving from one medium to another. In the following we are only interested in non-magnetic materials where χ^{m} is negligible.

4.3.2. Dielectric function in d dimensions

Another linear response of matter is the relation between currents and the generating electric fields known as Ohm's Law

$$j^a = \sigma^a{}_b E^b, \tag{4.131}$$

Inserting Ohm's Law into the magnetic field equation (4.128) yields

$$\epsilon^{abc}\partial_a H_b = \tilde{\epsilon}^c{}_d \partial_0 E^d + 4\pi j^c = \left(\tilde{\epsilon}^c{}_d \partial_0 + 4\pi\sigma^c{}_d\right) E^d. \tag{4.132}$$

Fourier transforming this equation and comparing to the homogeneous equation, *i.e.* $j^a_{\text{free}} = 0$, gives us the definition of the complex dielectric tensor[14]

$$\epsilon^{abc}\mathrm{i}k_a H_b = \left(\tilde{\epsilon}^c{}_d(-\mathrm{i}\omega) + 4\pi\sigma^c{}_d\right) E^d \overset{!}{=} -\mathrm{i}\omega\hat{\epsilon}^c{}_d E^d,$$

$$\Rightarrow \quad -\mathrm{i}\omega\hat{\epsilon}^c{}_d = -\mathrm{i}\omega\tilde{\epsilon}^c{}_d + 4\pi\sigma^c{}_d \qquad \Rightarrow \quad \hat{\epsilon}^c{}_d = \tilde{\epsilon}^c{}_d + \frac{4\pi\mathrm{i}}{\omega}\sigma^c{}_d. \tag{4.133}$$

Additionally, there can be a phase shift between j_a and E_a due to a delay in the response of the medium to the electric field which renders the conductivity to be complex as well, so in general this will give a complex susceptibility $\hat{\chi}$

$$\hat{\epsilon}^c{}_d = \tilde{\epsilon}^c{}_d + \frac{4\pi\mathrm{i}}{\omega}\hat{\sigma}^c{}_d, \tag{4.134}$$

with

$$\hat{\epsilon}^c{}_d = \mathrm{Re}\,\epsilon^c{}_d + \mathrm{i}\,\mathrm{Im}\,\epsilon^c{}_d, \qquad \hat{\sigma}^c{}_d = \mathrm{Re}\,\sigma^c{}_d + \mathrm{i}\,\mathrm{Im}\,\sigma^c{}_d. \tag{4.135}$$

Inserting (4.135) into (4.134) the real and complex part of $\hat{\epsilon}$ and $\hat{\sigma}$ are related

$$\begin{aligned} \mathrm{Re}\,\epsilon^c{}_d &= 1 - \frac{4\pi}{\omega}\,\mathrm{Im}\,\sigma^c{}_d, & \mathrm{Im}\,\epsilon^c{}_d &= \frac{4\pi}{\omega}\,\mathrm{Re}\,\sigma^c{}_d, \\ \mathrm{Re}\,\sigma^c{}_d &= \frac{\omega}{4\pi}\,\mathrm{Im}\,\epsilon^c{}_d, & \mathrm{Im}\,\sigma^c{}_d &= \left(1 - \mathrm{Re}\,\epsilon^c{}_d\right)\frac{\omega}{4\pi}. \end{aligned} \tag{4.136}$$

[13] In general we have an antisymmetric magnetization tensor M_{ab} and also an antisymmetric magnetic field tensor H_{ab} which can be reduced with the help of the total antisymmetric symbol ϵ^{abc}.

[14] Following the notation in [226] hatted symbols denote complex quantities, *e.g.* $\hat{\epsilon} \in \mathbb{C}$.

We see that $\mathrm{Im}\,\sigma^c{}_d$ describes dispersive processes/change of phase which are/is related to energy transport, whereas $\mathrm{Re}\,\sigma^c{}_d$ describes absorption processes/loss of energy which are/is related to dissipation. As a last remark we note that we can decompose the complex dielectric tensor into a longitudinal and a transverse part

$$\hat{\epsilon}^c{}_d = \hat{\epsilon}_\mathrm{L}\frac{k_c \otimes k_d}{k^2} + \hat{\epsilon}_\mathrm{T}\left(\delta^c{}_d - \frac{k_c \otimes k_d}{k^2}\right). \tag{4.137}$$

The following discussions of the Drude model, the Kubo formula for the optical conductivity, Kramers-Kronig relations, and sum rules depend only on time derivatives and are independent of the spatial dimensions D. Therefore, we will omit the indices and work with scalar quantities since restoring the tensorial character is straightforward.

4.3.3. Drude-Sommerfeld model

The Drude-Sommerfeld model describes the properties of metals (*i.a.* electrical/thermal conductivities, heat capacities) by a simple model incorporating the behavior of the underlying charge carriers. The original Drude model is a purely classical model describing a gas of electrons diffusing through a fixed lattice of ions. These generate a positively charge background to balance the negative charge of the electron gas. Even after the discovery of quantum mechanics, the Drude model can still be used but some modifications are needed: The electrons are described by a fermionic gas obeying Fermi-Dirac statistics. This extension of the original model is usually called Drude-Sommerfeld model. There are several ways to arrive at the Drude formula each with their own set of approximations. Essentially, there are three approaches:

i. A classical approach assuming the existence of an average relaxation time describing the relaxation to equilibrium after turning off an external electric field, *i.e.* the relaxation time approximation which operationally replaces the collision integral by a linearized approximation including only the relaxation time scale and the Maxwell-Boltzmann distribution in the kinetic/Boltzmann transport equation. Strictly speaking, this derivation is borrowed from hydrodynamics where the collisions refer to a gas of weakly interacting particles.

ii. A semi-classical approach taking into account the quantum nature of the electron gas. Thus the free mean path is determined by the Fermi velocity of the electrons $\ell = v_\mathrm{F}\tau$ and only electrons near the Fermi surface can participate.

iii. A full microscopic approach considering an interacting electron gas employing Fermi liquid theory in combination with a diagrammatic expansion (and additional approximations such as the random phase approximation). Here the assumptions of Fermi liquid theory, in particular adiabatic continuity, are needed. Furthermore, it is useful to introduce an effective frequency dependent mass $m^*(\omega)$ for the quasi-particles of Fermi liquid theory, incorporating the effects of electron-phonon and electron-electron interactions, as well as a frequency dependent effective time scale $\tau^*(\omega)$. However, in the case of impurity scattering the ratio τ^*/m^* is identical to the bare values since the renormalization of the lifetime cancels the renormalization of the mass. This can be explicitly seen in a diagrammatic calculation of the current-current correlator using the Kubo formula. Here the mass renormalization cancels since the diagrams included in the self-energy are also included in the two particle diagrams. This is in agreement with Fermi liquid theory stating that the current of the quasi particles is independent of the interaction.

Since we do not know in general if there are really quasi-particles involved in strongly correlated systems (apart from heavy Fermi liquids), it seems to be a good strategy not to attempt to explain our holographic duals microscopically, but to take the "effective field theory" philosophy that focuses on the macroscopic rather than the microscopic degrees of freedom. In particular dealing with "Planckian dissipation", as hinted at in the introduction of this thesis, there is no particle transport and we are primarily interested in quantum critical transport at finite density. Therefore, we may follow the standard derivation using the Kubo formula without resorting to the aforementioned technicalities and make use of all the linear response concepts laid out in Section 2.2. A nice exposition of this derivation can be found in [226]. Here we will just state the main ideas and the result. We start with an interaction Hamiltonian

$$\mathcal{H}_{\text{int}} = -\frac{1}{c}\mathbf{J}\cdot\mathbf{A}, \tag{4.138}$$

and use the Kubo formula for the conductivity, *c.f.* (2.70)

$$\sigma(\omega,\mathbf{k}) = \sum_s \frac{1}{\hbar\omega}\int \mathrm{d}t \langle\, s \,|\, \mathbf{J}(0,\mathbf{k})\cdot\mathbf{J}(t,\mathbf{k})^* \,|\, s \,\rangle\, \mathrm{e}^{-\mathrm{i}\omega t}\,, \tag{4.139}$$

where the system's response is given by the current density operator $\mathbf{J}$ that can be rewritten in terms of the momentum operator. Assuming an exponential decay with a single time scale for all current-current correlators, *i.e.* the relaxation time approximation, and the dipole approximation, *i.e.* the external electric field is constant over the characteristic length scale which is surely valid for $v_{\text{F}} \ll c$, we arrive at

$$\sigma(\omega) = \frac{e^2\tau}{m^*}\frac{f}{1-\mathrm{i}\omega\tau}, \tag{4.140}$$

where f describes the oscillator strength measuring the transition probability between two states given by

$$f = 2\sum_{j,s,s'} \frac{\left|\langle\, s \,|\, \mathbf{p}_j \,|\, s' \,\rangle\right|^2}{m^*\hbar(\omega_s-\omega_{s'})}. \tag{4.141}$$

Furthermore the oscillator strength can be evaluated under the assumption of free electrons *i.e.*

$$m^*\hbar(\omega_s-\omega_{s'}) = \frac{\hbar^2\mathbf{k}^2}{2} \qquad \text{and} \qquad \sum_{s,s'}\left|\langle\, s \,|\, \mathbf{p}_j \,|\, s' \,\rangle\right|^2 = \langle\, \mathbf{p}_j^2 \,\rangle = \frac{\hbar^2\mathbf{k}^2}{4}, \tag{4.142}$$

since the self-interaction or electron-lattice interactions are already taken care of in the renormalization of the mass $m^*(\omega)$ and the relaxation rate $\tau^{-1}(\omega) = \tau^{-1}_{\text{impurity}} + \tau^{-1}_{\text{el-ph}} + \tau^{-1}_{\text{el-el}}$. Inserting (4.142) into (4.141) the oscillator strength f is given by the electron (or charge carrier) density n and thus

$$\sigma(\omega) = \frac{ne^2\tau}{m^*}\frac{1}{1-\mathrm{i}\omega\tau} = \frac{\omega_{\text{p}}^2}{4\pi}\frac{1}{\frac{1}{\tau}-\mathrm{i}\omega}, \tag{4.143}$$

using the definition of the plasma frequency (4.221) which in the limit of $\omega \to 0$ reduces to (4.145). If we assume the correction of $\tau_{\text{el-ph}}$ and $\tau_{\text{el-el}}$ to be small compared to τ_{impurity} we can follow the reasoning presented in point *iii* and replace τ^*/m^* by τ/m. The maximum of the real part of the optical conductivity (4.143) at $\omega = 0$ is called the Drude peak, whereas the imaginary part shows a maximum at $\omega = 1/\tau$. The generic behavior of the Drude model is displayed in Figure 4.4. We can rewrite the optical Drude conductivity in terms of the DC conductivity as follows

$$\sigma(\omega) = \frac{\omega_{\text{p}}^2}{4\pi}\frac{1}{\frac{1}{\tau}-\mathrm{i}\omega} = \frac{\omega_{\text{p}}^2\tau}{4\pi}\frac{1+\mathrm{i}\omega\tau}{1+\omega^2\tau^2} = \frac{\sigma_{\text{DC}}}{1-\mathrm{i}\omega\tau} = \frac{1+\mathrm{i}\omega\tau}{1+\omega^2\tau^2}\sigma_{\text{DC}}, \tag{4.144}$$

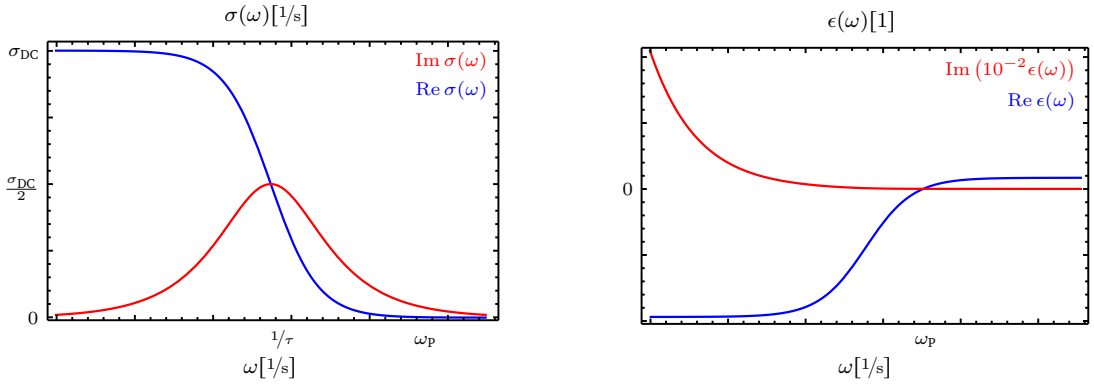

Figure 4.4. In the left panel, we see that $\mathrm{Re}\,\sigma(\omega)$ is maximal at $\omega = 0$ and drops to half its maximal value at the inverse relaxation time $1/\tau$, where $\mathrm{Im}\,\sigma(\omega)$ is maximal. At the plasma frequency ω_P the real part of $\sigma(\omega)$ has dropped to $(1 + 4\pi\sigma_{DC})^{-1}$ of its initial maximal value. The right panel shows the real part of the dielectric function changes sign at ω_P since $\mathrm{Re}\,\epsilon(\omega) = 0$ yields the condition $\omega = \sqrt{\omega_P^2 - \frac{1}{\tau^2}} \approx \omega_P$, whereas the imaginary part approaches one and subsequently falls off to zero.

so by comparing with (4.143) we find

$$\sigma_{DC} = \frac{\omega_P^2 \tau}{4\pi}. \tag{4.145}$$

The dielectric function of the Drude model reads

$$\begin{aligned}\epsilon(\omega) &= 1 + \frac{4\pi i}{\omega}\frac{\omega_P^2}{4\pi}\left(\frac{1}{\frac{1}{\tau} - i\omega}\right) = 1 - \frac{\omega_P^2}{\omega^2 + \frac{i\omega}{\tau}} \\ &= 1 - \frac{\omega_P^2}{\omega^2 + \tau^{-2}} + \frac{i}{\omega\tau}\frac{\omega_P^2}{\omega^2 + \tau^{-2}} = 1 - \frac{\omega_P^2\tau^2}{1 + \omega^2\tau^2} + \frac{i\tau}{\omega}\frac{\omega_P^2}{1 + \omega^2\tau^2}.\end{aligned} \tag{4.146}$$

We can distinguish three different regimes listed in Table 4.3, which are separated by the two scales in the system, namely the relaxation time of the quasi particles and the plasma frequency, *i.e.* the frequency above charged particles cannot respond to the fast changes in the external electric field anymore, *c.f.* Figure 4.4. The computation of the plasma frequency and its relation to the dielectric function and the Kramers-Kronig relation will be discussed in the subsequent sections.

4.3.4. Different ways of computing the plasma frequency

In principle, we are looking for the $1/\omega^2$ term in the high-frequency expression of the dielectric function, *c.f.* Table 4.3. In order to arrive at this expression there are two different approaches with different approximations/assumptions made:

- Using the random phase approximation where $\epsilon(\omega, \mathbf{k}) = 1 - \frac{4\pi}{\mathbf{k}^2}\chi(\omega, k)$ with $\chi(\omega, \mathbf{k})$ denoting the charge density correlation function.
- Using the dipole approximation where $\epsilon(\omega, \mathbf{k}) = 1 + \frac{4\pi i}{\omega}\sigma(\omega, \mathbf{k})$ with the conductivity calculated from current-current correlation functions.

Hagen-Rubens $\omega \ll \frac{1}{\tau}$	Relaxation $\frac{1}{\tau} \ll \omega \ll \omega_\mathrm{p}$	Transparent $\omega_\mathrm{p} \ll \omega$
$\mathrm{Im}\,\epsilon = \frac{\omega_\mathrm{p}^2\tau}{\omega}$	$\mathrm{Im}\,\epsilon = \frac{\omega_\mathrm{p}^2}{\omega^3\tau}$	$\mathrm{Im}\,\epsilon = \frac{\omega_\mathrm{p}^2}{\omega^3\tau} \approx 0$
$\mathrm{Re}\,\epsilon = 1 - \omega_\mathrm{p}^2\tau^2$	$\mathrm{Re}\,\epsilon = 1 - \frac{\omega_\mathrm{p}^2}{\omega^2}$	$\mathrm{Re}\,\epsilon = 1 - \frac{\omega_\mathrm{p}^2}{\omega^2} \approx 1$
$\mathrm{Im}\,\sigma = \frac{\omega_\mathrm{p}^2}{4\pi}\omega\tau^2 = \sigma_\mathrm{DC}\omega\tau$	$\mathrm{Im}\,\sigma = \frac{\omega_\mathrm{p}^2}{4\pi}\frac{1}{\omega} = \frac{\sigma_\mathrm{DC}}{\omega\tau}$	$\mathrm{Im}\,\sigma = \frac{\omega_\mathrm{p}^2}{4\pi}\frac{1}{\omega} \approx 0$
$\mathrm{Re}\,\sigma = \frac{\omega_\mathrm{p}^2\tau}{4\pi} = \sigma_\mathrm{DC}$	$\mathrm{Re}\,\sigma = \frac{\omega_\mathrm{p}^2}{4\pi}\frac{1}{\omega^2\tau} = \frac{\sigma_\mathrm{DC}}{\omega^2\tau^2}$	$\mathrm{Re}\,\sigma = \frac{\omega_\mathrm{p}^2}{4\pi}\frac{1}{\omega^2\tau} \approx 0$

Table 4.3. Dielectric function and conductivity in the three different regimes depending on the scales ω_p and τ. Note that the precise form of the relations depends on the physical assumptions encoded in the Drude-Sommerfeld model.

In general the conductivity and the polarization/Lindhard function are related by the Einstein relation following from the fluctuation-dissipation theorem

$$\chi(\omega, \mathbf{k}) = -\frac{\mathrm{i}\mathbf{k}^2}{\omega}\sigma(\omega, \mathbf{k}) = D^{-1}\sigma(\omega, \mathbf{k}), \tag{4.147}$$

whereas the conductivity is given by the retarded current-current Green function

$$\sigma(\omega, \mathbf{k}) = \frac{\mathrm{i}}{\omega}G^\mathrm{R}(\omega, \mathbf{k}). \tag{4.148}$$

As a further alternative the plasma frequency can be calculated with the help of the sum rules (4.162) and Kramers-Kronig relations (4.149) to be explained in the following.

4.3.5. Sum rules and Kramers-Kronig relations

According to the derivation in Section 2.2.3 and stated in Kramers-Kronig Relation on page 37, the Kramers-Kronig relations for arbitrary response functions can be written as

$$\hat{G}(\omega) = \frac{1}{\mathrm{i}\pi}\mathcal{P}\int_{-\infty}^{\infty}\mathrm{d}\omega'\,\frac{\hat{G}(\omega')}{\omega' - \omega}, \tag{4.149}$$

where $\mathcal{P}$ reminds us to take the principal value of the integral. Written out in real and imaginary parts we have

$$\mathrm{Re}\,G(\omega) = \frac{1}{\pi}\mathcal{P}\int_{-\infty}^{\infty}\mathrm{d}\omega'\,\frac{\mathrm{Im}\,G(\omega')}{\omega' - \omega}, \qquad \mathrm{Im}\,G(\omega) = -\frac{1}{\pi}\mathcal{P}\int_{-\infty}^{\infty}\mathrm{d}\omega'\,\frac{\mathrm{Re}\,G(\omega')}{\omega' - \omega}. \tag{4.150}$$

In order to remove the unphysical negative frequencies we can use the reality condition of the response functions

$$\hat{G}(\omega) = \hat{G}(-\omega)^* \quad \Rightarrow \quad \mathrm{Re}\,G(-\omega) = \mathrm{Re}\,G(\omega), \qquad \mathrm{Im}\,G(-\omega) = -\,\mathrm{Im}\,G(\omega), \tag{4.151}$$

where we see that the real part is an even function and the imaginary part an odd function of ω and the relation

$$\mathcal{P}\int_{-\infty}^{\infty}\mathrm{d}\omega'\,\frac{f(\omega')}{\omega' - \omega} = \mathcal{P}\int_{0}^{\infty}\mathrm{d}\omega'\,\frac{\omega'\left[f(\omega) - f(-\omega')\right] + \omega\left[f(\omega') + f(-\omega')\right]}{\omega'^2 - \omega^2}, \tag{4.152}$$

to read off

$$\mathrm{Re}\,G(\omega) = \frac{2}{\pi}\mathcal{P}\int_{0}^{\infty}\mathrm{d}\omega'\,\frac{\omega'\,\mathrm{Im}\,G(\omega')}{\omega'^2 - \omega^2}, \qquad \mathrm{Im}\,G(\omega) = -\frac{2\omega}{\pi}\mathcal{P}\int_{0}^{\infty}\mathrm{d}\omega'\,\frac{\mathrm{Re}\,G(\omega')}{\omega'^2 - \omega^2}. \tag{4.153}$$

Example: Conductivity and dielectric function

For $\hat{G} \equiv \hat{\sigma}$ equation (4.153) is a relation between absorption $\mathrm{Re}\,\sigma$ and dispersion $\mathrm{Im}\,\sigma$. In the case of $\hat{G} \equiv \hat{\epsilon}$ we have to take $(\mathrm{Re}\,\epsilon - 1)$ and $\mathrm{Im}\,\epsilon$ since the polarization as a response to the applied electric field is given by $4\pi P(\omega) = (\hat{\epsilon}(\omega) - 1)E(\omega)$. A convenient form to write the Kramers-Kronig relations for the dielectric function is

$$\begin{aligned} \mathrm{Re}\,\epsilon(\omega) - 1 &= \frac{2}{\pi}\mathcal{P}\int_0^\infty \mathrm{d}\omega'\,\frac{\omega'\,\mathrm{Im}\,\epsilon(\omega')}{\omega'^2 - \omega^2}, \\ \mathrm{Im}\,\epsilon(\omega) &= -\frac{2}{\pi\omega}\mathcal{P}\int_0^\infty \mathrm{d}\omega\,\frac{\omega'^2\,(\mathrm{Re}\,\epsilon(\omega') - 1)}{\omega'^2 - \omega^2}. \end{aligned} \tag{4.154}$$

If there is no absorption, $\mathrm{Im}\,\epsilon = 0$, then $\hat{\epsilon}$ has no ω dependence and is constant, *i.e.* $\hat{\epsilon} = 1$. With the help of

$$\mathcal{P}\int_0^\infty \mathrm{d}\omega'\,\frac{1}{\omega'^2 - \omega^2} = 0, \tag{4.155}$$

we can rewrite $\mathrm{Im}\,\epsilon$ in the form (see [226] for the explicit calculation)

$$\mathrm{Im}\,\epsilon(\omega) = -\frac{2}{\pi\omega}\mathcal{P}\int_0^\infty \mathrm{d}\omega'\left[\left(\mathrm{Re}\,\epsilon(\omega') - 1\right) - \frac{\omega^2\,\mathrm{Re}\,\epsilon(\omega')}{\omega'^2 - \omega^2}\right]. \tag{4.156}$$

Using the relation between $\hat{\epsilon}$ and $\hat{\sigma}$ given in (4.136), we write for σ_{DC},

$$\sigma_{\mathrm{DC}} = \frac{1}{2\pi^2}\int_0^\infty \mathrm{d}\omega'(1 - \mathrm{Re}\,\epsilon(\omega')), \tag{4.157}$$

and finally

$$\mathrm{Im}\,\epsilon(\omega) = \frac{4\pi\sigma_{\mathrm{DC}}}{\omega} - \frac{2\omega}{\pi}\mathcal{P}\int_0^\infty \mathrm{d}\omega'\,\frac{\omega'\,\mathrm{Re}\,\epsilon(\omega')}{\omega'^2 - \omega^2}. \tag{4.158}$$

Here we can read off some interesting properties, *e.g.* for non-insulating materials, $\sigma_{\mathrm{DC}} \neq 0$, the imaginary part of the dielectric function diverges in the limit of vanishing frequency, *i.e.* all the energy is dissipated until a static equilibrium is reached. For $\omega \to \infty$, we see that we have an ideal metal described by an electron gas (in the case of the Drude model this state is reached already for $\omega \gg \omega_{\mathrm{p}}$), since there are no losses/absorption.

Kramers-Kronig relations and physical assumptions

Combining the Kramers-Kronig relations with physical input will give rise to the sum rules for $\hat{\omega}$. First, we look at the special case for high frequencies, *i.e.* $\omega \gg \omega'$,

$$\frac{1}{\omega'^2 - \omega^2} = -\frac{1}{\omega^2}\frac{1}{1 - \frac{\omega'^2}{\omega^2}} \approx -\frac{1}{\omega^2}. \tag{4.159}$$

Thus, the relation (4.154) for $\mathrm{Im}\,\epsilon$ can be simplified to

$$\mathrm{Re}\,\epsilon(\omega) - 1 \approx -\frac{2}{\pi\omega}\int_0^\infty \mathrm{d}\omega'\,\omega'\,\mathrm{Im}\,\epsilon(\omega') = -\frac{8}{\omega^2}\int_0^\infty \mathrm{d}\omega'\,\mathrm{Re}\,\sigma(\omega'), \tag{4.160}$$

where we used $\mathrm{Im}\,\epsilon = (4\pi/\omega)\,\mathrm{Re}\,\sigma$ from (4.136). As a reasonable physical assumption we can take $\mathrm{Re}\,\epsilon$ to be of the form

$$\mathrm{Re}\,\epsilon \approx 1 - \frac{\omega_{\mathrm{p}}^2}{\omega^2} \qquad \longrightarrow \qquad \mathrm{Re}\,\epsilon - 1 \approx -\frac{\omega_{\mathrm{p}}^2}{\omega^2}, \tag{4.161}$$

so that we approach the constant dielectric function characteristic of an insulator in the high frequency regime, since here we have an ideal metal without any dissipation, *i.e.* $\operatorname{Im}\epsilon(\omega \gg \omega') = 0$. We take ω_{p} to be the scale where the frequency ω can be considered as large. This particular scale can be calculated from the conductivity or the dielectric function comparing (4.160) with (4.161)

$$\frac{\omega_{\mathrm{p}}^2}{8} = \int_0^\infty \mathrm{d}\omega \operatorname{Re}\sigma(\omega) = \frac{1}{4\pi}\int_0^\infty \mathrm{d}\omega\, \omega \operatorname{Im}\epsilon(\omega), \tag{4.162}$$

which is called the sum-rule for conductivities. This is an important relation since the conductivity may depend on many physical properties of the system under consideration, *e.g.* interactions between charged particles, band structures, and so on. Rigorously, this relation holds for any charged excitation in a quantum mechanical system, that can be described by creation and annihilation operators. This can be derived using the general Kubo formula for quantum field operators, *c.f.* [227]. In terms of the so called oscillator strength, *e.g.* measuring transition probability between different quantum states, we find a more general expression of the sum rule re-expressed in the following way

$$\int_0^\infty \mathrm{d}\omega \operatorname{Re}\sigma(\omega) = \frac{\pi}{2}\sum_i \frac{q_i^2}{m_i}, \tag{4.163}$$

where q_i denotes the charge and m_i the mass of the excitation. In general there can be a collective excitation involving n_i charged particles with charge e_i and mass m_i.

Superconductivity, superfluid density & plasma-frequency

Let us give a brief overview over the plasma frequency and the relations to the dielectric function and its role in terms of the superfluid density. Formally, according to (4.162), the plasma frequency is defined as

$$\frac{\omega_{\mathrm{p}}^2}{8} = \int_0^\infty \mathrm{d}\omega \operatorname{Re}\sigma(\omega), \tag{4.164}$$

using the optical sum rule. Inserting the relations between the complex dielectric function $\epsilon(\omega)$ and the complex optical conductivity $\sigma(\omega)$,

$$\epsilon = \epsilon_\infty + \frac{4\pi \mathrm{i}}{\omega}\sigma(\omega) \qquad \Rightarrow \qquad \operatorname{Re}\sigma(\omega) = \frac{\omega}{4\pi}\operatorname{Im}\epsilon(\omega), \tag{4.165}$$

where we slightly generalize the dielectric functions to allow for interband screening effects, we may rewrite the plasma frequency in terms of the dielectric function as

$$\omega_{\mathrm{p}}^2 = \frac{2}{\pi}\int_0^\infty \mathrm{d}\omega\, \omega \operatorname{Im}\epsilon(\omega). \tag{4.166}$$

With the help of the Kramers-Kronig relation for non-negative frequencies

$$\operatorname{Re} f(\omega) = \frac{2}{\pi}\mathcal{P}\int_0^\infty \mathrm{d}\omega' \frac{\omega' \operatorname{Im} f(\omega')}{\omega'^2 - \omega^2}, \qquad \operatorname{Im} f(\omega) = -\frac{2\omega}{\pi}\mathcal{P}\int_0^\infty \mathrm{d}\omega' \frac{\operatorname{Re} f(\omega')}{\omega'^2 - \omega^2}, \tag{4.167}$$

we may relate $\operatorname{Im}\epsilon(\omega)$ to $\operatorname{Re}\epsilon(\omega) - 1$. Note that for the dielectric function the polarization $P(\omega)$ is the response to the applied electric field $E(\omega)$,

$$4\pi P(\omega) = (\epsilon(\omega) - 1)\, E(\omega). \tag{4.168}$$

Therefore a convenient form to write the Kramers-Kronig relation for the dielectric function is to include the additional -1 in the real part of $\epsilon(\omega)$,

$$\operatorname{Re}\epsilon(\omega) - 1 = \frac{2}{\pi}\mathcal{P}\int_0^\infty \mathrm{d}\omega' \, \frac{\omega' \operatorname{Im}\epsilon(\omega')}{\omega'^2 - \omega^2} = -\frac{2}{\pi}\frac{1}{\omega^2}\mathcal{P}\int_0^\infty \mathrm{d}\omega' \, \frac{\omega' \operatorname{Im}\epsilon(\omega')}{1 - \frac{\omega'^2}{\omega^2}}$$

$$\overset{\omega \gg \omega'}{=} -\frac{2}{\pi}\frac{1}{\omega^2}\int_0^\infty \mathrm{d}\omega' \, \omega' \operatorname{Im}\epsilon(\omega') = -\frac{\omega_{\mathrm{P}}^2}{\omega^2}, \tag{4.169}$$

where we are interested in the high frequency regime, $\omega \gg 1/\tau$, since the sum rule is strictly valid only for $\omega \to \infty$. In experiments we deal with finite frequencies only, and thus it is possible to extract the plasma frequency by the following extrapolation of experimental data,

$$\omega_{\mathrm{P}}^2 = \lim_{\omega \to 0}\left(-\omega^2 \operatorname{Re}\epsilon(\omega)\right). \tag{4.170}$$

As explained in more detail in the following section on Homes' law the superconducting plasma frequency determines the frequency above which the superconductors becomes "transparent" in analogy to the normal metal plasma frequency. The reason for this terminology follows from the fact that photons can only penetrate the superconductor for length scales smaller than the London penetration depth λ_{L} which corresponds to ω_{Ps}. Here, the superconducting plasma frequency should be understood with the aforementioned analogy to normal metals in mind, described by the Drude-Sommerfeld form of the optical conductivity (4.143). In this case the superconducting plasma frequency is given by

$$\omega_{\mathrm{Ps}}^2 = 8\frac{ne^2}{m}\int_0^\infty \mathrm{d}(\omega\tau)\,\frac{1}{1+(\omega\tau)^2} = 8\frac{ne^2}{m}\arctan(\omega\tau)\Big|_0^\infty = 4\pi\frac{ne^2}{m} = \lambda_{\mathrm{L}}^{-2}. \tag{4.171}$$

Experimentally, we cannot reach infinite frequencies and thus the sum rule is modified by a cut-off frequency ω_c, sometimes called the partial optical sum rule of the Drude-Sommerfeld form

$$\int_0^{\omega_{\mathrm{c}}} \mathrm{d}(\omega\tau)\,\frac{1}{1+(\omega\tau)^2} = 8\frac{ne^2}{m}\arctan(\omega\tau)\Big|_0^{\omega_{\mathrm{c}}} = \frac{\omega_{\mathrm{P}}^2}{4\pi}\arctan(\omega_{\mathrm{c}}\tau). \tag{4.172}$$

Expanding the inverse tangent function for $\omega_c \to \infty$, we get a series expansion in the relaxation rate $1/\tau$ which reads

$$\arctan\left(\omega_{\mathrm{c}}\tau\right) = \frac{\pi}{2} - \frac{1}{\omega_{\mathrm{c}}\tau} + \mathcal{O}\left(\frac{1}{\omega_{\mathrm{c}}^3\tau^3}\right), \tag{4.173}$$

and thus

$$\int_0^{\omega_{\mathrm{c}}} \mathrm{d}\omega \operatorname{Re}\sigma(\omega) \approx \frac{\omega_{\mathrm{P}}^2}{8}\left(1 - \frac{2}{\pi}\frac{1}{\omega_{\mathrm{c}}\tau}\right), \tag{4.174}$$

from which we recover (4.164) for $\omega_{\mathrm{c}} \to \infty$.

4.3.6. Holographic description of the normal metallic phase

Let us apply the holographic Einstein-Maxwell model to the normal metallic phase and calculate optical/electrodynamic properties of the holographic metal such as the refractive index computed in [228] or charge diffusion constants [229–231]. We will fist focus on the conductivity and move on to diffusion in the next section which will be an interesting candidate for an explanation of Homes' law.

Analytic solutions to normal phase equations of motion for the gauge field fluctuations

Choosing the gauge $a_u = 0$ which takes into account the fact that we do not consider fluctuations of the gauge field with different "energy scales" u, we want to solve the equations of motion (4.81), (4.82), and (4.83) in the special case of $\Phi(u) = 0$, *i.e.*

$$a_t''(u) - \frac{d-3}{u} a_t'(u) - \frac{\mathbf{k}^2}{f(u)} a_t(u) - \frac{\omega}{f(u)} \mathbf{k} \cdot \mathbf{a}(u) = 0, \tag{4.175}$$

$$\mathbf{a}''(u) + \left(\frac{f'(u)}{f(u)} - \frac{d-3}{u} \right) \mathbf{a}'(u) + \left(\frac{\omega^2}{f(u)^2} - \frac{\mathbf{k}_\perp^2}{f(u)} \right) \mathbf{a}(u) + \frac{\omega}{f(u)^2} \mathbf{k} a_t(u) + \frac{\mathbf{k}}{f(u)} \left(\mathbf{k}_\perp \cdot \mathbf{a}(u) \right) = 0, \tag{4.176}$$

$$\frac{\omega}{f(u)} a_t'(u) + \mathbf{k} \cdot \mathbf{a}'(u) = 0. \tag{4.177}$$

Furthermore, in the case $\mathbf{k} = \mathbf{0}$, which implies $\mathbf{k}_\perp = \mathbf{0}$, the spatial and time components of the gauge field fluctuations decouple and the time component can be trivially solved, since the constraint (4.177) then reads

$$\frac{\omega}{f(u)} a_t'(u) = 0 \quad \overset{(4.175)}{\Rightarrow} \quad a_t''(u) = 0 \quad \Rightarrow \quad a_t = \text{const.} \tag{4.178}$$

The only remaining equation of motion is (4.176)

$$\mathbf{a}''(u) + \left(\frac{f'(u)}{f(u)} - \frac{d-3}{u} \right) \mathbf{a}'(u) + \frac{\bar{\omega}^2}{u_H^2 f(u)^2} \mathbf{a}(u) = 0, \tag{4.179}$$

where

$$\bar{\omega} = \omega u_\mathrm{H} = \frac{d}{4\pi} \frac{\omega}{T}. \tag{4.180}$$

Response function of the current-current correlator

The asymptotic behavior at the horizon and the boundary will fix the solution for the $\langle \mathbf{jj} \rangle$ correlator of the field theory as prescribed in detail in Section 3.5.1. Inserting the AdS-Schwarzschild redshift function $f(u)$ into (4.179) yields

$$\mathbf{a}''(u) + \underbrace{\left[\frac{d \left(\frac{u}{u_\mathrm{H}} \right)^{d-1}}{1 - \left(\frac{u}{u_\mathrm{H}} \right)^d} - \frac{d-3}{u} \right]}_{a(u, u_\mathrm{H}, d)} \mathbf{a}'(u) + \underbrace{\frac{\bar{\omega}^2}{u_\mathrm{H}^2 \left[1 - \left(\frac{u}{u_\mathrm{H}} \right)^d \right]^2}}_{b(u, u_\mathrm{H}, d, \bar{\omega})} \mathbf{a}(u) = 0. \tag{4.181}$$

The asymptotic behavior at the horizon is found by a series expansion around u_H up to order n

$$\mathbf{a}_\mathrm{H}(u) = (u - u_\mathrm{H})^\gamma \sum_{i=0}^{n} a_i (u - u_\mathrm{H})^i, \tag{4.182}$$

by plugging in the above series as Ansatz into the differential equation (4.181) multiplied by $(u_H - u)^{-\mathrm{i}\bar{\omega}/d}$ and solving for the coefficients a_i. The index γ is fixed by the ingoing boundary

conditions at the horizon and should be purely imaginary and negative. Up to linear order we have

$$\mathbf{a}_{\mathrm{H}}(u) = (u-u_{\mathrm{H}})^{-\frac{i\bar{\omega}}{d}}\left(1+\omega\frac{-id^2+d(2u_{\mathrm{H}}\omega+5i)-2u_{\mathrm{H}}\omega}{2d(d-2iu_{\mathrm{H}}\omega)}(u-u_{\mathrm{H}})\right)+\mathcal{O}\big((u-u_{\mathrm{H}})^2\big), \quad (4.183)$$

where we have set the second initial condition parameter to one since we are dealing with a linear equation, hence this parameter is appears linearly in all terms of the expansion. The asymptotic behavior at the boundary is given by $u \to 0$, *i.e.* the coefficient functions $a(u, u_{\mathrm{H}}, d)$ and $b(u, u_{\mathrm{H}}, d, \bar{\omega})$ of the differential equation (4.181) are reduced to

$$\lim_{u\to 0} a(u,u_{\mathrm{H}},d) = \lim_{u\to 0}\left(\frac{f'(u)}{f(u)}-\frac{d-3}{u}\right) = -\lim_{u\to 0}\left(\frac{d-3}{u}\right), \quad (4.184)$$

$$\lim_{u\to 0} b(u,u_{\mathrm{H}},d,\bar{\omega}) = \lim_{u\to 0}\left\{\frac{\bar{\omega}^2}{u_{\mathrm{H}}^2\left[1-\left(\frac{u}{u_{\mathrm{H}}}\right)^d\right]^2}\right\} = \frac{\bar{\omega}^2}{u_{\mathrm{H}}^2}, \quad (4.185)$$

where we used the regularity condition $f(u_{\mathrm{H}}) = 1$. The equation of motion then reads

$$\mathbf{a}''(u) - \frac{d-3}{u}\mathbf{a}'(u) + \frac{\bar{\omega}^2}{u_H^2}\mathbf{a}(u) = 0, \quad (4.186)$$

which is solved by a linear combination of Bessel function, *c.f.* [187] (10.13.4) with $\lambda^2 = {}^{\bar{\omega}^2}/_{u_{\mathrm{H}}^2}$ and $2\nu - 1 = d - 3$,

$$\mathbf{a}_{\mathrm{B}}(u) = C_1 u^{\frac{d-2}{2}}\mathcal{J}_{\frac{d-2}{2}}\left(\frac{\bar{\omega}u}{u_{\mathrm{H}}}\right) + C_2 u^{\frac{d-2}{2}}\mathcal{Y}_{\frac{d-2}{2}}\left(\frac{\bar{\omega}u}{u_{\mathrm{H}}}\right), \quad (4.187)$$

where $\mathcal{J}$ denotes the Bessel function of first kind and $\mathcal{Y}$ the Bessel function of second kind. In order to see the asymptotic behavior more clearly, we can take the $u \to 0$ limit of (4.187)

$$\lim_{u\to 0}\mathbf{a}_{\mathrm{B}}(u) = -\frac{C_2\left(\frac{\omega}{2}\right)^{-\frac{d-2}{2}}\Gamma\left(\frac{d-2}{2}\right)}{\pi} + \frac{\left(\frac{\omega}{2}\right)^{\frac{d-2}{2}}\left(C_1\pi + C_2\cos\left(\frac{d\pi}{2}\right)\Gamma\left(1-\frac{d}{2}\right)\Gamma\left(\frac{d}{2}\right)\right)}{\pi\Gamma\left(\frac{d}{2}\right)}u^{d-2}. \quad (4.188)$$

The dimensionality d of the system is a natural number and therefore we can simplify the cosine function to

$$\cos\left(\frac{d\pi}{2}\right) = \begin{cases} 0 & d \text{ odd} \\ (-1)^{d/2} & d \text{ even}, \end{cases} \quad (4.189)$$

The Green function is proportional to the ratio of the coefficient of the normalizable mode to the non-normalizable mode, so we get the ratio of the two terms in (4.188). Because of (4.189) we need to split the Green function into an odd and even part[15]

$$G^{\mathrm{R}}_{\mathrm{odd}}(\omega,\mathbf{0}) = \frac{C_1}{C_2}\frac{\pi}{\Gamma\left(\frac{d}{2}\right)\Gamma\left(\frac{d}{2}-1\right)}\left(\frac{\omega}{2}\right)^{d-2}, \qquad \text{with} \qquad \omega = \frac{\bar{\omega}}{u_H}. \quad (4.190)$$

[15] Note that the Green functions are the negative of the correlation functions of the fluctuations (*c.f.* generalized Kubo formula and the discussion in [205]), thus the additional minus sign cancels.

In case of the even Green function we can further simplify

$$\Gamma\left(1-\frac{d}{2}\right)\Gamma\left(\frac{d}{2}\right)=\pi\csc\left(\frac{d\pi}{2}\right)=\frac{\pi}{\sin\left(\frac{d\pi}{2}\right)}, \tag{4.191}$$

so finally we find

$$\begin{aligned} G^{\mathrm{R}}_{\mathrm{even}}(\omega,\mathbf{0}) &= \frac{\pi\left(\frac{\omega}{2}\right)^{d-2}}{\Gamma\left(\frac{d}{2}\right)\Gamma\left(\frac{d}{2}-1\right)}\left[\frac{C_1}{C_2}+(-1)^{\frac{d}{2}}\csc\left(\frac{d\pi}{2}\right)\right] \\ &= G^{\mathrm{R}}_{\mathrm{odd}}(\omega,\mathbf{0})+\#\frac{(-1)^{\frac{d}{2}}\pi\csc\left(\frac{d\pi}{2}\right)}{\Gamma\left(\frac{d}{2}\right)\Gamma\left(\frac{d}{2}-1\right)}. \end{aligned} \tag{4.192}$$

We see that the second term will always diverge in case of even dimensionality d since $\sin(d\pi/2)=0$ but this term is identical for all values of C_1 and C_2, so it is safe to ignore this additional term. In the end we can consider the odd Green function $G^{\mathrm{R}}(\omega)=G^{\mathrm{R}}_{\mathrm{odd}}(\omega)$ only. In order to determine C_1 and C_2, we need to solve the full equations of motion with ingoing boundary conditions at the horizon. In fact, these boundary conditions will give us a relation between C_1 and C_2 and the remaining overall factor amounts to a normalization of the complete solution.

Analytic solution in three dimensions

As a test for our general solution, we solve (4.181) for $d=3$ and $d=4$ explicitly, as the two easy cases of odd and even Green functions. For $d=3$ we have

$$\mathbf{a}''(u)+\frac{f'(u)}{f(u)}\mathbf{a}'(u)+\frac{\bar{\omega}}{u_H^2 f(u)^2}\mathbf{a}(u)=0. \tag{4.193}$$

To solution is given by

$$\mathbf{a}^{(d=3)}(u)=C_1\cos\big(g(u,u_{\mathrm{H}},\bar{\omega})\big)+C_2\sin\big(g(u,u_{\mathrm{H}},\bar{\omega})\big), \tag{4.194}$$

with[16]

$$g(u,u_{\mathrm{H}},\bar{\omega})=\frac{\bar{\omega}}{6}\left[2\sqrt{3}\arctan\left(\frac{2u+u_{\mathrm{H}}}{\sqrt{3}u_{\mathrm{H}}}\right)-2\ln(u-u_{\mathrm{H}})+\ln\left(u^2+uu_{\mathrm{H}}+u_{\mathrm{H}}^2\right)\right]. \tag{4.195}$$

We have to fix the two integration constants by imposing the ingoing boundary condition at the horizon $u=u_{\mathrm{H}}$,

$$\lim_{u\to u_{\mathrm{H}}} g(u,u_{\mathrm{H}},\bar{\omega})=\frac{\bar{\omega}}{6}\left[-2\ln(u-u_{\mathrm{H}})+\frac{2\pi}{\sqrt{3}}+\ln(3u_{\mathrm{H}}^2)\right]=-\frac{\bar{\omega}}{3}\ln(u-u_{\mathrm{H}})+C_3. \tag{4.196}$$

For ingoing boundary condition the sign of the exponent near the horizon

$$(u-u_{\mathrm{H}})^{\pm\frac{\mathrm{i}\bar{\omega}}{3}}=\mathrm{e}^{\pm\frac{\mathrm{i}\bar{\omega}}{3}\ln(u-u_{\mathrm{H}})}, \tag{4.197}$$

is chosen such that the phase is constant and the wave is propagating into the black brane horizon for increasing time t. This follows from the fact that

$$(u-u_{\mathrm{H}})^{\mathrm{i}\omega\varphi}\,\mathrm{e}^{-\mathrm{i}\omega t}=\mathrm{e}^{\mathrm{i}\omega[\varphi\ln(u-u_{\mathrm{H}})-t]}. \tag{4.198}$$

[16] Here the complex logarithm is defined on the first Riemann sheet, thus $\mathrm{Ln}(-1)=\mathrm{i}\pi$. Therefore we will assume that the argument of the logarithm is positive and we will only consider $\ln(|x|)$.

The maximum of the wave packet propagates with a constant phase, so $\gamma = \mathrm{i}\omega\varphi$ must be purely imaginary and depending on the behavior of the logarithm positive or negative. In our case the sign must be negative, *i.e.* the coefficient of the negative exponential near the horizon must vanish, since there is an additional minus sign coming from the function $g(u, u_H, \bar{\omega})$

$$\begin{aligned}\mathbf{a}_{\mathrm{H}}^{(d=3)}(u) &= C_1 \cos\big(g(u,u_{\mathrm{H}},\bar{\omega})\big) + C_2 \sin\big(g(u,u_{\mathrm{H}},\bar{\omega})\big) \\ &= \frac{1}{2}(C_1 - \mathrm{i}C_2)\,\mathrm{e}^{\mathrm{i}g(u,u_{\mathrm{H}},\bar{\omega})} + \frac{1}{2}(C_1 + \mathrm{i}C_2)\,\mathrm{e}^{-\mathrm{i}g(u,u_{\mathrm{H}},\bar{\omega})}\,. \end{aligned} \tag{4.199}$$

This yield the relation $C_1 + \mathrm{i}C_2 = 0$ which is satisfied by $C_1 = 1$ and $C_2 = \mathrm{i}$. Since we have a linear equation we can pull out the overall constant factor $C_1\,\mathrm{e}^{C_3}$, which finally gives rise to

$$\mathbf{a}_{\mathrm{H}}^{(d=3)}(u) = \mathrm{e}^{-\mathrm{i}\frac{\bar{\omega}}{3}\ln(u_{\mathrm{H}}-u)}\,, \tag{4.200}$$

which is in perfect agreement with the generic behavior (4.183) for $d = 3$. Having fixed the integration constants we can look at the limit at the boundary of AdS-Space, *i.e.* $u \to 0$, or more precisely the series expansion around $u = 0$,

$$\mathbf{a}_{\mathrm{B}}^{(d=3)}(u) = \cos\left(\frac{\sqrt{3}\pi\bar{\omega}}{18}\right) + \mathrm{i}\sin\left(\frac{\sqrt{3}\pi\bar{\omega}}{18}\right) + \left[\mathrm{i}\bar{\omega}\cos\left(\frac{\sqrt{3}\pi\bar{\omega}}{18}\right) - \bar{\omega}\sin\left(\frac{\sqrt{3}\pi\bar{\omega}}{18}\right)\right]\frac{u}{u_{\mathrm{H}}}. \tag{4.201}$$

The retarded Green function in this case reads

$$G(\omega, \mathbf{0}) = \frac{\mathrm{i}\bar{\omega}}{u_{\mathrm{H}}} = \mathrm{i}\omega, \tag{4.202}$$

which also agrees with the general result (4.190) for $d = 3$. This can be confirmed by inserting $d = 3$ in the general solution (4.187) and expanding around $u = 0$, which gives rise to

$$\mathbf{A}_B(u) \approx -\sqrt{\frac{2u_{\mathrm{H}}}{\pi\bar{\omega}}}C_2 + \sqrt{\frac{2u_{\mathrm{H}}}{\pi\bar{\omega}}}C_1 u, \qquad \text{and} \qquad G(\omega,\mathbf{0}) = \frac{C_1}{C_2}\frac{\bar{\omega}}{u_{\mathrm{H}}}. \tag{4.203}$$

Note that the minus sign in the ratio of leading to subleading term is absorbed into the definition of the response function (2.70). Finally, the conductivity takes the constant value $\sigma(\omega) = {}^{\mathrm{i}G^{\mathrm{R}}(\omega)}/_{\omega} = 1$ and thus the plasma frequency is zero since there is no ${}^{1}/_{\omega^2}$ term in the dielectric function (4.158). Alternatively, the sum rule integral (4.162) is not converging which implies that the plasma frequency is not well defined or infinity in that case. This fits into our expectation of looking at a strongly correlated theory without well-defined quasi particles. Our result is also in agreement with the general result of the optical conductivity of a physical system described by a CFT[17] [10, 181]

$$\sigma(\omega) = \frac{e^2}{\hbar}\mathscr{C}\left(\frac{\hbar\omega}{k_{\mathrm{B}}T}\right), \tag{4.204}$$

Since we are working in the probe limit the generically undetermined dimensionless function $\mathscr{C}$ is simply one. In order to find non-trivial solutions we need to resort to backreacted numerical solutions as conducted and discussed in Section 4.4.

[17] We have reinstated the physical constants $\hbar$, k_{B} and e removed by our choice of units.

Analytic solution in four dimensions

Following [232], we have to transform the equation of motion to new coordinates defined by

$$\bar{x} = 1 - \frac{r_{\mathrm{H}}^2}{r^2} = 1 - \frac{u^2}{u_{\mathrm{H}}^2}, \tag{4.205}$$

using the relations (A.18). The Green function is then given by[18]

$$G^{\mathrm{R}}(\omega, \mathbf{0}) = \frac{N_c^2 T^2}{8}\left\{\mathrm{i}\frac{\bar{\omega}}{2} + \frac{\bar{\omega}^2}{4}\left[\mathrm{LI}\left(\frac{(1-\mathrm{i})\bar{\omega}}{4}\right) + \mathrm{LI}\left(-\frac{(1+\mathrm{i})\bar{\omega}}{4}\right)\right]\right\}. \tag{4.206}$$

The terms involving the logarithmic derivative of the Γ-function, here denoted by $\mathrm{LI} = {}^{\Gamma'(z)}/_{\Gamma(z)}$, can be written as

$$\mathrm{LI}\,(-z^*) + \mathrm{LI}(z), \qquad \text{with} \qquad z = -\frac{(1+\mathrm{i})\bar{\omega}}{4}. \tag{4.207}$$

Under complex conjugation of the argument the LI-function changes sign *i.e.* $\mathrm{LI}(-z^*) = -\mathrm{LI}\,(-z)$, so (4.207) reduces to $\mathrm{LI}(z) - \mathrm{LI}(-z)$. Using the reflection and recurrence property of the LI-function

$$\mathrm{LI}(1-z) - \mathrm{LI}(z) = \pi\cot(\pi z), \qquad \mathrm{LI}(1+z) + \mathrm{LI}(z) = \frac{1}{z}, \tag{4.208}$$

we can write by replacing $z \longrightarrow -z$ in the recurrence formula

$$\mathrm{LI}(1-z) - \mathrm{LI}(z) = \pi\cot(\pi z) \qquad \Rightarrow \qquad \mathrm{LI}(-z) - \mathrm{LI}(z) = \pi\cot(\pi z) + \frac{1}{z}, \tag{4.209}$$

and thus the Green function reads

$$G^{\mathrm{R}}(\omega) = \frac{N_c^2 T^2}{8}\left\{\mathrm{i}\frac{\bar{\omega}}{2} + \frac{\bar{\omega}^2}{4}\left[-\pi\cot\left(-\pi\frac{(1+\mathrm{i})\bar{\omega}}{4}\right) + \frac{4}{(1+\mathrm{i})\bar{\omega}}\right]\right\}. \tag{4.210}$$

Inserting (4.210) into the dielectric function (4.134)

$$\epsilon(\omega) = 1 - \frac{4\pi}{\bar{\omega}^2\pi^2 T^2} G^{\mathrm{R}}(\omega) = 1 - \frac{N_c^2}{4\pi}\left[\frac{1}{\bar{\omega}} + \frac{\pi}{2}\cot\left(\pi\frac{(1+\mathrm{i})\bar{\omega}}{4}\right)\right]. \tag{4.211}$$

The $\omega \to \infty$-limit of the cot-function is $-\mathrm{i}$ and the ${}^1/_{\bar{\omega}}$-term is vanishing, so we finally arrive at

$$\lim_{\omega\to\infty} \epsilon(\omega) = 1 + \mathrm{i}\frac{N_c^2}{8}. \tag{4.212}$$

The $d = 4$ conductivity is given by

$$\sigma(\omega) = \frac{\mathrm{i}}{\bar{\omega}\pi T} G^{\mathrm{R}}(\omega) = \mathrm{i}\frac{N_c^2 T}{16\pi} + \mathrm{i}\frac{N_c^2 T}{32}\bar{\omega}\cot\left(\pi\frac{(1+\mathrm{i})\bar{\omega}}{4}\right). \tag{4.213}$$

Expanding this expression for small ω

$$\sigma(\omega) \approx \frac{N_c^2 T}{8\pi}\left(\frac{1}{2} + \mathrm{i}\right) + \frac{N_c^2 T\pi}{384}(1+\mathrm{i})\bar{\omega}^2, \tag{4.214}$$

[18] Here, we reinstated the overall factors of N_c and the temperature T to make the comparison to the literature easier.

Table 4.4.
Values of the dielectric function $\epsilon(\omega)$ and the conductivity $\sigma(\omega)$ for $d = 3, 4$. Looking at the real part of the dielectric function we see that the plasma frequency is vanishing, whereas the conductivity seems to indicate that the plasma frequency is diverging, due to the fact that the relaxation time is zero. The most striking deviation from the Drude model can be seen for $d = 4$ since here $\mathrm{Im}\,\epsilon(\omega) \neq 0$ and $\sigma(\omega) \sim \omega$.

	$\epsilon(\omega)$		$\sigma(\omega)$	
	$d=3$	$d=4$	$d=3$	$d=4$
Re	1	1	1	∞
Im	0	$\frac{N_c^2}{8}$	0	$\frac{N_c^2 T}{16\pi}$

we see a clear deviation from the Drude model and the dominating $\bar{\omega}^2$ term that can be found in numerical solutions for the conductivity in four dimensions. For $\bar{\omega} \to \infty$ or $\omega \gg T$, respectively, we find a linearly diverging real part and a constant imaginary part due to the limit of the cot-function. This is again in agreement with the general conformal limit result derived from (4.192) given by

$$\sigma(\omega) \sim \bar{\omega}^{d-3} = \left(\frac{d}{4\pi}\frac{\omega}{T}\right)^{d-3}. \tag{4.215}$$

Compare dielectric functions of different spacetime dimensionality

A comparison of the dielectric function in three and four dimensions reveal the structure already predicted by the Green function (4.190) found from the general solution for arbitrary dimensionality d. Taking a naïve look at the scaling of the Green function with ω one could conclude that we actually should have a non-vanishing plasma frequency in two dimensions. Unfortunately the solution for $d = 2$ is quite different — due to the behavior of the Bessel functions — and so the Green function in this case again scales with ω^2. Therefore, the only conclusion we can draw from this analysis is that the plasma frequency ω_{P} is not well defined for a holographic system since the UV boundary behavior possess a conformal symmetry that forbids the existence of an scale set by the plasma frequency ω_{P}. Therefore, the quasi particle interpretation of the Drude model cannot be applied to describe holographic charged particles as can be seen in Table 4.4. One might ask the question why is there no ω^2 term in the Drude model and how does the cut-off scale ω_{P} arise. A simple picture is the existence of massive quasi particles which defines a resonance frequency. Way above this resonance frequency the system is not able to respond to the external excitations anymore, due to the inertia of the massive quasi particles. This "classical" picture underlies the "classical" derivation of the Drude model and also the semi-classical derivation of the Drude-Sommerfeld model since the quantum nature of the Fermi gas do not change the functional form of the conductivity. Here we see even more clearly why we have massive quasi particles because we have to take into account the underlying interaction with the discrete lattice, *e.g.* the electron-phonon interaction, as well as the electron-electron interaction. Thus, our charged quasi-particles will have an effective mass that cannot be zero. Even if we take a "full" microscopic approach and derive the Drude-model from linear response with the help of the Kubo formula, as done in Section 4.3.3, we assume that we have microscopic harmonic oscillators with a finite mass defining the so called oscillator strength.

Conformal symmetry does not allow an underlying lattice as well as an additional scale set by ω_{P}. This is equivalent to have charge carrier with vanishing mass. An interesting picture is given by a harmonic oscillator in the limit of vanishing mass. For a periodic external excitation the

resonance frequency is given by

$$\omega_{\mathrm{R}} = \sqrt{\frac{k}{m} - \frac{c^2}{2m^2}}, \tag{4.216}$$

follows from

$$m\ddot{\xi}(t) + c\dot{\xi}(t) + k\xi(t) - F(t) = 0. \tag{4.217}$$

In the limit of small masses the resonance frequency will diverge while keeping c/m fixed, which just fixes the external damping parameter. Would we look at this mechanical problem with $m = 0$ from the beginning the solution allows for no real resonance frequency at all. This can be interpreted as a resonance frequency that is zero, although (4.216) might suggest it is infinite. As expected the quasi particle picture seems to give contradictory explanations. This is a recurring theme signaling the breakdown of the naïve quasi particle picture, *c.f.* [10, 173]. In any case looking at harmonic oscillators with zero mass resembles the case of having no oscillator at all since we can view it as a dumbbell — the spring becoming so stiff that there are no oscillations possible — and hence a cut-off frequency, above which there are no oscillation, does not have any meaning anymore.

Looking explicitly at the $d = 3$ case, we see that we have a frequency independent conductivity $\sigma = \sigma_{DC} = 1$. This can be explained by the properties of the probe limit, where we have dissipation for all frequencies since we do not take the deformations of the geometry into account. This can be viewed as an energy flow into the geometry which gives rise to a dominant dissipation and thus the relaxation time effectively vanishes *e.g.* $\tau \to 0$. On the other hand, we have a finite DC conductivity which allows for charge transport at any frequency. Thus, we conclude that the plasma frequency should be infinite, *e.g.* $\omega_{\mathrm{P}} \to \infty$. If we look at the dielectric function we can use the same argument to find exactly the opposite, *i.e.* $\tau \to \infty$ and $\omega_{\mathrm{P}} \to 0$. This would suggest that we have no dissipation at all due to the diverging mean free path of the quasi particles.

$$\left.\begin{array}{rcl} \mathrm{Re}\,\sigma = 1 & \Rightarrow & \sigma_{\mathrm{DC}} = 1 \\ \mathrm{Im}\,\sigma = 0 & \Rightarrow & \tau = 0 \end{array}\right\} \Rightarrow \omega_{\mathrm{P}} = \infty, \qquad \left.\begin{array}{rcl} \mathrm{Re}\,\epsilon = 1 & \Rightarrow & \omega_{\mathrm{P}} = 0 \\ \mathrm{Im}\,\epsilon = 0 & & \end{array}\right\} \Rightarrow \tau = \infty. \tag{4.218}$$

In the $d = 4$ case the situation is more complicated as shown in Figure 4.5 and cannot be explained by the properties of the probe limit alone. Nevertheless, we essentially find the same two possible explanations for τ and ω_{P} looking at the asymptotic behavior of the dielectric function for $\omega \to \infty$

$$\left.\begin{array}{rcl} \mathrm{Re}\,\epsilon = 1 & \Rightarrow & \omega_{\mathrm{P}} = 0 \\ \sigma_{\mathrm{DC}} \neq 0 & & \end{array}\right\} \Rightarrow \tau = \infty, \qquad \left.\begin{array}{rcl} \mathrm{Im}\,\epsilon = \dfrac{1}{8} & \Rightarrow & \omega_{\mathrm{P}} = \infty \\ \sigma_{\mathrm{DC}} \neq 0 & & \end{array}\right\} \Rightarrow \tau = \infty. \tag{4.219}$$

Compared to the harmonic oscillator (4.216), the two cases would be represented by $m \to 0$ and $m \to \infty$. The case $m \to 0$ or $k \to \infty$ looks like a dumbbell which could be viewed as a free particle with center of mass motion. The case $m \to \infty$ or $k \to 0$ looks essentially like two free particles again. So what we can learn from interpreting this solution that the Drude-Sommerfeld model is not accurate to describe the plasma frequency in a conformal theory. This is to be expected since the quasi particle picture will break down at strong coupling. Possible resolutions of this problem involve holographic systems with explicit lattices [33–35, 233] or the very intriguing system, where the lattice arises dynamically in analog to a Abrikosov lattice in real superconductors [36].

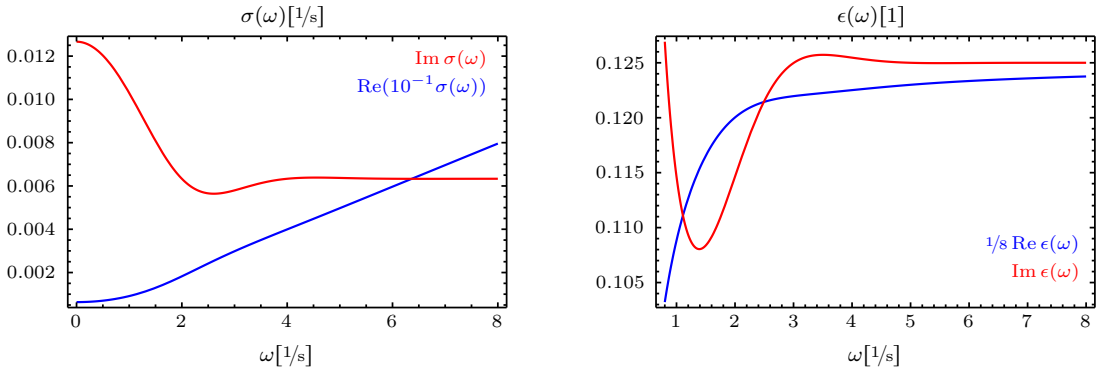

Figure 4.5. In the left panel we see that the four dimensional conductivity, $\mathrm{Re}\,\sigma(\omega) \sim \omega^2$ for small ω, whereas for large ω we find a $\mathrm{Re}\,\sigma(\omega) \sim \omega$ dependence. Here the relaxation time should be diverging since the maximum of $\mathrm{Im}\,\sigma(\omega)$ is located at 0. In the right panel the four dimensional dielectric function $\mathrm{Re}\,\epsilon(\omega)$ is not changing sign, so the plasma frequency should be either infinity or zero. Interestingly, the real part converges to one, whereas the imaginary part converges *not* to zero, but to the finite value of $1/8$.

4.4. Towards a Holographic Realization of Homes' Law

Overview

- Universal features of real world superconductors related to "Planckian dissipation", quantum critical regions, perfect fluids & strange metals.
- Empirically determined relation known as "Homes' law" is not theoretically explained/modeled yet.
- Modification of empiric Homes' law to model a holographic version of Homes' law feasible for holographic computations.

Finally we turn to Homes' law, one of the central results of this thesis. Let us start with a small introduction to Homes' law, perfect fluid and the concept of "Planckian dissipation". In this section, we outline how Homes' law may be implemented in holography. We follow a simple approach which allows to demonstrate the validity of Homes' law in the absence of backreaction of the matter fields on the geometry. We also find that our straightforward approach requires modifications in the presence of backreaction. We present and discuss possible generalizations and indicate directions for further research. In Section 4.4.1 we give a self-contained exposition of Homes' law and discuss related condensed matter concepts and their holographic realization. In the Sections 4.1 and 4.2 we discussed the holographic s-wave and p-wave superconductors, respectively. In particular, we focused on the effects that arise from the backreaction of the gravitational interaction with the matter fields onto the geometry, governing the gravity dual. For our Homes' law calculation, we numerically determine the phase diagram where we use the strength of the backreaction as parameter in addition to the ratio of temperature and chemical potential. This sets the ground for the calculations of various diffusion constants, which are discussed for the s-wave superconductor in Section 4.5.3 and for the p-wave superconductor in Section 4.5.4. We focus on the critical diffusion and associated time scales, *i.e.* the diffusion

at the critical ratio of temperature and chemical potential depending on the backreaction at which the system transits to the superconducting phase. We find that a particular version of Homes' law is satisfied if the backreaction is absent, while further work is required for the case with backreaction, as we explain. A detailed summary of the results can be found in Chapter 6 and additionally some possible explanations are given why Homes' law is not confirmed in the approach considered here. Some extensions of our original setup to remedy these problems are also discussed in Section 6.1.2 of that chapter along with some new perspectives on holographic superfluids/superconductors that might be of interest to pursue on their own.

4.4.1. Homes' law in condensed matter

An interesting phenomenon to look for universal behavior in condensed matter systems, as advertised in the introduction to this chapter, is the universal scaling law for superconductors empirically found by Homes et al. [42] by collecting experimental results. This so-called *Homes' law* describes a relation between different quantities of conventional and unconventional superconductors, *i.e.* the superfluid density ρ_s at zero temperature and the conductivity σ_{DC} times the critical temperature T_c,

$$\rho_s = C\sigma_{DC}(T_c)T_c, \tag{4.220}$$

where Homes et al. report two different values of the constant C in units $[\mathrm{cm}]^{-2}$ for the different cases considered in [43]. The value $C = 35$ is true for in-plane cuprates and elemental BCS superconductors, whereas for the cuprates along the c-axis and the dirty limit BCS superconductors they find $C = 65$. The superfluid density ρ_s is a measure for the number of particles contributing to the superfluid phase. It can be thought of as the square of the plasma frequency[19] of the superconducting phase ω_{Ps}^2, because the superconductor becomes "transparent" for electromagnetic waves with frequencies larger than

$$\rho_s \equiv \omega_{Ps}^2 = \frac{4\pi n_s e^2}{m^*}. \tag{4.221}$$

Here n_s denotes the superconducting charge carrier density which describes the number of superconducting charge carriers per volume (and is very different from the superfluid density ρ_s), e is the elementary charge and m^* is the effective mass of the charge carrier renormalized due to interactions. Another way to think about the superfluid density ρ_s is the London penetration depth λ_L which is basically the inverse of the superconducting plasma frequency, such that frequencies larger than ω_{Ps} correspond to length scales smaller than λ_L, *i.e.* $\rho_s \equiv \lambda_L^{-2}$. The critical temperature T_c is determined by the onset of superconductivity. The conductivity σ_{DC} and the superconducting plasma frequency ω_{Ps} are for instance obtained from reflectance measurements by extrapolation to the $\omega \to 0$ limit of the complex optical conductivity $\sigma(\omega)$,

$$\sigma_{DC} = \lim_{\omega\to 0} \mathrm{Re}\,\sigma(\omega), \qquad \omega_{Ps}^2 = \lim_{\omega\to 0}\big(-\omega^2\,\mathrm{Re}\,\epsilon(\omega)\big), \tag{4.222}$$

since the high frequency limit of the real part of the dielectric function $\epsilon(\omega)$ is given by

$$\mathrm{Re}\,\epsilon(\omega) = \epsilon_\infty - \frac{\omega_{Ps}^2}{\omega^2}. \tag{4.223}$$

where ϵ_∞ is set by the screening due to interband transitions.

Alternatively, the superconducting plasma frequency may be obtained from the optical conduc-

[19] The definition of the plasma frequency and its relations to the dielectric function and superconductivity is discussed in detail in Section 4.3.5.

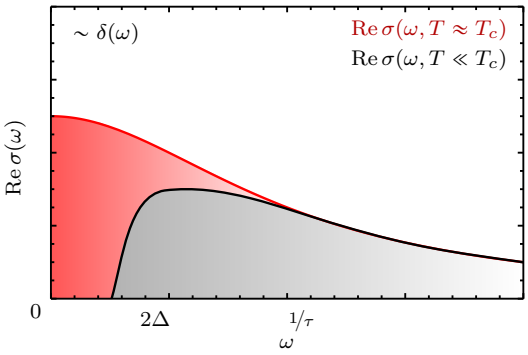

Figure 4.6.
Schematic plots of the optical conductivity above the critical temperature T_c and near the absolute zero $T = 0$ for a dirty BCS superconductor. In the superconducting phase a gap develops for frequencies $\omega < 2\Delta$. Note that in the dirty limit the quasi-particle scattering rate $1/\tau$ is larger than 2Δ. The missing area (red shaded region) *i.e.* the difference between the area under the curve of $\mathrm{Re}\,\sigma(\omega, T \approx T_c)$ and $\mathrm{Re}\,\sigma(\omega, T \ll T_c)$ which condenses into the δ-peak at $\omega = 0$ and thus the superfluid strength (being the coefficient of the $\delta(\omega)$-function) is proportional to the missing area. Following the definitions given in (4.225) we see that the area under the $\mathrm{Re}\,\sigma(\omega, T \ll T_c)$ curve determines N_s whereas the red shaded area yields $N_\mathrm{n} - N_\mathrm{s}$.

tivity measured above and below the critical temperature with the help of the oscillator strength sum rule

$$\frac{\omega_\mathrm{p}^2}{8} = \int_0^\infty \mathrm{d}\omega\, \mathrm{Re}\,\sigma(\omega), \tag{4.224}$$

for the optical conductivity. This gives rise to an alternative definition of the superfluid density as compared to (4.222). We define the spectral weight in the normal and superconducting phase as follows,

$$N_\mathrm{n} = \int_0^\infty \mathrm{d}\omega\, \mathrm{Re}\,\sigma(\omega)\Big|_{T>T_c} = \frac{\omega_\mathrm{pn}^2}{8}, \qquad N_\mathrm{s} = \int_{0^+}^\infty \mathrm{d}\omega\, \mathrm{Re}\,\sigma(\omega)\Big|_{T<T_c}. \tag{4.225}$$

The superfluid density ρ_s describes the degrees of freedom in the superconducting phase which have condensed into a Dirac δ-peak at zero frequency, where ρ_s can be viewed as the coefficient of $\delta(\omega)$. This δ-peak in the real part of the conductivity gives rise to an infinite DC conductivity or zero resistivity. The superfluid density is equal to the difference between the integral over the optical conductivity (4.224) evaluated for $T < T_c$ and $T > T_c$ and generally yields identical values as compared to (4.222). Using the definitions of the spectral weight (4.225) we find

$$\rho_\mathrm{s} = 8\,(N_\mathrm{n} - N_\mathrm{s})\,. \tag{4.226}$$

This is the *Ferrell-Glover-Tinkham sum rule*. Note that in the definition of N_s we have excluded the δ-peak at $\omega = 0$ because the oscillator strength sum rule (4.224) requires that the area under the optical conductivity curve is identical above and below T_c, *i.e.* in the superconducting and normal state. Thus (4.226) determines the missing area of the spectral weight that condensed into the δ-peak at $\omega = 0$, as illustrated in Figure 4.6. Although the gap describes the creation of Cooper pairs, it is really the missing area which gives rise to superconductivity, since according to (4.226) the missing area is equal to the degrees of freedom which condense at zero frequency, thus forming a new coherent macroscopic ground state with off-diagonal long range order. Semiconductors for instance are systems exhibiting an energy gap in their spectrum as well, but are

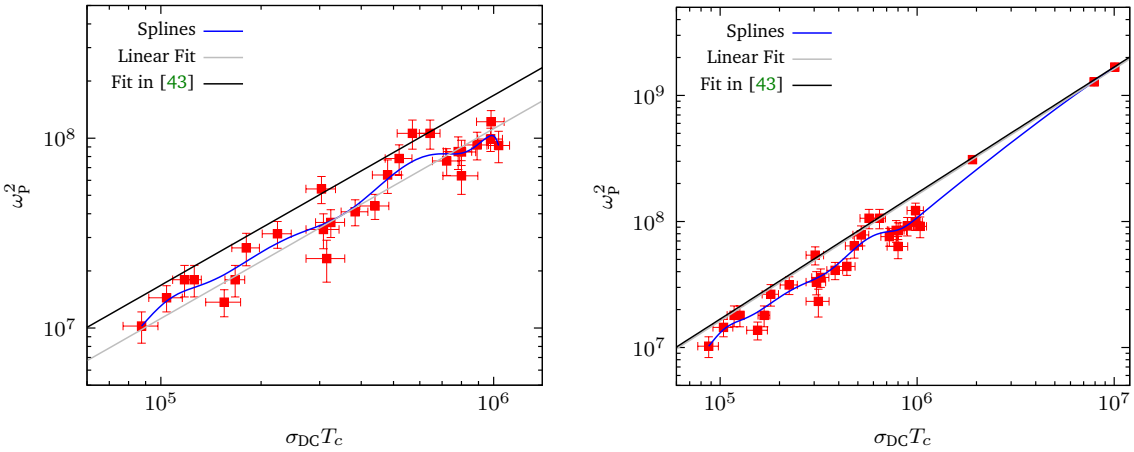

Figure 4.7. Plots of the complete data in Table 1 in [43]. The error bars are calculated by $\Delta(\omega_p^2) = 2\omega_p\Delta\omega_p$ and $\Delta(\sigma_{DC}T_c) = T_c\Delta\sigma_{DC}$. The left plot shows data from high T_c superconductors and for $Ba_{1-x}K_xBiO_3$, while the one on the right includes three data points from elemental superconductors. As shown on the right the elemental conventional superconductors, two data points for Nb and one coming from the Pb superconductor, actually give Homes' law as stated in [43]. If these three data points are ignored, as shown in the left panel, the linear fit is shifted and the data points are below the Homes' law line.

not necessarily superconducting since there is no missing area and hence no new ground state, let alone a phase transition. On the other hand, superconductors retain their properties even if the energy gap is removed (*e.g.* by magnetic impurities) due to the missing area under the $\mathrm{Re}\,\sigma(\omega)$ curve. As a caveat, let us note that high temperature superconductors may not satisfy the Ferrell-Glover-Tinkham sum rule, while it is expected to hold for dirty BCS superconductors.[20]

In order to see clearly the relation between superfluid density and the product of the conductivity at the critical temperature and the critical temperature expressed by Homes' law in (4.220), we have reproduced Table I from [43] with and without the elemental superconductors niobium Nb and lead Pb in Figure 4.7. According to [43] the constant is $C = 35.2$. Despite the original claim by Homes et al., the relation (4.220) seems not to be entirely independent of the doping. Some interesting deviations from the Homes' scaling line has been discussed in [234] along with possible explanations of the origin of this relation. It would be interesting to test/check if Homes' law strictly holds for optimally doped superconductors. Furthermore, in [40, 42, 43, 234] some possible explanations are given concerning the origin of Homes' law: Conventional dirty-limit superconductors, marginal Fermi-liquid behavior, for cuprates a Josephson coupling along the c-axis or unitary-limit impurity scattering. Moreover, the authors discuss limits where the relation breaks down, which is true in the overdoped region of cuprates. For dirty limit BCS superconductors, Homes' law can be explained by the very broad Drude-peak[21] which is condensing into the

[20] Experimentally, it is not possible to "integrate" up to $\omega \to \infty$ since a measurement cannot be done at arbitrary high frequencies, so in reality we need to introduce a cut-off frequency ω_c. For high temperature superconductors this cut-off frequency may be higher than the experimentally accessible frequencies and thus these superconductors may not satisfy the Ferrell-Glover-Tinkham sum rule, *c.f.* [43].

[21] The Drude peak is located at zero frequency where the real part of $\sigma(\omega)$ reaches its global maximum, see for example Figure 4.6 (and for more details on the Drude model see Section 4.3.3).

superconducting δ-peak at $\omega = 0$. The spectral weight of the condensate may then be estimated by an approximate rectangle of area $\rho_s \approx \sigma_{DC} \cdot 2\Delta$ in an optical conductivity plot, similar to Figure 4.6, where the gap in the energy of the superconducting state is denoted by 2Δ and σ_{DC} is the maximum of the curve at $\omega = 0$. According to the BCS model, the energy gap in the superconducting phase is proportional to the critical temperature T_c and thus $\rho_s \sim \sigma_{DC} T_c$. For high T_c temperature superconductors the most striking argument can be found in [40] which links the universal behavior to the "Planckian dissipation" giving rise to a perfect fluid description of the "strange metal phase" with possible universal behavior, comparable to the viscosity of the quark-gluon plasma. The argument, reproduced here for completeness, relies on the fact that the right structure of ρ_s, σ_{DC} and T_c may be worked out by dimensional analysis: First, as already stated above (4.221) the superfluid density must be proportional to the density of the charge carriers in the superconducting state. The natural dimension for this quantity is $(\text{time})^{-2}$ so the product of σ_{DC} and T_c should have the same physical dimension. Second, the normal state possesses two relevant time scales, the normal state plasma frequency ω_{Pn} and the relaxation time scale τ, which describes the dissipation of internal energy into entropy by inelastic scattering. One of the simplest combinations is the product of the two time scales which will yield the dimension $(\text{time})^{-1}$. Therefore, we may take the optical conductivity to be of the Drude-Sommerfeld form given by

$$\sigma_{DC} = \frac{\omega_{Pn}^2 \tau}{4\pi} = \frac{n_n e^2 \tau}{m^*}. \tag{4.227}$$

The last and most crucial step is to convert the critical temperature into the dimension $(\text{time})^{-1}$. Energy and time are related by Heisenberg's uncertainty principle and thus quantum physics and the idea of "Planckian dissipation" will enter,

$$\tau_\hbar (T_c)^{-1} = \frac{k_B T_c}{\hbar}. \tag{4.228}$$

This time scale is the lowest possible dissipation time for a given temperature. For smaller time scales the system will only allow for quantum mechanical dissipationless motion. Interestingly, at finite temperature the lower bound can only be reached if the system is in a quantum critical state [6]. This implies that high T_c superconductors exhibit a quantum critical region above the superconducting dome, which is supported by experimental evidence [7, 235]. The "Planckian dissipation" time scale can be compared to the ratio of shear viscosity over entropy density of a perfect quantum fluid. The shear viscosity is the constant connecting the shear force applied to a fluid layer to the resulting velocity gradient and hence its units are given by the units of

$$\frac{\frac{\text{force}}{\text{Area}}}{\frac{\text{velocity}}{\text{length}}} = \text{pressure} \times \text{time} = \text{energy density} \times \text{time}. \tag{4.229}$$

Therefore, we see that the viscosity is proportional to the relaxation time τ, where ε describes the energy density

$$\eta \sim \varepsilon \tau_\eta, \tag{4.230}$$

so the "Planckian dissipation" describes a perfect fluid in the sense of the viscosity of the quark-gluon-plasma and black branes[22]. It seems that the quantum critical region, that might be above the superconducting dome, is described by the relaxation time being the "Planckian dissipation" time (4.228), so the "strange metal" phase is an almost perfect fluid with possible universal

[22] Note that in [40] there is a confusing statement about the viscosity of a Planckian dissipative process stating that it is maximally viscous. According to [8] the author is aware of this lapse.

behavior. This can be compared to the universal behavior in the quark-gluon plasma [220] where one finds

$$\frac{\eta}{s} = \frac{1}{4\pi}\frac{\hbar}{k_{\mathrm{B}}} = \frac{1}{4\pi}. \tag{4.231}$$

Furthermore, to connect the expression on the right-hand-side of (4.220) with the left-hand-side, we can employ Tanner's law [236] which states that

$$n_{\mathrm{s}} \approx \frac{1}{4} n_{\mathrm{n}}, \tag{4.232}$$

relating the superfluid density to the normal state plasma frequency, as can be seen from (4.221) and (4.227). This "explanation" of Homes' law will guide us in order to find a holographic realization. We will expand on this idea in the following section.

4.4.2. Homes' law in holography

An obstacle towards checking Homes' law directly within holography is that due to the conformal symmetry and the absence of a lattice, the Drude peak of the conductivity is given by a delta distribution even at finite temperatures above the critical temperature, *i.e.*

$$\mathrm{Re}\,\sigma(\omega) \sim \delta(\omega) \qquad \Leftrightarrow \qquad \mathrm{Im}\,\sigma(\omega) \sim \frac{1}{\omega}. \tag{4.233}$$

Thus, it is not possible to evaluate ρ_{s} directly, which is related only to the superconducting degrees of freedom condensing at $\omega = 0$. We therefore rewrite Homes' law in such a way that it becomes accessible to simple models of holography. As we now discuss, this can be achieved by using the idea of Planckian dissipation following [40] for high temperature superconductors, as outlined above at the end of Section 4.4.1, or by employing the Ferrell-Glover-Tinkham sum rule (4.226) for dirty BCS superconductors as can be found in [234].

For simplicity, let us make two assumptions about holographic superconductors: First, let us assume that they satisfy the sum rule which requires that the area under the optical conductivity curve is identical in the superconducting phase and the normal phase. Second, we assume that all degrees of freedom condense in the superconducting state. Using the definition of the spectral weight in the normal phase N_{n} (4.225) and the definition of the superconducting plasma frequency (4.221), we see that both plasma frequencies must be equal

$$\omega_{\mathrm{Ps}}^2 = \omega_{\mathrm{Pn}}^2, \tag{4.234}$$

which implies that $N_{\mathrm{s}} = 0$ in (4.226). Here we clearly neglect possible missing spectral weight as explained in the second paragraph of Section 4.4.1. In the holographic context, similar sum rules have been investigated in [237–239]. Alternatively, we may assume that the holographic superconductors obey Tanner's law (4.235)

$$n_{\mathrm{s}} = B n_{\mathrm{n}}, \tag{4.235}$$

where n_{s} and n_{n} denotes the charge carrier density in the superconducting and the normal phase, respectively, and B is a numerical constant. With either one of these two assumptions, we may rewrite Homes' law in such a way that it becomes accessible to holography. Let us begin with the assumption that holographic superconductors fulfill the sum rule and that all degrees of freedom are participating in the superconducting phase: Starting from

$$\rho_{\mathrm{s}} \equiv \omega_{\mathrm{Ps}}^2 = C\sigma_{\mathrm{DC}}(T_c)T_c, \tag{4.236}$$

and assuming that the Drude-Sommerfeld model is still a useful approximation we can replace the conductivity by a characteristic time scale and the plasma frequency in the normal conducting phase

$$\sigma_{DC} = \frac{\omega_{\text{Pn}}^2 \tau}{4\pi}, \tag{4.237}$$

and thus (4.236) reads

$$\omega_{\text{Ps}}^2 = C \frac{\omega_{\text{Pn}}^2}{4\pi} \tau_c T_c, \tag{4.238}$$

where τ_c denotes $\tau(T_c)$. Equation (4.238) can be simplified using the assumption (4.234),

$$\tau_c T_c = \frac{4\pi}{C}. \tag{4.239}$$

Equation (4.239) holds if there is no missing spectral weight and that all the spectral weight associated with the charge carriers condenses in the superconducting phase and hence contributes to the δ-peak. This enables us to identify the plasma frequencies in the two different phases. Alternatively, we can use the assumption that the charge carrier densities in both states are proportional to each other. Starting again with

$$\rho_{\text{s}} \equiv 4\pi \frac{n_{\text{s}} e^2}{m^*} = C \sigma_{\text{DC}}(T_c) T_c, \tag{4.240}$$

and inserting the Drude-Sommerfeld optical conductivity in terms of the charge carrier density n_{n}

$$\sigma_{DC} = \frac{n_{\text{n}} e^2}{m^*} \tau, \tag{4.241}$$

we may write (4.240) as

$$n_{\text{s}} = \frac{C}{4\pi} n_{\text{n}} \tau_c T_c. \tag{4.242}$$

Assuming that the holographic superconductors obey (4.235) we arrive at

$$\tau_c T_c = \frac{4\pi B}{C}. \tag{4.243}$$

Note that the proportionality constants in (4.239) and in (4.243) may not coincide. If they do not, this will indicate that holographic superconductors behave either more like in–plane high temperature superconductors or like dirty-limit BCS superconductors. In any case the above simplifications allow us to circumvent the need to calculate spectral weights in the superconducting phase or the plasma frequency in either phase (some obstructions are discussed in Section 4.4.3), and to perform the calculation solely in the normal phase. Therefore, we will extract the time scales in the normal phase of the s- and p-wave superconductors from diffusion constants, basically the momentum and R-charge diffusion denoted by D_{M} and D_{R}, respectively. In particular, since $D(T_c) \sim \tau_c$ we obtain

$$D(T_c) T_c = \text{const.} \tag{4.244}$$

This relation is directly accessible to holography. In fact, without including the backreaction of the gauge and matter fields on gravity, the diffusion constants are given by [14, 166, 229]

$$D_{\mathrm{M}} = \frac{1}{4\pi T}, \qquad D_{\mathrm{R}} = \frac{1}{4\pi T}\frac{d}{d-2}, \tag{4.245}$$

such that

$$D_{\mathrm{M}} T = \frac{1}{4\pi} = \text{const.}, \qquad D_{\mathrm{R}} T = \frac{1}{4\pi}\frac{d}{d-2} = \text{const.}, \tag{4.246}$$

where d denotes the dimensionality of the spacetime, and thus Homes' law is trivially satisfied in this case. This can be derived simply by dimensional analysis as is done in [220]. Extending the calculation of the diffusion constants to include backreaction we checked analytically and numerically that our results reduce to the known results in the limit where the backreaction vanishes, for details see Section 4.5.2.

4.4.3. The Drude-Sommerfeld model & holography

Let us shorty recall the key results of the previous section. The optical conductivity of the Drude-Sommerfeld model (4.227)

$$\sigma_{DC} = \frac{\omega_{\mathrm{Pn}}^2 \tau}{4\pi} = \frac{n_{\mathrm{n}} e^2 \tau}{m^*}. \tag{4.247}$$

possesses two scales, the plasma frequency ω_{Pn}^2 setting the scale above which electromagnetic waves can enter the metal and the relaxation time scale τ, connected to the mean free path $l = v_{\mathrm{F}}\tau$ of the charge carriers, where the charge carrier density is denoted by n. Interactions between the charge carriers are included by the renormalization procedure generating effective masses m^* and correction to the relaxation time. The inverse of the real part of the optical conductivity describes absorption processes/loss of energy which is related to dissipation, whereas the imaginary part describes dispersive processes/change of phase which is related to energy transport. The resistivity is defined as $(\mathrm{Re}\,\sigma(\omega = 0))^{-1}$ and is the inverse of the maximum of the real part, the so called Drude peak. The width of the Drude peak is set by the relaxation rate τ^{-1}. The imaginary part of (4.247) is a Lorentzian-shaped curve with maximal energy transport at resonance for $\omega = \tau^{-1}$. For very high frequencies $\omega > \omega_{\mathrm{Pn}}$ the charge carriers are not able to follow the external excitation and thus the optical conductivity must approach zero.

Comparing our holographic setup to the above condensed matter discussion, we first notice that we do not have an underlying lattice. This implies that the Drude peak turns into a delta distribution (or δ-peak) at $\omega = 0$ since momentum conservation does not allow any dissipative process. In the large frequency limit, the optical conductivity approaches the non-vanishing conformal result, *i.e.* $\sigma(\omega \to \infty) = \text{const.}$, since the conformal symmetry does not permit any scale. In this sense there is no well-defined plasma frequency above which the system will become transparent, but a finite absorption due to the non-vanishing real part of the optical conductivity will be retained. A possible workaround is to define a regulated plasma frequency [237] which obey the Kramers-Kronig relations and thus the sum-rules. Moreover, we cannot compute effective masses m^* or more generally, we cannot describe any physical parameter related to the lattice. Additionally, interesting physics is hidden in the zero frequency limit of the optical conductivity, which cannot be resolved without a lattice due to the δ-peak arising from momentum conservation.[23]

[23] Technically, momentum conservation can be broken by neglecting the effects of backreaction onto the geometry on the gravity side. Physically this is not very helpful since the fixed geometry introduces an artificial dissipative reservoir.

One way to remedy these problems is to introduce a lattice explicitly as is done in different ways in [33–35, 233]. One of the results in [33] is the emergence of the Drude-Sommerfeld conductivity (4.143) in the low-frequency limit and – even more excitingly – in the mid-frequency range they find scaling behavior similar to cuprate superconductors. The use of an explicit lattice may be avoided by using the simplified form of Homes' law stated in (4.239) or (4.243) which assumes either the validity of the sum rule or Tanner's law, respectively. This fits in our overall scheme of looking at universal scaling behavior which should not be affected by an underlying microscopic lattice.

4.5. Holographic Realization of Homes' Law in s- & p-Wave Superconductivity

Overview

- Quasi-normal mode analysis of the linearized fluctuations to determine instabilities/condensed phases.
- Numerically determined phase diagram depending on the backreaction fixes the critical values of the temperature.
- Explicit calculation of R-charge and momentum diffusion to determine universal time scale related to "Planckian dissipation" time.

In this section we give a self-contained exposition of the solution to the equations of motion derived from the Einstein-Maxwell action minimally coupled to a charged scalar field. For obtaining a family of holographic s-wave superconductors, we include the backreaction of the gauge field and the scalar field on the metric into our analysis. We will employ a quasi-normal-mode analysis in order to determine the onset of the spontaneous condensation of the operator dual to the charged scalar field. For this purpose, we expand the action up to quadratic order in the fluctuations about the background and derive the corresponding equations of motion. Finally, we determine the R-charge and momentum diffusion related to the gauge field fluctuations and the metric fluctuations, respectively. This allows us to calculate the function relevant for testing Homes' law at finite backreaction.

4.5.1. Quasi-normal-mode analysis & phase diagram

In general the numerical solution to a system of coupled linear differential equation is found by setting the initial values and numerically integrating its evolution. Alternatively, boundary conditions can be set and thus one is sometimes forced to vary the boundary conditions on one "side" of the integration domain to match the wanted values on the other "side". This is usually done using a shooting method which additionally employs a root finding algorithm as explained in Section 4.1 for the s-wave superconductor. In our case we will follow a slightly different strategy. For 2^{nd} order phase transitions the critical temperature/chemical potential can be found by looking at the background solution with vanishing fields but non-vanishing fluctuations about this particular background solution, such that the overall value of the field is $\Phi \longrightarrow \Phi + \delta\phi = \delta\phi$. The condensation of the scalar field is triggered by an instability which can be seen from the poles of the Green function being located in the upper complex ω plane. In particular, the pole is moving through the origin of the complex ω-plane located at $\omega = 0$, exactly when the

temperature reaches the critical value T_c. The appearance of a zero mode is indicating a global symmetry breaking that generates a massless mode according to the Goldstone's Theorem on page 46. Decreasing the temperature further leads to the breakdown of the effective field theory constructed by the saddle-point solution and thus to a negative mass squared of the fluctuations causing acausal behavior. In practice the instability and the critical temperature can be found by:

- Find solution to the linearized fluctuation equations with $\omega = 0$ (zero mode) and $\mathbf{k} = \mathbf{0}$ (zero momentum). Finite momenta characterize transport processes beyond the thermodynamic validity, *e.g.* hydrodynamic properties of the system.
- Vary the chemical potential/temperature and look for poles in the Green function at the origin of the complex ω plane for vanishing momenta.

In the case of $\omega = 0$ and $\mathbf{k} = \mathbf{0}$ we see that the linearized fluctuation equations (4.97) are identical to the scalar equation for the background field Φ (4.68) and the poles of the Green function correspond to solutions of the background equations with vanishing source (*e.g.* the leading term of the boundary expansion of the background field is zero which corresponds to the denominator of the fluctuation Green function). Generically, this is only true for a special choice of the background scalar field potential, namely a quadratic potential . Since we are probing with small fluctuations about the $\Phi = 0$ solution up to quadratic order in the action, all that remains of the full-fledged potential is its leading quadratic term. After fixing u_H, the only parameter left to vary is T/μ. For the fluctuation equations in the probe limit we have $\bar{\mu}$ as an external parameter coming from the solutions of the background fields Φ and A_t. For a second order differential equation in $\delta\phi$ we have two free parameters. These are fixed by the infalling boundary condition at the horizon for the fluctuations $\delta\phi$ and the overall normalization (which can be set to one since it is linear in all terms of the expansion at the horizon). Therefore the Green function for $\omega = 0$ and $\mathbf{k} = \mathbf{0}$ only depends on the dimensionless parameter $\bar{\mu} = \mu u_\mathrm{H} \sim \mu/T$. Taking the backreaction into account we get an additional external parameter α which determines the strength of the backreaction. Therefore we have to determine for each α the corresponding $\bar{\mu}_c$ and take care of not running into temperatures that are non-positive since here the relation between μ, T and α is more complicated, *e.g.* see (4.52).

$$\frac{T}{\mu} = \frac{d - \frac{(d-2)^2}{d-1}\bar{\mu}^2\alpha^2}{4\pi\bar{\mu}} \qquad \longrightarrow \qquad \frac{T}{\mu}\Big|_{\alpha=0} = \frac{d}{4\pi\bar{\mu}}$$

$$\Rightarrow \quad \bar{\mu} = \frac{-2(d-1)\pi\frac{T}{\mu} + \sqrt{4(d-1)^2\pi^2\left(\frac{T}{\mu}\right)^2 + d(d-1)(d-2)^2\alpha^2}}{(d-2)^2\alpha^2} = \sqrt{\frac{d-1}{d-2}}\frac{\bar{Q}}{\alpha}. \tag{4.248}$$

Setting $\alpha = 0$ we recover the probe limit relation of T/μ and $\bar{\mu}$, see (4.67). Including the backreaction we use the holographic dissipation-fluctuation theorem in order to determine the complex-valued Green function of scalar fluctuations about the fixed scalar background in the normal phase. For convenience we state again the equation of motion for the scalar field fluctuations (4.97) in the normal phase

$$\delta\phi''(u) + \left(\frac{f'(u)}{f(u)} - \frac{d-1}{u}\right)\delta\phi'(u) + \left[\frac{(\omega + A_t)^2}{f(u)^2} - \frac{\mathbf{k}^2}{f(u)} - \frac{L^2m^2}{u^2 f(u)}\right]\delta\phi(u) = 0, \tag{4.249}$$

with the Reissner-Nordström black brane blackening factor (4.49) and the background gauge field (4.48). After fixing the incoming wave condition at the horizon of the AdS-Reissner-Nordström black brane, we integrate out to the boundary of AdS-space and fit the numerical

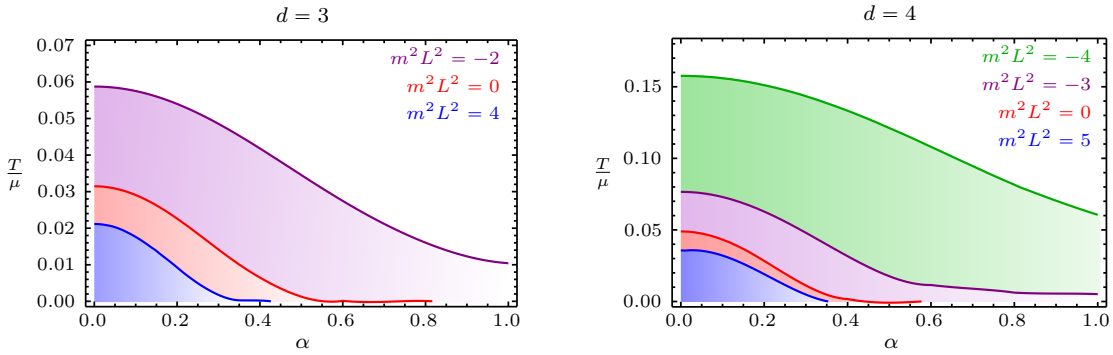

Figure 4.8. Phase diagram of the holographic s-wave superconductor for $d = 4$ and $d = 3$ as a function of the backreaction parameter α, depending on the scalar field mass. Colored regions (for $d = 3$ are encoded as $m^2L^2 = 4$, $m^2L^2 = 0$, $m^2L^2 = -2$ and for $d = 4$ we have $m^2L^2 = 5$, $m^2L^2 = 0$, $m^2L^2 = -3$, $m^2L^2 = -4$) show phases where the scalar field condenses yielding a superfluid phase. Due to the large N_c limit, the Coleman-Mermin-Wagner Theorem on page 53 is evaded in $d = 2 + 1$ dimensions allowing for a phase transition to happen. Quantum fluctuations arise only in the $1/N_c$ corrections. On the gravity side the Anderson-Higgs mechanism for removing gauge symmetries is not subject to any constraint, formally the lower critical dimension is ∞ due to Elitzur's theorem.

solution to the boundary expansion given in (4.42). Finally, we read off the Green function and determine the critical values of T/μ for a given value of the strength of the backreaction α yielding critical curves as shown in Figure 4.8. Additionally, we can also vary the mass of the scalar field related to the scaling dimension of the dual operator via

$$\Delta_\pm = \frac{1}{2}\left(d \pm \sqrt{d^2 + 4L^2m^2}\right), \qquad m^2L^2 = \Delta_\pm\left(\Delta_\pm - d\right). \tag{4.250}$$

Note that for positive masses, *i.e.* $m^2L^2 > 0$ the dual operator becomes relevant in the UV which would drastically alter the UV conformal theory. Since this operator is not sourced, the RG flow to the UV fixed point is not affected by the non-zero profile of the scalar field with positive masses in the bulk.

Analytic value of α_c at zero temperature

In the case of vanishing temperature, we can find an analytic solution for the critical value of the strength of the backreaction. The charge of the extremal Reissner-Nordström black brane for $T = 0$ can be determined from (4.248) to be

$$\bar{Q}^2 = \frac{d}{d-2} \qquad \Rightarrow \qquad T = 0. \tag{4.251}$$

with finite black brane horizon u_H following from (4.50),

$$u_\mathrm{H} = \frac{\sqrt{d(d-1)}}{d-2}\frac{1}{\alpha\mu}. \tag{4.252}$$

Curiously, the entropy density remains finite in this case. Taking the definition of the entropy given in (4.62) and inserting the zero temperature black brane horizon u_H we find

$$s = \frac{S}{V_{d-1}} = \frac{4\pi}{2\kappa^2}\frac{L^{d-1}}{u_\mathrm{H}^{d-1}} = \frac{4\pi}{2\kappa^2}\frac{L^{d-1}\alpha^{d-1}\mu^{d-1}}{\left[\frac{d(d-1)}{(d-2)^2}\right]^{\frac{(d-1)}{2}}} = 2\pi\left[\frac{(d-2)^2}{d(d-1)}\right]^{(d-1)/2} L^{d-3}\alpha^{d-3}\frac{\mu^{d-1}}{e^2} \tag{4.253}$$

where in the last equality κ^2 has been replaced via the definition of the backreaction $\alpha^2 L^2 = \kappa^2/e^2$. In $d = 3$ and $d = 4$ dimensions the zero-temperature entropy density reduces to

$$s\big|_{d=3} = \frac{\pi\mu^2}{3e^3}, \qquad s\big|_{d=4} = \frac{2\pi}{3\sqrt{3}}\frac{L\alpha\mu^3}{e^2}. \tag{4.254}$$

In the zero temperature limit, the near horizon limit of the blackening factor reads

$$f(u) = 1 - \left(\frac{d}{d-2}+1\right)\frac{u^d}{u_\mathrm{H}^d} + \frac{d}{d-2}\frac{u^{2(d-1)}}{u_\mathrm{H}^{2(d-1)}} \approx \frac{d(d-1)}{u_\mathrm{H}^2}(u-u_\mathrm{H})^2,$$

which gives rise to an AdS_2 metric

$$\begin{aligned} \mathrm{d}s^2 &\approx \frac{L^2}{u_\mathrm{H}^2}\left(-\frac{d(d-1)}{u_\mathrm{H}^2}(u-u_\mathrm{H})^2\,\mathrm{d}t^2 + \frac{u_\mathrm{H}^2}{d(d-1)(u-u_\mathrm{H}^2)}\,\mathrm{d}\,(u-u_\mathrm{H})^2 + \mathrm{d}\mathbf{x}^2\right) \\ &= \frac{L^2}{d(d-1)}\left(-\frac{d^2(d-1)^2}{u_\mathrm{H}^4}(u-u_\mathrm{H})^2\,\mathrm{d}t^2 + \frac{\mathrm{d}\,(u-u_\mathrm{H})^2}{(u-u_\mathrm{H})^2} + \frac{d(d-1)}{u_\mathrm{H}^2}\,\mathrm{d}\mathbf{x}^2\right). \end{aligned} \tag{4.255}$$

Redefining the coordinate $\varrho = (u-u_\mathrm{H})^{-1}$ and rescaling t and $\mathbf{x}$ by a constant accordingly, (4.255) looks like an $\mathrm{AdS}_2 \times \mathbb{R}^{d-1}$ metric

$$\mathrm{d}s^2 = \frac{L^2_{\mathrm{AdS}_2}}{\varrho^2}\left(\mathrm{d}\tilde{t}^2 + \mathrm{d}\varrho^2\right) + \mathrm{d}\tilde{\mathbf{x}}^2 = \mathrm{d}s^2_{\mathrm{AdS}_2} + \mathrm{d}\mathbb{E}^{d-1}, \tag{4.256}$$

where the AdS_2 radius is is related to the AdS_{d+1} radius by

$$L^2_{\mathrm{AdS}_2} = \frac{L^2}{d(d-1)}. \tag{4.257}$$

The gauge field/chemical potential for vanishing temperature is given by

$$A = \frac{\sqrt{d(d-1)}}{(d-2)}\frac{1}{u_\mathrm{H}\alpha}\left(1 - \frac{u^{d-2}}{u_\mathrm{H}^{d-2}}\right)\mathrm{d}t, \tag{4.258}$$

and the near horizon expansion of $A_t(u)^2$ up to leading order reads

$$A_t(u)^2 \approx \frac{d(d-1)}{u_\mathrm{H}^4\alpha^2}(u-u_\mathrm{H})^2. \tag{4.259}$$

For the near horizon expansion of (4.249) we need to insert the near horizon expansions of $f(u)$ and $A_t(u)^2$ which up to leading order yields

$$\delta\phi''(u-u_{\mathrm{H}}) + \left(\frac{2}{u-u_{\mathrm{H}}} - \frac{d-1}{u_{\mathrm{H}}}\right)\delta\phi'(u-u_{\mathrm{H}}) + \left[\frac{d(d-1)}{d^2(d-1)^2\alpha^2(u-u_{\mathrm{H}}^2)} - \frac{L^2m^2}{d(d-1)(u-u_{\mathrm{H}})^2}\right]\delta\phi(u-u_{\mathrm{H}}) = 0,$$

$$\delta\phi''(u-u_{\mathrm{H}}) + \left(\frac{2}{u-u_{\mathrm{H}}}\right)\delta\phi'(u-u_{\mathrm{H}}) - \frac{1}{d(d-1)}\left(L^2m^2 - \frac{1}{\alpha^2}\right)\frac{\delta\phi(u-u_{\mathrm{H}})}{(u-u_{\mathrm{H}})^2} = 0. \tag{4.260}$$

The effective mass term in (4.260) can be read off by comparing to the scalar field equation in AdS_2[24]

$$\delta\phi''(r) + \frac{2}{r}\delta\phi'(r) - \frac{L^2_{\mathrm{AdS}_2}m^2}{r^2}\delta\phi(r) = 0, \tag{4.261}$$

and compare it to the Breitenlohner-Freedman stability bound in one dimension since we are in $\mathrm{AdS}_{d+1=2}$-space

$$L^2_{\mathrm{AdS}_2}m^2_{\mathrm{eff}} = \frac{1}{d(d-1)}\left(L^2m^2 - \frac{1}{\alpha^2}\right) \leqslant L^2_{\mathrm{AdS}_2}m^2_{\mathrm{BF}} = -\frac{1}{4}, \tag{4.262}$$

which indicates, that the stability bound for the effective scalar field mass m_{eff} is lowered by the strength of the backreaction α. This is true in general since the minimal coupling of the scalar field to the $U(1)$ gauge field gives rise to an effective mass term. Looking at (4.8) we see

$$\nabla_a\nabla^a\Phi + \mathrm{i}\nabla_a A^a\Phi - \left(m^2 + A_aA^a\right)\Phi = 0. \tag{4.263}$$

Of course, there is still the possibility for more complicated potentials which may lead to more complicated mass terms in the first place. Assuming that we only have a non-zero time component of the gauge field dependent on the radial coordinate, (4.263) can be rewritten as

$$\nabla_a\nabla^a\Phi - \left(m^2 + g^{tt}A_tA_t\right)\Phi = 0. \tag{4.264}$$

Thus, there could be a critical value of α where the scalar field condenses in the near horizon region. Solving (4.262) for α gives rise to the condition that scalar field condensation occurs

$$\frac{1}{\alpha^2} \geqslant \frac{d(d-1)}{4} + L^2m^2, \qquad \text{or} \qquad \alpha^2 \leqslant \frac{1}{\frac{d(d-1)}{4} + L^2m^2}. \tag{4.265}$$

In the case of $d = 3, 4$ we find the critical value to be *c.f.* Figure 4.9

$$\alpha_c^2\Big|_{d=3} = \frac{1}{\frac{3}{2} + L^2m^2}, \qquad \alpha_c^2\Big|_{d=4} = \frac{1}{3 + L^2m^2}. \tag{4.266}$$

We see if the mass is already below the AdS_2 Breitenlohner-Freedman bound, there is no critical value for α and hence no quantum critical point or phase transition at zero temperature between the condensed phase and the normal phase. The different masses used in the numerical calculation and the corresponding values for the scaling and the critical backreaction strength are listed in Table 4.5. This is true for all m^2L^2 we have chosen for $d = 3, 4$, ($m^2L^2 = -2, -3, -4 < -1/4$)

[24] It is easier to work in the coordinates $r = u - u_{\mathrm{H}}$ with the AdS_2 metric $\mathrm{d}s^2_{\mathrm{AdS}_2} = L^2\left(r^2\,\mathrm{d}\tilde{t} + \mathrm{d}r^2/r^2\right)$ in order to compare with the original AdS_{d+1} Schwarzschild metric in u coordinates since the double zeros of the blackening factor give rise to the metric structure.

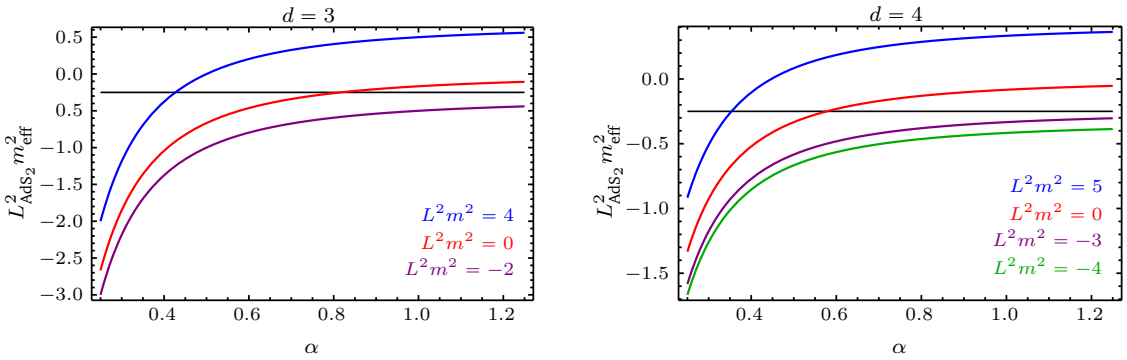

Figure 4.9. The left plot shows the effective AdS_2 mass in $d = 3$ for different masses of the scalar field. The black constant line denotes the Breitenlohner-Freedman bound in one dimension. In the case of $m^2L^2 = 0, 4$, the mass of the scalar field is above the BF bound where the intersection determines α_c. In $d = 4$ dimensions, shown on the right, we see that only for $m^2L^2 = 0, 5$ the masses are above the Breitenlohner-Freedman bound in the IR and so there is a critical value α_c.

so the superfluid phase is extended along the $T = 0$ axis for all values of α. Finally, we can calculate the corresponding critical value of $\bar{\mu}$ via (4.50) to be

$$\bar{\mu}_c = \sqrt{\frac{d(d-1)}{d-2}}\frac{1}{\alpha_c} \qquad \longrightarrow \qquad \mu_c\Big|_{d=3} = \frac{\sqrt{6}}{\alpha_c}, \quad \text{and} \quad \mu_c\Big|_{d=4} = \frac{\sqrt{3}}{\alpha_c}, \tag{4.267}$$

which upon insertion into T/μ given in (4.248) will give zero. Our results as displayed in Figure 4.8 show that the critical temperature decreases with increasing backreaction strength α. Moreover, if the scalar mass is larger than a critical value, the critical temperature goes to zero for a finite value of α. This is the case most reminiscent of a real high T_c superconductor, when the dome in Figure 4.8 has similarities with the right hand side of the dome in the phase diagram of a high T_c superconductor.

Physical interpretation of the holographic superconductor

The physical interpretation of α is that it corresponds to the ratio of the number of $SU(2)$ charged degrees of freedom over all degrees of freedom [219]. The phase diagrams above indicate that an increase of α reduces the numbers of degrees of freedom which can participate in pair formation and condensation, such that T_c is lowered. A similar mechanism also seems to be at work when adding a double trace deformation to the holographic superconductor [240], and has been discussed within condensed matter physics using a BCS approach in [241]. For holographic superconductors, this mechanism is most clearly visible for the top-down holographic superconductors involving D7 brane probes [215, 217] in which the dual field theory Lagrangian and thus the field content of the condensing operator is known. In these models, there is a $U(2)$ symmetry which factorizes into an $SU(2)_I \times U(1)_B$, *i.e.* into an isospin and a baryonic symmetry. A chemical potential is switched on for the $SU(2)_I$ isospin symmetry and the condensate is of ρ-meson form,

$$J_x{}^1 = \bar{\psi}\sigma^1\gamma_x\psi + \bar{\phi}\sigma^1\partial_x\phi = \bar{\psi}_\uparrow\gamma_x\psi_\downarrow + \bar{\psi}_\downarrow\gamma_x\psi_\uparrow + \text{bosons}, \tag{4.268}$$

where $\psi = (\psi_\uparrow, \psi_\downarrow)$ and $\phi = (\phi_\uparrow, \phi_\downarrow)$ are the quark and squark doublets, respectively, which involve up and down flavors, with σ^i the Pauli matrices in isospin space and γ_μ the Dirac matrices.

	$d=3$			$d=4$			
m^2L^2	4	0	-2	5	0	-3	-4
Δ_-	-1	0	1	-1	0	1	2
Δ_+	4	3	2	5	4	3	2
α_c^2	$\frac{2}{11}$	$\frac{2}{3}$	-2	$\frac{1}{8}$	$\frac{1}{3}$	∞	-1

Table 4.5. List of the critical values for the strength of the backreaction α for different masses in three and four dimensions. Note that the instability condition is satisfied for $\alpha < \alpha_c$. In particular, for the negative values we do not have a critical value of $\alpha \in \mathbb{R}$, so in this case for $T = 0$ we always find a condensed/superfluid phase. $\Delta_\pm$ describes the scaling of the dual operator according to the boundary expansion $\Phi \approx \Phi_{\text{source}} u^{\Delta_-} + \langle O_{\Delta_+} \rangle u^{\Delta_+}$. For $d = 3$ and $m^2L^2 = -2$ an alternative quantization scheme yields the operator O_{Δ_-}. For $d = 4$ with saturated Breitenlohner-Freedman bound we need to introduce an additional implicit UV cut-off $\ln(u/\delta)$.

As an additional control parameter, a chemical potential μ_B for the baryonic $U(1)_B$ symmetry may be turned on. This leads to a decrease of T_c [222], see also [242], which may be understood as follows: Under the $U(1)_B$ symmetry, ψ and $\bar{\psi}$ have opposite charge. The same applies to ϕ and $\bar{\phi}$. Turning on μ_B leads to an excess of ψ over $\bar{\psi}$ degrees of freedom, which implies that less degrees of freedom are available to form the pairs (4.268). The same applies to ϕ and $\bar{\phi}$ degrees of freedom. Thus in this case, charge carriers in the normal state are also present in the superconducting phase, leading to the formation of a pseudo-gap.

Let us comment on the RG picture of the holographic superconductors, pictorially shown in Figure 4.10. The conformal UV fixed point is deformed by a relevant operator J^t which scaling field is associated with the boundary value of $A_{t\,\mathrm{B}} = \mu$. According to Table 3.3, a massless vector field with $p = 1$ and $m = 0$ is always a relevant scaling field with $y_\mu = d - \Delta_J > 0$. More generally, the UV relevant operator J^t, driving the system out of the conformal UV fixed point, generates a RG flow where the $U(1)$ gauge symmetry is removed and Lorentz invariance is broken. The deep interior IR geometry is stabilized by the scalar field condensate. In the zero temperature case discussed above, the emergent $\mathrm{AdS}_2 \times \mathbb{R}^{d-2}$ of the extremal AdS-Reissner-Nordström black brane allows for a stable scale invariant solution of the scalar field by choosing a suitable IR potential such that the ground state yields a irrelevant scalar deformation [245]. For the operator J^t there are two possibilities, either J^t becomes irrelevant in the IR, restoring Lorentz symmetry which gives rise to a AdS_4 spacetime [246–248], or the operator's anomalous dimension allows a more intricate IR fixed point geometry. In general, these solutions involve so-called Lifshitz geometries [158] with arbitrary dynamical scaling exponent z, defined in (2.159). In the case $z = 1$ we find a relativistic AdS_4 geometry, whereas the extremal AdS-Reissner-Nordström black brane is recovered in the limit $z \to \infty$. Lifshitz solution with finite z describe completely discharged black brane geometries, where the charged scalar condensate sources the boundary field theory charge density $\langle J^t \rangle$. A nice overview of the low-temperature behavior of the holographic condensed phases are given in [249]. More details of the related fermionic story described by electron stars can be found in [177]. Let us conclude with two open questions:

- What is the origin of the $\mathrm{AdS}_2 \times \mathbb{R}^{d-2}$ instability close to the quantum critical point at α_c?

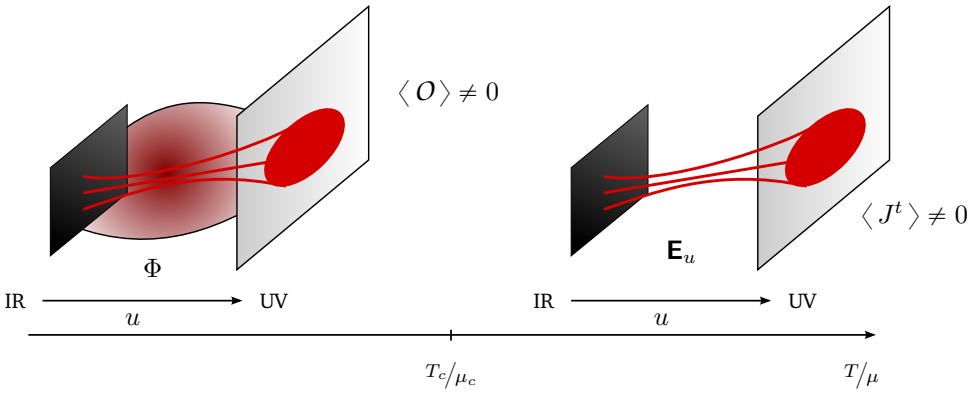

Figure 4.10. In the normal phase $T/\mu > T_c/\mu_c$ the charge density of the boundary theory $\langle J^t \rangle$ is sourced completely by the electric flux through the black brane horizon connected to the electric field $\mathbf{E}_\mathrm{H} = A'_{t\,\mathrm{H}}(u)$. A charged pair producing instability characterizes the onset of the superconducting phase below T_c/μ_c generating a charged condensate $\langle O \rangle$ that contributes to the boundary field theory charge density. For extremely low temperatures $T \ll \mu$ the IR geometry becomes more intricate. As we already discussed in the main text at zero temperature, the extremal Reissner-Nordström black brane gives rise to an emergent $\mathrm{AdS}_2 \times \mathbb{R}^{d-2}$ IR geometry. More "exotic" IR fixed point geometries are possible which allow for a completely discharged and thus vanishing black brane, where the charge density is sourced entirely by the electric flux generated by the charged condensate. In a wider sense, geometries with charges "hidden" behind the black brane horizon are called fully fractionalized, whereas charge distributions inside and outside of the black brane are known as partially fractionalized. An electric flux sourced completely by charges in the bulk are called cohesive; well-known examples are bosonic holographic superconductors and fermionic electron stars [243, 244].

- How do quantum corrections in $1/N_c$ affect the large N_c holographic picture? Clearly, on the field theory side we expect an instability due to the diverging entropy (4.254) allowing for a high ground state degeneracy. More importantly, in $d = 3$ dimensions we expect that the phase of the condensate is totally randomized due to quantum fluctuations, restoring the $U(1)$ as explained in Section 2.3.4.

Parts of these questions are tried to answered in a zero temperature finite density top-down setup discussed in Chapter 5.

4.5.2. Momentum & charge diffusion constants

After extensively discussing the phase diagram, let us come back to the holographic analysis of Homes' law. As explained in Section 4.4, the analysis of Homes' law requires the definition of a relevant time scale. Possible candidates for time scales are associated with diffusive processes. We may determine two different types of diffusion, momentum diffusion D_M and R-charge diffusion D_R, respectively. The former can be related to the shear viscosity by studying hydrodynamic modes

$$D_\mathrm{M} = \frac{\eta}{\varepsilon + P}, \tag{4.269}$$

such that it can be solely described by thermodynamic quantities using the famous result (1.1). The latter, however, cannot be calculated solely by thermodynamic quantities in general, such that an independent calculation for each background is necessary. Usually the charge diffusion constant can be read off from the dispersion relation $\omega = -\mathrm{i}D\mathbf{k}^2$ of the conserved current, which can be derived from Fick's law and the continuity equation

$$\mathbf{j} = -D\nabla\rho, \qquad \text{and} \qquad \dot{\rho} + \nabla\cdot\mathbf{j} = 0, \qquad \longrightarrow \qquad \dot{\rho} - D\nabla^2\rho = 0. \tag{4.270}$$

Fortunately, this work has already been done by [229] without backreaction.

Momentum diffusion with backreaction

Since we are working with a fixed chemical potential, we take the grand canonical ensemble to describe the momentum diffusion in the thermodynamic limit. Using the gauge/gravity duality the grand canonical potential is given by

$$\Omega = \frac{1}{\beta} I = TI, \tag{4.271}$$

where I denotes the regularized Euclidean on-shell action given by

$$I = -\frac{L^{d-1}}{2\kappa^2}\frac{V_{d-1}}{T}\frac{1}{u_{\mathrm{H}}^d}\left(1+\bar{Q}^2\right). \tag{4.272}$$

According to the gauge/gravity dictionary, we derive the charge density, the energy density and the entropy density from (4.271), with the help of the relations defined in (4.58)–(4.60)

$$\begin{aligned} s &= \frac{4\pi}{2\kappa^2}\frac{L^{d-1}}{u_{\mathrm{H}}^{d-1}}, \\ \varepsilon &= \frac{d-1}{2\kappa^2 L^{d-1}}\frac{1+\bar{Q}^2}{u_{\mathrm{H}}^d}, \\ n &= \sqrt{(d-1)(d-2)}\frac{L^{d-1}}{\kappa^2}\frac{\alpha\bar{Q}}{u_{\mathrm{H}}^{d-1}}. \end{aligned} \tag{4.273}$$

The black brane horizon u_{H} should be understood as a function of μ or T, respectively, defined by solving either (4.50) or (4.51) for u_{H}, whereas $\bar{Q}$ is a function of T/μ defined by the inversion of (4.53). Starting from the definition of the momentum diffusion and using the relations (1.1) and the first law of thermodynamics $\varepsilon = Ts - P + \mu n$, we find

$$D_{\mathrm{M}} = \frac{\eta}{\varepsilon + P} = \frac{\frac{s}{4\pi}}{Ts + \mu n} = \frac{1}{4\pi T}\frac{1}{1+\frac{\mu}{T}\frac{n}{s}}. \tag{4.274}$$

The relation for μ/T is stated in (4.52) and following (4.273) we find

$$\frac{n}{s} = \frac{\alpha\bar{Q}}{2\pi}\sqrt{(d-1)(d-2)}. \tag{4.275}$$

Inserting (4.52) and (4.275), the momentum diffusion written in terms of Q reads

$$D_{\mathrm{M}} = \frac{1}{4\pi T}\left(1+\frac{4\pi}{\alpha}\frac{\sqrt{\frac{d-1}{d-2}}\bar{Q}}{d-(d-2)\bar{Q}^2}\frac{\sqrt{(d-1)(d-2)}}{2\pi}\alpha\bar{Q}\right)^{-1}$$
$$= \frac{1}{4\pi T}\left(1+\frac{2(d-1)\bar{Q}^2}{d-(d-2)\bar{Q}^2}\right)^{-1} \tag{4.276}$$

R-charge diffusion with backreaction

As explained in the previous subsection it is not straightforward to generalize the R-charge diffusion with backreaction to arbitrary dimensions. To our knowledge the functional dependence on the backreaction of D_{R} in $d=3$ dimensions is not known yet, let alone for arbitrary dimensions d. Surely, this would be an interesting result which is beyond the scope of this work. In $d=4$ the R-charge diffusion with backreaction is determined in [231]. Converting the expression

$$D_{\mathrm{R}} = \frac{1+\bar{M}}{4\bar{M}R} = \frac{1}{2R}\frac{2+\bar{Q}^2}{2(1+\bar{Q}^2)}, \tag{4.277}$$

into the form given by our conventions, we can use the relation (4.50) between mass and charge of the AdS-Reissner-Nordström black brane we can rewrite the R-charge diffusion constant in terms of the charge $\bar{Q}$ only. In order to transform (4.277) into our coordinates, we apply the following replacement $R \longrightarrow \frac{1}{u_{\mathrm{H}}}$. We then have

$$\bar{Q}=0 \quad \Rightarrow \quad T=\frac{1}{\pi u_{\mathrm{H}}}, \qquad \text{and} \qquad D_{\mathrm{R}}=\frac{1}{2\pi T} \quad \Rightarrow \quad D_{\mathrm{R}}=\frac{u_{\mathrm{H}}}{2}. \tag{4.278}$$

Comparing with (4.277) for $\bar{Q}=0$ we find $1/2R \longrightarrow u_{\mathrm{H}}/2$ and thus

$$D_{\mathrm{R}} = \frac{u_{\mathrm{H}}}{2}\frac{2+\bar{Q}^2}{2(1+\bar{Q}^2)} = \frac{1}{4\pi T}\frac{(2-\bar{Q}^2)(2+\bar{Q}^2)}{2(1+\bar{Q}^2)}, \tag{4.279}$$

where the dimensionless black brane charge is defined in (4.50) and we use (4.51) to eliminate u_{H}. Furthermore, we may look at the ratio of the two different diffusion constants,

$$\frac{D_{\mathrm{R}}}{D_{\mathrm{M}}} = \frac{(2-\bar{Q}^2)(2+\bar{Q}^2)}{2(1+\bar{Q}^2)} + \frac{3\bar{Q}^2(2+\bar{Q}^2)}{2(1+\bar{Q}^2)} = 2+\bar{Q}^2. \tag{4.280}$$

Evaluated for the two cases $\alpha=0$ and $\alpha=\infty$ we find

$$\left.\frac{D_{\mathrm{R}}}{D_{\mathrm{M}}}\right|_{\substack{Q=0\\ \alpha=0}} = 2, \qquad \left.\frac{D_{\mathrm{R}}}{D_{\mathrm{M}}}\right|_{\substack{Q=\sqrt{2}\\ \alpha=\infty}} = 4. \tag{4.281}$$

4.5.3. Diffusion constants in s-wave superconductivity

Finally, we discuss the diffusion constants determined by our numerical results. Therefore, we insert the s-wave solutions, where we trace the critical line in the s-wave phase diagram Figure 4.8 fixing $\bar{\mu}$ and α and plot the behavior of the diffusion constant.

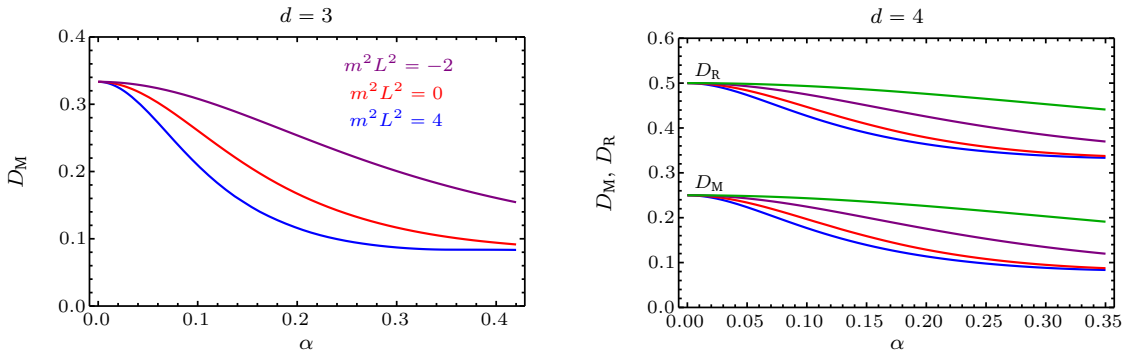

Figure 4.11. Plots of momentum diffusion constant D_M for $d = 3$ (left panel) and R-charge diffusion D_R and momentum diffusion D_M for $d = 4$ (right panel) versus the backreaction strength α. The color coding of the different scalar field masses follows Figure 4.8. The probe limit properties for $\alpha = 0$ are reproduced, *i.e.* for $d = 3$ we find $D_M = 1/3$ and in the case of $d = 4$, $D_M = 1/4$ and $D_R = 1/2$, independently of the scalar field mass.

Diffusion without backreaction for arbitrary d

First of all we check our results by taking the limit of vanishing backreaction, *i.e.* setting α and $\bar{Q}$ to zero in (4.276) and (4.279). We see that the dimensionless temperature $\bar{T}$ (4.52) has the fixed value of $d/4\pi$ and thus

$$\bar{D}_M = \frac{1}{4\pi\bar{T}} = \frac{1}{d}, \tag{4.282}$$

is equal for all masses of the scalar field. Similarly, the R-charge diffusion is given by [220]

$$\bar{D}_R = \frac{1}{4\pi\bar{T}}\frac{d}{d-2} = \frac{1}{d-2}, \tag{4.283}$$

and the ratio is given by

$$\frac{D_R}{D_M} = \frac{d}{d-2}. \tag{4.284}$$

Comparing these results to our numerical solutions shown in Figure 4.11, we see that for $\alpha = 0$, we obtain for $d = 3$ dimensions a dimensionless value of $1/3$ for $\bar{D}_M$. This is consistent with the values obtained form the analytic calculation without backreaction (4.282). In particular, we see that the momentum diffusion does not depend on the mass of the background scalar field since all diffusion constants for different masses, indicated in the figure by different colors, converge to the same value. Similarly for $d = 4$, we check our numerical values for the momentum and the R-charge diffusion by comparing to the results without backreaction. As is displayed in Figure 4.11, we find that $\bar{D}_M = 1/4$ and $\bar{D}_R = 1/2$ as stated in (4.282) and (4.283), as well as the correct value of the ratio $D_R/D_M = 2$. Again our numerical results are consistent with the analytic solutions without backreaction and we see the same convergence effect for the different masses of the scalar field for each diffusion constant displaying the independence on the scalar fields' mass.

Momentum diffusion for $d = 3$

Inserting the critical values for T/μ at a fixed α, we may check how much the momentum diffusion is varying with respect to α.

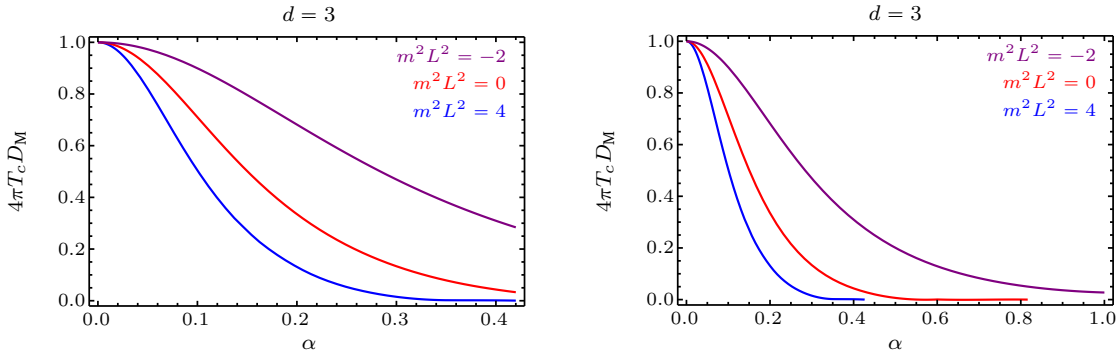

Figure 4.12. The constant C_M related to momentum diffusion D_M for $d = 3$ and different masses of the scalar field (color coded as $m^2L^2 = 4$, $m^2L^2 = 0$ and $m^2L^2 = -2$) plotted depending on the strength of the backreaction α, defined in (4.6). The left panel shows the numerical values found by a minimization algorithm up to the α where poles of higher excitations in the Green function overlay with the lowest modes, thus leading to a breakdown of the algorithm. Only in the case of $m^2L^2 = -2$, we have tested our algorithm up to $\alpha = 1$. In the right panel we included the analytically determined critical points α_c for $m^2L^2 = 4$ and $m^2L^2 = 0$ given in Table 4.5 which corresponds to the zero temperature case with $\bar{Q}^2 = {}^{d}/_{(d-2)}$ and thus $C_M = 0$. Due to the reduced number of data points we use an interpolation function in the region $\alpha \in [0.35, \sqrt{2/3} \approx 0.82]$. For this reason the curves for $m^2L^2 = 4$ and $m^2L^2 = 0$ should not be trusted to be very accurate. Since for $m^2L^2 = -2$ there is no critical value of α, so C_M approaches zero asymptotically.

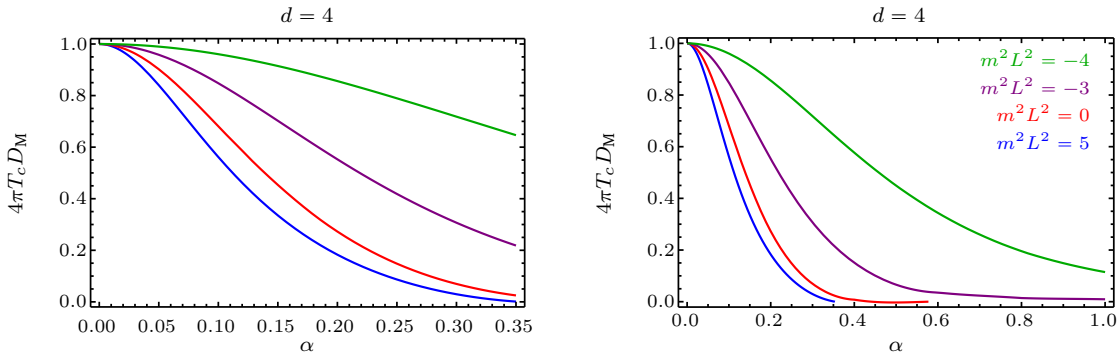

Figure 4.13. Dimensionless momentum diffusion in $d = 4$ dimensions given by C_M depending on the backreaction α (for different masses of the scalar field color coded as $m^2L^2 = 5$, $m^2L^2 = 0$, $m^2L^2 = -3$ and $m^2L^2 = -4$). As already explained in Figure 4.12, the endpoint in the curves for scalar field mass $m^2L^2 = 5$ and $m^2L^2 = 0$ as shown in the right panel is set by the critical values of α listed in Table 4.5. Due to the interpolation these curves should be taken with a grain of salt in the vicinity of the critical point α_c.

As shown in Figure 4.12, there is a mild variation of the momentum diffusion in the sense that we are approaching the values for $\alpha = 0$ in a linear way. In order to compare our numerical results to the constant governing Homes' law rewritten in the form (4.239) or (4.243), we introduce the

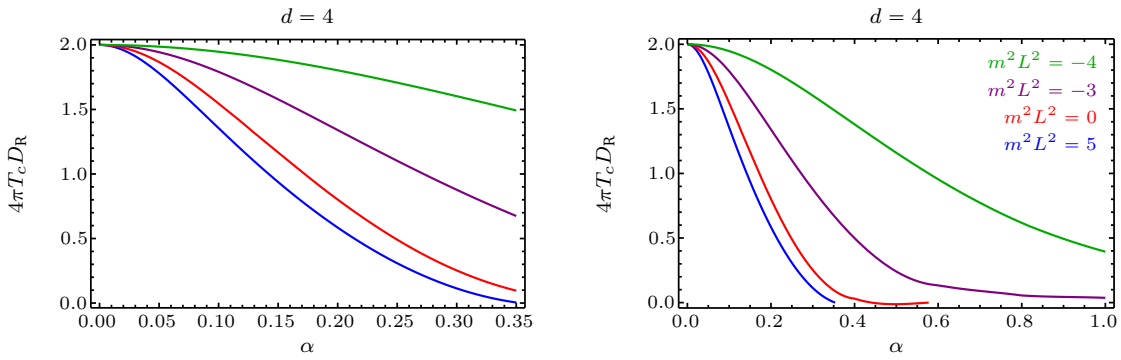

Figure 4.14. Dimensionless R-charge diffusion given by $C_R = 4\pi T_c D_R$. Note that we have used the same prefactor in the definition (4.286) as for the dimensionless momentum C_M, which leads to the probe limit value of two. The color coding of the scalar field masses is identical to Figure 4.13.

function

$$C_M = 4\pi T_c D_M(T_c) = \left(1 + \frac{4\bar{Q}^2}{3 - \bar{Q}^2}\right)^{-1}, \tag{4.285}$$

plotted in Figure 4.12. Here we assume that the diffusive process is proportional to a time scale $\tau_c \sim D_M(T_c)$, such that the proportionality does not depend on $\bar{Q}$ or α.

R-charge diffusion and momentum diffusion for $d = 4$

We now repeat the discussion of the previous subsection for the four-dimensional case. In addition to the momentum diffusion, we may also calculate the R-charge diffusion which will give us an additional time scale to choose. The constant related to $4\pi\tau_c T_c$ for the R-charge diffusion reads

$$C_R = \frac{(2 - \bar{Q}^2)(2 + \bar{Q}^2)}{2(1 + \bar{Q}^2)}. \tag{4.286}$$

Note that this function is running from 2 to 0 for $\alpha \in [0, \alpha_c]$ since the R-charge diffusion without backreaction is given by $1/(2\pi T)$ see (4.283). For $d = 4$, the constant for the momentum diffusion reads

$$C_M = \left(1 + \frac{3\bar{Q}^2}{2 - \bar{Q}^2}\right)^{-1}. \tag{4.287}$$

Note also that the ratio C_R/C_M is given by 2 in compliance with the ratio for the diffusion constants (4.284). The plots of C_M and C_R are shown in Figure 4.13 and Figure 4.14, respectively. We see that the numerically solutions are virtually the same as in the three dimensional case. In both dimensions the numerical solutions display the same properties:

- Instead of the behavior $D(T_c)T_c = $ const. predicted by Homes' law in combination with the sum rules as discussed in Section 4.4.2, we observe a decrease of this quantity with increasing backreaction strength α. We discuss possible explanations for this behavior in Chapter 6.

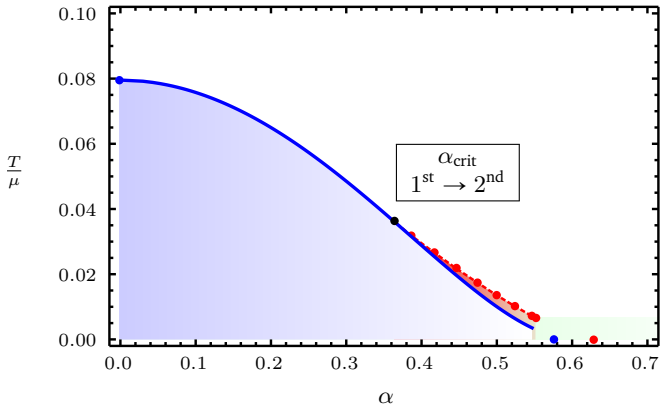

Figure 4.15. Phase structure of the p-wave superconductor theory: In the blue and red region the broken phase is the thermodynamically preferred phase, while in the white region the Reissner-Nordström black brane is the ground state. In the blue region the Reissner-Nordström black brane is unstable and the transition from the white to the blue region is second order. In the red region the Reissner-Nordström black brane is still stable. The transition form the white to the red region is first order. The black dot determines the critical point where the order of the phase transition changes. In the green region we cannot trust our numerics.

- A test on our calculations is provided by the fact that numerically, we reproduce the results known from probe limit calculations where by definition C_{M} and C_{R} are one or two, respectively.
- The region where our minimization algorithm is working safely is approximately given by $\alpha \approx 0.35$. For higher values we use an interpolation function for the curves associated to the non-negative scalar field masses including the zero temperature values obtained analytically.
- At the endpoints where we encounter a quantum critical point with vanishing critical temperature, C_{M} and C_{R} are zero since these points correspond to the critical α stated in Table 4.5. For the negative masses there exists no critical α and the curves are reaching zero only asymptotically.

4.5.4. Diffusion constants in p-wave superconductivity

In this section we discuss the Einstein-Yang-Mills theory including backreaction in asymptotically AdS_5 which give rise to a holographic p-wave superfluid at low temperatures. Redoing exactly the same steps conducted for the s-wave calculation, *i.e.* determining the phase diagram shown in Figure 4.15 from the fluctuation equation close to the phase transition in the AdS-Reissner-Nordström background with

$$f(r) = 1, \qquad \sigma(r) = 1, \tag{4.288}$$

and

$$m(r) = \frac{1}{2} + \frac{1}{3}\alpha\mu^2\left(1 - \frac{1}{r^2}\right), \qquad \phi(r) = \mu\left(1 - \frac{1}{r^2}\right). \tag{4.289}$$

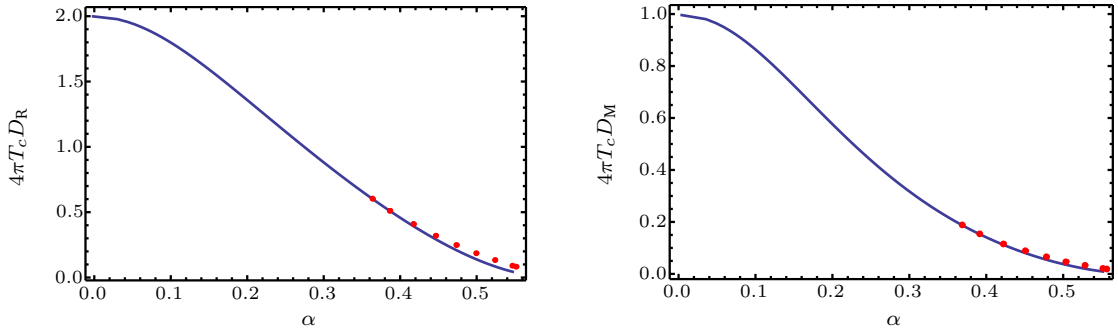

Figure 4.16. $C_R = 4\pi T_c D_R(T_c)$ and $C_M = 4\pi T_c D_M(T_c)$ related to charge diffusion $D_{\rm R}$ and momentum diffusion $D_{\rm M}$ depending on the strength of the backreaction α for the holographic p-wave superfluid with $d = 4$. The blue line corresponds to the constants evaluated at the temperature at which the Reissner-Nordström black brane becomes unstable (see blue line in Figure 4.15). The red dots corresponds to the constants evaluated at the critical temperature at which the superfluid phase is thermodynamically preferred (see red dots in Figure 4.15).

The onset of the instability is controlled by the scalar fluctuation equation given by

$$a_x^{1\prime\prime}(r) + \left(\frac{1}{r} - \frac{2f'(r)}{f(r)} + \frac{N'(r)}{N(r)} + \frac{\sigma'(r)}{\sigma(r)}\right) a_x^{1\prime}(r) + \frac{r^2 f(r)^2(\omega - \phi(r))^2}{N(r)\sigma(r)^2} a_x^1(r) = 0, \tag{4.290}$$

with

$$N(r) = -\frac{2m(r)}{r^2} + \frac{r^2}{L^2}. \tag{4.291}$$

The critical line in the p-wave phase diagram is used to fix the critical value of μ and α and inserted into the diffusion formula for $D_{\rm R}$ (4.279). As far as Homes' law is concerned, we observe very similar dependence of $D(T_c)T_c$ on the backreaction as in the s-wave case.

p-wave phase diagram

Let us now discuss the phase structure of this theory. At temperature below the critical temperature the thermodynamically favored phase is the holographic superfluid. By varying the parameter α, the critical temperature changes. In addition in [219] it was found that the order of the phase transition depends on the ratio of the coupling constants α. For $\alpha \leqslant \alpha_c = 0.365$, the phase transition is second order while for larger values of α the transition becomes first order. The critical temperature decreases as we increase the parameter α. The quantitative dependence of the critical temperature on the parameter α is given in Figure 4.15. The broken phase is thermodynamically preferred in the blue and red region while in the white region the Reissner-Nordström black hole is favored. The Reissner-Nordström black brane is unstable in the blue region and the phase transition from the white to the blue region is second order. In the red region, the Reissner-Nordström black brane is still stable, however the state with non-zero condensate is preferred. The transition from the white to the red region is first order. In the green region we cannot trust our numerics. At zero temperature, the data is obtained as described in [250, 251].

P-wave diffusion constants

We now determine the diffusion constants at the critical temperature. Since the system is still described by a Reissner-Nordström black brane as in the holographic s-wave superfluid and thus the equations of motion for the fluctuations coincide, we can use the same expressions to calculate the diffusion constants for the holographic p-wave superfluid. The only change is the dependence of the critical temperature on the parameter α. The numerical results are shown in Figure 4.16. Comparing the phase diagram of Figure 4.15 and the diffusion constants of Figure 4.16, we see that they are virtually identical. Furthermore, the analytical expression converting the curve of critical values of T/μ into the product $D(T_c)T_c$ is the same for both holographic superconductors. Thus, it is not surprising that we will find answers that have a very large resemblance. Moreover, the same is true for the s-wave superconductors and the comparison between the s-wave and the p-wave superconductor: All curves for $D(T_c)T_c$ are very similar in both cases.

A detailed summary and some possible extension to remedy the problems encountered to uncover Homes' law completely are given in Chapter 6. Suffice it to say, dissipative effects should be coupled to breaking the translational symmetry of holographic duals [33, 34, 37, 38] and a deeper understanding of the emerging AdS_2 spacetime related to the quantum critical point α_c. It has been shown that naïvely adding a lattice might not be enough to understand Homes' law completely [39]. In my view, the key to unravel this mystery lies in the understanding how to distinguish an ideal conductor from a superconductor holographically. Since the Meißner-Ochsenfeld effect is not accessible directly, the IR geometry is not enough to clearly see the effective difference between these two physical systems since both show a depletion of spectral weight for $\omega \ll T$ and a redistribution into a δ-peak or Drude peak at $\omega = 0$.

5
Cold Holographic Matter

In the previous chapter, we employed a so-called bottom-up holographic model starting with a simple bulk action including only a few couplings that capture the essential physical properties of the problem at hand. In return, we do not know the full microscopic field theory but rather an effective low-energy theory. In order to have a faithful one-to-one mapping, a so-called top-down construction allows the precise knowledge of the field theory and a true comparison with weak coupling strength calculations. However, the top-down construction usually involves a large number of bulk fields and coupling arising from a more complicated D_q/D_p-brane setup as well as a more intricate field theory involving possibly unwanted/unnecessary fields. The art of model building demands to identify the correct setup encoding the effects which are crucial to the physical problem. In this chapter we construct an explicit top-down model to understand the nature of ultracold strongly coupled matter. As we have already seen in Chapter 4 there is an intriguing quantum phase transition involving the critical AdS-Reissner-Nordström black brane with an extremal horizon with finite charge but vanishing temperature (*c.f*. Figure 4.10). Thus, we have a system with finite entropy density indicating a large degeneracy of correlated microstates induced by the finite chemical potential. Any small perturbation allows the system to settle in a possibly lower non-degenerate ground state, displaying a instability of the physical system. This instability is intimately connected to the quantum critical point discussed in Section 4.5.1. The emerging AdS_2 spacetime is one of the various potential stable ground state geometries of the extremal AdS-Reissner-Nordström black brane, stabilized by the Breitenlohner-Freedman bound as shown in Figure 4.9. in this case the extremal horizon is replaced by a scalar condensate or "scalar hair". In bottom-up models there exist a plethora of different scaling geometries such as the Lifshitz geometries or AdS_4 Poincaré discussed in [249]. Additionally, the AdS-Reissner-Nordström black hole shows simple perfect quantum fluid behavior, *e.g*. saturating the viscosity over entropy density bound for isotropic fluids $\eta/s = 1/4\pi$ [252] and a sound mode controlled by pure scale invariance, *i.e*. $v^2 = 1/d$ [253]. This is surprising since we would expect a breakdown of the effective hydrodynamic theory in the limit of $T/\mu \to 0$ where the mean free path diverges. An approach to understand the nature of this effective theory in the Wilsonian RG formalism is undertaken in [254]. Moreover, taking the gauge/gravity duality seriously, we may uncover a different state of quantum matter that *does not* belong to the known categories, *i.e*. bosonic superfluid or fermionic non-Fermi liquid. In this chapter we are trying to unravel

some of the mysteries by employing a stability analysis of a top-down holographic model describing compressible matter. Apart from the intricate models involving many non-trivial coupled fields [255–258], we may use a simpler yet more tractable model: probe D_p-branes embedded in a D_3 background. As explained in Section 5.1 fundamental matter may be added by embedding a single D_7-brane in $\text{AdS}_5 \times S^5$, wrapping the $\text{AdS}_5 \times S^3$ directions [140]. The corresponding dual field theory is an $\mathcal{N} = 4$ supersymmetric $SU(N_c)$ Yang-Mills theory coupled to a single fundamental $\mathcal{N} = 2$ hypermultiplet describing flavor fields. In particular we will study the zero-temperature, finite baryon density case with baryon number chemical potential μ associated to the global $U(1)_\text{B}$ flavor symmetry and a mass M for the $\mathcal{N} = 2$ hypermultiplet. This system describe a compressible state of matter for $\mu > M$ which is subject to a quantum critical point at $\mu = M$. This field theory configurations are described by black hole embeddings as shown in Figure 5.1. For $\mu < M$ we are below the mass gap, so we do not find any condensates or finite densities. In this case we find a general anti-brane/brane embedding which can be reduced to simple Minkowski embeddings [259].

This chapter will discussed the aforementioned points in the following order: first in Section 5.1.1, we introduce fundamental flavor matter in AdS/CFT and discuss a specific setup, the D_3/D_7-brane construction yielding an extension to the holographic dictionary. Then, solutions of different D_p-brane embeddings with finite mass, density and temperature are studied in Section 5.1.4. In order to determine the instabilities, we employ a quasi-normal mode analysis of the fluctuations about the background solutions. As a warm-up, we first determine the fluctuations in the trivial zero-density/Minkowski embedding following [260] and finally we will redo the same calculation with a non-trivial zero-temperature, but finite density D_7-brane embedding. The central result of this chapter laid out in Section 5.3 is the stability analysis of the fluctuating modes in this D_3/D_7-brane system background in order to understand the nature of the peculiarities mentioned above, *i.e.* the finite entropy density at zero temperature, the condensate of charged scalars resembling a bosonic coherent state such as a Bose-Einstein condensate or a superfluid and in principle the fermionic sector may exhibit non-trivial inhomogeneous ground states such as chiral density waves. These fluctuating modes correspond to mesonic field theory operators uncharged under the global baryonic $U(1)_\text{B}$ symmetry and hence our analysis is not sensitive to superfluid instabilities. In order to uncover instabilities yielding inhomogeneous ground states we conduct a stability analysis in finite frequencies *and* momenta. All calculations listed below have been performed by myself, independent of the other authors of our publication [2] in order to have a "blind test" concerning the correctness of the mathematical expressions. Furthermore, all numerical computations have been carried out using an independently coded *Mathematica* program, see Mathematica Code D.4 for the core parts of our numerical procedure. According to [261], holographic Fermi surfaces generally exist, so we do not expect fermionic instabilities. Therefore our stability analysis is complete covering all bosonic fluctuations of the D_7-branes.

5.1. AdS/CFT with Fundamental Matter

Overview

- Adding matter fields, transforming in the fundamental representation of $SU(N_c)$, by putting probe branes into a fixed background geometry.
- State of the system is described by the embedding function of the N_f probe brane in a N_C D_3-background geometry.

Table 5.1.
Considering D_3/D_p-brane constructions with finite separations in the common transverse directions yields the following supersymmetry preserving possibilities. The • denotes directions wrapped by the brane, whereas – denotes transverse directions. Note that only for the D_3/D_7-brane setup we find a $3+1$ dimensional field theory. All other D_p-brane embeddings yield lower dimensional defect theories. The ten dimensional directions are labeled by Arabic numbers, where 01234 denotes the AdS_5 and 56789 the S^5-directions, respectively.

	0	1	2	3	4	5	6	7	8	9
N_c $D3$	•	•	•	•	–	–	–	–	–	–
N_f $D7$	•	•	•	•	•	•	•	•	–	–
N_f $D7$	•	•	–	–	•	•	•	•	•	•
N_f $D5$	•	•	•	–	•	•	•	–	–	–
N_f $D5$	•	–	–	–	•	•	•	•	•	–
N_f $D3$	•	•	–	–	•	•	–	–	–	–

- Fluctuations of probe branes correspond to mesonic operators in the dual field theory.

In this section we will give a short overview of top-down construction with flavor degrees of freedom. Additionally, we will work out the full background geometry, the full embedded D_p-brane action, and the embedding functions with finite baryon density and temperature. The explicit calculations are deferred to Section 5.1.4 in order to focus on the conceptual ideas and the symmetries of the dual field theory.

5.1.1. Adding fundamental flavor degrees of freedom to AdS/CFT

The matter fields in the $\mathcal{N}=4$ vector multiplet (*c.f.* Table 3.2) transform in the adjoint representation of the gauge group $SU(N_c)$. On the gravity side, the adjoint representation corresponds to the open strings connecting N_c coincident D_3-branes as shown in Figure 3.9. In order to generate a fundamental representation in N_c we need a setup where strings stretch between the stack of coincident D_3-branes and additional separated D_p-branes. Preserving the R-symmetry of supersymmetric field theories, we need to take D_p-brane constructions such that the there are common directions in the ten-dimensional spacetime transverse to both the D_3 and the D_p-branes, which leaves us with three possibilities: $p=3$, $p=5$ and $p=7$. In Table 5.1 the possible supersymmetry preserving D_3/D_p-brane constructions are listed. Note that for D_5-branes, only defect theories in the $3+1$ dimensional spacetime are possible. Let us denote the number of additional D_p-branes by N_f where the subscript f reminds us of the number of flavors analogous to QCD with effective flavor symmetry. In the following we will call the fields transforming under the fundamental representation of the gauge group $SU(N_c)$ quarks. If the N_f D_p-branes are separated from the stack of D_3-branes, the quarks acquires a finite mass given by $m_q = {}^{L}/_{2\pi\alpha'}$.[1] Furthermore, the strings connecting N_f coincident D_p-branes transform in the adjoint representation of the quark global $U(N_f)$ flavor symmetry and thus can be identified with mesonic

[1] In this chapter we will denote the distance between the D_p-branes and the stack of D_3-branes by L, whereas R will denote the AdS_5 or S^5 radius, respectively.

degrees of freedom. More specifically, the fluctuations of the D_p-brane about the background geometry will be dual to mesons in the gauge field theory.

Let us construct specifically the D_3/D_7-brane version of the AdS/CFT correspondence in the probe limit $N_f \ll N_c$ by retracing the steps taken in Section 3.2.2. The probe limit ensures that the quantum fluctuations of the flavor fields are suppressed and thus there is no running of the coupling. In particular at weak 't Hooft coupling λ the probe limit can be understood in a perturbative diagrammatic expansion where all flavor field loop diagrams are discarded. On the gravity side, the probe limit allows for a fixed background metric generated solely by the stack of N_c D_3-branes in the near horizon limit (3.51),

$$\mathrm{d}s^2 = G_{AB}\,\mathrm{d}x^A\,\mathrm{d}x^B = \frac{r^2}{R^2}\left(-\,\mathrm{d}t^2 + \mathrm{d}\mathbf{x}^2\right) + \frac{R^2}{r^2}\left(\mathrm{d}r^2 + r^2\,\mathrm{d}\Omega_5{}^2\right). \tag{5.1}$$

The probe D_7-branes wraps the AdS_5 part and the S^3 of the S^5, so the common transverse directions are the x^8 and x^9 directions. The original $SO(6)$ symmetry arising from the transverse directions of the D_3-brane is broken into $SO(4) \times SO(2)$. As mentioned above the quark mass m_q is given by the string tension times the string length L *i.e.* the distance between the D_3- and D_7-branes. In principle, the mass arises from a linear combination of x^8 and x^9 with a relative angle in the 89-plane. Thus we conclude there is a $U(1)_{\mathrm{R}} \cong SO(2)$ symmetry associated with rotations in the 89-plane leaving the quark mass invariant. The $SO(4)$ of the 4567 directions transverse only to the D_3-brane gives rise to a $SU(2)_{\text{scalar}} \times SU(2)_{\mathrm{R}}$.

All these symmetries are related to the following field theory setup: in addition to the vector multiplet of the $\mathcal{N} = 4$ supersymmetric $SU(N_c)$ gauge theory we have N_f hypermultiplets transforming in the fundamental representation of the gauge group $U(N_f)$ with baryon number one under the baryonic $U(1)_{\mathrm{B}} \subset U(N_f)$ subgroup. The content of the $\mathcal{N} = 4$ vector multiplet can be decomposed into an $\mathcal{N} = 2$ hypermultiplet and a $\mathcal{N} = 2$ vector multiplet as listed in Table 3.2. Technically, the four scalars related to the four transverse directions to the D_3, *i.e.* 4567 are combined into the two scalars, $\Phi^1 \sim x^4 + \mathrm{i}x^5$ and $\Phi^2 \sim x^6 + \mathrm{i}x^7$ of the $\mathcal{N} = 2$ hypermultiplet, whereas the directions transverse to the D_7-brane 89 are combined to the scalar of the $\mathcal{N} = 2$ vector multiplet, $\Phi^3 \sim x^8 + \mathrm{i}x^9$. Therefore the $SU(4)_{\mathrm{R}} \cong SO(6)_{\mathrm{R}}$ is broken to a $SO(4) \times U(1)_{\mathrm{R}} \cong SU(2)_{\text{scalar}} \times SU(2)_{\mathrm{R}} \times U(1)_{\mathrm{R}}$, where the $SU(2)_{\mathrm{R}} \times U(1)_{\mathrm{R}}$ part acts as $\mathcal{N} = 2$ R-symmetry group and the $SU(2)_{\text{scalar}}$ rotates the scalars Φ^1, Φ^2 of the $\mathcal{N} = 2$ hypermultiplet. For massive flavor fields the chiral $U(1)_{\mathrm{R}}$ is explicitly broken analogous to the chiral symmetry breaking in QCD. Note also that the finite quark mass m_q breaks the conformal symmetry of the four dimensional field theory $SO(2,4)$ to the Lorentz group $SO(1,3)$. The four fermions of the $\mathcal{N} = 4$ vector multiplet are distributed equally among the $\mathcal{N} = 2$ hyper- and vector multiplet. The fermions of the N_f $\mathcal{N} = 2$ hypermultiplets are quarks denoted by ψ while the supersymmetric partners, *i.e.* the squarks, are complex scalars denoted by q and $\tilde{q}$. The $\mathcal{N} = 4$ originates from the strings connecting the stack of D_3-branes, dubbed $3-3$ strings, whereas the $\mathcal{N} = 2$ hypermultiplets are induced by the strings stretching between the D_3/D_7 branes, the $3-7$ or $7-3$ strings.[2] Taking the near horizon/large N_c limit, the $7-7$ strings connecting D_7-branes decouple from the other $3-3$ and $3-7$ strings, since the eight dimensional 't Hooft coupling of the D_7-branes, using (3.49), is given by

$$\frac{\lambda_{D_p}}{\lambda_{D_3}} = (2\pi)^4 \frac{N_c}{N_f}\alpha'^{(p-3)/2} \qquad \Rightarrow \qquad \frac{\lambda_{D_7}}{\lambda_{D_3}} = (2\pi)^4 \frac{N_c}{N_f}\alpha'^2 \xrightarrow[\ell_s \to 0]{\alpha' \to 0} 0 \tag{5.2}$$

[2] We define the $3-7$ strings to transform in the fundamental representation, while the $7-3$ strings transform in the anti-fundamental representation of $SU(N_c)$

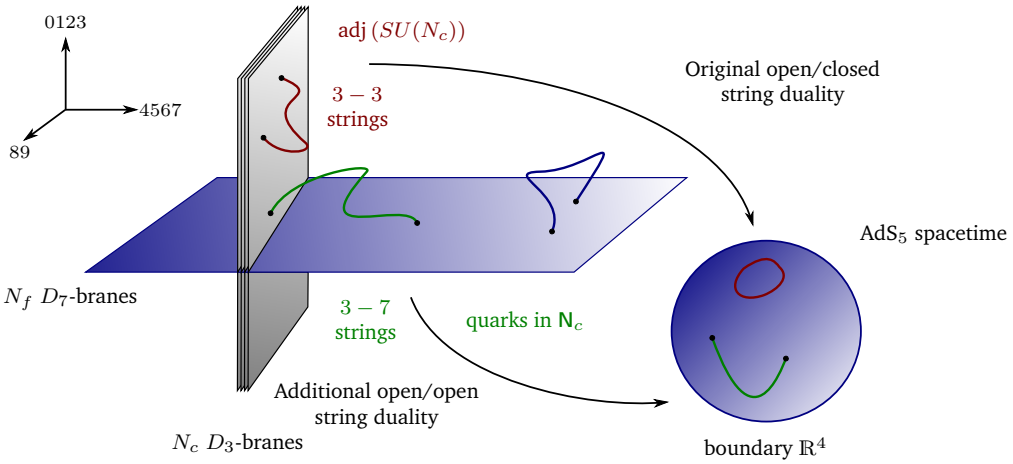

Figure 5.1. Adding fundamental matter to the original AdS$_5$/CFT$_4$ correspondence amounts to adding $N_f \ll N_c$ D_p-branes to the stack of N_c D_3-branes. Specifically, we show the case for $p = 7$, where the D_7-brane extends in the 0123456 directions of the ten-dimensional AdS$_5 \times S^5$ spacetime, wrapping the S^3 of the S^5 directions. The $3-3$ strings describe the adjoint matter in the original AdS/CFT correspondence. Additionally, the $3-7$ strings stretching from the D_3 to the D_7 brane are in the fundamental representation of the $SU(N_c)$ gauge group $\mathbf{N}_c$ and hence called quarks. For a finite distance L of the branes, the quarks acquire a mass $m_q \sim L$. The $7-7$ strings decouple in the low-energy limit, whereas the $3-3$ strings are mapped to closed strings in the sense of the open/closed viewpoint of D-branes. The $3-7$ open strings are mapped to open strings on the D_7 brane which asymptotically wraps the AdS$_5 \times S^3$. Note that the S^3 and S^5 are not shown in the picture. Fluctuations of the D_7 brane about the background embedding describe mesonic excitations which corresponds to open string excitations on the brane.

for λ_{D_3} and N_f fixed. Thus, we are left with an effective four dimensional low-energy theory with a global $U(N_f)$ gauge group due to $N_f \ll N_c$. Pictorially, the decoupling limit is shown in Figure 5.1. Typically, one deals with the simplest probe brane embedding, *i.e.* $N_f = 1$ where the precise action of the D_7 brane is known to be the DBI action (3.40) supplemented with the Chern-Simons term (3.42). So far, the full generalization of the DBI action to non-Abelian gauge groups with $N_f > 1$ is not understood completely. The same derivation can be conducted with all other D_3/D_p-brane constructions listed in Table 5.1. For example, in the D_3/D_5-brane setup we can retrace all steps above yielding a $2+1$ dimensional field theory with conformal symmetry $SO(2,3)$ for $m_q = 0$ and the Lorentz symmetry $SO(1,2)$ in the case of $m_q \neq 0$. The $\mathcal{N} = 2$ R-symmetry follows again from the transverse directions to the D_3-brane, *i.e.* $SO(3)_{456} \times SO(3)_{678} \cong SU(2)_{\mathrm{V}} \times SU(2)_{\mathrm{H}}$ where the subscripts stand for vector and hyper, respectively.

5.1.2. Ten-dimensional background fields

First, we need to determine the ten-dimensional background fields, *i.e.* the AdS$_5 \times S^5$ metric in r and u coordinates, including zero- and finite temperature geometries. Furthermore, the type IIB supergravity in the AdS$_5 \times S^5$ background includes N_c units of the Ramond-Ramond (RR) five form flux on the S^5. Thus we need to determine the corresponding $C_{(4)}$ form, such that

$F_{(5)} = \mathrm{d}C_{(4)}$, whereas the other RR fields $C_{(0)}$ and $C_{(2)}$ can be set to zero consistently.

Background metric induced by D_3-branes

The D_3 background field is described by an $\mathrm{AdS}_5 \times S^5$-Schwarzschild metric in the near horizon approximation

$$\begin{aligned}\mathrm{d}s^2 &= H^{-\frac{1}{2}}(r)\,\mathrm{d}^2 s\left(\mathbb{E}^{(1,3)}\right) + H^{-\frac{1}{2}}(r)\,\mathrm{d}\mathbf{Y}\cdot\mathrm{d}\mathbf{Y} \\ &= H^{-\frac{1}{2}}(r)\eta_{\mu\nu}\,\mathrm{d}x^\mu\,\mathrm{d}x^\nu + H^{-\frac{1}{2}}(r)\delta_{ab}\,\mathrm{d}Y^a\,\mathrm{d}Y^b,\end{aligned} \tag{5.3}$$

with[3]

$$H(r) = 1 + \frac{R^4}{r^4} \approx \frac{R^4}{r^4}, \qquad \text{and} \qquad r^2 = \sum_{a=1}^{6}(Y^a)^2 = |\mathbf{Y}|^2, \tag{5.4}$$

where R corresponds to the AdS_5 curvature[4] and r denotes the transverse distance to the D_3-brane. The Minkowski metric is $\eta_{\mu\nu} = \mathrm{diag}(-1,1,1,1)$. Inserting $H(r)$ into the metric (5.3) and introducing six dimensional spherical coordinates we find

$$\begin{aligned}\mathrm{d}s^2 &= \frac{r^2}{R^2}\eta_{\mu\nu}\,\mathrm{d}x^\mu\,\mathrm{d}x^\nu + \frac{R^2}{r^2}\left(\mathrm{d}r^2 + r^2\,\mathrm{d}\Omega_5^2\right) \\ &= \underbrace{\frac{r^2}{R^2}\eta_{\mu\nu}\,\mathrm{d}x^\mu\,\mathrm{d}x^\nu + \frac{R^2}{r^2}\,\mathrm{d}r^2}_{\mathrm{AdS}_5\text{-Part}} \underbrace{+R^2\,\mathrm{d}\Omega_5^2}_{S^5\text{-Part}},\end{aligned} \tag{5.5}$$

The first part of (5.5) can be rewritten as a true AdS_5 metric with the help of the coordinate transformation

$$u = \frac{R^2}{r} \qquad \longrightarrow \qquad r = \frac{R^2}{u}, \tag{5.6}$$

$$\mathrm{d}r = \frac{\partial\left(R^2/u\right)}{\partial u}\,\mathrm{d}u = -\frac{R^2}{u^2}\,\mathrm{d}u\,. \tag{5.7}$$

Reinserting the coordinate transformation (5.6) into the metric (5.5) leads to[5]

$$\begin{aligned}\mathrm{d}s^2 &= \left(\frac{R^2}{u}\right)^2\frac{1}{R^2}\eta_{\mu\nu}\,\mathrm{d}x^\mu\,\mathrm{d}x^\nu + R^2\left(\frac{u}{R^2}\right)^2\left(-\frac{R^2}{u^2}\right)^2\mathrm{d}u^2 + R^2\,\mathrm{d}\Omega_5^2 \\ &= \frac{R^2}{u^2}\left(\mathrm{d}u^2 + \eta_{\mu\nu}\,\mathrm{d}x^\mu\,\mathrm{d}x^\nu\right) + R^2\,\mathrm{d}\Omega_5^2,\end{aligned} \tag{5.8}$$

[3] The index convention in this section is as follows: D_3-brane/field theory directions are labeled by Greek indices $\mu,\nu,\ldots$, the ten-dimensional background coordinates by capital Latin indices $A,B,\ldots$, the coordinates on the S^5 by lower case Latin indices $i,j,\ldots$ and last, but not least the D_p-brane world volume indices are denoted by lower case Latin letters from the beginning of the alphabet, *i.e.* $a,b,\ldots$.

[4] In fact the curvature scalar of AdS_5 is given by $-20/R^2$

[5] Since the AdS_5-part scales with the same "radius" as the S^5-part we find that the curvature scalar of S^5 is $20/R^2$ and so the total curvature of $\mathrm{AdS}_5 \times S^5$ vanishes.

where **x** denotes the spatial part of the D_3-brane, *i.e.* x, y, z. In the same way we can derive the full $\mathrm{AdS}_5 \times S^5$-Schwarzschild background metric

$$\mathrm{d}s^2 = \frac{R^2}{u^2}\left(-f(u)\,\mathrm{d}t^2 + \mathrm{d}\mathbf{x}^2 + \frac{\mathrm{d}u^2}{f(u)}\right) + R^2\,\mathrm{d}\Omega_5^2, \tag{5.9}$$

with

$$f(u) = 1 - \left(\frac{u}{u_\mathrm{H}}\right)^4. \tag{5.10}$$

where u_H denotes the horizon of the Schwarzschild black hole defined by $f(u_h) = 0$ and temperature $T = {}^1\!/_{(\pi u_\mathrm{H})}$. The AdS_5-Schwarzschild metric can be written as

$$(G_{AB})_{\mathrm{AdS}_5} = \begin{pmatrix} -\frac{R^2}{u^2}\left(1-\frac{u^4}{u_\mathrm{H}^4}\right) & 0 & 0 & 0 & 0 \\ 0 & \frac{R^2}{u^2} & 0 & 0 & 0 \\ 0 & 0 & \frac{R^2}{u^2} & 0 & 0 \\ 0 & 0 & 0 & \frac{R^2}{u^2} & 0 \\ 0 & 0 & 0 & 0 & \frac{R^2}{u^2\left(1-\frac{u^4}{u_\mathrm{H}^4}\right)} \end{pmatrix}. \tag{5.11}$$

The S^5 is parametrized in the following way

$$\begin{aligned} \mathrm{d}\Omega_5^2 &= \mathrm{d}\theta^2 + \sin^2\theta\,\mathrm{d}\phi^2 + \cos^2\theta\,\mathrm{d}\Omega_3^2, \\ \mathrm{d}\Omega_3^2 &= \mathrm{d}\psi^2 + \sin^2\psi\,\mathrm{d}\Omega_2^2, \\ \mathrm{d}\Omega_2^2 &= \mathrm{d}\vartheta^2 + \sin^2\vartheta\,\mathrm{d}\varphi^2, \end{aligned} \tag{5.12}$$

yielding the S^5 metric

$$(G_{AB})_{S^5} = \begin{pmatrix} R^2 & 0 & 0 & 0 & 0 \\ 0 & R^2\sin^2\theta & 0 & 0 & 0 \\ 0 & 0 & R^2\cos^2\theta & 0 & 0 \\ 0 & 0 & 0 & R^2\sin^2\psi\cos^2\theta & 0 \\ 0 & 0 & 0 & 0 & R^2\sin^2\psi\sin^2\vartheta\cos^2\theta \end{pmatrix}. \tag{5.13}$$

The complete $\mathrm{AdS}_5 \times S^5$ is the direct sum of (5.11) and (5.13), *i.e.* $(g_{MN})_{\mathrm{AdS}_5} \oplus (g_{mn})_{S^5}$.

Temperature

The pure $\mathrm{AdS}_5 \times S^5$ does not have any temperature since there is no scale to associate a period for wrapping up the time direction on a circle. So for zero temperature calculations it is convenient to choose the r coordinates which ranges from the deep AdS_5 interior at $r = 0$ up to the boundary at $r \to \infty$. on the other hand for finite temperature calculations, it is more useful to introduce the u coordinates as done in (5.6) where the horizon of the Schwarzschild black hole is set at u_H and the boundary is located at $u = 0$. The Hawking temperature can be determined from the

surface gravity, *c.f*. Section 3.1.1, employing the Unruh effect or alternatively from the condition to eliminate the conical singularity in the imaginary time circle by choosing an appropriate period

$$T = \frac{1}{\pi u_{\mathrm{H}}}, \qquad \Leftrightarrow \qquad u_{\mathrm{H}} = \frac{1}{\pi T}. \tag{5.14}$$

The scale u_{H} will be used to rewrite the equations of motion in dimensionless quantities by a rescaling of all dimensionful quantities with appropriate factors of T.

Self-dual five form $F_{(5)}$

In type IIB supergravity the self-dual five form is defined as

$$F_{(5)} = \mathrm{d}C_{(4)} + \underbrace{H_{(3)}}_{=0} \wedge \underbrace{C_{(2)}}_{=0} = \mathrm{d}C_{(4)}, \tag{5.15}$$

where in our case it can be purely written as the exterior derivative of the $C_{(4)}$-form

$$C_{(4)} = H^{-1}\,\mathrm{d}x^0 \wedge \mathrm{d}x^1 \wedge \mathrm{d}x^2 \wedge \mathrm{d}x^3\,. \tag{5.16}$$

Therefore we end up with total antisymmetric differential form of maximal degree with respect to the AdS_5 coordinates and hence is proportional to the unique volume form

$$\Omega \equiv \mathrm{vol}_n = \sqrt{|g|}\,\mathrm{d}x^0 \wedge \cdots \wedge \mathrm{d}x^n = \star\mathbb{1}, \tag{5.17}$$

with the proportionality factor $4/L$, where L denotes the radius of the AdS_5 space, *i.e*.

$$\begin{aligned} F_{(5)} &= \mathrm{d}H^{-1} \wedge \mathrm{d}x^0 \wedge \mathrm{d}x^1 \wedge \mathrm{d}x^2 \wedge \mathrm{d}x^3 \\ &= \frac{4}{L}\sqrt{|\det(g_{\mathrm{AdS}_5})|}\,\mathrm{d}x^0 \wedge \mathrm{d}x^1 \wedge \mathrm{d}x^2 \wedge \mathrm{d}x^3 \wedge \mathrm{d}x^4 \\ &= \frac{4}{L}\,\mathrm{vol}\,(\mathrm{AdS}_5)\,. \end{aligned} \tag{5.18}$$

We will explicitly calculate the self-dual five form when needed in coordinate representation below. The self-duality condition has to be imposed by hand, so we need to calculate the Hodge dual and add it to (5.18) to obtain a self-dual form. For a five form in a ten-dimensional space, the Hodge dual is given according to the definition[6]

$$\star F_{(p)} = \frac{1}{p!(n-p)!}\sqrt{|\det g|}\,\epsilon_{a_1 a_2 \ldots a_{n-p} b_1 b_2 \ldots b_p} F^{b_1 b_2 \ldots b_p}\,\mathrm{d}x^{a_1} \wedge \mathrm{d}x^{a_2} \wedge \cdots \wedge \mathrm{d}x^{a_{n-p}}, \tag{5.19}$$

[6] This is a definition commonly found in string theory texts *e.g*. in [109]. An alternative definitions often used by general relativists is

$$\bar{\star} F_{(p)} = \frac{1}{p!(n-p)!}\sqrt{|\det g|}\,\epsilon_{b_1 b_2 \ldots b_p a_1 a_2 \ldots a_{n-p}} F^{b_1 b_2 \ldots b_p}\,\mathrm{d}x^{a_1} \wedge \mathrm{d}x^{a_2} \wedge \cdots \wedge \mathrm{d}x^{a_{n-p}},$$

where the ordering of the set of contracted indices with the set of the free indices is reversed, see [70]. Thus the two different definitions of the Hodge dual are related by

$$\star = (-1)^{p(n-p)}\bar{\star}.$$

Except from the inner product of two forms (where also the order of the arguments needs to be reversed) all formulae should be independent of the chosen definition.

which is a five form as well, since $(n-p) = (10-5) = 5$. The additional determinant in the definition (5.19) is needed because the total antisymmetric epsilon symbol $\epsilon_{a_1a_2\ldots a_{n-p}b_1b_2\ldots b_p}$ should be replaced by an odd tensor density[7] of weight -1, *i.e.* it transforms with an additional factor of $|\det g|^{-1/2}$ under general coordinate transformations. Therefore we find

$$\begin{aligned}\star F_{(5)} &= \frac{4}{L}\sqrt{|\det(g_{\mathsf{AdS}_5})|}\star\left(\mathrm{d}x^0\wedge\mathrm{d}x^1\wedge\mathrm{d}x^2\wedge\mathrm{d}x^3\wedge\mathrm{d}x^4\right)\\ &= \frac{1}{5!5!}\sqrt{|\det g|}\epsilon_{b_1b_2b_3b_4b_5}{}^{a_1a_2a_3a_4a_5}F_{a_1a_2a_3a_4a_5}\,\mathrm{d}\Theta^{b_1}\wedge\mathrm{d}\Theta^{b_2}\wedge\mathrm{d}\Theta^{b_3}\wedge\mathrm{d}\Theta^{b_4}\wedge\mathrm{d}\Theta^{b_5},\end{aligned} \tag{5.20}$$

where the Θ^i denote the angles of S^5. Note that the first five indices of the epsilon tensor density are upper indices because the components of the original five form $F_{(5)}$ are covariant. The five angles of the S^5 are denoted by Θ^i. Since $F_{(5)}$ is proportional to the volume form of AdS_5 only one component is non zero, namely the 01234 component. Using the fact that $\epsilon^{a_1a_2a_3a_4a_5}{}_{b_1b_2b_3b_4b_5}$ is totally antisymmetric $\star F_{(5)}$ must be proportional to the volume form of S^5 and therefore the only non vanishing component remaining after summing over a_i and b_i is

$$\begin{aligned}\star F_{(5)} &= \frac{4}{L}\sqrt{|\det(g_{\mathsf{AdS}_5})|}\sqrt{|\det g|}\epsilon^{01234}{}_{56789}\,\mathrm{d}\Theta^5\wedge\mathrm{d}\Theta^6\wedge\mathrm{d}\Theta^7\wedge\mathrm{d}\Theta^8\wedge\mathrm{d}\Theta^9\\ &= \frac{4}{L}\sqrt{|\det(g_{\mathsf{AdS}_5})|}\sqrt{|\det(g_{\mathsf{AdS}_5})|}\sqrt{|\det(g_{S^5})|}g^{0n}g^{1p}g^{2q}g^{3r}g^{4t}\epsilon_{npqrt56789}\\ &\quad\cdot\mathrm{d}\Theta^5\wedge\mathrm{d}\Theta^6\wedge\mathrm{d}\Theta^7\wedge\mathrm{d}\Theta^8\wedge\mathrm{d}\Theta^9\,.\end{aligned} \tag{5.21}$$

Note that $\det g = \det(g_{\mathsf{AdS}_5}\oplus g_{S^5}) = \det g_{\mathsf{AdS}_5}\det g_{S^5}$. The determinant of a bilinear object, and its inverse, such as the metric tensor can be written with the help of the epsilon symbol as

$$\det g = \epsilon^{npqrt}g_{0n}g_{1p}g_{2q}g_{3r}g_{4t},\qquad\qquad \det g^{-1} = \epsilon_{npqrt}g^{0n}g^{1p}g^{2q}g^{3r}g^{4t}, \tag{5.22}$$

This can be derived from the definition of the determinant of a $n\times n$ matrix written in terms of epsilon symbols

$$\det A = \frac{1}{n!}\epsilon_{i_1\ldots i_n}\epsilon_{j_1\ldots j_n}a_{i_1j_1}\cdots a_{i_nj_n}. \tag{5.23}$$

For the metric, we have

$$\epsilon^{abcde}\det g = \epsilon^{npqrt}g_{an}g_{bp}g_{cq}g_{dr}g_{et}\qquad\Leftrightarrow\qquad \det g = \frac{1}{5!}\epsilon^{abcde}\epsilon^{npqrt}g_{an}g_{bp}g_{cq}g_{dr}g_{et}. \tag{5.24}$$

[7] The epsilon symbol ϵ gives rise to an (odd) tensor density defined as $\varepsilon_{a_1\ldots a_n} = \sqrt{|g|}\epsilon_{a_1\ldots a_n}$ and $\varepsilon^{a_1\ldots a_n} = {}^1\!/\!\sqrt{|g|}\epsilon^{a_1\ldots a_n}$, such that ε behaves as a true tensor, *i.e.* $\varepsilon^{a_1\ldots a_n} = g^{a_1b_1}\cdots g^{a_nb_n}\varepsilon_{b1\ldots b_n}$. Alternatively, we can choose a different convention for the epsilon symbol, which manifestly shows the odd tensor density character

$$\varepsilon^{012\ldots} = 1\qquad\Leftrightarrow\qquad \varepsilon_{012\ldots} = \operatorname{sign} g\,|g|\,.$$

In general an even tensor density of weight w is defined as

$$\mathfrak{E}_{a_1\ldots a_n} = \left|\det\left(\frac{\partial x'^{b_1}}{\partial x^{a_1}}\cdots\frac{\partial x'^{b_n}}{\partial x^{a_n}}\right)\right|^w\mathfrak{E}_{b_1\ldots b_n},$$

whereas an odd tensor density depends on the sign of the determinant of the local transformation

$$\mathfrak{O}_{a_1\ldots a_n} = \operatorname{sign}\left[\det\left(\frac{\partial x'^{b_1}}{\partial x^{a_1}}\cdots\frac{\partial x'^{b_n}}{\partial x^{a_n}}\right)\right]\left|\det\left(\frac{\partial x'^{b_1}}{\partial x^{a_1}}\cdots\frac{\partial x'^{b_n}}{\partial x^{a_n}}\right)\right|^w\mathfrak{O}_{b_1\ldots b_n}.$$

The determinant of the metric g is not an invariant since it transforms under general coordinate transformations

$$\begin{aligned}\det g &= \frac{1}{n!}\epsilon^{a_1\dots a_n}\epsilon^{b_1\dots b_n} g_{a_1 b_1}\cdots g_{a_n b_n}\\ &= \frac{1}{n!}\epsilon^{a_1\dots a_n}\epsilon^{b_1\dots b_n}\frac{\partial x'^{p_1}}{\partial x^{a_1}}\cdots\frac{\partial x'^{p_n}}{\partial x^{a_n}}\frac{\partial x'^{q_1}}{\partial x^{b_1}}\cdots\frac{\partial x'^{q_n}}{\partial x^{b_n}}\\ &= \det\left(g'\left[\frac{\partial x'^{p}}{\partial x^{a}}\right]\left[\frac{\partial x'^{q}}{\partial x^{b}}\right]\right) = \det g' \det\left(\left[\frac{\partial x'}{\partial x}\right]^2\right).\end{aligned} \tag{5.25}$$

This result is also consistent with the above statement that ε is an odd tensor density. Using (5.22) leads to the simplification

$$\begin{aligned}\star F_{(5)} &= \frac{4}{L}\left|\det g_{\mathsf{AdS}_5}\right|\sqrt{\left|\det(g_{S^5})\right|}\det g_{\mathsf{AdS}_5}^{-1}\,\mathrm{d}\Theta^5\wedge\mathrm{d}\Theta^6\wedge\mathrm{d}\Theta^7\wedge\mathrm{d}\Theta^8\wedge\mathrm{d}\Theta^9\\ &= \frac{4}{L}\underbrace{\frac{\left|\det g_{\mathsf{AdS}_5}\right|}{\det g_{\mathsf{AdS}_5}}}_{=-1}\underbrace{\sqrt{\left|\det(g_{S^5})\right|}}_{L^5\sqrt{\widetilde{g}_{S^5}}}\mathrm{d}\Theta^5\wedge\mathrm{d}\Theta^6\wedge\mathrm{d}\Theta^7\wedge\mathrm{d}\Theta^8\wedge\mathrm{d}\Theta^9\\ &= -4L^4\,\mathrm{vol}\left(S^5\right),\end{aligned} \tag{5.26}$$

where $\widetilde{g}_{S^5}$ denotes the round metric[8] of S^5. The Hodge dual of $F_{(5)}$ is proportional to the volume form of S^5. The final result for the self-dual five form for $\mathsf{AdS}_5\times S^5$ is

$$F_{(5)} = \frac{4}{L}\,\mathrm{vol}\left(\mathsf{AdS}_5\right) - 4L^4\,\mathrm{vol}\left(S^5\right) = \frac{4}{L}\left(\mathrm{vol}\left(\mathsf{AdS}_5\right) - L^5\,\mathrm{vol}\left(S^5\right)\right). \tag{5.27}$$

Note that the particular prefactor $4/L$ may differ in other coordinate representations.

Self-Dual Five Form in $\mathsf{AdS}_5\times S^5$ and $\mathsf{AdS}_5\times S^5$-Schwarzschild Coordinates

The expressions for the five form $F_{(5)}$ (5.18) and its dual $\star F_{(5)}$ (5.18) are coordinate independent. In particular if we use the determinant of the AdS_5-part of the metric (5.5) we find

$$\det g_{\mathsf{AdS}_5} = -\left(\frac{r^2}{L^2}\right)^4\left(\frac{L^2}{r^2}\right) = -\frac{r^6}{L^6} \qquad\longrightarrow\qquad \sqrt{\left|\det(g_{\mathsf{AdS}_5})\right|} = \frac{r^3}{L^3}, \tag{5.28}$$

and hence the volume form of the AdS_5 space given by

$$\mathrm{vol}\left(\mathsf{AdS}_5\right)_r = \frac{r^3}{L^3}\,\mathrm{d}x^0\wedge\mathrm{d}x^1\wedge\mathrm{d}x^2\wedge\mathrm{d}x^3\wedge\mathrm{d}r\,. \tag{5.29}$$

Compared with an explicit calculation of the coordinate representation of the five form $F_{(5)}$ starting from its definition

$$F_{(5)}(r) = \mathrm{d}C_{(4)} = \mathrm{d}\left(H(r)^{-1}\,\mathrm{d}x^0\wedge\mathrm{d}x^1\wedge\mathrm{d}x^2\wedge\mathrm{d}x^3\right), \tag{5.30}$$

where

$$H(r)^{-1} = \frac{r^4}{L^4} \qquad\longrightarrow\qquad \mathrm{d}H(r)^{-1} = 4\frac{r^3}{L^4}\,\mathrm{d}r\,. \tag{5.31}$$

[8] The round metric of a sphere is defined without the overall radial factor, in this case L^2.

Inserting $H(r)^{-1}$ into $F_{(5)} = \mathrm{d}C_{(4)}$ gives rise to

$$\begin{aligned} F_{(5)}(r) &= \mathrm{d}H(r)^{-1} \wedge \mathrm{d}x^0 \wedge \mathrm{d}x^1 \wedge \mathrm{d}x^2 \wedge \mathrm{d}x^3 \\ &= 4\frac{r^3}{L^4}\,\mathrm{d}r \wedge \mathrm{d}x^0 \wedge \mathrm{d}x^1 \wedge \mathrm{d}x^2 \wedge \mathrm{d}x^3 \\ &= 4\frac{r^3}{L^4}(-1)^4\,\mathrm{d}x^0 \wedge \mathrm{d}x^1 \wedge \mathrm{d}x^2 \wedge \mathrm{d}x^3 \wedge \mathrm{d}r, \end{aligned} \tag{5.32}$$

which does agree with the coordinate independent formulation. The corresponding Hodge dual is given by

$$\star\, F_{(5)}(r) = -4L^4\,\mathrm{vol}\left(S^5\right)_r . \tag{5.33}$$

The complete self-dual five form thus reads

$$\begin{aligned} F_{(5)}(r) &= F_{\mathrm{AdS}_5}(r) + F_{S^5}(r) \\ &= \frac{4}{L}\left(\mathrm{vol}\left(\mathrm{AdS}_5\right)_r - L^5\,\mathrm{vol}\left(S^5\right)_r\right) \\ &= \frac{4r^3}{L^4}\,\mathrm{d}x^0 \wedge \mathrm{d}x^1 \wedge \mathrm{d}x^2 \wedge \mathrm{d}x^3 \wedge \mathrm{d}r \\ &\quad - \left(4L^4\cos^3\theta\sin\theta\sin^2\psi\sin\vartheta\right)\mathrm{d}\theta \wedge \mathrm{d}\phi \wedge \mathrm{d}\psi \wedge \mathrm{d}\vartheta \wedge \mathrm{d}\varphi . \end{aligned} \tag{5.34}$$

In the AdS_5-Schwarzschild metric case (5.11) we see that we end up with the same expression (up to an overall minus sign) for $F_{(5)}$ as in the pure AdS_5 coordinates. As mentioned below (5.27) the proportionality factor may still depend on the explicit coordinate representation. The determinant is given by

$$\det g_{\mathrm{AdS}_5} = -\left(\frac{L^2}{u^2}f(u)\right)\left(\frac{L^2}{u^2}\right)^3\left(\frac{L^2}{u^2 f(u)}\right) = -\frac{L^{10}}{u^{10}}, \tag{5.35}$$

Applying the coordinate transformation (5.6), namely $u = {}^{L^2}\!/_r$, we find

$$H(u)^{-1} = \frac{L^4}{u^4} \quad\longrightarrow\quad F_{(5)}(u) = -\frac{4L^4}{u^5}\,\mathrm{d}x^0 \wedge \mathrm{d}x^1 \wedge \mathrm{d}x^2 \wedge \mathrm{d}x^3 \wedge \mathrm{d}u = -\frac{4}{L}\,\mathrm{vol}\left(\mathrm{AdS}_5\right)_u . \tag{5.36}$$

and for the corresponding Hodge dual

$$\star\, F_{(5)}(u) = 4L^4\,\mathrm{vol}\left(S^5\right)_u , \tag{5.37}$$

accordingly. So in the $\mathrm{AdS}_5 \times S^5$-Schwarzschild metric (5.11) and (5.13) the self-dual five form reads

$$\begin{aligned} F_{(5)}(u) &= F_{\mathrm{AdS}_5}(u) + F_{S^5}(u) \\ &= -\frac{4}{L}\left(\mathrm{vol}\left(\mathrm{AdS}_5\right)_u - L^5\,\mathrm{vol}\left(S^5\right)_u\right) \\ &= -\frac{4L^4}{u^5}\,\mathrm{d}x^0 \wedge \mathrm{d}x^1 \wedge \mathrm{d}x^2 \wedge \mathrm{d}x^3 \wedge \mathrm{d}u \\ &\quad + \left(4L^4\cos^3\theta\sin\theta\sin^2\psi\sin\vartheta\right)\mathrm{d}\theta \wedge \mathrm{d}\phi \wedge \mathrm{d}\psi \wedge \mathrm{d}\vartheta \wedge \mathrm{d}\varphi . \end{aligned} \tag{5.38}$$

Background gauge field in the AdS$_5 \times S^5$-Schwarzschild metric

For probe-brane D_p/D_q-systems a finite density does not backreact onto the geometry and may be included by solving the decoupled Maxwell equation in this background. The Maxwell equations in curved space are given by

$$\nabla^a F^{\mathrm{B}}_{ab} = g^{ac}\nabla_a F^{\mathrm{B}}_{cb} = 0 \tag{5.39}$$

where the superscript B distinguishes the background gauge field from the gauge field living on the D-brane worldvolume determined in Section 5.1.3. Allowing only for a finite charge density, we can set all components of the gauge field to zero, except for the time component. In the dual field theory a non-zero value of A^{B}_t at the boundary will set the chemical potential that sets the corresponding charge density. Assuming that the gauge field only depends on the radial coordinate

$$A^{\mathrm{B}}_{(1)} = A^{\mathrm{B}}_t(u)\,\mathrm{d}t, \qquad F^{\mathrm{B}}_{(2)} = \mathrm{d}A^{\mathrm{B}}_{(1)} = -\partial_u A^{\mathrm{B}}_t(u)\,\mathrm{d}t\wedge\mathrm{d}u, \tag{5.40}$$

and thus we have only a single non-trivial equation for $b = t$

$$g^{uu}\nabla_u F^{\mathrm{B}}_{ut} = \frac{uf(u)}{L^2}\left(uA^{\mathrm{B}\prime\prime}_t(u) - A^{\mathrm{B}\prime}_t(u)\right) = 0. \tag{5.41}$$

Solving (5.41) yields the general solution

$$A^{\mathrm{B}} = C_1 + \frac{C_2}{2}u^2\,\mathrm{d}t\,. \tag{5.42}$$

The leading term is the background field theory chemical potential μ^{B}, so we want to impose the condition $A^{\mathrm{B}}_t(0) = \mu^{\mathrm{B}}$ on (5.42)

$$A^{\mathrm{B}} = \mu^{\mathrm{B}} + \frac{C_2}{2}u^2\,\mathrm{d}t\,. \tag{5.43}$$

Using the regularity condition $A^{\mathrm{B}}_t(u_{\mathrm{H}}) = 0$ for the one-form to be well-defined at the black hole horizon u_{H}, the solution reads

$$A^{\mathrm{B}}(u) = \mu^{\mathrm{B}}\left(1 - \frac{u^2}{u^2_{\mathrm{H}}}\right)\mathrm{d}t\,. \tag{5.44}$$

where the chemical potential μ^{B} is related to the charge density d^{B} by

$$d^{\mathrm{B}} = -\frac{2\mu^{\mathrm{B}}}{u^2_{\mathrm{H}}}. \tag{5.45}$$

5.1.3. Bosonic sector of D_3/D_p-systems with flat zero temperature embeddings

In this section we consider massless embeddings of D_p-branes that will wrap the AdS$_P$ and S^Q subspaces of the full ten-dimensional AdS$_5 \times S^5$ spacetime. Thus, we have to pullback the spacetime metric and the background gauge field onto the Dp-brane worldvolume. In the following we will consider a flat embedding of the D_p-brane, *i.e.* a flat hyperplane which give rise to $\partial_a x^m = \delta_a{}^A$ since we can identify the curved spacetime coordinate functions x^A with the D_p-brane coordinate functions ξ^a. The remaining embedding functions in the transverse direction are set to zero. This flat embedding corresponds to a massless quark hypermultiplet (and is therefore called a massless background) since the distance $L = 0$ at the boundary of the AdS-space is proportional to the quark masses $L \sim m_q$. First we need to solve the bosonic sector

of the D_p-brane action. It will be more convenient to write $p = 2n + 1$ since we are mainly interested in $p = 5$ and $p = 7$ which corresponds to $n = 2$ and $n = 3$. The bosonic sector of the D_{2n+1}-brane consists of the DBI-term (3.40) and the CS-term (3.42). In both cases the CS-term

$$S^{\text{CS}}_{D_{2n+1}} = T_{D_{2n+1}} \frac{(2\pi\alpha')^2}{2} \int \sum_{2q}^{2n} \mathcal{P}\left[C_{(2q)}\right] \wedge \operatorname{tr}\left(\mathrm{e}^{\mathscr{F}}\right) = 0. \tag{5.46}$$

vanishes since the only non-vanishing RR form $C_{(4)}$ introduces all field theory directions. In general, for D_p-branes all directions transverse to the brane are scalars and can be set to a constant value, yet the direction forms still remain, so all the $U(1)$ worldvolume field strength two form will have at least a common direction with the $C_{(4)}$ form. To be specific, the D_7 $C_{(4)}$ form takes the form

$$C_{(4)} = \frac{r^4}{R^4}\, \mathrm{d}x^0 \wedge \mathrm{d}x^1 \wedge \mathrm{d}x^2 \wedge \mathrm{d}x^3 - R^4 \cos^4\theta\, \mathrm{d}\phi \wedge \mathrm{d}\Omega_3, \tag{5.47}$$

where the transverse S^2 directions are considered as scalars allowing us to choose $\sin\psi = 1$ and $\sin\theta = 1$. So we only have to solve the equations of motions coming from the DBI action

$$\begin{aligned} S^{\text{DBI}}_{D_{2n+1}} &= -N_f T_{D_{2n+1}} \int \mathrm{d}^{2n+2}\, \xi\, \mathrm{e}^{-\tilde{\Phi}} \sqrt{-\det(\mathcal{P}[G] + \mathscr{F})} \\ &= -N_f T_{D_{2n+1}} \int \mathrm{d}^{2n+2}\, \xi\, \mathrm{e}^{-\tilde{\Phi}} \sqrt{-\det\left(g_{ab} + (2\pi\alpha') f_{ab}\right)}. \end{aligned} \tag{5.48}$$

As mentioned above in the case of flat embeddings we can simply restrict the ten-dimensional background metric to the subspace spanned by the D_p-branes hypersurface. Considering zero temperature background, we take the $\text{AdS}_5 \times S^5$-Schwarzschild metric (5.9) with vanishing horizon $u_{\text{H}} \to 0$ and the worldvolume gauge field Ansatz $A = A_t(u)\, \mathrm{d}t$. Let us first start with the D_5-brane calculation. Setting $B_{(2)} = 0$ and $\tilde{\Phi} = 0$ allow us to reduce the DBI-action to

$$\begin{aligned} S^{\text{DBI}}_{D_5} &= -N_f T_{D_5} \int \mathrm{d}t\, \mathrm{d}^2\mathbf{x}\, \mathrm{d}u\, \mathrm{d}\theta\, \mathrm{d}\phi \sqrt{\frac{R^8}{u^8} \sin^2\theta \Big[R^4 - u^4 (2\pi\alpha' A_t'(u))^2\Big]} \\ &= -N_f T_{D_5} V \int \mathrm{d}u\, \mathrm{d}\theta\, \mathrm{d}\phi\, \frac{R^4}{u^4} \sin\theta \sqrt{R^4 - u^4 (2\pi\alpha' A_t'(u))^2} \\ &= -R^4 \underbrace{N_f T_{D_5} V 4\pi}_{\mathscr{N}_{D_5}} \int \mathrm{d}u\, \underbrace{u^{-4} \sqrt{R^4 - u^4 (2\pi\alpha' A_t'(u))^2}}_{\mathscr{L}}. \end{aligned} \tag{5.49}$$

Here we will abbreviate the prefactor by $\mathscr{N}_{D_5}$. The action has a cyclic variable $A_t'(u)$ so under variation of the action we find a first integral

$$\frac{1}{(2\pi\alpha')} \frac{\delta\mathscr{L}}{\delta A_t{}'(u)} = -\frac{R^4 \mathscr{N}_{D_5} (2\pi\alpha') A_t'(u)}{\sqrt{R^4 - u^4 (2\pi\alpha' A_t'(u))^2}} = d, \tag{5.50}$$

with the conserved charge d which can be viewed as some charge density related to the $U(1)$ gauge symmetry. Solving (5.50) for $A_t'(u)$ we can integrate this first order differential equation

$$A_t'(u) = \frac{1}{2\pi\alpha'} \frac{R^2 d}{\sqrt{d^2 u^4 + R^8 \mathscr{N}_{D_5}}}, \tag{5.51}$$

and obtain a solution in terms of elliptic integrals

$$A_t(u) = \frac{1}{2\pi\alpha'}\sqrt{\frac{d}{\mathcal{N}_5}}\mathscr{E}_{\mathrm{F}}\left(\operatorname{arcsinh}\left(\sqrt{\frac{d}{R^4\mathcal{N}_5}}\right)u;1\right), \tag{5.52}$$

where $\mathscr{E}_{\mathrm{F}}$ denotes the Legendre incomplete elliptic integral of the first kind see [187] Chapter 19, (19.2.4) defined as

$$\mathscr{E}_{\mathrm{F}}(\phi;k) = \int_0^{\phi}\frac{\mathrm{d}\theta}{\sqrt{1-k^2\sin^2(\theta)}}. \tag{5.53}$$

The solution (5.52) can be converted into a hypergeometric function using its integral representations stated in [187] Section 15.6,

$$A_t(u) = \frac{du}{2\pi\alpha' R^2\mathcal{N}_{D_5}}\,{}_2F_1\left(\frac{1}{4},\frac{1}{2};\frac{5}{4};-\frac{d^2u^4}{R^8\mathcal{N}_{D_5}}\right) \tag{5.54}$$

with ${}_2F_1$ denoting the hypergeometric function. The D_7-brane calculation can be done analogously. Curiously, the corresponding gauge field equations of motions are easier to solve in r coordinates. The solution reads

$$A_t(u) = \frac{1}{2\pi\alpha'}\frac{d^{1/3}}{2\cdot 3^{1/4}\mathcal{N}_7^{1/3}}\mathscr{E}_{\mathrm{F}}\left(\arccos\left(\frac{d^{2/3}+\left(1-\sqrt{3}\right)\mathcal{N}_7^{2/3}r^2}{d^{2/3}+\left(1+\sqrt{3}\right)\mathcal{N}_7^{2/3}r^2}\right);\frac{2+\sqrt{3}}{4}\right), \tag{5.55}$$

and correspondingly in terms of a hypergeometric function

$$A_t(r) = \frac{r}{2\pi\alpha'}\,{}_2F_1\left(\frac{1}{6},\frac{1}{2};\frac{7}{6};-\frac{\mathcal{N}_7^2r^6}{d^2}\right). \tag{5.56}$$

The boundary asymptotic allows us to fix the constant of motion d in terms of physical quantities since the boundary value of the worldvolume gauge field is identified with the baryon chemical potential $A_{t\,\mathrm{B}} = \mu/(2\pi\alpha')$. The D_5-brane boundary expansion of (5.54) reads

$$A_t(u_{\mathrm{B}}) = \frac{\sqrt{d}\Gamma\left(\frac{1}{4}\right)\Gamma\left(\frac{5}{4}\right)}{2\pi\alpha'\sqrt{\pi}\sqrt{\mathcal{N}_{D_5}}} + \mathcal{O}\left(\frac{1}{\rho}\right), \tag{5.57}$$

written in r coordinates for better comparison to the D_7-brane boundary expansion of (5.56)

$$A_t(u_{\mathrm{B}}) = \frac{\sqrt[3]{d}\Gamma\left(\frac{1}{3}\right)\Gamma\left(\frac{7}{6}\right)}{2\pi\alpha'\sqrt{\pi}\sqrt[3]{\mathcal{N}_{D_7}}} + \mathcal{O}\left(\frac{1}{\rho}\right). \tag{5.58}$$

Identifying the leading term at the boundary $\rho\to\infty$ with $\mu/(2\pi\alpha')$ we obtain

$$d\big|_{D_5} = \frac{\pi\mathcal{N}_{D_5}}{\Gamma\left(\frac{1}{4}\right)^2\Gamma\left(\frac{5}{4}\right)^2}\mu^2, \qquad d\big|_{D_7} = \frac{\pi^{3/2}\mathcal{N}_{D_7}}{\Gamma\left(\frac{1}{3}\right)^3\Gamma\left(\frac{7}{6}\right)^3}\mu^3. \tag{5.59}$$

with $\mathcal{N}_{D_5} = 4\pi N_f T_{D_5}V$ and $\mathcal{N}_{D_7} = 2\pi^2 N_f T_{D_7}V$. Replacing d in the solutions enables us to generate the appropriate background by dialing the baryonic chemical potential μ. Finite density and finite temperature embeddings are not known analytically, but have been studied numerically [262, 263]. The reason lies in the additional constraint that the gauge field needs to vanish at the black hole horizon. Thus, the boundary expansion of our solutions (5.54) and (5.56)

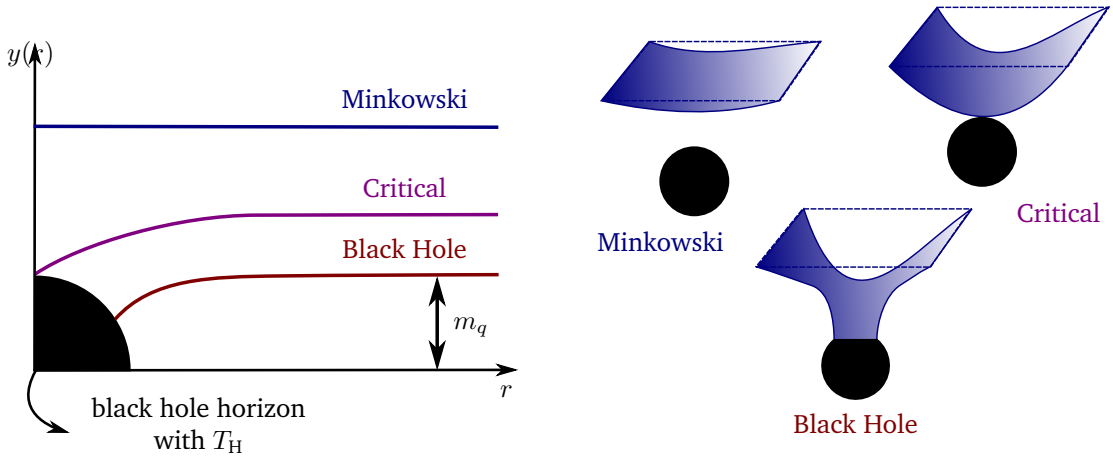

Figure 5.2. For zero baryon density all three embeddings are possible, but for finite baryon chemical potential inducing a finite baryon density only black hole embeddings are consistent solutions, see [262]. The boundary separation yields the quark mass m_q and the temperature is controlled by the black hole horizon. The finite baryon density is controlled by turning on a chemical potential by considering a non-trivial worldvolume gauge field with the diagonal $U(1)_{\rm B} \subset U(N_f)$ gauge group.

cannot be solved for the constant of motion d, but must be determined by a numerical shooting method, for instance. In general, for finite temperature black hole backgrounds, there are three possible embeddings: flat or Minkowski embeddings, critical embeddings and black hole embeddings shown in Figure 5.2. Note that in the finite temperature case a massless embedding can only be a flat black hole embedding. Zero-temperature backgrounds allow also a zero quark mass Minkowski embedding, where the embedding function is strictly zero as well as the black hole horizon.

5.1.4. Zero temperature and finite density embedding of D_p-branes

Finally, we want to generalize the zero temperature background D_{2n+1}-brane to arbitrary embeddings. It is convenient to introduce the split $\mathrm{AdS}_5 \times S^5$-metric

$$\begin{aligned} \mathrm{d}s^2 &= \frac{r^2}{R^2}\eta_{\mu\nu}\,\mathrm{d}x^\mu\,\mathrm{d}x^\nu + \frac{R^2}{r^2}\left(\mathrm{d}r^2 + r^2\,\mathrm{d}\Omega_5\right) \\ &= \frac{r^2}{R^2}\eta_{\mu\nu}\,\mathrm{d}x^\mu\,\mathrm{d}x^\nu + \frac{R^2}{r^2}\left(\mathrm{d}\rho^2 + \rho^2\,\mathrm{d}\Omega_n + \mathrm{d}\mathbf{Y}\cdot\mathrm{d}\mathbf{Y}\right) \end{aligned} \tag{5.60}$$

where the transverse directions to the D_3-brane are denoted by r and the transverse directions of the D_{2n+1}-brane, wrapping the S^n of the S^5, are given by $\mathbf{Y}^2$, *i.e.*

$$r^2 = \rho^2 + \mathbf{Y}^2, \qquad \mathbf{Y}^2 = \sum_{i=1}^{5-n} y^i, \tag{5.61}$$

with $d-(2n+2)=8-2n$ embedding functions[9] depending on all worldvolume coordinates ξ^a. Imposing the conditions that the embedding must not break Lorentz invariance in the field theory directions 0123 and the rotational symmetry of the wrapped S^n directions, the embedding functions $y^i(\rho)$ can only depend on the radial worldvolume coordinate ρ of the pullback metric on the D_{2n+1}-brane. Using the rotational symmetry of the transverse direction to the D_{2n+1}-brane, we can set all embedding function to zero, consistently, except for one embedding function which will be denoted simply by $y(\rho)$ in the following.

Let us do the calculation for the D_7-brane embedding with $n=3$, explicitly. The pullback of the split metric (5.60) onto the D_7-worldvolume is given by

$$g_{ab}=(\mathcal{P}[G])_{ab}=\frac{\partial x^A}{\partial\xi^a}\frac{\partial x^B}{\partial\xi^b}G_{AB}, \tag{5.62}$$

where the only non-trivial entry of the pullback metric $g_{\rho\rho}$ comes from

$$g_{\rho\rho}=\frac{\partial\rho}{\partial\rho}\frac{\partial\rho}{\partial\rho}G_{\rho\rho}+\frac{\partial y(\rho)}{\partial y(\rho)}\frac{\partial y(\rho)}{\partial y(\rho)}G_{yy}. \tag{5.63}$$

The total metric, including the gauge field strength $\mathscr{F}=(2\pi\alpha')F$ reads

$$g_{ab}+(2\pi\alpha')F_{ab}=\begin{pmatrix} -\frac{\rho^2+R^2}{R^2} & & & & -(2\pi\alpha')A_t'(\rho) & \\ & \frac{\rho^2+R^2}{R^2} & & & & \\ & & \frac{\rho^2+R^2}{R^2} & & & \\ & & & \frac{\rho^2+R^2}{R^2} & & \\ (2\pi\alpha')A_t'(\rho) & & & & \frac{R^2}{\rho^2+R^2}\left(1+y'(\rho)^2\right) & \\ & & & & & \frac{R^2}{\rho^2+R^2}\rho^2\widetilde{g}_{ij}^{(3\times3)} \end{pmatrix} \tag{5.64}$$

where $\widetilde{g}_{ij}^{(3\times3)}$ is the S^3 round metric defined as

$$\widetilde{g}_{ij}=\begin{pmatrix} 1 & & \\ & \sin^2\psi & \\ & & \sin^2\vartheta\sin^2\psi \end{pmatrix} \tag{5.65}$$

according to (5.12). Thus, the full DBI action of the D_7-brane reduces to

$$S_{D_7}=-\mathscr{N}_{D_7}\int \mathrm{d}\rho\,\rho^3\sqrt{1+y'(\rho)^2-(2\pi\alpha')^2A_t'(\rho)^2}. \tag{5.66}$$

The action is again independent of the fields $y(\rho)$ and $A_t(\rho)$, so we find two simple first integrals or conserved charges

$$\begin{aligned} \frac{\delta\mathscr{L}}{\delta y'(\rho)}&=-\frac{\mathscr{N}_{D_7}\rho^3y'(\rho)}{\sqrt{1+y'(\rho)^2-2\pi\alpha'A_t'(\rho)^2}}=-c,\\ \frac{1}{2\pi\alpha'}\frac{\delta\mathscr{L}}{\delta A_t'(\rho)}&=\frac{\rho^3\mathscr{N}_{D_7}(2\pi\alpha')A_t'(\rho)}{\sqrt{1+y'(\rho)^2-2\pi\alpha'A_t'(\rho)^2}}=d. \end{aligned} \tag{5.67}$$

[9] Note that D_5-embeddings describe defect theories where some of the D_3 directions are transverse to the D_5-branes and hence needed to described the full embedding, *c.f.* Table 5.1.

The corresponding equations of motion are given by

$$y'(\rho) = \frac{c}{\sqrt{(d^2 - c^2 + \mathscr{N}_{D_7}\rho^6)}}, \qquad A_t'(\rho) = \frac{1}{2\pi\alpha'}\frac{d}{\sqrt{d^2 - c^2 + \mathscr{N}_{D_7}\rho^6}}. \tag{5.68}$$

and according to [259] are solved by incomplete Beta functions

$$\begin{aligned} y(\rho) &= \frac{c^{-1/3}\mathscr{N}_{D_7}}{6}\left(\frac{d^2}{(2\pi\alpha')^2} - c^2\right)^{-1/3} B\left(\frac{\mathscr{N}_{D_7}\rho^6}{\mathscr{N}_{D_7}^2\rho^6 + d^2 - c^2}; \frac{1}{6}, \frac{1}{3}\right), \\ A_t(\rho) &= \frac{d}{(2\pi\alpha')c}y(\rho). \end{aligned} \tag{5.69}$$

For further convenience we define the parameter ε to be

$$(2\pi\alpha')A_t'(\rho) = \frac{1}{\varepsilon}y'(\rho) \qquad \Rightarrow \qquad \frac{y'(\rho)}{A_t'(\rho)} = (2\pi\alpha')\varepsilon \tag{5.70}$$

such that the ratio of (5.68) and (5.69) can be written as

$$\frac{y'(\rho)}{A_t'(\rho)} = \frac{(2\pi\alpha')c}{d} = \frac{y(\rho)}{A_t(\rho)} \qquad \Rightarrow \qquad \varepsilon = \frac{c}{d}. \tag{5.71}$$

Furthermore, the conserved charges c and d can be written in terms of physical parameters of the field theory by expanding the solutions (5.69) at the boundary and reading off the leading terms

$$\lim_{\rho\to\infty} y(\rho) = \frac{\Gamma\left(\frac{1}{6}\right)\Gamma\left(\frac{1}{3}\right)}{6\sqrt{\pi}\sqrt[3]{\mathscr{N}_{D_7}}}\frac{c}{\sqrt[3]{d^2 - c^2}}, \qquad \lim_{\rho\to\infty} A_t(\rho) = \frac{\Gamma\left(\frac{1}{6}\right)\Gamma\left(\frac{1}{3}\right)}{6\sqrt{\pi}\sqrt[3]{\mathscr{N}_{D_7}}}\frac{(2\pi\alpha')d}{\sqrt[3]{d^2 - c^2}}. \tag{5.72}$$

Following the holographic dictionary, the boundary values of the bulk fields $y(\rho)$ and $A_t(\rho)$

$$\lim_{\rho\to\infty} y(\rho) = y\big|_{\partial(\text{AdS})} = m_q, \qquad \lim_{\rho\to\infty} A_t(\rho) = A_t\big|_{\partial(\text{AdS})} = \frac{\mu}{(2\pi\alpha')}. \tag{5.73}$$

are related to the sources of the corresponding dual operators,

$$\langle\, \mathcal{O}_m \,\rangle = -\frac{\delta S_{D_7}}{\delta y\big|_{\partial(\text{AdS})}} = c, \qquad \left\langle\, J^t \,\right\rangle = -\frac{\delta S_{D_7}}{\delta A_t\big|_{\partial(\text{AdS})}} = (2\pi\alpha')d \tag{5.74}$$

Therefore, the parameter c is identified as the condensate of the operator

$$\mathcal{O}_m = \mathrm{i}\overline{\psi}\psi + q^\dagger\left(m_q + \sqrt{2}\Phi^3\right)q + \tilde{q}\left(m_q + \sqrt{2}\Phi^3\right)\tilde{q}^\dagger + \text{Hermitian conjugate}, \tag{5.75}$$

where q, $\tilde{q}$ are the squarks, two complex scalars and ψ, $\overline{\psi}$ the quarks, or a single Dirac fermion of the $\mathcal{N} = 2$ hypermultiplet. The only R-charged scalar to be included, comes form the decomposition of the $\mathcal{N} = 4$ vector multiplet, *i.e.* $\Phi^3 \sim x^8 + \mathrm{i}x^9$. Similarly, we may identify the parameter d as the density of the current

$$J^t = \psi^\dagger\psi + \mathrm{i}\left(q^\dagger\,\mathrm{D}_t\,q - (\mathrm{D}_t\,q)^\dagger q\right) + \mathrm{i}\left(\tilde{q}(\mathrm{D}_t\,\tilde{q})^\dagger - \mathrm{D}_t\,\tilde{q}\tilde{q}^\dagger\right) \tag{5.76}$$

As expected the microscopic Lagrangian is of the general form for scalars and fermions, schematically written as $\mathscr{L} = \mathrm{i}\overline{\psi}\not{D}\psi + \mathrm{D}_\mu\, q(\mathrm{D}^\mu\, q)^*$, where D denotes the $SU(N_c)$ gauge invariant derivative. Comparing (5.74) with (5.72) allows us to express the condensate c and the density d in terms of physical field theory quantities as

$$\begin{aligned} c &= \frac{216\pi^{3/2}\mathscr{N}_{D_7}}{\Gamma\left(\frac{1}{6}\right)^3\Gamma\left(\frac{1}{3}\right)^3}\left(\frac{\mu^2}{(2\pi\alpha')^4} - m_q^2\right) m_q, \\ d &= \frac{216\pi^{3/2}\mathscr{N}_{D_7}}{\Gamma\left(\frac{1}{6}\right)^3\Gamma\left(\frac{1}{3}\right)^3}\left(\frac{\mu^2}{\alpha'^4} - m_q^2\right)\frac{\mu}{\alpha'^2}. \end{aligned} \tag{5.77}$$

In particular, the parameter ε can be viewed as the ratio of quark mass to chemical potential due to

$$\varepsilon = (2\pi\alpha')\frac{\langle\, O_m\,\rangle}{\langle\, J^t\,\rangle} = \frac{c}{d} = (2\pi\alpha')^2\frac{m_q}{\mu}. \tag{5.78}$$

The holographic dictionary identifies the on-shell bulk action $S_{\text{on-shell}}$ with the grand canonical potential $\Omega(T, V, \mu)$ Tuning the chemical potential μ in the grand canonical ensemble enables us to resolve the phase diagram of the theory. As extensively discussed in [259], there is a quantum phase transition at the critical value $\mu_c = m_q$. For $\mu < m_q$ the thermodynamically preferred state is given by a flat embedding, describing a zero density theory with $\langle\, O_m\,\rangle = 0$ and $\langle\, J^t\,\rangle = 0$, as expected for a system below its mass gap. For $\mu > m_q$ we find the zero temperature, finite density state with $\langle\, O_m\,\rangle = c$ and $\langle\, J^t\,\rangle = (2\pi\alpha')d$ where the condensate c and the density d are determined by (5.77). Under this quantum phase transition, the embedded D_7-brane configuration changes from a flat $y(\rho) = L$ to a non-trivial curved embedding function. Moreover, the parameter ε takes only values between 0 and 1 corresponding to the massless case $m_q = 0$ and the critical zero density case $\mu = m_q$, respectively. In the following section, we are investigating the mesonic spectrum of the theory, where the mesons are determined by the D_7-brane fluctuations about the background solution (5.69). The spectrum can be determined by a quasinormal mode analysis, searching for standing waves with endpoints on the D_7-brane and the AdS_5 boundary, which show up as poles in the correlation functions of the dual operators. The mesonic states can be viewed as deeply bound states since they are not related to confinement or chiral symmetry breaking unlike their real world QCD cousins.

5.2. Stability & Fluctuations

Overview

- Instabilities are expected due to zero temperature finite entropy density
  $\longrightarrow$ ground state highly degenerate.
- Instabilities are signaled by poles of the retarded correlation function
  in the lower complex frequency plane.
- Zero sound mode in gauge field fluctuations.

As explained in the introduction to this chapter, the finite density state, most generally described by a AdS-Reissner-Nordström black hole in holographic duals, displays a quantum phase transition. It is unclear, however, if there is a yet unknown stable phase associated with this critical point. There are many reasons to expect instabilities:

- Non zero entropy density at zero temperature *c.f.* (4.254) signaling the high ground state degeneracy.
- Presence of charged fermionic and bosonic degrees of freedom. A chemical potential may trigger a Bose-Einstein condensation of the charged scalars q and $\tilde{q}$, in particular a chemical potential larger than the scalar field mass $\mu > m_q$ leads to a second order phase transition to a broken phase of the global $U(1)$. The fermions of the $\mathcal{N} = 2$ hypermultiplet may form a Fermi surface and a corresponding Cooper instability. Interestingly, as we explicitly show in Section 5.2.2 the finite density system exhibit a zero sound mode known from Fermi liquids. On the other hand for $T \ll \mu$ the heat capacity scales as $c_V \sim T^6$ unlike any quantum liquid known so far [264, 265]. According to [266] the system seems to be stable at low temperatures indicating a peculiar zero-temperature state which is not describe by a Bose or Fermi liquid.
- Another question concerns symmetry breaking instabilities. In our holographic setup we focus on mesonic operators, characterized by D_7-brane fluctuations, that are gauge invariant under $SU(N_c)$ and $U(1)_{=B}$. This leaves us with symmetry breaking instabilities of the remaining global $SU(2)_{\text{scalar}} \times SU(2)_{\text{R}}$ symmetry and in the case of massless quarks $m_q = 0$, the $U(1)_{\text{R}}$ symmetry.

Apart from expecting an instability, there remains the question if the squarks q, $\tilde{q}$ may already form a Bose-Einstein condensate with non-zero $\langle J^t \rangle$ and $\langle O_m \rangle$. Intuitively, such a squark condensate should break the $SU(N_c) \times SU(2)_{\text{R}} \times U(1)_{\text{B}}$, yet the condensing operators are uncharged and the solution (5.69) preserves these global symmetries. A condensation process without symmetry breaking might be a feature strongly correlated, compressible quantum matter as suggested in the introduction chapter of this thesis. At any rate, the understanding of the quasi-normal modes will help to unveil parts of these mysteries. So in the following we conduct a stability analysis: at first we determine the mesonic spectrum at zero density and then move on to finite densities. Instabilities in the mesonic spectrum will be determined by quasi-normal modes of the D_7-brane fluctuations in the *lower*[10] complex frequency half plane, corresponding to poles in the correlation functions of the dual mesonic operators.

5.2.1. Fluctuations in zero density backgrounds

Before generalizing the quasi-normal analysis to the zero temperature and finite density embedding, let us first discuss the meson spectrum of the D_3/D_7-theory. Following [260], we consider the trivial embedding with $y(\rho) = L$ and $A_t(rho) = 0$. The pullback of the background metric is simply given by

$$\mathrm{d}s^2 = \frac{\rho^2 + L^2}{R^2}\,\mathrm{d}s^2\left(\mathbb{E}^{(1,3)}\right) + \frac{R^2}{\rho^2 + L^2}\left(\mathrm{d}\rho^2 + \rho^2\,\mathrm{d}\Omega_3^2\right). \tag{5.79}$$

We will adopt the following labeling scheme: Greek indices denote Minkowski spacetime coordinates, ρ denotes the radius of the spherical coordinates of the 4567-space and Latin indices denote the coordinates on the S^3. The determinant of the induce metric (5.79) is

$$\det g = -\left(\frac{\rho^2 + L^2}{R^2}\right)^4 \left(\frac{R^2}{\rho^2 + L^2}\right)^4 \rho^6 \sin^4\psi \sin^2\vartheta = -\rho^6 \det\tilde{g}, \tag{5.80}$$

[10] The alert reader may wonder how the contradiction to Section 2.2 arise. The reason lies in a different convention for the Fourier transform *i.e.* in this chapter we use $\mathrm{e}^{\mathrm{i}k_\mu x^\mu} = \mathrm{e}^{\mathrm{i}\omega t - \mathrm{i}\mathbf{k}\cdot\mathbf{x}}$ instead of $\mathrm{e}^{-\mathrm{i}k_\mu x^\mu}$. Thus, all statements in Section 2.2 concerning correlation functions must be converted by $\omega \longrightarrow -\omega$.

where $\det \tilde{g}$ denotes the determinant of the S^3 round metric. There are two types of fluctuations we can investigate: Scalar fluctuations about $x^8 = y^1 = L$ and $x^9 = y^2 = 0$ and gauge field fluctuations about $A_a = 0$.

Scalar field fluctuations

The $D7$-brane is embedded in the 89-space as follows

$$y^1 = L, \qquad y^2 = 0. \tag{5.81}$$

The respective scalar field fluctuations are given by χ and φ being functions of all worldvolume coordinates ξ^a

$$y^1 = L + 2\pi\alpha'\chi(\xi), \qquad y^2 = 2\pi\alpha'\varphi(\xi). \tag{5.82}$$

Since the background gauge fields are zero, the Chern-Simons term of the full action vanishes and we are left with a simple worldvolume action

$$S_{D_7} = -T_{D_7}\int \mathrm{d}^8\xi\,\sqrt{-\det \mathcal{P}[G]}. \tag{5.83}$$

Expanding the action in scalar fluctuations up to quadratic order, we need to expand in the induced metric g_{ab} via

$$\delta\sqrt{-\det g_{ab}} = \frac{1}{2}\sqrt{-\det g_{ab}}g^{ab}\delta g_{ab}. \tag{5.84}$$

It is sufficient to expand $\sqrt{-\det g_{ab}}$ to first order, since the background scalar field embedding are constant functions and hence the induced metric in terms of scalar fluctuations is given by

$$\begin{aligned}
\delta g_{ab} = \delta\mathcal{P}[G]_{ab} &= \frac{\partial\left(x^A + \delta x^A\right)}{\partial\xi^a}\frac{\partial\left(x^B + \delta x^B\right)}{\partial\xi^B}G_{AB} - \frac{\partial x^A}{\partial\xi^a}\frac{\partial x^B}{\partial\xi^b}G_{AB} \\
&= \left(\frac{\partial x^A}{\partial\xi^a}\frac{\partial\delta x^B}{\partial x i^b} + \frac{\partial\delta x^a}{\partial\xi^a}\frac{\partial x^B}{\partial\xi^b} + \frac{\partial\delta x^A}{\partial\xi^a}\frac{\partial\delta x^B}{\partial\xi^b}\right)G_{AB} \\
&= (2\pi\alpha')^2\left(\frac{\partial\chi}{\partial\xi^a}\frac{\partial\chi}{\partial\xi^b}G_{88} + \frac{\partial\varphi}{\partial\xi^a}\frac{\partial\varphi}{\partial\xi^b}G_{99}\right) \\
&= (2\pi\alpha')^2\frac{R^2}{r^2}\left(\partial_a\chi\partial_b\chi + \partial_a\varphi\partial_b\varphi\right),
\end{aligned} \tag{5.85}$$

where we inserted the split background metric (5.60). The effective action in quadratic fluctuations reads

$$S = -T_{D_7}\int \mathrm{d}^8\xi\,\sqrt{-\det g}\left[1 + \frac{1}{2}\left(2\pi\alpha'\right)^2\frac{R^2}{r^2}g^{cd}\left(\partial_c\chi\partial_d\chi + \partial_c\varphi\partial_d\varphi\right)\right]. \tag{5.86}$$

Calculating the equations of motions with the help of the Euler-Lagrange equations

$$\frac{\delta S}{\delta\varphi} = \partial_a\left(\frac{\partial\mathscr{L}}{\partial(\partial_a\varphi)}\right) - \frac{\partial\mathscr{L}}{\partial\varphi} = 0, \tag{5.87}$$

we see that the second term of (5.87) is vanishing because $\mathscr{L}$ does not depend on the scalar fields χ and φ explicitly

$$\partial_a\left[-\frac{1}{2}T_{D_7}\left(2\pi\alpha'\right)^2\frac{R^2\sqrt{-\det g}}{r^2}\frac{\partial}{\partial(\partial_a\Phi)}\left(g^{cd}\partial_c\chi\partial_d\chi + \partial_c\varphi\partial_d\varphi\right)\right] = 0, \tag{5.88}$$

where Φ denotes the scalar field χ and φ. We see that the equations of motions are identical for both scalar fluctuations. Therefore, (5.88) can be simplified to

$$\partial_a\left(\frac{\rho^3\sqrt{\det\widetilde{g}}}{\rho^2+L^2}g^{ab}\partial_b\varphi\right)=0, \tag{5.89}$$

where we have inserted the expression for r in terms of worldvolume coordinates (5.61) and the determinant of the induced metric given in equation (5.80) reading $\sqrt{-\det g}=\sqrt{\rho^6\det\widetilde{g}}$. The equations of motion can be split in a four dimensional Minkowski spacetime part and the spherical coordinate part of the 4567-space

$$\partial_\mu\left(\frac{\rho^3\sqrt{\det\widetilde{g}}}{\rho^2+L^2}\underbrace{g^{\mu\nu}}_{\frac{R^2}{\rho^2+L^2}\eta^{\mu\nu}}\partial_\nu\varphi\right)+\partial_\rho\left(\frac{\rho^3\sqrt{\det\widetilde{g}}}{\rho^2+L^2}\underbrace{g^{\rho\rho}}_{\frac{\rho^2+L^2}{R^2}}\partial_\rho\varphi\right)+\partial_i\left(\frac{\rho^3\sqrt{\det\widetilde{g}}}{\rho^2+L^2}\underbrace{g^{ij}}_{\frac{\rho^2+L^2}{R^2}\frac{1}{\rho^2}\widetilde{g}^{ij}}\partial_i\varphi\right)=0$$

$$\rho^3\sqrt{\det\widetilde{g}}\frac{R^2}{(\rho^2+L^2)^2}\eta^{\mu\nu}\partial_\mu\partial_\nu\varphi+\frac{1}{R^2}\sqrt{\det\widetilde{g}}\partial_\rho\left(\rho^3\partial_\rho\varphi\right)+\rho^3\frac{1}{\rho^2R^2}\partial_i\left(\sqrt{\det\widetilde{g}}\widetilde{g}^{ij}\partial_j\varphi\right)=0$$

$$\Rightarrow\quad\frac{R^4}{(\rho^2+L^2)^2}\partial_\mu\partial^\mu\varphi+\frac{1}{\rho^3}\partial_\rho\left(\rho^3\partial_\rho\varphi\right)+\frac{1}{\rho^2}\underbrace{\frac{1}{\sqrt{\det\widetilde{g}}}\partial_i\left(\sqrt{\det\widetilde{g}}\widetilde{g}^{ij}\partial_j\varphi\right)}_{\nabla_i\nabla^i\varphi}=0, \tag{5.90}$$

where ∇ denotes the covariant derivative on the three sphere. This differential equation can be separated in two modes, the plan waves in four dimensional Minkowski spacetime and the scalar spherical harmonics on the three sphere, satisfying the following eigenvalue equation

$$\nabla_i\nabla^i\mathcal{Y}^\ell=-\ell(\ell+2)\mathcal{Y}^\ell, \tag{5.91}$$

where $\mathcal{Y}^\ell(S^3)$ transform in the $(\ell/2,\ell/2)$-representation of $SO(4)$. Therefore we can write as Ansatz for the solution of (5.90)

$$\Phi=\phi(\rho)\,\mathrm{e}^{\mathrm{i}k\cdot x}\,\mathcal{Y}^\ell, \tag{5.92}$$

where the scalar product of two four vectors is denoted by a dot, *e.g.* $k\cdot x\equiv k_\mu x^\mu$. Inserting the Ansatz (5.92) into the differential equation (5.90) yields

$$\frac{R^4}{(\rho^2+L^2)^2}\mathrm{i}k_\mu\mathrm{i}k^\mu\Phi+\frac{1}{\rho^3}\Big[\rho^3\partial_\rho\phi(\rho)\Big]\mathrm{e}^{\mathrm{i}k\cdot x}\,\mathcal{Y}^\ell+\frac{1}{\rho^2}\Big[-\ell(\ell+2)\Big]\Phi=0. \tag{5.93}$$

With the help of the following redefinitions rendering the equations of motion dimensionless

$$\begin{aligned}\varrho&=\frac{\rho}{L}, & \bar{M}^2&=-\frac{k^2R^4}{L^2},\\ \partial_\rho&=\frac{1}{L}\partial_\varrho, & \partial_\rho^2&=\frac{1}{L^2}\partial_\varrho^2,\end{aligned} \tag{5.94}$$

we can rewrite equation (5.93) as

$$\left[-\frac{R^4}{\left(\frac{\rho^2}{L^2}+1\right)^2L^4}k^2-\frac{\ell(\ell+2)}{L^2\frac{\rho^2}{L^2}}\right]\Phi+\left[\underbrace{\frac{3}{\rho^3}\rho^2}_{\frac{1}{L}\frac{\rho}{L}}\partial_\rho\phi(\rho)+\partial_\rho^2\phi(\rho)\right]\mathrm{e}^{\mathrm{i}k\cdot x}\,\mathcal{Y}^\ell=0\qquad\Big|\cdot\frac{L^2}{\mathrm{e}^{\mathrm{i}k\cdot x}\,\mathcal{Y}^\ell} \tag{5.95}$$

$$\frac{3}{\varrho}\underbrace{L\partial_\rho}_{\partial_\varrho}\phi(\varrho)+\underbrace{L^2\partial_\rho^2}_{\partial_\varrho^2}\phi(\varrho)+\left[\frac{\bar{M}^2}{(1+\varrho^2)^2}-\frac{\ell(\ell+2)}{\varrho^2}\right]\phi(\varrho)=0$$

$$\Rightarrow\quad \partial_\varrho^2\phi(\varrho)+\frac{3}{\varrho}\partial_\varrho\phi(\varrho)+\left[\frac{\bar{M}^2}{(1+\varrho^2)^2}-\frac{\ell(\ell+2)}{\varrho^2}\right]\phi(\varrho)=0 \tag{5.96}$$

The equations of motion can be solved in terms of hypergeometric functions

$$\varphi(\rho)=\frac{\rho^\ell}{(\rho^2+L^2)^\alpha}\,{}_2F_1\left(-\alpha,-\alpha;\ell+2;-\frac{\rho^2}{L^2}\right), \tag{5.97}$$

where the parameter α is related to the dimensionless mass $\bar{M}$ via

$$\alpha=\frac{\sqrt{1+\bar{M}^2}-1}{2}. \tag{5.98}$$

The regularity conditions at the origin $\rho\to 0$ and the normalization condition at the boundary fixes the parameter α in terms of two natural numbers ℓ and n, *i.e.* $\alpha=n+\ell+1$ such that the mesonic mass spectrum is given by

$$M(n,\ell)=\frac{2L}{R^2}\sqrt{(n+\ell+1)(n+\ell+2)}. \tag{5.99}$$

As expected we find a true mass gap coming from $M(0,0)$

$$m_{\text{gap}}=2\sqrt{2}\frac{L}{R^2}=\frac{4\pi}{\sqrt{g^2_{\text{YM}}N_c}}m_q, \tag{5.100}$$

where we have inserted the definition of the AdS radius R and the quark mas m_q. For further discussion on the ramifications of the mesons spectrum see [260].

Fluctuations of the Gauge Fields

For the fluctuations of the gauge field we need to expand the full action including the Chern-Simons term

$$S_{D7}=-T_{D7}\int \mathrm{d}^8\xi\,\sqrt{-\det\left(P[G]_{ab}+2\pi\alpha' F_{ab}\right)}+\frac{(2\pi\alpha')^2}{2}T_{D7}\int\mathcal{P}\left[C^{(4)}\right]\wedge F\wedge F, \tag{5.101}$$

where the pullback of the four form (5.47) is given by

$$\begin{aligned}\mathcal{P}\left[C_{(4)}\right]&=\frac{\partial x^A}{\partial\xi^a}\frac{\partial x^B}{\partial\xi^b}\frac{\partial x^C}{\partial\xi^c}\frac{\partial x^D}{\partial\xi^d}\frac{C_{ABCD}}{4!}\,\mathrm{d}\xi^a\wedge\mathrm{d}\xi^b\wedge\mathrm{d}\xi^c\wedge\mathrm{d}\xi^d\\&=\frac{(\rho^2+L^2)^2}{R^4}\,\mathrm{d}x^0\wedge\mathrm{d}x^1\wedge\mathrm{d}x^2\wedge\mathrm{d}x^3\\&\quad+\underbrace{\frac{\partial\phi}{\partial\xi^a}}_{=0}\frac{\partial\psi}{\partial\xi^b}\frac{\partial\vartheta}{\partial\xi^c}\frac{\partial\phi}{\partial\xi^d}C_{\varphi\psi\vartheta\phi}\,\mathrm{d}\xi^a\wedge\mathrm{d}\xi^b\wedge\mathrm{d}\xi^c\wedge\mathrm{d}\xi^d.\end{aligned} \tag{5.102}$$

Note that the azimuthal angle of the S^5 is independent of the D_7 worldvolume and thus the entire S^3 part of the $C_{(4)}$ drops out. The bulk metric of the brane's worldvolume is given by the induced metric (5.79). The complete action of the $D7$-brane can then be written as

$$\begin{aligned} S_{D7} = & -T_{D_7}\int \mathrm{d}^8\xi\,\sqrt{-\det\left(g_{ab}+2\pi\alpha' F_{ab}\right)} \\ & + \frac{(2\pi\alpha')^2}{2}T_{D_7}\int \mathrm{d}x^0\wedge\mathrm{d}x^1\wedge\mathrm{d}x^2\wedge\mathrm{d}x^3\wedge F\wedge F\frac{(\rho^2+L^2)^2}{R^4}. \end{aligned} \tag{5.103}$$

In the following the gauge field fluctuations are denoted by A in order to keep the notation simple since the background gauge field is zero. The directions transverse to the D_3 brane, the *i.e.* 4567 space are denoted by Y^i. The Chern-Simons term can be simplified by inserting the definition of the two form field strengths $F = \mathrm{d}A$ as exterior derivative of the one form gauge fields

$$A = A_i\,\mathrm{d}Y^i \longrightarrow \mathrm{d}A = \frac{1}{2}\sum_{j=1}^{4}\frac{\partial A_i}{\partial Y^j}\,\mathrm{d}Y^j\wedge\mathrm{d}Y^i, \tag{5.104}$$

and therefore the four form $F\wedge F$ is given by

$$\mathrm{d}A\wedge\mathrm{d}A = \frac{1}{4}\sum_{j,l=1}^{4}\frac{\partial A_i}{\partial Y^j}\frac{\partial A_l}{\partial Y^l}\,\mathrm{d}Y^j\wedge\mathrm{d}Y^i\wedge\mathrm{d}Y^l\wedge\mathrm{d}Y^k\,. \tag{5.105}$$

Because our worldvolume of the $D7$-brane is eight dimensional, the complete eight form $\mathrm{d}^4x\wedge\mathrm{d}A\wedge\mathrm{d}A$ is proportional to the eight dimensional pseudoscalar and we can split the complete eight dimensional differential form in a Minkowski spacetime part and the 4567-space part

$$\begin{aligned} \mathrm{d}x^0\wedge\mathrm{d}x^1\wedge\mathrm{d}x^2\wedge\mathrm{d}x^3\wedge F\wedge F = & \frac{1}{4}\sum_{j,l=1}^{4}\frac{\partial A_i}{\partial Y^j}\frac{\partial A_l}{\partial Y^l}\,\mathrm{d}x^0\wedge\mathrm{d}x^1\wedge\mathrm{d}x^2\wedge\mathrm{d}x^3 \\ & \wedge\mathrm{d}Y^j\wedge\mathrm{d}Y^i\wedge\mathrm{d}Y^l\wedge\mathrm{d}Y^k, \end{aligned} \tag{5.106}$$

whereas the 4567-space part consist of a pseudoscalar. Finally the complete action (5.103) can be written as

$$S_{D7} = -T_{D_7}\int \mathrm{d}^8\xi\,\sqrt{-\det\left(g_{ab}+2\pi\alpha' F_{ab}\right)} + \frac{1}{8}T_{D_7}(2\pi\alpha')^2\int \mathrm{d}^4x\,\frac{(\rho^2+L^2)^2}{R^4}\epsilon^{jilk}F_{ji}F_{lk}. \tag{5.107}$$

The DBI term of the action can be approximated by an expansion of the determinant up to second order. Therefore we need to factor out the metric g_{ab} in the square root

$$\sqrt{-\det\left(g_{ab}+2\pi\alpha' F_{ab}\right)} = \sqrt{-\det g_{ac}\det\left(\delta^c{}_b+2\pi\alpha' F^c{}_b\right)}. \tag{5.108}$$

Using the identity (A.10) in Appendix A.1.2, we can expand the determinant of $\mathbb{1}+\mathcal{M}$ up to second order in $\mathcal{M}$

$$\det(\mathbb{1}+\mathcal{M}) \approx 1+\operatorname{tr}\mathcal{M}-\frac{1}{2}\operatorname{tr}\left(\mathcal{M}^2\right)+\frac{1}{2}\left(\operatorname{tr}\mathcal{M}\right)^2. \tag{5.109}$$

Furthermore, we need to expand the square root up to second order as well

$$\sqrt{1+x} \approx 1+\frac{x}{2}-\frac{x^2}{8}, \tag{5.110}$$

which finally leads to

$$\sqrt{\det(\mathbb{1}+\mathcal{M})} \approx \sqrt{1+\operatorname{tr}\mathcal{M}-\frac{1}{2}\operatorname{tr}\left(\mathcal{M}^2\right)+\frac{1}{2}\left(\operatorname{tr}\mathcal{M}\right)^2}$$
$$\approx 1+\frac{1}{2}\operatorname{tr}\mathcal{M}-\frac{1}{4}\operatorname{tr}\left(\mathcal{M}^2\right)+\frac{1}{8}\left(\operatorname{tr}\mathcal{M}\right)^2, \tag{5.111}$$

Setting $\mathcal{M} = 2\pi\alpha' F^c{}_b$, we see that the trace in the above expression is vanishing, since $F^c{}_b$ is antisymmetric and we are left with

$$\sqrt{\det(\mathbb{1}+M)} \approx 1-\frac{1}{4}\operatorname{tr}\left(M^2\right). \tag{5.112}$$

The formal mathematical expression for a matrix using the Einstein summation convention is $M^a{}_b$, so we can safely assume that $F^c{}_b$ is really a matrix where the identity (A.10) holds. But one should be aware that the Einstein summation convention can not account for splitting the determinant of a product of two matrices into a product of two determinants. Therefore the right hand side of equation (5.108) is a little bit misleading, since we cannot sum over the upper index c anymore, because after the splitting we are dealing with a simple product of determinants, *i.e.* these are purely scalar numbers, that involves no summation at all. In the following, we just use the indices to denote the mathematical object and to do some neat calculations. Starting with the insertion of (5.112) into (5.108) we find

$$\sqrt{-\det g_{ab}\det\left(\delta^c{}_d+2\pi\alpha' F^c{}_d\right)} \approx \sqrt{-\det g_{ab}}\left[1-\frac{1}{4}(2\pi\alpha')^2\operatorname{tr}\left(F\cdot F\right)\right]$$
$$= \sqrt{-\det g_{ab}}\left[1-\frac{(2\pi\alpha')^2}{4}\operatorname{tr}\left(g_{ce}F^c{}_d F^e{}_f\right)\right]$$
$$= \sqrt{-\det g_{ab}}\left(1-\frac{(2\pi\alpha')^2}{4}g_{ce}g^{df}F^c{}_d F^e{}_f\right)$$
$$= \sqrt{-\det g_{ab}}\left(1-\frac{(2\pi\alpha')^2}{4}F_{cd}F^{cd}\right). \tag{5.113}$$

The Dirac-Born-Infeld action up to second order is thus given as

$$S_{\text{DBI}} \approx -T_{D_7}\int \mathrm{d}^8\xi\,\sqrt{-\det g}\left(1-\frac{(2\pi\alpha')^2}{4}F_{cd}F^{cd}\right), \tag{5.114}$$

and the complete action is

$$S_{D7} \approx -T_{D_7}\int \mathrm{d}^8\xi\,\sqrt{-\det g}\left(1-\frac{(2\pi\alpha')^2}{4}F_{cd}F^{cd}\right)+\frac{1}{8}T_{D_7}(2\pi\alpha')^2\int \mathrm{d}^4x\,\frac{(\rho^2+L^2)^2}{R^4}\epsilon^{ijkl}F_{ij}F_{kl}. \tag{5.115}$$

In order to calculate the variation of the gauge fields A_b we use the Euler-Lagrange equations (5.87) with $\phi \equiv A_b$

$$\frac{\delta S_{D7}}{\delta A_b} = \partial_a\left(\frac{\partial\mathscr{L}}{\partial(\partial_a A_b)}\right)-\frac{\partial\mathscr{L}}{\partial A_b} = 0. \tag{5.116}$$

The second term is again vanishing because $\mathscr{L}$ does not depend on the gauge fields A_b directly, but only on the field strengths $F = \mathrm{d}A$. With the help of equation (A.13) in Appendix A.2 we

find for the variation of the Born-Infeld action

$$\begin{aligned}
\frac{\delta S_{\text{DBI}}}{\delta A_b} &= \partial_a \left[\left(\delta_c{}^a \delta_d{}^b - \delta_d{}^a \delta_c{}^b\right) \sqrt{-\det g} T_{D_7} \frac{(2\pi\alpha')^2}{4} \frac{\partial}{\partial F_{cd}} \left(F_{cd} F^{cd}\right) \right] \\
&= \partial_a \left[\left(\delta_c{}^a \delta_d{}^b - \delta_d{}^a \delta_c{}^b\right) \sqrt{-\det g} T_{D_7} \frac{(2\pi\alpha')^2}{4} \left(F^{cd} + F_{cd} \frac{\partial F^{cd}}{\partial F_{cd}} \right) \right] \\
&= T_{D_7} (2\pi\alpha')^2 \frac{1}{4} \partial_a \left\{ \sqrt{-\det g} \left[F^{ab} - F^{ba} + \left(\delta_c{}^a \delta_d{}^b - \delta_d{}^a \delta_c{}^b\right) F_{cd} g^{ce} g^{df} \frac{\partial F_{ef}}{\partial F_{cd}} \right] \right\} \\
&= T_{D_7} (2\pi\alpha')^2 \frac{1}{4} \partial_a \left\{ \sqrt{-\det g} \left[2F^{ab} + \left(\delta_c{}^a \delta_d{}^b - \delta_d{}^a \delta_c{}^b\right) \underbrace{F^{ef} \delta_e{}^c \delta_f{}^d}_{F^{cd} \longrightarrow F^{ab} - F^{ba}} \right] \right\} \\
&= T_{D_7} (2\pi\alpha')^2 \partial_a \left(\sqrt{-\det g} F^{ab} \right),
\end{aligned} \tag{5.117}$$

and for the Chern-Simons term in the action

$$\begin{aligned}
\frac{\delta S_{\text{CS}}}{\delta A_b} &= \frac{1}{8} T_{D_7} (2\pi\alpha')^2 \partial_a \left[\left(\delta_c{}^a \delta_d{}^b - \delta_d{}^a \delta_c{}^b\right) \frac{(\rho^2 + L^2)^2}{R^4} \frac{\partial}{\partial F_{cd}} \epsilon^{ijkl} F_{ij} F_{kl} \right] \\
&= \frac{1}{8} T_{D_7} (2\pi\alpha')^2 \partial_a \left[\left(\delta_c{}^a \delta_d{}^b - \delta_d{}^a \delta_c{}^b\right) \frac{(\rho^2 + L^2)^2}{R^4} \epsilon^{ijkl} \left(\delta_i{}^c \delta_j{}^d F_{kl} + F_{ij} \delta_k{}^c \delta_l{}^d \right) \right] \\
&= \frac{1}{8} T_{D_7} (2\pi\alpha')^2 \partial_a \left[\left(\delta_c{}^a \delta_d{}^b - \delta_d{}^a \delta_c{}^b\right) \frac{(\rho^2 + L^2)^2}{R^4} \left(\epsilon^{cdkl} F_{kl} + \underbrace{\epsilon^{ijcd} F_{ij}}_{\epsilon^{cdkl} F_{kl}} \right) \right] \\
&= \frac{1}{4} T_{D_7} (2\pi\alpha')^2 \partial_a \left[\left(\delta_c{}^a \delta_d{}^b - \delta_d{}^a \delta_c{}^b\right) \frac{(\rho^2 + L^2)^2}{R^4} \epsilon^{cdij} F_{ij} \right] \\
&= \frac{1}{4} T_{D_7} (2\pi\alpha')^2 \partial_a \left[\frac{(\rho^2 + L^2)^2}{R^4} \left(\underbrace{\epsilon^{abij} F_{ij} - \epsilon^{baij} F_{ij}}_{2\epsilon^{abij} F_{ij}} \right) \right] \\
&= \frac{1}{2} T_{D_7} (2\pi\alpha')^2 \partial_a \left[\frac{(\rho^2 + L^2)^2}{R^4} \epsilon^{abij} F_{ij} \right].
\end{aligned} \tag{5.118}$$

The indices of ϵ^{abij} run only over the spherical coordinates of the 4567-space, *i.e.* the indices can only take ρ and ijk, since for the Minkowski spacetime indices the eight form in the Chern-Simons term of the action (5.106) is vanishing because of the occurrence of two identical Minkowski spacetime indices. Therefore we can split equation (5.118) in two parts

$$\begin{aligned}
\frac{\delta S_{\text{WZ}}}{\delta A_b} &= \frac{1}{2} T_{D_7} (2\pi\alpha')^2 \left\{ \partial_\rho \left[\frac{(\rho^2 + L^2)^2}{R^4} \epsilon^{\rho bij} F_{ij} \right] + \frac{(\rho^2 + L^2)^2}{R^4} \partial_k \left(\epsilon^{kbij} F_{ij} \right) \right\} \\
&= \frac{1}{2} T_{D_7} (2\pi\alpha')^2 \left[\frac{4\rho(\rho^2 + L^2)}{R^4} \epsilon^{\rho bij} F_{ij} + \frac{(\rho^2 + L^2)^2}{R^4} \left(\epsilon^{\rho bij} \partial_\rho F_{ij} + \epsilon^{kbij} \partial_k F_{ij} \right) \right],
\end{aligned} \tag{5.119}$$

where the index b remains free, as it should be. We see that the second term are the source free Maxwell equations written in coordinate language

$$\mathrm{d}\mathrm{d}A = 0, \qquad \partial_\delta \epsilon^{\alpha\beta\gamma\delta} F_{\alpha\beta} = 0, \tag{5.120}$$

so we can rewrite equation (5.119)

$$\begin{aligned}
\frac{\delta S_{\text{CS}}}{\delta A_b} &= \frac{1}{2} T_{D_7} (2\pi\alpha')^2 \left(\frac{4\rho(\rho^2+L^2)}{R^4} \epsilon^{\rho bij} F_{ij} + \frac{(\rho^2+L^2)^2}{R^4} \underbrace{\partial_{:\rho,k:} \epsilon^{:\rho,k:bij} F_{ij}}_{=0} \right) \\
&= \frac{1}{2} T_{D_7} (2\pi\alpha')^2 \frac{4\rho(\rho^2+L^2)}{R^4} \epsilon^{\rho bij} \left(\underbrace{\partial_i A_j - \partial_j A_i}_{2\epsilon^{\rho bij}\partial_i A_j} \right) \\
&= T_{D_7} (2\pi\alpha')^2 \frac{4\rho(\rho^2+L^2)}{R^4} \epsilon^{\rho bij} \partial_i A_j,
\end{aligned} \tag{5.121}$$

where the colon denotes the combination of the two indices to one index. Finally the equations of motions are

$$\begin{aligned}
\frac{\delta S_{D7}}{\delta A_b} &= \frac{\delta S_{\text{DBI}}}{\delta A_b} + \frac{\delta S_{\text{CS}}}{\delta A_b} \\
&= T_{D_7} (2\pi\alpha')^2 \left[\partial_a \left(\sqrt{-\det g} F^{ab} \right) + \frac{4\rho(\rho^2+L^2)}{R^4} \epsilon^{\rho bij} \partial_i A_j \right] = 0 \\
\Rightarrow \qquad & \partial_a \left(\sqrt{-\det g} g^{ac} g^{bd} F_{cd} \right) + \frac{4\rho(\rho^2+L^2)}{R^4} \epsilon^{\rho bij} \partial_i A_j = 0.
\end{aligned} \tag{5.122}$$

Because of the different structure regarding the indices in the equation of motions (5.122), it is useful to separately write drown the equations of motions for the three different cases where $b = \nu$, $b = \rho$ and $b = k$. In the first case we will only look at the spacetime indices of the four dimensional Minkowski spacetime and therefore the second term is vanishing. The last two cases are described by the indices of the spherical coordinates of the 4567-space, namely the radius ρ and the three angles of S^3. We start with the first case

$\underline{b = \nu}$:

$$\partial_\mu \left(\sqrt{-\det g} g^{\mu c} g^{\nu d} F_{cd} \right) + \partial_\rho \left(\sqrt{-\det g} g^{\rho c} g^{\nu d} F_{cd} \right) + \partial_i \left(\sqrt{-\det g} g^{ic} g^{\nu d} F_{cd} \right) = 0. \tag{5.123}$$

Inserting the induced metric (5.79) on the $D7$-brane worldvolume as well as its inverse and rewriting the square root of the determinant of g with the help of equation (5.80) leads to

$$\begin{aligned}
0 = \partial_\mu & \left[\rho^3 \sqrt{\det \widetilde{g}} \left(\frac{R^2}{\rho^2+L^2} \right) \eta^{\mu\sigma} \left(\frac{R^2}{\rho^2+L^2} \right) \eta^{\nu\tau} F_{\sigma\tau} \right] \\
+ \partial_\rho & \left[\rho^3 \sqrt{\det \widetilde{g}} \left(\frac{\rho^2+L^2}{R^2} \right) g^{\rho\rho} \left(\frac{\rho^2+L^2}{R^2} \right) \eta^{\nu\tau} F_{\rho\tau} \right] \\
+ \partial_i & \left[\rho^3 \sqrt{\det \widetilde{g}} \left(\frac{\rho^2+L^2}{R^2} \right) g^{ij} \left(\frac{R^2}{\rho^2+L^2} \right) \eta^{\nu\tau} F_{j\tau} \right],
\end{aligned} \tag{5.124}$$

where we used the fact that the induced metric (5.79) is of block-diagonal form and we can insert for every type of index (ν, ρ and k) the corresponding block of the coordinate representation of the induced metric. Further simplifications give rise to

$$\begin{aligned}
0 &= \rho^3\sqrt{\det\widetilde{g}}\eta^{\nu\tau}\eta^{\mu\sigma}\left(\frac{R^2}{\rho^2+L^2}\right)^2\partial_\mu\left(\partial_\sigma A_\tau-\partial_\tau A_\sigma\right)+\sqrt{\det\widetilde{g}}\eta^{\nu\tau}\partial_\rho\left[\rho^3\left(\partial_\rho A_\tau-\partial_\tau A_\rho\right)\right]\\
&\quad+\rho^3\eta^{\nu\tau}\partial_i\left[\sqrt{\det\widetilde{g}}\frac{\widetilde{g}^{ij}}{\rho^2}\left(\partial_j A_\tau-\partial_\tau A_j\right)\right] \qquad \Big|\cdot\frac{\eta_{\lambda\nu}}{\rho^3\sqrt{\det\widetilde{g}}}\\
0 &= \underbrace{\eta_{\lambda\nu}\eta^{\nu\tau}}_{\delta_\lambda{}^\tau}\eta^{\mu\sigma}\left(\frac{R^2}{\rho^2+L^2}\right)^2\partial_\mu\left(\partial_\sigma A_\tau-\partial_\tau A_\sigma\right)+\underbrace{\eta_{\lambda\nu}\eta^{\nu\tau}}_{\delta_\lambda{}^\tau}\frac{1}{\rho^3}\partial_\rho\left[\rho^3\left(\partial_\rho A_\tau-\partial_\tau A_\rho\right)\right]\\
&\quad+\underbrace{\eta_{\lambda\nu}\eta^{\nu\tau}}_{\delta_\lambda{}^\tau}\frac{1}{\rho^2}\frac{1}{\sqrt{\det\widetilde{g}}}\partial_i\left[\sqrt{\det\widetilde{g}}\frac{\widetilde{g}^{ij}}{\rho^2}\left(\partial_j A_\tau-\partial_\tau A_j\right)\right].
\end{aligned} \tag{5.125}$$

Finally setting $\lambda=\nu$ we arrive at

$$\begin{aligned}
0 &= \frac{R^4}{(\rho^2+L^2)^2}\eta^{\mu\sigma}\partial_\mu\left(\partial_\sigma A_\nu-\partial_\nu A_\sigma\right)+\frac{1}{\rho^3}\partial_\rho\Big[\rho^3\left(\partial_\rho A_\nu-\partial_\nu A_\rho\right)\Big]\\
&\quad+\frac{1}{\rho^2}\frac{1}{\sqrt{\det\widetilde{g}}}\partial_i\left[\sqrt{\det\widetilde{g}}\widetilde{g}^{ij}\left(\partial_j A_\nu-\partial_\nu A_j\right)\right].
\end{aligned} \tag{5.126}$$

The case $b=\rho$ is nearly identical to the previous case, but because of the antisymmetry of the field strength, the term with partial derivatives with respect to ρ will vanish

$\underline{b=\rho}$:

$$\begin{aligned}
0 &= \partial_\mu\left(\sqrt{-\det g}g^{\mu c}g^{\rho d}F_{cd}\right)+\partial_\rho\left(\sqrt{-\det g}g^{\rho c}g^{\rho d}F_{cd}\right)+\partial_i\left(\sqrt{-\det g}g^{ic}g^{\rho d}F_{cd}\right)\\
0 &= \partial_\mu\left(\sqrt{-\det g}\left(\frac{R^2}{\rho^2+L^2}\right)\eta^{\mu\nu}\left(\frac{\rho^2+L^2}{R^2}\right)F_{\nu\rho}\right)+\partial_\rho\left[\sqrt{-\det g}\left(\frac{R^2}{\rho^2+L^2}\right)^2\underbrace{F_{\rho\rho}}_{=0}\right]\\
&\quad+\partial_i\left(\sqrt{-\det g}\left(\frac{R^2}{\rho^2+L^2}\right)^2\frac{1}{\rho^2}\widetilde{g}^{ij}F_{j\rho}\right)\\
0 &= \frac{R^4}{(\rho^2+L^2)^2}\eta^{\mu\nu}\partial_\mu F_{\nu\rho}+\frac{1}{\rho^2}\frac{1}{\sqrt{\det\widetilde{g}}}\partial_i\left(\sqrt{\det\widetilde{g}}\widetilde{g}^{ij}F_{j\rho}\right).
\end{aligned} \tag{5.127}$$

Inserting the field strength $F_{\mu\nu}$ gives rise to

$$0=\frac{R^4}{(\rho^2+L^2)^2}\eta^{\mu\nu}\partial_\mu\left(\partial_\nu A_\rho-\partial_\rho A_\nu\right)+\frac{1}{\rho^2}\frac{1}{\sqrt{\det\widetilde{g}}}\partial_i\left[\sqrt{\det\widetilde{g}}\widetilde{g}^{ij}\left(\partial_j A_\rho-\partial_\rho A_j\right)\right]. \tag{5.128}$$

Finally, we examine the case where $b = k$, where k is an index running over the S^3 coordinates. Therefore the last term in equation (5.122) will not vanish

$\underline{b = k}$:

$$
\begin{aligned}
0 &= \partial_\mu \left[\rho^3 \sqrt{\det \widetilde{g}} \left(\frac{R^2}{\rho^2+L^2}\right) \eta^{\mu\nu} \left(\frac{\rho^2+L^2}{R^2}\right) \frac{1}{\rho^2} \widetilde{g}^{km} F_{\nu m}\right] \\
&\quad + \partial_\rho \left[\rho^3 \sqrt{\det \widetilde{g}} \left(\frac{\rho^2+L^2}{R^2}\right) g^{\rho\rho} \left(\frac{\rho^2+L^2}{R^2}\right) \frac{1}{\rho^2} \widetilde{g}^{km} F_{\rho m}\right] \\
&\quad + \partial_i \left[\rho^3 \sqrt{\det \widetilde{g}} \left(\frac{\rho^2+L^2}{R^2}\right) \frac{1}{\rho^2} \widetilde{g}^{ij} \left(\frac{R^2}{\rho^2+L^2}\right) \frac{1}{\rho^2} \widetilde{g}^{km} F_{jm}\right] + \frac{4\rho(\rho^2+L^2)}{R^4} \epsilon^{\rho kij} \partial_i A_j \\
0 &= \rho \sqrt{\det \widetilde{g}} \widetilde{g} \widetilde{g}^{km} \eta^{\mu\nu} \partial_\mu F_{\nu m} + \sqrt{\det \widetilde{g}} \widetilde{g}^{km} \partial_\rho \left[\rho \left(\frac{\rho^2+L^2}{R^2}\right)^2 F_{\rho m}\right] \\
&\quad + \left(\frac{\rho^2+L^2}{R^2}\right)^2 \frac{1}{\rho} \partial_i \left(\sqrt{\det \widetilde{g}} \widetilde{g} \widetilde{g}^{ij} \widetilde{g}^{km} F_{jm}\right) + \frac{4\rho(\rho^2+L^2)}{R^4} \epsilon^{\rho kij} \partial_i A_j \qquad \Big| \cdot \frac{\widetilde{g}_{nk}}{\rho \sqrt{\det \widetilde{g}}} \\
0 &= \underbrace{\widetilde{g}_{nk} \widetilde{g}^{km}}_{\delta_n{}^m} \eta^{\mu\nu} \partial_\mu F_{\nu m} + \delta_n{}^m \frac{1}{\rho} \partial_\rho \left(\frac{\rho(\rho^2+L^2)^2}{R^4} F_{\rho m}\right) \\
&\quad + \frac{(\rho^2+L^2)^2}{R^4} \frac{1}{\rho^2} \widetilde{g}_{nk} \frac{1}{\sqrt{\det \widetilde{g}}} \partial_i \left(\sqrt{\det \widetilde{g}} \widetilde{g}^{ij} \widetilde{g}^{km} F_{jm}\right) + \frac{4}{R^2} (\rho^2+L^2) \widetilde{g}_{nk} \frac{\epsilon^{\rho kij}}{\sqrt{\det \widetilde{g}}} \partial_i A_j .
\end{aligned}
\tag{5.129}
$$

Setting $n = \ell$ and inserting the field strength $F_{\mu\nu}$ we find

$$
\begin{aligned}
0 &= \eta^{\mu\nu} \partial_\mu \left(\partial_\nu A_\ell - \partial_\ell A_\nu\right) + \frac{1}{\rho} \partial_\rho \left[\frac{\rho(\rho^2+L^2)^2}{R^4} \left(\partial_\rho A_\ell - \partial_\ell A_\rho\right)\right] \\
&\quad + \frac{(\rho^2+L^2)^2}{R^4} \frac{1}{\rho^2} \widetilde{g}_{k\ell} \frac{1}{\sqrt{\det \widetilde{g}}} \partial_i \left[\sqrt{\det \widetilde{g}} \widetilde{g} \widetilde{g}^{ij} \widetilde{g}^{km} \left(\partial_j A_m - \partial_m A_j\right)\right] \\
&\quad + \frac{4}{R^2} (\rho^2+L^2) \widetilde{g}_{k\ell} \frac{\epsilon^{\rho kij}}{\sqrt{\det \widetilde{g}}} \partial_i A_j .
\end{aligned}
\tag{5.130}
$$

The term $\widetilde{g}_{k\ell} (\det \widetilde{g})^{-1/2} \epsilon^{\rho kij}$ can be considered as $\epsilon^{\rho}{}_{kij}$ since $\epsilon^{\rho kij}$ is a tensor density of weight -1 and therefore the indices of the above term can be raised and lowered as for an true tensor. A second property of the epsilon tensor is its total antisymmetry in all its indices which leads to a representation of the determinant of the metric while lowering or raising the indices. But since we will strictly stick to the Einstein summation convention, we will not use this simplifications. In order to solve these three types of equations of motion, we introduce three types of modes listed in Table 5.2. For the first type we need vector spherical harmonics that come in three

Type I	$A_\mu = 0$	$A_\rho = 0$	$A_i = \phi^\pm_{\text{I}}(\rho)\, \mathrm{e}^{\mathrm{i}k\cdot x}\, \mathcal{Y}^{\ell,\pm}_i(S^3)$
Type II	$A_\mu = \zeta_\mu \phi_{\text{II}}(\rho)\, \mathrm{e}^{\mathrm{i}k\cdot x}\, \mathcal{Y}^{\ell}(S^3)$	$A_\rho = 0$	$A_i = 0$
Type III	$A_\mu = 0$	$A_\rho = \phi_{\text{III}}(\rho)\, \mathrm{e}^{\mathrm{i}k\cdot x}\, \mathcal{Y}^{\ell}(S^3)$	$A_i = \tilde{\phi}_{\text{III}}(\rho)\, \mathrm{e}^{\mathrm{i}k\cdot x}\, \nabla_i \mathcal{Y}^{\ell}(S^3)$

Table 5.2. Overview of the three types of modes used to solve the three different types of equations of motion. Note that for the modes of type I, we use vector spherical harmonics listed in (5.131a)– (5.131c) whereas for Type II & III scalar spherical harmonics introduced in (5.91) are used. For the type II modes there is also an additional constraint regarding the polarization of the modes ζ_μ, namely we use transverse polarized waves, *i.e.* $k \cdot \zeta = 0$; for details see [260].

different classes

$$\nabla_i \nabla^i \mathcal{Y}^{\ell,\pm}_j - R^k{}_j \mathcal{Y}^{\ell,\pm}_l = -(\ell+1)^2 \mathcal{Y}^{\ell,\pm}_j, \tag{5.131a}$$

$$\epsilon_{ijk} \nabla_j \mathcal{Y}^{\ell,\pm}_k = \pm(\ell+1) \mathcal{Y}^{\ell,\pm}_i, \tag{5.131b}$$

$$\nabla^i \mathcal{Y}^{\ell,\pm}_i = 0, \tag{5.131c}$$

where $\mathcal{Y}^{\ell,\pm}_i$ with $\ell \leqslant 1$ transform in the $(\ell \mp 1/2, l \pm 1/2)$-representation and $R^i{}_j = 2\delta^i{}_j$ is the Ricci tensor of the S^3. The second equations (5.131b) should strictly be understand with raised indices on the epsilon tensor (density), but as has been remarked earlier, we can identify it with the expression in the last term of (5.130). With these preliminaries in mind we can insert the type I Ansatz in all three equations of motions $b = \nu$ (5.126), $b = \rho$ (5.128) and $b = k$ (5.130), leading to

Type I $b = \nu, \rho$:

$$\begin{aligned} \frac{1}{\sqrt{\det \tilde{g}}} \partial_i \left(\sqrt{\det \tilde{g}} \tilde{g}^{ij} \partial_\nu A_j \right) &= \partial_\nu \underbrace{\frac{1}{\sqrt{\det \tilde{g}}} \partial_i \left(\sqrt{\det \tilde{g}} \tilde{g}^{ij} A_j \right)}_{\nabla_i A^i} \\ &= \partial_\nu \nabla_i A^i = \partial_\nu \Big[\phi^\pm_{\text{I}}(\rho)\, \mathrm{e}^{\mathrm{i}k\cdot x}\, \underbrace{\nabla^i \mathcal{Y}^{\ell,\pm}_i(S^3)}_{=0} \Big] = 0, \end{aligned} \tag{5.132}$$

where we have used the identity of the covariant divergence of a vector field $\tilde{g}^{ij} A_j$, see (A.14) in Appendix A.2, and the identity of the vector spherical harmonics (5.131b). The equation of motion for $b = \rho$ is identical with equation (5.132) in the case of an Ansatz of type I and is trivially fulfilled as well. The remaining equation of motion is

Type I $b = k$:

$$0 = \eta^{\mu\nu} \partial_\mu \partial_\nu A_\ell + \frac{1}{\rho} \partial_\rho \left(\frac{\rho(\rho^2 + L^2)^2}{R^4} \partial_\rho A_\ell \right) \tag{5.133}$$

$$+\frac{(\rho^2+L^2)^2}{R^4\rho^2}\widetilde{g}_{k\ell}\frac{1}{\sqrt{\det\widetilde{g}}}\partial_i\left[\sqrt{\det\widetilde{g}}\widetilde{g}^{ij}\widetilde{g}^{km}\left(\partial_j A_m-\partial_m A_j\right)\right]+\frac{4}{R^2}(\rho^2+L^2)\widetilde{g}_{k\ell}\frac{\epsilon^{\rho kij}}{\sqrt{\det\widetilde{g}}}\partial_i A_j. \tag{5.134}$$

Let us insert the type II Ansatz in the three equations of motions starting with

Type II $b=\nu$:

$$\begin{aligned}
0=&\frac{R^4}{(\rho^2+L^2)^2}\Big[\eta^{\mu\sigma}\partial_\mu\partial_\sigma A_\nu-\partial_\nu(\underbrace{\eta^{\mu\sigma}\partial_\mu A_\sigma}_{=0})\Big]+\frac{1}{\rho^3}\partial_\rho\left(\rho^3\partial_\rho A_\nu\right)\\
&+\frac{1}{\rho^2}\underbrace{\frac{1}{\sqrt{\det\widetilde{g}}}\partial_i\left(\sqrt{\det\widetilde{g}}\widetilde{g}^{ij}\partial_j\ A_\nu\right)}_{=\nabla_i\nabla^i}\\
0=&\frac{R^4}{(\rho^2+L^2)^2}\zeta_\mu\phi_{\rm II}(\rho)\partial_\mu\partial^\mu\left(\mathrm{e}^{\mathrm{i}k\cdot x}\right)\mathcal{Y}^\ell(S^3)+\frac{1}{\rho^3}\zeta_\mu\partial_\rho\left(\rho^3\partial_\rho\phi_{\rm II}(\rho)\right)\mathrm{e}^{\mathrm{i}k\cdot x}\mathcal{Y}^\ell(S^3)\\
&+\frac{1}{\rho^2}\zeta_\mu\phi_{\rm II}(\rho)\,\mathrm{e}^{\mathrm{i}k\cdot x}\underbrace{\nabla_i\nabla^i\mathcal{Y}^\ell(S^3)}_{-\ell(\ell+2)\mathcal{Y}^\ell(S^3)},
\end{aligned} \tag{5.135}$$

where the constraint $k\cdot\zeta=0$ is translated into $\partial_\mu A^\mu=0$ and we have used the definition of the covariant Laplace-Beltrami operator (A.15) for scalar functions, which applies here because the vector field A_ν is only defined on the Minkowski spacetime and can therefore be regarded as a scalar with respect to the coordinates on the S^3

$$\begin{aligned}
&\frac{R^4}{(\rho^2+L^2)^2}\mathrm{i}k\mathrm{i}k\phi_{\rm II}(\rho)+\frac{1}{\rho^3}\partial_\rho\left(\rho^3\partial_\rho\phi_{\rm II}(\rho)\right)-\frac{\ell(\ell+2)}{\rho^2}\phi_{\rm II}(\rho)=0\\
&-\left[\frac{k^2R^4}{(1+\frac{\rho^2}{L^2})^2L^4}+\frac{\ell(\ell+2)}{L^2\frac{\rho^2}{L^2}}\right]\phi_{\rm II}(\rho)+\frac{1}{L^3\frac{\rho^3}{L^3}}\partial_\rho\left(L^3\frac{\rho^3}{L^3}\partial_\rho\phi_{\rm II}(\rho)\right)=0 \qquad \Big|\cdot L^2\\
&\left[-\frac{k^2R^4}{(1+\varrho^2)^2L^2}-\frac{\ell(\ell+2)}{\varrho^2}\right]\phi_{\rm II}(\varrho)+\frac{1}{L}\frac{1}{\varrho^3}\frac{1}{L}\partial_\varrho\left(L^3\varrho^3\frac{1}{L}\partial_\varrho\phi_{\rm II}(\varrho)\right)=0\\
&\Rightarrow\quad\frac{3}{\varrho}\partial_\varrho\phi_{\rm II}(\varrho)+\partial_\varrho^2\phi_{\rm II}(\varrho)+\left[\frac{\bar{M}}{(1+\varrho^2)^2}-\frac{\ell(\ell+2)}{\varrho^2}\right]\phi_{\rm II}(\varrho)=0,
\end{aligned} \tag{5.136}$$

After inserting the redefinitions (5.94) we see that equation (5.136) is identical to equation (5.96) and therefore possesses the same solution.

Type II $b=\rho,k$:

$$\eta^{\mu\nu}\partial_\mu\partial_\rho A_\nu=\partial_\rho\left(\eta^{\mu\nu}\partial_\mu A_\nu\right)=0, \tag{5.137}$$

which is trivially fulfilled by virtue of the constraint $k\cdot\zeta=0$ and $\partial_\mu A^\mu=0$, respectively. The same is true for $b=k$ so we are finished with the Ansatz of type II. Finally we need to insert the Ansatz type III in all three equations

Type III $b = \nu$:

$$-\frac{1}{\rho^3}\partial_\rho\left(\rho^3\partial_\nu A_\rho\right) - \frac{1}{\rho^2}\frac{1}{\sqrt{\det\widetilde{g}}}\partial_i\left(\sqrt{\det\widetilde{g}}\widetilde{g}^{ij}\partial_\nu A_j\right) = 0$$

$$\frac{1}{\rho^3}\partial_\rho\left(\rho^3\phi_{\text{III}}(\rho)\right)\mathrm{i}k\,\mathrm{e}^{\mathrm{i}k\cdot x}\,\mathcal{Y}^\ell(S^3) + \frac{1}{\rho^2}\frac{1}{\sqrt{\det\widetilde{g}}}\partial_i\left(\sqrt{\det\widetilde{g}}\widetilde{g}^{ij}\nabla_j\mathcal{Y}^\ell(S^3)\right)\mathrm{i}k\tilde{\phi}_{\text{III}}(\rho)\,\mathrm{e}^{\mathrm{i}k\cdot x} = 0 \quad \Big| \cdot \frac{\rho^2}{\mathrm{i}k\,\mathrm{e}^{\mathrm{i}k\cdot x}}$$

$$\frac{1}{\rho}\partial_\rho\left(\rho^3\phi_{\text{III}}(\rho)\right)\mathcal{Y}^\ell + \underbrace{\frac{1}{\sqrt{\det\widetilde{g}}}\partial_i\left(\sqrt{\det\widetilde{g}}\widetilde{g}^{ij}\nabla_j\mathcal{Y}^\ell(S^3)\right)}_{\nabla_i\nabla^i\mathcal{Y}^\ell=-\ell(\ell+2)\mathcal{Y}^\ell}\tilde{\phi}_{\text{III}}(\rho) = 0$$

$$\Rightarrow \quad \frac{1}{\rho}\partial_\rho\left(\rho^3\phi_{\text{III}}(\rho)\right) - \ell(\ell+2)\tilde{\phi}_{\text{III}}(\rho) = 0. \tag{5.138}$$

So we have found a relation between $\phi_{\text{III}}(\rho)$ and $\tilde{\phi}_{\text{III}}(\rho)$.

Type III $b = \rho$:

$$0 = \frac{R^4}{(\rho^2+L^2)^2}\eta^{\mu\nu}\partial_\mu\partial_\nu A_\rho + \frac{1}{\rho^2}\frac{1}{\sqrt{\det\widetilde{g}}}\partial_i\left[\sqrt{\det\widetilde{g}}\widetilde{g}^{ij}\left(\partial_i A_\rho - \partial_\rho A_j\right)\right]$$

$$0 = -\frac{R^4k^2}{(\rho^2+L^2)^2}\phi_{\text{III}}(\rho)\,\mathrm{e}^{\mathrm{i}k\cdot x}\,\mathcal{Y}^\ell(S^3) + \frac{1}{\rho^2}\frac{1}{\sqrt{\det\widetilde{g}}}\partial_i\Big\{\sqrt{\det\widetilde{g}}\widetilde{g}^{ij}\left[\partial_i\left(\phi_{\text{III}}(\rho)\mathcal{Y}^\ell(S^3)\right)\right.$$

$$\left.-\partial_\rho\left(\tilde{\phi}_{\text{III}}(\rho)\nabla_i\mathcal{Y}^\ell(S^3)\right)\right]\Big\}\mathrm{e}^{\mathrm{i}k\cdot x} \qquad \Big| \cdot \mathrm{e}^{-\mathrm{i}k\cdot x}$$

$$0 = -\frac{R^4k^2}{(\rho^2+L^2)^2}\phi_{\text{III}}(\rho)\mathcal{Y}^\ell(S^3) + \frac{1}{\rho^2}\frac{1}{\sqrt{\det\widetilde{g}}}\partial_i\Big[\sqrt{\det\widetilde{g}}\widetilde{g}^{ij}\underbrace{\partial_j\mathcal{Y}^\ell(S^3)}_{\nabla_j\mathcal{Y}^\ell(S^3)}\Big]\phi_{\text{III}}(\rho)$$

$$-\frac{1}{\rho^2}\frac{1}{\sqrt{\det\widetilde{g}}}\partial_i\left[\sqrt{\det\widetilde{g}}\widetilde{g}^{ij}\nabla_i\mathcal{Y}^\ell(S^3)\right]\partial_\rho\tilde{\phi}_{\text{III}}(\rho)$$

$$0 = -\frac{R^4k^2}{(\rho^2+L^2)^2}\phi_{\text{III}}(\rho)\mathcal{Y}^\ell(S^3) + \frac{1}{\rho^2}\underbrace{\nabla_i\nabla^i\mathcal{Y}^\ell(S^3)}_{-\ell(\ell+2)\mathcal{Y}^\ell(S^3)}\phi_{\text{III}}(\rho) - \frac{1}{\rho^2}\underbrace{\nabla_i\nabla^i\mathcal{Y}^\ell(S^3)}_{-\ell(\ell+2)\mathcal{Y}^\ell(S^3)}\partial_\rho\tilde{\phi}_{\text{III}}(\rho) \quad \Big| \cdot \frac{\rho^2}{\mathcal{Y}^\ell(S^3)}$$

$$0 = -\frac{R^4\rho^2k^2}{(\rho^2+L^2)^2}\phi_{\text{III}}(\rho) - \ell(\ell+2)\phi_{\text{III}} + \partial_\rho\left[\ell(\ell+2)\tilde{\phi}_{\text{III}}(\rho)\right], \tag{5.139}$$

where we have used the fact, that for scalar spherical harmonics $\mathcal{Y}^\ell(S^3)$ the covariant derivative and the partial derivative are identical, *i.e.* $\nabla_i\mathcal{Y}^\ell(S^3) \equiv \partial_i\mathcal{Y}^\ell(S^3)$. Now we can insert relation (5.138) derived from $b = \nu$ into equation (5.139) which leads to a equation where only have to solve for $\phi_{\text{III}}(\rho)$

$$-\frac{R^4\rho^2k^2}{(\rho^2+L^2)^2}\phi_{\text{III}}(\rho) - \ell(\ell+2)\phi_{\text{III}} + \partial_\rho\left[\frac{1}{\rho}\partial_\rho\left(\rho^3\phi_{\text{III}}(\rho)\right)\right] = 0. \tag{5.140}$$

With the help of the replacements (5.94) we finally can write

$$-\frac{R^4k^2\frac{\rho^2}{L^2}L^2}{(1+\frac{\rho^2}{L^2})L^4}\phi_{\rm III}(\rho)-\ell(\ell+2)\phi_{\rm III}(\rho)+\partial_\rho\left[\frac{1}{L\frac{\rho}{L}}\partial_\rho\left(L^3\frac{\rho^3}{L^3}\phi_{\rm III}(\rho)\right)\right]=0$$

$$\frac{\bar{M}^2\varrho^2}{(1+\varrho)^2}\phi_{\rm III}(\varrho)-\ell(\ell+2)\phi_{\rm III}(\varrho)+\frac{1}{L}\partial_\varrho\left[\frac{1}{L\varrho}\frac{1}{L}\partial_\varrho\left(L^3\varrho^3\phi_{\rm III}(\varrho)\right)\right]=0$$

$$\Rightarrow\quad \frac{\bar{M}^2\varrho^2}{(1+\varrho)^2}\phi_{\rm III}(\varrho)-\ell(\ell+2)\phi_{\rm III}(\varrho)+\partial_\varrho\left[\frac{1}{\varrho}\partial_\varrho\left(\varrho^3\phi_{\rm III}(\varrho)\right)\right]=0. \tag{5.141}$$

As in the scalar case, the solutions are given by hypergeometric functions and the corresponding mass spectra (*c.f.* [260])

$$M_{\rm I}^{+}=\frac{2L}{R^2}\sqrt{(n+\ell+2)(n+\ell+3)},\qquad \ell\leqslant 1, \tag{5.142a}$$

$$M_{\rm I}^{-}=\frac{2L}{R^2}\sqrt{(n+\ell)(n+\ell+1)},\qquad \ell\leqslant 1, \tag{5.142b}$$

$$M_{\rm II}=\frac{2L}{R^2}\sqrt{(n+\ell+1)(n+\ell+2)},\qquad \ell\leqslant 0, \tag{5.142c}$$

$$M_{\rm III}=\frac{2L}{R^2}\sqrt{(n+\ell+1)(n+\ell+2)},\qquad \ell\leqslant 1, \tag{5.142d}$$

and $n\in\mathbb{N}_0$. In the next section we move on to finite density backgrounds and employ the quasi-normal mode analysis in order to search for possible instabilities.

5.2.2. Fluctuations of D7-brane in zero temperature, finite density backgrounds

The rather technical calculation presented in the last section is retraced, but this time the spectrum of fluctuations of bosonic D7-brane worldvolume fields are ascertained in the zero temperature, finite density background given by (5.69). Again the procedure will closely follow [260], as presented in the previous section, where the finite-mass meson spectrum for zero density states was computed by solving the fluctuation equations about the constant background solution $y(\rho)=L$ and $A_t(\rho)=0$. The fluctuations are dependent on all spacetime directions of the D_7-brane, *i.e.* the Minkowski directions, the radial directions and the angles on the S^3. In particular, we introduce the fluctuations of the embedding functions $y(\rho)$ and ϕ, which can be viewed as the polar coordinates of the remaining S^2 after the splitting of the S^5, and the worldvolume gauge field A_b

$$y(\rho)\longrightarrow y(\rho)+(2\pi\alpha')\chi(\xi)\qquad \phi\longrightarrow 0+(2\pi\alpha')\varphi\qquad A_b\longrightarrow\delta^t_bA_t+\delta A_b. \tag{5.143}$$

Note that in terms of the background scalar fields the azimuthal angle ϕ of the S^5 can be written as

$$\frac{y^2}{y^1}=\frac{\sin\phi}{\cos\phi}\quad\Rightarrow\quad\phi=\arctan\left(\frac{y^2}{y^1}\right). \tag{5.144}$$

First, we expand the induced metric and the $U(1)$ field strength in the fluctuations χ, ϕ and δA_b up to quadratic order. Using (5.85) we find for the induced metric

$$\begin{aligned}\delta g_{ab} &= \left(\frac{\partial x^A}{\partial \xi^a}\frac{\partial \delta x^B}{\partial x i^b} + \frac{\partial \delta x^a}{\partial \xi^a}\frac{\partial x^B}{\partial \xi^b} + \frac{\partial \delta x^A}{\partial \xi^a}\frac{\partial \delta x^B}{\partial \xi^b}\right) G_{AB} \\ &= \left(\frac{\partial y(\rho)}{\partial \xi^a}\frac{\partial (2\pi\alpha')\chi}{\partial \xi^b} + \frac{\partial (2\pi\alpha')\chi}{\partial \xi^a}\frac{\partial y(\rho)}{\partial \xi^b} + \frac{\partial (2\pi\alpha')\chi}{\partial \xi^a}\frac{\partial (2\pi\alpha')\chi}{\partial \xi^b}\right) G_{88} \\ &\quad + \frac{\partial (2\pi\alpha')\varphi}{\partial \xi^a}\frac{\partial (2\pi\alpha')\varphi}{\partial \xi^b} G_{99} \\ &= (2\pi\alpha')\frac{y'}{r^2}(\partial_a\chi\delta^\rho_b + \partial_b\chi\delta^\rho_a) + (2\pi\alpha')^2\frac{1}{r^2}(\partial_a\chi\partial_b\chi + \partial_a\varphi\partial_b\varphi). \end{aligned} \tag{5.145}$$

Due to the appearance of F^2 in the action, it is sufficient to expand the field strength in linear order of the $U(1)$ gauge field fluctuations

$$\delta F_{ab} = \partial_a \delta A_b - \partial_b \delta A_a. \tag{5.146}$$

Similarly, the pullback of the four-form is needed only linearly in the fluctuations. Using (5.102) the expansion in fluctuations read

$$\begin{aligned}\delta P[C^{(4)}] &= \delta\left(\frac{\partial x^0}{\partial \xi^a}\frac{\partial x^1}{\partial \xi^b}\frac{\partial x^2}{\partial \xi^c}\frac{\partial x^3}{\partial \xi^c}\right) C_{0123}\,\mathrm{d}x^0\wedge\mathrm{d}x^1\wedge\mathrm{d}x^2\wedge\mathrm{d}x^3\wedge \\ &\quad + \delta\left(\frac{\partial \phi}{\partial \xi^a}\frac{\partial \theta^1}{\partial \xi^b}\frac{\partial \theta^2}{\partial \xi^c}\frac{\partial \theta^3}{\partial \xi^c}\right) C_{\phi\theta^1\theta^2\theta^3}\,\mathrm{d}\xi^a\wedge\mathrm{d}\xi^b\wedge\mathrm{d}\xi^c\wedge\mathrm{d}\xi^d. \end{aligned} \tag{5.147}$$

The first term vanishes since there are no fluctuations in the Minkowski directions and the last term yields six entries of the fluctuating four form for $a = 0,\ldots,6$ due to the dependence of the fluctuation ϕ on all worldvolume coordinates ξ. Using (5.144) we find

$$\begin{aligned}\delta P[C^{(4)}] &= \delta\left(\frac{\partial \phi}{\partial \xi^a}\right) C_{\phi\theta^1\theta^2\theta^3}\,\mathrm{d}\xi^a\wedge\mathrm{d}\Omega_3 \\ &= (2\pi\alpha')\cos^4\theta\left(-\frac{\varphi}{y^2}\frac{\partial y}{\partial \xi^a} + \frac{1}{y}\frac{\partial \varphi}{\partial \xi^a}\right)\mathrm{d}\xi^a\wedge\mathrm{d}\Omega_3 \\ &= (2\pi\alpha')\cos^4\theta\left[\partial_\rho\left(\frac{\varphi}{y}\right)\mathrm{d}\rho\wedge\mathrm{d}\Omega_3 + \frac{1}{y}\partial_t\varphi\,\mathrm{d}t\wedge\mathrm{d}\Omega_3 + \frac{1}{y}\nabla\varphi\,\mathrm{d}x\wedge\mathrm{d}\Omega_3\right]. \end{aligned} \tag{5.148}$$

Furthermore, we define the generalized background as follows

$$\eta_{ab} \equiv g_{ab} + (2\pi\alpha')F_{ab} = \begin{pmatrix} -r^2 & -\frac{1}{\varepsilon}y' & & & \\ \frac{1}{\varepsilon}y' & \frac{1}{r}^2(1+y'^2) & & & \\ & & r^2\delta_{\mu\nu} & & \\ & & & \frac{\rho^2}{r^2}\widetilde{g}_{ij} & \end{pmatrix}, \tag{5.149}$$

where we have reordered the coordinates as $(t,\rho,\mathbf{x},\theta^1,\theta^2,\theta^3)$ where $\mu,\nu,\ldots$ denote the Minkowski directions and $i,j,\ldots$ the coordinates on the S^3. This ordering is particularly suitable for our

numerical computations in Section 5.3.3. Note that we have replaced $A_t'(\rho)$ by $y(\rho)$ using (5.70). Due to the coupling it is useful to work with the full generalized metric η_{ab} and its inverse η^{ab} with symmetric and antisymmetric parts defined as

$$\eta_S^{ab} = \frac{1}{2}\left(\eta^{ab} + \eta^{ba}\right), \qquad \eta_A^{ab} = \frac{1}{2}\left(\eta^{ab} - \eta^{ba}\right), \tag{5.150}$$

where the only non-vanishing element of the inverse metric η_A^{ab} is $\eta_A^{\rho t} = -\eta_A^{t\rho}$. The action (5.115) expanded up to quadratic fluctuations does not contain a linear term upon the insertion of (5.146) and (5.148), as expected, since the background fields are on-shell. Dropping the overall factors, *e.g.* $(2\pi\alpha')T_{D_7}$, that do not affect the fluctuation equations of motion, the effective action reads

$$\begin{aligned} oprrL_{D7}^{\mathcal{O}(\delta^2)} \sim\ & -\sqrt{-\eta}\frac{1}{2}\eta^{ba}\frac{1}{r^2}(\partial_a\chi\partial_b\chi + \partial_a\varphi\partial_b\varphi) - \sqrt{-\eta}\left(\frac{1}{8}\eta^{ba}\eta^{dc} - \frac{1}{4}\eta^{da}\eta^{bc}\right) \\ & \times\left[\frac{y'}{r^2}(\partial_a\chi\delta_b^\rho + \partial_b\chi\delta_a^\rho) + \partial_a\delta A_b - \partial_b\delta A_a\right]\left[\frac{y'}{r^2}(\partial_c\chi\delta_d^\rho + \partial_d\chi\delta_c^\rho) + \partial_c\delta A_d - \partial_d\delta A_c\right] \\ & + r^4(\partial_\rho\delta A_i - \partial_i\delta A_\rho)\partial_j\delta A_k\epsilon^{ijk} - \frac{(2\pi\alpha')}{\varepsilon}\cos^4\theta\frac{y'}{y}\partial_\alpha\varphi(\partial_\beta\delta A_\gamma - \partial_\gamma\delta A_\beta)\epsilon^{\alpha\beta\gamma}. \end{aligned} \tag{5.151}$$

Varying (5.151) with respect to φ, χ, A_ρ, A_t, A_α, and A_i yield the following equations of motion

$$0 = \partial_a\left(\sqrt{-\eta}\eta_S^{ab}\frac{1}{\rho^2+y^2}\partial_b\varphi\right), \tag{5.152a}$$

$$\begin{aligned} 0 = {} & \partial_a\left(\sqrt{-\eta}\eta_S^{ab}\frac{1}{\rho^2+y^2}\partial_b\chi\right) - \sqrt{-\eta}(\eta^{\rho t})^2\frac{y'^2}{(\rho^2+y^2)^2}\partial_t^2\chi - \partial_a\left(\sqrt{-\eta}\eta^{\rho\rho}\eta_S^{ab}\frac{y'^2}{(\rho^2+y^2)^2}\partial_b\chi\right) \\ & + \partial_a\left(\sqrt{-\eta}\eta^{\rho t}\eta_S^{ab}\frac{y'}{\rho^2+y^2}\partial_b\delta A_t\right) - \partial_a\left(\sqrt{-\eta}\eta^{\rho t}\eta_S^{ab}\frac{y'}{\rho^2+y^2}\partial_t\delta A_b\right), \end{aligned} \tag{5.152b}$$

$$0 = \sqrt{-\eta}\eta^{\rho\rho}\eta^{\rho t}\frac{y'}{\rho^2+y^2}\partial_\rho\partial_t\chi + \partial_a\left(\sqrt{-\eta}\eta^{\rho\rho}\eta_S^{ab}\partial_\rho\delta A_b\right), \tag{5.152c}$$

$$\begin{aligned} 0 = {} & \sqrt{-\eta}\eta^{\rho t}\eta^{tt}\frac{y'}{\rho^2+y^2}\partial_t^2\chi - \partial_a\left(\sqrt{-\eta}\eta^{\rho t}\eta_S^{ab}\frac{y'}{\rho^2+y^2}\partial_b\chi\right) - \partial_a\left(\sqrt{-\eta}\eta^{tt}\eta_S^{ab}\partial_b\delta A_t\right) \\ & + \partial_a\left(\sqrt{-\eta}\eta^{tt}\eta_S^{ab}\partial_t\delta A_b\right), \end{aligned} \tag{5.152d}$$

$$0 = \sqrt{-\eta}\eta^{\rho t}\eta^{xx}\frac{y'}{\rho^2+y^2}\partial_t\nabla\chi + \partial_a\left(\sqrt{-\eta}\eta^{xx}\eta_S^{ab}\nabla\delta A_b\right) - \partial_a\left(\sqrt{-\eta}\eta^{xx}\eta_S^{ab}\partial_b\delta\mathbf{A}\right) \tag{5.152e}$$

$$\begin{aligned} 0 = {} & \sqrt{-\eta}\eta^{\rho t}\eta^{ij}\frac{y'}{\rho^2+y^2}\partial_t\partial_j\chi + \partial_a\left(\sqrt{-\eta}\eta_S^{ab}\eta^{ij}\partial_j\delta A_b\right) - \partial_a\left(\sqrt{-\eta}\eta^{ij}\eta_S^{ab}\partial_b\delta A_j\right) \\ & + 4(\rho^2+y^2)(\rho+yy')\epsilon^{ijk}\partial_j\delta A_k. \end{aligned} \tag{5.152f}$$

We are working explicitly in the "radial" gauge $\delta A_\rho = 0$, so the equation of motion for δA_ρ (5.152c) imposes a constraint on the remaining fields. Due to the anti-symmetry of ϵ^{ijk}, the last

term in (5.151) drops out in the equations of motions, *i.e.* the Chern-Simons term only affect the S^3 gauge field fluctuations A_i in contrast to [267] where the Chern-Simons term shows up in the full AdS_5 gauge field equations of motion. Note that the equations of motion reduce to (5.90) and (5.126) if we set $F_{ab} = 0$ and $y'(\rho) = 0$, albeit in a different gauge: in the zero-density calculation we implicitly applied the gauge $\partial \cdot A = -\partial_t \delta A_t + \partial_\mu \delta A_\mu = 0$. Due to the rotational and translational symmetry of our background solution in the field theory directions we employ the Fourier decomposition in plane waves, where we may choose a finite momentum in x^3 direction. Thus, in our conventions adopted in this chapter the plane wave modes take the form $\mathrm{e}^{\mathrm{i}\omega t - \mathrm{i}kx^3}$. Let us emphasize again that in this convention the stable modes will appear in the *upper* complex ω half-plane. The Fourier transformed equations of motion of the the transverse gauge field fluctuations δA_1 and δA_2 decouple from all other fluctuations and are reduced to a scalar equation, identical to the equation (5.152a) for φ. As in Section 5.2.1 we decompose the fluctuations into S^3 scalar and vector spherical harmonics denoted by $\mathcal{Y}^\ell$ and $\mathcal{Y}_i^{\ell,\pm}$, respectively[11] obeying the relations

$$\begin{aligned}
\nabla^i \nabla_i \mathcal{Y}^\ell &= -\ell(\ell+2)\mathcal{Y}^\ell, \\
\nabla^i \nabla_i \mathcal{Y}^{\ell,\pm} - R^k{}_j \mathcal{Y}^{\ell,\pm} &= -(\ell+1)^2 \mathcal{Y}_j^{\ell,\pm}, \\
\epsilon^{ijk} \nabla_j \mathcal{Y}_k^{\ell,\pm} &= \pm(\ell+1)\sqrt{\widetilde{g}}\widetilde{g}^{ij}\mathcal{Y}_j^{\ell,\pm}, \\
\nabla^i \mathcal{Y}_i^{\ell,\pm} &= 0,
\end{aligned} \tag{5.153}$$

where ∇^i denotes the curved space covariant derivative. Note that the Ricci tensor $R^i{}_j = 2\delta^i{}_j$ due to the maximal symmetric nature of S^3 manifold. The scalar harmonics $\mathcal{Y}^\ell$ transform in the $(\frac{\ell}{2}, \frac{\ell}{2})$ representation for $\ell \geqslant 0$ with respect to the $SO(4) = SU(2)_{\mathrm{R}} \times SU(2)_{\mathrm{L}}$ isometry of the S^3, whereas the vector harmonics $\mathcal{Y}_i^{\ell,\pm}$ transform in the $(\frac{\ell\mp1}{2}, \frac{ell\pm1}{2})$ representation, with $\ell \geqslant 1$. Similarly to the decomposition shown in Table 5.2, we may choose the following Ansatz to decouple the full system of coupled equations of motion. Again, the scalar fields φ, χ and the gauge fields A_i can be decomposed into scalar and vector spherical harmonics, respectively. Therefore we generalize the Ansatz in Table 5.2 by defining

$$\delta A_i = 0, \quad \delta A_t = \varepsilon\chi, \quad \delta A_3 = -\frac{\omega}{k}\varepsilon\chi, \qquad \chi = \Phi(\rho)\,\mathrm{e}^{\mathrm{i}\omega t - \mathrm{i}kx^3}\,\mathcal{Y}^\ell, \tag{5.154a}$$

$$\chi = 0, \quad \delta A_t = 0, \quad \delta A_3 = 0, \qquad \delta A_i = \Phi^\pm(\rho)\,\mathrm{e}^{\mathrm{i}\omega t - \mathrm{i}kx^3}\,\mathcal{Y}^{\ell,\pm}, \tag{5.154b}$$

$$\chi = 0, \quad \delta A_t = 0, \quad \delta A_3 = \Phi(\rho)\,\mathrm{e}^{\mathrm{i}\omega t - \mathrm{i}kx^3}\,\mathcal{Y}^\ell, \quad \delta A_i = \frac{-\mathrm{i}k\eta^{xx}}{\ell(\ell+2)\eta^{S3}}\Phi(\rho)\,\mathrm{e}^{\mathrm{i}\omega t - \mathrm{i}kx^3}\,\nabla_i\mathcal{Y}^\ell, \tag{5.154c}$$

with the definitions of $\eta^{ij} = \eta^{S3}\widetilde{g}^{ij} = \frac{r^2}{\rho^2}\widetilde{g}^{ij}$. The scalar harmonics Ansatz (5.154a) and the vector harmonics Ansatz (5.154b) decouple from each other since they transform in different representation of the $SO(4)$. On the contrary, the Ansatz (5.154c) entails a coupling between the scalar and vector harmonics. Moreover, for all other scalar equations φ, δA_1, and δA_2 we use the Ansatz(5.154a). Inserting the Ansatz (5.154) into the equations of motion, (5.152a) to

[11] Corresponding to (5.92) and (5.131), respectively.

(5.152f) as well as $A_t(\rho) = \frac{1}{(2\pi\alpha')}\frac{1}{\varepsilon}y(\rho)$ (*c.f.* (5.70)), we find

$$0 = \partial_a\left(\sqrt{-\eta}\eta_S^{ab}\frac{1}{\rho^2+y^2}\partial_b\chi\right), \tag{5.155a}$$

$$0 = \partial_k\left(\sqrt{-\eta}\eta^{kl}\eta^{ij}\partial_j\delta A_l\right) - \partial_a\left(\sqrt{-\eta}\eta^{ij}\eta_S^{ac}\partial_c\delta A_j\right) + 4\left(\rho^2+y^2\right)(\rho+yy')\epsilon^{ijk}\partial_j\delta A_k, \tag{5.155b}$$

$$0 = \partial_a\left(\sqrt{-\eta}\eta_S^{ab}\frac{1}{\rho^2+y^2}\partial_b\delta A_3\right). \tag{5.155c}$$

In particular, we see that (5.155a) and (5.155c) are identical to the equations of motion of χ and of course, φ, δA_1, and δA_2. Thus, all scalar fluctuations and the gauge field fluctuations in Minkowski directions obey the same equation of motion, as expected, since all these fluctuations are build from scalar spherical harmonics $\mathcal{Y}^\ell$ or $\nabla_i\mathcal{Y}^\ell$ on the S^3. The radial dependent part of all these fluctuations will be collectively denoted by $\Phi(\rho)$. For the fluctuations arising from vector spherical harmonics $\mathcal{Y}^{m,\pm}$ (5.155b), we find two different equations of motion denoted by $\Phi^+(\rho)$ and $\Phi^-(\rho)$. Using the relations (5.153) for the spherical harmonics the equations of motion can be reduced to

$$\begin{aligned}
0 &= \partial_\rho\left(\sqrt{-\eta}\eta^{\rho\rho}\eta^{xx}\partial_\rho\Phi\right) - \sqrt{-\eta}\left(\omega^2\eta^{tt}\eta^{xx} + k^2(\eta^{xx})^2 + \ell(\ell+2)\eta^{S3}\eta^{xx}\right)\Phi,\\
0 &= \partial_\rho(\sqrt{-\eta}\eta^{S3}\eta^{\rho\rho}\partial_\rho\Phi^\pm) - \Big(\sqrt{-\eta}\left(\eta^{S3}(\omega^2\eta^{tt}+k^2\eta^{xx}) + (\eta^{S3})^2(\ell+1)^2\right)\\
&\quad \pm 4\left(\rho^2+y^2\right)(\rho+yy')(\ell+1)\sqrt{\widetilde{g}}\Big)\Phi^\pm,
\end{aligned} \tag{5.156}$$

The first equation follows from (5.155a) and the second from (5.155b). Recalling the interpretation of the AdS_5 radial coordinate as a field theory energy scale, the background solutions $y(\rho)$ and $A_t(\rho)$ describe a RG flow. The coupling of some of the fluctuations corresponds to a mixing of the dual field theory operators under the background field induced RG flow. From the fact that χ, δA_t and δA_3 are coupled, we may infer that the dual field theory operators O_M, J^t, and J^{x^3} are mixed as well, whereas all other fluctuations are decoupled and so the dual meson operators do not mix with any other meson operator.

To check the validity of (5.156) let us compare to the zero density calculation. In this case the scalar fluctuations decouple form all other fluctuations, as can be seen in (5.89). In the finite density case the φ fluctuations are identical to the zero density case φ fluctuations, (5.152a) but the χ fluctuations do arise from different background fields, namely $y(\rho) = L$ and the finite density background solution (5.69). In particular for $m_q = 0$ the parameter ε vanishes and according to (5.154a) decoupling χ from all other fluctuations. Since φ and χ are the only fields on the D_7-brane worldvolume that are charged under the chiral $U(1)_\mathrm{R}$ symmetry, we expect that these fluctuations are decouple from the uncharged fields being in different representations of the $U(1)_\mathrm{R}$. For $m_q \neq 0$ the $U(1)_\mathrm{R}$ is broken so the χ fluctuation may couple to other fluctuations as can be seen in (5.154a) with $\varepsilon > 0$ and we may consider (5.154a) as the generalization to finite density of Table 5.2. Hoverer, due to the symmetries of the S^3 spherical harmonics the scalar fluctuations χ does decouple eventually, *c.f.* (5.155a). Comparing to Table 5.2 we see that (5.154b) describes type I gauge field fluctuations, whereas the type III gauge field fluctuations are modified by our different gauge choice and generalized to finite density in (5.154c). The type II gauge field fluctuations are characterized by scalar harmonics on the S^3 only in the Minkowski components, whereas in our case the finite density explicitly breaks Lorentz invariance to spatial rotation and translations. Thus, only the fluctuations of the gauge field components δA_1 and δA_2

still decouple, but for finite quark masses δA_t and δA_3 are coupled to χ.

The special case $\ell = 0$ yields an ill-defined Ansatz in (5.154c), similarly to the type III fluctuations. Equation (5.152b) and (5.152f) can be viewed as constraint equations arising from $\delta A_\rho = 0$ and $\delta A_i = 0$, respectively, which are trivially fulfilled in the case $\ell = 0$ and hence eliminating one of the constraints. The reduction in the constraints gives rise to an additional degree of freedom that can be identified with the zero sound mode. Therefore as an additional sanity check of our system of equations of motion (5.152), let us re-derive the zero sound mode found in [264, 268, 269].

Zero sound mode

The field theory zero sound mode appears as pole in the correlation functions of the dual $U(1)_\mathrm{B}$ current, which are singlets under the global $SO(4)$ symmetry. On the gravity side, the fluctuations of δA_t and δA_3 with $\ell = 0$ describe zero modes on the S^3. For finite flavor masses we have a non-trivial D_7-brane embedding which additionally allows a coupling to the $\ell = 0$ mode of the fluctuation χ [268]. Therefore our Ansatz (5.154a) should include a zero sound mode. Unfortunately, (5.152f) is trivially satisfied for $\ell = 0$ since the derivatives with respect to the S^3 directions are zero. Since we can view (5.152f) as a constraint equation for $\delta A_i = 0$, we expect to find an additional physical degree of freedom which is independent of the fluctuations following from (5.154a). Thus, we may take the simplest Ansatz involving only $\ell = 0$ S^3, plane-wave fluctuations χ, δA_t, and δA_3. Let us first define two functions, f_1 and f_2 given by

$$f_1 = \delta A_t - \varepsilon\chi, \qquad f_2 = \omega\eta^{\rho t}y'\chi + \omega\frac{\eta^{tt}}{\eta^{xx}}\delta A_t - k\delta A_3, \tag{5.157}$$

such that the constraint equation (5.152c) can be written as

$$\partial_\rho f_2 = \omega\partial_\rho\left(\frac{\eta^{tt}}{\eta^{xx}}\right) f_1, \tag{5.158}$$

and the relevant equations of motion (5.152b) and (5.152d) read

$$\begin{aligned} 0 = {}& \partial_a\left(\sqrt{-\eta}\eta_S^{ab}\eta^{xx}\left(1-\eta^{\rho\rho}\eta^{xx}y'^2\right)\partial_b\chi\right) + \partial_a\left(\sqrt{-\eta}\eta_S^{ab}\eta^{xx}\eta^{\rho t}y'\partial_b\delta A_t\right) \\ & + \omega\sqrt{-\eta}\left(\eta^{xx}\right)^2\eta^{\rho t}y' f_2, \end{aligned} \tag{5.159a}$$

$$0 = \partial_a\left(\sqrt{-\eta}\eta_S^{ab}\eta^{xx}\eta^{\rho t}y'\partial_b\chi\right) + \partial_a\left(\sqrt{-\eta}\eta_S^{ab}\eta^{xx}\left(\frac{\eta^{tt}}{\eta^{xx}}\right)\partial_b\delta A_t\right) + \omega\sqrt{-\eta}\eta^{tt}\eta^{xx}f_2. \tag{5.159b}$$

Constructing the linear combinations $-{}^1\!/_{(\eta^{\rho\rho}\eta^{xx})}\left[(5.159a) + \varepsilon(5.159b)\right]$ and using the identities

$$\eta^{\rho t}y' = \frac{1}{\varepsilon}\eta^{\rho\rho}\eta^{xx}y'^2 = -\varepsilon\left(1+\frac{\eta^{tt}}{\eta^{xx}}\right) = -\frac{1}{\varepsilon}\left(\eta^{\rho\rho}\eta^{xx}+\frac{\eta^{tt}}{\eta^{xx}}\right), \tag{5.160}$$

we obtain a simplified equation of motion for f_1,

$$\left(\varepsilon^2-1\right)\partial_\rho\left(\eta^{tt}/\eta^{xx}\right)\sqrt{-\eta}\partial_\rho f_1 + \partial_a\left(\sqrt{-\eta}\eta_S^{ab}\eta^{xx}\partial_b f_1\right) + \omega\sqrt{-\eta}\left(\eta^{xx}\right)^2 f_2 = 0. \tag{5.161}$$

Since the fields f_1 and f_2 are not gauge-invariant we need to take pure gauge solutions into account [270]. As an advantage of our approach we have to deal only with one dynamical equation (5.161) in contrast to [268]. As explained below (5.156) in the $m_q = 0$ or $\varepsilon = 0$ case

the chiral $U(1)_{\rm R}$ symmetry is restored and so χ decouples in (5.157) since it transforms in a different representation as the uncharged gauge field fluctuations δA_t and δA_3. In this case the scalar and gauge field fluctuations can be viewed as a finite-density generalization of the type II fluctuations in Table 5.2.

Following [264,268] we determine the zero sound dispersion relation by matching two solutions in different limits in their overlapping regime. First we solve the equation in the near horizon limit $\rho \to 0$ and expand this solution for small frequencies $\omega \ll \rho$ and momenta $k \ll \rho$ while keeping ω/k fixed. Secondly, we solve the equation in the low-frequency and low-momentum limit and then conduct a near horizon expansion of the solution. The infalling solutions near the horizon with rescaling $\omega \longrightarrow \omega\sqrt{1-\varepsilon^2}$ are given by

$$f_1 = c_1\, \mathrm{e}^{-\frac{\mathrm{i}\omega}{\rho}}\, \rho^7(1+\mathcal{O}(\rho)), \qquad f_2 = c_2\, \mathrm{e}^{-\frac{\mathrm{i}\omega}{\rho}}\, \rho^2(1+\mathcal{O}(\rho)), \tag{5.162}$$

where the horizon normalization constants are related by

$$c_2 = -\mathrm{i}\frac{6c}{\sqrt{1-\varepsilon^2}\varepsilon^2\mathscr{N}_{D_7}^2}c_1, \tag{5.163}$$

This is in agreement with the fact that we deal only with one dynamical equation, so to be consistent one of the two integration constants must be eliminated.

Taking the low-frequency and low-momentum limit of (5.161) we find

$$(1-\varepsilon^2)\partial_\rho\left(\frac{\eta^{tt}}{\eta^{xx}}\right)\sqrt{-\eta}\partial_\rho f_1 - \partial_\rho\left(\sqrt{-\eta}\eta_S^{\rho\rho}\eta^{xx}\partial_\rho f_1\right) = 0. \tag{5.164}$$

Introducing the dimensionless radial coordinate $\bar{\rho}$ defined as

$$\bar{\rho}^6 \equiv \rho^6\left(\frac{\mathscr{N}_{D_7}}{c}\right)^2\left(\frac{1}{\varepsilon^2}-1\right)^{-1}, \tag{5.165}$$

(5.164) is solved by

$$f_1(\bar{\rho}) = C\int_0^{\bar{\rho}} \mathrm{d}\bar{\rho}'\, \frac{\bar{\rho}'^6}{(\bar{\rho}'^6+1)^{3/2}}, \tag{5.166}$$

with C being an undetermined constant. Note that we can add an arbitrary constant to f_1 to generate a new solution since (5.164) depends only on $\partial_\rho f_1$. This constant has been already fixed by the matching condition of the near horizon limit and the low-frequency limit of the solution in (5.162) as explained above. Equation (5.166) can be converted into an incomplete Beta function or a hypergeometric function given by

$$f_1(\bar{\rho}) = -\frac{3\bar{\rho}^6+1}{6\bar{\rho}^5\sqrt{\rho^6+1}} + \frac{\sqrt{\bar{\rho}^6+1}}{6\bar{\rho}^5}\,{}_2F_1\left(-\frac{1}{3},1;\frac{1}{6};-\rho^6\right). \tag{5.167}$$

The function $f_2(\bar{\rho})$ can be determined by integrating the constraint equation

$$f_2(\bar{\rho}) = \omega\int_0^{\bar{\rho}} \mathrm{d}\bar{\rho}'\, \frac{6}{\bar{\rho}'^7(1-\varepsilon^2)}f_1(\bar{\rho}'). \tag{5.168}$$

The expansion of f_1 and f_2 near the AdS$_5$ boundary yields

$$\lim_{\rho\to\infty} f_1 = C\frac{\Gamma(\frac{7}{6})\Gamma(\frac{4}{3})}{\sqrt{\pi}}, \qquad \lim_{\rho\to\infty} f_2 = C\frac{2\omega}{1-\varepsilon^2}\frac{\Gamma(\frac{7}{6})\Gamma(\frac{4}{3})}{\sqrt{\pi}}. \tag{5.169}$$

The gauge-dependent fields change under gauge transformations of the following form $\delta A_b \to \delta A_b + \partial_b \alpha$. In order to preserve the gauge choice $\delta A_\rho = 0$, the pure gauge solution cannot depend on ρ and must be of plane-wave type, *i.e.*

$$\chi = 0, \qquad \delta A_t = \mathrm{i}\omega\, \mathrm{e}^{\mathrm{i}\omega t - ikx_3}\,, \qquad \delta A_3 = -\mathrm{i}k\, \mathrm{e}^{\mathrm{i}\omega t - ikx_3}\,. \tag{5.170}$$

Using the definitions of f_1 and f_2 in (5.157), the boundary expansion of the pure-gauge solution with $\eta^{tt}/\eta^{xx} \to -1$ reads

$$\lim_{\rho\to\infty} f_1 = \mathrm{i}\omega, \qquad \lim_{\rho\to\infty} f_2 = -\mathrm{i}(\omega^2 - k^2). \tag{5.171}$$

Near the boundary the leading contribution will be given by a linear combination of (5.169) and (5.171) that sources the dual field theory operators. For quasi-normal modes the leading contribution will vanish which amounts to the condition

$$\det \begin{pmatrix} C\frac{\Gamma(\frac{7}{6})\Gamma(\frac{4}{3})}{\sqrt{\pi}} & C\frac{2\omega}{1-\varepsilon^2}\frac{\Gamma(\frac{7}{6})\Gamma(\frac{4}{3})}{\sqrt{\pi}} \\ \mathrm{i}\omega & -\mathrm{i}(\omega^2 - k^2) \end{pmatrix} = \mathrm{i}C\frac{\Gamma(\frac{7}{6})\Gamma(\frac{4}{3})}{\sqrt{\pi}}\left(k^2 - \omega^2 - \frac{2\omega^2}{1-\varepsilon^2}\right) = 0, \tag{5.172}$$

from which we can read off the dispersion relation of the leading term contribution

$$\frac{\omega^2}{k^2} = \frac{1-\varepsilon^2}{3-\varepsilon^2} = \frac{\mu^2 - (2\pi\alpha')^4 m_q^2}{3\mu^2 - (2\pi\alpha')^4 m_q^2}, \tag{5.173}$$

This is in agreement with the zero sound dispersion relation found in [268] for finite m_q and [264] for $m_q = 0$ reading

$$\omega(k) = \pm\frac{1}{\sqrt{3}}k + \mathrm{i}\frac{k^2}{6\mu} + \mathcal{O}\left(k^3\right). \tag{5.174}$$

After gaining confidence in the correctness of our fluctuation equations by re-deriving the zero sound mode, we move on to further simplify the equations of motion in order to bring them in a suitable form for numerical treatments. Let us first introduce dimensionless variables in addition to (5.165), defined in terms of $barN \equiv \mathcal{N}_{D7}/c$ with length dimension three, *i.e.* $\left[\bar{N}\right]_{\text{length}} = 3$ following from (5.77) where $\left[m_q\right]_{\text{length}} = -1$. Thus, we define

$$\begin{aligned} \bar{\rho}^6 &\equiv \rho^6 \bar{N}^2 \left(\frac{1}{\varepsilon^2} - 1\right)^{-1}, & \bar{y}^6 &\equiv y^6 \bar{N}^2 \left(\frac{1}{\varepsilon^2} - 1\right)^{-1}, \\ \bar{\omega}^2 &\equiv \omega^2 \left[\bar{N}^2 / \left(\frac{1}{\varepsilon^2} - 1\right)\right]^{1/3}, & \bar{k}^2 &\equiv k^2 \left[\bar{N}^2 / \left(\frac{1}{\varepsilon^2} - 1\right)\right]^{1/3}. \end{aligned} \tag{5.175}$$

The background solution can be rewritten in terms of the dimensionless variables as

$$\bar{y}(\bar{\rho}) = \frac{1}{6}\left(\frac{1}{\varepsilon^2} - 1\right)^{-1/2} B\left(\frac{\bar{\rho}^6}{\bar{\rho}^6 + 1}; \frac{1}{6}, \frac{1}{3}\right), \tag{5.176}$$

$$\bar{y}'(\bar{\rho}) \equiv \frac{d\bar{y}}{d\bar{\rho}} = \frac{1}{\sqrt{(\bar{\rho}^6 + 1)\left(\frac{1}{\varepsilon^2} - 1\right)}}. \tag{5.177}$$

Rewriting the equations of motion in a form susceptible for a singular point analysis, the final version of our system of equations (5.156) reads

$$\Phi'' + p_1(\bar{\rho})\Phi' + q_1(\bar{\rho},\bar{\omega},\bar{k},\ell)\Phi = 0, \tag{5.178a}$$

$$\Phi^{\pm\prime\prime} + p_2(\bar{\rho})\Phi^{\pm\prime} + q_2^{\pm}(\bar{\rho},\bar{\omega},\bar{k},\ell)\Phi^{\pm} = 0, \tag{5.178b}$$

where

$$p_1(\bar{\rho}) = \frac{3\bar{\rho}^5}{1+\bar{\rho}^6}, \tag{5.179a}$$

$$q_1(\bar{\rho},\bar{\omega},\bar{k},\ell) = \frac{-\ell(\ell+2)\bar{\rho}^4}{1+\bar{\rho}^6} + \frac{\bar{\omega}^2(1+\bar{y}'^2)}{(\bar{\rho}^2+\bar{y}^2)^2} - \frac{\bar{k}^2\bar{\rho}^6}{(1+\bar{\rho}^6)(\bar{\rho}^2+\bar{y}^2)^2}, \tag{5.179b}$$

$$p_2(\bar{\rho}) = \frac{\bar{\rho}^2(2+5\bar{\rho}^6)+(-2+\bar{\rho}^6)\bar{y}^2+4\bar{\rho}(1+\bar{\rho}^6)\bar{y}\bar{y}'}{\bar{\rho}(1+\bar{\rho}^6)(\bar{\rho}^2+\bar{y}^2)}, \tag{5.179c}$$

$$\begin{aligned} q_2^{\pm}(\bar{\rho},\bar{\omega},\bar{k},\ell) = & -\frac{(\ell+1)^2\bar{\rho}^4}{1+\bar{\rho}^6} \mp 4(\ell+1)\sqrt{\frac{\bar{\rho}^6}{1+\bar{\rho}^6}}\frac{\bar{\rho}+\bar{y}\bar{y}'}{\bar{\rho}(\bar{\rho}^2+\bar{y}^2)} \\ & + \frac{\bar{\omega}^2(1+\bar{y}'^2)}{(\bar{\rho}^2+\bar{y}^2)^2} - \frac{\bar{k}^2\bar{\rho}^6}{(1+\bar{\rho}^6)(\bar{\rho}^2+\bar{y}^2)^2}. \end{aligned} \tag{5.179d}$$

The numerical solutions and in particular the quasi-normal mode analysis conducted in Section 5.3 allows us to obtain insights into the physical nature of the modes and the existence of any instabilities as explained above.

Finally, we want to elucidate the connection between the fluctuations and the near horizon AdS_2 region [254, 271–273] arising in the limit $\bar{\rho} \to 0$.

$$\bar{y}(\bar{\rho}) = \frac{\bar{\rho}}{\sqrt{\frac{1}{\varepsilon^2}-1}} + \mathcal{O}\left(\bar{\rho}^7\right). \tag{5.180}$$

Let us first consider the equation (5.178a) for $\Phi(\bar{\rho})$. The scaling behavior of (5.179b) is as follows: the dominant term in $q_1(\bar{\rho},\bar{\omega},\bar{k},\ell)$ scales at leading order as $\bar{\omega}^2/\bar{\rho}^4$, followed by $\ell(\ell+2)\bar{\rho}^4$ and $\bar{k}^2\bar{\rho}^6$. Since only the time and radial coordinates appear in the AdS_2 we expect an suppression of the linear momenta of the Minkowski directions and the angular momenta of the S^3 directions. According to (5.179a) in the near horizon limit $p_1(\bar{\rho}) \to 3\bar{\rho}^5$ is only of sub-leading order and hence can be removed from (5.178a). Therefore, in the near horizon limit $\bar{\rho} \to 0$ (5.178a) is given at leading order as

$$\Phi'' + \frac{\bar{\omega}^2}{\bar{\rho}^4}(1-\varepsilon^2)\Phi = 0. \tag{5.181}$$

With the rescaling $\Phi(\bar{\rho}) \equiv \bar{\rho}\hat{\Phi}(\bar{\rho})$ (5.181) can be written as

$$\hat{\Phi}'' + \frac{2}{\bar{\rho}}\hat{\Phi}' + \frac{\bar{\omega}^2}{\bar{\rho}^4}(1-\varepsilon^2)\hat{\Phi} = 0, \tag{5.182}$$

which is identical to the equation of motion for a massless scalar in AdS_2 (4.261), with frequency $\bar{\omega}\sqrt{1-\varepsilon^2}$.

Similarly, the near horizon limit $\bar{\rho} \to 0$ of the $\Phi^{\pm}(\bar{\rho})$ equation (5.178b) is constructed by looking at the leading contribution in $q_2(\bar{\rho}, \bar{\omega}, \bar{k}, \ell)$ (5.179d) which yields the identical result as before. The coefficient function $p_2(\bar{\rho})$ behaves in the near horizon limit $\bar{\rho} \to 0$ as $p_2(\bar{\rho}) \to 2/\bar{\rho}$ and thus to leading order (5.178b) reads

$$\Phi^{\pm\prime\prime} + \frac{2}{\bar{\rho}}\Phi^{\pm\prime} + \frac{\bar{\omega}^2}{\bar{\rho}^4}(1-\varepsilon^2)\Phi^{\pm} = 0, \tag{5.183}$$

which is identical to (5.182) and again a massless scalar equations in AdS_2 with frequency $\bar{\omega}\sqrt{1-\varepsilon^2}$, where the rescaling by a factor of $\bar{\rho}$ is not even necessary. The emergent near horizon AdS_2 region is intimately related to a non-trivial profile of $A_t(\bar{\rho})$ which corresponds to a finite density on the field theory side. Zero density solutions are Lorentz invariant, hence the spatial momentum $\mathbf{k}$ cannot be suppressed in the near horizon limit with respect to the frequency ω, since $-k_\mu k^\mu = \omega^2 - \mathbf{k}^2$. Due to the appearance of a massless scalar field in the emergent AdS_2 spacetime which cannot violated the AdS_2 BF bound given by $-1/4$, we cannot obtain an instability in (5.182) and (5.183) for all values of $\bar{k}$, ε, and ℓ. Nonetheless, there are two known deformations that are capable of triggering instabilities without violating the AdS_2 BF bound: a sufficiently large $U(1)_B$ magnetic field, introducing a spontaneous breaking of the chiral $U(1)_R$ symmetry for massless flavor fields [274–276], and an enhancement of the flavor symmetry to include an isospin chemical potential via the Cartan generator of $U(1)_B \times SU(2)$. In the latter case an additional coincident D_7-brane needs to be introduced which causes vector meson condensation and leads to a p-wave superconductor or superfluid state [215–217, 222]. Further evidence comes from bosonic worldvolume fluctuations with zero sound modes, that "see" an effective AdS_2 near horizon region [254]. This follows from the fact that after rescaling f_1' by a factor of ρ^7 and f_2 by a factor of ρ^2 the fluctuations obey again an equation of motion identical to a massless scalar in AdS_2.

5.3. The Spectrum of Quasi-Normal Modes in Finite Density Systems

Overview

- Matching method of inner and outer horizon used for small frequency and momentum expansion.
- Irregular singular points in equations of motion
  ⟶ Zig-Zag method devised to disentangle in-going and out-going boundary conditions at the horizon.
- No instabilities found ⟶ existence of "R-spin" diffusive mode.

Mesonic operators of the dual field theory correspond to fluctuation of the D_7-brane worldvolume fields. According to the holographic dictionary of the gauge/gravity duality or more precisely, the AdS/CFT correspondence the on-shell bulk action is identified with the field theory generating functional for correlation functions. The dual two-point functions are established by the linearized solutions the to bulk equations of motion for the fluctuations (5.178a) and (5.178b). In the real-time formalism the Lorentz signature allows for two different correlators, the advanced and the retarded Green function which corresponds to different near horizon

boundary conditions of the bulk field, namely out-going and in-going waves, respectively. Physically, we are interested in retarded Green functions therefore we will impose in-going boundary conditions in the near-horizon region corresponding to waves propagating into the deep interior of AdS_5 [78]. Since we are only interested in the stability of our ground state, *i.e.* the given fixed gravity background describing finite density at zero temperature, it is sufficient to compute the eigenfrequencies of the linear operators in (5.178a) and (5.178b), instead of the full correlator. In general the eigenfrequencies are related to quasi-normal modes with complex eigenvalues due to the "leakage" of the standing wave across the AdS_5 Poincaré horizon. This is in agreement with the field theory expectation of mesons with finite lifetime in a finite density background. The quasi-normal modes are dual to poles in the retarded Green functions and hence an instability appears as a pole in the lower complex frequency half-plane[12] yielding a fluctuation with uncontrolled exponential amplitude. Technically, the main difficulty arise from the presence of irregular singular points in (5.178a) and (5.178b) in order to apply the known recipes to compute quasi-normal modes. Therefore, we need to deal with the irregular singular points by employing a tricky combination of analytical and numerical techniques. The analytical low-frequency form of the correlators are determined by a matching technique following [261], which is explained in detail in Section 5.3.1. Furthermore, in Section 5.3.2, we discuss the nature of the singular points and review one of the main approaches to deal with such points namely, Leaver's method, and explain the difficulties that arise in employing this method for the case at hand. Finally, we present our own numerical method geared towards the computation of the quasi-normal mode spectra, which are discussed in the final Section 5.3.3

5.3.1. Low-frequency expansion of fluctuations

Instabilities are signaled by quasi-normal modes crossing into the lower-half of the complex frequency plane at small absolute frequency. Following [261] the exact from of the retarded Green functions can be obtained in the low-frequency limit as follows: Divide the radial direction into two regions dubbed the "inner" and the "outer" regions which are defined as $\bar{\rho} \ll 1$ and $\Omega/\bar{\rho} \ll 1$, respectively, and the overlap of both regions is given for small frequencies $\Omega \ll 1$.. Note that the inner region is given by the emergent AdS_2 near horizon geometry, suggesting the emergence of a finite-density $(0+1)$-dimensional effective CFT at low energies. Applying the holographic dictionary to the AdS_2 geometry itself, yields for every AdS_2 field a dual operator of the $(0+1)$-dimensional CFT living at the outer boundary which is matched to the outer region. Massless fields in the inner AdS_2 region are related to marginal dimension one scalar operators of the $(0+1)$-dimensional CFT with Green functions encoding the low-frequency behavior of the full Green function as will be explicitly shown. As derived in the last section, *all* bosonic fluctuations of the D_7-brane fields obeyed identical equations of motion of a massless scalar in the AdS_2 region independent of their other quantum numbers, such as the spin, linear momentum in the Minkowski directions or angular momentum in the S^3 directions. Therefore, the field theory mesonic operators are dual to a marginal scalar operators of an effective low-energy $(0+1)$-dimensional CFT independent of their spin, momentum or $SO(4)$ charges.

Let us start with the equation of motion for $\Phi(\bar{\rho})$ in the inner region given by (5.181). Using the rescaled version (5.182) with $\Phi(\bar{\rho}) \longrightarrow \bar{\rho}\Phi(\bar{\rho})$ the in-going solution expanded $\Omega \ll \bar{\rho}$ in reads

$$\hat{\Phi}(\bar{\rho}) = \mathrm{e}^{-\frac{\mathrm{i}\Omega}{\bar{\rho}}} = 1 - \frac{\mathrm{i}\Omega}{\bar{\rho}} + \mathcal{O}\left(\frac{\Omega^2}{\bar{\rho}^2}\right), \qquad \Omega \equiv \bar{\omega}\sqrt{1-\varepsilon^2}. \tag{5.184}$$

[12] Note again the different sign convention, such that stable modes appear in the upper-half of the complex frequency plane, conversely to the conventions in Section 2.2.

We find a massless AdS_2 scalar, dual to a dimension-one operator in the non-normalizable leading term and according to the holographic dictionary we identify the coefficient of the normalizable sub-leading term as the expectation value of the dimension one-operator. The two-point correlator for linearized equations or more precisely in linear response is given by the ratio of the coefficient of the normalizable to the non-normalizable mode which yields the expected result of $\mathrm{i}\Omega$ [261]. The complete inner region expansion yields

$$\Phi(\bar{\rho}) = \bar{\rho}\,\mathrm{e}^{-\frac{i\Omega}{\bar{\rho}}}\,(1+\mathcal{O}(\bar{\rho}^5)), \tag{5.185}$$

which can be approximated for small frequencies as

$$\Phi(\bar{\rho}) \approx \bar{\rho} - i\Omega. \tag{5.186}$$

The outer region expansion is obtained by the the leading-order small-frequency solution from (5.178a) in the limit $\bar{\omega} \to 0$ with two linearly independent solutions denoted by $\Phi_0(\bar{\rho})$ and $\Phi_1(\bar{\rho})$. A generic solution may be constructed by linear combinations of $\Phi_0(\bar{\rho})$ and $\Phi_1(\bar{\rho})$, with arbitrary coefficients depending on all parameters, *i.e.* $(\Omega, \bar{k}, \varepsilon, \ell)$. Imposing the matching conditions between the inner region and outer region given by $\Phi_0(\bar{\rho}) \to 1$ and $\Phi_1(\bar{\rho}) \to \bar{\rho}$ as $\bar{\rho} \to 0$ fixes the Ω-dependence of the ratio of the coefficients, so at small frequencies we find

$$\Phi(\bar{\rho}) = \Phi_1(\bar{\rho}) - \mathrm{i}\Omega\Phi_0(\bar{\rho}). \tag{5.187}$$

We find a normalizable and a non-normalizable solution in the vicinity of the AdS_5 boundary denoted by $\Phi_{\mathrm{V}}(\bar{\rho})$ identified as the source and $\Phi_{\mathrm{S}}(\bar{\rho})$ identified as the vacuum expectation value, respectively. In general, the boundary solutions are connected to the horizon by a linear map of the following form

$$\begin{aligned} \Phi_1(\bar{\rho}) &= a_1\Phi_{\mathrm{S}}(\bar{\rho}) + b_1\Phi_{\mathrm{V}}(\bar{\rho}), \\ \Phi_0(\bar{\rho}) &= a_0\Phi_{\mathrm{S}}(\bar{\rho}) + b_0\Phi_{\mathrm{V}}(\bar{\rho}), \end{aligned} \tag{5.188}$$

where the $(\bar{k}, \varepsilon, m)$-dependence of the coefficients a_1, b_1, a_0, b_0 is omitted. Close to the AdS_5 boundary (5.187) reduces to

$$\Phi(\bar{\rho}) = (a_1 - \mathrm{i}\Omega a_0)\Phi_{\mathrm{S}}(\bar{\rho}) + (b_1 - \mathrm{i}\Omega b_0)\Phi_{\mathrm{V}}(\bar{\rho}), \tag{5.189}$$

where the coefficient of the first term is related to the source and the coefficient of the second term to the expectation value. Thus, the retarded Green function $G(\Omega)$ is given by the ratio

$$G(\Omega) = \frac{b_1 - \mathrm{i}\Omega b_0}{a_1 - \mathrm{i}\Omega a_0}. \tag{5.190}$$

Note that the retarded Green function additionally depends on all the omitted parameters $(\bar{k}, \varepsilon, \ell)$. The leading small frequency behavior of all fluctuations in (5.178a) is completely determined by (5.190) which in turn is controlled by the $(0+1)$-dimensional CFT Green function given by $-\mathrm{i}\Omega$.

For the other fluctuations the analysis is virtually identical, with the main difference that in the inner region we do not need to rescale the field by a factor of $\bar{\rho}$, so (5.184) is the inner region solution instead of (5.186). Again the outer region expansion with $\Phi_0^{\pm}(\bar{\rho})$ and $\Phi_{-1}^{\pm}(\bar{\rho})$ is matched with the inner region solution and we can relate the the normalizable and non-normalizable solutions in terms of a linear transformation

$$\begin{aligned} \Phi_0^{\pm}(\bar{\rho}) &= a_0^{\pm}\Phi_{\mathrm{S}}^{\pm}(\bar{\rho}) + b_0^{\pm}\Phi_{\mathrm{V}}^{\pm}(\bar{\rho}), \\ \Phi_{-1}^{\pm}(\bar{\rho}) &= a_{-1}^{\pm}\Phi_{\mathrm{S}}^{\pm}(\bar{\rho}) + b_{-1}^{\pm}\Phi_{\mathrm{V}}^{\pm}(\bar{\rho}). \end{aligned} \tag{5.191}$$

The corresponding retarded Green function for small frequencies read

$$G^{\pm}(\Omega) = \frac{b_0^{\pm} - \mathrm{i}\Omega b_{-1}^{\pm}}{a_0^{\pm} - \mathrm{i}\Omega a_{-1}^{\pm}}. \tag{5.192}$$

All coefficients a_1, a_0, b_1, b_0 and $a_0^{\pm}$, $a_{-1}^{\pm}$, $b_0^{\pm}$, $b_{-1}^{\pm}$ are necessarily real, which follows directly from the zero frequency forms of (5.178a) and (5.178b). In order to determine these coefficient, we need to find the solution of $\Phi(\bar{\rho})$ and $\Phi(\bar{\rho})^{\pm}$. We succeeded only to determine their numerical solution by the standard prescription which allows us to determine the coefficient at vanishing frequency $\Omega = 0$, applied extensively in Section 4.5. Luckily, in the zero frequency case the irregular singular point $\bar{\rho} = 0$ reduces to a regular singular point in (5.178a) and (5.178b), that can be solved without introducing any special mathematical methods. Thus, we numerically compute the coefficient for different values of $(\bar{k}, \varepsilon, \ell)$ and check for instabilities via pole structure of the Green functions (5.190) and (5.192). Taking the $\Omega \to 0$ limit into account we find poles crossing the real line for ${}^{a_1}\!/_{a_0} \to 0^-$ or ${}^{a_0^{\pm}}\!/_{a_{-1}^{\pm}} \to 0^-$. Our numerical analysis is restricted to modes with $\ell \leqslant 2$ related to the dimension of the dual operator such that a larger ℓ corresponds to a higher dual operator dimension. Heuristically, in field theories we expect instabilities to be triggered by the most relevant operators, *i.e.* the operators with the lowest scaling dimension. This is in general true for phase transitions, where the critical point is controlled by a CFT, *e.g.* quantum critical points and related quantum critical regions. If relevant deformations fail to induce a RG flow from the mixed fixed point, describing the critical point, to a stable fixed point, describing a different phase of matter (*c.f.* Figure 2.4), it is highly unlikely that less relevant operators might succeed. Thus, we do note expect instabilities in higher ℓ modes. Studying numerically the parameter range of $\epsilon \in (0, 0.9)$ and $\bar{k} \in (0, 50)$ of the $\ell = 0, 1$ modes of $\Phi(\bar{\rho})$, the $\ell = 1$ mode of $\Phi^{+}(\bar{\rho})$ and the $\ell = 1, 2, 3$ modes of $\Phi^{-}(\bar{\rho})$, we did not detect any instabilities. In fact the results for $\Phi(\bar{\rho})$ and $\Phi^{+}(\bar{\rho})$ do not exhibit any particularly interesting features. However, the modes $\ell = 1, 2, 3$ of $\Phi^{-}(\bar{\rho})$ yields an interesting dispersion relation coming from

$$\frac{a_0^-}{a_{-1}^-} \to D(\varepsilon)\bar{k}^2 > 0 \quad \text{for} \quad \bar{k} \to 0. \tag{5.193}$$

This is a typical diffusion mode with dispersion relation $\Omega = \mathrm{i}D(\varepsilon)\bar{k}^2$ and numerically computable diffusion constant $D(\varepsilon)$ as shown in Figure 5.3 For example the dual operator to $\Phi^{-}(\bar{\rho})$ with $m = 1$ is a dimension two scalar operator in the $SU(2)_{\mathrm{R}}$ vector representation [260] and hence can be written explicitly in terms of a $SU(2)_{\mathrm{R}}$ doublet of squarks

$$O^I = Q^{\alpha\dagger}\sigma^I_{\alpha\beta}Q^{\beta}, \tag{5.194}$$

where the doublet is defined as $Q^{\alpha} = (q, \tilde{q}^{\dagger})^{\mathsf{T}}$ and $\sigma^I_{\alpha\beta}$ denote the $SU(2)_R$ Pauli matrices.

5.3.2. A Numerical method for irregular singular points: The zig-zag method

The presence of irregular singular points in (5.178a) and (5.178b) is a main obstacle to compute the quasi-normal modes numerically, by the usual recipe. More precisely, the irregular singular point arises at $\bar{\rho} = 0$ since the coefficients $p_1(\bar{\rho})$ and $p_2(\bar{\rho})$ possess a simple pole but $q_1(\bar{\rho}, \bar{\omega}, \bar{k}, \ell)$ and $q_2(\bar{\rho}, \bar{\omega}, \bar{k}, \ell)$ a quartic pole. In the near horizon limit of $\Phi(\bar{\rho})$ (5.181) we find two solutions $\bar{\rho}\,\mathrm{e}^{\pm \mathrm{i}\Omega/\bar{\rho}}$, one in-going with negative sign and the out-going with positive sign. Applying our recipe of imposing the in-going wave boundary condition at a small yet finite $\bar{\rho}$, and numerically integrate the equation of motion we find a solution that is extremely sensitive under variations of

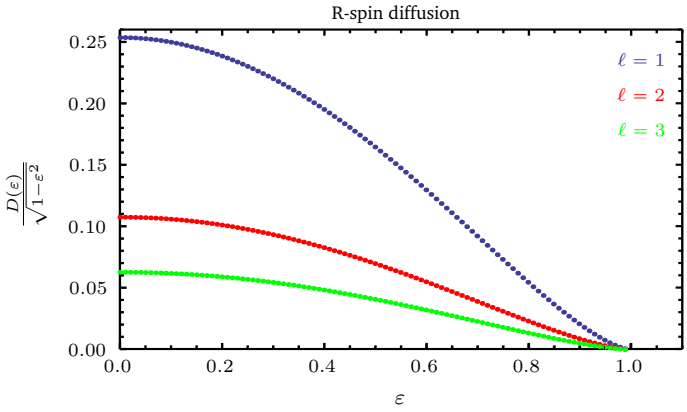

Figure 5.3. The "diffusion constant" $D(\varepsilon)/\sqrt{1-\varepsilon^2}$ defined in (5.206) found in the $\ell = 1, 2, 3$ quasi-normal modes of $\Phi^-(\bar{\rho})$ for $\bar{k} \to 0$ plotted against the ratio $\varepsilon = (2\pi\alpha')m_q/\mu$. The corresponding dual operator is a Lorentz scalar in the vector representation of the $SU(2)_{\mathrm{R}}$. Thus, physically we may view this mode as a "R-spin diffusion" adding to the zero sound mode evidence that holographic quantum critical matter may be described by an effective theory resembling hydrodynamics very closely. Furthermore, we can even draw an analogy to "spin diffusion" modes in real world itinerant electron systems in the spirit of [277, 278]. Low energy electronic systems exhibit strong suppression of the spin-orbit interaction and thus spin rotations decouple entirely from spacetime rotations, rendering the electron spin an internal $SU(2)$ quantum number and hence a global symmetry with a well-defined rate of expansion/diffusion.

the deep interior starting point $\bar{\rho}$. Thus, the solutions still depend on the deep interior properties of the equation of motion and hence are unphysical. For quasi-normal modes with complex frequencies, we find an exponentially growing in-going solution while the out-going solution is exponentially suppressed as $\bar{\rho} \to 0$. However, the near horizon series expansion

$$\Phi(\bar{\rho}) = \bar{\rho}\, \mathrm{e}^{-\frac{\mathrm{i}\Omega}{\bar{\rho}}} \left(1 + \mathcal{O}\left(\bar{\rho}^5\right)\right), \tag{5.195}$$

is only accurate for sufficiently small $\bar{\rho}$ and thus the numerical error is effectively susceptible to the exponentially suppressed solution out-going solution rendering the initial values of the integration inaccurate. To deal with such problems some techniques have been invented [261, 279–282] *i.a.* the already used matched asymptotic expansions at small frequency. The matrix, determinant or Leaver's method [279, 281] generically allows to deal with arbitrary frequencies. For example, extracting the leading behavior of $\Phi(\bar{\rho})$ near each singular point, we may set $\Phi(\bar{\rho}) = \bar{\rho}\, \mathrm{e}^{-\mathrm{i}\Omega/\bar{\rho}}\, \tilde{\Phi}(\bar{\rho})$ and insert this Ansatz into (5.178a) to obtain an equation for $\tilde{\Phi}(\bar{\rho})$. Solving this equation by choosing a non-singular point, such that the series expansion of $\tilde{\Phi}(\bar{\rho})$ about this point has an radius of convergence which includes the the two singular points at the horizon and at the boundary. Choosing a general Ansatz for the series expansion with coefficients c_p depending on $\bar{\omega}$, $\bar{k}$, ε, and ℓ, up to order n,

$$\tilde{\Phi}(\bar{\rho}) = \sum_{p=0}^{n} c_p (\bar{\rho} - \tilde{\rho})^p, \tag{5.196}$$

we obtain $n + 1$ equations for the $n + 1$ unknown coefficients c_p that may be written as a linear transformation of the form

$$\sum_{p=0}^{n} \mathcal{M}_{qp} c_p = 0, \tag{5.197}$$

with the matrix $\mathcal{M}_{qp}$ being dependent on $\bar{\omega}$, $\bar{k}$, ε, and ℓ. The quasi-normal modes are determined by the roots of the determinant, *i.e.* $\det \mathcal{M}_{qp} = 0$, and for sufficiently large n the results should converge to trustworthy values, which we identify with the actual physical values. This method is working perfectly for fields in the extremal AdS-Reissner-Nordström black hole [253,281,283] due to the fact that for charged fields the coefficients c_p, up to some order n, exhibit a nine-term recurrence relation yielding a diagonal band matrix $\mathcal{M}_{qp}$ with a width of nine and hence allow for an fast and efficient calculation of $\det \mathcal{M}_{qp} = 0$ even for large values of n. Yet in our case a difficulty arise: the matrix $\mathcal{M}_{qp}$ is generically an upper triangular matrix such that the computation of its determinant becomes increasingly difficult for larger values of n. In order to have more efficient numerics we devised an method adapted to our specific problem.

i. Choose an arbitrary value for the frequency $\bar{\omega} = \bar{\omega}^{\text{test}}_{\text{QNM}}$ which needs to be tested if it is a quasi-normal mode.,

ii. Analytically continue the radial coordinate $\bar{\rho}$ to complex values in such a way that the phase of the radial coordinate coincides with the phase of the arbitrary chosen frequency, *i.e.* $\arg \bar{\rho} = \arg \bar{\omega}^{\text{test}}_{\text{QNM}}$. This reduces the exponent of $\bar{\rho} e^{\pm i\Omega/\bar{\rho}}$ to purely real values, such that the in-going and the out-going solutions become purely oscillatory and hence are simple to disentangle.

iii. Specify a contour that connects the origin of the complex $\bar{\rho}$ plane with infinity on the real $\bar{\rho}$ axis in such a way that we start with the phase given by $\arg \bar{\rho} = \arg \bar{\omega}^{\text{test}}_{\text{QNM}}$ and avoid any branch cuts appearing in the complex $\bar{\rho}$ plane.

Unfortunately, there are branch cuts introduced by the background solution $\bar{y}(\bar{\rho})$ of (5.177) in the coefficients $p_2(\bar{\rho})$, $q_1(\bar{\rho}, \bar{\omega}, \bar{k}, m)$, and $q_2(\bar{\rho}, \bar{\omega}, \bar{k}, m)$. The solution (5.177) written in terms of an incomplete Beta function, can be transformed into a hypergeometric function

$$B\left(\frac{\bar{\rho}^6}{\bar{\rho}^6+1}; \frac{1}{6}, \frac{1}{3}\right) = \frac{6\bar{\rho}}{(1+\bar{\rho}^6)^{1/6}} {}_2F_1\left(\frac{1}{6}, \frac{2}{3}; \frac{7}{6}; \frac{\bar{\rho}^6}{1+\bar{\rho}^6}\right). \tag{5.198}$$

The hypergeometric function exhibit a branch cuts for arguments running from one to infinity. In the complex $\bar{\rho}$ plane we thus find six branch cuts corresponding to $\bar{\rho} = \infty$ and $\bar{\rho}^6 + 1 = 0$. In order to avoid crossing these branch cuts, the integration contour follows a "zig-zag" line , where for small values of $|\bar{\rho}|$ we follow the $\arg \bar{\rho} = \arg \bar{\omega}^{\text{test}}_{\text{QNM}}$ line up to the point where the contribution from the out-going solution is negligible, but still smaller than the starting point of the branch cut $|\bar{\rho}| = 1$. Then, we turn to the real $\bar{\rho}$ axis moving along a segment of a circle with fixed radius $|\bar{\rho}|$ until we reach $\arg \bar{\rho} = 0$. The final segment of the integration contour is simply given by the real $\bar{\rho}$-axis to $\bar{\rho} = \infty$. For the actual numerical integration we will stop at a sufficiently large value of $\bar{\rho}$. The complete integration contour along with the branch cuts of the hypergeometric function is displayed in Figure 5.4. At each of the turning points $\bar{\rho}_1$ and $\bar{\rho}_2$ we need to specify matching conditions for combining the solutions on the three segments of the integration contour. For an analytical solution in the complex $\bar{\rho}$ plane the matching condition at the turning points of a second order differential equation read

$$\begin{aligned} \Phi_{\text{I}}(\bar{\rho}_1) &= \Phi_{\text{II}}(\bar{\rho}_1), & \Phi'_{\text{I}}(\bar{\rho}_1) &= \Phi'_{\text{II}}(\bar{\rho}_1), \\ \Phi_{\text{II}}(\bar{\rho}_2) &= \Phi_{\text{III}}(\bar{\rho}_2), & \Phi'_{\text{II}}(\bar{\rho}_2) &= \Phi'_{\text{III}}(\bar{\rho}_2), \end{aligned} \tag{5.199}$$

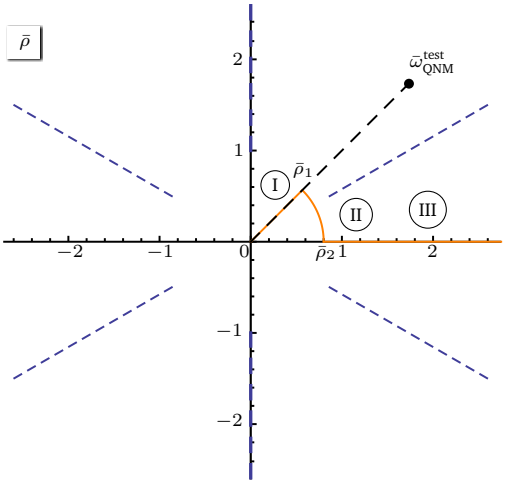

Figure 5.4.
Illustration of the zig-zag contour: The complex branch cuts of the coefficients from equations (5.178a) and (5.178b) displayed as dashed blue lines (- - -) in the complex $\bar{\rho}$ plane. The contour of integration is indicated by the solid orange curve (—) and the respective segments are labeled as I, II and III between the turning points denoted by $\bar{\rho}_1$ and $\bar{\rho}_2$. The "test" quasi-normal frequency with finite phase $\arg\left(\bar{\omega}^{\text{test}}_{\text{QNM}}\right)$ is shown as dashed black line (- - -) that ends at the dot labeled $\bar{\omega}^{\text{test}}_{\text{QNM}}$.

where the derivatives are taken along the direction of the corresponding segment of the contour. As an example, let is explicitly illustrate our method by considering $\Phi(\bar{\rho})$. First, we determine the near horizon expansion of $\Phi(\bar{\rho})$ given by

$$\Phi(\bar{\rho}) = \mathrm{e}^{-\mathrm{i}\frac{\bar{\omega}}{\bar{\rho}}}\left(\bar{\rho} + \sum_{p=6}^{\infty} \alpha_p \bar{\rho}^p\right), \tag{5.200}$$

where the constant coefficients are recursively computed, starting from α_6 up to the order p_{max}. For our numerical integration the coefficients up to α_{12} are sufficient to start the computation at finite $\bar{\rho} \leqslant 0.1$. As we explicitly checked, the numerical results are extremely stable under variations of the starting value. After integrating the equations of motion numerically along the zig-zag contour shown in Figure 5.4, we read off the leading normalizable and subleading non-normalizable solution at the AdS_5 boundary by fitting the numerical solution for sufficiently large $\bar{\rho}$ to the boundary expansion

$$\Phi(\bar{\rho}, \bar{\omega}, \bar{k}) \approx A(\bar{\omega}, \bar{k})\Phi_{\text{S}}(\bar{\rho}) + B(\bar{\omega}, \bar{k})\Phi_{\text{V}}(\bar{\rho}), \tag{5.201}$$

with

$$\Phi_S(\bar{\rho}) = 1 + \frac{(\bar{\omega}^2 - \bar{k}^2)\log\bar{\rho}}{2\bar{\rho}^2} + \mathcal{O}(\bar{\rho}^{-3}), \qquad \Phi_V(\bar{\rho}) = \bar{\rho}^{-2} + \mathcal{O}(\bar{\rho}^{-3}). \tag{5.202}$$

for $\ell = 0$. For general ℓ, the boundary expansion reads

$$\Phi_{\text{S}}(\bar{\rho}) \approx \bar{\rho}^{\ell}, \qquad \Phi_{\text{V}}(\bar{\rho}) \approx \bar{\rho}^{-\ell-2} \tag{5.203}$$

which agrees with the boundary expansion of the scalar and type II and III gauge fluctuations in the zero density case. The coefficients $A(\bar{\omega}, \bar{k})$ and $B(\bar{\omega}, \bar{k})$ in (5.201) are identified with the source and the vacuum expectation value of the dual operator, respectively. According to the holographic dictionary linear response functions are defined as the ratio of the expectation value and the source. The poles of the retarded Green function is thus given by $B(\bar{\omega},\bar{k})/A(\bar{\omega},\bar{k})$ and the quasi-normal modes are located at the zeros of $|A(\bar{\omega},\bar{k})/B(\bar{\omega},\bar{k})|$. The quasi-normal search is conducted by a minimization procedure implemented in Mathematica Code D.4 over the complex $\bar{\omega}$ plane for different fixed values of $(\bar{k}, \epsilon, \ell)$. The overall accuracy we aimed for so far, allows us

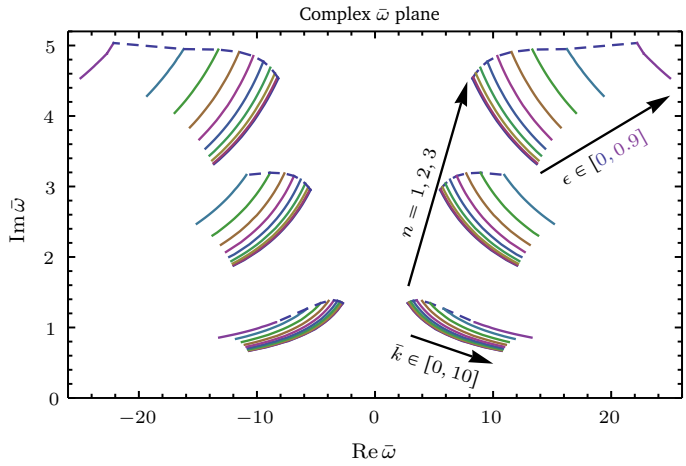

Figure 5.5. The curves show the location of the first three quasi normal modes of $\Phi(\bar{\rho})$ for $\ell = 0$, labeled by $n = 1, 2, 3$. Upon varying the momentum $\bar{k}$ indicated by the solid colored lines the quasi-normal modes are shifted sideways while for discrete variations in $\varepsilon \sim {}^{m_q}/_{\mu}$ (ten for $n = 1, 3$ and nine for $n = 2$ running from 0 to 0.9, and 0.8, respectively, with a step size of 0.1) we choose different colors. The dashed line indicates the behavior of the quasi-normal modes for vanishing momenta as ε is increased. There are no quasi-normal modes in the lower complex $\bar{\omega}$ half-plane indicating a stable ground state of the system. Since only $\bar{\omega}^2$ enters the equations of motion, we find a mirror symmetric spectrum in the complex $\bar{\omega}$ plane.

to treat values between 10^{-4} and 10^{-2} as sufficiently small to be considered zero, effectively.

The computational procedure of $\Phi^{\pm}(\bar{\rho})$ follows exactly the same steps, except that the boundary expansion of $\Phi^{\pm}(\bar{\rho})$for arbitrary ℓ is given by

$$\Phi^{+}_{\mathrm{S}}(\bar{\rho}) \approx \bar{\rho}^{\ell+1}, \qquad \Phi^{+}_{\mathrm{V}}(\bar{\rho}) \approx \bar{\rho}^{-\ell-5}, \tag{5.204}$$

$$\Phi^{-}_{\mathrm{S}}(\bar{\rho}) \approx \bar{\rho}^{\ell-3}, \qquad \Phi^{-}_{\mathrm{V}}(\bar{\rho}) \approx \bar{\rho}^{-\ell-1}. \tag{5.205}$$

As expected the leading behaviors of $\Phi^{\pm}_{\mathrm{V}}(\bar{\rho})$ agree with the type I fluctuations of Table 5.2.

The zig-zag method proved to be extremely stable under variations of the initial starting value $\rho \tilde{\approx} 10^{-1}$. As a more rigorous test of the stability of the zig-zag method we compare our numerically determined quasi-normal modes of $\Phi^{-}(\bar{\rho})$ to the R-spin diffusion mode arising in $G^{-}(\Omega)$ of (5.192). At small frequencies the solution of the zig-zag method perfectly agrees with the dispersion relation $\Omega = \mathrm{i}D(\varepsilon)k^2$ of the R-spin diffusion mode.

5.3.3. Numerical results

The spectrum of the quasi-normal modes for $\ell = 0$, $\varepsilon \in [0, 0.9]$ and $\bar{k} \in [0, 10]$ of $\Phi(\bar{\rho})$ is shown in Figure 5.5. Higher values of $\bar{k}$ were not accessible to our numerical procedure since the value of $|{}^{A(\bar{\omega},\bar{k})}/_{B(\bar{\omega},\bar{k})}|$ in the vicinity of its zeros was increasing drastically, rendering a stable minimization procedure impossible and thus the identification of the precise location of the zero failed for the required accuracy.

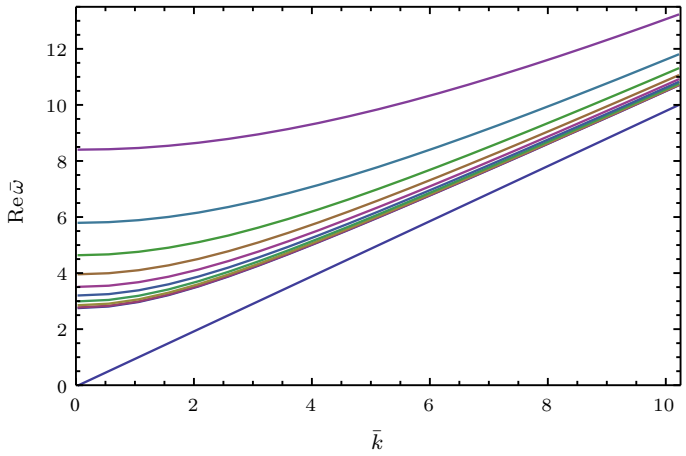

Figure 5.6. Investigating the real part of the first quasi-normal frequency of $\Phi(\bar{\rho})$ for $\ell = 0$ given by the $n = 1$ point in Figure 5.5, yields the curves shown for values of epsilon $\varepsilon = 0, 0.1, 0.2, 0.3, 0.4, 0.5, 0.6, 0.7, 0.8, 0.9$ from bottom to top. For increasing momentum $\bar{k}$ the modes approaches the lightcone given by the solid blue line (—) intersecting the origin. For $\bar{k} = 10$ the asymptotic velocities given by the slope $^{\mathrm{Re}\,\bar{\omega}}/_{\bar{k}}$ are within 10% of v_{light}.

There are no instabilities in the system arising from quasi-normal modes crossing into the lower complex $\bar{\omega}$ half-plane. Still there is a peculiarity visible in Figure 5.5, the imaginary part of the quasi-normal mode decreases for increasing momentum $\bar{k}$ in contrast to the zero sound dispersion relation (5.174). In the large momentum limit $\bar{k} \to \infty$ we should recover a ultra relativistic theory where the slope of the real part of the dispersion relation should reach the speed of light, *i.e.* $\mathrm{Re}\,\bar{\omega} = v_{\text{light}}\bar{k}$. As plotted in Figure 5.6, the slope of our numerical solution reaches about 10% of the speed of light at the largest values of $\bar{k} \approx 10$ accessible in our numerical procedure. Similar results are found in the case $\ell = 1$ in particular no instability occurred as well for all values of ε and $\bar{k}$ numerically explored. The results for the quasi-normal modes of $\Phi^+(\bar{\rho})$ with $\ell = 1$ are presented in Figure 5.7. Due to numerical problems in locating the precise position of the poles of the corresponding Green function, only the lowest lying quasi-normal mode could be resolved with satisfying accuracy. Since there is no instability in the lowest laying quasi-normal mode, it is highly unlikely that any instability might arise for higher excitations. Heuristically, the most relevant modes should be sensitive to a true physical instability. As reasoned in Section 5.3.1, we are interested in the ground state instabilities therefore we may also rule out instabilities arising from $\ell > 1$ quasi-normal modes corresponding to operators with higher scaling dimension. In Figure 5.8 the results of the first three quasi normal modes of $\Phi^-(\bar{\rho})$ with $\ell = 1$ are displayed. Qualitatively, the results are similar to the quasi-normal modes encountered for $\Phi(\bar{\rho})$ and again there are no instabilities in the studied range of momenta. The asymptotic velocities are quite similar to the results found for the $\Phi(\bar{\rho})$, $\ell = 0$ quasi-normal modes displayed in Figure 5.6. The R-spin diffusion mode (5.193) is found in the quasi-normal mode spectrum of $\Phi^-(\bar{\rho})$ located directly on the imaginary axis of the complex $\bar{\omega}$ plane for small momentum $\bar{k}$. For larger values of the momentum the mode is shifted away from the imaginary axis in a circular fashion as illustrated in Figure 5.9. Employing a numerical fit of the form

$$\bar{\omega} = \mathrm{i}\frac{D(\varepsilon)}{\sqrt{1-\varepsilon^2}}\bar{k}^2 + E(\varepsilon)\bar{k}^3 + \mathcal{O}(\bar{k}^4), \tag{5.206}$$

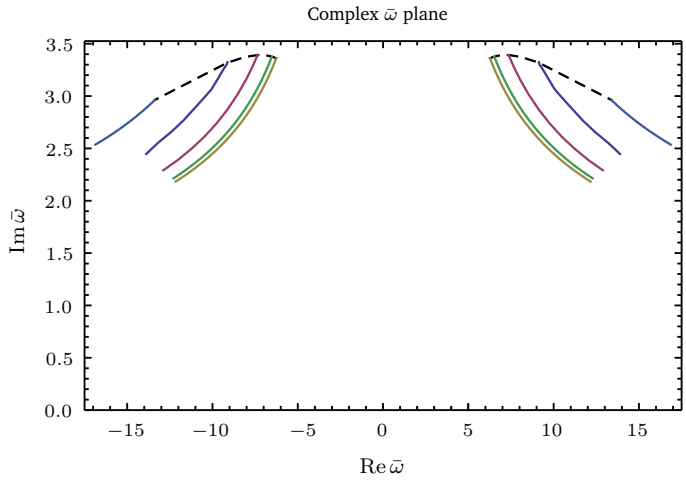

Figure 5.7. Using the same labeling conventions as in Figure 5.5 the first quasi-normal mode of $\Phi^+(\bar{\rho})$ with $\ell = 1$ for $\varepsilon = (0, 0.2, 0.4, 0.6, 0.8)$ and $\bar{k} \in (0, 10)$ is shown. Higher quasi-normal modes with $n > 1$ are located above the first quasi-normal mode, so we do not expect to find any instabilities (*c.f.* Figure 5.5). Unfortunately, our numerical code is not sophisticated enough to resolve the exact locations of the these quasi-normal modes in the complex $\bar{\omega}$ plane. Again we do not find any instability or quasi-normal mode crossing the real axis in the explored ranges of ε and $\bar{k}$.

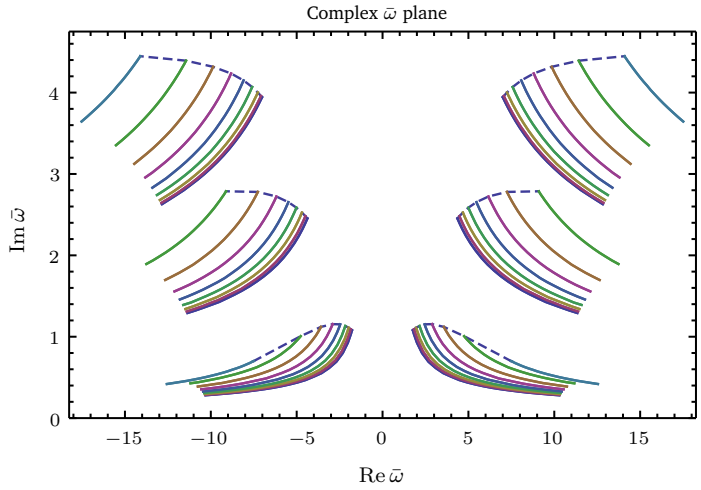

Figure 5.8. The curves show the first three quasi-normal modes of $\Phi^-(\bar{\rho})$ with $\ell = 1$ under variations of ε and $\bar{k}$. The identical convention and interpretation as in Figure 5.5 is used with the following exceptions: For the $n = 1$ and $n = 3$ the range of ε is reduce to $[0, 0.8]$ and for the $n = 2$ quasi normal mode to $[0, 0.7]$. The range of $\bar{k}$ is again $[0, 10]$.

enables us to numerically compute the functions $D(\varepsilon)$ and $E(\varepsilon)$ for sufficiently small momenta $\bar{k}$. This can be done quite analogously for the cases $\ell = 2$ and $\ell = 3$. The numerical determined values of $D(\varepsilon)$ are shown in Figure 5.3. Let us conclude this chapter with a last remark: the fluc-

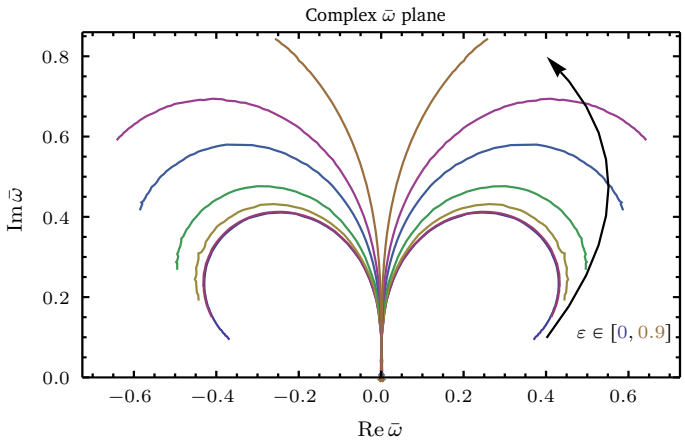

Figure 5.9. The $\ell = 1$, $\Phi^-(\bar{\rho})$ quasi-normal modes starting on the imaginary axis for small $\bar{k}$ and different $\varepsilon \sim {}^{M}/_{\mu} = (0, 0.1, 0.3, 0.5, 0.7, 0.8, 0.9)$, which is identified with the R-spin diffusion mode discussed in Section 5.3.1. The reason for its gaplessness is explained in a follow up publication [284], stemming from emergent moduli spaces related to $U(1)$ instantons in the probe limit case $N_f = 1$.

tuation $\Phi^-(\bar{\rho})$ with $\ell = 1$ is dual to the scalar operator in (5.194) which allows the interpretation of the conserved current diffusion mode as R-spin diffusion comes as a surprise. Since there are no perturbative instabilities the question arises what kind of symmetry principle protects the massless $SU(2)_{\mathrm{R}}$ R-spin diffusion mode. An answer to this question is given in [284] where the gapless mode is protect by an emergent moduli space at finite density, hinting at $U(1)$ instantons.

6 Conclusion & Outlook

The central results of this thesis are the numerical determination of the diffusion constants in holographic superconductors and the related timescales in order to realize a theoretical description of the empirical found Homes' law in real world superconductors. Secondly, a thorough stability analysis of all bosonic fluctuations in a top-down model of holographic quantum critical matter has been conducted. In the process, we needed to devise a new numerical scheme to deal with irregular singular points and found an interesting unexpected additional mode which we interpreted as R-spin diffusion. Let us give a review over the main results of each of the two projects and an outlook for future research.

6.1. Homes' Law

Let us summarize the main results of the Homes' law calculation: motivated by Homes' law we have analyzed the diffusion constants in holographic s- and p-wave superconductors with backreaction. In particular, we have discussed the temperature and density dependence of the momentum and R-charge diffusion for various masses of the scalar field, in the s-wave case, and for different strengths of the backreaction. We have found that the diffusion constants decrease with increasing backreaction and that the decay of the diffusion constants increases with increasing mass of the scalar field. For non-negative masses of the s-wave superconductor scalar field, we find an emerging AdS_2 at zero temperature which defines a critical strength of the backreaction α_c. Above this critical backreaction there is no phase transition to the superfluid/condensed phase, thus implying that α_c defines a quantum phase transition between the normal and the condensed phase.

6.1.1. Overview of Homes' law results

Let us now discuss these results in relation to Homes' law: we have found that without backreaction, holographic superconductors obey Homes' law since $\tau_c T_c = \text{const.}$ in all spacetime dimensions greater than two. In the case of s-wave superconductors, this holds for all scalar

field masses. Without backreaction, the result $\tau_c T_c = \text{const.}$ is almost automatic since the diffusion constant D scales as $1/T$. Turning on the backreaction, we find that $D(T_c)T_c$ is no longer constant, but decreases with increasing backreaction strength. Both for s-wave and p-wave holographic superconductors, we obtain virtually the same curves for the various diffusion constants in three and four dimensions. In particular, the s-wave superconductor shows this behavior in three and four dimensions for different masses of the scalar field. This is a strong indication that there is a universal principle at work, although we do not find a true constant. There are several possibilities how corrections may arise:

i. The simplest explanation is the fact that we cannot assume the validity of the assumption (4.234) for holographic superconductors. As discussed at the end of Section 4.5.3, increasing the backreaction α leads to the formation of a pseudo-gap and there are normal state charge carriers present in the superconducting phase as well. The dependence of the pseudo-gap on the backreaction has been studied holographically in [285], where it was found that the pseudo-gap arising in the superconducting phase becomes larger with increasing backreaction, as is clearly visible in Figure 4 of [285]. Assuming that the Ferrell-Glover-Tinkham sum rule (4.226) is still valid in the presence of the pseudo-gap, N_s in (4.226) is no longer zero. This leads to correction terms to (4.234) and (4.239),

$$\omega_{\text{Ps}}^2 = \omega_{\text{Pn}}^2 - 8N_\text{s} \qquad \Leftrightarrow \qquad \tau_c T_c = \frac{4\pi}{C}\left(1 - \frac{N_\text{s}}{N_\text{n}}\right). \tag{6.1}$$

Thus, we would expect the "constant" in (4.243) to decrease and this is exactly what we see in Figure 4.12, 4.13, 4.14 and 4.16.

ii. Even more dramatically, the sum rule (4.226) may not be valid for holographic superconductors in the presence of the backreaction. In this case Homes' law will be implied by Tanner's law (4.235) which applies to high T_c superconductors. It would be interesting to study Tanner's law in a holographic context, regardless of its relevance to Homes' law. Our result leads to the conjecture that the relation between the superconducting charge carrier and the normal state charge carrier concentration is dependent on the strength of the backreaction

$$n_\text{s} = B(\alpha) n_\text{n}, \tag{6.2}$$

such that (4.243) is modified by the monotonically decreasing function $B(\alpha)$ yielding

$$\tau_c T_c = 4\pi \frac{B(\alpha)}{C}. \tag{6.3}$$

iii. The proportionality between the time scale and the diffusion constant could in principle depend on α and $\bar{Q}$, *i.e.* a function $A(\alpha)$, say. In this case the question arises if there might be some additional dynamics concerning diffusion in holographic superfluids/superconductors which would have to be taken into account. This would lead to the modified version of (4.244),

$$D(T_c)T_c = \frac{4\pi}{A(\alpha)C}. \tag{6.4}$$

iv. From a condensed matter point of view, we should look at the dominant time scale which is given by the energy relaxation time. This needs not necessarily to be the same as the

momentum time scale. However, the Einstein-Higgs models obey relativistic symmetries and therefore the momentum diffusion/time scales are related to the energy diffusion/-time scales. In fact, the energy diffusion constant is identical to the momentum diffusion, as expected from the symmetries, up to a factor depending on the spacetime dimensions: conformal symmetry implies that the bulk viscosity vanishes, which ensures that hydrodynamic modes corresponding to energy and momentum diffusion are related.[1] So the natural choice is indeed to look at momentum and R-charge diffusive processes to determine the relevant time scales, as done in Section 4.4. Nevertheless, this issue deserves further investigation.

A more speculative and interesting correction could originate from the fact that we already have an infinite Drude peak in the normal phase,indicating an ideal conductor, *i.e.* $\mathrm{Re}\,\sigma(\omega) \sim \delta(\omega)$, since there is no lattice present in our model. Entering the superconducting phase seems to add additional spectral weight due to the condensation of the scalar field. This in turn implies that the perfect conducting metal in the normal state *does not* turn into a superconductor but that the ideal conductor and the superconductor coexist in the superconducting phase. Here we would again expect a violation of equal spectral weight, or of the Ferrell-Glover-Tinkham sum rule (4.226), as well as having a simple relation between the normal state charge carrier concentration and the one in the superconducting state. In order to really understand what happens in the superconducting phase, one needs to determine the behavior of ρ_s for small temperatures and to check that only the contribution to the superconducting state is considered. It is believed that exactly at $T = 0$ the normal state δ-shaped Drude peak vanishes and the coefficient of the delta distribution is really the superfluid strength, yet to our knowledge this is not explicitly shown so far.

6.1.2. Outlook

As is explained in the previous section, the most striking explanation for corrections to $\tau_c T_c =$ const. in the backreacting case comes from additional degrees of freedom in the pseudo-gap. Let us give a list of open questions which needs to be addressed to make further progress:

- An explicit calculation to verify the validity of the sum rules of holographic superconductors is in itself an interesting question. Therefore, one needs to calculate the superfluid density including its dependence on the backreaction at zero temperature as well as the optical conductivity above the critical temperature and near zero temperature. The conceptual setting is quite clear, but the numerical implementation might be challenging.

- In order to confirm the assumptions made in (4.235) one needs to check if the holographic superconductors show a relation between n_s and n_n, *i.e.* Tanner's law. The same challenges might arise as in the aforementioned point.

- It would be interesting to understand if the holographic superconductors consists of an ideal metal coexisting with a superconductor following the speculative point made in the conclusion. If so, one needs to devise a scheme to calculate the superfluid strength by removing the influence of the perfectly conducting metal. There are several ways to achieve this: First of all it would be interesting to look for the Meißner-Ochsenfeld effect, *i.e.* to calculate the transverse response of the gauge field which is only sensitive to the

[1] A natural candidate for energy diffusion is the sound attenuation Γ following from the dispersion relation $\omega(k) = v_\mathrm{sound} k - \mathrm{i}\Gamma k^2$. For a conformal fluid, Γ is determined by the momentum diffusion via $\Gamma = \frac{d-2}{d-1} D_\mathrm{M}$.

superfluid strength deep in the superconducting phase. Alternatively, a further idea is to change the geometry such that the degrees of freedom of the normal state become very massive and are thus "gapped out" of the spectrum. Possible candidates are the hard-wall geometry, studied in the condensed matter context in [286], or a more smooth realization emerging in the AdS-soliton solutions [287], focusing in particular on the AdS-soliton to AdS-soliton superconductor transition. A suppression of normal low energy spectral weight has also been observed recently in a different context in [288]. It will also be interesting to consider holographic systems with lattice structure, such as [33] and [34], in the context explained here. These do not have the δ-peak in the normal phase, as expected for a system with an underlying lattice.

- Since within condensed matter physics, energy diffusion is relevant to Homes' law, a systematic investigation of the relation between energy diffusion and momentum diffusion in the holographic context appears to be highly desirable, in particular in the presence of finite density and backreaction. As explained in the conclusion, our assumption that energy and momentum diffusion are related within holography is well-motivated. Nevertheless this is a crucial issue which requires systematic study.

- It would also be useful to calculate the dependence of fermionic excitations on the backreaction, for instance by generalizing the work of [251] and [289].

In any case it is very important to disentangle the different contributions to the δ-peak in the superconducting phase in order to learn the differences which arise in holographic superfluids/superconductors as compared to "real world" systems.

6.2. Cold Holographic Matter

6.2.1. Main results of the holographic analysis

The stability of holographic quantum matter near criticality has been studied in a top-down fashion by embedding a single probe D_7-brane in $AdS_5 \times S^5$ spacetime. The non-trivial embedding characterizes the physical zero temperature, finite baryon density state of the single flavor $\mathcal{N} = 2$ hypermultiplet coupled to the $\mathcal{N} = 4$ SYM theory, described by the non-trivial D_7-brane worldvolume gauge fields. The mesonic spectrum is computed by determining the spectrum of the D_7-brane fluctuations. For the numerically analyzed range of momenta, no instabilities were detected. There are three main results: First, we showed that all bosonic worldvolume fluctuations effectively "see" a AdS_2 near horizon geometry induced by the non-trivial background of the worldvolume fields. In the corresponding dual field theory picture, for finite-density states, a $(0+1)$-dimensional CFT emerges as effective low-energy theory. Secondly, we devised a new numerical procedure, dubbed the "zig-zag" method, which may be applied to any quasi-normal mode calculation involving irregular singular points in the bulk differential equations of motion. Thirdly, we discovered a purely imaginary mode reminiscent to a diffusive mode of a conserved current correlator. More specifically, the dual operator of the correlation function exhibiting the diffusive mode, is a dimension-two scalar operator transforming under a vector representation of $SU(2)_{\mathrm{R}}$, *c.f.* (5.194). A natural interpretation of this $SU(2)_{\mathrm{R}}$ symmetry as electronic spin allows to draw an analogy to itinerant electronic systems with decoupled spin-orbit coupling and thus as a R-spin diffusion mode. Generalizing to higher values of ℓ, the dual operators form an $(\ell+2)$-dimensional representation of the $SU(2)_{\mathrm{R}}$ symmetry. Numerically, we computed the diffusion constant of this mode for values of $\ell = 1, 2, 3$ and expect that this mode is generically found for arbitrary ℓ.

6.2.2. Future research directions

There are several possibilities to extend the analysis of cold holographic quantum matter:

- An immediate interesting extensions is to redo the quasi-normal mode stability analysis for $N_f > 1$. In this case the flavor symmetry is given by $U(1)_{\rm B} \times SU(N_f)$, where we may introduce an isospin chemical potential for each Cartan generator of $SU(N_f)$. As we already discussed in Section 4.2, the zero temperature ground state is described by a holographic p-wave superfluid consisting of a condensate of vector mesons [215–217, 222]. Apart from the stability one may search for emergent scale invariant low energy effective theories, *e.g.* a $(0+1)$-dimensional CFT, and of course a generalization of the R-spin diffusion mode. It is known that at finite temperature an isospin chemical potential give rise to a squark condensation instability [290] for constant worldvolume gauge fields. So far it is not clear how this result is modified by a non-trivial profile of the gauge-field.

- Another possibility is the extension of the analysis to other D_3/D_p probe brane systems as listed in Table 5.1. In particular, the probe brane embedding of a D_5-brane extended along $\text{AdS}_4 \times S^2$ inside $\text{AdS}_5 \times S^5$ [291–293] seems to be tractable since an exact solution of the background fields similar to (5.69) is known. The dual field theory describes a $(2+1)$-dimensional defect. Again the spectrum includes a zero sound mode [264] and there are reasons to expect an emergent $(0+1)$-dimensional CFT [271]. D_5-branes in external $U(1)_{\rm B}$ magnetic fields exhibit an instability arising from the violation of the AdS_2 BF bound [271, 294], so one could anticipate instabilities in the spectrum of fluctuations.

- In [284] the nature of the gaplessness of the R-spin diffusion mode has been unraveled, which is related to moduli spaces at finite density. Similar work has been done in the D_3/D_5-probe brane system in [295]. Furthermore, there is a conjecture to find a classification of compressible states arising in the probe brane systems at finite temperature. It would be very tempting to relate this classification to quantum order found in table-top experiments.

- Another pressing question is the nature of the effective low energy theory of compressible states. We already know that this theory must include the zero sound and R-spin diffusion modes. Additionally, the low-temperature heat capacity scales as $c_V \sim T^6$ and there is a finite entropy density. It seems that the ground state cannot be understood in terms of known Fermi or Bose quantum liquids. Adding more properties might give a clue what kind of microscopic state could exhibit such exotic properties.

- Studying the fermionic degrees of freedom of D_3/D_p probe brane systems [296]. Are there any Fermi surfaces and how do they relate to the hyperscaling violation found in [198]? This is actually work in progress and the author hopes to complete tentatively survey of top-down fermions to find more intriguing answers and questions.

A

Some Useful Relations Concerning Determinants & Derivatives

A.1. Series Expansions

A.1.1. Series expansion of analytic functions

Using the analytic expression given for the geometric series

$$\frac{1}{1-x} = \sum_{n=0}^{\infty} x^n \qquad \longrightarrow \qquad \frac{1}{1+x} = \sum_{n=0}^{\infty} (-1)^n x^n, \tag{A.1}$$

and integrating it over the whole positive real domain, we find the series expansion of the natural logarithm

$$\ln(1+x) = \sum_{n=0}^{\infty} (-1)^n \frac{x^{n+1}}{n+1}. \tag{A.2}$$

Using Taylor's formula for series expansion around the real point x_0 given by

$$f(x_0) = \sum_{n=0}^{\infty} \left. \frac{f^{(n)}}{n!} \right| (x-x_0)^n, \tag{A.3}$$

where $f^{(n)}$ denotes the n^{th} derivative of the function f. We can find the series expansion around $x_0 = 0$ for the exponential function immediately, since the derivative of the exponential function at $x_0 = 0$ is always one to all orders. Thus, we can write

$$\mathrm{e}^x = \sum_{n=0}^{\infty} \frac{x^n}{n!}. \tag{A.4}$$

Now with the help of these two elementary series expansions we are able to generate more complicated series expansions.

A.1.2. Expansions of determinants

The determinant of a regular, diagonalizable and invertible matrix $\mathcal{M}$ can be written in terms of analytic function of $\mathcal{M}$ and its trace. Since the matrix $\mathcal{M}$ is diagonalizable we can write

$$\det(\,\mathrm{e}^{\mathcal{M}}\,) = \prod_{i=1}^{N} \tilde{\lambda}_i = \prod_{i=1}^{N} \mathrm{e}^{\lambda_i} \;=\; \mathrm{e}^{\det \mathcal{M}}\,, \tag{A.5}$$

where $\tilde{\lambda}$ denotes the eigenvalues of the matrix $\mathrm{e}^{\mathcal{M}}$ that can be expressed by the eigenvalues λ of $\mathcal{M}$, because the diagonalization of the matrix $\mathcal{M}$ is carried over to the diagonalization of $\mathrm{e}^{\mathcal{M}}$

$$\mathrm{e}^{\mathcal{D}} \;=\; \mathrm{e}^{\mathcal{Q}^{-1}\mathcal{M}\mathcal{Q}} \;=\; \sum_{n=0}^{\infty} \frac{(\mathcal{Q}^{-1}\mathcal{M}\mathcal{Q})^n}{n!} = \mathcal{Q}^{-1} \sum_{n=0}^{\infty} \frac{\mathcal{M}^n}{n!} \mathcal{Q} = \mathcal{Q}^{-1}\,\mathrm{e}^{\mathcal{M}}\,\mathcal{Q} = \widetilde{\mathcal{D}}. \tag{A.6}$$

We can write the matrices $\mathrm{e}^{\mathcal{D}}$ and $\widetilde{\mathcal{D}}$ as

$$\mathrm{e}^{\mathcal{D}} \;=\; \begin{pmatrix} \mathrm{e}^{\lambda_1} & & \\ & \ddots & \\ & & \mathrm{e}^{\lambda_N} \end{pmatrix}, \qquad \text{and} \qquad \widetilde{\mathcal{D}} = \begin{pmatrix} \tilde{\lambda}_1 & & \\ & \ddots & \\ & & \tilde{\lambda}_N \end{pmatrix}, \tag{A.7}$$

respectively. We can easily read off the relation between the eigenvalues of the two matrices, namely $\tilde{\lambda}_i = \mathrm{e}^{\lambda_i}$. Therefore we can write

$$\det(e[\mathcal{M}]) = \prod_{i=1}^{N} \mathrm{e}^{\lambda_i} \;= \mathrm{e}^{\sum_{i=1}^{N} \lambda_i} \;=\; \mathrm{e}^{\mathrm{tr}(\mathcal{M})}\,, \tag{A.8}$$

and after replacing $\mathrm{e}^{\mathcal{M}}$ with $\widetilde{\mathcal{M}}$ and splitting it intoa sum consisting of an identity matrix and a matrix $\mathcal{M}' = \widetilde{\mathcal{M}} - \mathbb{1}$, we arrive at

$$\det(\mathbb{1} + \mathcal{M}) = \;\mathrm{e}^{\mathrm{tr}[\ln(\mathbb{1}+\mathcal{M})]}\,. \tag{A.9}$$

This formula is also valid for non-diagonalizable matrices. Finally one can write equation (A.9) as a series expansion with the help of the series expansion (A.2) and (A.4),

$$\det(\mathbb{1} + \mathcal{M}) = \sum_{m=0}^{\infty} \frac{1}{m!} \left[\sum_{n=0}^{\infty} \frac{(-1)^n}{n+1} \left(\mathrm{tr}\, M^{n+1}\right) \right]^m. \tag{A.10}$$

A.2. Several Useful Relations Between Derivatives

In order to vary actions depending on gauge fields, it is useful to find a derivative of the field strengths $F^{ab} = \partial_a A_b - \partial_b A_a$ with respect to the gauge fields A_c. Naturally, the partial derivative is a covariant vector, so the derivative with respect to a covariant field or one form A_c is a vector since

$$\frac{\partial}{\partial x_a} = \frac{\partial}{\partial x^b}\frac{\partial x^b}{\partial x_a} = \frac{\partial}{\partial x^b}\frac{\partial g^{bc} x_c}{\partial x_a} = \frac{\partial}{\partial x^b}\left(\delta_c{}^a g^{bc} + \frac{\partial g^{bc}}{\partial x_a}\right). \tag{A.11}$$

For a flat metric, *i.e.* g^{bc} is not dependent on the coordinates, *e.g.* the Minkowski metric η^{bc} (otherwise the partial derivative would be itself no covariant vector because of the additional term appearing in (A.11)), the index of the partial derivative can be raise to yield a vector

$$\partial^a \equiv \frac{\partial}{\partial x_a} = \eta^{ab} \frac{\partial}{\partial x^b} = \eta^{ab} \partial_b. \tag{A.12}$$

Thus, the derivative with respect to a covariant field or one form, yields a vector. With this knowledge we can define the derivative of $\partial_a A_b$ in terms of its two form field strength as

$$\frac{\partial}{\partial(\partial_a A_b)} = \frac{\partial F_{cd}}{\partial(\partial_a A_b)} \frac{\partial}{\partial F_{cd}} = \left(\frac{\partial(\partial_c A_d)}{\partial(\partial_a A_b)} - \frac{\partial(\partial_d A_c)}{\partial(\partial_a A_b)} \right) \frac{\partial}{\partial F_{cd}} = \left(\delta_c{}^a \delta_d{}^b - \delta_d{}^a \delta_c{}^b \right) \frac{\partial}{\partial F_{cd}}. \tag{A.13}$$

Another useful relation is to rewrite the Laplace-Beltrami operator in arbitrary coordinates. With the help of the metric g^{ab} and the square root of its negative determinant $\sqrt{-\det g}$, we can rewrite the divergence of a vector field v^i as

$$\operatorname{div} v^i \equiv \nabla_i v^i = \frac{1}{\sqrt{|\det g|}} \partial_i \left(\sqrt{|\det g|} v^i \right). \tag{A.14}$$

For an scalar function the partial derivative is identical to the covariant derivative, *i.e.* $\nabla_i f \equiv \partial_i f$. As stated in (A.12) we have to raise the index of the partial derivative, since the derivative "expects" a vector field as argument or in our case the gradient of the scalar function f which is defined to be a vector field, *i.e.* $\operatorname{grad} f \equiv g^{ij} \partial_j f$. The Laplace-Beltrami operator thus reads

$$\nabla^2 f = \nabla_i \nabla^i f = \frac{1}{\sqrt{|\det g|}} \partial_i \left(\sqrt{|\det g|} g^{ij} \partial_j f \right), \tag{A.15}$$

which is equal to the usual "$\operatorname{div} \operatorname{grad} f$" of a scalar function. This is also true in case of applying ∇^2 to every component of a vector x^a.

A.3. Coordinate Transformation of 2nd Order Differential Equations

It is useful to transform the equation (4.181) into different coordinates which might be more suitable for a given dimensionality. Consider a second order differential equation of the following form

$$\phi''(x) + a(x)\phi'(x) + b(x)\phi(x) = 0, \tag{A.16}$$

to transform into

$$\ddot{\phi}(y) + a(y)\dot{\phi}(y) + b(y)\phi(y) = 0. \tag{A.17}$$

For an arbitrary bijective coordinate transformation $y = h(x)$, the coefficient functions a and b are transforming as

$$\begin{aligned} a(y) &= \left(\frac{h''(x)}{h'(x)^2} + \frac{a(x)}{h'(x)} \right) \Bigg|_{x=h^{-1}(y)}, \\ b(y) &= \frac{b(x)}{h'(x)^2} \Bigg|_{x=h^{-1}(y)}. \end{aligned} \tag{A.18}$$

Note, that any expression occuring in $a(x)$ or $b(x)$ involving derivatives must be transformed in a similar fashion. In particular, terms involving first derivatives, *e.g.* $f'(x)$ in $a(x)$ can be replaced directly by $\dot{f}(y)$ in $a(y)$ since the two factors arising from the transformation will cancel.

B

Gaussian Integrals, Wick's Theorem & Thermal Averages

B.1. Gaussian Integrals & Wick's Theorem

If we define the partition function of the multivariate normal distribution to be

$$Z \equiv (2\pi)^{-\frac{d}{2}} \int \mathrm{d}^{\mathrm{d}}x \; \mathrm{e}^{-\frac{1}{2}(x-\mu)\cdot\boldsymbol{\Sigma}^{-1}(x-\mu)} \; = \sqrt{\det \Sigma}, \tag{B.1}$$

we can explicitly calculate

$$\frac{\partial^2 \ln Z}{\partial \Sigma_{ij} \partial \Sigma_{kl}} = \frac{\partial}{\partial \Sigma_{ij}} \left(\frac{1}{Z} \frac{\partial Z}{\partial \Sigma_{kl}} \right) = -\frac{1}{Z^2} \frac{\partial Z}{\partial \Sigma_{ij}} \frac{\partial Z}{\partial \Sigma_{kl}} + \frac{1}{Z} \frac{\partial^2 Z}{\partial \Sigma_{ij} \partial \Sigma_{kl}}, \tag{B.2}$$

with the help of

$$\mathrm{d}\boldsymbol{M}^{-1} = -\boldsymbol{M}^{-1} \, \mathrm{d}\boldsymbol{M} \boldsymbol{M}^{-1}, \tag{B.3}$$

or

$$\begin{aligned} \frac{\partial \left(\boldsymbol{M}^{-1}\right)_{ij}}{\partial M_{kl}} &= -\left(\boldsymbol{M}^{-1}\right)_{in} \frac{\partial M_{nm}}{\partial M_{kl}} \left(\boldsymbol{M}^{-1}\right)_{mj} \\ &= -\left(\boldsymbol{M}^{-1}\right)_{in} \left(\delta_{nk}\delta_{ml}\right) \left(\boldsymbol{M}^{-1}\right)_{mj} \\ &= -\left(\boldsymbol{M}^{-1}\right)_{ik} \left(\boldsymbol{M}^{-1}\right)_{lj}, \end{aligned} \tag{B.4}$$

and

$$\mathrm{d}\left(\det \boldsymbol{M}\right) = \mathrm{tr}\left(\mathrm{adj}\, \boldsymbol{M} \, \mathrm{d}\boldsymbol{M}\right) = \det \boldsymbol{M} \, \mathrm{tr}\left(\boldsymbol{M}^{-1} \, \mathrm{d}\boldsymbol{M}\right), \tag{B.5}$$

or

$$\frac{\partial \det \boldsymbol{M}}{\partial M_{ij}} = \det \boldsymbol{M} \operatorname{tr}\left[\left(\boldsymbol{M}^{-1}\right)_{kl} \frac{\partial M_{lm}}{\partial M_{ij}}\right]$$
$$= \det \boldsymbol{M} \left(\boldsymbol{M}^{-1}\right)_{kl} \left(\delta_{li}\delta_{mj}\right) \delta_{km} = \det \boldsymbol{M} \left(\boldsymbol{M}^{-1}\right)_{ji} . \tag{B.6}$$

For a symmetric matrix $\boldsymbol{M}$ the derivative needs to be symmetrized, *i.e.* we need to write $1/2(\delta_{ni}\delta_{mj} + \delta_{nj}\delta_{mi})$. First we rewrite

$$\frac{\partial Z}{\partial \Sigma_{kl}} = \frac{1}{2\sqrt{\det \boldsymbol{\Sigma}}} \frac{\partial \det \boldsymbol{\Sigma}}{\partial \Sigma_{kl}} = \frac{1}{2} \sqrt{\det \boldsymbol{\Sigma}} \left(\boldsymbol{\Sigma}^{-1}\right)_{lk} . \tag{B.7}$$

Taking another derivative of the above equation yields

$$\frac{\partial^2 Z}{\partial \Sigma_{ij} \partial \Sigma_{kl}} = \frac{1}{2} \underbrace{\frac{\partial \sqrt{\det \boldsymbol{\Sigma}}}{\partial \Sigma_{ij}}}_{\frac{1}{2}\sqrt{\det \boldsymbol{\Sigma}} \left(\boldsymbol{\Sigma}^{-1}\right)_{ji}} \left(\boldsymbol{\Sigma}^{-1}\right)_{lk} + \frac{1}{2} \sqrt{\det \boldsymbol{\Sigma}} \frac{\partial \left(\boldsymbol{\Sigma}^{-1}\right)_{lk}}{\partial \Sigma_{ij}}$$
$$= \frac{1}{4} \sqrt{\det \boldsymbol{\Sigma}} \left(\boldsymbol{\Sigma}^{-1}\right)_{ji} \left(\boldsymbol{\Sigma}^{-1}\right)_{lk} - \frac{1}{4} \sqrt{\det \boldsymbol{\Sigma}} \left[\left(\boldsymbol{\Sigma}^{-1}\right)_{li} \left(\boldsymbol{\Sigma}^{-1}\right)_{jk} + \left(\boldsymbol{\Sigma}^{-1}\right)_{lj} \left(\boldsymbol{\Sigma}^{-1}\right)_{ik}\right] . \tag{B.8}$$

Putting everything together in (B.2) gives rise to

$$\frac{\partial^2 \ln Z}{\partial \Sigma_{ij} \partial \Sigma_{kl}} = -\frac{1}{4} \left[\left(\boldsymbol{\Sigma}^{-1}\right)_{ik} \left(\boldsymbol{\Sigma}^{-1}\right)_{jl} + \left(\boldsymbol{\Sigma}^{-1}\right)_{il} \left(\boldsymbol{\Sigma}^{-1}\right)_{jk}\right] . \tag{B.9}$$

This is the general version of Wick's theorem, the full series can be constructed by taking further derivatives of (B.9).

B.2. Connected Green Functions & Thermal Averages

First let us check

$$\frac{\partial}{\partial \lambda^i} \operatorname{tr}\left(\mathrm{e}^{-\lambda^j x_j}\right) = \operatorname{tr}\left(-x_i \, \mathrm{e}^{-\lambda^j x_j}\right) , \tag{B.10}$$

This is true due to the linearity and cyclicity properties of the trace. Rewriting the left hand side we find

$$\frac{\partial}{\partial \lambda^i} \operatorname{tr}\left(\mathrm{e}^{-\lambda^j x_j}\right) = \sum_k \operatorname{tr}\left(\frac{\partial}{\partial \lambda^i} \frac{\left(\lambda^j x_j\right)^k}{k!}\right) . \tag{B.11}$$

For each fixed k in the above sum, we can bring x_i to the front by cyclic permutation inside the trace, *e.g.*

$$x_i + \operatorname{tr}\left(\frac{1}{2} x_i \left(\lambda^j x_j\right) + \frac{1}{2} \left(\lambda^j x_j\right) x_i\right)$$
$$+ \operatorname{tr}\left(\frac{1}{6} x_i \left(\lambda^j x_j\right)^2 + \frac{1}{6} \left(\lambda^j x_j\right) x_i \left(\lambda^j x_j\right) + \frac{1}{6} \left(\lambda^j x_j\right)^2 x_i\right) \tag{B.12}$$
$$+ \cdots + \operatorname{tr}\left(\frac{k}{k!} \left(\lambda^j x_j\right)^{k-\ell} \cdots x_i^{(\ell)} \cdots \left(\lambda^j x_j\right)^{\ell-1}\right) + \ldots ,$$

such that we find

$$\frac{\partial}{\partial\lambda^i}\operatorname{tr}\left(\mathrm{e}^{-\lambda^j x_j}\right)=\sum_k{}'\operatorname{tr}\left[\frac{x_i\left(\lambda^j x_j\right)^k}{(k-1)!}\right]=\operatorname{tr}\left(x_i\,\mathrm{e}^{-\lambda^j x_j}\right). \tag{B.13}$$

Calculating thermal averages via derivatives of the partition function

$$\begin{aligned}\frac{\partial}{\partial\lambda^i}\ln Z&=\frac{1}{Z}\frac{\partial Z}{\partial\lambda^i}=\frac{1}{Z}\frac{\partial}{\partial\lambda^i}\operatorname{tr}\left(\mathrm{e}^{-\lambda^j x_j}\right)\\&=-\frac{1}{Z}\operatorname{tr}\left(x_i\,\mathrm{e}^{-\lambda^j x_j}\right)=-\operatorname{tr}\left(\rho x_i\right)=-\langle\, x_i\,\rangle.\end{aligned} \tag{B.14}$$

Calculating the mixed second derivative is not possible since in that case the chain rule (B.13) fails

$$\begin{aligned}\frac{\partial^2}{\partial\lambda^i\partial\lambda^j}\ln Z&=\frac{\partial}{\partial\lambda^i}\left[\frac{1}{Z}\frac{\partial Z}{\partial\lambda^j}\right]=\frac{\partial}{\partial\lambda^i}\left[\frac{1}{Z}\operatorname{tr}\left(-x_j\,\mathrm{e}^{-\lambda^k x_k}\right)\right]\\&=\frac{1}{Z^2}\frac{\partial Z}{\partial\lambda^i}\operatorname{tr}\left(x_j\,\mathrm{e}^{-\lambda^k x_k}\right)-\frac{1}{Z}\operatorname{tr}\left(-x_j\frac{\partial}{\partial\lambda^i}\,\mathrm{e}^{-\lambda^k x_k}\right).\end{aligned} \tag{B.15}$$

The first term can be written as

$$\frac{1}{Z}\frac{\partial Z}{\partial\lambda^i}\cdot\frac{1}{Z}\operatorname{tr}\left(x_j\,\mathrm{e}^{-\lambda^k x_k}\right)=-\langle\, x_i\,\rangle\langle\, x_j\,\rangle, \tag{B.16}$$

whereas the second term the cyclicity of the trace is of no help and thus we would end up with the very intricate expression of (infinite) commutators. Physically, one cannot make any sense of such an expression and therefore we find

$$\frac{1}{Z}\operatorname{tr}\left(x_j\frac{\partial}{\partial\lambda^i}\,\mathrm{e}^{-\lambda^k x_k}\right)\neq\frac{1}{Z}\operatorname{tr}\left(x_j x_i\,\mathrm{e}^{-\lambda^k x_k}\right)=\langle\, x_j x_i\,\rangle. \tag{B.17}$$

The resolution of this puzzle is to use the Bogoliubov inner product which is well defined for bounded operators of finite quantum systems[1]

$$\langle\!\langle\, xy\,\rangle\!\rangle_f=\frac{1}{Z_f}\operatorname{tr}\left[\int_0^1\mathrm{d}s\left(y\,\mathrm{e}^{-sf}\,x\,\mathrm{e}^{sf}\right)\mathrm{e}^{-f}\right], \tag{B.18}$$

where f is an bounded self-adjoint operator and x, y are non-commuting with f and each other. Z_f denotes the partition function of f

$$Z_f=\operatorname{tr}\,\mathrm{e}^{-f}, \tag{B.19}$$

and the thermal average of an operator is given by

$$\langle\, g\,\rangle_f=\frac{1}{Z_f}\operatorname{tr}\left(g\,\mathrm{e}^{-f}\right). \tag{B.20}$$

[1] Here we stick to a very strict and pedantic notation in order to make sure everything is correct.

Actually, the Bogoliubov inner product is the same as the usual thermal average of two operators as can be seen for bounded self adjoint operators

$$\begin{aligned}\langle xy\rangle_f &= \frac{1}{Z_f}\operatorname{tr}\left(xy\,\mathrm{e}^{-f}\right)\\ &= \frac{1}{Z_f}\operatorname{tr}\left[x\left(\mathrm{e}^{f}\;\mathrm{e}^{-f}\right)y\,\mathrm{e}^{-f}\right] = \frac{1}{Z_f}\operatorname{tr}\left[y\left(\mathrm{e}^{-f}\,x\,\mathrm{e}^{f}\right)\;\mathrm{e}^{-f}\right]\\ &= \left\langle y\left(\mathrm{e}^{-f}\,x\,\mathrm{e}^{f}\right)\right\rangle_f . \end{aligned} \tag{B.21}$$

Defining

$$\mathcal{D}_f[x] = \mathrm{e}^{-f}\,x\,\mathrm{e}^{f}\,, \tag{B.22}$$

and

$$\mathcal{I}_f[x] = \int_0^1 \mathrm{d}s\;\mathrm{e}^{-sf}\,x\,\mathrm{e}^{sf}\,, \tag{B.23}$$

which are equivalent when acting on the eigenvectors of f,

$$\begin{aligned} y\langle\varphi\,|\,\mathcal{I}_f[x]\,|\,\varphi\rangle &= y\left\langle\varphi\,\middle|\left(\int_0^1 \mathrm{d}s\;\mathrm{e}^{-sf}\,x\,\mathrm{e}^{sf}\right)\middle|\,\varphi\right\rangle\\ &= y\int_0^1 \mathrm{d}s\;\mathrm{e}^{-sf(\varphi)}\,\langle\varphi\,|\,x\,|\,\varphi\rangle\,\mathrm{e}^{sf(\varphi)}\\ &= y\langle\varphi\,|\,x\,|\,\varphi\rangle = y\left\langle\varphi\,\middle|\,\mathrm{e}^{-sf}\,x\,\mathrm{e}^{sf}\,\middle|\,\varphi\right\rangle\\ &= y\langle\varphi\,|\,\mathcal{D}_f[x]\,|\,\varphi\rangle, \end{aligned} \tag{B.24}$$

we can rewrite (B.21) with the help of (B.22) as well as (B.18) using (B.23)

$$\langle xy\rangle_f = \langle y\mathcal{D}_f[x]\rangle_f\,, \qquad\qquad \langle\!\langle xy\rangle\!\rangle_f = \langle y\mathcal{I}_f[x]\rangle_f\,, \tag{B.25}$$

and thus $\langle xy\rangle_f = \langle\!\langle xy\rangle\!\rangle_f$. Note that

$$\langle x\rangle_f = \langle\mathcal{D}_f[x]\rangle_f\,, \qquad \langle\!\langle x\rangle\!\rangle_f = \langle\mathcal{I}_f[x]\rangle_f\,, \tag{B.26}$$

so strictly there is no need for the double angle bracket notation, but it adds to clarify in which order and on what operators are acting. This excess notation allows us to define a quantum chain rule that automatically takes care of the non-commutative nature of our operators and thus enables us to calculate the second derivative of $\ln Z$. In order to derive the quantum chain rule, we calculate what we already know from (B.13), *i.e.* the first order derivative of the exponential operator

$$\left\langle \mathrm{d}\,\mathrm{e}^{-f}\right\rangle_f = -\frac{1}{Z_f}\operatorname{tr}\left(\mathrm{d}f\;\mathrm{e}^{-f}\right) = -\langle\mathrm{d}f\rangle_f\,, \tag{B.27}$$

but we also know that

$$\left\langle \mathrm{d}\,\mathrm{e}^{-f}\right\rangle_f = -\langle\!\langle\,\mathrm{d}f\,\rangle\!\rangle_f = -\frac{1}{Z_f}\operatorname{tr}\left(\int_0^1 \mathrm{d}s\;\mathrm{e}^{-sf}\;\mathrm{d}f\;\mathrm{e}^{sf}\;\mathrm{e}^{-f}\right). \tag{B.28}$$

Therefore we can conclude that[2]

$$\mathrm{d}\,\mathrm{e}^{-f} = -\mathcal{I}_f[\mathrm{d}f]\,\mathrm{e}^{-f}\,. \tag{B.29}$$

Let us derive the quantum chain rule for an arbitrary bounded operator x,

$$\begin{aligned}\mathrm{d}\Big(Z_f\,\langle\, x\,\rangle_f\Big) &= (\mathrm{d}Z_f)\,\langle\, x\,\rangle_f + Z_f\,\mathrm{d}\langle\, x\,\rangle_f \\ \Rightarrow \mathrm{d}\langle\, x\,\rangle_f &= \frac{\mathrm{d}\Big(Z_f\,\langle\, x\,\rangle_f\Big) - (\mathrm{d}Z_f)\,\langle\, x\,\rangle_f}{Z_f}.\end{aligned} \tag{B.30}$$

The first term in the numerator is given by

$$\begin{aligned}\mathrm{d}\Big(Z_f\,\langle\, x\,\rangle_f\Big) &= \mathrm{d}\big[\mathrm{tr}\,(x\,\mathrm{e}^{-f})\big] = \mathrm{tr}\,(\mathrm{d}x\;\mathrm{e}^{-f}) + \mathrm{tr}\,(x\,\mathrm{d}\,\mathrm{e}^{-f}) \\ &= \mathrm{tr}\,(\mathrm{d}x\;\mathrm{e}^{-f}) - \mathrm{tr}\,(x\,\mathcal{I}[\mathrm{d}f]\,\mathrm{e}^{-f}) = Z_f\,\langle\,\mathrm{d}x\,\rangle_f - Z_f\,\langle\, x\,\mathcal{I}_f[\mathrm{d}f]\,\rangle_f \\ &= Z_f\,\Big(\langle\,\mathrm{d}x\,\rangle_f - \langle\!\langle\,\mathrm{d}f\,x\,\rangle\!\rangle_f\Big)\,,\end{aligned} \tag{B.31}$$

and the second term gives rise to

$$\begin{aligned}-\,\mathrm{d}Z_f &= -\,\mathrm{tr}\,(\mathrm{d}\,\mathrm{e}^{-f}) = \mathrm{tr}\,(\mathcal{I}[\mathrm{d}f]\,\mathrm{e}^{-f}) \\ &= Z_f\,\langle\,\mathcal{I}[\mathrm{d}f]\,\rangle_f = Z_f\,\langle\!\langle\,\mathrm{d}f\,\rangle\!\rangle_f = Z_f\,\langle\,\mathrm{d}f\,\rangle_f\,.\end{aligned} \tag{B.32}$$

The full quantum chain rule of an operator reads

$$\mathrm{d}\langle\, x\,\rangle_f = \langle\,\mathrm{d}x\,\rangle_f - \langle\!\langle\,\mathrm{d}f\,x\,\rangle\!\rangle_f + \langle\,\mathrm{d}f\,\rangle_f\,\langle\, x\,\rangle_f\,. \tag{B.33}$$

Applying the quantum chain rule to $\ln Z_f$ will give us the desired result

$$\mathrm{d}(\ln Z_f) = \frac{1}{Z_f}\,\mathrm{d}Z_f = -\langle\,\mathrm{d}f\,\rangle_f\,. \tag{B.34}$$

Higher thermal averages/cumulants are calculated by taking higher order derivatives

$$\mathrm{d}^2(\ln Z_f) = -\,\mathrm{d}\langle\,\mathrm{d}f\,\rangle_f = -\big\langle\,\mathrm{d}^2 f\,\big\rangle_f + \langle\!\langle\,\mathrm{d}f\,\mathrm{d}f\,\rangle\!\rangle_f - \langle\,\mathrm{d}f\,\rangle_f\,\langle\,\mathrm{d}f\,\rangle_f\,, \tag{B.35}$$

or for the mixed second derivative

$$\begin{aligned}\mathrm{d}_i\,\mathrm{d}_j\,(\ln Z_f) &= -\,\mathrm{d}_i\langle\,\mathrm{d}_j\,f\,\rangle_f \\ &= -\langle\,\mathrm{d}_i\,\mathrm{d}_j\,f\,\rangle_f + \langle\!\langle\,\mathrm{d}_i\,f\,\mathrm{d}_j\,f\,\rangle\!\rangle_f - \langle\,\mathrm{d}_i\,f\,\rangle_f\,\langle\,\mathrm{d}_j\,f\,\rangle_f\end{aligned} \tag{B.36}$$

Written in common physicist notation we find for $f = \lambda^i x_i$,

$$\begin{aligned}\frac{\partial^2}{\partial\lambda^i\partial\lambda^j}\ln Z &= -\underbrace{\left\langle\,\frac{\partial}{\partial\lambda^i}\frac{\partial}{\partial\lambda^j}f\,\right\rangle}_{=0} + \underbrace{\left\langle\,\frac{\partial f}{\partial\lambda^i}\frac{\partial f}{\partial\lambda^j}\,\right\rangle}_{\langle\, x_i x_j\,\rangle} - \underbrace{\left\langle\,\frac{\partial f}{\partial\lambda^i}\,\right\rangle\left\langle\,\frac{\partial f}{\partial\lambda^j}\,\right\rangle}_{\langle\, x_i\,\rangle\langle\, x_j\,\rangle} \\ &= \langle\, x_i x_j\,\rangle - \langle\, x_i\,\rangle\langle\, x_j\,\rangle - \langle\, x_i\,\rangle\langle\, x_j\,\rangle + \langle\, x_i\,\rangle\langle\, x_j\,\rangle \\ &= \langle\,(x_i - \langle\, x_i\,\rangle)\,(x_j - \langle\, x_j\,\rangle)\,\rangle\,.\end{aligned} \tag{B.37}$$

[2] A proper way to derive the chain rule involves a bit more trickery, *e.g.* we need to check if it is true on the boundaries of the integration domain.

As an aside, applying the Bogoliubov norm to the relative entropy yields a quantum version of the Fisher information metric [297].

B.3. Self Adjoint vs. Hermitian Operators

Transferring results obtained for finite dimensional operators to infinite dimensional spaces yields surprises like [298]

$$\mathrm{tr}\left([p,q]\right) = \mathrm{tr}(pq) - \mathrm{tr}(qp) = \mathrm{tr}(qp) - \mathrm{tr}(qp) = 0, \tag{B.38}$$

while on the other hand we find

$$\mathrm{tr}\left([p,q]\right) = -\,\mathrm{tr}\left(\mathrm{i}\hbar\mathbb{1}\right) \neq 0. \tag{B.39}$$

What is wrong? The reason why (B.39) fails is that we have to deal with an infinite dimensional space where the trace of the identity does not exist. But this is not enough. At least one of the operators needs to be unbounded in order to avoid the replacement of the finite sum by an infinite integral. We thus conclude that the one of the two operators cannot be defined on the entire infinite dimensional Hilbert space $\mathcal{H}$. So which one is it? In order to discuss this question we need to resort to more mathematical rigor.

Definition of an operator:

An operator consists of an pair $(x, \mathcal{D}(x))$ such that

$$\begin{aligned} \mathcal{D}(x) &\longrightarrow \mathcal{H}, \\ |\,\psi\,\rangle &\longmapsto x\,|\,\psi\,\rangle, \end{aligned} \tag{B.40}$$

where $\mathcal{D}(x) \subset \mathcal{H}$ is the domain of the operator. This is physically important since we can have operators acting the same way on the Hilbert space but with different domains, depending on the physical system. Thus to operators are only equal if

$$(x, \mathcal{D}(x)) = (y, \mathcal{D}(y)) \qquad \Rightarrow \qquad x\,|\,\psi\,\rangle = y\,|\,\psi\,\rangle, \qquad |\,\psi\,\rangle \in \mathcal{D}(x) = D(y). \tag{B.41}$$

Self-adjoint vs. hermitian operators:

An hermitian operator $x^\dagger$ acts in the same way as x on $\mathcal{D}(x)$, with a possible larger domain $\mathcal{D}(x^\dagger)$, i.e.

$$x^\dagger\,|\,\psi\,\rangle = x\,|\,\psi\,\rangle, \qquad \mathcal{D}(x^\dagger) \neq \mathcal{D}(x). \tag{B.42}$$

An self-adjoint operator is defined as $x^\dagger = x$ or more precisely $\left(x^\dagger, \mathcal{D}(x^\dagger)\right) = (x, \mathcal{D}(x))$. Therefore we can conclude that any self-adjoint operator is hermitian but not every hermitian operator is self-adjoint. Only if we throw away the crucial information on which domain an operator is defined, we can come to the wrong conclusion that hermitian operators are identical to self-adjoint operators.[3]

An prominent example is the momentum operator p which is hermitian but not self-adjoint.

[3] On finite Hilbert spaces all operators are defined on the entire space $\mathcal{D}(x) = \mathcal{H}$ and thus there is no difference between Hermitian and self-adjoint operators.

One can show that $\mathcal{D}(p) \subset \mathcal{D}(p^\dagger)$, so $\left(p^\dagger, \mathcal{D}(p^\dagger)\right) \neq (p, \mathcal{D}(p))$. This is very important since only self-adjoint operators possess an real spectrum with orthogonal proper and generalized eigenfunctions that form a complete set. On the other hand, hermitian operators do not allow to define proper and generalized eigenfunctions in a strict sense.[4] In general the spectrum of a Hilbert space operator consists of three parts: proper eigenvalues, general eigenvalues and the so-called residual spectrum, which is zero for a self-adjoint operator. Roughly speaking, the residual spectrum contains the eigenvalues/functions x^* that belong to $x^\dagger$ but not to x. The trace over the residual spectrum will yield/cancel the "contribution" from the trace over the identity such that $\mathrm{tr}\left([p,q]\right) = 0$. Finally, let us calculate the residual spectrum of p. Taking the representation

$$p = -\mathrm{i}\hbar\,\mathrm{d} = p^\dagger, \qquad \mathcal{D}(p) \subset \mathcal{D}(p^\dagger), \tag{B.43}$$

where $\mathcal{D}(p)$ has to respect that its eigenfunctions need to be square integrable *e.g.* bounded on some interval. This is sufficient also for the operator $p^\dagger$ and thus its domain is not "constrained". The residual spectrum is then given by all the eigenvalues of the eigenfunctions that are not square integrable, i.e.

$$\mathcal{D}(p^\dagger) \ni \psi(q) = \mathrm{e}^{\frac{\mathrm{i}}{\hbar}pq} \qquad \Rightarrow \qquad p^\dagger\psi(q) = p^*\psi(q). \tag{B.44}$$

Therefore we conclude that the residual spectrum is given by $\mathbb{C}$ (since p is the real physical momentum) and our calculation of $\mathrm{tr}\left([p,q]\right)$ was wrong in the first place. The correct result is given by

$$\mathrm{tr}\left([p,q]\right) = \mathrm{tr}\left(pq\right) - \mathrm{tr}\left(pq\right)^\dagger = 0 - \hbar\dim\mathbb{C} = \mathrm{tr}\left(-\mathrm{i}\hbar\mathbb{1}\right). \tag{B.45}$$

[4] This is the reason why physical observables must be self-adjoint and hermitian operators must be made self-adjoint if possible in order to get the right answers to compare with experiments

C

Full Set of Equations of Motion for Holographic S-Wave Superconductor

C.1. Scalar Field Fluctuation Equations of Motion

The Fourier transformed backreacted scalar field fluctuation $\delta\phi$ equations of motion including all gauge field fluctuations a_a and metric fluctuations h_{ab} reads

$$\begin{aligned}
&\delta\phi''(u) + \left(\frac{f'(u)}{f(u)} - \frac{\chi'(u)}{2} - \frac{d-1}{u}\right)\delta\phi'(u) + \left[\frac{\mathrm{e}^{\chi(u)}\,(\omega + A_t(u))^2}{f(u)^2} - \frac{\mathbf{k}^2}{f(u)} - \frac{L^2 m^2}{u^2 f(u)}\right]\delta\phi(u) \\
&\qquad + \left[\mathrm{e}^{\chi(u)}\,\left(\frac{\omega + 2A_t(u)}{f(u)^2}\right)a_t(u) + \frac{1}{f(u)}\mathbf{k}\cdot\mathbf{a}(u)\right]\Phi(u) \\
&\qquad - \mathrm{i}\Phi a_u'(u) - \mathrm{i}\left[\left(\frac{f'(u)}{f(u)} - \frac{\chi'(u)}{2} - \frac{d-1}{u}\right)\Phi(u) + 2\Phi'(u)\right]a_u(u) \\
&\qquad + \mathrm{e}^{\chi(u)}\,\left(\frac{\mathrm{i}A_t(u)\Phi(u) - \Phi'(u)}{2f(u)^2}\right)h_{tt}'(u) + \mathrm{e}^{\chi(u)}\,\left(\frac{\mathrm{i}u^2 A_t(u)\Phi(u)}{L^2 f(u)}\right)h_{tu}'(u) \\
&\qquad - \frac{\mathrm{i}A_t(u)\Phi(u) - \Phi'(u)}{2f(u)}\sum_{i=1}^{d-1}h_{ii}'(u) + \frac{1}{2}\left[\left(1 + \frac{2u^2 f(u)}{L^2}\right)\Phi'(u) - \mathrm{i}A_t(u)\Phi(u)\right]h_{uu}'(u) \\
&\qquad - \frac{\mathrm{e}^{\chi(u)}}{2f(u)^2}\left\{\Phi''(u) + \left[\mathrm{i}\left(\sum_{i=1}^{d-1}k_i - \omega\right) - \frac{d-1}{u} - \frac{f'(u)}{f(u)} + \frac{\chi'(u)}{2} - 2\mathrm{i}A_t(u)\right]\Phi'(u)\right. \qquad \text{(C.1)}
\end{aligned}$$

$$+\left[A_t(u)\left(\sum_{i=1}^{d-1}k_i-\omega\right)+\frac{\mathrm{i}(d-1)A_t(u)}{u}+\frac{2u^2\omega\,\mathrm{e}^{\chi(u)}\,A_t(u)}{L^2f(u)}+\frac{\mathrm{i}f'(u)}{f(u)}A_t(u)\right.$$
$$\left.-\left(1-\frac{2u^2\,\mathrm{e}^{\chi(u)}}{L^2f(u)}\right)A_t(u)^2-\mathrm{i}A_t'(u)-\frac{\mathrm{i}}{2}A_t(u)\chi'(u)\right]\Phi(u)\Bigg\}h_{tt}(u)$$
$$-\frac{u^2\,\mathrm{e}^{\chi(u)}\,A_t(u)\Phi(u)}{L^2f(u)^2}\sum_{i=1}^{d-1}h_{ti}k_i+\frac{\mathrm{i}u^2\,\mathrm{e}^{\chi(u)}}{L^2f(u)}\left[(\omega+2A_t(u))\Phi'(u)\right.$$
$$\left.+\left(A_t'(u)-\frac{\chi'(u)}{2}-\frac{d-3}{u}A_t(u)\right)\Phi(u)\right]h_{tu}(u)$$
$$+\frac{1}{2f(u)}\left\{\Phi''(u)+\left[\mathrm{i}\left(\sum_{i=1}^{d-1}k_i-\omega\right)-\frac{d-1}{u}-\frac{\chi'(u)}{2}-2\mathrm{i}A_t(u)\right]\Phi'(u)\right.$$
$$\left.+\left[A_t(u)\left(\sum_{i=1}^{d-1}k_i-\omega\right)+\frac{\mathrm{i}(d-1)A_t(u)}{u}-A_t(u)^2-\mathrm{i}A_t'(u)+\frac{\mathrm{i}}{2}A_t(u)\chi'(u)\right]\Phi(u)\right\}\sum_{i=1}^{d-1}h_{ii}(u)$$
$$+\frac{\mathrm{i}u^2\Phi'(u)}{L^2}\sum_{i=1}^{d-1}h_{ui}(u)k_i+\frac{1}{2}\left\{\left(1+\frac{2u^2f(u)}{L^2}\right)\Phi''(u)+\left[\mathrm{i}\left(\sum_{i=1}^{d-1}k_i-\omega\right)-\frac{d-1}{u}\right.\right.$$
$$\left.\left.-2\mathrm{i}A_t(u)+\frac{f'(u)}{f(u)}+\frac{4u^2f'(u)}{L^2}-\left(\frac{1}{2}+\frac{u^2f(u)}{L^2}\right)\chi'(u)-\frac{2(d-3)uf(u)}{L^2}\right]\Phi'(u)\right.$$
$$+\left[A_t(u)\left(\sum_{i=1}^{d-1}k_i-\omega\right)+\frac{\mathrm{i}(d-1)A_t(u)}{u}-\frac{\mathrm{i}f'(u)A_t(u)}{f(u)}-A_t(u)^2\right.$$
$$\left.\left.-\mathrm{i}A_t'(u)+\frac{\mathrm{i}}{2}A_t(u)\chi'(u)\right]\Phi(u)\right\}h_{uu}(u)=0. \quad \text{(C.2)}$$

The complex conjugated equation for $\delta\phi^*$ can be obtained by replacing $\omega\longrightarrow-\omega$ and $\mathbf{k}\longrightarrow-\mathbf{k}$. There are possible gauge choices for the gauge field and metric fluctuations that allows to set a_u and h_{au} to zero.

C.2. Gauge Field Fluctuation Equations of Motion

The d equations of motions for the spacetime components of the gauge field fluctuations are given by

$$a_t''(u)+\left(\frac{\chi'(u)}{2}-\frac{d-3}{u}\right)a_t'(u)-\left(\frac{\mathbf{k}^2}{f(u)}+\frac{2L^2\Psi(u)}{u^2f(u)}\right)a_t(u)-\frac{\omega}{f(u)}\mathbf{k}\cdot\mathbf{a}(u)$$
$$-\frac{L^2}{u^2f(u)}\Big[\big(\omega+2\Phi(u)\big)\delta\psi(u)-\big(\omega-2\Phi(u)\big)\delta\psi^*\Big]\Psi(u)+\mathrm{i}\omega\left[a_u'(u)+\left(\frac{\chi'(u)}{2}-\frac{d-3}{u}\right)a_u(u)\right] \quad \text{(C.3)}$$

$$
\begin{aligned}
&-\frac{3u^2\,\mathrm{e}^{\chi(u)}\,\Phi'(u)}{2L^2 f(u)}h'_{tt}(u)+\frac{u^2\Phi'(u)}{2L^2}\sum_{i=1}^{d-1}h'_{ii}(u)+\frac{3u^2 f(u)\Phi'(u)}{2L^2}h'_{uu}(u)\\
&-\left\{\frac{\left(L^2 f(u)-2u^2\right)\Phi(u)\Psi(u)^2}{u^2 f(u)}+\frac{3}{2}\frac{u^2\,\mathrm{e}^{\chi(u)}}{L^2 f(u)}\left[\Phi''(u)-\left(\frac{f'(u)}{f(u)}-\frac{3\chi'(u)}{2}+\frac{d-5}{u}\right)\Phi'(u)\right]\right\}h_{tt}(u)\\
&+\left[\frac{L^2\,\mathrm{e}^{-\chi(u)}\,\Phi(u)\Psi(u)^2}{u^2}+\frac{u^2}{2L^2}\left(\Phi''(u)+\left(\frac{\chi'(u)}{2}-\frac{d-5}{u}\right)\Phi'(u)\right)\right]\sum_{i=1}^{d-1}h_{ii}(u)+\frac{\mathrm{i}u\Phi'(u)}{L^2}\sum_{i=1}^{d-1}h_{ui}(u)k_i\\
&+\left\{\frac{L^2 f(u)\,\mathrm{e}^{-\chi(u)}\,\Phi(u)\Psi(u)^2}{u^2}+\frac{3}{2}\frac{u^2 f(u)}{L^2}\left[\Phi''(u)+\left(\frac{f'(u)}{f(u)}+\frac{\chi'(u)}{2}-\frac{d-5}{u}\right)\Phi'(u)\right]\right\}h_{uu}(u)=0,
\end{aligned}
\tag{C.4}
$$

$$
\begin{aligned}
&\mathbf{a}''(u)+\left(\frac{f'(u)}{f(u)}-\frac{\chi'(u)}{2}-\frac{d-3}{u}\right)\mathbf{a}'(u)+\left(\frac{\mathrm{e}^{\chi(u)}\,\omega^2}{f(u)^2}-\frac{\mathbf{k}_\perp^2}{f(u)}-\frac{2L^2\Psi(u)^2}{u^2 f(u)}\right)\mathbf{a}(u)+\frac{\mathbf{k}}{f(u)}\left(\mathbf{k}_\perp\cdot\mathbf{a}(u)\right)\\
&+\frac{\mathrm{e}^{\chi(u)}\,\omega\mathbf{k}}{f(u)^2}a_t(u)+\frac{L^2\mathbf{k}}{u^2 f(u)}\left(\delta\psi(u)-\delta\psi^*(u)\right)\Psi(u)-\mathrm{i}\mathbf{k}\left[a'_u(u)+\left(\frac{f'(u)}{f(u)}-\frac{\chi'(u)}{2}-\frac{d-3}{u}\right)a_u(u)\right]\\
&-\frac{u^2\,\mathrm{e}^{\chi(u)}\,\Phi'(u)}{L^2 f(u)}\mathbf{h}'_t(u)+\frac{L^2 e[\chi(u)]\Phi(u)\Psi(u)^2}{u^2 f(u)^2}h_{tt}(u)+\mathrm{e}^{\chi(u)}\left[\frac{2\Phi(u)\Psi(u)^2}{f(u)^2}\right.\\
&\left.-\frac{u^2}{L^2 f(u)}\left(\Phi''(u)+\frac{\chi'(u)}{2}-\frac{d-5}{u}\Phi'(u)\right)\right]\mathbf{h}_t(u)-\frac{L^2\Phi(u)\Psi(u)^2}{u^2 f(u)}\sum_{i=1}^{d-1}h_{ii}\\
&-\frac{\mathrm{i}u^2\omega\,\mathrm{e}^{\chi(u)}\,\Phi'(u)}{L^2 f(u)}\mathbf{h}_u(u)-\frac{L^2\Phi(u)\Psi(u)^2}{u^2}h_{uu}(u)=0,
\end{aligned}
\tag{C.5}
$$

and finally the constraint equation arising from a_u

$$
\begin{aligned}
&\frac{\mathrm{e}^{\chi(u)}\,\omega}{f(u)}a'_t(u)+\mathbf{k}\cdot\mathbf{a}'(u)-\mathrm{i}\left(\mathbf{k}^2-\frac{\mathrm{e}^{\chi(u)}\,\omega^2}{f(u)}+\frac{2L^2\Psi(u)^2}{u^2}\right)a_u(u)\\
&-\frac{L^2}{u^2}\left[\left(\delta\psi(u)-\delta\psi^*(u)\right)\Psi'(u)-\left(\delta\psi'(u)-\delta\psi'^*(u)\right)\Psi(u)\right]\\
&+\mathrm{e}^{\chi(u)}\left(\frac{\mathrm{i}L^2\Phi(u)\Psi(u)^2}{u^2 f(u)^2}-\frac{3}{2}\frac{u^2\omega\Phi'(u)}{L^2 f(u)^2}\right)h_{tt}(u)-\frac{u^2\,\mathrm{e}^{\chi(u)}\,\Phi'(u)}{L^2 f(u)}\sum_{i=1}^{d-1}h_{ti}k_i\\
&+\frac{2\mathrm{i}\,\mathrm{e}^{\chi(u)}\,\Phi(u)\Psi(u)^2}{f(u)}h_{tu}(u)-\left[\frac{\mathrm{i}L^2\Phi(u)\Psi(u)^2}{u^2 f(u)}-\frac{u^2\omega\,\mathrm{e}^{\chi(u)}\,\Phi'(u)}{2L^2 f(u)}\right]\sum_{i=1}^{d-1}h_{ii}(u)\\
&-\left[\frac{\mathrm{i}L^2\Phi(u)\Psi(u)^2}{u^2}-\frac{3}{2}\frac{u^2\omega\,\mathrm{e}^{\chi(u)}\,\Phi'(u)}{L^2}\right]h_{uu}(u)=0.
\end{aligned}
\tag{C.6}
$$

"Computer are like Old Testament gods:
lots of rules and no mercy."

– Joseph Campbell

D

Listings of *Mathematica*-Code

D.1. Solutions to Holographic Background Equations in the Probe Limit

The boundary and horizon asymptotic of a set of coupled differential equations is computed using the Frobenius method. The final answer is written to a file. The respective *Mathematica* code is listed below:

Mathematica Code D.1 Asymptotic.nb

```
IR/UV Asymptotic for the Background Fields Psi, Phi
in the Probe Limit
SetDirectory["/home/steffen/Dropbox/Holographic␣Superconductors/s-wave/data"
    ];
$Assumptions={Element[d,Integers]&&d>0&&Element[{u,uH},Reals]&& u>0 && uH>0};
Differential Equations Phi, Psi
AdS-Schwarzschild black hole in d dimensions with temperature T=d/(4pi
    Subscript[u, H])
f[u_,uH_,d_]=1-u^d/uH^d;
f'[u_,uH_,d_]=D[f[u,uH,d],u];
Definition of differential equations
eqPsi[u_,uH_,m_,d_]=Psi''[u]+(f'[u,uH,d]/f[u,uH,d]-(d-1)/u)Psi'[u]+(Phi[u]^2/
    f[u,uH,d]^2-m^2/(u^2 f[u,uH,d]))Psi[u];
eqPhi[u_,uH_,m_,d_]=Phi''[u]-(d-3)/u Phi'[u]-2 Psi[u]^2/(u^2 f[u,uH,d]) Phi[u
    ];
```

```
Asymptotics near the horizon Subscript[u, H] up to 4th order
Clear[alpha,beta,aPsi,aPhi,d,m];
Index and Expansion
u0=uH=1;
hord=4;
PsiH[u_]=(u-u0)^alpha Sum[aPsi[i](u-u0)^i,{i,0,hord}];
PhiH[u_]=(u-u0)^beta Sum[aPhi[i](u-u0)^i,{i,0,hord}];
Calculation of horizon expansion
expansionPsi=Simplify[(u-u0)^-alpha eqPsi[u,u0,m,d]/.{Psi->Function[{u},PsiH[
    u]],Phi->Function[{u},(u-u0)^-beta PhiH[u]]}];
expansionPhi=Simplify[(u-u0)^-beta eqPhi[u,u0,m,d]/.{Psi->Function[{u},(u-u0)
    ^-alpha PsiH[u]],Phi->Function[{u},PhiH[u]]}];
hPsi=Simplify[Series[expansionPsi,{u,u0,hord}]];
hPhi=Simplify[Series[expansionPhi,{u,u0,hord}]];
Set free boundary parameters and fix index alpha
Solve[{Coefficient[hPsi,u-u0,-2]==0,Coefficient[hPhi,u-u0,-2]==0},{alpha,beta
    ,aPsi[0],aPhi[0]}]
Solve::svars: Equations may not give solutions for all "solve" variables. >>
{{alpha->0,aPhi[0]->0},{beta->0,aPsi[0]->0},{beta->1,aPsi[0]->0},{beta->0,
    aPhi[0]->-I d alpha},{beta->1,aPhi[0]->-I d alpha},{beta->0,aPhi[0]->I d
    alpha},{beta->1,aPhi[0]->I d alpha},{aPsi[0]->0,aPhi[0]->0}}
alpha=beta=0;
aPsi[0]=CPsiH;
aPhi[0]=0;
Simplify[Coefficient[hPsi,u-u0,-2]]
Simplify[Coefficient[hPhi,u-u0,-2]]
0
0
solution=Solve[{Coefficient[hPsi,u-u0,-1]==0,Coefficient[hPhi,u-u0,-1]==0},{
    aPsi[1],aPhi[1]}]
Solve::svars: Equations may not give solutions for all "solve" variables. >>
{{aPsi[1]->-((CPsiH m^2)/d)}}
aPsi[1]=-((CPsiH m^2)/d );
aPhi[1]=CPhiH;
Simplify[Coefficient[hPsi,u-u0,-1]]
Simplify[Coefficient[hPhi,u-u0,-1]]
```

```
0
0
Determine asymptotic in terms of free boundary parameters
For[i=2,i<=hord,i++,
solution=Solve[{Coefficient[hPsi,u-u0,i-2]==0,Coefficient[hPhi,u-u0,i
    -2]==0},{aPsi[i],aPhi[i]}][[1]];
aPsi[i]=Simplify[aPsi[i]/.solution[[1]]];
aPhi[i]=Simplify[aPhi[i]/.solution[[2]]];
Print[Union[Simplify[{Coefficient[hPsi,u-u0,i-2],Coefficient[hPhi,u-u0,i
    -2]}]][[1]]]
]
0
0
0
Write out asymptotic expansion to external file
stream=OpenWrite["AsymptoticBackgroundHorizon4.dat"];
Write[stream,Table[{aPsi[i],aPhi[i]},{i,0,hord}]];
Close[stream];
Asymptotics near the boundary Subscript[u, B]
Clear[alpha,beta,aPsi,aPhi,d,m];
Modify differential equations for boundary computation (equations decouple ->
     find simple solution)
f[u_,uH_,d_]=1;
f'[u_,uH_,d_]=D[f[u,uH,d],u];
eqPsi[u_,uH_,m_,d_]=Psi''[u]+(f'[u,uH,d]/f[u,uH,d]-(d-1)/u)Psi'[u]+(Phi[u]^2/
    f[u,uH,d]^2-m^2/(u^2 f[u,uH,d]))Psi[u];
eqPhi[u_,uH_,m_,d_]=(Phi''[u]-(d-3)/u Phi'[u]-2 Psi[u]^2/(u^2 f[u,uH,d]) Phi[
    u])/.Psi[u]->0;
Index and Expansion
u0=uB=0;
bord=2;
PsiB[u_]=(u-u0)^alpha Sum[aPsi[i](u-u0)^i,{i,0,bord}];
PhiB[u_]=(u-u0)^beta Sum[aPhi[i](u-u0)^i,{i,0,bord}];
Calculation of horizon expansion
expansionPsi=Simplify[(u-u0)^-alpha eqPsi[u,u0,m,d]/.{Psi->Function[{u},PsiB[
    u]],Phi->Function[{u},(u-u0)^-beta PhiB[u]]}];
```

```
expansionPhi=Simplify[(u-u0)^-beta eqPhi[u,u0,m,d]/.{Psi->Function[{u},(u-u0)
    ^-alpha PsiB[u]],Phi->Function[{u},PhiB[u]]}];
hPsi=Simplify[Series[expansionPsi,{u,u0,bord}]];
hPhi=Simplify[Series[expansionPhi,{u,u0,bord}]];
Set free boundary parameters and fix index alpha, beta
Solve[{Coefficient[hPsi,u-u0,-2]==0,Coefficient[hPhi,u-u0,-2]==0},{alpha,beta
    ,aPsi[0],aPhi[0]}]
Solve::svars: Equations may not give solutions for all "solve" variables. >>
{{alpha->1/2 (d-Sqrt[d^2+4 m^2]),beta->0},{alpha->1/2 (d-Sqrt[d^2+4 m^2]),
    beta->-2+d},{alpha->1/2 (d-Sqrt[d^2+4 m^2]),aPhi[0]->0},{alpha->1/2 (d+
    Sqrt[d^2+4 m^2]),beta->0},{alpha->1/2 (d+Sqrt[d^2+4 m^2]),beta->-2+d},{
    alpha->1/2 (d+Sqrt[d^2+4 m^2]),aPhi[0]->0},{beta->0,aPsi[0]->0},{beta
    ->-2+d,aPsi[0]->0},{aPsi[0]->0,aPhi[0]->0}}
alpha=1/2 (d-Sqrt[d^2+4 m^2]);
beta=0;
aPsi[0]=CPsiB ;
aPhi[0]=CPhiB;
Simplify[Coefficient[hPsi,u-u0,-2]]
Simplify[Coefficient[hPhi/.CPsiB->0,u-u0,-2]]
0
0
alpha=1/2 (d+Sqrt[d^2+4 m^2]);
beta=0;
aPsi[0]=CPsiB ;
aPhi[0]=CPhiB;
Simplify[Coefficient[hPsi,u-u0,-2]]
Simplify[Coefficient[hPhi/.CPsiB->0,u-u0,-2]]
0
0
alpha=1/2 (d-Sqrt[d^2+4 m^2]);
beta=d-2;
aPsi[0]=CPsiB ;
aPhi[0]=CPhiB;
Simplify[Coefficient[hPsi,u-u0,-2]]
Simplify[Coefficient[hPhi/.CPsiB->0,u-u0,-2]]
0
```

```
0
alpha=1/2 (d+Sqrt[d^2+4 m^2]);
beta=d-2;
aPsi[0]=CPsiB ;
aPhi[0]=CPhiB;
Simplify[Coefficient[hPsi,u-u0,-2]]
Simplify[Coefficient[hPhi/.CPsiB->0,u-u0,-2]]
0
0
Boundary asymptotic
PsiB[u_]=Simplify[CPsiB [0](u-u0)^(1/2 (d-Sqrt[d^2+4 m^2]))+CPsiB [1](u-u0)
    ^(1/2 (d+Sqrt[d^2+4 m^2]))]
PhiB[u_]=Simplify[CPhiB[0](u-u0)^0-CPhiB[1](u-u0)^(-2+d)]
u^(1/2 (d-Sqrt[d^2+4 m^2])) (CPsiB[0]+u^Sqrt[d^2+4 m^2] CPsiB[1])
CPhiB[0]-u^(-2+d) CPhiB[1]
Check with DSolve
f[u_,uH_,d_]=1;
f'[u_,uH_,d_]=D[f[u,uH,d],u];
eqPsi[u_,uH_,m_,d_]=Psi''[u]+(f'[u,uH,d]/f[u,uH,d]-(d-1)/u)Psi'[u]+(Phi[u]^2/
    f[u,uH,d]^2-m^2/(u^2 f[u,uH,d]))Psi[u];
eqPhi[u_,uH_,m_,d_]=(Phi''[u]-(d-3)/u Phi'[u]-2 Psi[u]^2/(u^2 f[u,uH,d]) Phi[
    u])/.Psi[u]->0;
solPhi=Simplify[DSolve[{eqPhi[u,u0,m,d]==0,Phi[1]==0},Phi,u]][[1]]
{Phi->Function[{u},-(((u^2-u^d) C[1])/((-2+d) u^2))]}
solPsi=Simplify[DSolve[{(eqPsi[u,u0,m,d]/.Phi->Function[u,mu])==0},Psi,u
    ]][[1]]
{Psi->Function[{u},u^(d/2) BesselJ[1/2 Sqrt[d^2+4 m^2],u mu] C[1]+u^(d/2)
    BesselY[1/2 Sqrt[d^2+4 m^2],u mu] C[2]]}
```

The coupled differential equations are solved by reading the asymptotic generated by Mathematica Code D.1, using the build in function ND Solve and fitting the solution near the boundary to the boundary expansion. For example the s-wave code for $m^2L^2 = -4$ and $d = 4$ is implemented as:

Mathematica Code D.2 SolutionBackground–d4–m2i.nb

```
Solution to the background fields Psi, Phi
in the Probe Limit
```

```
SetDirectory["/home/steffen/Dropbox/Holographic␣Superconductors/s-wave/data/"
    ];
$Assumptions={Element[d,Integers]&&d>0&&Element[{u,uH},Reals]&& u>0 && uH>0};
SetOptions[Plot,PlotRange->Full,PlotStyle->Evaluate[Directive[#,Thickness
    [.005]]&/@{Blue,Red}],FrameStyle->Thickness[.005],FrameLabel->{"x","y"},
    PlotLabel->"Caption",Frame->True,Axes->False];
SetOptions[ListLinePlot,PlotRange->Full,PlotStyle->Evaluate[Directive[#,
    Thickness[.005]]&/@{Blue,Red}],FrameStyle->Thickness[.005],FrameLabel->{"
    x","y"},PlotLabel->"Caption",Frame->True,Axes->False];
Differential Equations Phi, Psi
AdS-Schwarzschild black hole in d dimensions with temperature T=d/(4pi )
f[u_,d_]=1-u^d;
f'[u_,d_]=D[f[u,d],u];
Definition of differential equations
eqPsi[u_,m_,d_]=Psi''[u]+(f'[u,d]/f[u,d]-(d-1)/u)Psi'[u]+(Phi[u]^2/f[u,d]^2-m
    ^2/(u^2 f[u,d]))Psi[u];
eqPhi[u_,m_,d_]=Phi''[u]-(d-3)/u Phi'[u]-2 Psi[u]^2/(u^2 f[u,d]) Phi[u];
Asymptotics near the horizon Subscript[u, H]
u0=uH=1;
hord=4;
alpha=beta=0;
asymptoticbackground=ReadList["AsymptoticBackgroundHorizon4.dat"];
asymptoticbackground=asymptoticbackground[[1]];
For[i=0,i<= hord,i++,
aPsi[i]=Part[asymptoticbackground[[i+1]],1];
aPhi[i]=Part[asymptoticbackground[[i+1]],2];
]
PsiH[u_,m_,d_,CPsiH_,CPhiH_]=(u-u0)^alpha Sum[aPsi[i](u-u0)^i,{i,0,hord}];
PhiH[u_,m_,d_,CPsiH_,CPhiH_]=(u-u0)^beta Sum[aPhi[i](u-u0)^i,{i,0,hord}];
DPsiH[u_,m_,d_,CPsiH_,CPhiH_]=D[PsiH[u,m,d,CPsiH,CPhiH],u];
DPhiH[u_,m_,d_,CPsiH_,CPhiH_]=D[PhiH[u,m,d,CPsiH,CPhiH],u];
Integration to boundary Subscript[u, B] = 0
IntegrateEOMs[EOMPsi_,Psi_,PsiH_,DPsiH_,EOMPhi_,Phi_,PhiH_,DPhiH_,m_,d_,CPsi_
    ,CPhi_,init_,end_]:=
Module[{eomPsi,eomPhi,BoundaryConditionPsi,BoundaryConditionPhi,
    DBoundaryConditionPsi,DBoundaryConditionPhi,solution},
```

```
eomPsi=EOMPsi[arg,m,d];
eomPhi=EOMPhi[arg,m,d];
BoundaryConditionPsi=PsiH[init,m,d,CPsi,CPhi];
BoundaryConditionPhi=PhiH[init,m,d,CPsi,CPhi];
DBoundaryConditionPsi=DPsiH[init,m,d,CPsi,CPhi];
DBoundaryConditionPhi=DPhiH[init,m,d,CPsi,CPhi];
solution=NDSolve[{eomPsi==0,eomPhi==0,Psi[init]==BoundaryConditionPsi,Psi'[
    init]==DBoundaryConditionPsi,Phi[init]==BoundaryConditionPhi,Phi'[init]==
    DBoundaryConditionPhi},{Psi,Phi},{arg,end,init},MaxSteps->inf,
    PrecisionGoal->12,AccuracyGoal->inf][[1]]
]
IntegrateToBoundaries[EOMPsi_,Psi_,PsiH_,DPsiH_,EOMPhi_,Phi_,PhiH_,DPhiH_,m_,
    d_,CPsi_,CPhi_,init_,end_]:=
Module[{eomPsi,eomPhi,BoundaryConditionPsi,BoundaryConditionPhi,
    DBoundaryConditionPsi,DBoundaryConditionPhi,solution},
eomPsi=EOMPsi[arg,m,d];
eomPhi=EOMPhi[arg,m,d];
BoundaryConditionPsi=PsiH[init,m,d,CPsi,CPhi];
BoundaryConditionPhi=PhiH[init,m,d,CPsi,CPhi];
DBoundaryConditionPsi=DPsiH[init,m,d,CPsi,CPhi];
DBoundaryConditionPhi=DPhiH[init,m,d,CPsi,CPhi];
solution=NDSolve[{eomPsi==0,eomPhi==0,Psi[init]==BoundaryConditionPsi,Psi'[
    init]==DBoundaryConditionPsi,Phi[init]==BoundaryConditionPhi,Phi'[init]==
    DBoundaryConditionPhi},{Psi,Phi},{arg,end,init},MaxSteps->inf,
    PrecisionGoal->12,AccuracyGoal->inf][[1]];
{Psi[end],Phi[end],Psi'[end],Phi'[end]}/.solution
]
SolutionAtBoundaries[EOMPsi_,Psi_,PsiH_,DPsiH_,EOMPhi_,Phi_,PhiH_,DPhiH_,m_,
    d_,CPsi_,CPhi_,init_,end_,epsilon_,n_]:=
Module[{Psi1,Psi2,Phi1,Phi2,solution,fitPsi,fitPhi,APsi,BPsi,APhi,BPhi},
solution=IntegrateEOMs[EOMPsi,Psi,PsiH,DPsiH,EOMPhi,Phi,PhiH,DPhiH,m,d,CPsi,
    CPhi,init,end];
fitPsi=FindFit[{#,#^-2/Log[# 10^-.413173] Psi[#]/.solution[[1]]}&/@Range[end,
    n[[1]] epsilon[[1]],epsilon[[1]]],{APsi-BPsi /Log[u]},{APsi,BPsi},u];
Psi1=APsi/.fitPsi[[1]];
Psi2=BPsi/.fitPsi[[2]];
```

```
fitPhi=FindFit[{#,Phi[#]/.solution[[2]]}&/@Range[end,n[[2]] epsilon[[2]],
    epsilon[[2]]],{ APhi-u^(-2+d) BPhi},{APhi,BPhi},u];
Phi1=APhi/.fitPhi[[1]];
Phi2=BPhi/.fitPhi[[2]];
{Psi1,Psi2,Phi1,Phi2}
]
Invoke binary search to find the interpolation function mapping (CPsiH,
    CPhiH)->(0,mu)
binsearch[start_,end_,bisections_,func_]:=
Module[{sign1,interval,dir,pos,sign2,i},
sign1=Sign[func[start]];
interval=end-start;
dir=1;
pos=start;
For[i=1,i<=bisections,i++,
pos=pos+dir interval/2^i;
sign2=Sign[func[pos]];
If[sign2!=sign1,dir=-dir];
sign1=sign2;
];
{pos,func[pos]}
]
SolutionAtBoundaries[eqPsi,Psi,PsiH,DPsiH,eqPhi,Phi,PhiH,DPhiH,m,d
    ,10^-10,4.210862533,uinit,uend,{epsilonPsi,epsilonPhi},{nPsi,nPhi}]
{3.08729*10^-20,-1.31182*10^-10,-2.10543,-2.10543}
SolutionAtBoundaries[eqPsi,Psi,PsiH,DPsiH,eqPhi,Phi,PhiH,DPhiH,m,d
    ,.17469361,4.19,uinit,uend,{epsilonPsi,epsilonPhi},{nPsi,nPhi}]
{-8.40561*10^-13,-0.229535,-2.11084,-2.14134}
data={};
AppendTo[data
    ,{10^-10,4.210862533,3.0872944720377906`*^-20,-2.1054312664999872`}];
AppendTo[data
    ,{.17469361,4.19,-8.405609541739523`*^-13,-2.1108398487301363`}];
init={.17469361,4.19};
inter=.1;
start=init[[1]]-inter;
```

```
end=init[[1]]+inter;
Monitor[
For[CPhi=(init[[2]]-.02),CPhi>=.1,CPhi-=.02,
func[CPsi_]:=SolutionAtBoundaries[eqPsi,Psi,PsiH,DPsiH,eqPhi,Phi,PhiH,DPhiH,m
    ,d,CPsi,CPhi,uinit,uend,{epsilonPsi,epsilonPhi},{nPsi,nPhi}][[1]];
root=binsearch[start,end,50,func];
mu=SolutionAtBoundaries[eqPsi,Psi,PsiH,DPsiH,eqPhi,Phi,PhiH,DPhiH,m,d,root
    [[1]],CPhi,uinit,uend,{epsilonPsi,epsilonPhi},{nPsi,nPhi}][[3]];
AppendTo[data,N[{root[[1]],CPhi,root[[2]],mu}]];
start=root[[1]]-inter;
end=root[[1]]+inter;
],N[{root[[1]],CPhi,root[[2]],mu}]]
Write out data to external file
stream=OpenWrite["datad4m2i.dat"];
Write[stream,dataC];
Close[stream];
stream=OpenWrite["datamuCPsid4m2i.dat"];
Write[stream,datamuCPsi];
Close[stream];
stream=OpenWrite["datamuCPhid4m2i.dat"];
Write[stream,datamuCPhi];
Close[stream];
```

These codes are quite generic and can be extended to arbitrary systems of second order ordinary differential equations, *e.g.* dealing with fluctuation and/or backreaction.

D.2. Different Root-Finding Algorithms

The following *Mathematica* code displays three typical root finding algorithms, the bisection method, the Newton methods and the secant method:

Mathematica Code D.3 Numerical–Methods.nb

```
Numerical Methods
Newton's Method
NewtonsMethod[start_,error_,imax_,f_]:=
Module[{x0,x1,i,xerror,fp},
tracking={};
```

```
i=0;
x0=start;
fp[x_]:=Evaluate[D[f[x],x]];
While[True,
x1=x0-N[f[x0]/fp[x0]];
xerror=Abs[x1-x0];
x0=x1;
i++;
AppendTo[tracking,xerror];
If[!((xerror>error)&& i<=imax),
Break[];
];
];
{x0,f[x0],error}
]
MultiDimensionalNewtonsMethod[start_,error_,imax_,f_,fp_]:=
Module[{x0,x1,i,d,xerror,errora},
(* fp[{x}_]:=Evaluate[D[f@@x,{x}]]; calculate fp in exactly this way with
    outside the module and supply it in the fp slot *)
tracking={};
i=0;
x0=start;
d=Length[x0];
errora=error IdentityMatrix[d];
While[True,
If[Det[fp@@x0]==0,
Print["Error: Jacobian has no inverse!"];
Break[];
];
x1=x0-N[Inverse[fp@@x0].f@@x0];
xerror=Abs[x1-x0];
x0=x1;
i++;
AppendTo[tracking,xerror[[1]]];
(* Find out how to compare the error *)
If[And@@Table[xerror[[j]]<errora[[j]],{j,d}]|| i>=imax,
```

```
41  Break[];
    ];
43  ];
    {x0,f@@x0,xerror}
45  ]
    Secant Method
47  SecantMethod[start_,stepsize_,error_,imax_,f_]:=
    Module[{x0,x1,i,xerror},
49  tracking={};
    i=0;
51  x0=start;
    While[True,
53  x1=x0-N[f[x0]stepsize/(f[x0+stepsize]-f[x0])];
    xerror=Abs[x1-x0];
55  x0=x1;
    i++;
57  AppendTo[tracking,xerror];
    If[!((xerror>error)&& i<=imax),
59  Break[];
    ];
61  ];
    {x0,f[x0],error}
63  ]
    MultiDimensionalSecantMethod[start_,stepsize_,error_,imax_,f_]:=
65  Module[{x0,x0h,x1,i,d,xerror,errora,fpx0},
    tracking={};
67  i=0;
    x0=start;
69  d=Length[x0];
    errora=error IdentityMatrix[d];
71  x0h[x_,n_]:=Table[x[[m]]+stepsize KroneckerDelta[n,m],{m,d}];
    While[True,
73  fpx0=Table[(f@@(x0h[x0,k])-f@@x0)[[j]],{j,d},{k,d}];
    If[Det[fpx0]==0,
75  Print["Error:␣Jacobian␣has␣no␣inverse!"];
    Break[];
```

```
77 ];
   x1=x0–N[stepsize Inverse[fpx0].f@@x0];
79 xerror=Abs[x1–x0];
   x0=x1;
81 i++;
   AppendTo[tracking,xerror[[1]]];
83 (* Find out how to compare the error *)
   If[And@@Table[xerror[[j]]<errora[[j]],{j,d}]|| i>=imax,
85 Break[];
   ];
87 ];
   {x0,f@@x0,xerror}
89 ]
   Binary Search
91 binsearch[start_,end_,bisections_,func_]:=
   Module[{sign1,interval,dir,pos,sign2,i},
93 sign1=Sign[func[start]];
   interval=end–start;
95 dir=1;
   pos=start;
97 For[i=1,i<=bisections,i++,
   pos=pos+dir interval/2^i;
99 sign2=Sign[func[pos]];
   If[sign2!=sign1,dir=–dir];
101 sign1=sign2;
   ];
103 {pos,func[pos]}
   ]
```

D.3. Three-Point Search Algorithm for Minimization

The three point step search employed to search for minima of the Green's function in the quasi-normal mode search is implemented as follows[1]:

Mathematica Code D.4 Step–Search–Method.nb

[1] Main parts of the code have been implemented by Jonathan Shock.

```
Step Search Method to Find Local Minima/Maxima
Definition of the Setp Search Method
left={cx-dist,cy};
right={cx+dist,cy};
top={cx,cy+dist};
bottom={cx,cy-dist};
centre={cx,cy};
coords[cx_,cy_,dist_]={right,top,left,bottom,centre};
pm[ar_]:=Position[ar,Min[ar]][[1,1]];
arrayminfirst[cx_,cy_,dist_]:=Module[{arr},
arr=Apply[func1,coords[cx,cy,dist],1];
(*Print[{pm[arr],Min[arr]}];*)
{pm[arr],Min[arr]}
]
(*newnumbers=Append[Most[RotateLeft[Range[4],Mod[#,4]]],5]&/@Range[-1,2];*)
newnumbers={{2,3,1,5},{1,4,2,5},{1,4,3,5},{2,3,4,5}};
posdep[cx_,cy_,dist_]=coords[cx,cy,dist][[#]]&/@Map[Most,newnumbers];
arraymin[cx_,cy_,dist_,from_,prevmin_]:=Module[{arr},
arr=Append[Apply[func1,posdep[cx,cy,dist][[from,#]]]&/@Range[3],prevmin];
{newnumbers[[from,pm[arr]]],Min[arr]}
]
newnumbers=Append[RotateLeft[Range[4],Mod[#,4]],5]&/@Range[0,3];
newnumbers={{2,3,1,5},{1,4,2,5},{1,4,3,5},{2,3,4,5}};
(*The first loop, enumerated by mit, looks in a grid of five points and
    determines which of the points has a minimum value of func. If the centre
     point (point 5) is chosen, the gridsize reduces and the five points are
    recalculated. This iteration can run until the grid size is the original
    distance/10^10 - very small. It's unlikely that it will ever get to this
    point unless there's an error.*)
FivePointSeek[firstx_,firsty_,distance_]:=Module[{fcontrol,posmin,mit,
    vardistance,newcentrest={firstx,firsty}},
vardistance=distance;
(*Print["into 5"];*)
For[fcontrol=5,fcontrol==5,
posmin=arrayminfirst[firstx,firsty,vardistance];
```

```
30  If[Log[10,vardistance]<=-acc,Break[]];
    If[Sqrt[(re1-firstx)^2+(im1-firsty)^2]>ranger,toofar=True;Break[]];
32  fcontrol=posmin[[1]];
    If[fcontrol==5,vardistance=vardistance/10,newcentrest=posdep[firstx,firsty,
        vardistance][[fcontrol,3]]];
34  ];
    {posmin,newcentrest,vardistance}
36  ]
    (*Here we use arraymin, which looks in a region of 4 points to decide which
        direction to go in.*)
38  ThreePointSeek[varnewcentres_,vardistance_,varposmin_]:=Module[{newposmin,nit
        ,renewcentres},
    {newposmin,renewcentres}={varposmin,varnewcentres};
40  fcontrol=newposmin[[1]];
    For[fcontrol,fcontrol!=5,
42  newposmin=arraymin[renewcentres[[1]],renewcentres[[2]],vardistance,fcontrol,
        newposmin[[2]]];
    fcontrol=newposmin[[1]];
44  If[fcontrol!=5,renewcentres=posdep[renewcentres[[1]],renewcentres[[2]],
        vardistance][[fcontrol,3]],Break[]];
    If[Sqrt[(re1-renewcentres[[1]])^2+(im1-renewcentres[[2]])^2]>ranger,toofar=
        True;Break[]];
46  ];
    {newposmin,renewcentres}
48  ]
    tracking={};
50  (*Some random function with a load of minima*)
    myfunc[wx_,wy_,nk_,neb_,nm_,ir_,uv_]=Sin[wx nk]+Cos[wy neb]+nm+ir uv;
52  twodstepsearch[firstx_,firsty_,vardistance_,nk_,neb_,nm_,ir_,uv_]:=Module[{
        bit,mit,nit,cit,try1,distance,newcentres},
    If[NumberQ[ranger],,ranger=10];
54  If[NumberQ[acc],,acc=5];
    warning=False;(*This variable is a flag which is printed at the end and tells
         us whether any of the possible errors have occured through the
        computation. If they have the data is likely not to be accurate*)
56  tracking={};
```

```
func1[wx_,wy_]:=myfunc[wx,wy,nk,neb,nm,ir,uv];(*((Abs[Re[#]]+Abs[Im[#]])&/@
    {DetHepsilon[c,d,wx-I wy,varq]})[[1]];*)(Abs[Re[#]]+Abs[Im[#]])&/@{
    DetHepsilon[c,d,wx-I wy,varq]}*)
(*func1[wx_,wy_]=wx^2+wy^2;*)
(*We here define the function which we would like to minimise. We use the
    logarithm simply so that we can see the order of magnitude*)
distance=vardistance;
(*distance is the first step size we will use for our grid. It will be
    reduced as we get closer to the minimum*)

(*the outputs of the first loop are try1 and newcentres. try1 tells us the
    direction of the minimum point on the grid (one of five options (top,
    left, right, bottom, centre)=(1,2,3,4,5)), and newcentres gives the
    position of the new centre position in the complex omega plane.*)

tempdistance=distance;
{try1,newcentres,distance}=FivePointSeek[firstx,firsty,tempdistance];
Clear[tempdistance];

(*Now we have the position of the next point to study - ie. we want to find
    the direction from the new point which will take us towards the local
    minimum*)
(*Print[newcentres];*)
(*The if statement makes sure that we haven't been stuck on the same centre
    point in the above loop. If we have, then try1 will give 5(=centre) and
    the warning flag will be turned to true. If try1 is not 5, we continue in
     the direcion of the minimum which we have found in the first loop, above
    *)
If[try1[[1]]!=5,
(*Here we make upto 50 steps iterated over bit, to move towards the local
    minimum*)

For[bit=1,bit<10,bit++,
(*Print[distance];*)
{tempnc,tempt1}={newcentres,try1};
{try1,newcentres}=ThreePointSeek[tempnc,distance,tempt1];
```

```
Clear[tempnc,tempt1];

(*Once we are in a minimum (given a specific gridsize) we decrease this
    stepsize to begin a more accurate search centered around this minimum*)
distance=distance/10;
(*If nit does not get to 50 then we have found a minimum and we have to redo
    everything with the new (smaller) gridstep.*)
{tempdistance,tempnc1,tempnc2}={distance,newcentres[[1]],newcentres[[2]]};

{try1,newcentres,distance}=FivePointSeek[tempnc1,tempnc2,tempdistance];

Clear[tempdistance,tempnc1,tempnc2];
If[Sqrt[(re1-newcentres[[1]])^2+(im1-newcentres[[2]])^2]>ranger,toofar=True;
    bit=50];
If[distance<=10^-acc,bit=50];
(*If the gridsize has decreased four times in a row without moving from the
    same position there is probably a problem and the warning flag is turned
    on*)
If[try1[[1]]==5,warning=True;bit=50;Print["yes4"]];

(*This is an accuracy check. We repeat the whole process (inside the bit loop
    ) until the logarithm becomes negative. If the loop runs 50 times and we
    still haven't achieved this accuracy we flag the warning.*)

If[bit>=7&&try1[[2]]<0,Print["yes3"];bit=50];
If[bit==10&&try1[[2]]>0,warning=True];

];
(*This is from the first if statement.*)
,warning=True;

];
```

“Emacs is like a laser guided missile.
It only has to be slightly misconfigured
to ruin your whole day.”

– Sean McGrath

E
Production Notes

This thesis was produced using mostly free software, except for *Mathematica*. The present digital version was typeset using LaTeX, more specifically the latest frozen TexLive 2012 version. In order to “compile” the LaTeXdocument the build automation tool *Make* was used to assemble the vast amount of information stored in the auxiliary files. The bibliography was generate with *Bibtex8*, the UTF-8 encoding extension of the original *Bibtex* program. The Figure 4.7 was generated by *Gnuplot* from the data taken from [43] and all pictures found in the figures were drawn in *Inkscape*. With the help of *Cairo* all svg files were converted to eps files, preserving the labels, in order to replace them with LaTeXtags using the package psfrag. The LaTeXsource file was created with *Emacs* using the *AucTex* extension for a better teXing experience and the *Ispell* spelling checker to minimize the number of typos. The author used *Xindy* to assemble a indexed list of symbols, which unfortunately could not be added to the final version due the lack of time. The author wants to express his gratitude to all people developing, maintaining and distributing free software in particular the possibility to employ the aforementioned software free of charge for non-commercial usage.

Bibliography

[1] J. Erdmenger, P. Kerner, and S. Müller, *Towards a Holographic Realization of Homes' Law*, JHEP **1210** (2012) 021, arXiv:1206.5305.

[2] M. Ammon, J. Erdmenger, S. Lin, S. Müller, A. O'Bannon, and J. P. Shock, *On Stability and Transport of Cold Holographic Matter*, JHEP **1109** (2011) 030, arXiv:1108.1798.

[3] C. Burgess and G. Moore, *The Standard Model: A Primer*. Cambridge University Press, 2007.

[4] X.-G. Wen, *Quantum Field Theory of Many-Body Systems: From the Origin of Sound to an Origin of Light and Electrons*. Oxford University Press, 2004.

[5] M. Z. Hasan and C. L. Kane, *Topological Insulators*, Rev.Mod.Phys **82** (Oct, 2010) 3045–3067, arXiv:1002.3895.

[6] S. Sachdev, *Quantum Phase Transition*. Cambridge University Press, 2011.

[7] S. Sachdev and B. Keimer, *Quantum Criticality*, Phys.Today **64N2** (2011) 29, arXiv:1102.4628.

[8] J. Zaanen, *A Modern, but way too short history of the theory of superconductivity at a high temperature*, arXiv (Dec, 2010) arXiv:1012.5461.

[9] S. Sachdev, *The Quantum phases of matter*, arXiv (2012) arXiv:1203.4565.

[10] S. Sachdev, *What can Gauge-Gravity Duality Teach us about Condensed Matter Physics?*, Ann.Rev.Condensed Matter Phys. **3** (2012) 9–33, arXiv:1108.1197.

[11] K. Rajagopal and F. Wilczek, *The Condensed Matter Physics of QCD*, Shifman, M. (ed.): At the Frontier of Particle Physics, Vol. 3 (2000) arXiv:hep-ph/0011333.

[12] M. G. Alford, A. Schmitt, K. Rajagopal, and T. Schäfer, *Color superconductivity in dense quark matter*, Rev.Mod.Phys. **80** (2008) 1455–1515, arXiv:0709.4635.

[13] M. Stephanov, *QCD phase diagram: An Overview*, PoS **LAT2006** (2006) 024, arXiv:hep-lat/0701002.

[14] P. Kovtun, D. T. Son, and A. O. Starinets, *Holography and Hydrodynamics: Diffusion on Stretched Horizons*, JHEP **0310** (2003) 064, arXiv:hep-th/0309213.

[15] A. Karch, *Recent Progress in Applying Gauge/Gravity Duality to Quark-Gluon Plasma Physics*, AIP Conf.Proc. **1441** (2012) 95–102, arXiv:1108.4014.

[16] V. Kaplunovsky, D. Melnikov, and J. Sonnenschein, *Baryonic Popcorn*, JHEP **1211** (2012) 047, arXiv:1201.1331.

[17] A. Buchel and J. T. Liu, *Universality of the Shear Viscosity in Supergravity*, Phys.Rev.Lett. **93** (2004) 090602, arXiv:hep-th/0311175.

[18] P. Kovtun, D. Son, and A. Starinets, *Viscosity in Strongly Interacting Quantum Field Theories from Black Hole Physics*, Phys.Rev.Lett. **94** (2005) 111601, arXiv:hep-th/0405231.

[19] N. Iqbal and H. Liu, *Universality of the Hydrodynamic Limit in AdS/CFT and the Membrane Paradigm*, Phys.Rev. **D79** (2009) 025023, arXiv:0809.3808.

[20] A. Sinha and R. C. Myers, *The Viscosity Bound in String Theory*, Nucl.Phys. **A830** (2009) 295C–298C, arXiv:0907.4798.

[21] J. Erdmenger, P. Kerner, and H. Zeller, *Non-universal shear viscosity from Einstein gravity*, Phys.Lett. **B699** (2011) 301–304, arXiv:1011.5912.

[22] J. Erdmenger, P. Kerner, and H. Zeller, *Transport in Anisotropic Superfluids: A Holographic Description*, JHEP **1201** (2012) 059, arXiv:1110.0007.

[23] A. Rebhan and D. Steineder, *Violation of the Holographic Viscosity Bound in a Strongly Coupled Anisotropic Plasma*, Phys.Rev.Lett. **108** (2012) 021601, arXiv:1110.6825.

[24] S. Sachdev and M. Müller, *Quantum Criticality and Black Holes*, J.Phys.Condens.Matter **21** (2009) 164216, arXiv:0810.3005.

[25] H. Liu, J. McGreevy, and D. Vegh, *Non-Fermi Liquids from Holography*, Phys.Rev. **D83** (2011) 065029, arXiv:0903.2477.

[26] M. Cubrovic, J. Zaanen, and K. Schalm, *String Theory, Quantum Phase Transitions and the Emergent Fermi-Liquid*, Science **325** (2009) 439–444, arXiv:0904.1993.

[27] N. Iqbal, H. Liu, and M. Mezei, *Lectures on Holographic Non-Fermi Liquids and Quantum Phase Transitions*, arXiv (2011) arXiv:1110.3814.

[28] S. A. Hartnoll, *Lectures on Holographic Methods for Condensed Matter Physics*, Class.Quant.Grav. **26** (2009) 224002, arXiv:0903.3246.

[29] C. P. Herzog, *Lectures on Holographic Superfluidity and Superconductivity*, J.Phys.A **A42** (2009) 343001, arXiv:0904.1975. 39 pages, 9 figures, lectures given at the Trieste Spring School on Superstring Theory and Related Topics.

[30] G. T. Horowitz, *Theory of Superconductivity*, Lect.Notes Phys. **828** (2011) 313–347.

[31] M. Kaminski, *Flavor Superconductivity & Superfluidity*, Lect.Notes Phys. **828** (2011) 349–393, arXiv:1002.4886.

[32] J.-H. She, B. J. Overbosch, Y.-W. Sun, Y. Liu, K. Schalm, J. A. Mydosh, and J. Zaanen, *Observing the Origin of Superconductivity in Quantum Critical Metals*, Phys.Rev. **B84** (2011) 144527, arXiv:1105.5377.

[33] G. T. Horowitz, J. E. Santos, and D. Tong, *Optical Conductivity with Holographic Lattices*, JHEP **1207** (2012) 168, arXiv:1204.0519.

[34] Y. Liu, K. Schalm, Y.-W. Sun, and J. Zaanen, *Lattice Potentials and Fermions in Holographic Non-Fermi Liquids: Hybridizing Local Quantum Criticality*, JHEP **1210** (2012) 036, arXiv:1205.5227.

[35] N. Iizuka and K. Maeda, *Towards the Lattice Effects on the Holographic Superconductor*, JHEP **1211** (2012) 117, arXiv:1207.2943.

[36] Y.-Y. Bu, J. Erdmenger, J. P. Shock, and M. Strydom, *Magnetic Field Induced Lattice Ground States from Holography*, JHEP **1303** (2013) 165, arXiv:1210.6669.

[37] A. Donos and S. A. Hartnoll, *Metal-insulator transition in holography*, arXiv (2012) arXiv:1212.2998.

[38] D. Vegh, *Holography without Translational Symmetry*, arXiv (2013) arXiv:1301.0537.

[39] G. T. Horowitz and J. E. Santos, *General Relativity and the Cuprates*, arXiv (2013) arXiv:1302.6586.

[40] J. Zaanen, *Superconductivity: Why the Temperature is High*, Nature **430** (Jul, 2004) 512–513.

[41] M. Ammon, *Gauge/Gravity Duality Applied to Condensed Matter Systems*, Fortsch.Phys. **58** (2010) 1123–1250.

[42] C. C. Homes, S. V. Dordevic, M. Strongin, D. A. Bonn, R. Liang, W. N. Hardy, S. Komiya, Y. Ando, G. Yu, N. Kaneko, X. Zhao, M. Greven, D. N. Basov, and T. Timusk, *A Universal Scaling Relation in High-Temperature Superconductors*, Nature **430** (Jul, 2004) 539–541.

[43] C. C. Homes, S. V. Dordevic, T. Valla, and M. Strongin, *Scaling of the Superfluid Density in High-Temperature Superconductors*, Phys. Rev. B **72** (Oct, 2005) 134517.

[44] H. Kleinert, *Path Integrals in Quantum Mechanics, Statistics, Polymer Physics, and Financial Markets*. World Scientific, 2009.

[45] J. Zinn-Justin, *Path Integrals in Quantum Mechanics*. Oxford University Press, 2006.

[46] C. Rovelli, *Quantum Gravity*. Cambridge University Press, 2004.

[47] T. Banks, *Modern Quantum Field Theory*. Cambridge University Press, 2008.

[48] M. E. Peskin and D. V. Schroeder, *An Introduction to Quantum Field Theory*. Perseus Books, 1995.

[49] M. Srednicki, *Quantum Field Theory*. Cambridge University Press, 2007.

[50] A. Zee, *Quantum Field Theory in a Nutshell*. Princton University Press, 2010.

[51] A. Altland and B. Simons, *Condensed Matter Field Theory*. Cambridge University Press, 2010.

[52] J. Rammer, *Quantum Field Theory of Non-Equilibrium States*. Cambridge University Press, 2007.

[53] D. Thouless, *Topological Quantum Numbers in Nonrelativistic Physics*. World Scientific, 1998.

[54] S. Weinberg, *The Quantum Theory of Fields. Vol. 1: Foundations*. Cambridge University Press, 1995.

[55] P. H. Frampton, *Gauge Field Theories: Third Revised and Improved Edition*. Wiley-VCH, Weinheim, Germany, 2008.

[56] M. Gaul and C. Rovelli, *Loop Quantum Gravity and the Meaning of Diffeomorphism Invariance*, Lect.Notes Phys. **541** (2000) 277–324, arXiv:gr-qc/9910079.

[57] S. Elitzur, *Impossibility of Spontaneously Breaking Local Symmetries*, Phys.Rev. **D12** (Dec, 1975) 3978–3982.

[58] M. Greiter, *Is Electromagnetic Gauge Invariance Spontaneously Violated in Superconductors?*, Annals of Physics **319** (2005), no. 1, 217–249.

[59] L. Landau, *On the Angular Momentum of a Two-Photon System*, Dokl.Akad.Nauk Ser.Fiz. **60** (1948) 207–209.

[60] C.-N. Yang, *Selection Rules for the Dematerialization of a Particle into Two Photons*, Phys.Rev. **77** (Jan, 1950) 242–245.

[61] C. Ruegg, B. Normand, M. Matsumoto, A. Furrer, D. McMorrow, K. W. Krämer, H. U. Güdel, S. N. Gvasaliya, H. Mutka, and M. Boehm, *Quantum Magnets under Pressure: Controlling Elementary Excitations in* $\mathrm{TlCuCl_3}$, Phys.Rev.Lett. **100** (May, 2008) 205701.

[62] M. Endres, T. Fukuhara, D. Pekker, M. Cheneau, P. Schauss, *et al.*, *The "Higgs" Amplitude Mode at the Two-Dimensional Superfluid-Mott Insulator Transition*, Nature **487** (2012) 454–458, arXiv:1204.5183.

[63] D. Podolsky, A. Auerbach, and D. P. Arovas, *Visibility of the Amplitude (Higgs) Mode in Condensed Matter*, Phys.Rev. **B84** (Nov, 2011) 174522, arXiv:1108.5207.

[64] D. Podolsky and S. Sachdev, *Spectral functions of the Higgs mode near two-dimensional quantum critical points*, Phys.Rev. **B86** (Aug, 2012) 054508, arXiv:1205.2700.

[65] S. Gazit, D. Podolsky, and A. Auerbach, *Fate of the Higgs mode near quantum criticality*, arXiv (2012) arXiv:1212.3759.

[66] L. Pollet and N. Prokof'ev, *The Higgs Mode in a Two-Dimensional Superfluid*, Phys.Rev.Lett. **109** (Jul, 2012) 010401, arXiv:1204.5190.

[67] A. Pelissetto and E. Vicari, *Critical Phenomena and Renormalization Group Theory*, Phys.Rept. **368** (2002) 549–727, arXiv:cond-mat/0012164.

[68] H. Nishimori and G. Ortiz, *Elements of Phase Transitions and Critical Phenomena*. Oxford University Press, 2011.

[69] P. Di Francesco, P. Mathieu, and D. Senechal, *Conformal Field Theory*. Springer, 1997.

[70] R. M. Wald, *General Relativity*. University of Chicago Press, 1984.

[71] M. A. Vasiliev, *Higher Spin Gauge Theories: Star Product and AdS Space*, arXiv (1999) arXiv:hep-th/9910096. Contributed article to Golfand's Memorial Volume, M. Shifman ed., World Scientific.

[72] M. Henkel and J. Unterberger, *Schrödinger Invariance and Space-Time Symmetries*, Nucl.Phys. **B660** (2003) 407–435, arXiv:hep-th/0302187.

[73] L. Huijse, S. Sachdev, and B. Swingle, *Hidden Fermi Surfaces in Compressible States of Gauge/Gravity Duality*, Phys.Rev. **B85** (2012) 035121, arXiv:1112.0573.

[74] J. M. Maldacena, *The Large N Limit of Superconformal Field Theories and Supergravity*, Adv.Theor.Math.Phys. **2** (1998) 231–252, arXiv:hep-th/9711200.

[75] S. Gubser, I. R. Klebanov, and A. M. Polyakov, *Gauge Theory Correlators from Noncritical String Theory*, Phys.Lett. **B428** (1998) 105–114, arXiv:hep-th/9802109.

[76] E. Witten, *Anti-de Sitter Space and Holography*, Adv.Theor.Math.Phys. **2** (1998) 253–291, arXiv:hep-th/9802150.

[77] I. R. Klebanov and E. Witten, *AdS/CFT Correspondence and Symmetry Breaking*, Nucl.Phys. **B556** (1999) 89–114, arXiv:hep-th/9905104.

[78] D. T. Son and A. O. Starinets, *Minkowski-Space Correlators in AdS/CFT Correspondence: Recipe and Applications*, JHEP **09** (2002) 042, arXiv:hep-th/0205051.

[79] C. Herzog and D. Son, *Schwinger-Keldysh propagators from AdS/CFT correspondence*, JHEP **0303** (2003) 046, arXiv:hep-th/0212072.

[80] B. S. DeWitt, *Quantum Theory of Gravity. I. The Canonical Theory*, Phys.Rev. **160** (Aug, 1967) 1113–1148.

[81] L. Susskind and J. Lindesay, *An Introduction to Black Holes, Information and the String Theory Revolution: The Holographic Universe*. World Scientific, 2005.

[82] E. Martin-Martinez, I. Fuentes, and R. B. Mann, *Using Berry's Phase to Detect the Unruh Effect at Lower Accelerations*, Phys.Rev.Lett. **107** (2011) 131301, arXiv:1012.2208.

[83] O. Lahav, A. Itah, A. Blumkin, C. Gordon, and J. Steinhauer, *Realization of a Sonic Black Hole Analogue in a Bose-Einstein Condensate*, Phys.Rev.Lett. **105** (Dec, 2010) 240401, arXiv:0906.1337.

[84] W. Wootters and W. Zurek, *A Single Quantum Cannot Be Cloned*, Nature **299** (Oct, 1982) 802–803.

[85] A. Almheiri, D. Marolf, J. Polchinski, and J. Sully, *Black Holes: Complementarity or Firewalls?*, JHEP **1302** (2013) 062, arXiv:1207.3123.

[86] R. Bousso, *Complementarity Is Not Enough*, arXiv (2012) arXiv:1207.5192.

[87] L. Susskind, L. Thorlacius, and J. Uglum, *The Stretched Horizon and Black Hole Complementarity*, Phys.Rev. **D48** (1993) 3743–3761, arXiv:hep-th/9306069.

[88] R. Price and K. Thorne, *Membrane Viewpoint on Black Holes: Properties and Evolution of the Stretched Horizon*, Phys.Rev. **D33** (1986) 915–941.

[89] E. Thorne, Kip S., E. Price, R.H., and E. Macdonald, D.A., *Black Holes: The Membrane Paradigm*. Yale University Press, 1986.

[90] D. Bigatti and L. Susskind, *TASI Lectures on the Holographic Principle*, arXiv (1999) 883–933, arXiv:hep-th/0002044.

[91] S. Weinberg and E. Witten, *Limits on Massless Particles*, Phys.Lett. **B96** (1980) 59–62.

[92] T. Thiemann, *Modern Canonical Quantum General Relativity*, arXiv (2001) arXiv:gr-qc/0110034.

[93] T. Thiemann, *Lectures on Loop Quantum Gravity*, Lect.Notes Phys. **631** (2003) 41–135, arXiv:gr-qc/0210094.

[94] H. Nicolai, K. Peeters, and M. Zamaklar, *Loop Quantum Gravity: An Outside View*, Class.Quant.Grav. **22** (2005) R193, arXiv:hep-th/0501114.

[95] J. Polchinski, *String Theory. Vol. 1: An introduction to the bosonic string*. Cambridge University Press, 1998.

[96] J. Polchinski, *String Theory. Vol. 2: Superstring Theory and Beyond*. Cambridge University Press, 1998.

[97] M. Blau and S. Theisen, *String theory as a theory of quantum gravity: A status report*, Gen.Rel.Grav. **41** (2009) 743–755.

[98] D. Tong, *String Theory*, arXiv (2009) arXiv:0908.0333.

[99] B. Zwiebach, *A First Course in String Theory*. Cambridge University Press, 2009.

[100] J. Aastrup and J. M. Grimstrup, *Intersecting Quantum Gravity with Noncommutative Geometry: A Review*, SIGMA **8** (2012) 018, arXiv:1203.6164.

[101] M. A. Levin and X.-G. Wen, *String-Net Condensation: A Physical Mechanism for Topological Phases*, Phys.Rev. **B71** (Jan, 2005) 045110, arXiv:cond-mat/0404617.

[102] M. A. Levin and X.-G. Wen, *A Unification of Light and Electrons Based on Spin Models*, arXiv (2004) arXiv:cond-mat/0407140.

[103] Z.-C. Gu and X.-G. Wen, *A Lattice Bosonic Model as a Quantum Theory of Gravity*, arXiv (2006) arXiv:gr-qc/0606100.

[104] T. Konopka, F. Markopoulou, and S. Severini, *Quantum Graphity: A Model of Emergent Locality*, Phys.Rev. **D77** (May, 2008) 104029, arXiv:0801.0861.

[105] T. Banks, W. Fischler, S. Shenker, and L. Susskind, *M Theory as a Matrix Model: A Conjecture*, Phys.Rev. **D55** (1997) 5112–5128, arXiv:hep-th/9610043.

[106] W. Taylor, *M(atrix) Theory: Matrix Quantum Mechanics as a Fundamental Theory*, Rev.Mod.Phys. **73** (2001) 419–462, arXiv:hep-th/0101126.

[107] J. Polchinski, *M theory and the light cone*, Prog.Theor.Phys.Suppl. **134** (1999) 158–170, arXiv:hep-th/9903165.

[108] J. Polchinski, *Dirichlet Branes and Ramond-Ramond Charges*, Phys.Rev.Lett. **75** (1995) 4724–4727, arXiv:hep-th/9510017.

[109] C. V. Johnson, *D-branes*. Cambridge University Press, 2003.

[110] K. Hashimoto, *D-Brane: Superstrings and New Perspective of our World*. Springer, 2012.

[111] I. Tyutin, *Gauge Invariance in Field Theory and Statistical Physics in Operator Formalism*, arXiv (1975) arXiv:0812.0580.

[112] C. Becchi, A. Rouet, and R. Stora, *Renormalization of Gauge Theories*, Annals Phys. **98** (1976) 287–321.

[113] P. Binétruy, *Supersymmetry: Theory, Experiment and Cosmology*. Oxford University Press, 2006.

[114] D. Z. Freedman and A. Van Proeyen, *Supergravity*. Cambridge University Press, 2012.

[115] E. Bogomolny, *Stability of Classical Solutions*, Sov.J.Nucl.Phys. **24** (1976) 449.

[116] M. Prasad and C. M. Sommerfield, *An Exact Classical Solution for the 't Hooft Monopole and the Julia-Zee Dyon*, Phys.Rev.Lett. **35** (Sep, 1975) 760–762.

[117] E. Witten and D. I. Olive, *Supersymmetry Algebras that Include Topological Charges*, Phys.Lett. **B78** (1978), no. 1, 97–101.

[118] J. D. Lykken, *Introduction to Supersymmetry*, arXiv (1996) 85–153, arXiv:hep-th/9612114.

[119] J. Bagger and J. Wess, *Supersymmetry and Supergravity*. Princton University Press, 1992.

[120] F. Gliozzi, J. Scherk, and D. I. Olive, *Supersymmetry, Supergravity Theories and the Dual Spinor Model*, Nucl.Phys. **B122** (1977) 253–290.

[121] G. Mussardo, *Statistical Field Theory*. Oxford University Press, 2010.

[122] K. Becker, M. Becker, and J. Schwarz, *String theory and M-theory: A modern introduction*. Cambridge University Press, 2007.

[123] O. Aharony, S. S. Gubser, J. M. Maldacena, H. Ooguri, and Y. Oz, *Large N Field Theories, String Theory and Gravity*, Phys.Rept. **323** (2000) 183–386, arXiv:hep-th/9905111.

[124] M. R. Douglas and S. Randjbar-Daemi, *Two Lectures on the AdS/CFT Correspondence*, arXiv (1999) arXiv:hep-th/9902022.

[125] J. L. Petersen, *Introduction to the Maldacena Conjecture on AdS/CFT*, Int.J.Mod.Phys. **A14** (1999) 3597–3672, arXiv:hep-th/9902131.

[126] P. Di Vecchia, *Large N Gauge Theories and AdS/CFT Correspondence*, arXiv (1999) arXiv:hep-th/9908148.

[127] S. Randjbar-Daemi, *Aspects of Gauge Theory/Gravity Correspondence*, arXiv (1999) 311–322, arXiv:hep-th/0004204.

[128] I. R. Klebanov, *TASI lectures: Introduction to the AdS/CFT Correspondence*, arXiv (2000) 615–650, arXiv:hep-th/0009139.

[129] E. Alvarez, J. Conde, and L. Hernandez, *Rudiments of Holography*, Int.J.Mod.Phys. **D12** (2003) 543–582, arXiv:hep-th/0205075.

[130] J. M. Maldacena, *TASI 2003 Lectures on AdS/CFT*, arXiv (2003) 155–203, arXiv:hep-th/0309246.

[131] H. Nastase, *Introduction to AdS/CFT*, arXiv (2007) arXiv:0712.0689.

[132] M. K. Benna and I. R. Klebanov, *Gauge-String Dualities and Some Applications*, arXiv (2008) 611–662, arXiv:0803.1315.

[133] S. R. Wadia, *Gauge/Gravity Duality and Some Applications*, Mod.Phys.Lett. **A25** (2010) 2859–2872, arXiv:1009.0212.

[134] J. Polchinski, *Introduction to Gauge/Gravity Duality*, arXiv (2010) arXiv:1010.6134.

[135] J. Maldacena, *The Gauge/Gravity Duality*, arXiv (2011) arXiv:1106.6073.

[136] M. Duff, *TASI Lectures on Branes, Black Holes and Anti-de Sitter Space*, arXiv (1999) arXiv:hep-th/9912164.

[137] E. D'Hoker and D. Z. Freedman, *Supersymmetric Gauge Theories and the AdS/CFT Correspondence*, arXiv (2002) 3–158, arXiv:hep-th/0201253.

[138] D. J. Smith, *Intersecting brane solutions in string and M theory*, Class.Quant.Grav. **20** (2003) R233, arXiv:hep-th/0210157.

[139] G. Arutyunov and S. Frolov, *Foundations of the $AdS_5 \times S^5$ Superstring. Part I*, J.Phys. **A42** (2009) 254003, arXiv:0901.4937.

[140] A. Karch and E. Katz, *Adding Flavor to AdS/CFT*, JHEP **0206** (2002) 043, arXiv:hep-th/0205236.

[141] J. Erdmenger, N. Evans, I. Kirsch, and E. Threlfall, *Mesons in Gauge/Gravity Duals - A Review*, Eur.Phys.J. **A35** (2008) 81–133, arXiv:0711.4467.

[142] T. Sakai and S. Sugimoto, *Low Energy Hadron Physics in Holographic QCD*, Prog.Theor.Phys. **113** (2005) 843–882, arXiv:hep-th/0412141.

[143] O. Aharony, O. Bergman, D. L. Jafferis, and J. Maldacena, *N=6 superconformal Chern-Simons-matter theories, M2-branes and their gravity duals*, JHEP **0810** (2008) 091, arXiv:0806.1218.

[144] M. Marino, *Lectures on Localization and Matrix Models in Supersymmetric Chern-Simons-Matter Theories*, J.Phys. **A44** (2011) 463001, arXiv:1104.0783.

[145] I. Klebanov and A. Polyakov, *AdS Dual of the Critical O(N) Vector Model*, Phys.Lett. **B550** (2002) 213–219, arXiv:hep-th/0210114.

[146] A. C. Petkou, *Evaluating the AdS Dual of the Critical O(N) Vector Model*, JHEP **0303** (2003) 049, arXiv:hep-th/0302063.

[147] S. Giombi and X. Yin, *On Higher Spin Gauge Theory and the Critical O(N) Model*, Phys.Rev. **D85** (2012) 086005, arXiv:1105.4011.

[148] S. Giombi and X. Yin, *The Higher Spin/Vector Model Duality*, arXiv (2012) arXiv:1208.4036.

[149] J. Sonnenschein, *What does the String/Gauge Correspondence Teach us about Wilson Loops?*, arXiv (1999) 219–269, arXiv:hep-th/0003032.

[150] M. Bertolini, *Four Lectures on the Gauge/Gravity Correspondence*, Int.J.Mod.Phys. **A18** (2003) 5647–5712, arXiv:hep-th/0303160.

[151] E. Imeroni, *The Gauge/String Correspondence Towards Realistic Gauge Theories*, arXiv (2003) arXiv:hep-th/0312070.

[152] L. F. Alday and R. Roiban, *Scattering Amplitudes, Wilson Loops and the String/Gauge Theory Correspondence*, Phys.Rept. **468** (2008) 153–211, arXiv:0807.1889.

[153] S. S. Gubser and A. Karch, *From Gauge-String Duality to Strong Interactions: A Pedestrian's Guide*, Ann.Rev.Nucl.Part.Sci. **59** (2009) 145–168, arXiv:0901.0935.

[154] G. T. Horowitz and J. Polchinski, *Gauge/Gravity Duality*, arXiv (2006) arXiv:gr-qc/0602037.

[155] Y. Tian, X.-N. Wu, and H. Zhang, *Poor Man's Holography: How far can it go?*, arXiv (2012) arXiv:1204.2029.

[156] D. Son, *Toward an AdS/Cold Atoms Correspondence: A Geometric Realization of the Schrödinger Symmetry*, Phys.Rev. **D78** (2008) 046003, arXiv:0804.3972.

[157] K. Balasubramanian and J. McGreevy, *Gravity Duals for Non-Relativistic CFTs*, Phys.Rev.Lett. **101** (2008) 061601, arXiv:0804.4053.

[158] S. Kachru, X. Liu, and M. Mulligan, *Gravity Duals of Lifshitz-like Fixed Points*, Phys.Rev. **D78** (2008) 106005, arXiv:0808.1725.

[159] U. Gursoy, *Gravity/Spin-Model Correspondence and Holographic Superfluids*, JHEP **1012** (2010) 062, arXiv:1007.4854.

[160] O. Aharony, *The Non-AdS/Non-CFT Correspondence, or Three Different Paths to QCD*, arXiv (2002) 3–24, arXiv:hep-th/0212193.

[161] M. Caselle, *Lattice Gauge Theories and the AdS/CFT Correspondence*, Int.J.Mod.Phys. **A15** (2000) 3901–3966, arXiv:hep-th/0003119.

[162] E. Iancu, *Partons and Jets in a Strongly-Coupled Plasma from AdS/CFT*, Acta Phys.Polon. **B39** (2008) 3213–3280, arXiv:0812.0500.

[163] R. A. Janik, *The Dynamics of Quark-Gluon Plasma and AdS/CFT*, Lect.Notes Phys. **828** (2011) 147–181, arXiv:1003.3291.

[164] B. Chen, *An Introduction to AdS/CFT Correspondence for Phenomenologists*, Commun.Theor.Phys. **56** (2011) 895–904.

[165] J. Casalderrey-Solana, H. Liu, D. Mateos, K. Rajagopal, and U. A. Wiedemann, *Gauge/String Duality, Hot QCD and Heavy Ion Collisions*, arXiv (2011) arXiv:1101.0618.

[166] D. T. Son and A. O. Starinets, *Viscosity, Black Holes, and Quantum Field Theory*, Ann.Rev.Nucl.Part.Sci. **57** (2007) 95–118, arXiv:0704.0240.

[167] M. Rangamani, *Gravity and Hydrodynamics: Lectures on the Fluid/Gravity Correspondence*, Class.Quant.Grav. **26** (2009) 224003, arXiv:0905.4352.

[168] V. E. Hubeny and M. Rangamani, *A Holographic view on physics out of equilibrium*, Adv.High Energy Phys. **2010** (2010) 297916, arXiv:1006.3675.

[169] J. Bhattacharya, S. Bhattacharyya, and S. Minwalla, *Dissipative Superfluid Dynamics from Gravity*, JHEP **1104** (2011) 125, arXiv:1101.3332.

[170] V. E. Hubeny, S. Minwalla, and M. Rangamani, *The Fluid/Gravity Correspondence*, arXiv (2011) arXiv:1107.5780.

[171] J. McGreevy, *Holographic Duality with a View Toward Many-Body Physics*, Adv.High Energy Phys. **2010** (2010) 723105, arXiv:0909.0518.

[172] S. A. Hartnoll, *Quantum Critical Dynamics from Black Holes*, arXiv (2009) arXiv:0909.3553.

[173] S. Sachdev, *Condensed Matter and AdS/CFT*, Lect.Notes Phys. **828** (2011) 273–311, arXiv:1002.2947.

[174] A. Pires, *AdS/CFT Correspondence in Condensed Matter*, arXiv (2010) arXiv:1006.5838.

[175] S.-S. Lee, *TASI Lectures on Emergence of Supersymmetry, Gauge Theory and String in Condensed Matter Systems*, arXiv (2010) arXiv:1009.5127.

[176] G. T. Horowitz, *Surprising Connections Between General Relativity and Condensed Matter*, Class.Quant.Grav. **28** (2011) 114008, arXiv:1010.2784.

[177] S. A. Hartnoll, *Horizons, Holography and Condensed Matter*, arXiv (2011) arXiv:1106.4324.

[178] F. Benini, *Holography and Condensed Matter*, Fortsch.Phys. **60** (2012) 810–821, arXiv:1202.6008.

[179] A. Adams, L. D. Carr, T. Schäfer, P. Steinberg, and J. E. Thomas, *Strongly Correlated Quantum Fluids: Ultracold Quantum Gases, Quantum Chromodynamic Plasmas, and Holographic Duality*, New J.Phys. **14** (2012) 115009, arXiv:1205.5180.

[180] S. S. Gubser, *TASI lectures: Collisions in Anti-de Sitter Space, Conformal Symmetry, and Holographic Superconductors*, arXiv (2010) arXiv:1012.5312.

[181] C. P. Herzog, P. Kovtun, S. Sachdev, and D. T. Son, *Quantum Critical Transport, Duality, and M-theory*, Phys.Rev. **D75** (2007) 085020, arXiv:hep-th/0701036.

[182] J. McGreevy, *Viewpoint: In Pursuit of a Nameless Metal*, Physics **3** (2010) 83.

[183] S. Sachdev, *Strange Metals and the AdS/CFT Correspondence*, J.Stat.Mech. **1011** (2010) P11022, arXiv:1010.0682.

[184] B.-H. Lee, D.-W. Pang, and C. Park, *A Holographic Model of Strange Metals*, Int.J.Mod.Phys. **A26** (2011) 2279–2305, arXiv:1107.5822.

[185] L. Huijse and S. Sachdev, *Fermi Surfaces and Gauge-Gravity Duality*, Phys.Rev. **D84** (2011) 026001, arXiv:1104.5022.

[186] G. 't Hooft, *A Planar Diagram Theory for Strong Interactions*, Nucl.Phys. **B72** (1974) 461.

[187] F. W. J. Olver, D. W. Lozier, R. F. Boisvert, and C. W. Clark, *NIST Handbook of Mathematical Functions*. Cambridge University Press, 2010.

[188] P. Breitenlohner and D. Z. Freedman, *Positive Energy in Anti-De Sitter Backgrounds and Gauged Extended Supergravity*, Phys.Lett. **B115** (1982) 197.

[189] L. Susskind and E. Witten, *The Holographic Bound in Anti-de Sitter Space*, arXiv (1998) arXiv:hep-th/9805114.

[190] K. Skenderis, *Lecture Notes on Holographic Renormalization*, Class.Quant.Grav. **19** (2002) 5849–5876, arXiv:hep-th/0209067.

[191] D. Freedman, S. Gubser, K. Pilch, and N. Warner, *Renormalization Group Flows from Holography Supersymmetry and a C-Theorem*, Adv.Theor.Math.Phys. **3** (1999) 363–417, arXiv:hep-th/9904017.

[192] N. Iqbal and H. Liu, *Real-Time Response in AdS/CFT with Application to Spinors*, Fortsch.Phys. **57** (2009) 367–384, arXiv:0903.2596.

[193] A. Adams, K. Balasubramanian, and J. McGreevy, *Hot Spacetimes for Cold Atoms*, JHEP **0811** (2008) 059, arXiv:0807.1111.

[194] S. Lee, S. Minwalla, M. Rangamani, and N. Seiberg, *Three Point Functions of Chiral Operators in $D = 4$, $N = 4$ SYM at large N*, Adv.Theor.Math.Phys. **2** (1998) 697–718, arXiv:hep-th/9806074.

[195] D. Z. Freedman, S. D. Mathur, A. Matusis, and L. Rastelli, *Correlation Functions in the CFT(d)/AdS(d+1) Correspondence*, Nucl.Phys. **B546** (1999) 96–118, arXiv:hep-th/9804058.

[196] D. Serban, *Integrability and the AdS/CFT Correspondence*, J.Phys. **A44** (2011) 124001, arXiv:1003.4214.

[197] N. Beisert, C. Ahn, L. F. Alday, Z. Bajnok, J. M. Drummond, *et al.*, *Review of AdS/CFT Integrability: An Overview*, Lett.Math.Phys. **99** (2012) 3–32, arXiv:1012.3982.

[198] M. Ammon, M. Kaminski, and A. Karch, *Hyperscaling-Violation on Probe D-Branes*, JHEP **1211** (2012) 028, arXiv:1207.1726.

[199] S. Weinberg, *Infrared Photons and Gravitons*, Phys.Rev. **140** (1965) B516–B524.

[200] V. Balasubramanian, P. Kraus, A. E. Lawrence, and S. P. Trivedi, *Holographic Probes of Anti-de Sitter Space-Times*, Phys.Rev. **D59** (1999) 104021, arXiv:hep-th/9808017.

[201] L. Keldysh, *Diagram Technique for Nonequilibrium Processes*, Zh.Eksp.Teor.Fiz. **47** (1964) 1515–1527.

[202] J. Zinn-Justin, *Quantum field theory and critical phenomena*, vol. 113. Oxford, 2002.

[203] K. Efetov, *Supersymmetry in Disorder and Chaos*. Cambridge University Press, 1997.

[204] A. Kamenev, *Field Theory of Non-Equilibrium Systems*. Cambridge University Press, 2011.

[205] K. Maeda, M. Natsuume, and T. Okamura, *On two Pieces of Folklore in the AdS/CFT Duality*, Phys.Rev. **D82** (2010) 046002, arXiv:1005.2431.

[206] S. S. Gubser, *Breaking an Abelian Gauge Symmetry near a Black Hole Horizon*, Phys.Rev. **D78** (2008) 065034, arXiv:0801.2977.

[207] S. A. Hartnoll, C. P. Herzog, and G. T. Horowitz, *Building a Holographic Superconductor*, Phys.Rev.Lett. **101** (2008) 031601, arXiv:0803.3295.

[208] S. S. Gubser and S. S. Pufu, *The Gravity Dual of a p-Wave Superconductor*, JHEP **0811** (2008) 033, arXiv:0805.2960.

[209] J.-W. Chen, Y.-J. Kao, D. Maity, W.-Y. Wen, and C.-P. Yeh, *Towards A Holographic Model of D-Wave Superconductors*, Phys.Rev. **D81** (2010) 106008, arXiv:1003.2991.

[210] F. Benini, C. P. Herzog, R. Rahman, and A. Yarom, *Gauge Gravity Duality for D-Wave Superconductors: Prospects and Challenges*, JHEP **1011** (2010) 137, arXiv:1007.1981.

[211] H.-B. Zeng, Z.-Y. Fan, and H.-S. Zong, *D-Wave Holographic Superconductor Vortex Lattice and Non-Abelian Holographic Superconductor Droplet*, Phys.Rev. **D82** (2010) 126008, arXiv:1007.4151.

[212] I. Amado, M. Kaminski, and K. Landsteiner, *Hydrodynamics of Holographic Superconductors*, JHEP **05** (2009) 021, arXiv:0903.2209.

[213] C. P. Herzog, *An Analytic Holographic Superconductor*, Phys. Rev. **D81** (2010) 126009, arXiv:1003.3278.

[214] H.-B. Zeng, X. Gao, Y. Jiang, and H.-S. Zong, *Analytical Computation of Critical Exponents in Several Holographic Superconductors*, JHEP **1105** (2011) 002, arXiv:1012.5564.

[215] M. Ammon, J. Erdmenger, M. Kaminski, and P. Kerner, *Superconductivity from Gauge/Gravity Duality with Flavor*, Phys.Lett. **B680** (2009) 516–520, arXiv:0810.2316.

[216] P. Basu, J. He, A. Mukherjee, and H.-H. Shieh, *Superconductivity from D3/D7: Holographic Pion Superfluid*, JHEP **0911** (2009) 070, arXiv:0810.3970.

[217] M. Ammon, J. Erdmenger, M. Kaminski, and P. Kerner, *Flavor Superconductivity from Gauge/Gravity Duality*, JHEP **0910** (2009) 067, arXiv:0903.1864.

[218] S. A. Hartnoll, C. P. Herzog, and G. T. Horowitz, *Holographic Superconductors*, JHEP **0812** (2008) 015, arXiv:0810.1563.

[219] M. Ammon, J. Erdmenger, V. Grass, P. Kerner, and A. O'Bannon, *On Holographic p-wave Superfluids with Back-Reaction*, Phys.Lett. **B686** (2010) 192–198, arXiv:0912.3515.

[220] P. Kovtun and A. Ritz, *Universal Conductivity and Central Charges*, Phys.Rev. **D78** (2008) 066009, arXiv:0806.0110.

[221] A. Chamblin, R. Emparan, C. V. Johnson, and R. C. Myers, *Charged AdS Black Holes and Catastrophic Holography*, Phys.Rev. **D60** (1999) 064018, arXiv:hep-th/9902170.

[222] J. Erdmenger, V. Grass, P. Kerner, and T. H. Ngo, *Holographic Superfluidity in Imbalanced Mixtures*, JHEP **1108** (2011) 037, arXiv:1103.4145.

[223] C. Herzog, P. Kovtun, and D. Son, *Holographic Model of Superfluidity*, Phys.Rev. **D79** (2009) 066002, arXiv:0809.4870.

[224] P. Basu and J.-H. Oh, *Analytic Approaches to Anisotropic Holographic Superfluids*, JHEP **1207** (2012) 106, arXiv:1109.4592.

[225] K. Skenderis and M. Taylor, *Branes in AdS and p p Wave Space-Times*, JHEP **0206** (2002) 025, arXiv:hep-th/0204054.

[226] M. Dressel and G. Grüner, *Electrodynamics of Solids*. Cambridge University Press, 2003.

[227] R. Kubo, *Statistical-Mechanical Theory of Irreversible Processes. I. General Theory and Simple Applications to Magnetic and Conduction Problems*, Journal of the Physical Society of Japan **12** (1957), no. 6, 570–586.

[228] A. Amariti, D. Forcella, A. Mariotti, and G. Policastro, *Holographic Optics and Negative Refractive Index*, JHEP **1104** (2011) 036, arXiv:1006.5714. 20+1 pages, 7 figures.

[229] D. T. Son and A. O. Starinets, *Hydrodynamics of R-Charged Black Holes*, JHEP **0603** (2006) 052, arXiv:hep-th/0601157.

[230] J. Erdmenger, M. Haack, M. Kaminski, and A. Yarom, *Fluid Dynamics of R-charged Black Holes*, JHEP **0901** (2009) 055, arXiv:0809.2488.

[231] N. Banerjee, J. Bhattacharya, S. Bhattacharyya, S. Dutta, R. Loganayagam, *et al.*, *Hydrodynamics from Charged Black Branes*, JHEP **1101** (2011) 094, arXiv:0809.2596.

[232] R. C. Myers, A. O. Starinets, and R. M. Thomson, *Holographic Spectral Functions and Diffusion Constants for Fundamental Matter*, JHEP **11** (2007) 091, arXiv:0706.0162.

[233] S. A. Hartnoll and D. M. Hofman, *Locally Critical Resistivities from Umklapp Scattering*, Phys.Rev.Lett. **108** (2012) 241601, arXiv:1201.3917.

[234] J. L. Tallon, J. R. Cooper, S. H. Naqib, and J. W. Loram, *Scaling Relation for the Superfluid Density of Cuprate Superconductors: Origins and Limits*, Phys. Rev. B **73** (May, 2006) 180504.

[235] D. v. d. Marel, H. J. A. Molegraaf, J. Zaanen, Z. Nussinov, F. Carbone, A. Damascelli, H. Eisaki, M. Greven, P. H. Kes, and M. Li, *Quantum Critical Behaviour in a High-Tc Superconductor*, Nature **425** (Sep, 2003) 271–274.

[236] D. Tanner, H. Liu, M. Quijada, A. Zibold, H. Berger, R. Kelley, M. Onellion, F. Chou, D. Johnston, J. Rice, D. Ginsberg, and J. Markert, *Superfluid and Normal Fluid Density in High-Tc Superconductors*, Physica B: Condensed Matter **244** (Jan, 1998) 1–8.

[237] J. Mas, J. P. Shock, and J. Tarrio, *Sum Rules, Plasma Frequencies and Hall phenomenology in Holographic Plasmas*, JHEP **1102** (2011) 015, arXiv:1010.5613.

[238] D. R. Gulotta, C. P. Herzog, and M. Kaminski, *Sum Rules from an Extra Dimension*, JHEP **1101** (2011) 148, arXiv:1010.4806.

[239] U. Gürsoy, E. Plauschinn, H. Stoof, and S. Vandoren, *Holography and ARPES Sum-Rules*, JHEP **1205** (2012) 018, arXiv:1112.5074.

[240] T. Faulkner, G. T. Horowitz, and M. M. Roberts, *Holographic Quantum Criticality from Multi-Trace Deformations*, JHEP **1104** (2011) 051, arXiv:1008.1581.

[241] J.-H. She and J. Zaanen, *BCS superconductivity in quantum critical metals*, Phys. Rev. B **80** (Nov, 2009) 184518.

[242] F. Bigazzi, A. L. Cotrone, D. Musso, N. P. Fokeeva, and D. Seminara, *Unbalanced Holographic Superconductors and Spintronics*, JHEP **1202** (2012) 078, arXiv:1111.6601.

[243] S. A. Hartnoll, J. Polchinski, E. Silverstein, and D. Tong, *Towards Strange Metallic Holography*, JHEP **1004** (2010) 120, arXiv:0912.1061.

[244] S. A. Hartnoll and A. Tavanfar, *Electron Stars for Holographic Metallic Criticality*, Phys.Rev. **D83** (2011) 046003, arXiv:1008.2828.

[245] S. S. Gubser and A. Nellore, *Ground States of Holographic Superconductors*, Phys.Rev. **D80** (2009) 105007, arXiv:0908.1972.

[246] S. S. Gubser and F. D. Rocha, *The Gravity Dual to a Quantum Critical Point with Spontaneous Symmetry Breaking*, Phys.Rev.Lett. **102** (2009) 061601, arXiv:0807.1737.

[247] J. P. Gauntlett, J. Sonner, and T. Wiseman, *Holographic Superconductivity in M-Theory*, Phys.Rev.Lett. **103** (2009) 151601, arXiv:0907.3796.

[248] S. S. Gubser, S. S. Pufu, and F. D. Rocha, *Quantum Critical Superconductors in String Theory and M-Theory*, Phys.Lett. **B683** (2010) 201–204, arXiv:0908.0011.

[249] C. Charmousis, B. Gouteraux, B. Kim, E. Kiritsis, and R. Meyer, *Effective Holographic Theories for Low-Temperature Condensed Matter Systems*, JHEP **1011** (2010) 151, arXiv:1005.4690.

[250] P. Basu, J. He, A. Mukherjee, and H.-H. Shieh, *Hard-Gapped Holographic Superconductors*, Phys.Lett. **B689** (2010) 45–50, arXiv:0911.4999.

[251] S. S. Gubser, F. D. Rocha, and A. Yarom, *Fermion Correlators in Non-Abelian Holographic Superconductors*, JHEP **1011** (2010) 085, arXiv:1002.4416.

[252] M. Edalati, J. I. Jottar, and R. G. Leigh, *Transport Coefficients at Zero Temperature from Extremal Black Holes*, JHEP **1001** (2010) 018, arXiv:0910.0645.

[253] M. Edalati, J. I. Jottar, and R. G. Leigh, *Holography and the Sound of Criticality*, JHEP **1010** (2010) 058, arXiv:1005.4075.

[254] D. Nickel and D. T. Son, *Deconstructing Holographic Liquids*, New J.Phys. **13** (2011) 075010, arXiv:1009.3094.

[255] M. Cvetic, M. Duff, P. Hoxha, J. T. Liu, H. Lu, *et al.*, *Embedding AdS Black Holes in Ten-Dimensions and Eleven-Dimensions*, Nucl.Phys. **B558** (1999) 96–126, arXiv:hep-th/9903214.

[256] A. Buchel and J. T. Liu, *Gauged Supergravity from Type IIB String Theory on Y**p,q Manifolds*, Nucl.Phys. **B771** (2007) 93–112, arXiv:hep-th/0608002.

[257] J. P. Gauntlett, E. O Colgain, and O. Varela, *Properties Of Some Conformal Field Theories with M-theory Duals*, JHEP **0702** (2007) 049, arXiv:hep-th/0611219.

[258] J. P. Gauntlett and O. Varela, *Consistent Kaluza-Klein Reductions for General Supersymmetric AdS Solutions*, Phys.Rev. **D76** (2007) 126007, arXiv:0707.2315.

[259] A. Karch and A. O'Bannon, *Holographic Thermodynamics at Finite Baryon Density: Some Exact Results*, JHEP **0711** (2007) 074, arXiv:0709.0570.

[260] M. Kruczenski, D. Mateos, R. C. Myers, and D. J. Winters, *Meson Spectroscopy in AdS/CFT with Flavour*, JHEP **07** (2003) 049, arXiv:hep-th/0304032.

[261] T. Faulkner, H. Liu, J. McGreevy, and D. Vegh, *Emergent Quantum criticality, Fermi surfaces, and* AdS_2, Phys.Rev. **D83** (2011) 125002, arXiv:0907.2694.

[262] S. Kobayashi, D. Mateos, S. Matsuura, R. C. Myers, and R. M. Thomson, *Holographic Phase Transitions at Finite Baryon Density*, JHEP **0702** (2007) 016, arXiv:hep-th/0611099.

[263] D. Mateos, S. Matsuura, R. C. Myers, and R. M. Thomson, *Holographic Phase Transitions at Finite Chemical Potential*, JHEP **0711** (2007) 085, arXiv:0709.1225.

[264] A. Karch, D. Son, and A. Starinets, *Zero Sound from Holography*, arXiv (2008) arXiv:0806.3796.

[265] A. Karch, M. Kulaxizi, and A. Parnachev, *Notes on Properties of Holographic Matter*, JHEP **0911** (2009) 017, arXiv:0908.3493.

[266] P. Benincasa, *Universality of Holographic Phase Transitions and Holographic Quantum Liquids*, arXiv (2009) arXiv:0911.0075.

[267] S. Nakamura, H. Ooguri, and C.-S. Park, *Gravity Dual of Spatially Modulated Phase*, Phys.Rev. **D81** (2010) 044018, arXiv:0911.0679.

[268] M. Kulaxizi and A. Parnachev, *Comments on Fermi Liquid from Holography*, Phys.Rev. **D78** (2008) 086004, arXiv:0808.3953.

[269] K.-Y. Kim and I. Zahed, *Baryonic Response of Dense Holographic QCD*, JHEP **0812** (2008) 075, arXiv:0811.0184.

[270] G. Policastro, D. T. Son, and A. O. Starinets, *From AdS/CFT Correspondence to Hydrodynamics. 2. Sound Waves*, JHEP **0212** (2002) 054, arXiv:hep-th/0210220.

[271] K. Jensen, A. Karch, D. T. Son, and E. G. Thompson, *Holographic Berezinskii-Kosterlitz-Thouless Transitions*, Phys.Rev.Lett. **105** (2010) 041601, arXiv:1002.3159.

[272] K. Jensen, *More Holographic Berezinskii-Kosterlitz-Thouless Transitions*, Phys.Rev. **D82** (2010) 046005, arXiv:1006.3066.

[273] N. Evans, K. Jensen, and K.-Y. Kim, *Non Mean-Field Quantum Critical Points from Holography*, Phys.Rev. **D82** (2010) 105012, arXiv:1008.1889.

[274] V. G. Filev, C. V. Johnson, R. Rashkov, and K. Viswanathan, *Flavoured Large N Gauge Theory in an External Magnetic Field*, JHEP **0710** (2007) 019, arXiv:hep-th/0701001.

[275] N. Evans, A. Gebauer, K.-Y. Kim, and M. Magou, *Holographic Description of the Phase Diagram of a Chiral Symmetry Breaking Gauge Theory*, JHEP **1003** (2010) 132, arXiv:1002.1885.

[276] K. Jensen, A. Karch, and E. G. Thompson, *A Holographic Quantum Critical Point at Finite Magnetic Field and Finite Density*, JHEP **1005** (2010) 015, arXiv:1002.2447.

[277] N. Iqbal, H. Liu, M. Mezei, and Q. Si, *Quantum Phase Transitions in Holographic Models of Magnetism and Superconductors*, Phys.Rev. **D82** (2010) 045002, arXiv:1003.0010.

[278] A. Karch, J. Maciejko, and T. Takayanagi, *Holographic Fractional Topological Insulators in 2+1 and 1+1 Dimensions*, Phys.Rev. **D82** (2010) 126003, arXiv:1009.2991.

[279] E. W. Leaver, *Quasinormal Modes of Reissner-Nordström Black Holes*, Phys.Rev. **D41** (1990) 2986–2997.

[280] A. Nunez and A. O. Starinets, *AdS / CFT Correspondence, Quasi-Normal Modes, and Thermal Correlators in $N = 4$ SYM*, Phys.Rev. **D67** (2003) 124013, arXiv:hep-th/0302026.

[281] F. Denef, S. A. Hartnoll, and S. Sachdev, *Quantum Oscillations and Black Hole Ringing*, Phys.Rev. **D80** (2009) 126016, arXiv:0908.1788.

[282] M. Kaminski, K. Landsteiner, F. Pena-Benitez, J. Erdmenger, C. Greubel, and P. Kerner, *Quasinormal Modes of Massive Charged Flavor Branes*, JHEP **1003** (2010) 117, arXiv:0911.3544.

[283] M. Edalati, J. I. Jottar, and R. G. Leigh, *Shear Modes, Criticality and Extremal Black Holes*, JHEP **1004** (2010) 075, arXiv:1001.0779.

[284] M. Ammon, K. Jensen, K.-Y. Kim, J. N. Laia, and A. O'Bannon, *Moduli Spaces of Cold Holographic Matter*, JHEP **1211** (2012) 055, arXiv:1208.3197.

[285] Q. Pan and B. Wang, *General Holographic Superconductor Models with Backreactions*, arXiv (2011) arXiv:1101.0222.

[286] S. Sachdev, *A Model of a Fermi Liquid using Gauge-Gravity Duality*, Phys.Rev. **D84** (2011) 066009, arXiv:1107.5321.

[287] T. Nishioka, S. Ryu, and T. Takayanagi, *Holographic Superconductor/Insulator Transition at Zero Temperature*, JHEP **1003** (2010) 131, arXiv:0911.0962.

[288] S. A. Hartnoll and E. Shaghoulian, *Spectral Weight in Holographic Scaling Geometries*, JHEP **1207** (2012) 078, arXiv:1203.4236.

[289] M. Ammon, J. Erdmenger, M. Kaminski, and A. O'Bannon, *Fermionic Operator Mixing in Holographic p-wave Superfluids*, JHEP **05** (2010) 053, arXiv:1003.1134.

[290] R. Apreda, J. Erdmenger, N. Evans, and Z. Guralnik, *Strong Coupling Effective Higgs Potential and a First Order Thermal Phase Transition from AdS/CFT Duality*, Phys.Rev. **D71** (2005) 126002, arXiv:hep-th/0504151.

[291] A. Karch and L. Randall, *Open and Closed String Interpretation of SUSY CFT's on Branes with Boundaries*, JHEP **0106** (2001) 063, arXiv:hep-th/0105132.

[292] O. DeWolfe, D. Z. Freedman, and H. Ooguri, *Holography and Defect Conformal Field Theories*, Phys.Rev. **D66** (2002) 025009, arXiv:hep-th/0111135.

[293] J. Erdmenger, Z. Guralnik, and I. Kirsch, *Four-Dimensional Superconformal Theories with Interacting Boundaries or Defects*, Phys.Rev. **D66** (2002) 025020, arXiv:hep-th/0203020.

[294] N. Evans, A. Gebauer, K.-Y. Kim, and M. Magou, *Phase Diagram of the D3/D5 System in a Magnetic Field and a BKT Transition*, Phys.Lett. **B698** (2011) 91–95, arXiv:1003.2694.

[295] H.-C. Chang and A. Karch, *Novel Solutions of Finite-Density D3/D5 Probe Brane System and Their Implications for Stability*, JHEP **1210** (2012) 069, arXiv:1207.7078.

[296] L. Martucci, J. Rosseel, D. Van den Bleeken, and A. Van Proeyen, *Dirac Actions for D-branes on Backgrounds with Fluxes*, Class. Quant. Grav. **22** (2005) 2745–2764, arXiv:hep-th/0504041.

[297] D. Petz and G. Toth, *The Bogoliubov Inner Product in Quantum Statistics*, Letters in Mathematical Physics **27** (1993), no. 3, 205–216.

[298] F. Gieres, *Dirac's Formalism and Mathematical Surprises in Quantum Mechanics*, arXiv (1999) arXiv:quant-ph/9907069.

Acknowledgments

The author would like to thank Johanna Erdmenger for her supportive and encouraging supervision of this thesis, the opportunity to write this doctoral thesis and the very nice and enjoyable working atmosphere in her group. I thank Dieter Lüst for the stimulating and productive working environment provided at the Max Planck Institute for Physics, reading through this thesis as a second supervisor and for his incredible short response time concerning email communication.

Furthermore, I like to thank my co-workers Martin Ammon for his patient and elucidating explanations at the beginning of my work, Shu Lin for the productive support concerning analytical calculations, Jonathan Shock for helping to code useful, fast and reliable *Mathematica* codes, Patrick Kerner for various discussion on Homes' law and holographic superconductors and Andy O'Bannon for inspiring ideas.

For carefully proofreading parts of my thesis and giving me suggestions and comments, I thank Federico Bonetti, Benedikt Herwerth, Max-Niklas Newizella, Migael Strydom, Hansjörg Zeller and Ann-Kathrin Straub. I am indebted to Martin Ammon, Mario Araujo, Federico Bonetti, Sophia Borowka, Yan-Yan Bu, Andreas Deser, Veselin Filev, Viviane Graß, Benedikt Herwerth, Benjamin Jurke, Patrick Kerner, Shu Lin, Noppadol Mekareeya, Hai Thanh Ngo, Thorsten Rahn, Oliver Schlotterer, Jonathan Shock, Charlotte Sleight, Stephan Steinfurt, Ann-Kathrin Straub, Migael Strydom, Matthias Weissenbacher and Hansjörg Zeller for the pleasant time spent together and for the many intriguing discussion, not only about physics.

Last but not least I would like to thank my wife for her unconditional support during the time of my doctoral studies.